International
Mine Water Association

2013 Annual Conference

MINE
WATER
TECHNOLOGY
RELIABLE

Golden, Colorado, USA
August 6 – 9, 2013

VOLUME
II

RELIABLE MINE WATER TECHNOLOGY
VOLUME II

Reliable Mine Water Technology

Volume II

Proceedings of the
International Mine Water Association
Annual Conference 2013

August 6 — 9, 2013

Golden, Colorado, USA

Editors

Adrian Brown

Linda Figueroa

Christian Wolkersdorfer

International Mine Water Association. Anual Conference (2013 : Golden, CO)
Reliable Mine Water Technology –Volume II
International Mine Water Association Annual Conference,
2013, Golden, Colorado, USA / Adrian Brown, Linda Figueroa, Christian Wolkersdorfer, editors.

ISBN 978-0-615-79385-6 Volume II

Cover Design ✒ Karoline Wolkersdorfer
Layout and Typesetting ✒ Prof. Dr. habil. Christian Wolkersdorfer

Cover Photographs
front Stephen W. Oachs ❧ Henk Coetzee ❧ Carleton R. Bern ❧ Arabella M. L. Moorhouse ❧ Christian Wolkersdorfer ❧ **back** Matthew T. Bailey ❧ Henk Coetzee ❧ Christian Wolkersdorfer

Themes Photographs
5 John Chahbandour ❧ **6** Naďa Rapantova ❧ **7** Christian Wolkersdorfer ❧ **8** Raymond Johnson

Typeset with QuarkXPress in TheAntiqua, TheMix, and TheSans from Lukas de Groot

Printed in the USA on recycled paper

www.IMWA.info

Organizers

International Mine Water Association

Colorado School of Mines

International Scientific Committee

Joel Adams, USA
Sandra Ainsworth, USA
Lena Alakangas, Sweden
Bert Allard, Sweden
Lee C. Atkinson, USA
Mattias Bäckström, Sweden
Jeff Bain, Canada
Andre Banning, Germany
Carleton R Bern, USA
Nico Bezuidenhout, South Africa
Colin J. Booth, USA
Hanna Braden, USA
Adrian Brown, USA
John Chahbandour, USA
Rosa Cidu, Italy
Wilhelm Georg Coldewey, Germany
David Dettrick, Australia
Enrico Dinelli, Italy
Craig Divine, USA
Scott Effner, USA
Linda Ann Figueroa, USA
Kay Florence, United Kingdom
Jennifer N. Geroni, United Kingdom
Jeff Gillow, USA
Jordi Guimera, Chile
James Edward Hanley, USA
Robert S Hedin, USA
Roger Lynn Howell, USA
Amy L. Hudson, USA
Ryan Jakubowski, Peru
Frans Knops, Netherlands
Natalie Alyssa Kruse Daniels, USA
Jorge Loredo, Spain
John Foriyes Lupo, USA
Clint McCullough, Australia
Broder Merkel, Germany
Thomas Metschies, Germany
Jacek Motyka, Poland
Kevin Myers, USA
Robert W. Nairn, USA
James Navratil, USA
Carmen Neculita, Canada
Nora Hilda Paños, Argentina
Walter Pohl, Austria
Volker Preuss, Germany
Naďa Rapantova, Czech Republic
Pierre Rousseau, Australia
Martin Schultze, Germany
Robert Seal, USA
Alison Sinclair, Australia
Kathleen S. Smith, USA
Mark Vancook, Canada
Rens Verburg, USA
Danie Vermeulen, South Africa
John Waterhouse, Australia
Daniel Weber, USA
Walter Weinig, USA
Phillip Whittle, Australia
Frank Winde, South Africa
Andrzej Witkowski, Poland
Christian Wolkersdorfer, Germany
Magdalena Worsa-Kozak, Poland

Local Organising Committee

Co-Chairs

Adrian Brown PE	President, International Mine Water Association, Denver, Colorado USA
Dr. Linda Figueroa	Associate Professor, Colorado School of Mines, Golden, Colorado USA

Members

Dr. Lee Atkinson	Atkinson Mine Water Consultants, Inc., Golden, Colorado USA
Dr. Carleton Bern	United States Geological Survey, Lakewood, Colorado USA
Dr. Raymond Johnson	United States Geological Survey, Lakewood, Colorado USA
Dr. Robert Kleinmann	CH2M Hill, Pittsburgh, Pennsylvania USA
Dr. John Lupo PE	Newmont Mining Corporation, Fiddlers Green, Colorado USA
Dr. Mei Lin Shelp	Barrick Mining Corporation, Toronto, Canada
Dr. Kathy Smith	United States Geological Survey, Lakewood, Colorado USA
Liz Swaim	Itasca Denver, Lakewood, Colorado USA
John Waterhouse	Golder Associates, Perth, Western Australia
Daniel Weber PG	Montgomery & Associates, Denver, Colorado USA
Dr. Christian Wolkersdorfer	International Mine Water Association, Freiberg, Germany

Administration

Melody Francisco	CSM Special Programs and Continuing Education, Golden, Colorado USA
Timothy O’Leary	CSM Special Programs and Continuing Education, Golden, Colorado USA

IMWA 2013 Sponsors

Silver Sponsor

Schlumberger
Water Services

Bronze Sponsors

AngloGold Ashanti
ANGLOGOLD ASHANTI NORTH AMERICA INC.

BARRICK

CC&V
Cripple Creek & Victor
Gold Mining Company
www.ccvgoldmine.com

DHI
The expert in WATER ENVIRONMENTS

Golder Associates

NEWMONT™

SiLi®
SIGMUND LINDNER

Other Sponsors

CH2MHILL®

CMA
COLORADO MINING ASSOCIATION

FEFLOW

Contents

Volume I ❧ Themes 1–4

1 Reliable Mine Water Permits and Regulation

2 Reliable Mine Water Hydrology

| 3 RELIABLE MINE WATER GEOCHEMISTRY

4 RELIABLE MINE WATER TREATMENT

| VOLUME II ❧ THEMES 5 – 8

| 5 RELIABLE MINE WATER OPERATIONS

| 6 RELIABLE MINE WATER CLOSURE

| 7 RELIABLE MINED HYDROCARBON WATER

8 FIELD TRIPS

LAGNIAPPE

5

RELIABLE MINE WATER OPERATIONS

RELIABLE
MINE WATER OPERATIONS

DROP Project: Leaching process optimization for reducing water consumption in copper mining

Ulrike Broschek, Jorge Lobos, Jorge Cornejo, Luis Bravo, Josué Lagos, Karien Volker

Fundación Chile, Av Parque Antonio Rabat Sur 6165, Vitacura, Santiago, Chile

Abstract The growing water shortage in the north of Chile and the projected growth of the mining sector has forced the initiation of efforts to optimize the use of water resources and to minimize water losses. The DROP Initiative, developed by Fundación Chile at a mine company, aimed to reduce fresh water consumption in the leaching process by the optimization of the sprinkler irrigation system. The results of the field tests performed on the leaching pads showed that the solution generated can meet the goal of reducing water losses defined at the beginning of the project of 5 L/s.

Keywords Water losses, leaching process, sprinkler irrigation, evaporation

Introduction

Copper mining takes place mainly in the North of Chile, where the availability of water resources is limited mainly due to low rainfall. This limited availability of water is exacerbated by, the growing increase in water demand from mining in conjunction with the changes in the water cycle caused by global climate change, particularly evident in recent years (Garredeau 2011). As a result of this situation the mining projects in the area, both old and new, are affected by this shortage which has led to the urgent need to develop optimization processes in current mining water consumption(Cochilco 2010). This is how project DROP emerged: an initiative led by the Water and Environment Department of Fundacion Chile alongside a mine company of northern Chile. This initiative is part of the Cluster World Class Provider Programme for the global mining industry, which seeks to encourage suppliers to develop greater technology and management in order to address the challenges that the mining industry has throughout the country and the world (Fundación Chile 2012).

Copper mining in Chile has two operational paths, depending on whether the copper ore is in a sulfide or oxidized state, holding constant the extraction stages. The sulfide milling process, involves; flotation, smelting and electro-refining. If oxidized, it will go through a leaching, solvent extraction and electro-winning process. Mining Company, through this latter process, operates under dynamic heaps, formed by mixtures of oxide-type materials and copper sulfides: representing a proportion of between forty to sixty percent of oxides. The project began by identifying the losses in the leaching process, specifically in the wetting of the heaps under nebulization, in order to achieve the goal of developing and evaluating the nebulized system in order to reduce water consumption by 5 L/s in the leaching process. This improvement was carried out keeping current copper extraction rates.

Operational and environmental critical factors in the process of nebulization:

For the leaching process to develop properly, one must consider a number of operational and critical environmental factors in the process of nebulization. These can be grouped into three categories: operational factors of process, design factors specific to the nebulization step, and environmental factors or (also known as) external factors.

The first category includes the permeability of the material to be leached and the efficiency of contact between the material and the leaching solution. The permeability of the material to be leached, and refining the solution must pass through the entire bed of material and make contact with it. The effectiveness of contact between the material and the leaching liquid depends on the surface area, porosity, particle size and roughness of the surfaces (Mellado, Galvez &Cisternas 2011) amongst other factors. During the application of the solution, refinement is applied as spray. The correct operation prevents water loss by crusting on the surface, avoiding superficial ponding and formation of preferential channels by promoting efficient leaching of ore on the heap. (Avendaño 2004).

The second group of operational factors, relating to the nebulization design, can be identified as: irrigated frame (nebulizers configuration), the height of the nozzle and pressure and nozzle diameter. The frame affects the correct overlap of nebulizers. If nebulizeres are spaced further apart, the dispersion of the cloud caused by the wind is more influential, avoiding a good wetting process. The height of the nozzle determines the residence time of the drop of water in the air, the higher the losses by wind drag and the evaporation due to residence time is greater. The pressure and the nozzle diameter determine the droplet size; smaller diameter, more evaporation.

Finally, in the third category, the environmental factors that promote the loss of water are: a) the temperature, b) air humidity, c) solar radiation, and d) wind flows.

In this research, efforts have focused on optimizing the irrigation matrix of the leaching process. To meet this goal, we studied the water loss in the current configuration, and furthermore each design factorswas studied (eg nozzle height, irrigation frame, drop size and use of cover, among others) individually. Then, we proceeded to optimize these design factors in order to reduce water losses and finally we quantified the effect on water loss of the entire process and also at the level of each design parameters.

Methodology

Experimental Design

Tests for water loss were performed *in situ* in the leach pads on the mine company. This was achieved on a quadrant of twenty meters long and eighty meters wide on a leach pad. The quadrant was divided into a 8-cell study plot of approximately ten by ten meters. Each unit contained seven nebulizers mounted on a triangular design distribution, as used by the mine (Fig. 1).

The evaporation and precipitation rate measurement was made using forty-eight catch cans around the center of nebulizer. Pressure and flow rates were monitored by a pressure gauge and a flowmeter, respectively, both located in the input line to each cell. The evaporation loss value was calculated as the difference between the rate of applied irrigation and water collected at the set of catch cans. Tests were conducted in three different

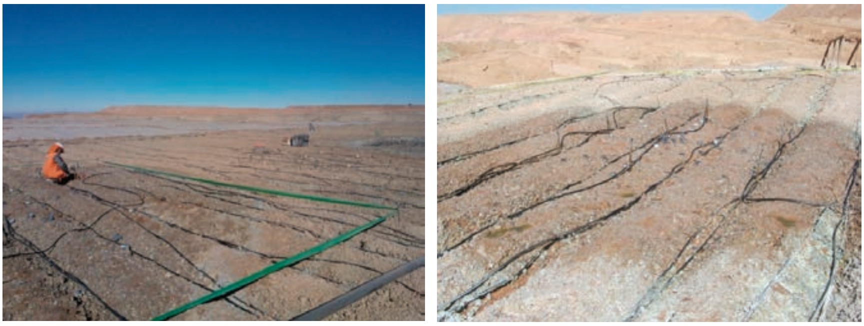

Fig. 1*.Configuring nebulizers on study plots*

time intervals: 9:30–11:00 am, 11:30am-13:00 pm and 15:00pm-16:30 pm each day in order to evaluate the effect of environmental variables on water loss. For statistical purposes, each test was repeated 3 times.

In addition to the sampling of environmental variables a weather station was mounted in a field at a fixed point of the leaching plant to generate a wind rose to determinate wind behavior and its influence on the losses and water savings achieved in conducted tests.

Optimizing process design parameters – nebulization

In relation to the operational and environmental variables a test matrix was used for evaluating their effects on potential water savings (Table 1).

Note that the current system configuration of nebulization is a 1.8 m separation between nebulizer, a 40 cm nozzle heightand no use cover. A mixture of measurements were also considered in order to verify synergy between them by means of a experimental factorial design 2^4.

Finally, in order to study the droplet size, a nebulizer was mounted inside a covered cell with a droplet size measuring station, which consisted of a 40 cm high nebulizer and water sensitive cards along the wet radius. These cards can capture various droplet sizes by changing from yellow to blue upon contact with the water, registering droplet size with a droplet finger print that is marked on the card. After the test, the cards were scanned and processed in the Steinmaster software that translates every mark and droplet size. Droplet size was measured for the current nebulizer and another alternative nebulizer, similar in operational parameters, in order to quantify the difference in droplet sizes.

Potential solutions	Unit	Test range
Nozzle height modification	Cm	40 - 20
Framemodification	M	1,4 - 1,8
Coversystem	--	Use/No use
Dropsize	µm	190-250

Table 1 *Potential measurementsto reducewater consumption*

Results and discussion

Base analysis

The results presented below are for the time interval of 15:30 to 17:00 hrs, Zone 3, where it was expected to be the most favorable condition for high evaporation.

Framework irrigation

The effect of frame irrigation did not influence the reduction of evaporation losses or drag. It's important to say that although a reduction was not observed in regards to evaporation losses,

There was an overall evaporation reduction, considering that if the distance is reduced between the nebulizers, more are needed in the same area, which consequently means a reduction of the pressure and flow rate to keep a constant flow rate. Taking into account this effect, the overall reduction is positive, which quantifies potential savings. Those savings compared to the rest of the measures are discussed in the following section.

Nozzle Height

The nozzle height did not show a favorable trend in relation to the reduction of evaporation losses and drag. The increase may be explained by wind turbulence on the areas close to the surface as the drops would remain in the air longer.

Covers

The use of a cover to isolate the spray from the environment is a desirable element in terms of evaporation. This can be seen in Fig. 1. Wind speed measurements within the cell showed that the wind reduced by 75 % (in regards to the wind outside), confirming the importance of protecting the nebulizers from the wind due to the influence on the process.

Droplet Size

In Fig. 2, the droplet size shows a difference of almost 10 % between the nebulizer and the alternating current due to the effect of the drop on evaporation. The small drop of the alternative nebulizer is more likely to be dragged due to their weight and increase evaporation due to the high surface area. Although the difference in size between drops was 60 µm, the trend is significant, demonstrating an important sensitivity in this parameter.

Environmental variables

The weather station worked during most of the study, recording data every 1 minute. This data was then processed and the values were reported hourly. This allowed information to be checked in relation to time intevals and to see how this variable influenced water losses. The main parameters are shown in Table 2

As seen in Table 2, zone 3 is the most unfavorable for nebulization due to a low relative humidity anda high wind speed and strong radiation, which is consistent with previous data.

It’s important to say the results of evaporation losses from the other two zones were not favorable, because the measurements did not show a positive trend in terms of reducing water consumption.

Integrating Optimization variables.

After a baseline analysis, a new analysis was introduced that integrated operational variables with the previous heap nebulizers results. This analysis was essential to connect the loss by evaporation and drag with the flow rate in order to compare it with the preferred flow rate. In this analysis we integrated the total amount of nebulizers, the flow emitted by each of them, the total nebulization area, the wetting ramp established, among other variables.

Considering this analysis aims to support the reduction of total water consumption, with respect to the four variables described above, the order of importance taking into account the greatest reduction is:

Frame irrigation> cover> height
> drop size

Considering the reduction goal of 5 L/s, four variables were able to overcome it. Of these, 3 are a combination of variables.

Cover + frame irrigation>
frame irrigation + cover + height >
frame irrigation>Frame irrigation + height

If the criteria are the costs associated with

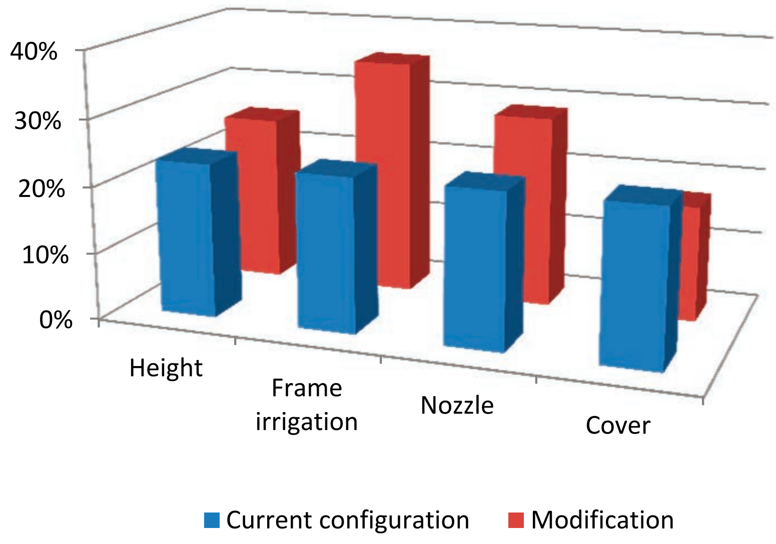

Fig. 2 *Effect of the proposed measures on the total losses*

Topic	Unit	Zone 1	Zone 2	Zone 3
Wind	m/s	1,3	2,5	3,6
RelativeHumidity	%	20	14	14
Radiation	W/m2	20	530	830

***Table 2** Environmental variables and ranges measures on field*

each variable, taking into account the highest cost, the optimized solution would be:

Cover + height + frame irrigation>
walls + height + frame irrigation >
frame irrigation + height> frame irrigation

Taking account the two previous criteria, frame irrigation and height are seen as cost-efficient options to reduce water losses.

Conclusions

From this analysis, the possibility to change the distance between the nebulizers and the use of covers, are the most interesting options with the potential for significant water savings.

The drop size was the most sensitive parameter, demonstrate its importance in terms of evaporation and drag. If the size is known, its possible modifying in order to reduce evaporation.

At the end of this project, Fundación Chile studied and considered the factors in this process comprehensively and articulated a methodology for nebulization irrigation. This provides insights for appropriate solutions to several operational realities, aiming to reduce water losses.

References

Avendano, C. (2004). ‘Revision de la Lixiviacion en Pilas de Minerales de Cobre’. PaperpresentedonLX UsersConference Chile, La Serena, Chile, Junio 2004

Cochilco (2010), Consumo de agua en la minería del cobre, Dirección de estudios y políticas públicas viewed 4 march 2013, www.cochilco.cl/productos/pdf/2011/INFORME_AGUA_2010.pdf

Fundación Chile (2012). Guía programa proveedores de clase mundial, InnovumCentro de innovación en capital humano,viewed 1 march 2013 www.fundacionchile.com/archivos/Gu_a_Programa_Proveedores_de_Clase_Mundial.pdf

Garreaud, R. (2011) Cambio Climático: Bases físicas e impactos en Chile. Revista Tierra Adento INIA-Chile, no. 93, pp 13–19

Hooghart, J. C. (1987). Evaporation and weather, 44th edn, Technical Meeting, Netherlands.

Mellado, M., Galvez, E., and Cisternas, L. (2011).On the optimization of flow rates on copperheapleaching-operations. International Journal of Mineral Processing. vol. 101 no. 1–4, pp 75–80.

Nin, R.A. (2008). Tecnologia del riego por aspersion estacionario. Calibración y validación de unmodelo de simulación. Universidad de Castilla-La Mancha, Espana

Tarjuelo, J.M. (2005). El riego por aspersion y su tecnología, 3rd edn, Mundiprensa, Espana.

Valiantzas, J. D. (2006). Simplified versions for the Penman evaporation equation using routineweather data.Journal of Hydrology, vol. 331, pp 690– 702

Reliable Mine Water Management – Connecting the Drops to Operate "Water Smart" Mines

John Chahbandour

MWH Global 1801 California St, Suite 2900 Denver, Colorado, USA, John.Chahbandour@mwhglobal.com

Abstract The effectiveness of management practices have a direct impact on a mining company's reputation, access to new reserves, financial performance and social license to operate. Water is a strategic asset for mining companies that has a business value significantly greater than the cost of procurement. Reliable Mine Water Management requires an integrated approach to promote operational efficiency and mitigate strategic and operational risks. "Water Smart" mines reflect a robust corporate governance framework that is flexible enough to manage variability while effectively mitigating risks. This paper provides an overview of the process for developing "Water Smart" mines.

Keywords Mine water management, strategic water risks, water management strategy

Introduction

No mine operates without managing water. The effectiveness of management practices can have a direct impact on a mining company's reputation, ability to access to new reserves, financial performance and social license to operate. Water is a strategic asset for mining companies that has a business value significantly greater than the cost of procurement. In addition, it is the single most important vector for potential environmental impacts throughout the mine life-cycle. Therefore, effective water management is critical to preserving value and exploiting opportunities.

There are numerous examples illustrating the reputational and financial impacts to mining companies resulting from mismanagement of this strategic operational resource. However, by taking an integrated approach to managing water (*i.e.* connecting the drops) operational risks can be can be mitigated in a manner that successfully prevents them from developing into enterprise impacts.

Why operating "Water Smart" mines is important

There are a range of drivers for operating "Water Smart" mines, ranging from global mega-trends to establishing shared-value with local host communities.

Big picture trends

There are several global trends that are driving the need for more intelligent mine water management.

- Population growth is putting increasing pressure on available resources and escalating competition for water. A growing emphasis on managing the water-energy-food nexus is being driven by population growth and mining will have to compete with these interests.
- Increased urbanization is impacting water quality/quantity which also is increasing competition for water between municipalities, agriculture and industry. This drives up costs for source water, decreases available supplies and increases the amount of water requiring treatment prior to use.
- Climate change and extreme weather variations resulting in droughts and floods have impacted operational continuity at numerous mines around the world.

Strategic risks

The three primary strategic risks are reputational, growth potential and maintaining social license to operate. All of these risks have some degree of financial consequence associated with them. For example, access to new reserves is a measure of a company's long-term growth potential, market share, and ultimately, investment attractiveness. Two major projects in Chile (El Morro) and Peru (Mina Conga) have been significantly delayed as a result of revocation or withdrawal of permitting documents, largely as a result of issues involving water resources.

Operational risks

Similar to risks at a strategic level, operational risks tie directly back to financial performance. Operational risks generally can be broadly categorized as outlined below.

- Security of supply is critical to avoid lost production and properly support mine expansions. In arid areas, water use efficiency and demand management are important components of improving security of supply.
- Excess inventory can lead to increased operating costs resulting from the need to treat water, reduced mineral recovery due to the need to use water not "fit to purpose", unauthorized discharges and increased closure costs.
- Inadequate water quality management can increase the amount of contact water that enters the process circuit resulting in elevated operating costs. Continued degradation of process water quality increases freshwater makeup demand and has the potential to impact operational efficiency due to reductions in mineral recovery.

The relationship between operational and strategic risk management

There is a direct link between operational and strategic risks. As illustrated in Fig. 1, effective management of water related risks is a function of:

1. the water management framework (both at a corporate and site level),
2. defining and measuring performance against appropriate metrics, and
3. the degree to which water is incorporated into stakeholder relations.

"Water Smart" mines successfully drive operational practices as they relate to each of

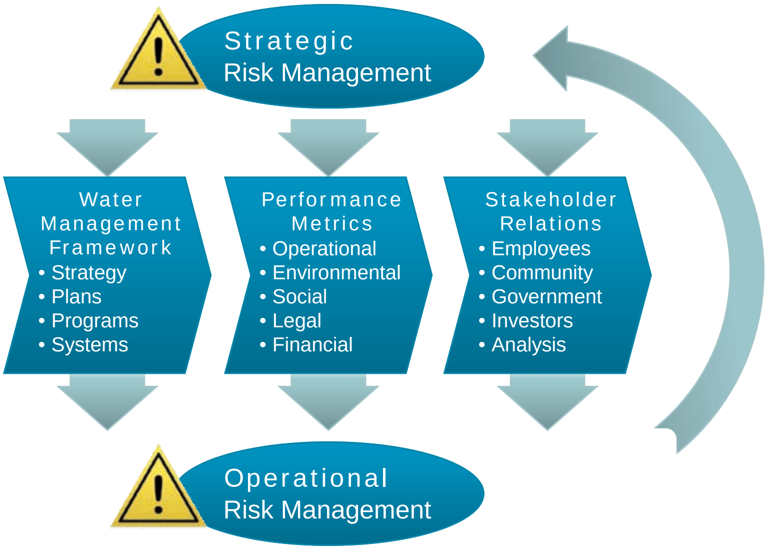

Fig. 1 *The relationship between operational and strategic risk management*

these elements in a manner that significantly reduces the water-related strategic risks a company may face.

Getting to "Water Smart"

At an operational level, getting to "Water Smart" requires developing an Integrated Mine Water Management Plan (IMWMP) tailored specifically for the mine site. However, as illustrated in Fig. 2, the IMWMP is also supported by the corporate water management strategy, guidance documents and site-specific operational procedures.

The purpose of the IMWMP is to:

1. Codify water-related operational practices across functional groups.
2. Define the hierarchy of water management priorities.
3. Establish the process and responsibilities for integrating the IMWMP with the mine plan.
4. Summarize monitoring requirements & environmental compliance standards.
5. Establish the framework for identifying and managing water-related risks (inside and outside the fence line).
6. Drive mitigation actions and continuous improvement.

An effective IMWMP can only be developed by:

1. Involving all operational departments and incorporating key mine facilities throughout the life-cycle.
2. Fully integrating the water management strategy with the mine plan and ensuring operational practices and infrastructure are consistent with the operating environment.
3. Understanding water-related risks both within and outside the fence line at a level of detail sufficient to preserve business value and financial performance.
4. Support the mines ability to meet both internal and external commitments (Fig. 3).

The process of developing in IMWMP begins with the steps illustrated in Fig. 4.

These steps are followed by the codification and continuous improvement phases. The codification phase establishes the organizational structure of the document, outlines key information for critical facilities, summarizes operational performance metrics and details mitigation actions that address material water-related risks. Because the IMWMP is a living document that gets updated in response to major changes in the mine plan, identification opportunities for continuous improvement is an important aspect that ensures the water management strategy consistently delivers business value to the operation. This is an essential aspect of ensuring that, as the end

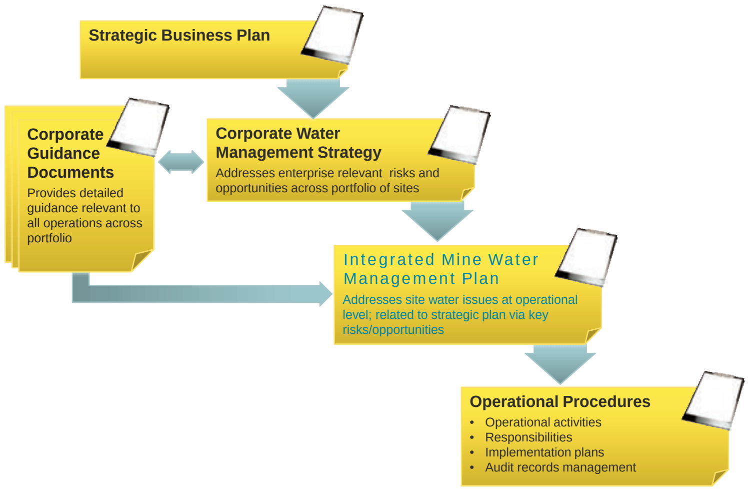

Fig. 2 *The relationship corporate and operational water management strategies (after MCMPR 2006)*

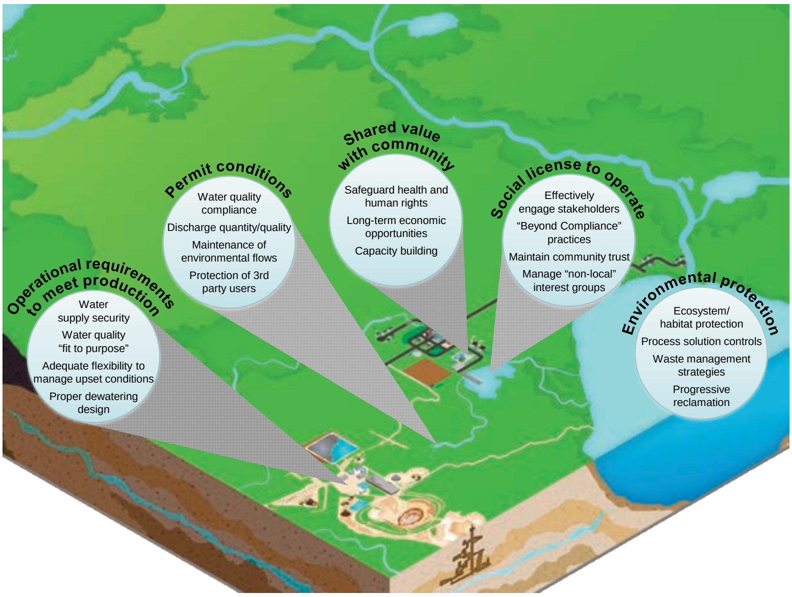

Fig. 3 *Internal and external commitments that the IMWMP must support*

of mine life approaches, operational practices support minimizing closure costs.

Case studies of success and failure

"Water Smart" principals beyond the fence line to create shared value

One of the largest copper mines in the world is located in an arid environment adjacent to a community experiencing rapid urban growth. Historically, the water supply for the mine, local agricultural users and the municipality was derived from reservoirs. The allocation of water to the principal users in the basin (in order of priority) was the municipality, agriculture and industry (including mining). All domestic and industrial wastewater was discharged directly to the local river which degraded surface water quality.

The mine plan called for an expansion that would triple production capacity and generate an additional US$88 billion in gross revenue over a period of 20 years. In order to support the expansion an additional 1 m^3/s of makeup water was required. However, because of the urban growth, increased agricultural production to support the growing population and arid climate there was insufficient basin yield to support the additional water required by the mine. It was possible to determine this because the mine had a clear understanding of the water resources situation outside their fence line. In addition, they had accurately defined the social and political risks associated with changing the operating rules for the reservoirs to secure the necessary water.

The solution was to build a municipal wastewater treatment plant and use a portion of the treated effluent as the makeup supply required for the increased mine production. Excess treated wastewater was discharged to the river which immediately improved surface water quality and the reliability of supply for downstream agricultural users. By taking an integrated approach to this water management challenge it was possible to establish a reliable supply that was economically, socially

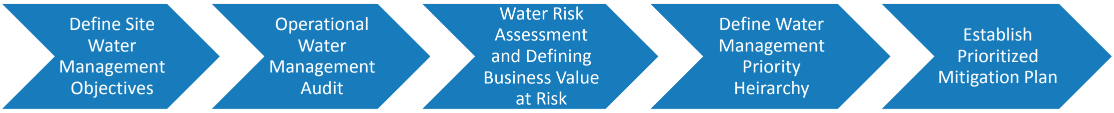

Fig. 4 *Initial steps in the IMWMP development process*

and politically sustainable.

Operational mismanagement leading to erosion of shareholder value

A uranium mine operated in an area subject to intense monsoonal rainfall was forced to shut down due to excess inventory and risk of a tailing dam failure. This was a direct result of inadequate operational management practices, and inadequate mine water control infrastructure. The mine, which had previously produced up to 10 percent of the world's uranium, was forced to suspend all operations for five months while a solution was implemented to deal with the excess water (Uranium News 2012).

As a result of the lost production the year on year net earnings before interest and tax went from AUS$68 million to a loss of AUS$61 million (Uranium News 2012a). The company also cut the size of its estimated reserves at the Ranger mine, wiping AUS$99 million of inventory value from its balance sheet. These events lead to a decrease in share value of approximately 80 % (Uranium News 2012b).

The potential financial loss could have been mitigated to some extent by incorporating adequate water management infrastructure consistent with the operating environment, establishing a clear set of operational water management priorities and robust contingency plans to deal with extreme weather events. The risks associated with excessive rainfall were known but the business value at risk resulting from inadequate mitigation measures was not factored into decision making. The cost of properly mitigating the risks associated with accumulation of excess water during a monsoon was likely a fraction of the lost business value.

Conclusions

Reliable Mine Water Management requires an integrated approach to promote operational efficiency and mitigate strategic (enterprise level) and operational risks. There is a direct link between effective management of operational risks and strategic risks. "Water Smart" mines reflect a robust corporate governance framework that is flexible enough to manage variability while effectively mitigating strategic risks. To effectively "connect the drops" reliable mine water management involves all operational departments working with a common understanding of the management objectives. This occurs when the water management strategy is fully integrated with the mine plan and is consistent with the operating environment. "Water Smart" mines utilize a water-specific risk management framework to identify and mitigate water-related risks inside and outside the fence line in order to preserve business value and enhance financial performance.

References

Uranium News (January 2012a) Ranger uranium mine in danger of floods.

Uranium News (April 2012b) The woes of Energy Resources of Australia leading to closure of Ranger uranium mine.

Ministerial Council on Mineral and Petroleum Resources (MCMPR) and Minerals Council of Australia (2006) Strategic Water Management in the Minerals Industry.

Dugald River Tailings Storage Facility and Process Water Dam – Robust Options Analyses

Nathan Clements[1], Craig Noske[2]

[1]*MMG, Level 23/28 Freshwater Place, Southbank, Victoria, Australia, nathan.clements@mmg.com*
[2]*ATCWilliams, 222 Beach Road, Mordialloc, Victoria, Australia, CraigN@atcwilliams.com.au*

Abstract The Dugald River Tailings Storage Facility and Process Water Dam are good examples of a robust options analysis. An initial options assessment, which considered the water management impacts of the pre-selected facility design helped produce a final facility design that has provided numerous benefits to the operation, including the reduction of reliance on external water sources by an average of 50 %. A detailed water balance model utilising a synthetic 1,000 year rainfall sequence was used to optimise the water storage requirements and achieve an outcome that would meet MMG's legislative and corporate risk requirements.

Keywords Tailings storage facility, water management, reuse

Introduction

Dugald River, one MMG Limited's (MMG) major development projects, is located in north-west Queensland, Australia, 85 km north-east of Mount Isa. The project will use conventional mechanised underground technology to mine zinc, lead and silver. The mine production will be approximately 2 Mt of ore per annum.

The Dugald River Tailings Storage Facility (TSF) and Process Water Dam (PWD) are integral components of the project from many perspectives.

Initial Studies and Assessment Criteria

Water Management Issues

The initial assessment of TSF and PWD site options was based on the following criteria:

1. Site Water Management Implications
2. Capital and Operating Costs
3. Operating and Maintenance Requirements
4. Risk of Failure
5. Site & Downstream Receiving Environment Environmental Sensitivity
6. Site Disturbance Footprint Implications
7. Expandability
8. Rehabilitation Requirements

Upon commencement of studies it became apparent that, as with other remote mine sites in northern Australia, water was likely to be the second most precious commodity after the mining resource itself. One of the main consumers of water on site will be the TSF, hence it will be desirable to recover water from the TSF and recycle it into the processing operations to the greatest extent possible (ATC Williams, March 2008).

The importance of water to the operation is also revealed as sub-criteria within each of the site options assessment criteria listed above. Key factors include:

- Climate – the tropical (wet/dry season) climate with average annual evaporation exceeding rainfall by a multiple of approximately six (500 mm rainfall and 3,000 mm evaporation).
- Rainfall seasonality and variability – around 80 % of the annual rainfall occurs between the months of December to March, and wet season rainfall variability is extreme (*e.g.* 0.01 annual exceedence probability (AEP) annual rainfall is

1,300 mm, whilst the 0.01 AEP 2-month rainfall is 1,100 mm). This means that the annual mine water balance switches between water surplus and water deficit across the year.

- Regulation of water management – these requirements preclude the off-site discharge of tailings process water, requiring adequate provision of storage for high wet season inflows in the TSF as well as PWD design. Depending on the TSF/PWD catchment characteristics, this can often require significant water storage dams, which nevertheless, due to the seasonal variability in the rainfall, cannot provide a guaranteed supply of process water throughout the life of the mine.

Options and Pre-Feasibility Studies

The TSF options analysis at Dugald River conducted by ATC Williams (2008), considered all possible options within the project area. Seven TSF sites were considered in this initial options study (Fig. 1), including locations within, to the west of, and to the east of the Knapdale Range, which runs in a north-south direction through the centre of the site. Each option varied in construction technique and operational methodology.

The Dugald River site is somewhat unique in that it contains a variety of topographic and geological conditions, ranging from gently sloping alluvial terraces to rugged ranges of hard, outcropping rock. This results in a variety of potential TSF configurations, including down-valley discharge, side-hill spigot discharge, and upstream-raised cells with perimeter spigot discharge. PWD options range from gravity-fed adjacent storages to separate pumped dams.

Each of the above configurations had unique water management benefits and drawbacks; some of which could have had significant impacts on project economics and risk management. There were, however, cases where smart engineering design could be used to convert a perceived drawback into an overall mine operation benefit.

For example, down-valley discharge TSF schemes can often involve significantly larger catchments than side-hill or cell configurations. If these catchments cannot be effectively diverted then the wet season inflows will introduce significant volumes of water into the storage system. If this water can be separated from the TSF into an adjacent PWD, the TSF at sites such as Dugald River (where external water supply is not straightforward as well as freely available), can form a valuable source of water for mine operations.

Conversely, with side hill or cell TSF designs, the aim is to minimize the contributing catchment so that the focus of the structure can be to maximize the evaporative beach drying of the deposited tailings.

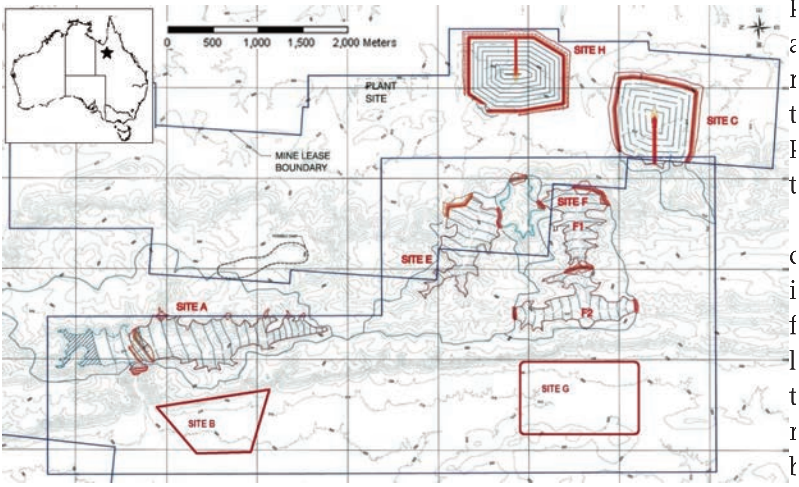

Fig. 1 Dugald River TSF Site Options – Initial Assessment

Common practice sees the initial options assessment focusing on the tailings storage issues (for example tailings thickening and delivery, embankments requirements and storage filling rates/densities). There is often insufficient attention given to the associated water management implications, which in reality can completely change the relative ranking of a particular scheme.

After this initial screening of the seven options, two very different sites and associated construction/operation methodologies were selected to proceed to the feasibility design stage. The two selected options included:

1. Down-valley discharge TSF/downstream PWD, located in a valley within the hard quartzite rocks of the Knapdale Range (known as Site A);
2. Upstream-raised cell, perimeter spigot discharge/separate PWD, located on the gently sloping alluvial grounds to the east of the Knapdale Range (known as Site H).

Site A was ranked the highest due to its tailings storage efficiency and potential for expansion, with water balance modeling required to investigate the issues involved in the sizing and operation of the PWD. Site Hwas also considered deserving of further study, given its proximity to the proposed process plant site (ATC Williams, March 2008).

Selected Option

Feasibility Study Outcomes

The feasibility studies examined the logistics of both sites, exposing some of the key benefits of the down-valley discharge option (Site A). These included the reduced capital cost through utilising the natural containment properties of the Knapdale Valley, expandability and the potential to delineate a large PWD for the mine. Site H was more restrictive from a sizing perspective (due to tight lease boundaries), and it did not contain the relatively impermeable natural formation that could be used as a natural barrier to seepage. Site A was therefore selected to proceed to detailed design.

Knapdale Valley Site (Site A) Overview

Dugald River tailings will be pumped to the Knapdale Valley TSF approximately four kilometers north-west of the processing plant. The TSF will be located within a long, narrow bifurcated valley running north-south on the western side of the Knapdale Ranges. The TSF concept will involve down-valley discharge of tailings to the TSF Embankment, with all decant and runoff water conveyed via a gravity decant structure to the PWD directly downstream.

The PWD will contain all water released from the deposited tailings, as well as storm water runoff from the 338 ha catchment. The PWD will potentially also need to provide storage for underground mine dewatering and additional mine site water inputs during wet season high rainfall periods, when other water storages on site approach their capacities.

The structural geology of the Knapdale Valley has indicated that there is no evidence of significant defects that could extend from the TSF – minimizing the risks of significant seepage occurring from the structure (ATC Williams 2011). Natural geology is mainly comprised of quartzite rock with a permeability of $k = 10^{-7}$ m/s over the upper five meters and reducing one to two orders of magnitude at greater depths. Any further benefits of reducing permeability by lining the structure were quickly ruled out due to the substantial capital costs.

The TSF embankment will be constructed of local rockfill. It has been designed to retain tailings but to allow some decant seepage through to the PWD. The PWD Embankment will be a water retaining structure constructed of rockfill with a thin, impermeable PVC geocomposite fitted to the upstream face. The adopted down-valley discharge and associated water management practices will facilitate timely rehabilitation, with the TSF capped with a low water flux, naturally self-shedding cover.

Water Balance Modeling

Objectives

Given the site configuration and water management benefits outlined above, a comprehensive water balance model was developed by ATC Williams for the Knapdale Valley TSF/PWD scheme. The model has been run on a daily, two-stage (TSF and separate PWD) mass balance approach over the life of mine, using actual daily climatic records. Inputs into the TSF system include tailings bleed and catchment runoff, with outputs being decant delivery to PWD and evaporation. PWD inputs include TSF decant and catchment runoff, with outputs comprising process water return and evaporation. The objectives of the water balance were to examine:

- The ability of the TSF decant to maintain the decant pond in a minimum condition;
- The water level fluctuation in the PWD due to the seasonal climatic impacts;
- The expected return water rates from the PWD to the Process Plant and continuity of supply due to the seasonal impacts; and
- The required capacity of the PWD to adequately provide for the regulatory Design Storage Allowance (DSA), which equates to the 100 year ARI, 2-month inflow. The prime management objective of the PWD is that it has sufficient capacity to store the DSA for the combined facility at the beginning of each wet season (taken to be 1st November).

Rainfall Analyses

A database of 123 years of daily rainfall and evaporation has been compiled for hydrological modeling of the Dugald River TSF/PWD site (ATC Williams 2011). The data was obtained from an Australian Bureau of Meteorology archive of interpolated rainfall and climate data (DSTITIA 2010). The interpolated data is synthetic, with no original meteorological station data left in the calculated grid fields. The prime advantage of the archive is that representative datasets can be interpolated for any set of coordinates in Australia.

From the rainfall data analyses it is apparent that the Dugald River climate is cyclic in nature. The 5-year moving average indicates pronounced cycles of “wet-wet” and “dry-wet” seasons, with the most recent 5 years being the highest 5-year sequence on record.

In order to provide a statistical check of the water balance results from the actual rainfall data, it was decided to synthesise further data. This provides a means of analyzing the potential for further such “wet-wet” sequences, and also allows such sequences to be placed at the beginning and middle of the 22 year Life Of Mine (LOM) simulation, rather than just at the end. This was achieved using specialized software to develop 1,000 years of daily rainfall data with the same statistical characteristics as the existing record.

Key Factors

Model inputs and outputs having a significant impact on the four defined objectives include inputs and outputs as follows:

Model Inputs – Catchment Runoff

Catchment runoff is the dominant source of water in the TSF/PWD system. TSF runoff collects in the Decant Pond, from where it is conveyed to the PWD via the decant system. The PWD has its own external catchment, contributing runoff directly to the storage.

Watershed modelling of the external catchments was conducted using the Boughton SFB model, which has been specifically developed for ungauged catchments by correlating real rainfall records and yields for catchments in Australia. It takes into account antecedent catchment conditions by separately assessing the residual moisture stored in the soil, migration of water down the soil strata to base flow, and migration of water up the soil strata to evaporation in order to calculate the total water available for runoff.

Given that no quantitative runoff data exists for the Knapdale Valley, a range of Boughton parameters were trialled to examine the sensitivity of the PWD volume response. This involved equivalent catchment yield factors ranging from 0.28 to 0.5, with 0.35 adopted for design.

Model Outputs – Process Return Water& Closure Implications

Preliminary water balance modelling indicted that without recycling, the PWD would run at a net water gain throughout the LOM, resulting in final storage volumes in excess of 10 GL. This is an unacceptable situation given the environmental issues with respect to facility closure and the discharge of potentially contaminated water, and would represent a significant economic legacy issue for MMG at the completion of mining.

It hence became clear that PWD water would need to be utilised to the maximum practicable extent in processing and related mine activities (*e.g.* dust sprays, mine service water streams), in order for the Knapdale Valley TSF/PWD scheme to be considered viable. Additional water for the operation, including for potable water supply, would be sourced from Lake Julius due to a lack of significant local groundwater resources in the area.

The proposed mining plan utilises campaign-based paste thickening, which would lead to a variable make-up water demand, ranging from 40 to 134 m^3/h (with an annual average of 68 m^3/h). The addition of a water treatment plant half way through the operation, which could supply cleaner water to other site uses (and bring the average annual reuse rate to 100 m^3/h), was found to reduce the modelled final PWD storage volume from an average of 1,200 ML (with no treatment plant) to 400 ML (with treatment after year 10).

Associated studies indicate that there is negligible impact on closure if the final PWD volume is less than 600 ML, but that closure may be delayed up to 5 years if the final volume is greater than 2,000 ML (ATC Williams 2011).

Design Storage Allowance & Required PWD Capacity

Design Storage Allowance and Adopted PWD Design

Queensland regulatory guidelines require operations to provide the DSA volume on 1st November each year, and one of the key objectives of the water balance modeling is to predict compliance of the proposed design. The guidelines discuss two methods of estimating the DSA, and hence the required storage capacity of the PWD. Both methods have been assessed using the synthetic 1,000 year rainfall database, for which 978 separate LOM simulations were conducted. The higher resultant 2-month wet season inflow (3,835 ML) was adopted as the DSA.

In order to then select an appropriate design PWD capacity, the DSA was added to the 1st November water balance volume with a chance of exceedence equivalent to once in the operational life (approximately 1 in 20), resulting in a design capacity of 8,360 ML.

Modelling Results

Various stochastic and simulated water balance outcomes are presented in Fig. 2. The stochastic data indicates a maximum simulated PWD volume of just under 6,000 ML, however the significantly lower 95th percentile outcomes show the sensitivity of the system to extreme wet season rainfall. The conservative nature of the DSA design approach is also apparent, with the design capacity almost 40 % higher than the maximum simulated PWD volume.

Fig. 2 also shows available water storage and DSA provision assessments. In reality there is significant additional flood water storage within the TSF. Whilst long-term storage on the tailings is not encouraged, it nevertheless needs to be included when assessing the risk aspects associated with the selection of the required PWD capacity. It is apparent from Fig. 2 that the maximum allowable 1st November PWD volume is always well in excess of the 95th percentile outcomes. However, given that

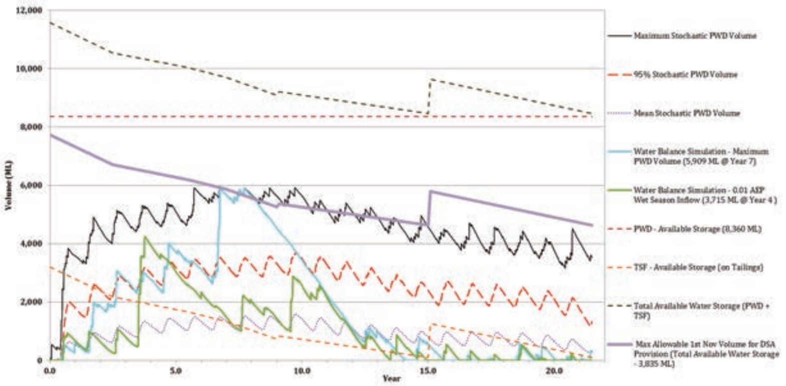

Fig. 2 *Dugald River Process Water Dam Stochastic and Simulated Volume Outcomes, Available Water Storage & DSA Provision over Life of Mine*

the severity of recent wet seasons has increased; it is considered that this additional capacity represents appropriate defensive design for a 22 year mine life.

The performance of the proposed TSF and PWD combination will be continuously assessed against its design assumptions. A rigorous monitoring program, including meteorological data, key inflows and outflows, and regional groundwater levels will be implemented, as will annual audits of the facility and calibration of the water and tailings balance model against actual processing tonnages, tailings volumes and densities.

Conclusions

The Dugald River Project TSF has provided MMG with an opportunity to utilize process water as a resource capable of providing approximately 50 % of the mine’s annual water requirements. A multi-faceted approach to selecting and sizing the PWD for the facility has been utilized to produce a combination that satisfies the site’s legal obligations and reduces the mine’s reliance on external water sources.

A robust water balance model was developed for the TSF and PWD that utilized both historical and synthetic climate data to predict and verify required storage volumes. The model accounted for sensitivities in catchment runoff and process water reuse rates, and conformed with the regulatory need to be able to store a specified DSA at 1st November in each year of operation.

This approach has led to a design that is “best-for-project”, providing optimal solutions across multiple assessment criteria. It has shown that, by including site water management impacts as a priority in initial options analysis and feasibility studies, TSF/PWD combinations may provide substantial benefits to project economics if properly managed.

References

ATC Williams (March 2008) Dugald River Project Feasibility Study Tailings Storage Facility Site Options Analysis. Mordialloc, Victoria

ATC Williams (2011) Dugald River Project Feasibility Study Tailings Storage Facility Final Report – Site A1. Mordialloc, Victoria

Queensland Department of Science, Information Technology, Innovation and the Arts (DSTITIA) (2010) SILO Climate Data, viewed May 2010, www.longpaddock.qld.gov.au/silo

Additional information can be found at http://bitly.com/IMWA2013_380

Water Quality and Compliance Monitoring of Treated Underground and Surface Water at the Grootvlei Proprietary Mines and the Blesbokspruit Wetland, Springs, South Africa

Louis de Wet[1], Sibusiso Sidu[2]

[1]*Waterlab (Pty) Ltd, PO Box 283, Persequor Park, 0020, Pretoria, South Africa, Ldewet@waterlab.co.za*
[2]*Gold One International Limited, PO Box 262, Petersfield, 1566, Springs, South Africa, sibusiso.sidu@gold1.co.za*

Abstract During 1996, Grootvlei Mine in Springs, on the East Rand Basin, Witwatersrand, discharged severely contaminated water into the Blesbokspruit Wetland. Subsequently, a HDS (High Density Sludge) plant had to be constructed to remove Iron and Suspended Solids to less than prescribed concentrations. Monitoring of the quality of the HDS effluent consisted of daily sampling and analyses of pH, Electrical Conductivity, Iron and Suspended Solids (SS). Compliance analyses to required standards showed the plant, over a period of approximately 3500 days, to achieve 83.4 % compliance for Iron, 80.8 % for SS, and 99 % for both pH and Electrical Conductivity.

Keywords Mine Water; Treatment; Monitoring; Compliance

Introduction

Acid Rock Drainage (ARD) is a major contributor of environmental degradation worlwide. This is also applicable to the pyrite (FeS_2) containing Witwatersrand gold-ores which have been mined for more than a hundred years in South Africa. Acid mine-water is the consequence of the oxidation of iron-pyrites with the subsequent formation of sulphuric acid (Unz & Dietz 1986). Consequently, effluents and seepage waters with high levels of metals, salts and sulphate are able to reach the aquatic environment. Various authors describe the relevant chemical reactions involved in the oxidation of pyrite into dissolved iron, sulphate and hydrogen (*e.g.* Wittmann & Förstner 1976; Johnson *et al.* 1979; Thompson 1980; Murray 1987; Usher *et al.* 2003).

Release of untreated ARD from the Grootvlei Mine No 3 Shaft into the Blesbokspruit, necessitated the construction of a HDS (High Density Sludge; van Staden 1979; Osuchowski 1992; Craddock 1997) plant (Fig. 1 in electronic attachment) to treat the contaminated undergroundwater, and reduce the concentrations of Iron and Suspended Solids being released into the Blesbokspruit wetland. Treatment of contaminated undergroundwater was achieved by the addition of oxygen which converted ferrous (Fe^{2+}) to ferric (Fe^{3+}) iron. Precipitation of the ferric hydroxide sludge was achieved through the addition of lime as neutralising agent. Ferric iron is a denser, handle able product, which settles out rapidly and produces an effluent with a suspended solids content of less than 25 mg/L.

Methods

Monitoring of the HDS plant at the Grootvlei No 3 Shaft consisted of the collection of daily composite (15 min intervals) samples of the treated effluent from the HDS plant. Samples collected were sent to Waterlab (Pty) Ltd for analyses of pH, Electrical Conductivity and Suspended Solids by Standard Methods for water (APHA 1995), and metals by ICP-OES (Inductively Coupled Plasma – Optical Emission Spectrophotometer). In addition, two samples from each monthly batch (bi-weekly) were selected and analysed for additional parameters (table 1). Untreated underground water was also collected once a month and subjected to a number of analyses as listed (table 1). A number of additional tests were also conducted, which included toxicity testing and chemical monitoring on the Blesbokspruit wetland.

Monthly reports evaluating the daily, biweekly and underground water quality were submitted to Grootvlei Mine, indicating the compliance for each water quality parameter. These reports were submitted to the Department of Water Affairs and Forestry (DWAF). Compliance evaluation consisted of comparisons of water quality data with parameters set by DWAF (table 2), and calculations of monthly compliance figures for each. For the purpose of this paper, data from 1998 to 2009 were consolidated into one compliance sheet, and is reported in Tables 3–10.

Results

Water quality results obtained for monthly monitoring of the untreated underground water show the pH to vary between 5.6 and 6.9, while varying concentrations of Total Dissolved Solids (TDS) were measured, ranging between 1986 and 4090 mg/L, with an average of 2689 mg/L (table 3). Sulphate concentrations in the underground water ranged between 1003 and 3554 mg/L, while Sodium concentration showed a concentration range of 147 – 267 mg/L and and average of 217 mg/L. High Iron-Fe concentrations were measured during this monitoring period, ranging between 33 – 311 mg/L, with an average of 142 mg/L. Manganese concentrations also showed unacceptably high concentration levels (Range: 1.9 – 6.4 mg/L : Average: 3.6 mg/L) which was not permitted to be released into the environment (table 3).

Analysis Requirements	Monitoring Frequency	Parameters
Underground Water : Chemical	Monthly	Temperature, DO, pH, EC, TDS, Cl, SO_4, Na, Ca, Mg, Fe, Mn, Al
HDS Plant Treated Effluent : Chemical	Daily	pH, EC, Fe, SS
HDS Plant Treated Effluent : Chemical	Bi-Weekly	TDS, Cl, SO_4, Na, Ca, Mg, Mn, Al
HDS Plant Treated Effluent : Toxicity (US EPA 2002)	Monthly	*Daphnia* Definitive: 24 & 48 h
Blesbokspruit : Chemical	Bi-Weekly	Temperature, DO, pH, EC, TDS, Cl, SO_4, Na, Ca, Mg, Fe, Mn, Al
Bio-Monitoring (Dallas 2005)	Bi-Weekly	Macro-Invertebrates, Fish

Table 1 *Monitoring requirements of Treated ARD at the Grootvlei HDS Plant.*

Water Quality Variable	Monitoring Frequency	DWAF Licence Objective
Electrical Conductivity (mS/m)	Daily	**400**
pH	Daily	**6.5 – 8.5**
Suspended Solids (mg/L)	Daily	**25**
Sodium-Na (mg/L)	Bi-Weekly	**290**
Sulphate-SO_4 (mg/L)	Bi-Weekly	**2200**
Chloride-Cl (mg/L)	Bi-Weekly	**210**
Iron-Fe (mg/L)	Daily	**1.0**
Manganese-Mn (mg/L)	Bi-Weekly	**1.0**
Aluminium-Al (mg/L)	Bi-Weekly	**0.5**

Table 2 *DWAF water quality objectives for the Grootvlei Mine HDS plant.*

Water Quality Parameter	Range (mg/L)	Average (mg/L)
pH	5.6 – 6.9	6.4 (Median)
Electrical Conductivity (mS/m)	240 - 377	293
Total Dissolved Solids	1986 - 4090	2689
Chloride as Cl	124 - 243	160
Sulphate as SO_4	1003 - 3554	1585
Sodium as Na	147 - 267	217
Iron as Fe	33 - 311	142
Manganese as Mn	1.9 – 6.4	3.6

Table 3 *Summarised water quality of underground water from Grootvlei Mine.*

Summarised water quantity and quality monitoring data from the HDS plant, over a period of nearly ten years, is presented in (table 4). The HDS plant produced an average of 92 ML of treated water per day (ML/d), but producing as low as 31 ML/d during the dry seasons, and up to 133 ML/d during the wet season, depending on the amount of surface recharge. When compared with the quality of the untreated undergroundwater (table 3), the treated effluent showed a significant increase in the range and median pH (6.4 to 7.6), due to neutralising agents being added during the HDS process. Although the EC of HDS effluent (289 mS/m) showed a slight decrease when compared to the undergroundwater (293 mS/m), the effect of the HDS plant in reducing salt concentrations was more pronounced when the TDS concentrations are compared. While TDS concentrations in the undergroundwater ranged between 1986 – 4090 mg/L, the TDS concentrations in the HDS plant effluent ranged between 445 – 3406 mg/L, with a decrease in the average concentrations from 2689 mg/L underground to 1860 mg/L in the HDS plant effluent (table 4).

Similar to TDS concentrations, a significant decrease in the average sulphate concentration in the HDS plant was encountered. While the undergroundwater showed a range of 1003 – 3554 mg/L (average: 1585 mg/L), the HDS plant treated effluent showed a slightly lower range (814 – 1951 mg/L) and average (1261 mg/L). In contrast to the above however, Chloride-Cl and Sodium-Na showed a somewhat opposite pattern, when the ranges and averages are compared. Chloride showed a slight increase in range for the undergroundwater (124 – 243 mg/L; average: 160 mg/L) to the treated HDS effluent (105 – 208 mg/L; average: 162 mg/L), while Sodium increased from a 217 mg/L average (147 – 267 mg/L) underground to a 219 mg/L average (114 – 289 mg/L; table 4). For all purposes, the concentrations of both these parameters remained relatively constant.

Removal of Iron-Fe from the undergroundwater showed the best results. Concentrations in the treated effluent ranged between 0.010 – 39 mg/L, with an average of 0.753 mg/L, as compared to the average of the undergroundwater of 142 mg/L (table 4). This represents a removal of Iron of 99.5 % from the undergroundwater over this period. Although high concentrations of Iron were periodically measured in the HDS plant effluent, it was of short duration, as it was mainly caused by either mechanical or electrical failures of minor magnitude. However, if a composite daily sample contained a sub-sample of for example 30 minutes of non-compliant water, the average of that particular sample would not comply with the 1 mg/L standard for Iron set by DWAF. Subsequently, numerous days were encountered where, due to a small failure on the plant, non-compliance for that particular day was encountered.

Similar to Iron, significant, but less successful removal of Manganese was obtained during the total monitoring period. Manganese, showing a concentration range of 0.200 – 1.20 mg/L and an average of 0.667 mg/L (table 4) in the HDS plant effluent, was less successful, representing a removal of

Water Quality Parameter	Range (mg/L)	Average (mg/L)
Volume Treated (ML/d)	31 – 133	92
pH	6.1 – 11.6	7.6 (Median)
Electrical Conductivity (mS/m)	54 – 524	289
Total Dissolved Solids	445 – 3406	1860
Chloride as Cl	105 – 208	162
Sulphate as SO_4	814 – 1951	1261
Sodium as Na	114 – 289	219
Iron as Fe	0.010 – 39	0.753
Manganese as Mn	0.200 – 1.20	0.667

Table 4 *Summarised volumes and water quality of treated water from the Grootvlei Mine HDS Plant.*

85.1 % from the undergroundwater. However, due to the difference in the chemical properties of Manganese, remaining for a longer period in solution, and the HDS process not designed particularly for the removal of Manganese, it was expected that the removal of that metal would be less successful.

Compliance analyses of the daily and biweekly samples obtained from the HDS plant for pH, Electrical Conductivity (EC), Fe, Mn and Suspended Solids (SS) yielded results of varing compliances and success rates. A compliance analysis for pH showed that for 3528 days, the pH of the treated effluent remained within the set range of 6.5 – 8.5 (97.6 %). For 1 day (<0.1 %), the pH was less than 6.5, while for 85 days, the pH of the treated effluent was higher than 8.5, representing a non-compliance of 2.4 % (table 5).

Electrical conductivity of the treated effluent, which showed relatively little variation, showed the best compliance, with concentrations being less than 400 mS/m for 3553 days, or 99.9 % of the time. Only on 4 days of the monitoring period, did the EC exceed the limit of 400 mS/m, representing a non-compliance of 0.1 % (table 6).

Compliance analyses for Iron consisted of more concentration categories, ranging between 0 and >10 mg/L for comparative purposes. In the 0 – 1 mg/L compliance range, which was the standard required by DWAF, 3009 of the samples analysed showed an Iron concentration of less than 1 mg/L, representing a compliance of 83.4 %. In the 1 -2 mg/L category, 474 samples were classified, representing a non-compliance of 13.1 %. The 2 – 5 mg/L category showed 104 samples (2.9 %) to be non-compliant, while the 5 – 10 mg/L (17 samples) and >10 mg/L resulted in non-compliance figures of 0.5 % and 0.1 % respectively (table 7).

Manganese removal from the undergroundwater, as mentioned, was less successful than Iron. Subsequently, in comparison with a discharge limit of 1 mg/L set by DWAF, only 220 of the 600 bi-weekly samples complied with that standard, representing a compliance success of only 36.7 %. Manganese concentrations exceeding the 1 mg/L were measured on 380 of the 600 days, representing a non-compliance of 63.3 % (table 8).

Nearly similar to Iron compliance, SS concentrations complied on 2917 days with the discharge limit of 25 mg/L, representing a success rate of 80.8 %. For 531 days, or 14.7 % of the

pH Compliance Ranges	Number of Days	Percentage Compliance
Within Range: 6.5 – 8.5	3528	97.6
Below Range: <6.5	1	<0.1
Above Range: >8.5	85	2.4

Table 5 *Compliance analysis of the pH of HDS plant effluents.*

EC Compliance Ranges (mS/m)	Number of Days	Percentage Compliance
<400	3553	99.9
>400	4	0.1

Table 6 *Compliance analysis of the EC of HDS plant effluents.*

Iron-Fe Compliance Ranges (mg/L)	Number of Days	Percentage Compliance
0 – 1	3009	83.4
1 – 2	474	13.1
2 – 5	104	2.9
5 – 10	17	0.5
>10	4	0.1

Table 7 *Compliance analysis of Iron concentrations in HDS plant effluents.*

Mn Compliance Ranges (mg/L)	Number of Days	Percentage Compliance
<1	220	36.7
>1	380	63.3

Table 8 *Compliance analysis of Mn concentrations in HDS plant effluents.*

time, SS concentrations ranged between 25 – 50 mg/L, while for 112 days (3.1 %), concentrations were non-compliant between 50 – 100 mg/L. Extremely high SS concentrations of higher than 100 mg/L were encountered during 52 days (1.4 %) of the monitoring period (table 9).

Based on the flow discharges from the HDS plant (table 4), which ranged between 31 – 133 ML/d with an average of 92 ML/d, load discharge figures show TDS loads to range between 39 – 300 t/d, with an average of 177 t/d, or 5302 t/month being released from the HDS plant, into the Blesbokspruit. Suspended Solids loads ranged between 0.03 – 70 t/d, with an average of 2.3 t/d, or an average of 70 t/month. Due to the efficient operation of the HDS plant, the Iron loads being released were limited to a range of 0.01 – 4.5 t/d, or an average of 0.09 t/d. This represented and average release of Iron of 2.70 t/month (table 10). The calculated annual release for each of the listed parameters are 64 508 t/a (TDS), 848 t/a (SS) and 33 t/a (Fe) respectively.

Discussion

Although attempts were made with the Grootvlei Mine HDS plant to remove as much as possible Iron, Suspended Solids and salts form the underground water, before being released into the Blesbokspruit wetland, significantly large amounts were discharged over the 10 year period of operation. Results show thousands of tonnes of salts discharged annually, while, even though a compliance of 83.4 % for Iron was achieved, an estimated amount of 33 t/a of Iron was still discharged into the Blesbokspruit wetland. Under these circumstances, and with the technology and funds available, the Grootvlei Mine still managed to achieve a reasonable performance, and avoid any repetition of the environmental disaster which occurred in 1996. Regular toxicity testing of water from the Blesbokspruit during discharge, and well as bio-monitoring of the system, focusing on the avian, fish and invertebrate fauna of the wetland has shown that even though these high loads of salts and metals were being discharged, the most significant impact was limited to a relatively small section of the wetland downstream of the discharge point. The wetland in fact sustains a large number of fish and bird species during this period, and even now, after purification and pumping operations have ceased.

Due to the closure of the Grootvlei Mine and the No 3 shaft HDS plant in 2009, purification of underground water has ceased. It is expected that due to surface recharge, the water in the East Rand Basin may rise at a rate of 1 m per day from a depth of approximately 800 m below surface. Once the contaminated underground water approaches the surface, or decants at sites not known yet, a variety of potentially devastating environmental impacts may manifest.

Should contaminated underground water decant on the surface and reach the Blesbokspruit again, the environmental impacts could be equally devastating as it was in 1996. The Marievale Bird Sanctuary, a RAMSAR site of approximately 1000 ha, which sustains approximately 280 bird species, and mammals such as the Cape Clawless Otter, Reedbuck, Blesbok,

SS Compliance Ranges (mg/L)	Number of Days	Percentage Compliance
0 – 25	2917	80.8
25 – 50	531	14.7
50 – 100	112	3.1
>100	52	1.4

Table 9 *Compliance analysis of SS concentrations in HDS plant effluents.*

Water Quality Parameter	Range : Average (t/d)	Average (t/30 day month)
Total Dissolved Solids	39 – 300 : 177	5302
Suspended Solids	0.03 – 70 : 2.3	70
Iron as Fe	0.01 – 4.5 : 0.09	2.70

Table 10 *Summarised loads released from the Grootvlei Mine HDS Plant.*

Cape Hare and three species of Mongoose, could be severely affected should untreated decant water reach it. Equally, the quality of underground water previously being utilized for potable water and agricultural purposes by numerous farmers in this area may be so severely affected that it is not suitable for any of that uses any more.

A report to the Inter-Ministerial Committee on Acid Mine Drainage (2012) compiled by various experts in the field of Acid Mine Drainage recognize the potential impacts of AMD on the Western-, Central- and Eastern Basins of the Witwatersrand Gold Field. Various options are discussed and anticipated in order to treat AMD, which include pH adjustment by lime, aeration, precipitation, clarification and finally thickening and disposal of sludge. Other treatment options include sulphate and salt reduction by biological passive treatment, High Pressure Reverse Osmosis and precipitation processes using barium and calcium. Depending on Private and Government funding, the Department of Water Affairs (DWA) anticipate selecting appropriate treatment technologies for each of the Basins, and implementing these measures in order to curb any more potential AMD contamination and environmental damage which has already been experienced.

Acknowledgements

The authors wish to thank the Petrex and Pamodzi Companies for their support during this study. Waterlab (Pty) Ltd is thanked for all water quality analyses conducted.

References

APHA (American Public Health Association) (1995) Standard Methods for the examination of Water & Wastewater. APHA, Washington.

Craddock M (1997) High-desnity sludge process for acid mine water treatment. Chemical Technology Mar-Apr '97:15-17.

Dallas HF (2005) River Health Programme: Site Characterisation Field-Manual and Field-Data Sheets. Resource Quality Services: Department of Water Affairs and Forestry.

Inter-Ministerial Committee on Acid Mine Drainage (2012) Mine Water Management in the Witwatersrand Godl Fields with special emphasis on Acid Mine Drainage.

Johnson DB, Kelso WI, Jenkins DA (1979) Bacterial streamer growth in a disused pyrite mine. Environ Pollut 18:107 – 118.

Murray KA (1987) Wastewater treatment and pollution control. Heer Printing Co. (Pty) Ltd, Pretoria.

Osuchowski R (1992) Advanced treatment of acid mine water. Technology SA – Chemical `92.

Thompson JG (1980) Acid mine waters in South Africa and their ameriolation. Water SA 6(3):130 – 134.

Unz RF, Dietz JM (1986) Biological applications in the treatment of acidic mine drainages. Biotechnology and Bioengineering Symp No. 16:163 – 170.

United States Environmental Protection Agency (US EPA) (2002) Method for measuring the acute toxicity of effluents and receiving waters to freshwater and marine organisms. EPA-821-R-02-012, 5th Edition. Office of Research and Development, Washington DC 20460.

Usher BH, Cruywagen L-M, de Necker E, Hodgson FDI (2003) On-site laboratory investigations of spoil in opencast collieries and the development of Acid-Base Accounting procedures. Water Research Commission Report No 1055/1/03. WRC, Pretoria.

Van Staden CM (1979) How ERPM uses lime to solve unique underground water problem. Coal Gold + Base Minerals of SA May '79: 100–109.

Wittmann GTW, Förstner U (1976) Metal accumulation in acidic waters from goldmines in South Africa. Geoforum 7:41 – 49.

An electronic attachment can be found at:
http://bitly.com/IMWA2013_501

Practical Technologies and Equipment for Preventing and Controlling Coal Mine Water Hazards in China

Shuning DONG[1], Hao WANG*[1], Zaibin LIU[1], Xianxin SHI[1]

[1]Xi'an Research Institute of China Coal Technology & Engineering Group Corp., 82.jinye 1st Road Xi'an, Shaanxi,710077, P.R. China, Dongshuning@cctegxian.com, wanghao@cctegxian.com

Abstract This paper presents some of the most successful technologies and equipment for preventing and controlling coal mine water hazards in China, as well as introduces the application of some technologies and equipment. In addition, China's coal mine water hazard types are summarized, and the practical technologies and equipment for preventing and controlling coal mine water hazards are divided into four categories: 1) exploration technologies and equipment; 2) monitoring technologies and equipment; 3) predicting technologies and equipment; 4) controlling technologies and equipment.

Keywords Coal Mine Water Hazard, Prevention and Control Technology and Equipment, Exploration, Monitoring, Prediction, Control

Introduction

China, with large amounts of coal resources, has vast experience with underground coal mines, some of which operate under extremely complex hydrogeological conditions. In recent years, coal mine water disasters have occurred frequently, which has restricted the sustainable development of China's coal industry. To prevent and control coal mine water hazards, Chinese hydrogeologists have developed some practical technologies and equipment.

The purpose of this paper is to systematically review practical technologies and equipment for preventing and controlling China's coal mine water hazards, as well as exchange engineering experiences with coal mine hydrogeologists from all over the world.

Summary of China's Coal Mine Water Hazard Types and Their Prevention and Control Technology

Based on different water source and water inrush channels, coal mine water hazards can be divided into different types. Coal mine water hazards are divided into four groups (Shuning *et al.* 2008), according to the positional relation of the groundwater inrush source and the mining space: 1) groundwater inrush from the roof of the mining space, 2) groundwater inrush from the floor of the mining space, 3) groundwater inrush from the goaf, and 4) groundwater inrush from surface water. In addition, water hazards are divided into: fault water hazards, sink hole hazards, and poorly sealed borehole water hazards, according to differences in the water inrush channels.

In general, water hazard preventing and controlling technologies are divided into four main categories (Shuning *et al.* 2008). The first category is exploration technology, including geophysical exploration, drilling exploration and hydrogeological tests. The second category is monitoring technology. This includes for example coal mine water real time monitoring system, coal seam floor and roof water hazard monitoring or early warning technologies. The third category is prediction technology, including technologies such as coal mine water inflow prediction technology, coal mine roof or floor water inrush prediction technology. The fourth is coal mine water inrush control technology. It is imperative to control coal mine water inrush as soon as it occurs.

Coal Mine Water Hazard Exploration Technology and Equipment

1. Three dimensional seismic exploration technology and equipment

Three-dimensional seismic exploration is the most effective geophysical prospecting technology for high-resolution exploration of geological structures. It uses sound waves to form sharp three-dimensional images of underground formations. Experts in the Xi’an Research Institute of China Coal Technology & Engineering Group have successfully used this technology not only to detect the faults whose throw is less than 3 m in plain area, but also to obtain good results in mountainous area and deserts.

Equipment used for three dimensional seismic technologies includes the ‘ARISE’ digital seismic exploration device and the ‘Geovecteur Plus’ data processing system.

2. Electromagnetic detection technology and equipment

Electromagnetic detection technologies usually require less rigid earth surface conditions than seismic exploration technologies. Practical electromagnetic detection technologies include magnetic dipole source technology, high resolution earth resistivity technology, high density resistivity technology, direct current electric technology, transient electromagnetic technology, and audio-frequency electrical penetration technology.

In the Shendong coal mining area, there have been several serious accidents caused by water inrush accompanied with sand collapse. Magnetic dipole source and high resolution earth resistivity techniques helped mining engineers pinpoint the distribution of quaternary water-bearing area. This is very helpful for designing working face layout.

In March 2010, a severe accident caused by Ordovician limestone water inrush occurred in the coal seam 16 mining roadway in the Luotuoshan Coal mine. Thirty-two coal miners died in this accident. Ground transient electromagnetic technology was applied to detect the water inrush channels. In Fig. 1, the red point is water inrush point, and the blue low resistivity areas clearly show the water inrush channels of Ordovician limestone. Some boreholes were drilled at the low resistivity areas, which proved the accuracy of transient electromagnetic technology.

The Taoyuan coal mine, located in eastern China, had a water inrush accident at the No.1022 working face. To drain the water, ten boreholes were drilled without using geophysical prospecting technology at the beginning. Unfortunately, most of them were dry. Then, high resolution direct current electric technology was adopted to pinpoint the anomaly water-bearing area. According to the low resistivity anomaly area detected, additional dewatering boreholes were designed and drilled. All

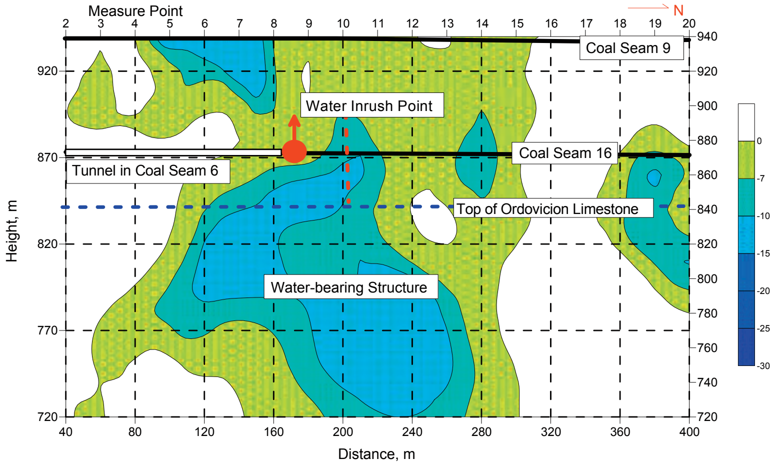

Fig. 1 *Diagrammatic cross-section of apparent resistivity for detecting water inrush channel*

of them worked well. This case proved the reliability of high resolution direct current electric technology.

3. Underground nearly-horizontal directional drilling technology and equipment

The underground nearly-horizontal directional drilling technology and equipment, which was first developed by Xi'an Research Institute of China Coal Technology & Engineering Group, is most advanced in the mining industry (Zhijun *et al.* 2011). The record of 1111 m drilling depth was made in underground in-seam directional drilling.

The calculation of borehole trajectory is the key to designing and constructing horizontal directional drilling boreholes. The calculation model of horizontal directional drilling borehole trajectory was established, with which three-dimensional trajectory can be obtained. Trajectory software was developed to arrange a uniform cluster of boreholes in the coal seam.

Directional drilling equipment came into use in 2008. Up to now, it has worked very well in China's coal mines. In the Hongliu coal mine, located in northwestern China, directional drilling technology was successfully used to explore undergroundwater-bearing areas which were near the mining roadway. In addition, in the Zhaogu coal mine, located in central China, directional drilling technology was employed to drill boreholes effectively which were used for underground grouting.

4. Dewatering test technology and equipment

Dewatering tests are an effective method in hydrogeological supplementary exploration of coal mines. The water source and water channels can be pinpointed, and countermeasures for preventing and controlling mine water hazard can be decided based on the tests. Furthermore, in order to pinpoint the groundwater recharge channel, dewatering tests are often combined with tracer tests which are based on hydrochemical analysis and environmental isotope technology. Successful dewatering tests can help coal mine hydrogeologists obtain important hydrogeological parameters, such as hydraulic conductivity, storage coefficient, and specific yield, so it is very popular in Chinese coal mines, especially in coal mines under very complex hydrogeological conditions.

For example, in the Feicheng mining area, which is seriously threatened by karst groundwater, dewatering tests of different scales have been conducted to explore hydrogeological conditions. With the data obtained in dewatering tests, numerical models were built to predict groundwater inflow. The equipment used in dewatering tests includes KJ117 monitoring system, water quality testing equipment, or groundwater modeling software.

Coal Mine Water Hazard Monitoring Technology and Equipment

1. Mine water real time monitoring system

Mine water real time monitoring system is a distributed serial digital communication network system based on Controller Area Network (CAN) technique. The monitoring system includes three parts: monitoring center (*e.g.* mainframe computer, printer, network communication adapter), monitoring substation (*e.g.* sensors, data acquisition unit, network communication interface) and data transmission network (Dewu *et al.* 2013).

The monitoring items include for example water level, water pressure, water temperature, precipitation, mine water inflow, maintenance condition of mine water facilities, real time condition of mine drainage system.

This system has been used in the Jiaozuo, Pingdingshan, Yongcheng coal mine areas in China in recent years. Main mine water monitoring equipment produced by Xi'an Research Institute of China Coal Technology & Engineering Group is KJ117 mine water monitoring system, YJSY(A) water level telemeter, YJSZ(A) water level recorder and YJS(A) mine water pressure recorder.

2. Coal seam roof water hazard monitoring and early warning

The roof water hazard monitoring and early warning system developed by Xi'an Re-

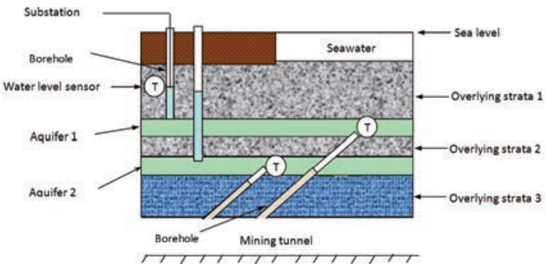

Fig. 2 *Roof water hazard monitoring system*

search Institute was successfully applied in the undersea working faces of the Beizao coal mine in Longkou, as shown in Fig. 2. Monitoring indexes of this monitoring system include water pressure, water quality, water temperature, and water inflow rate.

Surface and underground boreholes were used to monitor water pressure, water temperature and water quality of target aquifers. Early warning thresholds of water quality indicators were determined by water matching tests.

3. Coal seam floor water hazard monitoring and early warning

The floor water inrush monitoring and early warning system consists of the water inrush point analysis system, the monitoring system, the early warning system and the contingency plan. The monitoring system is a multi-parameter and multi-channel sensor system whose hardware system includes a mainframe computer, underground line, converter boxes, and sensors of water temperature, water pressure and stress.

The coal seam floor water inrush monitoring and early warning system developed by the Xi'an Research Institute of China Coal Technology & Engineering Group has been successfully used in the Liuqiao and Dongpang coal mines.

Coal Mine Water Hazard Prediction Technology and Equipment

Coal mine water hazard prediction technology includes coal mine roof water inrush prediction technology, coal mine floor water inrush prediction technology, and coal mine water inflow prediction technology. In this paper, the last of these is introduced. The most practical methods for predicting coal mine water inflow in China's coal mines include hydrogeological analogue method, Q-S extrapolation method, analytical method, artificial neural network method and groundwater modeling method.

If a coal mine under construction has similar hydrogeological condition and mining method to some operating coal mines, Chinese hydrogeologists often use hydrogeological analogue method to predict the water inflow of the coal mine under construction. The limiting condition of this method is that these operating coal mines must have long-term observed water inflow data. In some older coal mine area located in Eastern China, the hydrogeological analogue method usually is the best choice for water inflow prediction, even better than groundwater modeling method.

An analytical method which is called 'big well' method is very popular in predicting coal mine water inflow. It conceptualizes the entire coal mine tunnel system as an ideal 'big well', and makes the area of the big well the same as tunnel system's. The water inflow of the 'big well' is equivalent to the whole tunnel system's inflow. Based on this information, the radius of the big well can be calculated according to geometric theory. This method is often used in preliminary exploration of coal mines.

With the rapid development of computer and hydrogeological exploration techniques, numerical modelling method is widely used to calculate coal mine water inflow. In engineering applications, geophysical prospecting, dewatering test and tracer test techniques are combined to support the numerical model. Some advanced groundwater modeling software, such as GMS (Groundwater modeling system), Visual Modflow, Feflow, are very popular in the process of coal mine water inflow prediction.

Coal Mine Water Hazard Control Technology and Equipment

1. Water-retaining wall construction technology

The Xi’an Research Institute of China Coal Technology & Engineering Group has carried out some sink hole water inrush control engineering in several coal mines, including the Donpang coal mine (2003–2006), the Jiulong coal mine (2008), the Huangsha coal mine (2010–2012), the Luotuoshan coal mine (2010), the Sangshuping coal mine (2011), the Shenjiazhuang coal mine (2012) and the Taoyuan coal mine (2013).

Generally, to control a sink hole water inrush, the first stage is to construct a water-retaining wall in the mining tunnel to stop flooding. The second stage is to construct a water stopper in the sink hole to seal the water inrush channel thoroughly.

There are four steps for constructing water-retaining wall. The first step is to inject aggregates into the running water to form an aggregate accumulation body; the second step is to use rotary jet grouting to form water-blocking concrete body; the third step is to drill additional boreholes for grouting, and build an intact water-retaining wall; and the fourth step is to increase grouting pressure to increase the wall’s strength and permeability resistance. These four steps for constructing water-retaining wall are shown in Fig. 3.

2. Sink hole water stopper construction technology

A sink hole water stopper is constructed successfully by grouting in a proper position to block the sink hole water inrush channel in the Dongpang coal mine (Shenghui *et al.* 2008). Grouting and monitoring boreholes were drilled with directional drilling technology to ensure designed trajectory. There are four grouting steps to construct a water stopper: regular grouting, pressure grouting, drainage grouting and reinforcement grouting. The effectiveness of water stopper can be evaluated by underground dewatering tests.

Fig. 4 shows a sink hole water stopper built in the Dongpang coal mine in northeastern China. The column stopper was built by Xi’an Research Institute of China Coal Technology & Engineering Group. The total grout volume of the water stopper was 49 340 m^3.

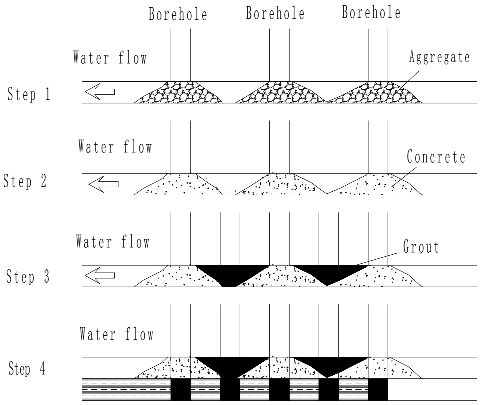

Fig. 3 *Four steps of constructing water-retaining wall*

3. (3) Technology of grouting controlled by drilling tool

Grouting controlled by drilling tool is a patented technology developed by Xi’an Research Institute of China Coal Technology & Engineering Group. This technology supplies a combined drilling tool hidden in a high strength non-woven fabric grout protection bag. The device can be sent to water inrush channel by drilling rig. The drilling fluid channel near the drilling bit will be plugged by a bowling method to push off the drilling rig and the grout protection bag. Rapid gel filling material will be injected to the grout protection bag through the drilling tool to form a controllable grouting body to seal water inrush channel.

This technology was applied in the Yubujie coal mine to seal a water inrush point in March 2012. Twenty-four grouting boreholes were drilled and twenty-four grout protection bags were used to grout 849 m^3 concrete. Compared with traditional grouting techniques, this technique can reduce construction cost and duration significantly.

Conclusion

Water hazard prevention and control technologies and equipment can be divided into

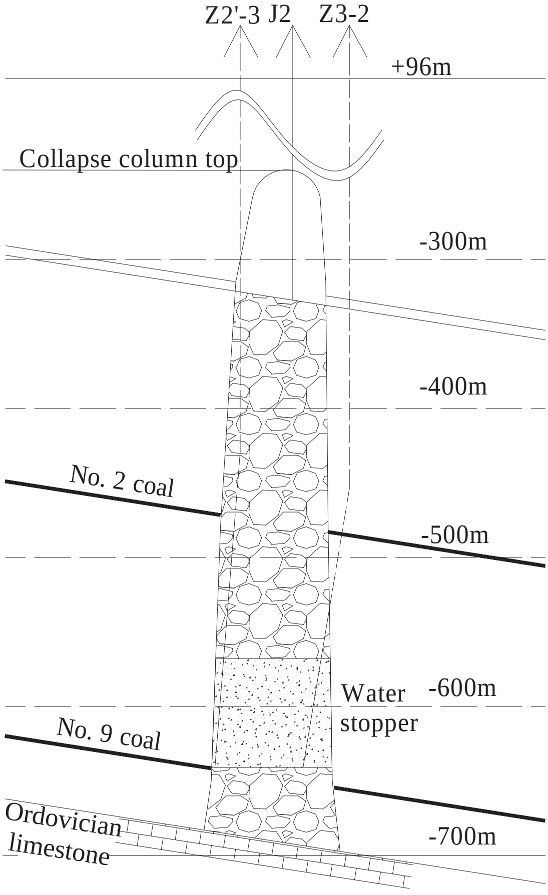

Fig. 4 *Water stopper in Dongpang Coal mine*

four categories, which are exploration, monitoring, prediction and control technologies and equipment.

Exploration technology and equipment, such as three dimensional seismic exploration, electromagnetic detection, underground nearly-horizontal directional drilling, and underground dewatering test, are very useful in underground structure and water-bearing anomaly area detection, as well as hydrogeological parameters identification. Monitoring technology and equipment, such as mine water real time monitoring system, coal roof and floor water hazard monitoring and early warning technology and equipment, which provide latest information of water level, water temperature, and surrounding rock to coal mine hydrogeologists, are the ‘underground eyes’ of coal mine hydrogeologists. Prediction technology and equipment, including coal roof & floor water inrush prediction, as well as coal mine water inflow prediction technology and equipment, if used properly, can help avoid most of coal mine water disasters. Control technology and equipment, containing water-retaining wall construction, sink hole water stopper construction and grouting controlled by drilling tool techniques and equipment, have been well developed to control water inrushes caused by sink holes, faults, and goaf water.

Acknowledgements

The authors gratefully thank IMWA and Colorado School of Mines for organizing and hosting the IMWA 2013 Conference, as well as hydrogeological department, geophysical prospecting research & development center, and drilling research & development center of Xi’an Research Institute of China Coal Technology & Engineering Group Corp for providing the research data. In addition, the paper’s English was greatly improved by Martha McGaughey from New York University.

References

Zhijun SH, Shuning D, Ningping Y, Dongzhuang T (2011) The underground directional drilling technology and equipment for kilometre deep borehole with MWD in coalmine. Procedia Earth and Planetary Science 3: 17–22

Dewu J, Yingfeng L, Zaibin L, Jianyuan C (2013) New progress of study on major water inrush disaster prevention and control technology in coal mine. Coal Science and Technology 41(1): 25–29

Shenghui N, Qinming J, Xiaoshan G, Kangkang L, Zaibin L, Lei S (2008) Construction technique of ground-water-preventing piston in Karst flow sink hole. Coal Geology and Exploration 36(4): 29–33

Surface water control in the bauxite mines of Porto Trombetas (Pará, Brazil)

Rafael Fernández Rubio[1], Helio Lazarim[2], David Lorca[1], Vinícius Vieira Ribeiro[2]

[1]FRASA Consulting Engineers. Luna 45, 28120 Ciudad Santo Domingo (Madrid, Spain).
rfrubio@gmail.com; d.lorca@gmail.com
[2]Mineracao Rio Norte, Porto Trombetas (Oriximiná, Pará, Brasil).
helio.lazarim@mrn.com.br; vinicius.ribeiro@mrn.com.br

Abstract MRN exploits large bauxite deposits by strip mining of plateaus in the Amazon rainforest. One important challenge is the control of water runoff, to minimize the entrainment of suspended solid material, and to avoid instability in the slopes at the plateau edge. These objectives have been achieved successfully after implementation and testing of micro-reservoirs installed across the mining areas. An important part of the micro-reservoir concept is that water infiltrates into a deep aquifer, reducing the amount of water that reaches the edges of the mining areas. Another advantage obtained with this methodology is the settling of suspended solids and colloids contained in the waters coming from mined areas.

Keywords Bauxite stripping mine, Amazon rainforest, suspended solid minimization, colloid removal, water infiltration, micro-reservoirs.

Geological context

The bauxite deposits of Porto Trombetas (State of Pará, Brazil) are sub-horizontal stratiform bodies of large regional extent, located at the top of the Upper Cretaceous Alter-do-Chão Formation, consisting of continental sediments deposited in a fluvial and lacustrine environment. These sediments are arranged in plane-parallel layers, with frequent interbedded clays. The thick sedimentary series overlies the Paleozoic rocks of the Amazon Basin, as shown in Fig. 1 (Mendes *et al.* 2012).

In detail, the Alter-do-Chão Formation comprises siltstone with interbedded sandstones, overlain by a sequence of more than 100 m thickness of indurate sediments, characterized by layered sandstone and conglomerates intercalated with mudstones, siltstones, sandstones, sandy clays and clayey sands (Cunha *et al.* 1993). The bauxite mineralization occurs as a result of weathering processes, where the tropical climate, with high levels of precipitation, humidity and drainage, were key factors in the hydrolysis and modification of layered primary ferruginous alumino-silicate minerals on top of the entire sedimentary body.

The intense erosion upstream caused a characteristic morphology of valleys and

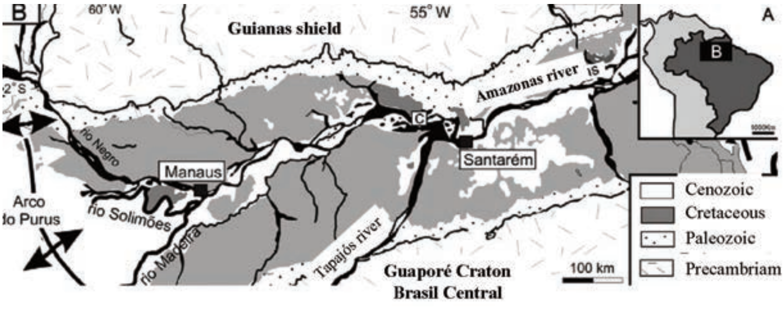

***Fig. 1** Exposure of the Alter-do-Chão Formation along the Amazon River.*

plateaus, which stand out in relief, and are jagged, indicating an immature geomorphological, non-stabilized stage (Fig. 2).

The bauxite deposits exist today as eroded remnants in these plateaus or “tablas” at the top of the Alter-do-Chão Formation, intersected by a dense network of surface drainages with dendritic patterns (Fig. 3).

The bauxite is in general restricted to the residual sub-horizontal plateaus, surfacing within or below the surficial topsoil and yellow clay. The higher hardness and erosion resistance of the bauxite causes it to form the edge of the plateau, as a morphological highlight (Fig. 4). On the slopes of the plateaus the overlying sedimentary materials outcrop over a significant length resulting from the depth of erosion achieved by the creeks. The hillsides have average slopes of less than 20 %, although locally they can be much steeper.

Hydroclimatic context

The average annual rainfall at the minesite is 2,189 mm, with annual maximums in excess of 3,000 mm. The site has an especially high rainfall period from December to May, with an average of 1,654 mm of rain. This represents a major water contribution to the runoff drainage basins, and creates great potential for soil erosion in deforested areas, or those areas with insufficient vegetative cover for its protection, providing significant amounts of suspended solids in runoff. Between June and November, the average rainfall is 532 mm, which is far from negligible. The maximum monthly rainfall occurred in March, 2005, with 637 mm. These rainfall rates have large spatial variability resulting from local convective-type storms. Monitoring of the precipitation has required installation of 24 rain gauges, 3 A-Class evaporation pans, and dozens of Piché-type evaporation gauges.

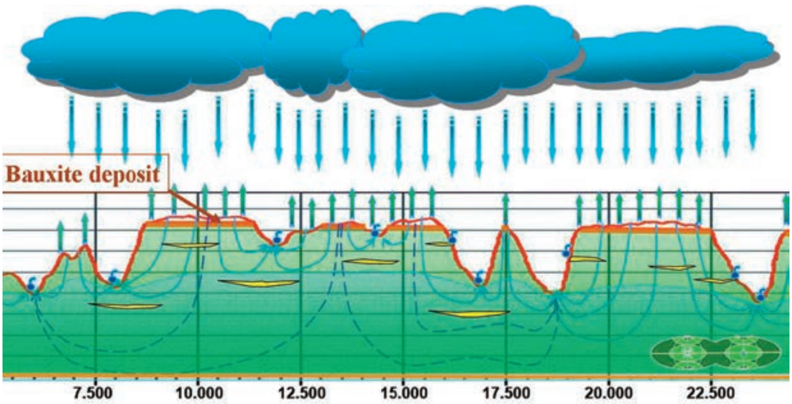

Fig. 2 *General morphology of the bauxite deposits and conceptual hydrologic model of Porto Trombetas.*

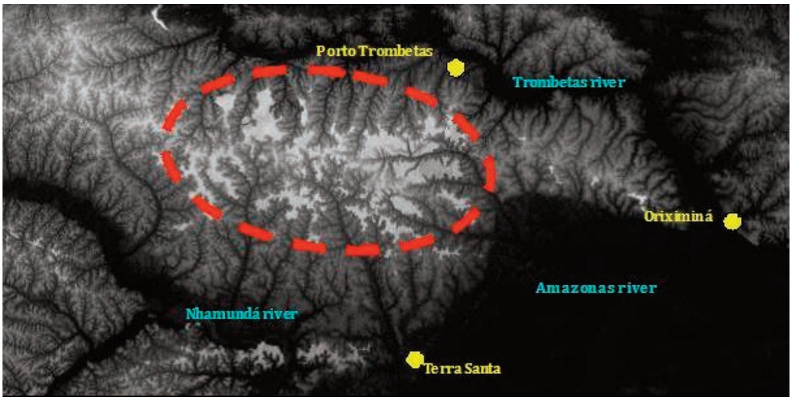

Fig. 3 *Tabular arrangement of the Porto Trombetas bauxites (satellite image).*

Hydrogeological context

A conceptual hydrogeological model has been developed for the project, with the support of a large number of shallow and deep piezometers. The model comprises three hydrostratigraphic units: isolated shallow aquifers; local suspended aquifers, and a regional deep aquifer (Fig. 5).

The sequence of lateritic and bauxitic horizons on top of the plateaus have reduced but not negligible permeability, causing most of the rainfall that is not evaporated to seep out into the plateaus under natural conditions. The infiltrated water can flow sub-horizontally to the periphery of the plateaus, giving rise to small temporal springs scattered around the edges of the plateau. Another important part of the hydrological system is that rainfall infiltrates vertically through the underlying clay and silt aquitard to the underlying local aquifers, and through them to the deep regional aquifer, which feeds the surface hydrological system by springs in incised streambeds.

Mining operation

The mining sequence in the plateaus consists of the following sequence:

1. Clearing the dense rainforest, which is supported by a thin layer of topsoil (usually less than 1 m thick).
2. Removal of topsoil, which is stockpiled for use in reforestation.
3. Mining of the silt and clay cover above the bauxite, with deposition into the mined-out adjacent strip, which is typically 30 m wide.

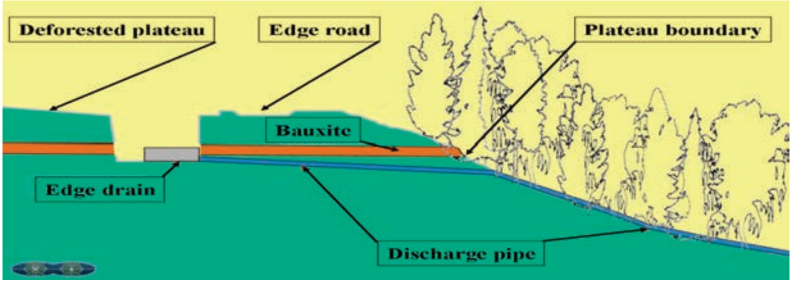

Fig. 4 Plateau edge morphology with drainage water system.

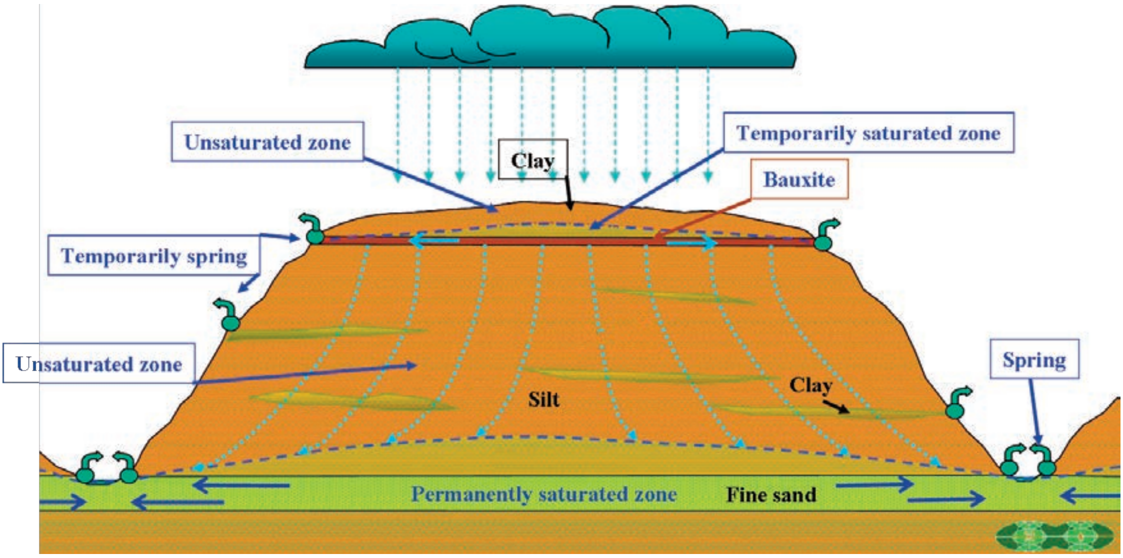

Fig. 5 Regional hydrogeological model.

4. Mining of the layer of bauxitic ore, leaving the zone of clay and silt beneath, which forms an aquitard, and contains the local suspended aquifer systems.

Following mining, the land is restored. This includes the installation of a protective fill berm around the edge of the mined area, with a minimum width of 10 to 30 m, higher elevation than that of the adjacent mining area, and a slope towards the interior of the mined area, so that the runoff from the exterior strip will always drain inward to the plateau.

Hydrological and environmental incidents

During prior operations, failure incidents occurred on the edges of the plateaus consisting of:

1. Erosion on the hillsides causing "bad-land" topography due to concentrated water flow and associated slope erosion, frequently leading to mud flow failures; and
2. Landslides near the edge of the plateau, due to relatively steep slopes and build-up of pore-water pressure due to precipitation.

In order to avoid slope failures, and to achieve better utilization of mining resources, we have designed a unique methodology that has allowed substantial progress towards stable, environmentally protective mining, and groundwater conservation.

Its application requires a detailed advance study of the edge conditions on the flanks of the plateaus, considering geotechnical, morphological, and hydrological parameters, edge conditions (whether natural or man-made), that may have an impact on stability. A final evaluation of the safety factor of the slope is made to establish the minimum edge border protection, which can vary between 5 and 30 m (added to by a 5 m wide service road).

A variety of methods are successfully applied to reduce the risk of erosion and landslides. This paper presents those aimed at surface water control and incremental infiltration of rainwater in the deep aquifer through artificial recharge, thus preventing the water from reaching drains at the edge of the plateau.

Runoff interception by micro-dams

The contribution of water to the edge drains is reduced by constructing a set of micro-dams for retention of water (Fig. 6), located in the mining areas and within the post-mining morphological reshaping within the plateau that is implemented during reclamation.

The effectiveness of this set of preventive structures for trapping water flow on the plateaus has been proven in all by noticeably reducing the intake of water to the edge drains, increasing infiltration of surface water to the deep regional aquifer system, increasing the evaporation rate, and also substantially reducing the discharge of suspended solids and colloids to creeks.

Mineração Rio do Norte has been building micro-dam structures on the plateaus in mining operations being reshaped for rehabilitation over the past three years, taking advantage of the excavation of drainage ditches and the movement of overburden materials. To date there has been no adverse hydrological or environmental incidents.

The micro-dams are constructed using transverse dikes extending away from the pe-

***Fig. 6** Micro-dam built on drainage channel.*

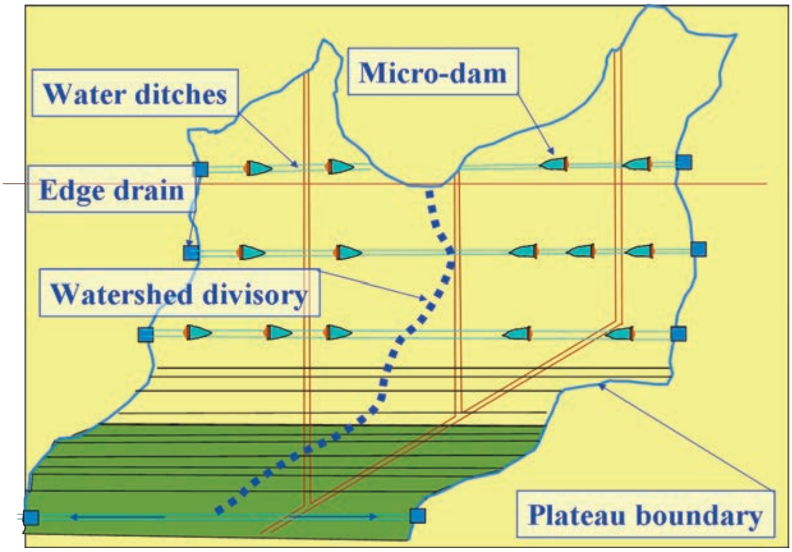

Fig. 7 *Schematic sketch of the location of micro-dams in drainage channels.*

riphery drains. These infrastructure features allow for retention of rainwater in local sub-basins, improving the safety of slopes by removing direct infiltration to the slope areas. Even though there are intense rainfall events, it has been shown to be practical to locally collect and store the stormwater flows on the mined-out surface during and after reclamation, thus preventing the storm surge of runoff from reaching the drains simultaneously (Fig. 7).

The implementation of micro-dams also favors sedimentation and settling of suspended solids, as well as retention of slash from processing and removal of tree trunks, branches and leaves. This retention results in the accumulation of material favorable to vegetative growth, and provision of a large number of seeds to begin that growth.

The crest height for each micro-dam dyke is located in a way that if it fills the water can overflow to the next micro-dam through a small side channel (effectively a spillway), directly on the rock base. This water finally reaches the drain, but with the flow peaks damped and the total flow peak substantially attenuated.

Other water retention structures

In addition to micro-dams, other intermediate settling boxes or small dams are constructed on the surface of the contributing mined basin, together with their servicing drains. While these have low capacity, they are very efficient for retaining rain-water and removing suspended solids.

Monitoring

In all main drainages rainfall is measured on a daily basis by local rain gauges. In addition, the height of water accumulated in front of the gabion-filter boxes is measured. These measurements demonstrate that the quantity of water received in the discharge drains has decreased very significantly, as shown in Fig. 8.

The reduction in water level is primarily the result of infiltration to the deep aquifer from the water pool in the micro-dams. The control of water flow has resulted in an important improvement in slope stability, in particular reducing the likelihood of landslides around the periphery of the bauxite mining area. In addition, the micro-dams have produced a total reduction in slope erosion accidents, and a very noticeable reduction in the contribution of solids in suspension to the drainage network.

In addition, piezometers were installed in micro-reservoirs to study the vertical filtration of stored water to the deep aquifer (Fig. 9).

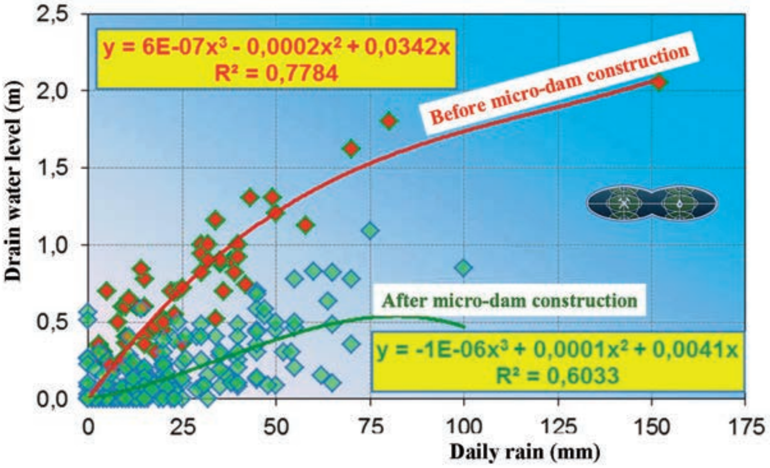

Fig. 8 Height of water next to the drain before and after the construction of the impoundments.

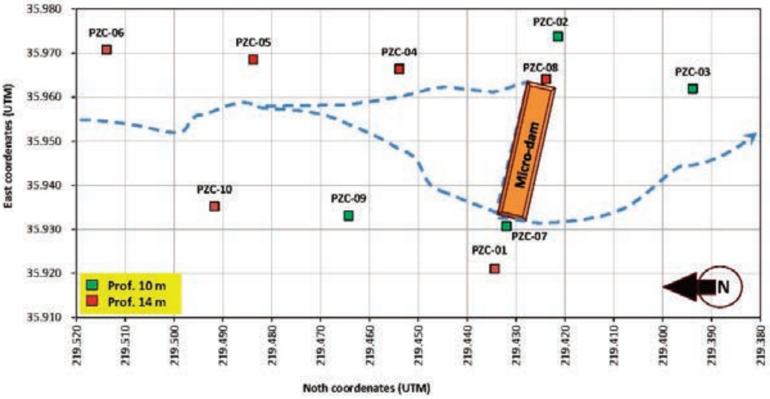

Fig. 9. Piezometers installed in micro-dam to study the vertical water infiltration.

Vegetal Cover

Another important aspect of micro-dams that was developed in this project is the reclamation of vegetation after mining. Revegetation comprising undergrowth, together with the planting of native forest trees was implemented, followed by the construction of "vegetal filters" immediately surrounding the drains, and placement of branches on drainage channels and in the vicinity of drains to provide surface stability and erosion protection.

Conclusions

A mini-dam program has been implemented in the Brazilian alumina mines in the Amazon basin to control the effects of very high rainfall. After three years of operation of the mini-dam program, they have been shown to be effective in reducing mine runoff and discharge, enhancing infiltration of water into the deep regional aquifer, and improving the stability of the plateau scarps surrounding the mined area. In this period no hydrological or environmental failures have occurred over the many kilometers of mine periphery along the edge of plateaus in operation or under rehabilitation.

References

Cunha FMB, Gonzaga FG, CoutinhoLFC &Feijó FJ (1994) Bacia do Amazonas. Bol. Geoc. Petrobras 8: 47-55.

Mendes AC, Truckenbrod W. & Rodrigues Nogueira AC (2012) Análise faciológica da Formação Alter-do-Chão (Cretáceo, Bacia do Amazonas), próximo à cidade de Óbidos, Pará, Brasil. Revista Brasileira de Geociências 42(1): 39-57.

Indirect implication of bacterial proteins in the biouptake of metals from aqueous solution

E. Fosso-Kankeu[1,2], A. F. Mulaba-Bafubiandi[1], T. G. Barnard[3], P. T. Campana[4]

[1]*Minerals Processing and Technology Research Center, Department of Metallurgy, School of Mining, Metallurgy and Chemical Engineering, Faculty of Engineering and the Built Environment, University of Johannesburg, PO Box 17011, Doornfontein 2028, Johannesburg, South Africa*
[2]*School of Chemical and Minerals Engineering, Faculty of Engineering, North West University, Potchefstroom Campus, Potchefstroom, South Africa, e-mail: 24838616@nwu.ac.za*
[3]*Water and Health Research Unit, Faculty of Health Sciences, University of Johannesburg, PO Box 17011, Doornfontein 2028, Johannesburg, South Africa*
[4]*Escola de Artes, Ciências e Humanidades, Universidade de São Paulo, Brazil*

Abstract To investigate the adsorptive role of proteins on the cell walls of four bacteria (*Bacillaceae bacteria, Bacillus subtilus, Escherichia coli* and *Pseudomonas aeruginosa*), they were mechanically disrupted and the cell residues used for adsorption of nickel. The effect of mechanical treatment on the biomasses was assessed using SDS-PAGE, specific protein assay kit and Fourier Transform Infrared Spectroscopy (FTIR). A decrease of the adsorption capacities of all the biomasses was observed following treatment. FTIR spectra showed slight shift in the signals of active groups on all the cells after treatment. Analysis confirmed removal of proteins from cells during treatment.

Keywords Biosorption, metal binding proteins, Gram-negative bacteria, Gram-positive bacteria, bioremediation, nickel

Introduction

Metal biosorption processes are exploited in the remediation of polluted water or recovery of values from mine solutions. Biosorbents often used are agricultural products, plants and, microorganisms reported to be more effective. Metal uptake by microorganisms occurs through two mechanisms namely passive and active mechanisms; in the active mechanism metal ions are transported across the membrane yielding to intracellular accumulation. This mechanism is often associated with an active defence system of microorganisms whereby metal binding proteins are induced in response to metals. Some metal ions (*e.g.* Mn^{2+}, Fe^{2+}, Co^{2+}, Ni^{2+}, Cu^{2+} and Zn^{2+}) have a role in a variety of important functions of proteins in microorganisms, however at higher concentrations even essential metals can become toxic (Roane and Pepper 2000). The control of intracellular metal ions is achieved by families of proteins including transmembrane transporters, metalloregulatory sensors and diffusible cytoplasmic metallochaperone proteins (Finney and Ohalloran 2003). Typical example of metalloproteins often found in yeast, fungi and algae are low molecular weight metallothioneins with a high cysteine content (Mejare and Bulow 2001; Ibrahim *et al.* 2001). The functions of metalloprotein in microbial cells are distinguishable, but all contribute in ensuring metal homeostasis in the cell, by influencing uptake, efflux, intracellular trafficking within compartments and storage (Tottey *et al.* 2008; Waldron and Robinson 2009).

Although the affinity for a metal ion in a metalloprotein is high if the function of the protein requires keeping the metal ion bound, conserved histidines, cysteines regions as well as other sites can be implicated in the binding

(Mejare and Bulow 2001; Pastore *et al.* 2007; Maret 2010; Passerini *et al.* 2006; Passerini *et al.* 2007; Shu *et al.* 2008). It is said that metalloproteins have affinity for specific metals to a certain extent, allowing them to bind the metals and move them across the cell (Ma *et al.* 2009).

Metalloproteins as part of the microbial cell membrane can affect its adsorption capacity and specificity. Acquisition of essential metal ions from the extracellular environment by the bacteria systems is made possible by cell membrane. The structure of bacterial cell membrane determines the ability of bacteria to uptake metal ions and meets cellular metal demands. Proteins, peptide, lipoproteins, polysaccharides and other extracellular polymeric substances of the cell wall can adsorb metals. It has been reported that proteins associated to microorganisms cell membranes play a crucial role in the removal of metals from solution (Fukushi *et al.* 1996; Bupp and Ghosh 1991; Ghosh and Bupp 1992). However the nature of the cell wall considerably varies between Gram-positive and Gram-negative bacteria. The cell wall of Gram-positive bacteria is mainly composed of peptidoglycan, while this polymer is thinner in Gram-negative bacteria but supplemented with lipopolysaccharide (Beveridge 1999; Vijayaraghavan and Yun 2008; Wang and Chen 2009).

For a better understanding of the influence of proteins on the adsorption capacity of microorganisms two types of cells, Gram-positive (*Bacillus subtilis* and *Bacillaceae bacterium*) and Gram-negative (P*seudomonas aeruginosa* and *Escherichia coli*) bacteria were studied.

Determination of the level of implication of membrane proteins in metal uptake by microorganisms will facilitate understanding of the mechanism of the process and also set a basis for the development of metal biosensors.

Methodology

Preparation of metal solutions

Analytical salts of copper and nickel sulphate were dissolved in distilled water to make stock solutions of 1000 mg/L.

Proteins extraction and characterization

To induce the production of metal binding proteins, cells of *Bacillaceae bacterium, Escherichia coli, Bacillus subtilis* and *Pseudomonas aeruginosa* were grown to early log phase and exposed to nickel (0, 40, 100 and 200 mg/L) in an aqueous solution at 37 °C for approximately four hours. Control and induced cells were both centrifuged at 8867 g for 5 min at 4°C and the pellets recovered. The cells were suspended in 1 mL phosphate buffer saline (NaCl: 0.138 M, KCl: 0.0027 M, pH 7.4) and a 3 mm bead was added. The cells were then lyzed by vortexing the mixture intermittently (1 min vortex and 1 min in ice) for 5 min using a Disruptor Genie machine (Scientific Industries, USA). Cell debris were then separated from the supernatant by centrifuging the mixture at 15600 g for 5 min. The supernatant was then collected and stored at 4 °C for the next experiment.

SDS-PAGE

Reagents were prepared according to manufacturers' specification. Prior to electrophoresis, presumptive protein fractions were added to equal volume of laemli buffer and a quarter of volume of 2-mercapto ethanol; the mixture was then heated at 95 °C for 5 min. The samples and SDS-PAGE pre-stained standard were loaded on pre-packed gels from Biorad and ran at 120 V for 45 min.

Quantification of proteins

For quantification of proteins present in the lysis extract, the Pierce BCA Protein Assay Kit (Thermo Scientific, SA) was used. Experiment was conducted in test-tubes according to the protocol provided by the manufacturer. The absorbance of all the samples was measured within 10 min at 562 nm. The standard curve was used to determine the protein concentration of each lysis extract.

FT-IR experiment

Freshly grown and lysed cells of *Bacillaceae bacteria, E. coli, B. subtilis* and *P. aeruginosa* were dried for 24 h in the oven at 50°C and then crushed in the mortar. Spectra of cell pellets were recorded within the wavenumber range of 400–4000 cm^{-1} with a Nicolet iS10 spectrometer (Thermo Fisher Scientific, SA).

Metal adsorption experiment

Cells of *Bacillaceae bacterium, Escherichia coli, Bacillus subtilis* and *Pseudomonas aeruginosa* were inoculated in nutrient broth ('Lab-Lemco' powder: 1.0 g/L; yeast extract 2.0 g/L; peptone 5.0 g/L; sodium chloride 5.0 g/L; pH 7.4 ± 0.2 at 25 °C; Merck Chemicals, SA) and incubated in incubator with shaker at 37 °C for 20 h. Cells were then harvested using a centrifuge at 8867 g for 5 min at 4°C.

Both freshly grown and lysed cells (0.1 g) were used for adsorption of nickel (10, 20, 30 and 40 mg/L) at 37 °C in an incubator with shaker (160 rpm, Labcon). Aliquot (5 mL) of the mixture was collected every 30 min of the duration of experiment (two hours). Collected samples were centrifuged at 15600 g for 5 min and the residual metal in the supernatant was measured using the Inductively Coupled Plasma Optical Emission Spectrometer (ICP-OES).

The adsorption capacity at equilibrium was determined using the following equation:

$$q_e = \frac{(C_o - C_e)V}{m} \qquad (1)$$

where: q_e is the absorption capacity in mg/g, C_o is the initial concentration of metal ions in solution (mg/L), C_e is the equilibrium of metal ions (mg/L), m is the biomass (g), V is the volume of the solution (L)

Results and discussion

Characterization and quantification of proteins

Visualization of isolated proteins on SDS-PAGE

This experiment was carried out in order to identify some of the proteins naturally produced by the cells but mostly to determine if other proteins were produced by bacteria in response to the presence of nickel. The Fig. 1 shows (head of arrows) that some additional proteins were produced during the exposure of cells to nickel. It could also be observed that the size of metal induced proteins varied per cells. This certainly implies the specificity of response with regard to the defence mechanism.

Relative quantity of specific proteins in the extract

The technique used for proteins' quantification was specific to proteins rich in four particular amino acids (cysteine, cystine, tryptophan and tyrosine). According to Passerini *et al.* (2012), high-throughput experimental techniques based on X-ray adsorption spectroscopy are effective in identifying metalloproteins, but do not allow detection of ligands involved in binding the metals. Metal binding proteins including metallothioneins and phytochelatins are reported to be rich in cysteine (Mejare and Bulow 2001; Passerini *et al.* 2012). It was therefore expected that cysteine bearing proteins will constitute the major part of proteins quantified in the extract isolated from bacteria cells. Results (not shown here) indicate that such proteins were mostly isolated from *E. coli* cell membrane (0.25 µg/mL). In

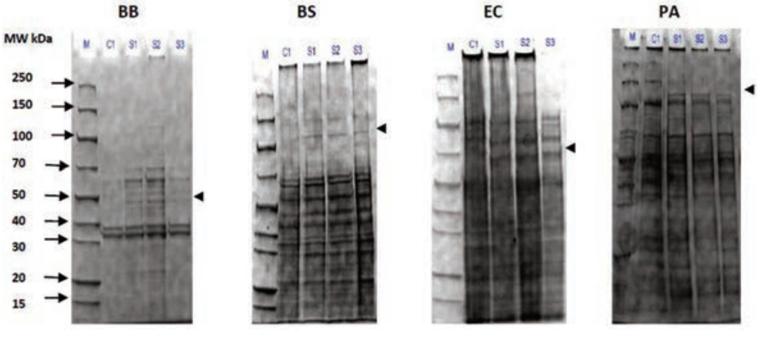

Fig. 1 *Isolated proteins observed on SDS-PAGE (M: marker, C1: cells non exposed to Ni, S1: Cells exposed to 40 mg/L Ni, S2: Cells exposed to 100 mg/L Ni, S3: cells exposed to 200 mg/L Ni). BB:* Bacillaceae bacterium, *BS:* B. subtilis, *EC:* E. coli, *PA:* P. aeruginosa.

general higher amount of proteins were removed from Gram-negative bacteria than Gram-positive bacteria. It has been reported that the proteins or peptides easily removed by mechanical disruptions are mostly part of the extracellular polymeric substances (EPS; Yee and Fein 2001; Vijayaraghavan and Yun 2008).

Active groups on treated and untreated cells (FTIR)

Discrepancies in the spectra of treated and untreated biomasses of Gram-negative bacteria were observed both in the region of 3300 – 2800 and 1700 – 750 cm^{-1} (Fig. 2) corresponding to the effect of mechanical disruption to the active groups. Such treatment affected the signals of active groups from E. coli (3265 cm^{-1}, 3065 cm^{-1}, 1300 cm^{-1} and 850 cm^{-1}) and mostly from *P. aeruginosa* (2900 cm^{-1}, 1600 cm^{-1}, 1100 cm^{-1} and 950 cm^{-1}).

For the Gram-positive bacteria, mechanical disruption also resulted in the bands’ shift of signals in *Bacillaceae bacterium* (2870 cm^{-1}, 1470 cm^{-1} and 1300 cm^{-1}) as well as *B. subtilis* (3290 cm^{-1} and 3070 cm^{-1}) biomasses spectra (Fig. 3).

The disappearance or reduction of signals mainly corresponding to the carboxylic and amine functional groups in the treated biomasses, implies that mechanical disruption certainly affected the peptide or proteins content of cells. It was observed that bands’ shift of signals were more pronounced with *P. aeruginosa* biomasses while *B. subtilis* biomasses were less affected.

Metal adsorption behaviour of treated and untreated biomasses

According to previous works an estimation of one-quarter to one-third of all proteins require metals, the exploitation of elements varying from cell to cell (Ferrer *et al.* 2007; Bertini and Cavallaro 2008; Waldron and Robinson 2009).

Adsorption behaviour as a function of metal concentration

The determination of adsorption behaviour of treated and untreated biomasses was carried out by plotting the adsorption capacity in a Langmuir model (C_e/q_e *vs.* C_e). It was observed (Fig. 4) that the adsorption behaviour of treated and untreated biomasses was similar; for both types of biomasses the adsorption capacity increased with an increase of equilibrium concentration, mainly due to mass transfer. The adsorption data showed acceptable fit with the Langmuir isotherm as indicated by the correlation coefficient for *Bacillaceae bacteria* (0.9594 and 0.9482), *B. subtilis* (0.9512 and 0.9648), *E. coli* (0.9805 and 0.9954) and *P. aeruginosa* (0.9724 and 0.9889) for untreated and treated biomasses respectively. However better adsorption of nickel by untreated bio-

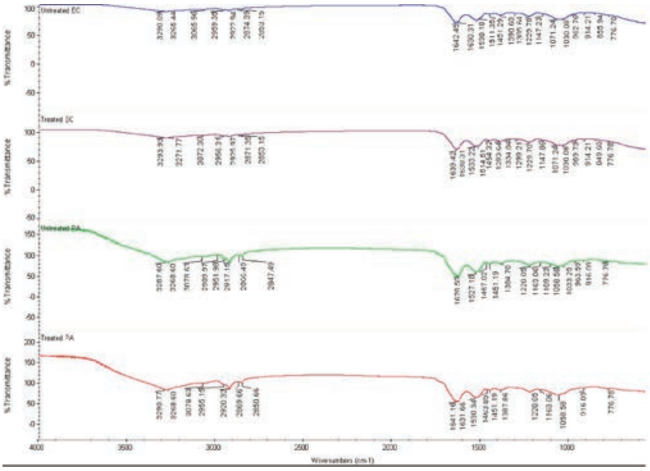

Fig. 2 *FTIR spectra of the treated and untreated Gram-negative bacteria biomasses; EC:* E. coli*, PA:* P. aeruginosa

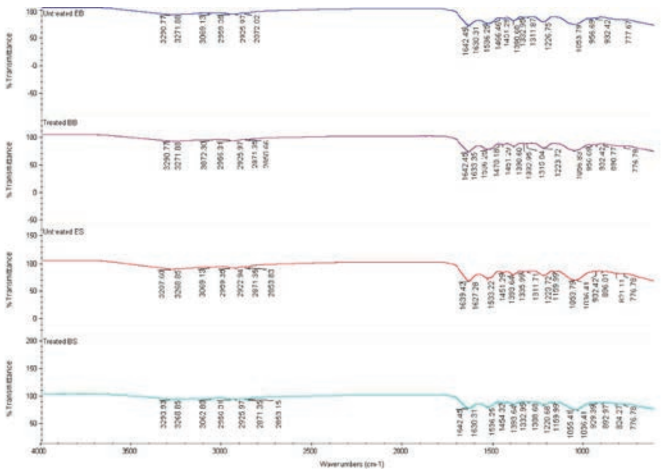

Fig. 3 FTIR spectra of treated and untreated Gram-positive bacteria biomasses; BB: Bacillaceae bacterium*, BS:* B. subtilis

masses compared to treated biomasses could be observed.

In previous study, Wei *et al.* (2011) also observed that removal of EPS from *B. subtilis* and *P. aeruginosa* reduced their affinity towards cadmium. In general, although the treatment affected mostly the adsorption capacity of Gram-positive biomasses, no significant difference was observed among the adsorption capacities of Gram-negative and -positive bacteria after treatment. According to Kulczycki *et al.* (2002), the difference in metal adsorption capacity between Gram-positive and -negative bacteria could not only ascribed to the differences between the sorptive functional groups of these bacteria, but also from variation in cell wall architecture.

Conclusion

Mechanical disruption of biomasses, has allowed to determine the indirect implication of proteins or peptides of the cell wall of Gram-negative (*E. coli* and *P. aeruginosa*) and -positive (*Bacillaceae bacterium* and *B. subtilis*) during nickel's adsorption; removal of proteins from cell walls led to reduction bacteria affin-

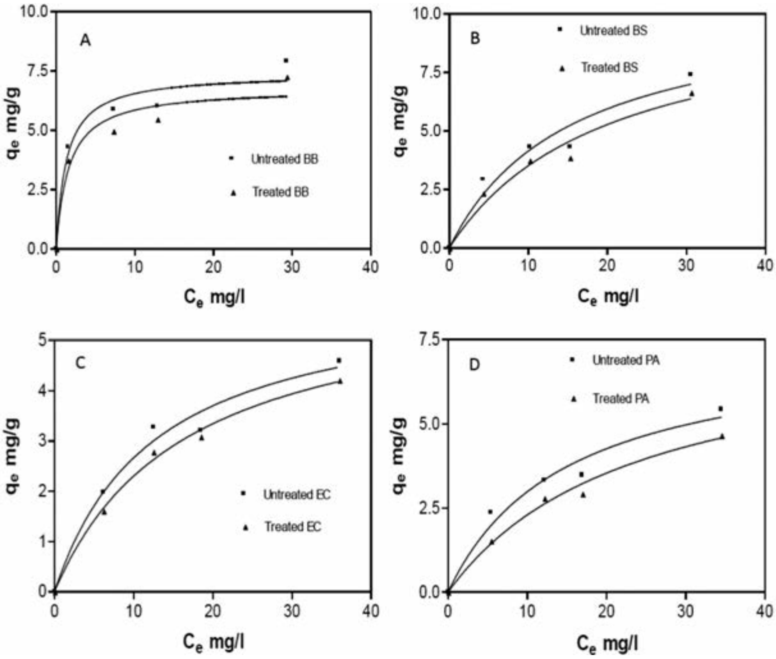

Fig. 4 Adsorption behaviour of treated and untreated biomasses during uptake of nickel. (A) Bacillaceae bacteria *"BB"; (B)* B. subtilis *"BS"; (C)* E. coli *"EC"; (D)* P. aeruginosa *"PA".*

ity towards nickel. Some of these proteins content a certain level of cysteine, which is an amino acid abundant in most of the metal binding proteins. Despite the chemical and physical differences among the cell walls of Gram-negative and -positive bacteria, no significant difference in the absorptive role of proteins on their cell wall was established in this study.

References

Beveridge TJ. 1999. Structures of Gram-negative cell walls and their derived membrane vesicles. J Bacteriol. 181: 4725–4733

Bupp S, Ghosh S. 1991. Heavy metal uptake by microbial protein complexation. Paper presented at the Research Symp., Annual WPCF Conf., Toronto, Canada, October.

Finney L.A., T.V. O'Halloran. 2003. Transition metal speciation in the cell: insights from the chemistry of metal ion receptors. Science, 300: 931–935.

Fukushi K, Chang D, Ghosh S. 1996. Enhanced heavy metal uptake by activated sludge cultures grown in the presence of biopolymer stimulators. Wat. Sci. Tech., 34(5–6): 267–272.

Ghosh S, Bupp S. 1991. Uptake of heavy metals by unacclimated aerobic culture. Prof. Conf. On Hazardous Waste Research, L. Erickson (ed.) Engineering Extension, Kansas State University, Manhattan, KS, pp 30.

Ibrahim Z., Azlina W., Baba A.B. 2001. Bioaccumulation of silver and the isolation of metal-binding protein from *P. diminuta*. Brazilian Archives of Biology and Technology, 44(3): 223–225.

Kulczycki E, Ferris FG, Fortin D. 2002. Impact of cell wall structure on the behaviour of bacterial cells as biosorbents of cadmium and lead. Geomicrobiology Journal. 19(6): 553–565.

Ma Z, Jacobsen FE, Giedroc DP. 2009. Metal Transporters and Metal Sensors: How Coordination Chemistry Controls Bacterial Metal Homeostasis. Chem. Rev. 109(10): 4644–4681.

Maret W. 2010. Metalloproteomics, metalloproteomes and the annotation of metalloproteins. Metallomics, 2: 117 – 125.

Mejare M, Bulow L. 2001. Metal-binding proteins and peptides in bioremediation and phytoremediation of heavy metals. Trends in Biotechnology. 19(2): 67–73.

Passerini A, Lippi M, Frasconi P. 2012. Predicting Metal Binding Sites from Protein Sequence. IEEE/ACM Transactions on Computational Biology and Bioinformatics. 9(1): 203–213.

Passerini A., Andreini C., Menchetti S., Rosato A., Frasconi P. 2007. Predicting zinc binding at the proteome level. BMC Bioinformatics, 8: p 39.

Passerini A., Punta M. Ceroni A., Rost B., Frasconi P. 2006. Identifying cysteines and histidines in transition-metal-binding sites using support vector machines and neural networks. Proteins, 65(2): 305 – 316.

Pastore C., Franzese M., Sica F., Temussi P., Pastore A. 2007. Understanding the binding properties of an unusual metal-binding protein – a study of bacterial frataxin. FEBS Journal, 274: 4199 – 4210.

Roane TM, Pepper IL. 2000. Microorganisms and metal pollutants. In: Maier, R.M., Pepper, I.L.,Gerba, C.P. (Eds.), Environmental Microbiology. Academic Press. San Diego, USA, 403–423.

Shu N, Zhou T, Hovmoller S. 2008. Prediction of zinc-binding sites in proteins from sequence. Bioinformatics, 24(6): 775 – 782.

Tottey S, Waldron KJ, Firbank SJ, Reale B, Bessant C, Sato K, Cheek TR, Gray J, Banfield MJ, Dennison C, Robinson NJ. 2008. Nature, 455–1138.

Vijayaraghavan K, Yun YS. 2008. Bacterial biosorbents and biosorption. Biotechnol. Adv. 26, 266–291.

Waldron KJ, Robinson NJ. 2009. How do bacterial cells ensure that metalloproteins get the correct metal? Nature Reviews. 6: 25–35.

Wang J, Chen C. 2009. Biosorbents for heavy metal removal and their future. Biotechnology Advances. 27, 195–226.

Wei X, Fang L, Cai P, Huang Q, Chen H, Liang W, Rong X. 2011. Influence of extracellular polymeric substances (EPS) on Cd adsorption by bacteria. Environmental Pollution. 159: 1369–1374.

Yee N, Fein J. 2001. Cd adsorption onto bacterial surfaces: a universal adsorption edge? Geochim Cosmochim Acta. 65: 2037–2042.

Consideration of Thermal Conditions in Year Round Heap Leach Operation in the Northern Desert Climates

Amy L. Hudson[1], Troy Meyer[2]

[1]*Tetra Tech, One Monarch Drive, Suite 202, Littleton, Massachusetts, 01460, USA,*
amy.hudson@tetratech.com
[2]*Tetra Tech, 120 West Park Drive, Suite 204, Grand Junction, Colorado, 80401, USA,*
troy.meyer@tetratech.com

Abstract Heap leach pad design and subsequent successful operation can be affected by many factors including material properties, ore grade, and climate. Often the climate component can be over looked, but in a northern desert environment that experiences extreme temperature shifts, the design must consider the pad thermal conditions not only for stacking, but also for solution application. The heap leach pad design and operational conditions for a project in northern Mongolia were developed through a combination of variably saturated flow modeling, thermal solution modeling within the heap, and thermal modeling of the solution pond. The project was constructed as designed, and has operated successfully using the suggested thermal conditions.

Keywords heap leach, modeling, unsaturated flow, thermal budget

Introduction

Modeling is often used during the design phase of a project to predict the operational and closure conditions of mining facilities. However, it is less common that the modeling results can be confirmed by the operations of the mine. This project used predictive modeling to design a heap leach pad and pond facility in the Selenge Province of northern Mongolia. The project is an operating gold mine that expanded their operation to include heap leaching, which allowed for the design to be implemented immediately, confirming the modeling results.

The location of the mine offers many challenges for designing the facilities due to the extreme climate of the mine. The temperature fluctuations from summer to winter can be from 40 °C to -40 °C. The goal of the mine was to be able to operate throughout the entire year, utilizing a heap leach pad to extract the gold. In order to accomplish this, the leach solution would have to maintain sufficient heat as it is applied to the facility surface, moves through the ore, and is temporarily held in the pregnant leach solution (PLS) pond. If too much heat is lost, the solution could freeze in the ore creating lenses of ice or rendering the PLS pond inoperable. In order to be conservative in the estimate of heat in the system, this study only considered the thermal conditions of the heap and the solution. Potential geochemical and biological heat sources were not considered.

The design parameters were determined through a series of models of the heap leach facility and the PLS pond. The models utilized were:

- Variably saturated flow modeling of solution application and flow through the heap;
- Thermal modeling of the solution application and transport through the heap; and
- Thermal modeling of the PLS pond.

Model Construction – Heap Leach Facility

VADOSE/W (GEO-SLOPE 2007), a finite-element model was used to simulate the fluid and thermal conditions of the heap leach pad. A combined variably saturated and thermal model was constructed for two cross-sections of the heap leach pad. Two cross-sections were used because of the geometry of the heap, which has areas that will be thinner and could be more susceptible to freezing than the thicker central portions of the heap. Fig. 1 presents the two cross-sections as modeled.

Conceptual model

Based on the design of this heap leach pad, the conceptual model is similar to other heap leach facilities. The water balance of the system consists of precipitation, evaporation, runoff, infiltration, and application of the leach solution. To prevent freezing of the emitter liners and the heap surface, the solution emitters were placed approximately 2.5 m below the top of the ore pile during winter operations to prevent freezing. Fig. 2 shows the conceptual model of the heap leach pad.

Modeling assumptions

As with any complex system, the modeling required some simplifying assumptions to complete the project. For this project, one of the key input parameters of the thermal modeling was the starting ore temperature of the heap. It was assumed that no ore would be placed on the heap during the winter months; however, leaching would continue. For this reason, the starting ore temperature is assumed to be equal to the average air temperature for the end of September/early October (the end of ore placement for the year). It is also assumed that no ice lenses will form within the heap material because the material will not be loaded on the pad during the winter months when snow could be trapped within the heap.

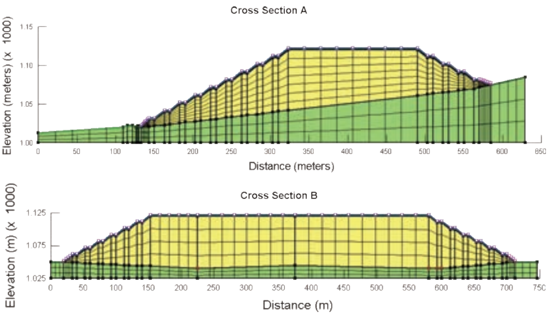

Fig. 1 *Facility cross-sections and model construction.*

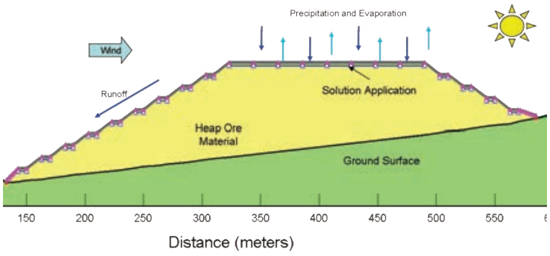

Fig. 2 *Conceptual model schematic.*

The heating of the leach solution is assumed to be 5 °C above the temperature at which it enters the boiler. This corresponds to the heating capacity of the boiler, and provides a target for determining if there is sufficient temperature gain. Two heating scenarios were considered in this modeling effort, a worst case and a typical operating case. As a worst-case scenario, it was assumed that the solution starting temperature would be approximately 0 °C and heated to 5 °C. For a typical operating scenario, it was assumed that the solution was heated from approximately room temperature (20 °C) to 25 °C.

Model input parameters

The following input parameters were incorporated into the VADOSE/W (GEO-SLOPE 2007) modeling:

- Site climate data;
- Solution application rate;
- Current heap leach facility design; and
- Unsaturated flow parameters for the ore material on the heap.

Material properties

The most important input parameters for the modeling are the physical properties of the ore placed on the heap and the ground surface under the heap leach pad facility. These parameters control the flow of water, air, and heat through the heap leach pad. The foundation soils were modeled using a saturated hydraulic conductivity of 10^{-15} m/s. This simulates the plastic liner that will be placed under the heap leach ore pile. The ore material was determined to have a saturated hydraulic conductivity of 10^{-4} m/s. This is equivalent to a uniform sand material which is comparable to the expected grind of the material prior to placement on the heap. The saturated volumetric water content of material will be 35 %. In addition, the thermal conductivity of the ore material was determined to be 9.83 kJ/d/m/°C with a specific heat equal to 1.32×10^3 kJ/m^3.

Boundary conditions

The next most significant input for the model simulations is the application of the boundary conditions. The boundary conditions necessary for this modeling were limited to the application of leach solution and the application of the climate data. The heap leaching operations involves the application of a combination of solutions to the heap surface for controlled infiltration and leaching of the ore. The application rate that will be used is 0.21 m/d. The solution will be applied to the heap using a 60 day leaching cycle (45 days of solution application and 15 days of drain-down). A boundary condition function was developed within the model to simulate this leaching cycle. Because the leach solution emitters will be placed 2.5 m below the surface of the heap, the boundary condition representing the solution application was also applied at that depth below the model surface. The climate boundary condition was applied to the surface of the model.

Climatology

Climate data from the Baruunkharaa meteorological station has a 30 year data set. This station is located approximately 19 km north of the site at an elevation of 810 m. In general, the climate at the mine is characterized by long cold winters and short hot summers. Winter air temperatures can reach -40 °C and summer temperatures can reach 40 °C. The average monthly temperatures range from -24.5 °C in January to 18.3 °C in July.

Model Construction – PLS Pond

A thermal model of the PLS pond was completed to determine how fast the water in the pond would freeze if the pond was stagnant. During operations it is expected that the PLS pond will have active inflow and outflow of solution, helping to keep the water from becoming thermally stagnant. However, the pond may become thermally stagnant if there is a problem with the boilers or the pumping system. Under these conditions, the pond could lose heat rapidly and freeze, severely limiting operations for the remainder of the winter. The thermal modeling of the pond was developed as a heat budget for the system. The heat budget equation used to model the PLS pond is:

$$dH/dt = \Theta_R + \Theta_E + \Theta_L + \Theta_{adv} + \Theta_B \qquad (1)$$

Where,
dH/dt = heat budget;
Θ_R = net radiation;
Θ_E = latent heat of exchange;
Θ_L = sensible heat exchange with atmosphere;
Θ_{adv} = net advective exchange;
Θ_B = conduction through bottom sediments.

By modeling the PLS pond using a heat budget approach, the sources of heat loss and gain, and engineering controls could easily be considered.

Modeling assumptions

For the modeling of the PLS pond, it was assumed that the primary engineering control that would be used to prevent heat loss from the pond would be plastic Bird Balls™. Bird

Balls are small, black hard plastic balls that float on the PLS pond surface, and are the most cost effective solution to year round operations. The Bird Balls™ are assumed to be a complete, single layer on the pond, covering approximately 91 % of the total water surface. The dark color of the balls maximizes the day time heating of the pond and minimizes the heat lost to the atmosphere at night. This can decrease the freezing point of the solution by 10 °C. In addition, the surface evaporation is decreased by 90 % due to the barrier created between the atmosphere and the solution surface. The decreased evaporation is an operational advantage in the winter by minimizing the heat loss, but is also an advantage for this mine during the summer. With potential summer temperatures in excess of 30 °C, the solution will not be subject to the same rate of evaporation as it would be without the cover. For comparison and to justify the added expense of the engineering control, the heat budget model was complete for the water surface of the PLS Pond both with and without the Bird Balls™. (Nelson Environmental, Inc. 2008)

Combined Heap and PLS Pond Thermal Models

The coupled variably saturated and thermal model of the heap leach pad and the heat budget model of the PLS pond were used in combination to optimize the design of the heap leach pad and to define the required operational conditions. The coupled variably saturated and thermal model defined the heat loss that is expected to occur within the heap due to contact with the ore during leaching and provided a starting temperature for the PLS pond. The heat budget model defines the expected heat loss while the solution is exposed to the extreme climatic conditions in the PLS pond.

Modeling results

The results of the coupled variably saturated and thermal modeling showed that the heating of the solution helped to maintain the heat near the emitters, even with near freezing starting ore temperatures and an average winter climate. The model results showed the surface of the heap is frozen during the winter months, but at a depth of 2.5 m there appears to be sufficient heat to prevent the emitters from freezing and becoming inoperable. Under both the typical conditions (heating from 20 °C to 25 °C) and the worst case conditions (heating from 0 °C to 5 °C), the solution lost between 3 °C and 5 °C within the heap material.

The goal of the heat budget model was to determine the amount of time it would take the upper one meter of the PLS pond to freeze if the system became thermally stagnant. Four possible scenarios of the PLS heat budget were modeled:

- Typical conditions with Bird Balls™ on pond surface;
- Typical conditions with open water surface;
- Worst case conditions with Bird Balls™ on pond surface; and
- Worst case conditions with open water surface.

Under the typical conditions heat budget model of the PLS pond, it was assumed that the solution exiting the heap will be at approximately 20 °C (the maximum heat loss resulting within the heap for the typical conditions simulation). Based on the results of the heat budget model, if the PLS pond became thermally stagnant, the upper meter of the pond will begin to freeze in approximately 18 hours. This is based on the pond having a single layer of Bird Balls™ on the surface. If the PLS pond surface is open to the atmosphere, the upper meter of the pond will freeze in approximately 1.5 hours. The model was simulated using 2 °C changes in the surface temperature of the solution. The results of this modeling are presented in Table 1 (PLS pond with Bird Balls™) and Table 2 (PLS pond without Bird Balls™) for the typical conditions scenario.

Ambient Air Temperature Kelvin	Water Surface Temperature Kelvin	Theta R W/m^2	Theta E W/m^2	Theta L W/m^2	$\frac{dH}{dt}$ $cal/m^2 \cdot sec$	Time to Lose 2°C minutes
253.3	293.15	-80	5.1	3965	930	35.8
253.3	291.15	-77	5.1	3766	883	37.8
253.3	289.15	-74	5.1	3567	836	39.9
253.3	287.15	-71	5.1	3368	789	42.2
253.3	285.15	-69	5.1	3169	742	44.9
253.3	283.15	-66	5.1	2970	695	47.9
253.3	281.15	-64	5.1	2771	648	51.4
253.3	279.15	-61	5.1	2572	601	55.4
253.3	277.15	-59	5.1	2373	554	60.1
253.3	275.15	-56	5.1	2174	507	65.7
253.3	273.15	-54	5.1	1975	460	72.4
253.3	271.15	-52	5.1	1776	413	80.6
253.3	269.15	-49	5.1	1577	366	91
253.3	267.15	-47	5.1	1378	319	104.4
253.3	265.15	-45	5.1	1179	272	122.4
253.3	263.15	-43	5.1	980	225	148
					Total time	18.3 hours

***Table 1** Results of typical conditions model for PLS pond with Bird Balls™*

Ambient Air Temperature K	Water Surface Temperature K	Theta *R* W/m^2	Theta *E* W/m^2	Theta *L* W/m^2	$\frac{dH}{dt}$ $cal/m^2 \cdot s$	Time to Lose 2°C minutes
253.3	293.15	-157	51	23790	5661	5.9
253.3	291.15	-146	51	22596	5378	6.2
253.3	289.15	-135	51	21402	5095	6.5
253.3	287.15	-124	51	20208	4812	6.9
253.3	285.15	-114	51	19014	4529	7.4
253.3	283.15	-104	51	17820	4246	7.8
253.3	281.15	-94	51	16626	3963	8.4
253.3	279.15	-84	51	15432	3680	9.1
253.3	277.15	-75	51	14238	3397	9.8
253.3	275.15	-66	51	13044	3114	10.7
253.3	273.15	-57	51	11850	2831	11.8
					Total time	1.5 hours

***Table 2** Results of typical conditions model for PLS pond with open water surface.*

Under the worst case conditions heat budget model of the PLS pond, it was assumed that the solution exiting the heap will be approximately 2 °C. Based on the results of the heat budget model, if the pond became thermally stagnant, the upper meter of the pond will begin to freeze in approximately 11 hours. This is based on the pond having a single layer of Bird Balls™ on the surface. If the PLS pond surface is open to the atmosphere, the upper meter of the pond will freeze in approximately half an hour. Even with these less than ideal conditions, the modeling showed sufficient heat to maintain operations if the pond does not remain stagnant for a long period of time. The results of the worst case conditions modeling are presented in Table 3 (PLS pond with Bird Balls™) and Table 4 (PLS pond without Bird Balls™).

This modeling only considered a single cycle through the system. Cumulative cooling impacts were not considered, but could impact the long term operation of the system. If too much heat is lost throughout the system, and it cannot be recovered through the use of a boiler, the time before the pond begins to freeze will be decreased. This is particularly important for the worst case conditions.

Conclusions

The modeling completed for the design of this heap leach facility suggested that even under the climatic conditions of Northern Mongolia, a heap leach pad can be operated year round if the proper engineering controls are utilized. It is critical that the solution be as warm as possible when applied to the heap, but the heat that is added by the boiler is expected to be

Ambient Air Temperature Kelvin	Water Surface Temperature Kelvin	Theta R W/m^2	Theta E W/m^2	Theta L W/m^2	$\frac{dH}{dt}$ cal/m^2·sec	Time to Lose 2ºC minutes
253.3	275.15	-56	5.1	2174	507	65.7
253.3	273.15	-54	5.1	1975	460	72.4
253.3	271.15	-52	5.1	1776	413	80.6
253.3	269.15	-49	5.1	1577	366	91
253.3	267.15	-47	5.1	1378	319	104.4
253.3	265.15	-45	5.1	1179	272	122.4
253.3	263.15	-43	5.1	980	225	148
					Total time	11.4 hours

Table 3 *Results of worst case conditions model for PLS pond with Bird Balls™.*

Ambient Air Temperature Kelvin	Water Surface Temperature Kelvin	Theta R W/m^2	Theta E W/m^2	Theta L W/m^2	$\frac{dH}{dt}$ cal/m^2·sec	Time to Lose 2ºC minutes
253.3	275.15	-66	51	13044	3114	10.7
253.3	273.15	-57	51	11850	2831	11.8
					Total time	22.5 min

Table 4 *Results of worst case conditions model for PLS pond with open water surface.*

completely lost before the solution exits the heap. If the solution exiting the heap is 20 °C, then the pond will not freeze unless it becomes thermally stagnant for a period of 18 hours with an air temperature of -20 °C. If the solution temperature is approximately 2 °C when it leaves the heap and the air temperature is -20 °C, then the time before freezing is reduced to 11 hours. The pond will be susceptible to freezing should a problem occur with the pumps or the boiler. For this reason, the pumps and a backup system are the most critical components of the leaching system for successful winter operations.

The heap leach pad and associated PLS pond were constructed as suggested by the modeling results and operated for a one year period. The constructed facility included the boiler to add 5 °C of heat to the leaching solutions, emitters buried 2.5 m below the surface to prevent freezing, and a single layer of BirBalls™ placed on the PLS pond surface. This combination of engineer controls proved to be an effective means of achieving year round operations, even under the extreme climate conditions of a northern desert.

References

GEO-SLOPE International Ltd. (2007). Vadose Zone Modeling with VADOSE/W: An Engineering Methodology. Alberta:GEO-SLOPE.

Nelson Environmental, Inc. (2008). Bird Ball™ Cover System. www.nelsonenvironmental.com/TechProd6_BirdBalls. Information verified 14 July 2008.

Mineral recovery from Lake Katwe brines using isothermal evaporation

Hillary KASEDDE[1,2], Matthäus U. BÄBLER[3], John Baptist KIRABIRA[2],
Anders TILLIANDER[1], Stefan JONSSON[1]

[1]KTH Royal Institute of Technology, Brinellvägen 23, SE-100 44 Stockholm, Sweden.
[2]School of Engineering, College of Engineering, Design, Art and Technology, Makerere University, P.O. Box 7062, Kampala, Uganda.
[3]KTH Royal Institute of Technology, Teknikringen 42, SE-100 44 Stockholm, Sweden.

Abstract Lake Katwe is a saline lake within the East African Rift system in Western Uganda, with a rich source of mineral salts. The present work aims at evaluating possibilities of future salt extraction from the lake deposit. An isothermal evaporation experiment was conducted on the lake brines. The precipitated salts were characterized by X-ray diffraction (XRD) and scanning electron microscopy (SEM) methods. Various economic salts such as thenardite, gypsum, mirabilite, burkeite, hanksite, anhydrite, trona, halite, nahcolite, thermonatrite, and soda ash precipitate from the lake brines. The experiments also reveal the sequence of mineral salt precipitation in the order sulfates→chlorides→carbonates.

Keywords Lake Katwe; Brine; Isothermal Evaporation; Sulfate salts; Chloride salts; Carbonate salts; XRD; SEM.

Introduction

Lake Katwe is a closed saline lake on the northern side of fresh water Lake Edward within the western branch of the East African Rift valley system, and about 15 km below the equator in western Uganda. The lake lies at an elevation of about 885 m, with a maximum area of 2.5 km^2, depth of less than 1.5 m, and measuring 9 km in circumference. The natural salt lake brines are highly alkaline and rich in Na^+, K^+, Cl^-, CO_3^{2-}, SO_4^{2-}, and HCO_3^- with lesser amounts of Mg^{2+}, Ca^{2+}, Br^-, and F^-. The surface brines are hydro-chemically of a carbonate type and represent an important source of mineral salts that are of great economic value. The salinity and density of the lake brines varies from 140 to 150 g/L and 1.15 to 1.23 g/mL respectively and depend on seasonal variations (Kasedde *et al.* 2012 submitted). The meteorological conditions in this region are generally semi-arid, with little rainfall, and a great capacity for evaporation. Because of these conditions, traditional solar pond evaporation techniques are currently used to extract salts from the surface brine resources of the lake. These salt extracts are composed of halite mixed with other impurities.

Since the 1960s, studies have been developed to exploit and utilize the lake’s mineral resources. Besides the study of the geological setting of the region and chemistry of the lake brines (Arad and Morton 1969), investigations were extended to studying the feasibility of salt extraction through estimation of the salt reserves (Morton and Old 1968, Dixon and Morton 1970, Morton 1973, UDC 1997), and the mineralogical composition of the evaporites (Nielsen 1999). Further studies involved devising techniques and concepts of improving salt mining and extraction from the lake resources (Kirabira *et al.* 2013) and characterization of the mineral salt raw materials from the salt lake deposit (Kasedde *et al.* 2012 submitted).

In the present investigation, an isothermal evaporation experiment was performed to determine the nature of mineral salts that can be recovered from Lake Katwe brines, and to study the sequence of their precipitation.

The study is essential for evaluating the possibilities for future comprehensive and sustainable utilization of the salt-lake brine resources.

Materials and methods

Apparatus and reagents

An FP12 thermostatic water bath (Julabo Labortechnik, GmbH, Seelback, Germany) was used for the isothermal evaporation experiment. The precision of temperature control was ±1 °C. The density of the liquid phase was measured by a portable densito-meter (DMA 35 Anton Paar, Graz Österreich, Austria) with an accuracy of ±0.001 g/cm^3. The salinity and electrical conductivity were measured by an electrode probe meter (HANNA instruments HI 98360, Woonsocket, RI, USA) with an accuracy of ±0.5 %. The pH value of the liquid phase was determined by a PC Titrator (Mantech). The mineralogy of the precipitated salts at each stage of evaporation was identified by X-ray diffractometry (XRD) using a D2 Phaser benchtop XRD system (Bruker Corporation, Massachusetts, USA) with a copper K_α radiation (λ = 1.5405 Å) operating at a voltage and current power of 30 kV and 10 mA. A diffraction interval between 2θ-10°-80° with step increments of 0.01° and a scan speed of 0.5 seconds were used. The morphology of the salts was examined by a Field Emission Gun Scanning Electron Microscope (FEG-SEM) using a LEO 1530 Gemini (Zeiss, Oberkochen, Germany) with settings at a voltage of 15 kV and aperture 60 µm. The images were taken with a secondary electron detector. A gold sputter coater (Emitech K550) was used to prepare the mineral salt samples before SEM analysis to make them electrically conductive. Double distilled water having a conductivity of 0.0182 S/m at 25 °C was used in the experiment.

Experimental methods

The dry season surface brine was sampled from Nambawu salt pans at Lake Katwe in August 2012 and was stored in plastic bottles at room temperature prior to the present study in October 2012. The brine had not been saturated since no solid precipitates were observed. For the isothermal evaporation experiment, one liter of the natural brine was filled in a glass beaker. The beaker was placed in a thermostatic water bath which was maintained at 30±1 °C. The evaporation conditions were close to those existing at Lake Katwe. The brine was left to evaporate without stirring in a ventilated environment at 30±1 °C with a continuous air flow of 1 m/s. The evolution of the brine evaporation was monitored on a daily basis for newly precipitated solid salts. When a sufficient amount of the solid salts appeared, they were separated from the solution by filtration. The salts were then dried and stored in small plastic sample bags and subsequently characterized with X-ray diffraction and scanning electron microscope techniques. At the same time, a 10 mL brine sample was taken from the liquid phase, diluted with distilled water to a final volume of 50 mL, then measurement of its physical properties were taken. The isothermal evaporation experiment was repeated for each sample until all the brine dried up.

Results and Discussion

The brine sample used in the evaporation experiment was the original brine from Lake Katwe. It’s chemical composition in g/L was 137 Na^+, 39.1 K^+, 0.00143 Mg^{2+}, 0.005 Ca^{2+}, 124 Cl^-, 43 SO_4^{2-}, 3.39 HCO_3^-, 61 CO_3^{2-}, and 0.082 F^-. In the course of the isothermal evaporation experiment, twelve liquid and twelve solid samples were collected. The physico-chemical parameters of the original brine (sample L_0) and the mother liquors (sample Ln, n representing the corresponding evaporation stage) are presented in Table 1.

The evolution of density and conductivity as given in Table 1 is shown graphically in Fig. 1. The original brine (sample L_0) is undersaturated and hence, upon evaporation of water from the original brine, both density and conductivity increase until the first salt precipitate is harvested at sample L_1. Thereafter, density

Sample	Evaporation Time(days)	Electrical Conductivity (mS/cm)	pH	Salinity (g/L)	Density (g/cm³)
L_0	0	140.1	10.2	70.0	1.306
L_1	6	147.3	10.7	73.8	1.315
L_2	12	138.3	10.7	69.2	1.316
L_3	15	133.5	10.7	66.6	1.322
L_4	20	132.3	10.7	66.1	1.326
L_5	25	134.5	10.8	67.4	1.320
L_6	29	130.5	10.9	65.3	1.325
L_7	33	123.6	10.9	62.1	1.336
L_8	36	116.6	10.8	58.4	1.343
L_9	40	99.6	11.1	49.8	1.360
L_{10}	43	95.2	11.1	47.4	1.361
L_{11}	47	93.0	11.2	44.0	1.355
L_{12}	50	-	-	-	-

Table 1 *Physico-chemical parameters of the liquid brine samples.*

and conductivity follow a different trend: while density tends to increase, conductivity gradually decreases. This indicates a change in the ionic composition of the brine as different ionic species contribute differently to density and conductivity. Furthermore, the local maxima of density, respectively the local minima of conductivity, observed for sample L_4 indicates a change in the precipitation sequence, as confirmed by analysis of the precipitates as outlined below.

The inset in Fig. 1 shows the evolution of pH during evaporation. After a sharp increase when moving from the original brine to the first sample, the pH assumes a constant value that lasts until sample L_4 after which a further increase is observed. This second period of increase culminates in a local maximum at sample L_6 and L_7, followed by a local minimum at sample L_8. Thereafter, a third increase is observed leading to plateau at sample L_9 and L_{10}. Likewise to the local extrema in density and conductivity, the different regions in the evolution of pH relate to the precipitation sequence.

The mineralogical composition of the recovered solids were analyzed by XRD and SEM. These measurements indicate the presence of various solid phases in each sample. A typical XRD measurement showing several characteristic peaks is shown in Fig. 2. Analyzing the XRD spectra allowed for identifying the solid

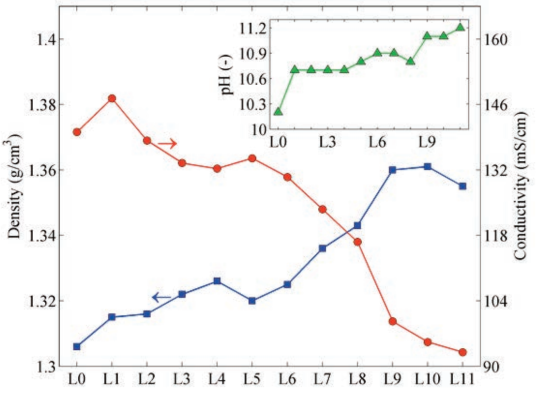

Fig. 1 *Evolution of brine density (square symbols), conductivity (circles), and pH (inset).*

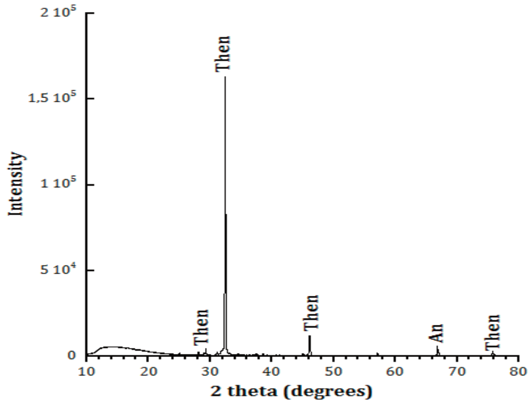

Fig. 2 *X-ray diffraction (XRD) results for salt sample S1 (Then-Thenardite, An-Anhydrite)*

Mineral phase		**Sample**											
		S_1	S_2	S_3	S_4	S_5	S_6	S_7	S_8	S_9	S_{10}	S_{11}	S_{12}
Thenardite (Then)	Na_2SO_4	X	X	X	X	X	X	X	X	X	X	X	X
Mirabilite (Mir)	$Na_2SO_4\cdot10H_2O$		X			X		X		X		X	
Burkeite (Bur)	$2Na_2CO_3\cdot Na_2SO_4$		X	X		X	X	X	X				
Hanksite (Han)	$9Na_2SO_4\cdot2Na_2CO_3\cdot KCl$		X	X		X		X	X	X		X	
Gypsum (Gy)	$CaSO_4\cdot2H_2O$			X		X	X	X		X			
Anhydrite (An)	$CaSO_4$	X			X								
Trona (Tr)	$Na_3(CO_3)(HCO_3)\cdot2H_2O$					X	X		X	X	X	X	X
Nahcolite (Nah)	$NaHCO_3$											X	X
Thermonatrite (Th)	$Na_2CO_3\cdot H_2O$												X
Soda ash (S)	Na_2CO_3											X	
Halite (Ha)	NaCl						X	X	X				

Table 2: *Mineralogical composition of the solid salts*

phases in each sample. Table 2 gives an overview of the identified solid phases.

From the data in Table 2 we can identify several precipitation stages. A first stage lasting from sample S_1 to S_4 is dominated by the precipitation of sulfates only, *i.e.* the XRD of the first four samples indicated the presence of the sodium sulfates thernardite and mirabilite, the carbonate containing sulfates burkeite and hansite, as well as the calcium sulfates gypsum and anhydrite. The corresponding mother liquors (sample L_1 to L_4 in Fig. 1) had a constant pH of 10.7, while the density and conductivity were increasing, respectively decreasing.

SEM micrographs of the salt sample in this first stage are shown in Fig. 3 (S1 to S4). Well faceted crystals with either elongated or platelet like shape together with long tubular crystals are seen in sample S1. Similar shape and sizes are seen in sample S2 which additionally contains some smaller less developed structures. Comparing the XRD measurements of the first two samples, the additional structures seen in the SEM of sample S2 can be related to the presence of hanksite, burkeite, and mirabilite in this sample. Considering sample S3 and S4, it is observed that the crystal sizes decreases while well faceted and elongated crystals together with platelets are also seen in these samples.

In a second precipitation stage, lasting from sample S_6 to S_8, sodium chloride crystallizing as halite precipitates together with sulfate minerals. In the physico-chemical parameters of the brine shown in Fig. 1, this stage is characterized by a strong increase in liquid density combined with a weak decrease in conductivity. The pH during this second stage goes through a local maximum as seen in the inset of Fig. 1. SEM micrographs are shown in Fig. 3 (S6 to S8). Small hexagonal crystals together with needles and some less well developed particles are observed. The typical cube like crystal shape of pure halite was not observed.

A third precipitation stage, lasting from sample S_9 to S_{12}, is characterized by the formation of sodium carbonates precipitating together with sulfates. Several sodium carbonates were identified by XRD, namely trona, nahcolite, thermonatrite, and soda ash. The mother liquors at this precipitation stage assumed fairly high densities, *i.e.* around 1.36 g/cm³ (Table 1), which can be explained by the relatively high solubility of the involved salts. On the other hand, conductivity was low while pH assumed values larger than 11. SEM micrographs of this last precipitation stage are shown in Fig. 3 (S9 to S12). While sample S_9 still shows many small crystals of various shape, sample S_{10} shows few large crystals together with some bulky material, identified as thenardite and trona, respectively. Sample S_{11} shows small prismatic crystals together with

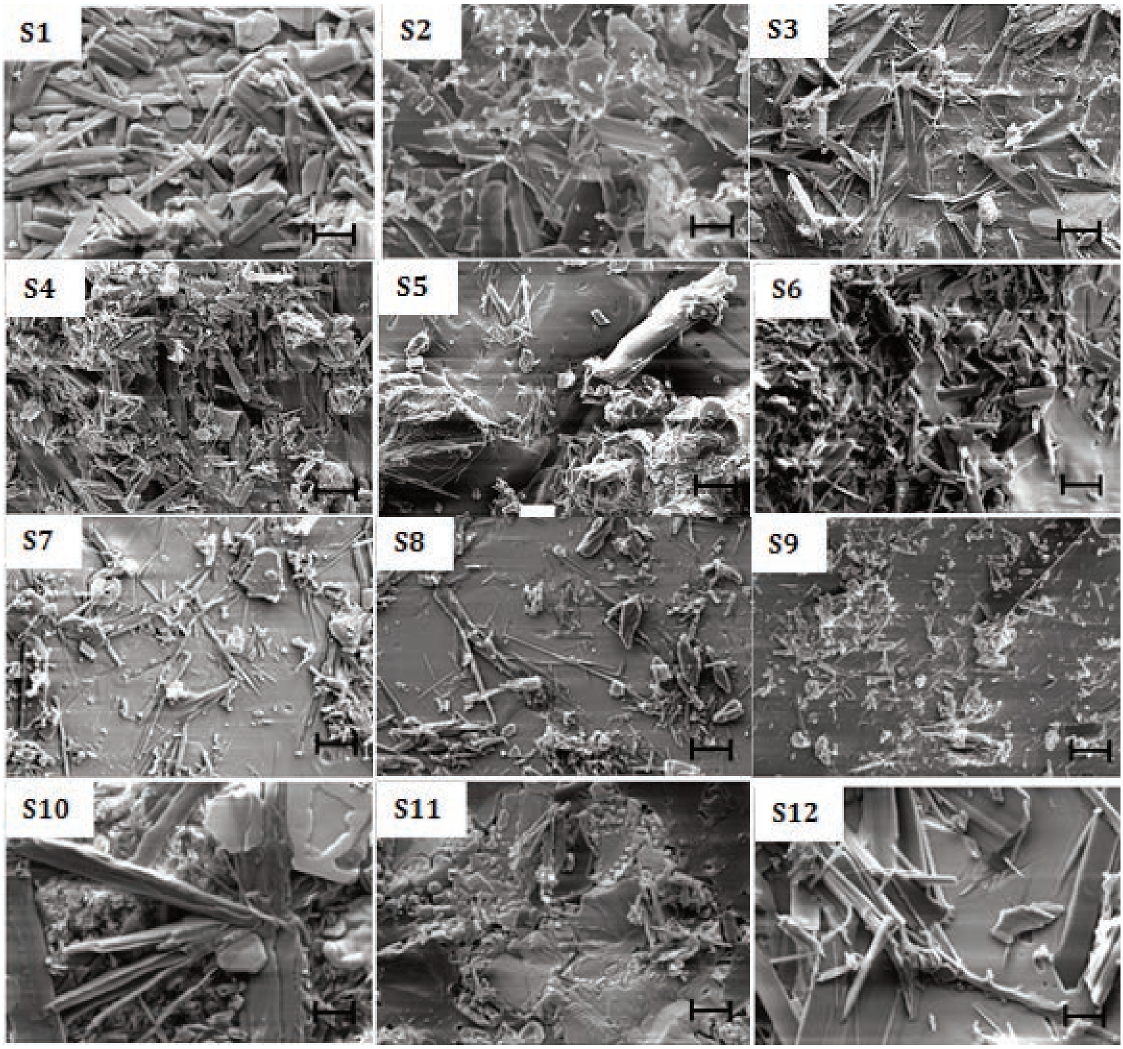

Fig. 3 *SEM micrographs of the recovered salts (S_1-S_{12}) during the isothermal evaporation experiment. Scale bars = 10 µm.*

large indistinguishable crystals which we relate to nahcolite and trona, respectively.

Conclusion

From the isothermal evaporation experiment of Lake Katwe brine, the following conclusions are drawn:

Precipitates show a rich variety of different mineral salts, *i.e.* upon evaporation of lake brines thenardite, anhydrite, mirabilite, burkeite, hanksite, gypsum, trona, halite, nahcolite, soda ash, and thermonatrite are formed. Thenardite precipitates during the entire evaporation process and its crystals were observed to be present in all samples.

The mineral salts precipitating from the lake brines follow the sequence sulfates→chlorides→carbonates. The evaporation pathway of Lake Katwe brines thus differs from that of modern sea water evaporation sequence.

The salts produced at Lake Katwe by traditional and artisanal techniques are composed of several mineral phases with limited production rates. The results from the present study can provide an important reference in the development of technologies for the extraction of various pure mineral salts from the natural brines of Lake Katwe. Understanding the sequence of salt precipitation from the brine helps to control its evolution during concentration and hence will lead to an improved operating design scheme of the current extraction process. However, to fully exploit the lake's brine resource, further work is required in studying its thermodynamics and the related phase equilibria.

Acknowledgements

This study was funded in part by the Swedish International Development Cooperation Agency (Sida) and Makerere University.

References

Arad A, Morton WH (1969) Mineral springs and saline lakes of the Western Rift Valley, Uganda Geochimica et Cosmochimica Acta 33:1169–1181

Dixon CG, Morton WH (1970) Thermal and Mineral Springs in Uganda. U.N Symposium on the Development and Utilization of Geothermal Resources, Pisa 1970. Vol. 2, Part 2

Kasedde H, Kirabira JB, Bäbler MU, Tilliander A, Jonsson S (2012) Characterization of brines and evaporites of Lake Katwe, Uganda. Manuscript submitted to Journal of African Earth Sciences

Kirabira JB, Kasedde H, Semukuuttu D (2013) Towards the improvement of salt extraction at Lake Katwe. International Journal of Scientific and Technology Research 2: 76–81

Morton WH, Old RA (1968) A composition and tonnage survey of the salt reserves of Lake Katwe. Uganda Geological Survey. Unpublished Report No. WHM 6/RAO 7

Morton WH (1973) Investigation of the brines and evaporite deposits of Lake Katwe, western Uganda. Overseas Geology and Mineral Resources, No. 41, Institute of Geological Sciences, 107–118.

Nielsen JM (1999) East African magadi (trona): fluoride concentration and mineralogical composition. Journal of African Earth Sciences 29:423–428.

UDC (1997) Feasibility study of the rehabilitation of Lake Katwe Salt Project. Uganda Development Cooperation, Republic of Uganda.

Glass Bead Filter Packs in Water Wells for Higher Efficiency and Reduced O & M costs

Reinhard Klaus

Sigmund Lindner GmbH,Oberwarmensteinacher Str., 95485 Warmensteinach, Germany,
klaus@sigmund-lindner.com

Abstract The selection of poor quality natural sand and gravel filter pack media for water supply wells leads to insufficient hydraulics, increased well clogging, higher electrical energy demand, reduced life-cycle, and increased Operations & Maintenance costs. Extensive comparative field and laboratory studies since 2008 proved, glass bead filter pack wells can achieve two figure savings for O & M at enhanced well performance and lifetime cycles.

Keywords Alternativefilter pack media, physical, hydrological properties, well performance

Introduction

Until late 2007 gravel and sand were exclusively used as filter pack media in water wells. Gravel and sand are natural minerals, their availability and quality is rapidly declining in the last years. This phenomenon can be detected globally. Apart from that, even material in accordance with industry norms causes a lot of problems in well construction and functionality. For instance the German industry norm DIN 4924 which determines the specifications of mineral sands and gravel for filter packs in water wells accepts 1 % of unclarified particles, 12 % of undersized and 15 % of oversized particles.

The amount of undersized particles is growing during transport of the material to the construction site due to disintegration because of insufficient crushing strength. A summary of negative effects on well construction and performance is given by Hermann and Stiegler 2008. Among others the main problems are:

- Jamming and bridging because of angular and edged grain (Fig. 1)
- High share of undersized particles and fines
- Cost intensive development work with limited effects
- Reduced porosity and permeability of the filter pack
- Clogged filter packs and well screens with gravel debris

Examinations in the Netherlands first proved fines in gravel packs are a major source for well aging by clogging and enhancing microbiological scaling with iron and manganese (Van Beek & Kooper 1980, Van Beek 1995, DeZwart 2007). Further indications on influencing or promoting factors of pack media for well aging or scaling are given by Treskatis & Houben 2003. Precisely they namegrain shape, inner surface (coarseness), size, geometry and

Fig. 1 *Clogged well screen with gravel debris after development pumping*

volume of pore channelsand fines (from formation and filter pack).

With average operation times of more than 40 years, operation and maintenance costs for frequent well rehabilitation to restore capacity loss by scaling are a major financial burden in total lifetime costs of a well. In addition there are added investment costs for the substitution of irreversible damaged wells.

Alternative filter pack media which will avoid these problems were in high demand. First quality characteristics in order to achieve better and more sustainablewell performance were identified by Treskatis *et al.* (2009; Tab. 1).

With regard to these demands, glass beads seemed to be a natural choice for a test.

Alternative filter pack media

In late 2007 soda lime glass beads from Sigmund Lindner were first applied in a 150 m deep well in the FrankonianKeupersandstone near Nuremberg. Wells in that formation have to cope with severe and fast well aging by iron and manganese encrustation. Gravel filter packs in former wells were irreversibly destroyed after some rehab cycles with high impact hydromechanicalcleaning technics. Promisingresults from handling and well performance gave way to a series of comparative R & D projects.

Physical properties

A major R & D project, funded by the German Federal Ministry of Economics and Technology was conducted from 2008 – 2009. The authors, Treskatis *et al.* (2010), performed comparative laboratory tests of several sizes and variations of natural gravel and glass beads for the parameters (Tab. 2). With the result: "Glass beads have mechanical and physical advantages compared to natural filter gravels and can make an important contribution to avoid clogging and to reduce incrustations when used in suitable unconsolidated sediments and bedrock, and thereby to an overall reduction in desanding and regeneration expenses" (Treskatis *et al.* 2010).

Figs. 2 and 3 give a clear indication about the amount of differences in relevant properties between gravel and glass beads.

Characteristic of the material	Quality goals
Washed and free from 'undersized particles'	Low material losses free from 'undersized particles' and compaction when developing the well; reduction of the development time
Well- rounded gravel grains	Increasing the porosity and hydraulic permeability compared with the aquifer; reduction of the lowering and pressure losses; improvement of the development ability and yield
High quartz share	Avoidance of volume changes through swellable or broken minerals
Smooth surface	Minimising deposits
Low irregular form	Low demixing when filling; avoidance of pressure losses through colmation

***Table 1** Quality characteristics for filter pack media (Treskatis et al. 2009)*

roundness	peak-to-valley heights
specific weight	surface relief
bulk density	surface profile
grading	specific surface
breaking load during static stress	abrasion resistivity
breaking properties during static stress	chemical resistance to rehabilitation solvents
breaking properties during dynamic stress	abrasion resistance

***Table 2** Tested parameters*

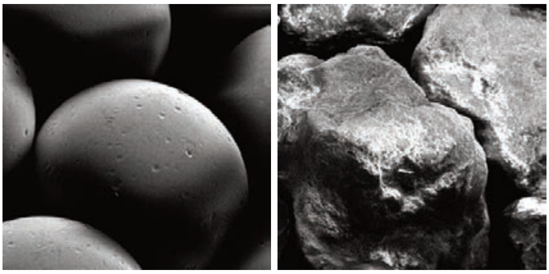

Fig. 2 *REM image of a glass bead compared to a filter gravel grain of the same grain size. The “smooth“ surface of the glass bead prevents the formation of tensile stress whenload is applied and reduces the agglomeration of incrustations (Treskatis et al. 2010).*

Hydraulic and Hydrodynamic properties

Comparative tests in the laboratory of Bau ABC (Federal Academy for Construction Professions) showed also better properties of glass beads for:

- Packing Properties/Compression Set
- Porosity
- Permeability

as well as better capabilities for sand discharge in the well development process at significantly higher efficiency. Glass beads generate a faster and, with regard to soil fines, more efficient sand discharge, while the limit of sand breakthrough, especially in uniform soils is already at a low leakage size. The grain larger than the characteristic grain is already mobilized on glass bead packs. Thus a comparatively rapid desanding is possible. A sand breakthrough occurs only when there is no supporting grain in the layer sequence. (Treskatis *et al.* 2011/2012)

Well aging caused by scaling

First column tests with gravel and glass beads in 2008 showed that in filter gravel, approx.

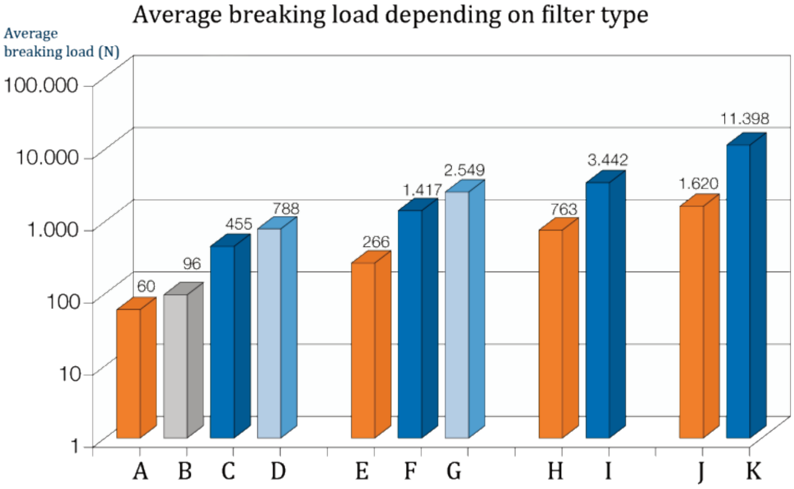

A	Filter gravel no.1 (1.4–2.2 mm)
B	filter gravel no.2 (1–2 mm)
C	glass bead type S (1.25–1.65 mm) part no.: 4505 #923033
D	glass bead type S (1.50±0.2) part no.: 4505-A #820029-1
E	filter gravel no.3 (2.0–3.15 mm);
F	glass bead type S (2.85–3.45 mm) part no.: 4511 #920032
G	glass bead type S (3.00±0.3) part no.: 4511-A #820022)
H	filter gravel no. 4 (5.6–8 mm)
I	glass bead type S (5–6 mm)
J	filter gravel no. 5 (8–12 mm)
K	glass bead type M (12 mm) part no.: 5018-99-24 #855057-20

Fig. 3 *Magnitudes of breaking loads for filter gravel and glass beads at different granulations and bead sizes and mixtures at static load handling (TRESKATIS et al. 2010)*

40 % more iron mass was embedded than in glass beads. Thus a clearly lower incrustation tendency could be expected in actual wells when using glass beads as filter pack media (Treskatis *et al.* 2009). Recent tests by the author *et al.* with actual wells in a test field and an extended laboratory set up with real heavy ferrous and manganiferousgroundwater proved that scaling of glass beads is delayed by factor 2 – 3 compared to natural gravel. The results will be published in late spring 2013. Fig. 4 shows the development of filter resistance over time in gravel and glass bead filled columns as a result of reduced porosity due to scaling processes.

Field results

To date more than 3000 t of glass beads were used in more than 100 water wells in Germany, Italy and the USA, covering the whole hydrogeologic spectrum from unconsolidated to solid rock and various groundwater chemistry, proving the laboratory results described above.

Further observations from contractors, technical consultants and well owners are:

- Easy application, no bridging or jamming during filling process
- Consolidated bedding after filling, no subsidence compared to gravel
- Time and volume for sand removal and clear pumping is down to 10 – 20 % compared to gravel
- Reduced drawdown of water table compared to former well layout
- Higher specific capacity
- Lower tendency of scaling in filter packs in exchange for higher rates inside the well screen.
- Intervals between rehabilitation can be stretched, which means lower expenses for O & M (The first water well equipped with glass beads in the town of Rosstal, near Nuremberg, still has not to be rehabilitated. The predecessor well in the same geologic setting had to be rehabilitated between every two years to once a year).

Meanwhile also 2 dewatering wells for mines in Colorado, one of them over 1.220 m. deep, are equipped with glass beads. Even under these demanding conditions the positive experience with handling or better filling could be proved.

Economic aspects

Based on local conditions, the investment costs for glass beads are between 2 and 5 times higher than for gravel. Regarding total costs of wells the surplus is between 0.5 %and 5 % depending for example on depth, diameter, screened area. But material price alone is no indicator for the efficiency of a well. Wells are long term investments with lifetime cycles far beyond 40 years. Operating costs, primarily for electrical energy and rehabilitation after iron and manganese scaling are the essential factor for efficiency. Due to higher specific capacity and delayed scaling, glass bead wells imply cost saving potential for O & M which will

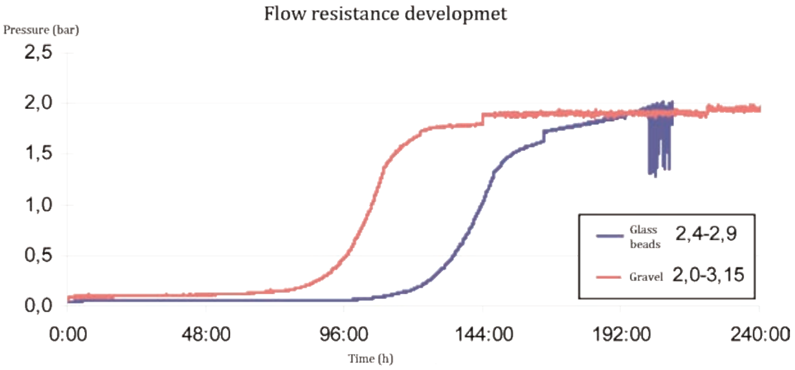

Fig. 4 *Pressure development in gravel packs 2.0 – 3.15 mm grading and glass beads packs grading 2.4 – 2.9 mm under continuous perfusion with iron and manganese containing groundwater*

more than compensate the initial higher investment.

Klaus & Walter 2011 did a first cost benefit analysis based on the then known facts. Even this first tentative approach on the base of 1 % savings for electric energy and 25 % for rehabilitation costs produced a total benefit of 8 % after 40 years considering interest and inflation.

Actual wells showed an increase in performance between 20 % and 300 % with corresponding savings for pumping energy. An updated calculation by Klaus & Walter 2012 brought savings for pumping costs between 50 and 80 % per year, which means a ROI in 3.5/8 years just on the base of cost savings for water pumping. A first extrapolation of the potential savings for rehabilitation based on the results of the recent scaling tests brings total lifetime savings up to more than 20 %.

Conclusions

Glass beads as substitute for mineral gravel in filter packs of water wells are successfully applied since 5 years. The field and laboratory results show, this application is a progress in well construction and shifts the state of the art to a higher level.

For the first time, physical, hydrological and chemical properties of a filter pack can stay consistent for the entire well lifetime cycle. Savings of electrical energy and O & M costs for rehabilitation are a major step towards real sustainability.

Promising results and positive feedback are coming also from the wastewater and water treatment sector.

Acknowledgements

The author thanks all participants who set the train in motion and keep it running with their commitment. In particular Mr. Frank Herrmann, Ochs Bohr GmbH, Nürnberg, for the initial idea and first pilot, Dr. Christoph Treskatis, Peter Walter and Lara Tholen for collegial cooperation and Gary Gin, City of Phoenix, for the first well in the USA, precious field research and valued discussions.

Not least the management at Sigmund Lindner and all coworkers for support. Notably Don Langlois for valuable input and strategic groundwork in the USA and Kathrin Benecke for support beyond regular office times.

References

van Beek, C. G. E. M. &Kooper, W.F. (1980): The clogging of shallow discharge wells in the Netherlands river region. Ground Water 18 (6): 578–586.

van Beek, C. G. E. M. (1995): Brunnenalterung und Brunnenregenerierung in den Niederlanden. gwf Wasser/Abwasser 136 (3): 128–137.

Herrmann, F. & Stiegler, X. (2008): Einsatz von Glaskugeln als Ersatz für Filterkies in Brunnen. bbr 05/2008: 48–53.

DeZwart, B.-R. (2007): Investigation of Clogging Process in Unconsolidated Aquifers near Water Supply Wells. – 200 p., Dissertation TU Delft.

Houben, G. & Treskatis, C. (2003): Regenerierung und Sanierung von Brunnen– 280 p.; München (Oldenbourg).

Klaus, R & Walter, P. (2011): Wirtschaftlichkeit von Glaskugeln im Brunnenbau. bbr 08/2011.

Klaus, R & Walter, P. (2012): Neubau von Brunnen mit Glaskugeln-Ergiebigkeiten/Einsparpotenzial. Energie/Wasser – Praxis (ewp) 04/2012: 30 – 33.

Treskatis, C., Hein., C., Peiffer, S. & Hermann, F. (2009): Brunnenalterung: Sind Glaskugeln eine Alternative zum Filterkies nach DIN 4924? bbr 04/2009: 36–44.

Treskatis, C., Danhof, M., Dressler, M. & Herrmann, F. (2010): Vergleich ausgewählterMaterialcharakteristiken von Glaskugeln und Filterkiesen für denEinsatz in Trinkwasserbrunnen. DVGW energie|wasser-praxis 1/2010: 26 –32.

Treskatis, C., Tholen, L. & Klaus, R. (2011): Hydraulische Merkmale von Filterkies und Glaskugelschüttungen im Brunnenbau – Teil 1. – Energie/Wasser – Praxis (ewp) 12/2011: 58 – 65.

Treskatis, C., Tholen, L. & Klaus, R. (2012): Hydraulische Merkmale von Filterkiesund Glaskugelschüttungen im Brunnenbau – Teil 2. – Energie/Wasser – Praxis (ewp) 01/2012: 40 – 43.

Assessing Water Availability for Life of Mine Operation Using Probabilistic Water Balance Model

Farshad Lotfiazad[1], Alejandro de Bary[2]

MMG Limited, Level 23/28 Freshwater Place, Southbank, Victoria, Australia,
[1]farshad.lotfiazad@mmg.com; [2]alejandro.debary@mmg.com

Abstract A dynamic probabilistic water balance model representing the water management system at Golden Grove mine located in Western Australia was developed and used to assess the availability of water for processing the minerals during the Life of Mine operation. The results showed that some risk existed of not achieving plant concentrate production due to water shortage as throughput increases and metal grades decrease during the simulation period. The model was then used to assess the effectiveness of several water management system upgrade options and estimate their costs.

Keywords water balance, probabilistic model, water shortage, system upgrade, Life of Mine

Introduction

The Golden Grove mine, operated by MMG Limited is a zinc/lead/copper metal mine located approximately 450 km northeast of Perth and 280 km east of Geraldton in Western Australia. Water is used in the process plant to produce concentrate from ore. The existing water management system of the plant (fig.1) consists of several ponds, pumps, pipes, bores, a mine water clarifier, underground mine dewatering, process plant, Cemented Hydraulic Fill (CHF) plant, Tailing Storage Facilities (TSF) and discharge to Lake Wownaminya.

Water inputs to the operation include groundwater inflow to the underground workings, groundwater abstraction from bores and direct rainfall on ponds. Tailings slurry produced during the process is discharged to TSF3 from where water is reclaimed (from decant pond and underdrain collection system) and pumped back to be reused in the process plant (GHD 2009). Water losses in the system include evaporation, water entrainment in the tailings, moisture in concentrate and water used for dust suppression and other mining activities. Excess water inputs are treated and discharged to Lake Wownaminya.

Data on water inflows and outflows of the system has been recorded since 2004. This data showed a trend of declining volume of water discharged to Lake Wownaminya, and raised questions on whether there would be sufficient water for production in future years. A study was commissioned to develop a dynamic water balance model, run the model to assess water availability for production for the existing system and to assess the cost and effectiveness of identified options to upgrade the water management system, estimating the NPV of each upgrade option and to then suggest the best solutions.

Water Balance Model

An integrated site water balance model was developed using GoldSim software (www.goldsim.com) to simulate inflows, outflows and internal transfers of water within the water management system (fig. 1). The simulation period covered 6 years and made use of the ore processing plans at the time (MMG Limited 2011). Dashboards were provided in the model as graphical interfaces to allow the user to enter and change the model input data, define settings and visualize the simulation results graphically.

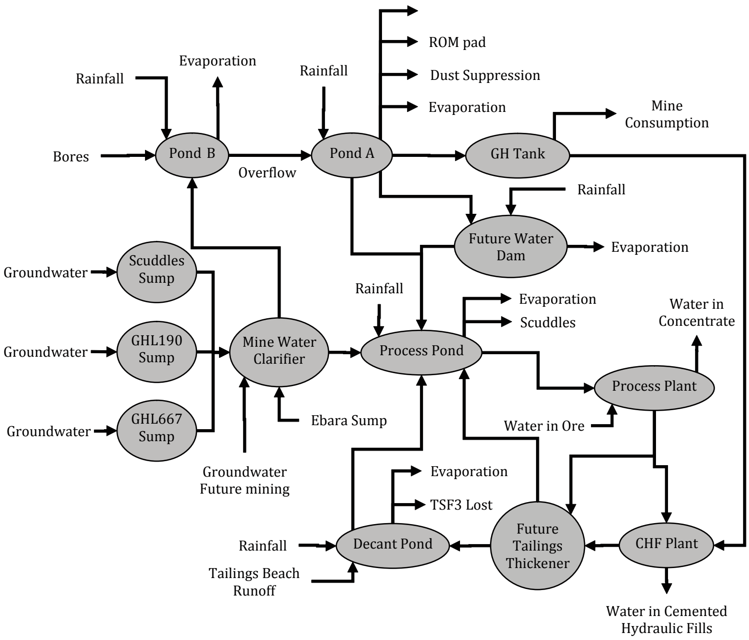

Fig. 1 *Schematic of Golden Grove water management system.*

Some of the key assumptions for setting up the model included:

- Ore processing rates and concentrate production rates were used from Golden Grove 2011 business plan;
- Evaporation pan factor was assumed to be 0.8;
- Solid content in tailings slurry was assumed to be constant 30 % w/w based on operation procedures;
- No seepage considered from ponds;
- No losses assumed in pumps, pipelines and tanks; and
- Starting and stopping of pumps were set based on water levels in sumps and ponds. Whilst in reality this is not an automatic process, it is representative of the operating philosophy.

Several key inflows and outflows of the water management system depend on rainfall and evaporation. Site specific long-term meteorological data used in the model has been obtained from the SILO (www.longpaddock.qld.gov.au/silo) data drill set for the geographical coordinates of 28°45′ S 116°57′ E. The data set covers the period of 1889–2010 for rainfall and evaporation.

Monthly rainfall and evaporation data for Golden Grove site was obtained for the period of 1987-2009 and 1999-2007 respectively from the Annual Aquifer Review report (URS 2010). Monthly average of rainfall and evaporation are calculated for SILO data and the results are compared with the Golden Grove site data (fig. 2 and fig. 3).

Based on the results there is a good agreement between SILO and Golden Grove monthly rainfall. But SILO evaporation is on average 25 % higher than that recorded onsite (but generally with a smaller percentage difference on the months with high evaporation). As rainfall and evaporation data were available for 121 years and the modelling period covered 6 years, the model was run for 117 rainfall and evaporation sequences using Monte Carlo simulation (Ang and Tang 1984). The results were presented based on average and 95 % of the 117 sequences.

The model results for the base case (no change to the existing water management system), showed water shortage leading to lower production especially in years with high evap-

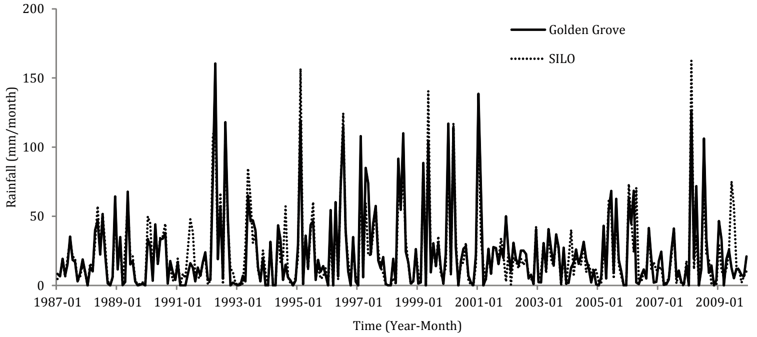

Fig. 2 *Comparison of SILO and Golden Grove rainfalls.*

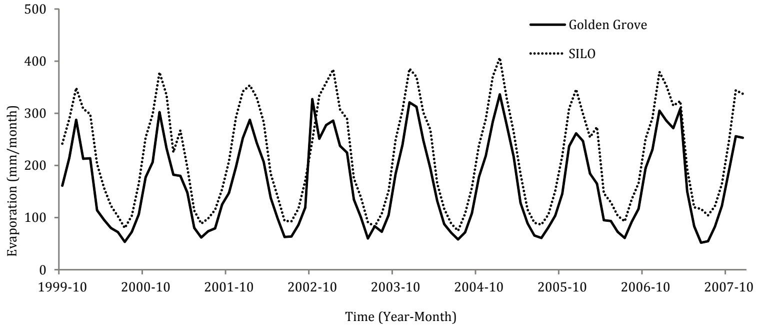

Fig. 3 *Comparison of SILO and Golden Grove evaporations.*

oration rate. Results of modeling are presented for average and 95 percentile of the 117 rainfall/evaporation sequences (fig. 4). As shown in the Fig. the concentrate production shortfall against plan would be higher in years 3 to 5 because of:

- Higher ore processing rate as the open pit becomes active; and
- Lower copper grade in the ore leading to production of greater volume of tailings.

Sensitivity Analysis

Sensitivity analysis was conducted to assess the effects of changes in the groundwater inflows to the system and reduced evaporation as these parameters had the biggest effect on inflows and outflows of the system. The model was run with modified groundwater inflows (-10 %, -20 %, +10 %; fig. 5). The results showed that 20 % decrease in groundwater inflow to the mines would reduce concentrate production by on average 7600 t/a. An increase in groundwater inflow rate however would not have any effect on concentrate production as the pumping capacity from pond A to the process pond constrained the availability of water for production and therefore any extra water would be discharged to Lake Wowaminya rather than being used in the process plant. An expansion of the pumping capacity however would have a beneficial impact on reducing production shortfall against plan.

As Golden Grove evaporation is about 25 % lower than SILO evaporation, the model

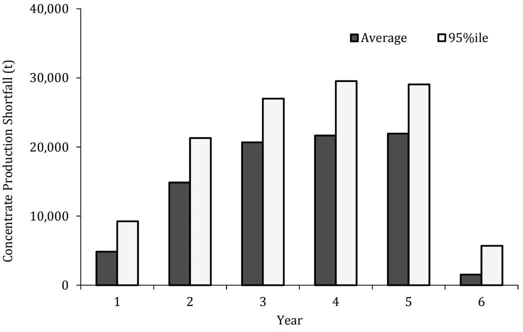

Fig. 4 *Concentrate production shortfall for Life of Mine period predicted by model for the base case.*

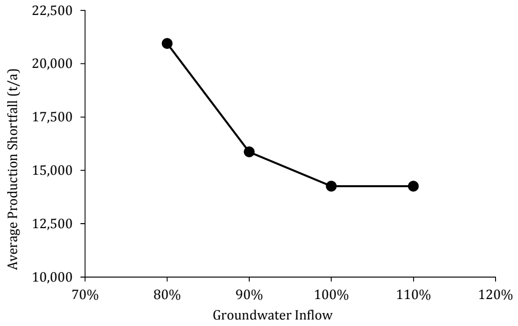

Fig. 5 *Effect of groundwater inflow changes on concentrate production shortfall.*

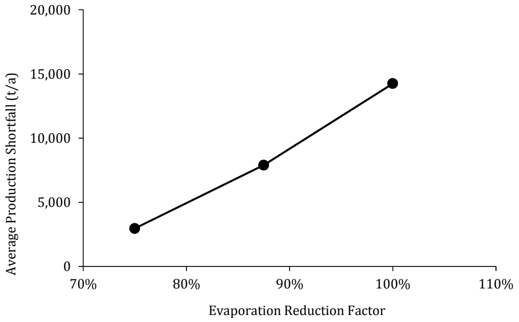

Fig. 6 *Effect of evaporation reduction on concentrate production loss.*

was run for the SILO evaporation reduced by 25 and 12.5 % (fig. 6). The results showed that if actual evaporation was 25 % lower than SILO sourced evaporation data the shortfall would drop from about 14,200 to 3,000 t/a. The sensitivity of production to evaporation highlighted importance of restarting measurement of evaporation on site.

Scenario Analysis

As objectives of this modelling study were finding solutions for potential water deficit in the future, it was decided to run the model for several water management system upgrade scenarios. After discussion with the mine site team 9 scenarios were defined (Table 1). Generally the scenarios are based on the following options:

- Storing the extra water in a water storage dam during the wet seasons rather than discharging the water to Lake Wownaminya and using the stored water later during the dry seasons. As evaporation depends on the area of the storage, three different storage areas and volumes are defined;
- Recycling some water from the tailings by using tailings thickeners before discharging tailings in TSF3. Two different outflow solid contents are defined and used;
- Supplying water from additional bores during the dry seasons;
- Upgrading pumping system from pond A to process pond to be able to transfer additional water supplied from bores; and
- Combination of two or more of above mentioned options.

Scenario	Description
A1	Do Nothing - No changes in the existing water management system
A2	1400 ML storage with 10 ha area
A3	1100 ML storage with 15 ha area
A4	1000 ML storage with 20 ha area
A5	Tailing thickeners with 40% w/w outflow solid content
A6	Tailing thickeners with 50% w/w outflow solid content
A9	Additional bores(4ML/d)
A10	Additional bores(4ML/d), Increasing pond A to process pond capacity to 6480 m^3/d
A12	Additional bores (2ML/d), Increasing Pond A to process pond (6,480 m^3/d), 50 ML Storage with 2.5 ha area

Table 1 *Description of defined scenarios.*

The developed water balance model was used to run all of the 9 scenarios for the 6 year period. For each scenario the model was run for 117 rainfall and evaporation sequences and the results were statistically analysed to predict the potential concentration production shortfall (fig. 7). The results show that if the water management system is not upgraded the annual mean and 95 percentile concentration production lost is estimated to be about 14,000 and 20,000 t. Storing water in the storage dam will not eliminate the production lost. With using the 15 and 20 ha dams which have a reasonable height, the lost production is still high (4,500 and 6,500 t). The 95 percentile lost is significantly higher than the mean lost (roughly about two times).

The results also show that tailings thickeners are very effective in reducing the risk of water shortage. Using tailings thickeners with 40 % w/w outflow solid content there would only be on average a 1,000 t annual production shortfall against plan, using tailings thickeners with 50 % w/w outflow solid contents there would be no production shortfall against plan.

Supplying water from additional bores with total yield of 4 ML/d would also be a very effective solution in reducing the risk of production shortfall against plan. In this case the capacity of the pumping system from Pond A to the process pond would need to be increased from 4320 to 6480 m^3/d. A better option would be to supply 2 ML/d from additional bores and storing the water in a relatively small storage (50 ML capacity).

The lost revenue from the production shortfall estimated based on production shortfall mass calculated in the previous section, the corporate economic assumptions for metal prices and the CAPEX and OPEX estimated for each system upgrade option were used to calculate the net present value for each option using a discount rate of 8 %. For each option the NPV was calculated for every one of the 117 rainfall and evaporation sequences and then the mean and 95 percentile of the results were determined (fig. 8).

Based on the results, the NPV for options which considered the water storage dams were positive but relatively low comparing to the scenarios which considered the use of tailings thickeners or additional bores. The reasons for this were:

- CAPEX of dam construction is very high; and
- These scenarios do not eliminate the production shortfall.

NPV of the scenario A9 is negative because it does not have a significant effect in reducing the production shortfall against plan as the water pumped from additional bores is not

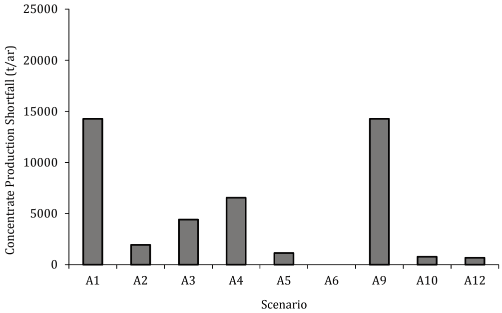

Fig. 7 *Mean concentrate production shortfalls for scenarios.*

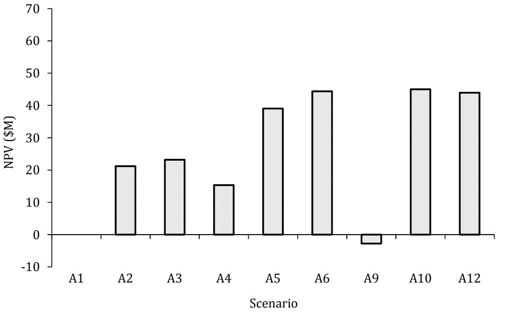

Fig. 8 *NPV for system upgrade options.*

transferred to the process pond because of limited capacity of the pumping system. NPV of options using tailings thickeners or additional bores are very close because both eliminate the water shortage and have relatively low CAPEX.

Conclusions

Assessing the water balance for Golden Grove has shown that a probabilistic dynamic water balance model can be successfully used to simulate the availability of water for the Life of Mine operations. It has also shown that the model has the capability to assess the effectiveness of solution scenarios when the production shortfall risk is present. Modeling can also be used to understand the information gaps and improve the water management and monitoring program.

Acknowledgements

The authors thank Colorado School of Mines for hosting the IMWA 2013 Conference.

References

Ang AH-S, Tang WH (1984) Probability concepts in engineering planning and design, Volume II: Design, risk and reliability, John Wiley & Sons, New York

MMG limited (2011) Golden Grove business plan

GHD (2009) Report for Golden Grove Tailings Storage Facility 3 Detailed Design

URS (2010) Golden Grove 2010 annual aquifer review

Keynote speech

Considerations for Mine Water Management in Operations

John Foriyes Lupo

Newmont Mining Corporation, Geotechnical and Hydrology, 6363 South Fiddler’s Green Circle, Suite 800, 80111, Greenwood Village, CO, United States; john.lupo@newmont.com

Abstract Mine water management plans at operating mines can be challenging to design and implement. The primary challenges to mine water management at stems from the fact that there are often multiple water sources to manage, such as:

- Open pit dewatering and de-pressurization
- Underground mine dewatering
- Process plants
- Tailings storage facilities
- Heap leach facilities
- Overburden storage areas
- Water storage reservoirs
- Run-off from precipitation

Water management of these (and other) sources consists of collection, routing, storage, treatment, and permitted discharge of water. However, the quantity and quality of water generally varies from source-to-source and over time, making the source water difficult to predict and manage. To address this variability (in quality and quantity), a robust mine water management plan should be developed to consider the natural dynamic process at mine operations. This means the plans must consider the inherent variability in mining operations and be able to adapt to the variability while still functioning.

This paper presents considerations for developing mine water management plans for operating mines, with a focus on the variability in sources of mine water and methods than can be used to effectively managing water.

Keywords Mine, Water, Management, Operations

Characterization of potential acid leachate from raw coal, discard coal, and slimes from a Colliery in the Witbank Coalfield, Mpumalanga Province, South Africa

Ntshengedzeni Obed NOVHE[1], Jannie MAREE[2], Jason Samuel OGOLA[3]

[1]*Council for Geoscience, Environmental Geosciences, 208 Pretoria, Silverton, 0001*
onovhe@geosciences.org.za
[2]*Tshwane University of Technology, Department of Environmental Water and Earth Science, Tshwane University of Technology, mareej@tut.ac.za*
[3]*School of Environmental Sciences, University of Venda, Private Bag X5050, Thohoyandou 0950, ogolaj@univen.ac.za*

Abstract Geochemical static and kinetic tests were conducted on raw and discard coal and slimes from a colliery in the Witbank coalfield, to characterize the potential leachate. Raw coal was found to be potential non-acid producers, whereas discard coal had the potential to produce acid. Based on column leaching tests, raw coal and slimes did not produce significant leachate, whereas discard coal produced acidic and sulphate rich leachate, especially at the initial stages of experiment, followed by cyclic buffering. The study recommended that there should be long-term environmentally acceptable strategies to treat discard coal in order to meet the regulatory requirements.

Keywords Witbank coalfield, raw and discard coal, slimes, static and kinetic tests, leachate

Introduction

An integral part of a mining project is the consideration of environmental impacts, particularly, acid mine drainage (AMD). The legacy of mining continues to affect the natural environment, such as surface and groundwater resources, agricultural soil, fauna and flora, long after mining operations have ceased (Arnesen and Iversen 1997). When sulphide-bearing coal with pyrite (FeS_2) is exposed to moisture and oxygen during mining, it results in the formation of AMD. The intensity and duration of AMD are complex functions of geology, mineralogy, hydrology, and the interaction of climatic conditions upon mine waste (White *et al.* 1999). In addition, the rate and degree by which AMD proceeds can be increased by the action of iron oxidizing bacteria, such as *Thiobacillus ferrooxidans* (Singer and Stumm 1970). Development of proper AMD management strategies in mining areas requires fundamental understanding of physiochemical and geological properties, as well as leaching behaviour of geologic formations such as coal beds and surrounding rocks prior to actual mining.

In South Africa, generation of contaminated water from abandoned coal mines remains a major environmental concern. The environmental impacts of AMD have been reported in the Witbank coal mines (Bell *et al.* 2001; Hobbs *et al.* 2008; Mey and van Niekerk 2009; Oberholster *et al.* 2010; McCarthy 2011).

The present work focuses on the characterisation of the potential acid leachate from raw coal, discard coal and slimes in a proposed colliery in the Witbank coalfield, Arnot North coal reserves, by means of geochemical static and kinetic techniques, and mineralogical study.

The coal seams in the Witbank Coalfield were formed in an epicontinental environment and occur within the Vryheid Formation, which forms the mid-part of the Ecca Group (Bell *et al.* 2001). The formation consists primarily of sandstone, siltstone, mudstone and shale, which represent the Ecca Group of the Karoo sequence. The economic coal seams are contained at depths from a few metres to about 300 m in the largely horizontal Ecca Series of the Karoo geological system. Five seams are developed in the Witbank Coalfield (Cairncross *et al.* 1990).

Materials and methods

Three types of representative samples of raw and discard coal, and slimes were studied. Both static and kinetic tests were done on the representative samples based on the procedures set by Sobek *et al.* (1978), APHA (1989), Lepakko (1994), Miller *et al.* (1995). Static tests included; paste pH, Neutralization Potential Analysis, Acid Potential Determination, and kinetic test was by column leaching for a period of 19 weeks. Geochemical composition determination was done using X-ray fluorescence spectrometry, and mineralogical analysis, using X-ray diffraction technique. In addition, sulphur and carbon content of raw and discard coal were determined using LECO induction furnace method.

Results interpretation

Geochemical data

Si_2O and Al_2O_3 were predominant in raw and discard coal, although the latter was also rich in Fe_2O_3 (Table 1). In lesser quantities were TiO_2, K_2O, Na_2O, MgO, MnO, and Cr_2O_3. Discard coal contained significant amounts of As, Cr, Pb, Ni, and Ce which are potential toxic metals, whereas raw coal was enriched in Sr, Ba, Co and Zn (Table 2). Raw coal and slimes contained the highest concentration of carbon (55–62.4 %) and lowest concentration of sulphur (0.3-0.6 %), whereas discard coal had the lowest concentration of carbon (20–29 %) and highest concentration of sulphur (0.6-3.7 %).

Mineralogical Data

Kaolinite ($Al_2Si_2O_5(OH)_4$) was the most abundant mineral in raw coal, whereas quartz (SiO_2) was dominant in discard coal. Discard coal contained also pyrite (FeS_2), siderite ($FeCO_3$), mica [$KAl_2(Si_3Al)O_{10}(OH, F)_2$], calcite ($CaCO_3$) and gypsum ($CaSO_4.2H_2O$). Pyrite which is a major acid producing mineral (Plumlee 1999) was found to be high and this conforms well to the LECO furnace sulphur content of 4.1 %. Kaolinite, mica and siderite are considered as potential acid neutralizers, but to a much lesser extent compared to carbonate minerals such as calcite (Jambor 2003; Blowes *et al.* 2003).

Acid base accounting

The calculated parameters, such as net neutralization potential (NNP as kg/ton $CaCO_3$), and net potential ratio (NPR) have been used as criteria to classify the acid producing potential of the coal. Paste pH for raw coal was about 6.3 and that of slimes was between 3.5–7.5, whereas discard coal had a pH between 2.2–3.8 (Table 3). A low pH may be indicative of sulphides that have reacted to produce acid, whereas a high paste pH could be indicative of a high concentration of alkaline minerals in coal.

A scatter plot for paste pH *vs.* sulphur content shows that paste pH increases with decreasing concentration of sulphur and vice versa (fig. 1). Based on this, the potential for raw coal and slimes to generate significant acid is low, whereas discard coal has high potential to generate acid. A classification of the samples based on the AP and NP ratio is presented in Fig. 2. Raw coal plotted at $NPR<2$, hence it is classified as potential non-acid generating, whereas slimes plotted at $1<NPR<1$, hence it is classified as both potential acid generating and in uncertain range.

Column leaching results

Considerable amount of acid and sulphate was leached from discard coal than in raw coal and slimes. In discard coal, 6,435 to 8,437 mg $CaCO_3$ of acid was leached per kg of discard coal in the first week of the column leaching test, whereas only 1,125 to 1, 500 mg $CaCO_3$ of acid was leached per kg of raw coal (fig.3). Considerable amount of sulphate load was also leached in

Oxides	***Raw coal wt%***	***Discard coal wt%***
SiO_2	10.49	38.14
TiO_2	0.32	0.94
Al_2O_3	5.14	11.9
Fe_2O_3(t)	0.22	6.8
MnO	0.022	0.04
MgO	0.05	0.16
CaO	0.14	0.59
Na_2O	0.07	0.28
K_2O	0.08	0.21
P_2O_5	0.18	0.04
Cr_2O_3	0.01	0.013
L.O.I.	81.88	39.66
TOTAL	98.61	98.78
H_2O^-	5.39	4.49

Table 1 *Chemical composition of raw coal and discard coal samples (wt %).*

Elements	Raw coal	Discard coal
As	<4	12
Ba	563	245
Br	4.7	101
Ce	56	103
Co	18	12
Cr	42	74
Ga	15	24
Ge	3.4	<1
La	29	51
Mo	<2	3.3
Nb	4	16
Nd	23	37
Ni	24	26
Pb	9	23
Rb	5	13
Sc	6.9	13
Se	<1	2.1
Sr	441	64
Th	4.2	16
U	4.4	3.1
V	40	61
Yb	<2	3.7
Zn	3.80	1.20
Zr	85	179

Table 2 *Trace elements in coal (mg/kg).*

the first week of column leaching test from discard samples (1,400–12,750 mg sulphate/kg), than in raw coal and slimes (175–1,700 mg sulphate/kg) (fig.4). Acid generation and sulphate rate in all samples decreases with time. After nineteen weeks of leaching test, 70 mg $CaCO_3$ of acid and 105 mg sulphate were leached per kg of discard coal, whereas 8 mg $CaCO_3$ of acid and74 mg sulphate leached per kg of raw coal.

Conclusions

In this study mineralogy and bulk geochemical analyses that were undertaken showed a clear variation in chemistry of the samples and this conforms to the likely leachate from the samples as determined by static and kinetic geochemical prediction techniques.

Based on wt % S, NPR, NNP, the raw coal from a colliery in the Witbank coalfield has no potential to generate acid as it contained low sulphur. The column test revealed that raw coal leaches neutral pH over a period of 19 weeks.

	Paste pH	wt% S	NP (as kg $CaCO_3$/t)	AP (as kg $CaCO_3$/t)	NNP (as kg $CaCO_3$/t)	NPR	NAG pH
Raw coal 1	6.28	0.3392	24.3	10.6	13.7	2.3	3.5
Raw coal 2	6.24	0.3488	23.3	10.9	12.4	2.1	3.74
Slimes 1	7.5	0.4	21.4	12.5	8.9	1.7	2.82
Slimes 2	3.51	0.5984	5.9	18.7	-12.8	0.3	1.86
Discard coal 1	3.83	0.5728	15.5	17.9	-2.4	0.9	2.31
Discard coal 2	3.05	3.6992	-4.6	115.6	-120.2	0.0	1.66
Discard coal 3	2.18	1.2992	-15.7	40.6	-56.3	-0.4	2.14
Discard coal 4	2.32	1.4496	-26.1	45.3	-71.4	0.0	1.62

Table 3 *Acid base accounting results for the samples.*

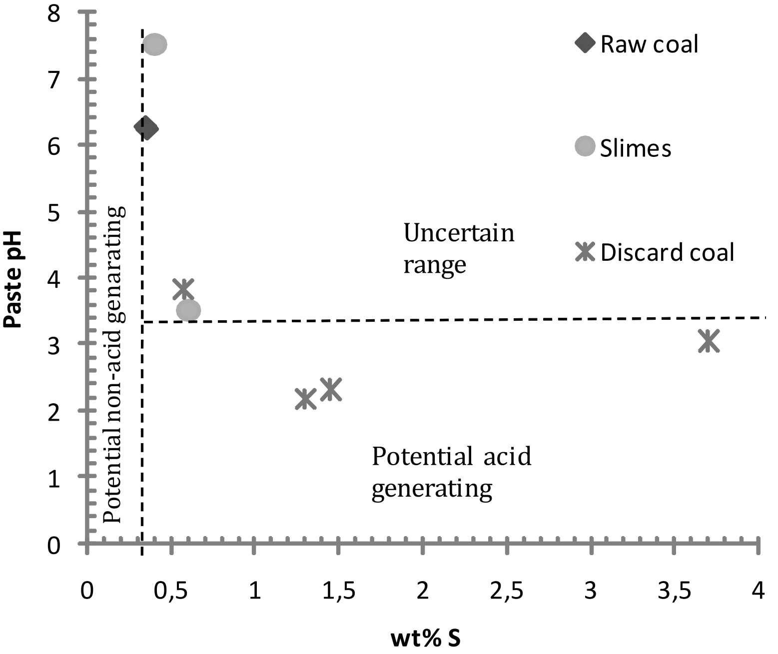

Fig. 1 Paste pH vswt % S indicating areas of potential acid generating, uncertain range and potential non-acid generating.

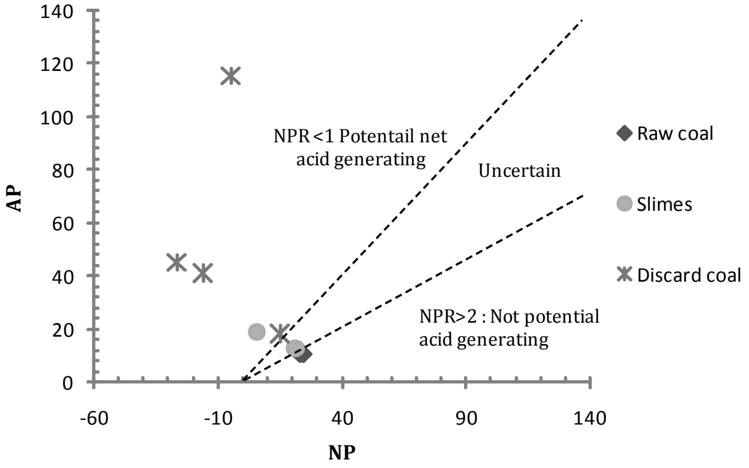

Fig. 2 Acid potential and Neutralisation potential graph indicating areas of potential acid generating, uncertain range and potential non-acid generating.

Discard coal was found to be a potential producer of acid upon leaching. X-ray diffraction analysis indicated that discard coal contained about 5 % of pyrite (acid producing mineral), and about 1 % of calcite (buffer mineral). In addition, kinetic test showed that discard coal produced acidic leachate upon leaching that occurred in two phases: the initial rapid acid leachate phase over a period of 1 to 7 days, followed by cyclic buffering due to dissolution of calcite and less reactive silicate minerals, notably kaolinite, mica and siderite.

Recommendations

The study showed that discard coal will produce significant acid leachate, especially during the initial stages of mining. Therefore, the main challenge of the company is to ensure that long-term, environmentally acceptable approaches are put in place to meet the stringent regulatory requirements and public concerns, and to reduce possible environmental contamination that may result from the discard dumps. Consequently, there is a need to carry out further work on the design of discard dumps to ensure minimal acid water generation.

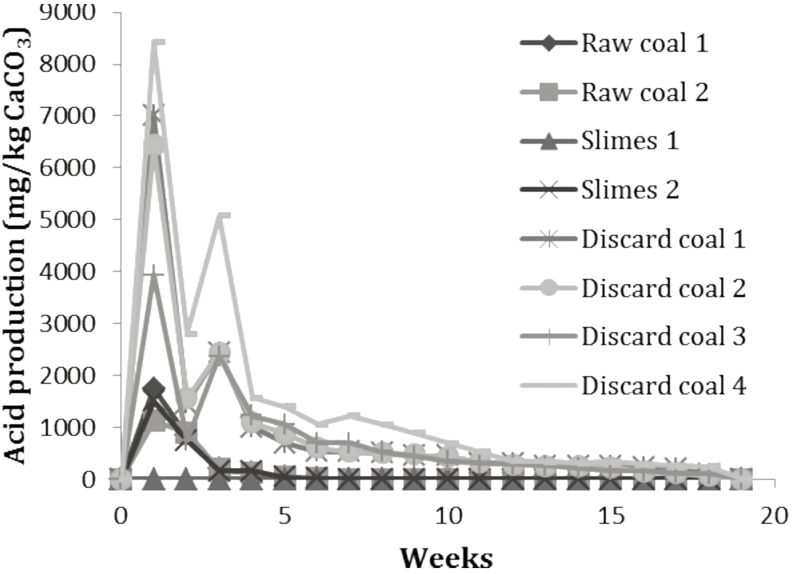

*Fig. **3*** *Rate of acid generation of samples during phase 2 column leaching test.*

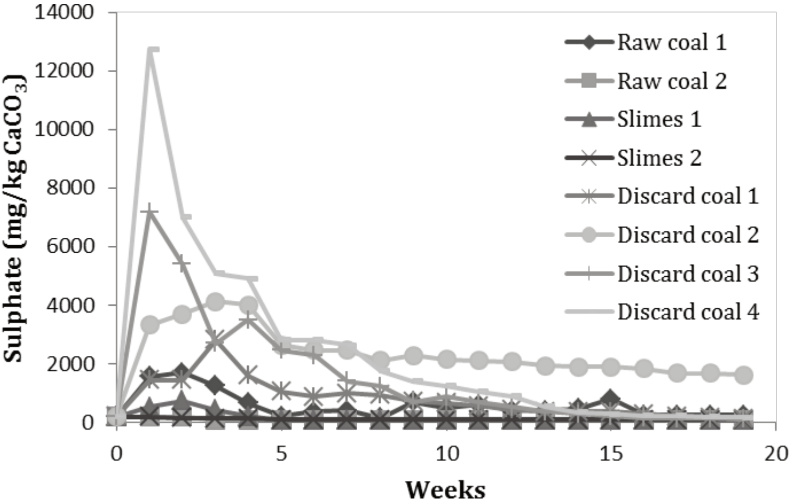

*Fig. **4*** *Rate of sulphate generation of samples during phase 2 column leaching test.*

Acknowledgements

This work was supported by the THRIP funds at the Council for Scientific and Industrial Research (CSIR) of South Africa, hence much appreciation for funding and the opportunity to conduct the work at the CSIR.

References

ALPHA (1989) Standard method for the examination of water and waste. American Public Health Association, 17 edit., Washington DC, p 44–90.

Arnesen RT, Iversen ER (1997) The Lokken Project – flooding a sulphide ore mine. Proceedings of 4th International Conference on Acid Rock Drainage, Vancouver, BC, Volume III: 1093–1107.

Bell FG, Bullock SET, Halbich TFJ, Lindsay P (2001) Environmental impacts associated with an abandoned mine in the Witbank Coal field, South Africa. International Journal of Coal Geology: 11–25.

Blowes DW, Ptacek CJ, Jamvor LJ, Weisener CG (2003) Geological prediction of metal leaching and acid Generation; geological control and baseline assessment. Geology and ore deposits; the Great Basin and Beyond, Proceedings, Vol. II: 8–20.

Cairncross B, Hart RJ, Willis JP (1990) Geochemistry and sedimentology of the coal seams from the Permian Witbank Coalfield, South Africa; a means of identification. International Journal of Coal Geology, 16: 309–325.

Hobbs P, Oelofse S, Rascher J (2008) Management of environmental impacts from coal mining in the Upper Olifants River Catchment as a function of age and scale. Water Resources Development, 24(3): p 417–431.

Jambor JL (2003) Mine-Waste Mineralogy and Mineralogical Perspectives of Acid-Base Accounting. In: JL, Jambor, DW Blowes and AIM Ritchie (Eds.), Environmental Aspects of Mine Wastes, Short Course Series Vol. 31, Mineralogical Association of Canada, 117–146.

Lepakko K (1994) Evaluation of neutralization potential determinations for metal mine waste and a

proposed alternative. In Intenational Land Reclamation and Mine Drainage Conference and Third International Conference on the Abatement of Acidic Drainage, PA, USA, US Bureau of Mines Special Publication, SP 06A-94, Vol. 1: 129–137.

McCarthy TS (2011) The impact of acid mine drainage in South Africa.South African Journal of Science, 107(5/6):1 – 7.

MeyWS, van Niekerk AM (2009) Evolution of mine water management in the Highveld coalfields.International Mine Water Conference, 19 – 23 October 2009, Pretoria, South Africa

Miller SD, Jeffery JJ, Murray GSC (1995) Identification and management of acid generating mine wastes; procedures and practices in Southeast Asia and the Pacific Regions. In Gadsby JW, Malick JA, Day SJ (eds.) Acid mine drainage designing for closure, Vancouver, BiTech Publishers Ltd., p 1–11.

Oberholster PJ, Myburgh JG, Ashton PJ, Botha AM (2010). Responses of phytoplankton upon exposure to a mixture of acid mine drainage and high levels of nutrient pollution in Lake Loskop, South Africa, Ecotoxicology and Environmental Safety, 73:326–335

Plumlee (1999)The Environmental Geology of Mineral Deposits. In: G.S. Plumlee and M.J. Logsdon (Eds.), The Environmental Geochemistry of Mineral Deposits, Part A: Processes, Techniques and Health Issues, Reviews in Economic Geology Vol. 6A, Society of Economic Geologists, Inc., 71–116.

Singer PC, Stumm W (1970). Acid Mine Drainage: the rate determining step Science: 167.1121-1123.

Sobek AA, Schuller WA, Freeman JR, Smith RM (1978) Field and laboratory methods applicable to overburdens and mine soil, WVU, EPA report No. 600/02-78-054: 47–50.

White WW, Lapakko KA, Cox RL (1999) Static test methods most commonly used to predict acid mine drainage: practical guidelines for use and interpretation. Society of Economic Geology., vol.7: 325–338.

The hydrogeological exploration and test technology to precisely determine the location of groundwater recharge channel in mining area

Guoying Pan[1], Yun Lin[2], Yazun Wu[3]

Institute of Resources & Environment, Henan Polytechnic University, Jiaozuo, 454003, China,
[1]pan-gy@hpu.edu.cn, [2]ylzz5211@sina.com, [3]wuyazun@163.com

Abstract Siwan mine is threatened seriously by water disasters. The Ordovician carbonate (O_2) water lateral recharges the second thin-bedded limestone aquifer (L_2) through F_8 fault. It is difficult to determine the cross section only by single method. The cross section on the fault was confirmed within fifty meters by a multiple method. It contains hydrogeological condition analysis, dewatering and tracing test, transient electromagnetic method and hydrology drilling. This result provides a target for the curtain grouting. Because of the accurate assessment, the water plugging effect is remarkable. The water discharge rate per unit drawdown dropped from 12.0 – 7.0 m^3/h/m, and the water yield reduced 600 m^3/h.

Keywords curtain grouting, dewatering test, tracing experiment, hydrology drilling, recharge channels.

Introduction

The North China coal basins, in which approximately 70 % of all the identified coal resources in China are deposited (Gao and Liu 1985), and the coal deposits were mainly formed in the Carboniferous to Permian periods (Han and Yang 1984). In the basin, there exist 11 thin-bedded limestone aquifers in the Taiyuan Group, those aquifers are sequentially named L_1 through L_{11} from the bottom to the top (Wu and Jin 1995), and an extremely thick Middle Ordovician carbonate aquifer (O_2 aquifer). Those aquifers are the main water filling aquifer of the coal basin. In particular, the O_2 aquifer stores abundant water and accepts a considerable recharge of precipitation. It developed lots of fracture and karst features, and wide distribution of outcrop areas. Thus, it serious threats the coal mining operations. Once the water which comes from O_2 aquifer discharge to the mine, it will lead to large scale water bursting hazards or inundation.

Hebi coalfield is located in alluvial plain of the Taihang Mountain in Henan province. The hydrogeological condition is very complex in this area. The eighth thin-bedded limestone aquifer (L_8), the second thin-bedded limestone aquifer (L_2) and the O_2 aquifer are main water-filling aquifers.

In the northeast of the Hebi coalfield there is the Siwan mine, in which the main coal mining seam is the bottom coal of the Taiyuan group. The coal seam, which roof is L_2 aquifer and floor is O_2 aquifer. In the mine, F_8 fault is one of a fault with water permeability. It is the channel that the O_2 water lateral recharges L_2 water in Siwan mine. The existence of this fault increases the risk of water inrush. Thus, the key point to control the recharge process is pouring grout curtain at this fault. At present, pouring the grout curtain alone the whole fault (2.3 km long) is impossible, that the important point to solve this problem is confirming the discharge cross section. The cross section was confirmed within fifty meters by many methods through hydrogeological condition analysis and experiment. This result provides a curtain grouting target for the following project. Because of the accurate assessment, the water plugging effect is remarkable.

The Hydrogeological Background

In Hebi coalfield, the L_2 aquifer with an average thickness of 7 m has a stably distributed, but the karst fissure is poor-developed and inhomogeneous, and the water abundance is greatly different in spatial. According to the pumping test data, the specific yield is 0.012-2.619 L/s/m, the hydraulic conductivity is 0.392-28.84 m/d. Because of the L_2 aquifer has limited outcrop area and no recharge source. The karst water is mainly static reserves and easy to drainage. However, O_2 water and L_2 water has hydraulic connection in some area by the faults. For example, F_8 fault caused the relationship between L_2 aquifer and O_2 aquifer, and the Ordovician carbonate water from east lateral recharge west L_2 water. The specific yield is 3.2 L/s/m, the water yield of Siwan mine is 1200-1400 m^3/h.

The O_2 aquifer, which thickness is 400 m and the karst fissure is well-developed. According to the single drilling pumping test data, the minimum value of specific yield is 0.67 L/s/m and the maximum value is 83.91 L/s/m, the average value is 14.02 L/s/m. The O_2 aquifer is widely outcropped in the Taihang Mountain area, and it accepts the recharge of precipitation infiltration. In addition, the river leakage recharges the groundwater through the karst fissure. After accepts the recharge in mountain area, the water flows to the piedmont from west to east, and discharges by karst spring and mine drainage.

The fault strike of F_9 fault (a normal fault) is NE22°, the dip is NW 63°, and it is the west boundary of the Siwan mine. According to the drilling data, the fault is a resistant water fault. The F_8 fault is the east boundary of the Siwan mine, and the strike is nearly north-south, the dip is W 63°-70°. The fault causes the L_2 aquifer joints with the O_2 aquifer. The O_2 water lateral recharges the L_2 water through the F_8 fault. It is the important recharge resource of L_2 limestone water (fig. 1).

Hydrogeological exploration and test

The channel that O_2 water recharged the L_2 on F_8 fault was confirmed within 50 m by a multiple method. It contains hydrogeological condition analysis, dewatering test, tracing test, transient electromagnetic method and hydrology drilling. This result provides a target for the curtain grouting. The whole exploration could be divided into three stages (fig. 2). The first was preliminary exploration stage, which from June 2006 to September 2007. Based on the data analysis, the water conductivity and the position of water channel of F_8 fault were confirmed by the hydrogeological exploration and testing. The second stage was curtain

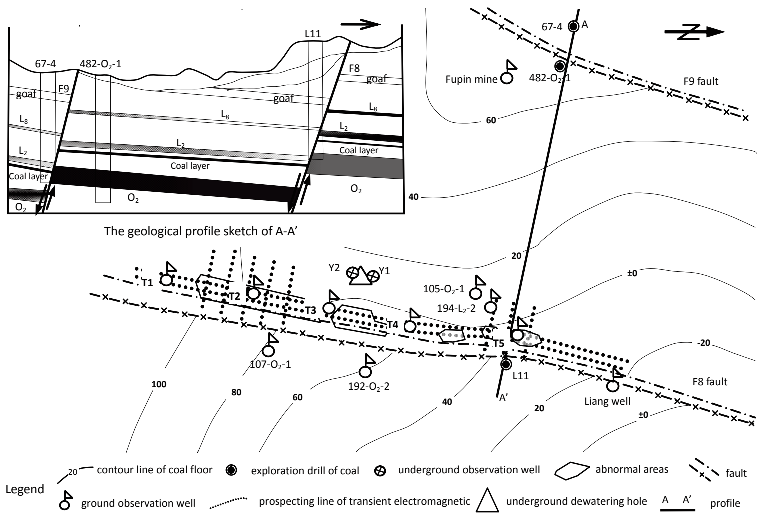

***Fig. 1** The layout sketch of hydrogeological exploration and experiment on F_8 fault.*

grouting, which from February 2008 to June 2008. The recharge channel on F_8 fault was plugged by the water plugging materials through ground drillings. The third stage was to verify the plugging effect, which from June 2008 to October 2008. It could be texted the effect of curtain grouting project for water plugging through comparing the dewatering test results before and after the grouting closure.

Dewatering test and tracing experiment

The dewatering tests were carried out 5 times. The first two tests were mainly to confirm the F_8 fault's transmissivity and position of the water channel, the purpose of the last three tests were to examine the effects of grouting for water plugging. In Siwan mine, There are twenty-one underground drillings, in which, two of them with manometer to observe water level (water pressure), the rest drillings to dewater the L_2 karst water when they turn on. Moreover, there have nine drillings on and under the ground to observe the dynamic of water level of the L_2 karst water and O_2 water. The unsteady flow dewatering test with three steps was carried on in June 2006. At the same time, two different tracer materials (potassium iodide and sodium fluoride) were input into two O_2 karst water observation drillings on the ground (192-O_2-2 and 105-O_2-1) at half an hour before the dewatering test (fig. 1). The tracers were pressed into the O_2 karst aquifer by continually injecting water in drillings. During the test, groundwater was sampled every two hours in dewatering well. The test was begun on 10:00 a.m., June 15 (tab. 1). Firstly, four dewatered holes were turn on. Steady water yield was 369.9 m^3/h. This stage lasted 72 hours. Secondly, five holes were increased on 10:00 a.m., June 20. Steady water yield was 674.4 m^3/h. This stage lasted 72 hours. Another three holes were turn on at 10:00 a.m., June 23. Steady water yield was 852.0 m^3/h. This stage lasted 72 hours. At last, all dewatered holes were closed on 10:00 a.m., June 25. The observation of water level was last 48 hours (Pan *et al.* 2007).

Bases on the experimental results, the water level in O_2 water observation drilling on the east side of F_8 fault (O_2-192-2) and the L2 water in Siwan mine (such as 194-L2-2) has the same decreasing trend. The maximum drawdown in dewatering hole is 73 m. Meanwhile, the water level descends 3.14 m in O_2 water drilling (O_2-192-2). In addition, the tracer KI was captured 58 hours later in 192-O_2-2 observation drilling. That means the O_2 water recharges L_2 karst water through the F_8 fault. The recharge channel of F_8 fault is estimated roughly which exists in a triangle-shaped area delimits by 192-O_2-2 hole, 107-O_2-1hole and dewatering area.

Hydrogeological drilling

At downthrown side of F_8 fault, along strike, the five hydrological exploration holes which

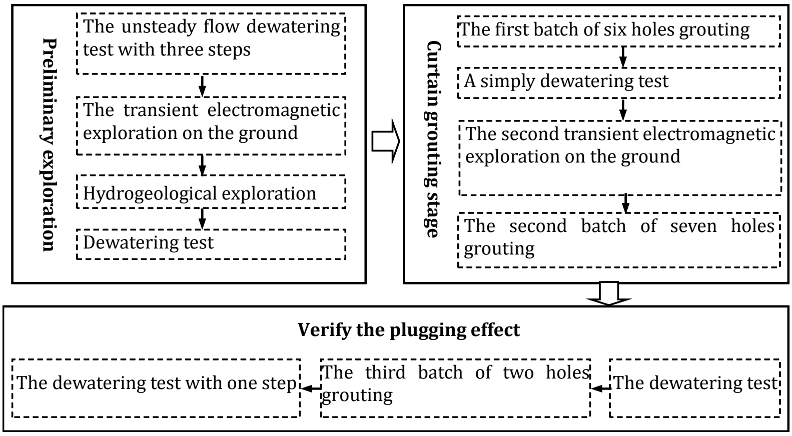

***Fig. 2** The flow chart of the curtain grouting for F_8 fault in siwan mine*

Dewatering Test stage	Water yield (m³/h)	The drawdown of L_2(m)				The drawdown of O_2(m)		
		Y1	Y2	194-L_2-2	Fupin mine	105-O_2-1	192-O_2-2	107-O_2-1
Ⅰ	366.9	17	21	15.48	11.73	0.09	1.10	0.38
Ⅱ	674.4	56	53	35.49	26.61	0.20	2.56	0.64
Ⅲ	852.0	73	67	44.34	33.08	0.34	3.14	0.72

Table 1 *Development of IMWA membership between January 2008 and December 2012.*

interval was 200 m were arranged (fig. 1). The finished stratum of the drill-hole was L_2 aquifer. Drilling results confirmed that the secondary fault and karst system well-developed between T_2 and T_4. The coal layer in T_3-hole is missing; stratigraphic sequence is confusing with broken rock. Solution fissure and small karst caves are developed which proves the existence of karst collapse column at this area. It is the runoff channel of karst water.

Transient electromagnetic method

The transient electromagnetic method was carried out two times. Based on the results of dewatering tests, two parallel transient electromagnetic survey lines along F_8 fault were arranged. The distance between the two lines was 20 m, the dot spacing was 5 m, the length of the survey lines was 1230 m, and the coordinate points were 494. Additional eight survey lines were arranged perpendicular to F_8 fault in the abnormal area of water-bearing. The dot spacing of these lines was 5 m, the length was 150 m, and the coordinate points were 248. The results of transient electromagnetic method shows that there are two recharge channels on F_8 fault, the one locate between T_1-hole and T_2-hole, the anther is between T_3-hole and T_4-hole.

Curtain grouting

Along the downthrown side of F_8 fault to form a continuous water-blocking curtain that can cut off the recharge channel (O_2 water recharges to L_2 water). There were 15 grouting holes which distribute between T_2 and T_4 hole to drill and grout by stages. The first batch of grouting holes focused on the recharge channel between T_2 and T_3 holes. There were 6 grouting holes (from Z_1 to Z_5 and an observation hole T_2) in this batch. In total, 1260 t of cement, 53.8 t of sodium silicate and 4.75 t of industrial salt were injected. Then the simply dewatering test was carried out. The result shows that the efficiency of grout is unobvious. The second batch of grouting holes focused on the water channel between T_3 and T_4 holes. At the same time, the grouting holes were increased between T_2 and T_3 holes. In this batch there were 7 grouting holes (Z_6-Z_9, Z_{11}, Z_{13} and an observation hole T_4), and in total, 991 t of cement, 41.1 tons of sodium silicate, and 5.15 t of industrial salt were injected. After this work, the water level of O_2 aquifer increased 0.5-0.8 m at 192-O_2-2 hole which located upthrown side of F_8 fault, and L_2 water level dropped 3-5m of the downthrown side. Then the dewatering test showed that water discharge rate per unit drawdown dropped from 12.0 – 7.9 m³/h/m. It proves that Z_{11} hole played an important role in water shut off. According to the results, Z10 and Z12 were arranged on both sides of the Z_{11}. In this stage, total 648 tons of cement, 32.2 t of sodium silicate and 3.2 t of industrial salt were injected.

Then the grout curtain project of water channel on F_8 fault was completed. This project had 13 grouting hole, and the amount of drilling works was 2912.03 m. 13 grouting hole and 2 observation holes were grouting, and the cumulative injected cement was 2,899 t, sodium silicate was 127.1 t, industrial salt was 13.1 t.

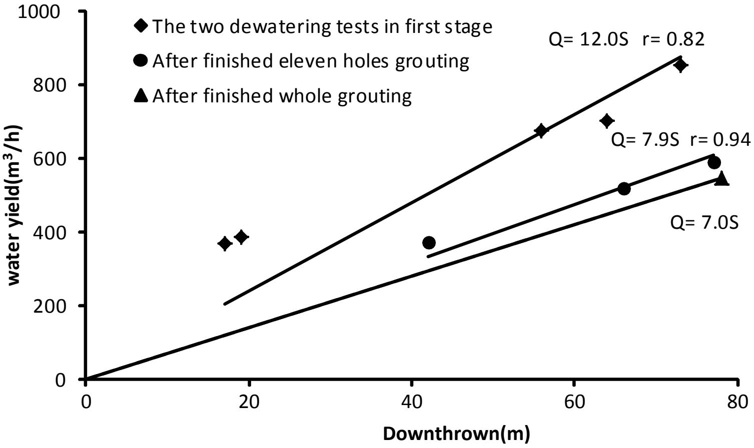

Fig. 3 *The relations of water level drawdown and water yield for previous dewatering tests.*

Examine the effect of grouting for water plugging

In order to examine the efficiency of curtain grouting, the dewatering tests were completed after each batch of grouting respectively. The results showed that, the water discharge rate per unit drawdown dropped from 12.0 – 7.0 $m^3/h/m$, decreasing amplitude was 42 % (fig.3). After grouting, the Siwan mine water yield dropped from 1400 m^3/h to 800m^3/h. Siwan mine was almost shut down due to the serious threat of O_2 aquifer before grouting. It began to resume production and the annual production of raw coal was 350 kt after grouting. Grouting project total investment was 600,000,000 yuan. The water yield reduced 600 m^3/h. The drainage cost was saved 1,000,000,000 yuan. It could reduce the waste of water resources.

Conclusion

The dewatering and tracing test confirmed that the F_8 fault was a water-conductive fault. Groundwater of O_2 aquifer recharged the L_2 aquifer through this fault.

The hydrogeological drilling and transient electromagnetic exploration determined the recharge channel on F_8 fault. It provided a target for curtain grouting.

Through a three stage curtain grouting, the water discharge rate per unit drawdown dropped from 12.0 — 7.0 $m^3/h/m$, and the water yield reduced 600 m^3/h. It provided the condition for Siwan mine safety mining.

Acknowledgements

The data were from the reports that the author presided. This study was funded by the Doctor Foundation of Henan Polytechnic University (No. B2012-034). We also thank Baoxiang Yue, Zhaoxia Liu, the Siwan Bay mine workers and Henan Polytechnic University students.

References

Gao H, Lin Z (1985) Regional characteristics of mine hydrogeological conditions of coal deposits in China. Hydrogeol Engg Geol 12(2):14–17

Han D, Yang Q (1984) China Coal Geology, 2nd edn. Publishing House of Coal Industry, Beijing

Pan GY, Xun JS, Yue BX, etc. (2007) The large dewatering test and tracing experiment based on GSM water level remote sensing system. J Henan Polytechnic University 26(2): 153–155

Wu Q, Jin Y (1995) Deciding system of preventing and curing mine water in Northern China Coalfield. Publishing House of Coal Industry, Beijing

Dewatering strategy for a copper mine in the Democratic Republic of Congo

Gideon Steyl[1], Gerrit van Tonder[2], Lordrif Chironga[3]

[1]Department of Chemistry, University of the Free State, Bloemfontein, South Africa, 9300; Golder Associates, Brisbane, Australia, 4064, gsteyl@golder.com.au
[2]Institute for Groundwater Studies, University of the Free State, Bloemfontein, South Africa, 9300, vTonderG@ufs.ac.za
[3] Institute for Groundwater Studies, University of the Free State, Bloemfontein, South Africa, 9300, lordchironga@gmail.com

Abstract Mining at the site is carried out in three pits and is located along a faulted overturned syncline composed of siltstones, argillites, sandstones and shales and covered by laterite. The operational problem at the mine site is the control of inflows of groundwater into the pits. This has resulted in failure of pit walls and flooding of mine operations during the wet season. Reducing these impacts requires a dewatering strategy which is cost effective. A detailed conceptual hydrogeological model was used to develop a site specific dewatering strategy to reduce pore pressures in the pit walls.

Keywords Conceptual model, dewatering strategies, permeability, faulting, management

Introduction

High-grade copper-cobalt mineralisation of the Central African Copperbelt and the scale of available ore bodies in the Democratic Republic of Congo (DRC) and Zambia are fast becoming the global 'hotspots' for international mining investment and exploitation activities (Lydall and Auchterlonie 2011). The mine, located in the Katanga Province, has a concession area of 15.7 km². Mining began in 2006 and is taking place in three pits from where copper ore is ferried to the mine plant while cobalt ore is stockpiled for processing in Zambia. The three pits are expected to reach terminal depth of 180 meters below ground level (mbgl) by year 2024.

Since the start of open pit operations in 2006, the single major problem at site has been the control of large inflows of groundwater into the pits. The rise of groundwater level at the mine site not only causes increases in water influx into the pit but also results in pit wall failures (fig. 1). The pit wall failure is due to increased pore water pressure behind the face of the wall and eventually results in the collapse of some pit walls.

The copper deposit occurs within the north east dipping layers of siliceous dolomitic schist in the local overturned syncline. Laterite deposits which cap the underlying formations at the site form a variable weathered residual overburden (regolith) layer which varies in thickness. The thickness of the regolith has an important effect on the occurrence of ground-

Fig. 1 *Rotational slide failure of Pit 2 walls at the mine site. Photo taken during dry season.*

water in both the fractured zones and above basement formations (Acworth 1987). Groundwater occurrence in the region can be correlated to the regional stress pattern that created faulting and folding (Acworth 1987).

The central African region had repeated episodes of compressive tectonism, involving at least four periods of wrench faulting separated by relaxation and dyke emplacement (Acworth 1987). Most lineaments in the region are faults or tectonically related joints forming as planes of tectonic shearing and hence could be considered as compressive features at the time of inception. The primary stress orientation in the region is along a NW-SE direction.

Groundwater flow in such deformed zones occurs both by matrix seepage and as fissure flow in discrete fracture channels, which could be part of an interconnected system. Open fractures below the water table surface have the capacity to store and channel water. Fractures that are under tensile and shear stresses are good targets for groundwater (Kellgren and Sander 2000).

The main focus of this paper is to evaluate the developed conceptual hydrogeological model. A numerical groundwater flow model was also developed but it will only be incorporated if required. A secondary objective is the achievement of pit slope stability by dewatering of the main fractured and weathered aquifer systems associated with the pit wall. Identification of groundwater flow from available remote sensing data and combining it with knowledge of the regional stress orientation, aquifer thickness from geophysical results (resistivity and drilling) results enabled groundwater quantification and design of dewatering strategies to be developed for the mine site.

The dynamic nature of a mine environment coupled with the heterogeneous and anisotropic distribution of hydrogeological parameters, make groundwater studies complex. The problem necessitates a well-planned programme of investigations. The programme should be tailored to suit the problem at hand.

Site description

The mine site is located in the Katanga Province of the Democratic Republic of Congo (DRC). Layout of the mine site is shown in Fig. 2. In the central part of the mine area are three pits located along the SE-NW striking Roan series aquifer. There are three waste rock dumps to the south-east, north-east and north-west of the pits. The tailings storage facility (TSF) and Coffer dam are located in the north-east corner and north-west of the area respectively, underlain by predominantly less transmissive sandstones and shales of the Kundelungu formation. The processing plant and mine offices are located between the TSF and the north-eastern waste rock dump.

Climate and drainage

The study area climate is typical of sub-tropical to tropical rainforest characterised by warm winters and hot and humid summers. Daily minimum and maximum temperatures vary from 15 °C and 26 °C (July) to 17 °C and 36 °C (October), respectively. The hottest months are September to November, when the mean daily temperature is typically in the region of 31 °C to 32 °C. Daytime temperatures can reach 36 °C which can fall to 34 °C at night. The rainfall sea-

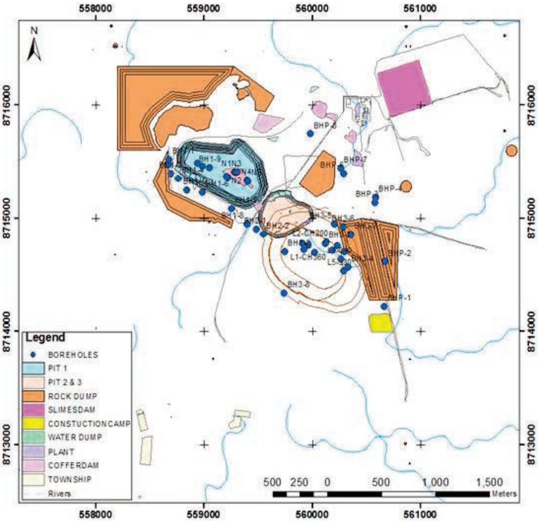

Fig. 2 *Location of mine site showing the main pits and tailings infrastructure.*

son stretches from late October to April at the site and annual rainfall ranges from 1000–2200 mm per annum.

The study area is drained by Luano River to the North West and Kebumba River to the North East. Groundwater has a short residence time after recharge as it discharges as baseflow into surface water. This phenomenon is proven by immediate water level rises and decline during the rainfall season and dry season, respectively. The catchment area of the Luano and Kebumba rivers is 5.1 km^2.

Regional geology

The mine site ore bodies are hosted by metasedimentary rocks of the 7000 m thick Neoproterozoic Katanga System. The area sits on the south end of the Katangan Copperbelt which together with the Zambian Copperbelt are located within the deformed SE-NW trending a fold-and-thrust belt called the Lufilian Arc which stretches into Namibia. This Copperbelt is 600 km long extending from Luanshya (Zambia) in the south-east to Kolwezi (DRC) in the north-west.

In the DRC, the Katangan Supergroup is preserved both as tightly folded, but relatively intact sequences and as complexly deformed dolomitic rocks namely the Roan strata (Straskraba 1991). The Katangan system is composed of sedimentary rocks of the late Proterozoic era, a succession of interbedded quartzites, sandstones, conglomerates, shales, siltstones, dolomites, limestones, argillites and dolomitic shales.

The mine site structural features are typically folded and brecciated, forming tight, steeply dipping synclinal and anticlinal structures. The vergence of the folds is variable; this is consistent with the interpretation of chaotic fragments within the breccia zone. The dip of the limbs is mainly steep from vertical to 85°, but also shallow down to 45° (GCS, 2006). In some places very shallow to sub horizontal dips occur. Fault displacements vary between 15–45 m.

Results

Hydrocensus and drilling campaign

A hydrocensus was carried out during the month of February 2010. Parameters that were collected during the hydrocensus include position of borehole; existing water supply equipment; current use; borehole status; reported yield; reported or measured borehole depth, static water level and photographs. The hydrocensus data was used in planning the next phase of the hydrogeological investigation, notably drilling, aquifer testing and water quality sampling. The highest hydraulic heads (1250–1272 mamsl) was observed on the southern side of the pits which coincided with the south west regional groundwater flow direction. The deepest hydraulic head (1222 mamsl) was recorded in Pit1 showing effects of continuous pumping for dewatering of the pit floor.

The objective of the drilling phase was to initially characterise rock units in terms hydrogeological properties. The hydrogeological properties of the rock units would then guide in establishing a dewatering plan for the mine. Blow yields were measured at 5 m intervals and the final blow yield at the end drilling. Groundwater physicochemical parameters were also measured during drilling which included water strikes (fig. 3). The top water strikes identified during drilling were also sealed off in some boreholes in order to measure the actual water strike yields in the lower formations.

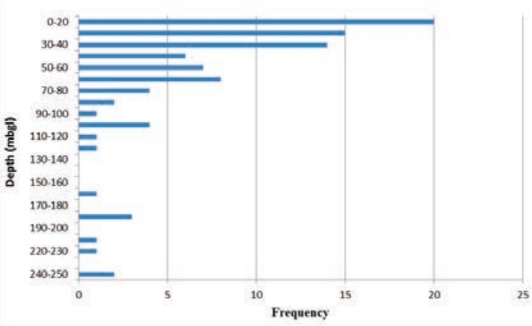

Fig. 3 *Water strike frequency during drilling campaign.*

The drilling data indicated multiple water strike positions, with shallower and less prolific water strikes in the depth range of 5–40 mbgl, mostly within the Kundelungu Formation and at depth range of 35–220 mbgl in the Roan Formation. The average yield of the Laterite aquifer was calculated to be 10 m^3/h. Blow yields for the Roan aquifer ranged between 15 and 400 m^3/h. It was noted that high yields were associated with the Roan lithologies located in the centre of Pit 1 and Pit 2. The southern side of the pits is underlain by predominantly semi-permeable and lowly yielding (<3 m^3/h) roches argillaceous talceus (RAT) and calcareous mineral noirs (CMN) formations.

Site Geology

Siliceous dolomitic shale (SDS) is the predominant rock type intersected in the deep boreholes. The weathered and altered dolomite namely the Black Ore Mineralised Zone (BOMZ) occurs as compartments in contact with the SDS.

Pit 1 intersected SDS and roches siliceuses feuilletees (RSF) of the Roan Formation and compartments of BOMZ. Difficult drilling conditions were encountered in the collapsing zones of the loose BOMZ. The SDS is separated into compartments by geological structures as evidenced by the presence of pockets of BOMZ. Drilling results indicate that periods of folding and associated faulting could have pushed the less permeable and older formations (*e.g.* RAT) closer to ground surface. Boreholes in Pit 2 intersected CMN, siliceous dolomitic siltstone and BOMZ. High blow yield in the BOMZ resulted in back-pressure and subsequent reduced penetration rates. Pit 3 area intersected Laterite underlain by RAT breccia. Below the RAT breccia is 15–20 m thick RAT underlain by 80–40 m thick SDS.

Weathering and associated alteration was encountered from ground surface to depths of approximately 80 mbgl in most boreholes. Fracturing was encountered at various depths and was encountered at 200 m depth in the deepest borehole at the mine. It was also noted that fracturing and weathering was associated with contact zones and bedding planes.

Hydraulic parameters

A graphical summary of estimated hydraulic conductivity values are given for Pit 1 in Fig. 4. The main features of each unit are briefly described below as it relates to permeability and storativity values.

The weathered regolith consists of weathered laterite in the pits area. Results from dewatering and groundwater monitoring drilling show that depths of weathering reach approximately 100 mbgl. The depth of weathering increases towards the south reaching 120 mbgl, where the topography is flat promoting infiltration during rainfall events. The estimated hydraulic conductivity of the upper weathered zone is approximately 7–15 m/d.

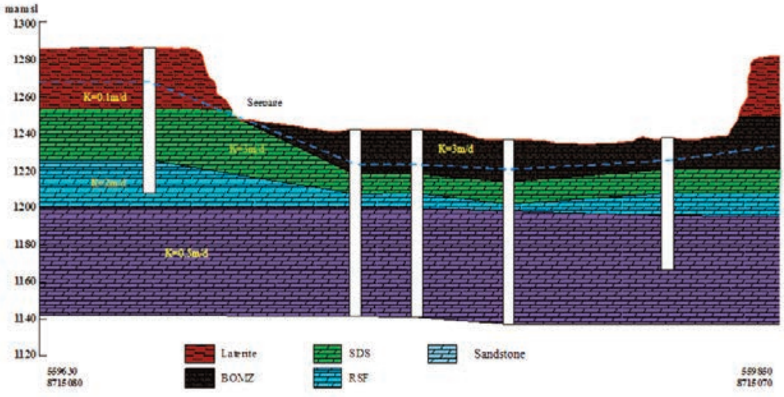

Fig. 4 *Pit 1 NE-SW cross section indicating the hydraulic conductivity zones.*

Weathered and altered dolomite (WAD) unit consists of 40 m thick highly weathered and decomposed dolomite and becomes moderately weathered to fresh with depth. Porosity for the unit was estimated to be 20–25 %, with moderate to high permeability within the weathered zones. Transmissivity of the unit was estimated to be 256 m^2/d with a storage coefficient of approximately 2.2×10^{-3}.

The RAT unit is interpreted to be a product of brittle failure when the Roan series was pushed over the Kundelungu series during the Katangan deformation. Yields within the RAT breccia range between 5–40 m^3/h. SDS unit consists of moderately weathered dolomitic shale, although highly weathered and friable horizons have been observed within the upper weathered zone. Sub-horizontal fracturing is dominant with estimated transmissivity values of approximately 252 m^2/d and a moderate-to-high porosity of 20–25 %. The RSF unit consists of relatively thin impersistent layers of foliated siliceous dolomite at the base of the Roan Formation. Porosity was estimated to be 15–25 % and transmissivity in the range of 200–400 m^2/d.

CMN was intersected by most boreholes drilled in the north-west of pits 1 and 2. Water logging conditions were observed in pit 2 north east areas underlain by CMN. Permeability is estimated to be low in orders of less than 0.001 m/d.

The water levels follow topography to a large extent indicating unconfined conditions. This could be an indication of a high degree of interconnectivity between shallow and deep aquifers and the system acts like a single aquifer.

Dewatering Strategy

At the current stage the magnitude of collapse of pit walls and flooding at the mine site depends primarily on the groundwater levels, the hydraulic conductivity of the rock units in the high walls and the local recharge to the groundwater system. The majority of modern mines use a combination of sump pumping, grouting and strategically designed active pumping and water interception systems.

The analysis of hydrogeology data gathered at the mine site demonstrates that an effective dewatering system for Pit 1 should consist of a combination of elements.

Recharge interception

The planned dewatering methods should cut off recharge from sandstones and from Luano River. However boreholes drilled in the sandstones south of the pit had low blow yields of approximately 5 m^3/h. Seepage mapping in Pit 1 identified a spring like type of flow with a flow rate of approximately 1 m^3/h. This represents significant recharge flow through fractures/conductive zones from the south. It is necessary to install a dewatering well along this fracture on the perimeter of the pit and intercept flow along the fracture/conductive zone.

Wells

Vertical in-pit and pit perimeter wells will be required for active dewatering. The wells will lower the phreatic surface below the working pit floor, and will have significant local effects on heads at the toe of the slope. The most prolific aquifer, the SDS, dips towards the North-East. Groundwater flow is expected along the bedding planes. Seepage mapping identified heavy seepage from the south-west of the pit.

Pumping wells located around the periphery of the pit may prove practical and economical. The wells should be installed to a depth in excess of 200 m and large diameters to accommodate bigger capacity pumps. The numerical model predicted a maximum inflow of 11000 m^3/d during the final year of mining in Pit 1. A total of six wells pumping on average of 100 m^3/h will have a total pumping volume of 14000 m^3/d. As of 2011 and early 2012 the water level had been maintained at approximately 5 m below the pit bottom, whilst pumping at an average rate of 9000 m^3/d. Monitoring wells located 25 m away from the pumping well showed quick response to pumping. As such borehole spacing of 25–30 m between pumping wells will be sufficient to create a compound cone of depression below the pit floor.

Three in-pit wells should be installed, one in the centre of the pit and the other two wells at about 30 m west and east of the central well. The wells should be screened in the BOMZ which deepens towards the east.

One pit perimeter well will be required on the north side of Pit 1 as it will be used to intercept any recharge from Luano River and its basin. The other pit perimeter well should be installed on the southern side of the pit preferably close to the high seepage/spring zone. The third perimeter well should be installed on the BOMZ-breccia contact zone and intercept flow along this zone. All the pit perimeter wells should be screened in the SDS, BOMZ and sandstone lithologies, which indicated a high hydraulic conductivity.

Pit sumps and drainage canal

In addition to drainage control within the pit itself, the control of surface drainage outside pit boundaries is necessary to ensure that surface water does not flow directly into the pit. If extra pumping capacity required, water flowing into the pit percolates into surface fractures and openings, many of which have been created by blasting, develops cleft water pressures. This aggravates pit wall collapse and the occurrence of local slides between benches.

As seepage and significant flow from the perched zones is expected in Fig. 4. Pit floor sumps should be constructed and harvest passive flow from the saturated perched zones. The sumps should be deep enough to accommodate submergible pumps. Pipelines from the sumps should preferably be connected to the pipelines from dewatering wells and discharge water to storage facilities like the Coffer Dam.

Conclusions

A full hydrogeological assessment of the mine site and surrounding environment was performed. A combination of dewatering methods has been implemented on site to address specific issues relating to mining and high wall stability. The site is located in a high rainfall area with high infiltration rates and overland flow, a combination of interception and higher pumping rates have proven to decrease the rate of influx into the mine site. In all instances an ongoing monitoring of strategies employed should be maintained as the mine floor is lowered over the next 10 years.

Acknowledgements

The authors thank Golder Associates, University of the Free State and the respective mine site for research funding.

References

Acworth RI (1987) The development of crystalline basement aquifers in a tropical environment. Quarterly J. Engineering Geology and Hydrogeology 20(4):265-272.

GCS (2006) GCS Report: 05.06-245/BFS/Final. Bankable Feasibility Study Hydrogeological Investigation.

Kellgren N and Sander P (2000) Benefits of incorporating remote sensing techniques as a methodological approach for improved borehole siting in fractured rock aquifers. In Sililo, O. *et al.* (eds.) 2000. Groundwater: Past Achievements and Future Challenges. Proceedings of the XXX IAH Congress, Cape Town, South Africa, 26 November – 1 December 2000. Balkema, Rotterdam. 1144 p

Lydall MI, Auchterlonie DA (2011) The Democratic Republic of Congo and Zambia: A Growing Global “Hotspot” for Copper-Cobalt mineral Investment and Exploitation: 25-33

Straskraba V (1991) Future Mine Dewatering Strategy for the Nkana Mine Area, Unpublished report for Zambia Consolidated Copper Mines, Ltd.

Evaluation and Depressurization of an Ordvician limestone confined aquifer in Xingcun coal mine

Sun Yajun, Sui Wanghua, Dong Guiming, Liu Shucai, Yu Jingcun

China University of Mining and Technology, 1 Daxue Road, Xuzhou, Jiangsu, 221116, China, syj@cumt.edu.cn

Abstract The maximum groundwater pressure of the Ordovician limestone aquifer is 12.97 MPa in the Xingcun coal mine. The coal mining is unavailable due to the risk of water inrush. In order to evaluate the depressurizing feasibility of the aquifer, a comprehensive method was proposed and applied. The time domain electromagnetic (TEM) exploration indicates the groundwater storage in the limestone with intensive nonhomogeneous karst development. Based on the hydrogeological test, the drawdown and its velocity were calculated. It shows the depressurizing of the aquifer is feasible. As a result of depressurization, the water pressure was finally reduced and the risk of water inrush was avoided.

Keywords depressurization, Ordovician limestone, confined aquifer, water inrush

Introduction

In the eastern part of China, the Ordovician limestone confined aquifer (OCA) is known for its intensive nonhomogeneous karst development, abundance of groundwater and high water pressure. For many coal mines, the OCA lies below the coal seam with thickness of 650-800 m (Wu 2006, Peng 2007). Generally, an aquifuge separates the aquifer and the coal seam and makes the mining available. But more than a thousand disasters of groundwater inrush into coal mines were induced because of high water pressure and insufficient aquifuge thickness. At least 35 coal mines were flooded and thousands people lost their life (Shi 2001). The maximum water inflow in a coal mine, Fangezhuang, has reached as much as 2053 m^3/min (Zhang 2005).

Dewatering and grouting are the technical choices to eliminate the possibility of water inrush and ensure the mining security, but dewatering or depressuring is generally not recommended due to expensive cost and environmental problems resulted consequently (Li 2006). In fact, it is difficult to generate effective drawdown for OCA with steady and sufficient recharge in most cases. If the aquifer is in an isolated hydrogeological unit with limited recharge, it can be achieved by dewatering OCA to depress the water level to the safe value corresponding to the aquifuge. With the practical example in Xingcun coal mine, this paper describe a comprehensive method involving geophysical exploration, hydrogeological test and calculation to evaluate the feasibility of depressurization of OCA.

Hydrogeological background

Located in Shandong, China, Xingcun coal mine is now mining the coal seam No. 3 in the lower Shanxi Group Formation of the Permian system, with thickness of 7.15 m and elevation from -1010 to -1100 m. The Ordovician limestone is below the coal seam with water level of +5.59 m. Regionally, the maximum groundwater pressure is 12.97 MPa, while the aquifuge thickness between the aquifer and the coal seam is 215.6 m.

E3206 is a work face in Xingcun coal mine, which is located in the hangingwall of fault DF39. The fault DF39 uplifts the Ordovician limestone in the footwall, making the distance between the work face and the opposite Ordovician limestone decreasing from 215.6 m to

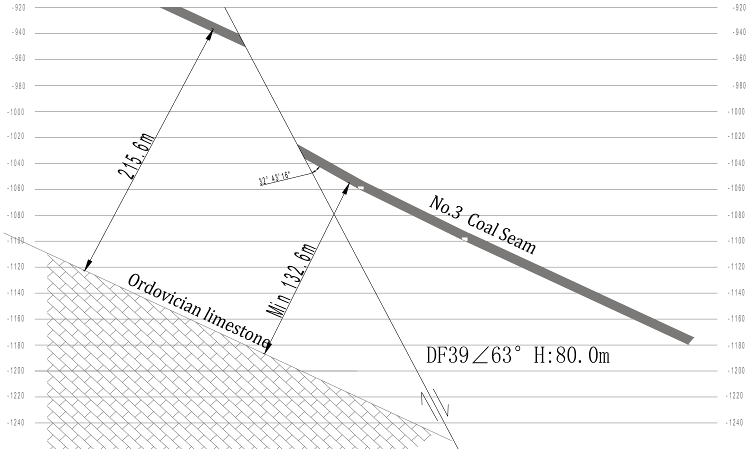

Fig. 1 *Hydrogeological profile of E3206*

132.6 m. Hydrogeological structure of the coal seam, work face, fault and the aquifer is schematically illustrated in Fig. 1. To the aquifuge of E3206, the water pressure reaches 12.97 MPa. The coal mining is under a ultra-high water pressure of confined aquifer as well as the complex tectonic conditions. The coal mining is therefore unavailable due to the risk of water inrush in this case, and the water level has to be depressed to a safe value before coal mining.

Methods and Analysis

In order to evaluate the depressurizing feasibility of the OCA with high pressure in the coal mine, we proposed and applied a comprehensive method involving geophysical exploration, hydrogeological test and calculation.

Geophysical exploration

Considering the nonhomogeneous karst development in the Ordovician limestone, the geophysical exploration of time domain electromagnetic methods was used in the E3206 to investigate the distribution of lower electrical resistance areas in the aquifer, which indicate the groundwater storage in the limestone. A total of 40 measuring points were designed by every 10 m along the E3206 track transportation tunnel. Each point investigates two directions towards floor and side. The result shows that the water stores only in the light grey area (Fig. 2).

Hydrogeological test

We conducted a hydrogeological test with a surface observation well (S5) and an under-

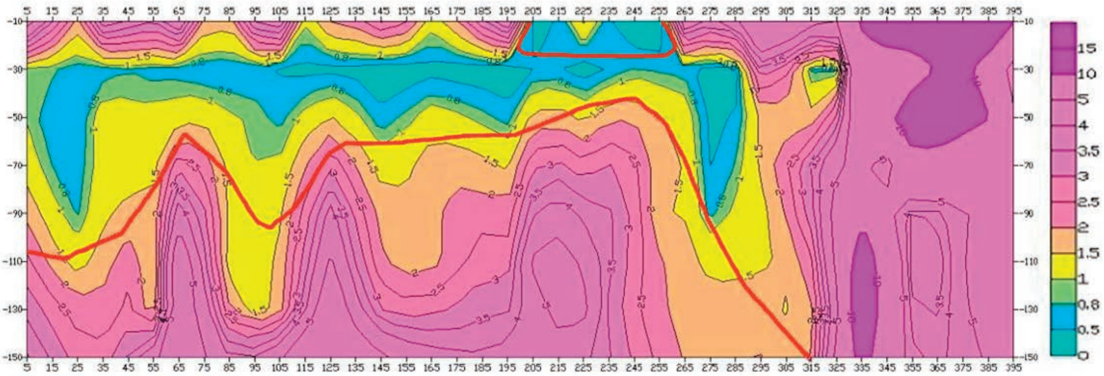

Fig. 2 *Apparent resistivity section of the floor of track tunnel for E3206 work face.*

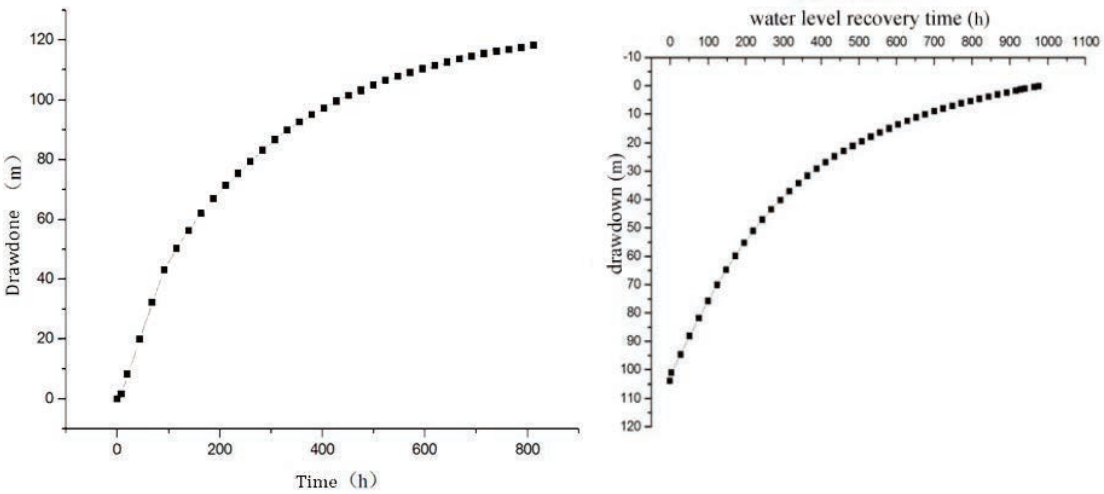

Fig. 3 *Curves of drawdown-time in S5 during the dewatering and recovery tests. left: dewatering; right: recovery.*

ground borehole (S2) in the coal mine to determine the groundwater abundance of the OCA and its hydrogeological parameters, such as the transmissivity (T) and the specific yield (q). The underground borehole S2 acted as the main dewatering drilled well of Ordovician limestone aquifer, and S5 as the water level observation well. We carried out two dewatering and two recovery tests. Some data of drawdown (water level) variation with time during the dewatering and recovery observed in S5 are as in Fig. 3.

Analysis of water abundance of Ordovician limestone

Fig.3 shows that the water level in S5 decreases gradually during the dewatering and rises slowly during the recovery in the two tests. So we can preliminarily draw the conclusion that the recharge of the Ordovician limestone aquifer is not sufficient. The parameters are calculated by Jacob linear distribution method and the water level recovery data. The results list in Tab. 1.

By the hydrogeological test, we obtained the specific yield of the aquifer as 0.01864 L/(m·s). The drawdown speed and the hydrogeological parameters indicate that the groundwater in the OCA in this coal mine is not as abundant as in other areas. We reasonably presume that the faults around the work face cut off some of the lateral recharge. This provides a very important basis for generating an enough drawdown by dewatering or drainage.

Parameters	Results in the first test	Results in the first recovery test	Results in the second test	Results in the second recovery test	Average results
Transmissivity T（m^2/h）	0.11	0.149	0.12	0.0643	0.115
storage coefficient S	1.71×10^{-5}		1.4×10^{-5}		1.56×10^{-5}

Table 1 *Parameters calculated by the hyrdrogeological tests*

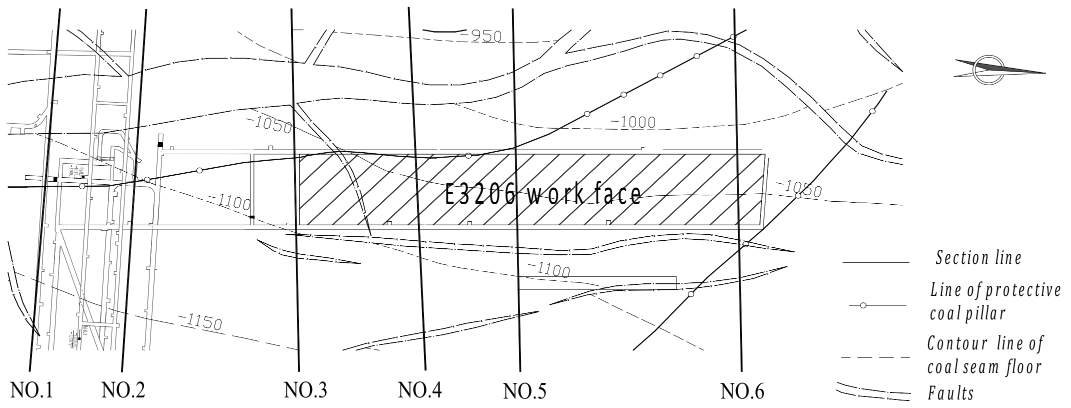

Fig. 4 *Distribution of the six section lines in E2306 work face*

Evaluation and Application

In order to evaluate the feasibility of depressuration of the OCA in this coal mine, we calculated the drawdown and time needed to eliminate the possibility of water inrush by two steps.

Calculating the drawdown needed

We calculated the water pressure which is in the safe range corresponding to the thickness of aquifuge. Considering that the water pressure and the thickness of aquifuge are not exactly the same at different locations due to the formation slope in E3206, six section lines were set up to determine the specific data for calculating the drawdown (Fig. 4).

We used the water inrush coefficient method (Eq. 1) to estimate if it is safe or dangerous in the cases of mining on a confined aquifer. By comparing with the critical value of water inrush coefficient, the water pressure allowed was calculated and then induced to the drawdown.

$$T = P/M \qquad (1)$$

Where T is the water inrush coefficient (MPa/m), P is the groundwater pressure of floor aquifer (MPa), and M is the aquifuge thickness between the confined aquifer and the coal seam (m). The critical values of water inrush coefficient is 0.06 MPa/m in the area of fault well developed and 0.1 MPa/m in others. According to the aquifuge thickness at the six section lines, we determined the safety drawdown required to avoid water inrush (Tab. 2).

Forecasting the groundwater field variation during depressurization

For an engineering application in coal mines, the feasibility of depressurization of OCA also depends on the time which is needed to lower the water level to a safe value, therefore the drawdown of the water level and the spreading velocity of the cone of depression were calculated based on the specific hydrogeological parameters and given flowing drainage wells. We designed several different dewatering plans with different number of wells and different flow quantity, and then forecasted the groundwater field variation in the Xingcun coal mine area by the methods of the Theis equation and numerical simulation.

By comparing the forecasting results of different drainage plans, we found that the drawdown would meet the requirement after 60 days with two drainage wells and flow quantity of 120 m^3/h in the area of E3206 work face. The maximum drawdown would reach 580 m at the centre of the cone of depression and 320 m at the end of the work face. The original flow field before drainage and the

Section line	Water pressure in Ordovician limestone （MPa）	Distance between Ordovician limestone and No.3 coal seam （m）	Water inrush coefficient （MPa/m）	Safety water pressure （MPa）	Safety drawdown （m）
No.1	12.975	150	0.087	9.00	405
No.2	12.775	143	0.089	8.58	428
No.3	12.39	145	0.085	8.70	376
No.4	12.39	171	0.072	10.26	123
No.5	12.39	191	0.065	11.46	95
No.6	12.78	215	0.059	12.90	0

***Table 2** Evaluation results by water inrush coefficient method*

forecasting drawdown after 60 days are illustrated in Figure 5.

Application result of depressurization

Two underground flowing drainage wells near the E3026 work face, S2 and S6 (the black circles in Fig. 5), were used to drainage the groundwater in the OCA. The flow quantity of S2 and S6 were respectively 39 m^3/h and 57 m^3/h. Finally, the water pressure of the Ordovician aquifer in E3206 was finally reduced to 2.2 MPa, and the risk of water inrush was avoided. The actual depressuring result of the aquifer is illustrated in Fig. 6. The coal mining finished successfully and safely by the end of 2012.

Conclusions

E3206 work face mining began on 5/29/2012 and ended on 11/18/2012 without water inrush caused by Ordovician limestone and faults. The mining and calculation results of drainage show that depressurization is an effective way to prevent and control the water inrush in this

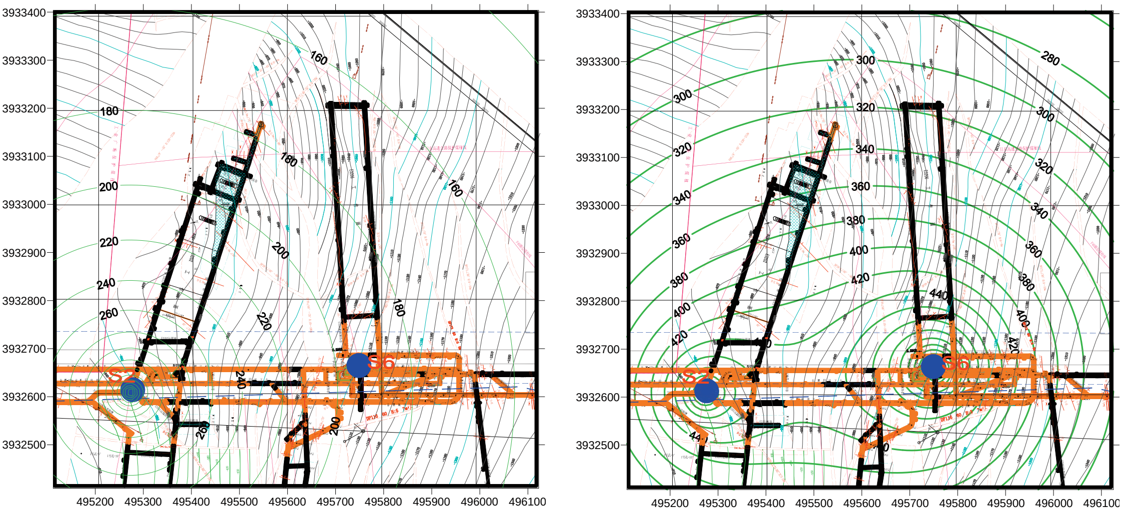

***Fig. 5** left: Contour map of drawdown before drainage in E2306 work face; right: Contour map of forecasting drawdown after 60 days of drainage*

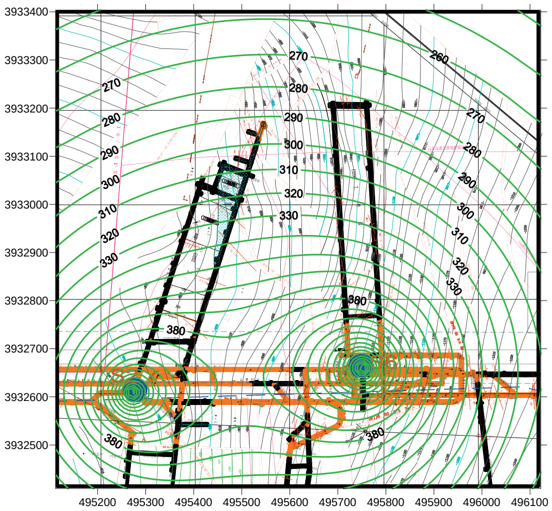

Fig. 6 *Contour map of drawdown after drainage and before mining in E2306 work face.*

region, and the comprehensive method with geophysical exploration, hydrogeological test and calculation is available to evaluate the feasibility of depressurization in the case of the limestone aquifer with high pressure and intensive nonhomogeneous karst development.

Acknowledgements

This work has been supported by National Basic Research Program of China, Research on basic theory about the mechanism of water inrush and its prevention in coal mines (No. 2007CB209401), and Basic research on geological disasters prevention and environment protection during intensive coal mining in the west of China (No. 2013CB227901).

References

Qiang Wu, Wanfang Zhou, Duo Li(2006) Management of karst water resources in mining area: dewatering in mines and demand for water supply in the Dongshan Mine of Taiyuan, Shanxi Province, North China, J Environmental Geology, 50(8): 1107–1117

Suping Peng, Jincai Zhang(2007) Engineering Geology for Underground Rocks – Vol 10, Mine strata failure and mining near aquifers – Water inrush and mining above confined aquifers. Springer-Verlag Berlin and Heidelberg GmbH & Co. K, 261–294 pp

Longqing Shi, R.N. Singh (2001) Study of Mine Water Inrush from Floor Strata through Faults, J Mine Water and the Environment, 20: 140–147

Jincai Zhang(2005) Investigations of water inrushes from aquifers under coal seams, J International Journal of Rock Mechanics and Mining Sciences, 42: 350–360

Wanfang Zhou, Gongyu Li(2001), Geological barrier – a natural rock stratum for preventing confined karst water from flowing into mines in North China, J Environmental Geology, 40(8): 1003–1009

Gongyu Li, Wanfang Zhou(2006), Impact of karst water on coal mining in North China, J Environmental Geology, 49(3): 449–457

Hydrogeological and Geochemical Evaluations in Support of Mine Water Management for the Jurong Rock Cavern Project, Singapore

Michael G. Wallace[1], Kathryn O. Johnson[2], John D. Osnes[3],
Eric L. Krantz[3], Crystal M. Hocking[3]

[1]*RESPEC, 5971 Jefferson NE, Suite 101 Albuquerque, New Mexico, 87109, USA, michael.wallace@respec.com*
[2]*Johnson Environmental 24054 Palmer Gulch Rd., Hill City, South Dakota, 57745, USA,kjohnson@johnsonenviro.com*
[3]*RESPC., 3824 Jet Drive, Rapid City, South Dakota, 57703, USA, john.osnes@respec.com, eric.krantz@respec.com, crystal.hocking@respec.com*

Abstract The Jurong Rock Cavern Project is a hydrocarbon cavern storage project in Singapore. Upon completion, the combined storage volume will exceed 1.5 Mm^3, sited as deep as 160 m beneath the overlying seabed, within a saturated groundwater environment. The project relies on the well-established principles of hydrodynamic containment. Ongoing hydrogeological and geochemical testing programs at the site are used to validate and inform groundwater and geochemical models. Results are relied upon for the final design and management of treated water injection curtains, grouting approaches, and groundwater monitoring and sampling systems associated with the project.

Keywords Jurong, hydrodynamic containment, hydrogeology, geochemistry, mine water

Introduction

The Jurong Rock Cavern (JRC) hydrocarbon storage facility is being excavated via drill and blast techniques underneath Banyan Basin, a bay located within a constructed island in an industrial zone off the coast of western Singapore. The underground facility reaches as deep as 185 m below sea level and consists of five separate storage caverns that are over 300 m long each. The entire cavern ensemble volume is sufficient to store over 1.5 Mm^3 of hydrocarbons. Two access shafts on either side of the rectangular bay and thousands of meters of auxiliary tunnels at two distinct levels facilitate the overall benching construction and the supporting infrastructure for cavern management, which includes an array of subsurface monitor systems, product and injection water pumps, and piping and headspace control. The overall project is divided into two levels. Level 1, which is approximately 90 m below sea level Admiralty Chart Datum (ACD), hosts the maintenance infrastructure and the network of water curtain galleries. Level 0, approximately -120 m ACD, hosts the construction tunnels used to excavate each storage cavern and haul rock. Caverns extend below Level 0. Once the cavern complex is fully constructed and tested, Level 0 will be sealed from each cavern and flooded.

The cavern complex will notably use the hydrodynamic containment principle to isolate the low vapor pressure products. The hydrodynamic containment principle involves isolating each cavern by taking advantage of natural water gradients that are augmented by artificial gradients provided by water curtain galleries, which are long specialty tunnels that are parallel to each cavern. Each gallery hosts approximately 50 individual boreholes, at various lengths (up to 60 m) and inclinations depending on hydrologic conditions, that inject treated water at pressure into the rock formations hosting the storage caverns. The successful design and operation of these galleries depends on a host of factors, and not the least of which includes a sound understanding of the hydrogeology and the geochemistry of the surrounding host rock formations.

Hydrogeological Setting and Investigation

The guiding principal of hydrodynamic containment is that a positive hydraulic gradient of water directed towards each cavern will prevent the stored hydrocarbon products from migrating away (Goodall *et al.* 1988; King 1999). Numerous storage cavern complexes throughout the world have operated over many decades using this approach. That guiding principal is reinforced by a suite of best industry practices that include groundwater and geochemical modeling and testing to optimize any system for long-term effectiveness and safety. Groundwater modeling aids in the synthesis of the available information to improve the design, estimate seepage rates, estimate water injection demands, interpret hydraulic tests, determine the best locations for monitor features (such as manometers), and facilitate knowledge transfer to the numerous technical and administrative team members. Geochemical modeling serves similar purposes but with a focus on the prevention of clogging of injection boreholes, which may be possible either through microbial action as well as through geochemical reactions between the injection water and the host rock.

A necessary condition for hydrodynamic containment is that the rock that overlies and surrounds each storage cavern must remain saturated with water throughout the excavation and operations periods. However, for construction purposes, caverns and tunnels must be kept relatively dry during excavation. Therefore developing best estimates of groundwater flow into those caverns and tunnels under excavation conditions is important to determine the size of the dewatering pumps and to design a rock grouting system and a water curtain injection system. Best estimates of the prevailing hydrogeological conditions during the operation phase must also be developed to evaluate the effectiveness of the proposed design for hydrodynamic containment. Hydrodynamic containment is designed for two objectives: (1) for preventing product migration from a cavern to operations tunnels (an essential component of worker safety) and (2) for preventing the mixing of products between storage caverns.

Given the challenging environment and objectives, there would likely never be too much information to work with. However, only near-surface, tidal, borehole and geophysical information was initially available for the preliminary designs that were developed. As additional information became available from excavations and additional surface and subsurface studies during the construction phase, the hydrodynamic containment parameters were continually re-evaluated.

The geological strata encountered in downward sequence in borehole drilling at the Banyan Basin locale include newly reclaimed sand, marine sediments, and sedimentary bedrocks of the Jurong Formation, such as siltstone; sandstone; conglomerate; limestone; and some intrusive rock dykes, sills, and veins. In addition, several joints and strike-slip faults were mapped. Within the layered sedimentary units, a shallow aquifer system includes the reclaimed sand aquifer, the marine sediments, and the weathered rock unit. The deeper fresh rock aquifer at the Level 0 and cavern horizons includes the low confined zone and the sedimentary rock zone. The structural features that include an acid dyke set, zones of perturbed rock associated with the dyke, and vertical and horizontal (thrusting) faults and fracture sets are found within these two zones.

Over the early period of construction in 2009 and 2010, we conducted preliminary hydrogeological and geochemical model activities based on this geologic model. Based on earlier interpretations, the three-dimensional steady state hydrogeological simulations using MODFLOW (Harbaugh *et al.* 2000) assumed that the vertical dike and fracture features were the most important water-bearing features at the cavern horizons. Our initial groundwater and geochemical models employed this early information to produce estimates for grouting targets, mine dewatering, and water treatment strategies and injection rates.

As excavation and testing progressed, it became clear that these vertical features are not important water-bearing zones over the scales of interest. Rather, sub-horizontal water-bearing features in or adjacent to the Level 1 horizon have been shown to significantly dominate the hydraulic flow regime. Although the lack of high-flow, water-bearing features in the cavern horizons is a benefit to the timely excavation of the caverns (so far), these water-bearing features posed significant obstacles, at times, to the excavation of tunnels in Level 1. As a result, some modifications to the cavern system were developed. Accordingly, revisions were made to the hydrogeological model to aid in developing alternative designs and new seepage and water curtain injection estimates (RESPEC 2013).

The previous models did not extend under land, but the new model does for a significant distance to allow, in part, the consideration of shoreline piezometer hydrographs (changes in measured depth to water over time). Those records were used to calibrate a recharge boundary condition (based on rainfall) applied over portions of the model that underlie the land. This allowed us to develop more realistic scenarios and to include a significant majority of the construction features in an integrated approach. In this capacity, the new boundary conditions and setup led to a hydrogeological model that closely matched the overall behavior of the system. Table 1 provides a sample comparison of the hydrogeological model results to historical mine seepage data. As the system is still under construction, we do not claim that our model's fidelity to the observed system is ideal, but so far the information does appear to show that our simulations are fair estimators of hydrodynamic performance.

The hydrogeological model has also been useful for considering various scenarios. One scenario concerned a hypothetical "marine clay" layer in the shallow seabed sediments. Such a layer might block natural recharge from the ocean. If that were the case, then additional overlying horizontal water curtains might be required. Through conservative model evaluations and an analysis of tidal perturbations on shoreline piezometers, we have been able to posit that such a marine clay layer, were it to exist over the cavern complex, would not adversely impact performance. Another scenario considered a high permeability arch that was postulated to connect cavern crowns to an overlying operations tunnel. Through the modeling exercise, a signature hydraulic pressure pattern was developed, which might indicate such a feature. If such a signature were to be observed as construction is advanced, then

Seepage inflow location	Measured seepage (m^3/hr)	Construction simulation of seepage (m^3/hr)
Level 1 and Level 0	234 and 20	241 and 14
Caverns CS 1/1, 1/2, and 1/3	13, 28, and 4	14, 26, and 26
WG 1/1 through 1/4 tunnels seepage	19, 15, 25, and 15	12, 10, 10, and 11
WG 1/1 through 1/4 curtain injection	-20, -20,-16, -22	-21, -19, -17, and -22
Entire excavation inflow	435	418

Table 1 *Selected preliminary comparisons of recent hydrogeological model results to in situ measurements over the mid-2012 time frame (RESPEC 2013).*

added grouting and water curtain borehole modifications could be employed to remediate any deficiencies in the containment system in advance. The possibility of seismic impacts to hydrodynamic containment was not directly addressed. Seismic disruption is considered to be a fairly unlikely scenario, due to the relatively low rate and degree of tectonic events in the locale (Balendra and Zi 2008).

Geochemical Setting and Investigation

Throughout the evolution of the project, different water sources for injection have been considered, including municipal fresh water, natural groundwater, and seawater. Currently, seawater is the injection liquid, and according to the hydrogeological model estimates, approximately 180 m^3/h of this water will be needed for injection on a continuous basis for containment needs. Early geochemical assessments identified the potential for clogging by chemical interactions between seawater injected into injection boreholes of the water curtain and the aquifer groundwater (Johnson 2011, RESPEC 2010).

The two potential causes of clogging that were identified by the geochemical assessments are (1) the precipitation of calcite caused primarily by pH changes and (2) the precipitation of iron hydroxide ($Fe(OH)_3$) in response to oxygen in the injection water. The precipitation of calcite depends on calcium concentration, pH, and temperature. Precipitation is favored under increasing pH conditions as well as increasing temperature. Under oxidizing conditions with Eh greater than approximately 200 mV (at pH conditions characteristic of the aquifer), iron hydroxide could precipitate and potentially reduce porosity and permeability.

To reach conclusive positions on the best long-term water-quality injection management strategy, a geochemical test was conducted. Three adjacent vertical boreholes spaced 10 m apart in a water curtain gallery were selected. All boreholes passed through an underlying subparallel, water-bearing feature approximately 10 m below the gallery invert. One borehole was used for injection, one for recovery, and the remaining borehole for added monitoring. All wells were monitored daily for pressure and water-quality parameters, including temperature, pH, ORP (later converted to Eh through standard practices), and electrical conductivity (EC). Samples of water from the injection and recovery boreholes were collected three times during the test and analyzed for a comprehensive list of parameters. Also, at three separate times, each well was subjected to a hydraulic test. Through this progression of hydraulic testing over the length of the test, it was believed that a pattern of decreasing hydraulic conductivity might be expressed if clogging was actually occurring.

The test was conducted in 2012 over a seven month period. Untreated seepage water recovered from the tunnels was injected over two months through the middle period of the test. Otherwise, treated and filtered seawater was injected. Some calibration and equipment issues prevented the full use of the data from the entire test period. However, the geochemical and hydraulic testing results, partly illustrated in Fig. 1, were sufficient in conjunction with some follow-up modeling calculations to determine that clogging by calcite precipitation was possible, and that this could likely be prevented through pH control of the injection fluid. Clogging by iron hydroxide precipitation, however, is no longer considered likely because of the significant presence of sulfite in the groundwater, which will consume any oxygen present in the injection water and, thereby, lower the Eh.

Summary and Conclusion

The Jurong Rock Cavern Project is a new underground hydrocarbon storage cavern facility being constructed under Banyan Basin in Singapore. It uses the principles of hydrodynamic containment for the effective storage of all hydrocarbons. These principals have guided the field investigations, ongoing data collection, and design and modeling studies for an integrated, hydrogeological and geochemical

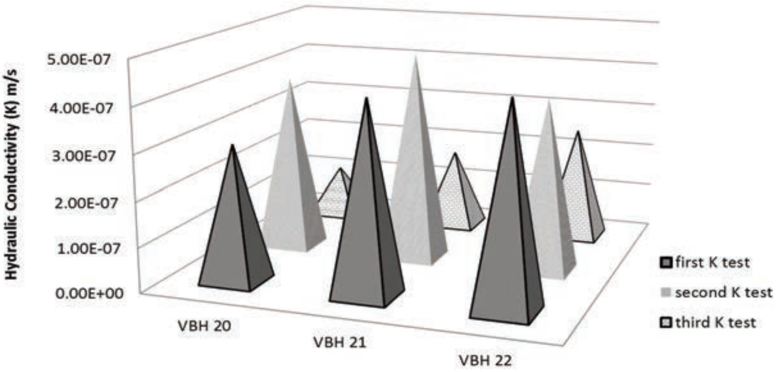

***Fig. 1** Results of hydraulic testing at boreholes (VHB 20 through VBH 22) used in geochemical test (RESPEC 2012).*

knowledge base that supports the project now and into the pending operations phase.

Acknowledgements

The authors gratefully acknowledge: Richard Abitz (now with Savannah River National Laboratory); Stephen Cormier, Tim Reichwein, and Bruce Russell (all with Parsons Brinkerhoff Energy Storage Services, Houston); Yung Kim, Eui Hong, Myung Kyu Song, Edward Armstrong, and Win Naing Ziziwar (all with Hyundai Engineering and Construction Limited, Singapore); Chin HwiGan, Mee Nee Lee, Hana Lee, and Ai Lin Teo (all of Parsons Brinkerhoff Pte Ltd. Singapore); Karla Lipp and Laura Fairhead (of RESPEC); Tim Ross of Agapito Associates; and the members of the JRC Project Team, including their reviewing engineers and scientists from Géostock.

References

Balendra T, Li Z. (2008) Seismic hazard of Singapore and Malaysia. Earthquake engineering in the low and moderate seismic regions of Southeast Asia and Australia. Electronic Journal of Structural Engineering (eJSE) Special Issue. eJSE International 2008.

Goodall DC, Aberg B, Brekke TL (1988) Fundamentals of gas containment in unlined rock caverns. Rock Mechanics and Rock Engineering, 21, 235–258

Harbaugh AW, Banta ER, Hill MC, McDonald MG (2000) Modflow-2000, The U.S. geological survey modular ground-water model–user guide to modularization concepts and the ground-water flow process, U.S. Geological Survey, Reston, Virginia

Johnson KO (2011) Jurong Geochemical Modeling. Memorandum to Michael Wallace, RESPEC. January

King J (1999) Hydrocarbon storage in mined caverns,a guide for state regulators. Interstate Oil and Gas Compact Commission, Oklahoma City, Oklahoma

RESPEC (2010) Geochemical model report for the Jurongrock cavern project. Topical Report RSI-2155 Revision 1. Prepared for PB Energy Storage Services, Inc. Houston, Texas. October

RESPEC (2012) Jurong preliminary analysis of geochemical test results. Memorandum prepared for PB Energy Storage Services, Inc. Houston, Texas. November

RESPEC (2013) Hydrogeological model report for the Jurongrock cavern project. Topical Report RSI-2115 Revision 5. Prepared for PB Energy Storage Services, Inc. Houston, Texas. January

Assessing the Applicability of Quaternary Sediments as Gravel Pack Material for Dewatering Wells

Christoph Weidner[1], Sebastian Henkel[2], Holger Schüttrumpf[2],
Thomas R. Rüde[1], Wiebke Klauder[3]

[1]RWTH Aachen University, Institute of Hydrogeology, Lochnerstraße 4–20, 52064 Aachen, Germany, weidner@hydro.rwth-aachen.de
[2]RWTH Aachen University, Institute of Hydraulic Engineering and Water Resources Management (IWW), Mies-van-der-Rohe-Straße, 52056 Aachen, Germany
[3]RWE Power AG, Water Resources Management, Zum Gut Bohlendorf, 50126 Bergheim, Germany

Abstract Installation of dewatering wells in the Rhenish lignite district requires huge amounts of gravel pack material, which is a limited natural resource. Even though opposing certain requirements on the quality of gravel pack material for wells in drinking water supply (no initial Fe-(hydr)oxides; minimum quartz-content), in this study, two Quaternary gravels have been considered for application in dewatering wells. Long-term hydrogeochemical exchange was estimated by column experiments, whereas Fe-clogging affinity was evaluated using the experimental model (Weidner *et al.* 2011). With this combined approach, no arguments against the application of these Quaternary materials could be found.

Keywords Quaternary gravel pack material, iron incrustation, experimental clogging model, long term metal release, elution column experiments

Introduction

The open-pit lignite mining in the Rhenish district requires a large number of wells for local dewatering of aquifers with well depths up to 750 m. This results in a high demand of easily accessible well materials, one of which is the gravel, used as filter material between screen and borehole wall. There are certain requirements on the quality of the gravel material, designed to reassure the general functions of the gravel pack: hydraulic permeability, prevention of sand erosion from the aquifer, mechanical integrity of borehole and well, and hydrochemical inertia (as little interaction with the groundwater like dissolution or precipitation of minerals or ionic exchange as possible). Regarding these criteria, quartz is one of the most suitable minerals. Thus, in Germany gravel used in drinking water supply has to contain at least 96 wt- % of quartz, as specified by DIN 4924 (German Institute of Standardization 1998). Furthermore, it is reported by several authors that high initial contents of ferric Fe minerals in the gravel might cause an acceleration or amplification of Fe(III)-(hydr)oxide precipitation and therefore well clogging (Tamura *et al.* 1976; Houben 2004; Geroni and Sapsford 2011).

The mining company RWE Power AG has been using gravel from a Tertiary deposit that fulfills the requirements of DIN 4924 and has no measurable initial content of Fe(III)-(hydr)oxides. However, as resources of this Tertiary gravel are limited, the question of applicability of cost-effective alternative materials, available in close vicinity to the location of use is of high interest. When considering wells for dewatering of open-pits, that question gains a special importance, since most available technical standards like DIN 4924 have been defined for wells in drinking water supply, for which construction and operating conditions are substantially different from those in mine dewatering (*e.g.* construction methods and dimensions, design life, drawdown depths, aeration of screen pipe and aquifers).

In this study, alternative gravel materials from two Quaternary deposits were considered for application in dewatering wells. As the two materials do not strictly fulfill the requirements given by DIN 4924, their properties and geochemical behavior in interaction with groundwater have to be evaluated before the gravel can actually be used for well assembly.

Firstly, the possible dissolution of minerals of the Quaternary gravel was investigated through column experiments by measurements of hydrochemical changes in water flowing through the gravel. Secondly, to preclude an increased clogging affinity due to the initial Fe content, experiments were conducted using a combined hydraulic/hydrochemical experimental clogging model developed at RWTH Aachen University (Weidner *et al.* 2012).

Materials

The gravel materials, considered in this study are produced in the Rhenish lignite mining district, near the three open-pits Garzweiler, Hambach and Inden (fig. 1). The production of the conventional material is situated in Weilerswist, around 25 km southeast of the open-pit Hambach, whereas the alternative materials are available in direct vicinity of either the open-pit Garzweiler (Frimmersdorf gravel pit) or Hambach (Dorsfeld gravel pit).

All three deposits consist of fluvial sediments from the river Rhine. One main difference between the conventional and alternative materials is the geologic time of their sedimentation. The conventional gravel consists of old, Tertiary sediments (Pliocene Kieseloolite Formation), which have been fluvially transported a long way from the Maas-Moselle-region and buried deep into the anoxic underground (Fliegel 1910, Kemna 2008), whereas the alternative materials are shallow Quaternary gravels, recently deposited in proximity to the source area under oxic conditions and covered by thin layers of loess (Fliegel 1910, Quaas 1908). Obviously, this results in a low level of maturity of the alternative materials including lower contents of quartz than claimed by DIN 4924 (< 96 %) and relatively high content of Fe(III)-(hydr)oxides (between 0.1 and 0.2 wt- % Fe) that can already be noticed optically.

Methods

Firstly, to estimate the likelihood of the gravel minerals to dissolve or react in contact with water, columns of PMMA (acrylic glass) of 60 cm length and 10 cm diameter were filled with the disturbed, wet gravel. The gravel was evenly compacted and provided with stabilizing filter plates at top and bottom of the columns. Both Quaternary gravels were assembled in two columns each, while for comparison a fifth column was filled with the conventional Tertiary gravel. Flow and pressure head were kept constant during the experiment except for two stop-flow periods. Tap water of Ca-HCO_3-type was used as inflow.

In the beginning of the column experiments, conservative tracer experiments with LiBr were conducted, to determine the effective porosity (pore volume: pv) of each col-

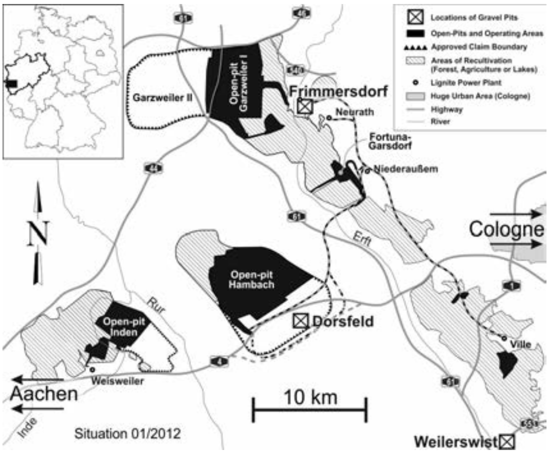

Fig. 1 *The Rhenish lignite mining district in western Germany and locations of the gravel deposits of the conventional material (Weilerswist) and the alternative Quaternary materials (Frimmersdorf, Dorsfeld; modified after DEBRIV 2012).*

umn. Subsequently, a continuous flow through the columns was applied over more than three months with two stop-flow periods, intended to study effects of diffusion controlled transport. The hydrochemistry of the in- and outflow water was characterized by daily measurements of pH and electrical conductivity (eC). Weekly samples were analyzed regarding their amounts of Fe, Mn, Al and Si via ICP-MS to quantify possible effects of dissolution or precipitation of minerals in the gravel. From the change of concentrations with time, the mass flow M_i per number of pore volumes exchanged (pv), normalized to the gravel mass in the column was calculated [mg t^{-1} pv^{-1}]:

$$M_i\,(pv) = \frac{\mu_i\,(pv)}{m_{gravel}} = \frac{\mu_i\,(\tau)\cdot V_{tot}\cdot n_e}{m_{gravel}\cdot Q\,(\tau)} = \frac{c_i\,(\tau)\cdot V_{tot}\cdot n_e}{m_{gravel}} \qquad (1)$$

with $\mu_\mathrm{i}(pv)$, $\mu_\mathrm{i}(\tau)$: mass flow rate [mg pv^{-1}] or [mg min^{-1}], respectively, with i = {Fe, Mn, Al or Si}, pv: number of pore volumes exchanged [-], τ: time [min], m_gravel: total gravel mass [t: metric ton], V_tot: total column volume [m^3], n_e: effective porosity [-], $Q(\tau)$: flow rate [m^3 min^{-1}], $c_\mathrm{i}(\tau)$: concentration [mg m^{-3}].

Secondly, to evaluate the clogging affinity of the two alternative gravel materials in comparison to the conventional gravel, the experimental model of a well section was used that was presented at the IMWA conference in 2011 (Weidner *et al.* 2011). In the model (PMMA flow channel; fig. 2), the process of Fe clogging was simulated in an accelerated way (Henkel *et al.* 2012).

Within each experiment, during the clogging step, incrustations were produced in the unsaturated zone ("clogging zone") by application of a low water level in the outflow chamber. Each experiment consisted of nine clogging steps of around 5 h net operation time (afternoon). In the evening, progression of Fe-precipitation in the gravel was successfully retained by saturating the clogging zone and stopping the flow through the channel (overnight shutdown). Each morning, flow through the clogging zone was enabled by applying a higher water level in the outflow chamber, to estimate the change in the hydraulic conductivity in the clogging zone from pressure measurements in the gravel during the evaluation step. The evaluation steps were also used to adjust the hydrochemical values that changed during the overnight shutdown periods. For the two segments of the gravel (I & II) at least 500 measurements of the hydraulic head were automatically recorded per evaluation step to calculate at least 150 single values of the hydraulic conductivity K per segment using Darcy equation:

$$K = \frac{Q}{A\cdot i} = \frac{Q}{b_{channel}\cdot(h_1+h_2)/2\cdot(h_1-h_2)/l} = \frac{2\cdot Q\cdot l}{b_{channel}\cdot(h_1^{\,2}-h_2^{\,2})} \qquad (2)$$

with K: hydraulic conductivity [m s^{-1}], Q: water volume flow [m^3 s^{-1}], A: flow cross section area in the middle between two pressure measurement points 1 and 2 [m], i: hydraulic gradient [-], b_channel: channel width [m], h_1, h_2: hydraulic head [m], l: distance between point 1 and 2 [m].

From the huge number of K-values one mean K-value was calculated per evaluation step. Furthermore, after the experiment the intensity of the clogging was evaluated by analysis of total Fe contents in the gravel by a hot oxalic acid extraction of Fe (hydr)oxides (Wen-

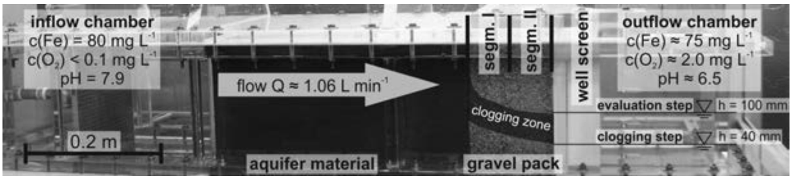

***Fig. 2** Unscaled well section model (flow channel). For a detailed description see Weidner et al. (2012).*

zel *et al.* 2001). With each of the three gravel materials, these clogging experiments were conducted at least twice, to allow for a quality control of the results.

Results

In the stationary operation phases of the column experiments, eC in the outflow remained unchanged with respect to the inflow, whereas the pH was decreased in contact with the gravel (fig. 3, left). During the stop-flow periods, higher contact times between water and gravel as well as diffusive transport were allowed in the columns, causing a decrease in pH and an increase in eC systematically in all columns. After resuming the column flow, pH and eC change back to the values recorded before the stop-flow period within at least one day.

The measurements of the (semi-)metals (fig. 3, right) in general revealed the tendency towards release of Al, Mn and Si from the gravel and capture of Fe in the gravel (negative mass flow difference ΔM_{Fe}). These effects were intensified, when higher contact times between gravel and water were admitted during the stop-flow periods, allowing for an increased hydrolysis of silica (decrease of pH). Surprisingly, in the conventional Weilerswist gravel release of Si, Al and Mn were even higher than in the alternative materials, resulting in the highest decrease of pH during stop-flow, whereas the Frimmersdorf gravel had the highest sorption of Fe and the highest increase of the electrical conductivity after the stop-flow periods. The Dorsfeld gravel only showed moderate reactions regarding pH, eC, Al, Si and Fe and no reaction at all regarding Mn. For the Frimmersdorf and Dorsfeld gravel the results of only one of the two columns were chosen for illustration, but except from the first value for (semi-)metal elution at the beginning of the experiments, the replicated experiments gave similar results.

The results of the clogging experiments (fig. 4) showed that the hydraulic conductivity of all three gravel materials decreased systematically with progression of clogging time (cumulative net operation time of the nine clogging steps). The comparison of all experiments revealed a scattering of the initial K-value, no matter if comparing different gravel materials with each other or comparing two experiments with the same gravel. These scattering effects most likely resulted from slight differ-

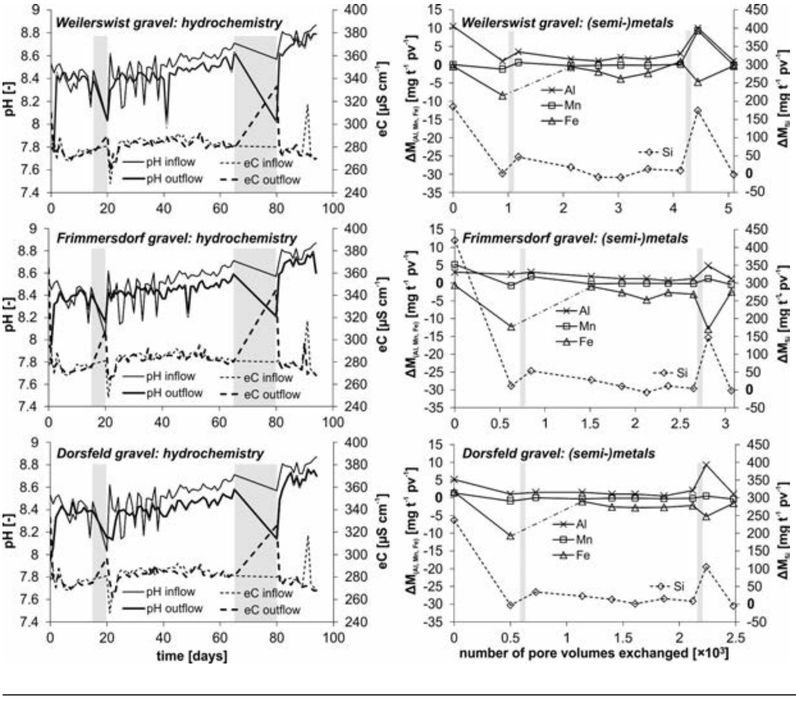

Fig. 3 *Development of pH and eC (left) and mass-flow difference ΔM*i *(outflow minus inflow) of (semi-)metal i released from the columns (right) during the long term elution experiments. Positive and negative values of ΔM*i *indicate release and capture of the considered element per metric ton of gravel material, respectively. Stop-flow periods are marked by grey areas.*

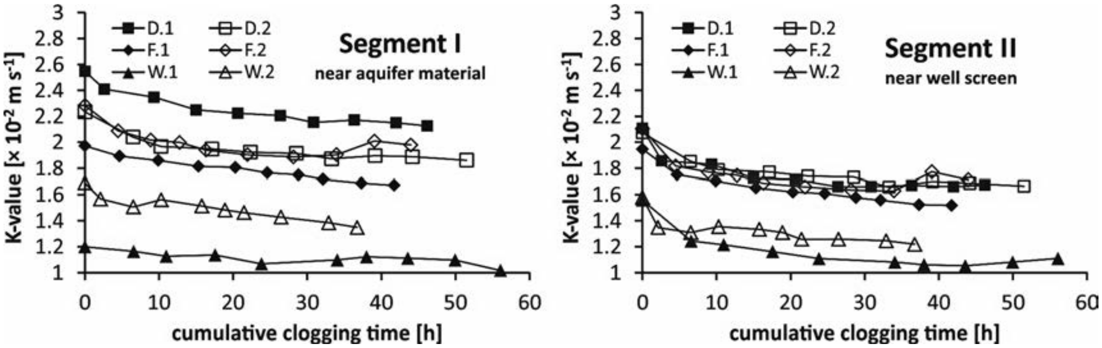

Fig. 4 Change in hydraulic conductivity K during the clogging experiments with the three considered gravel materials (D: Dorsfeld gravel, F: Frimmersdorf gravel, W: Weilerswist gravel). Repetitions of experiments with the same gravel are indicated by open symbols (D.2, F.2 and W.2).

ences in the assembly of the gravel pack in the model and were more prominent in segment I of the gravel (near the aquifer material). This could be due to vertical flow components of the near boundary flow field, varying between the assemblies of several experiments. In both segments the general level of hydraulic conductivity was somewhat lower in the conventional Weilerswist gravel in comparison to the Quaternary materials, which might be caused by a shift in the granulometry of the Weilerswist gravel towards smaller grains.

Set aside the variations in the initial situation, the hydraulic conductivity decreased more or less in the same manner and dimension in all six experiments. As the experimental duration was not exactly the same in all experiments, the initial hydraulic conductivity K_{initial} is compared to the K-value after 35 h cumulative clogging time $K_{35\mathrm{h}}$ (Table 1). Obviously the mean relative loss in hydraulic conductivity ΔK_{mean} is highest in the conventional Weilerswist gravel.

However, the increase of Fe in the gravel pack in relation to the cumulative clogging time $\Delta c(\mathrm{Fe})/\Delta t$ was very similar for all five considered experiments, with slightly less Fe attaching to the Frimmersdorf gravel. In experiment W.1, no samples for analysis of the Fe content could be taken, but the same calculation of a third experiment with the Weilerswist gravel not further described, led to an increase of iron concentration with time of 0.19 g kg^{-1} h^{-1}.

Conclusions

In comparison to the Tertiary Weilerswist gravel, the Quaternary Frimmersdorf and Dorsfeld gravels seem to possess very similar properties with respect to long term elution as well as clogging affinity. In some respects, the alternative materials seem to perform even better than the conventional DIN-conform Weilerswist gravel. The Weilerswist gravel showed the highest hydrochemical interaction with tap water within the column experi-

Parameter	Unit	D.1		D.2		F.1		F.2		W.1		W.2	
Segment		I	II	I	II	I	II	I	II	I	II	I	II
K_{initial}	×10^{-2} m s^{-1}	2.55	2.11	2.23	2.07	1.97	1.94	2.28	2.10	1.20	1.56	1.69	1.57
$K_{35\mathrm{h}}$	×10^{-2} m s^{-1}	2.17	1.67	1.88	1.67	1.70	1.54	1.93	1.66	1.10	1.08	1.35	1.22
Δ K	%	14.9	20.9	15.7	19.3	13.7	20.6	15.4	21.0	8.3	30.8	20.1	22.3
ΔK_{mean}	**%**	**17.7**				**17.7**				**20.4**			
$c(\mathrm{Fe})_{\mathrm{initial}}$	g kg^{-1}	1.10		1.10		2.03		2.03		< 0.01		< 0.01	
$c(\mathrm{Fe})_{\mathrm{max\ final}}$	g kg^{-1}	10.65		11.22		9.63		10.47		n.a.		7.93	
Δ c(Fe)	g kg^{-1}	9.55		10.12		7.60		8.44		n.a.		7.93	
Clogging time	h	46.2		51.5		41.7		44.0		56.1		36.7	
Δ c(Fe)/Δ t	**g kg^{-1} h^{-1}**	**0.21**		**0.20**		**0.18**		**0.19**		**n.a.**		**0.21**	

Table 1 Results of the clogging experiments. D: Dorsfeld gravel, F: Frimmersdorf gravel, W: Weilerswist gravel, 1: experiment 1, 2: experiment 2, n.a.: not analyzed.

ments, the lowest initial hydraulic conductivity and a somewhat higher loss in the K-value after 35 h (average of 20.4 %) in the clogging experiments.

The Frimmersdorf gravel had the second highest interaction with the tap water, especially concerning electrical conductivity and Fe sorption, while the Dorsfeld gravel showed the lowest interaction with tap water. The clogging experiments with the Quaternary materials showed no recognizably higher clogging affinity (both 17.7 % average loss in the *K*-value after 35 h) or measurable autocatalytic effect of the clogging reaction, even though high initial Fe-contents in the alternative materials were found.

Altogether, with this combined approach no substantial drawbacks for the application of the alternative gravel materials could be found. In most respects, an even better performance can be expected of the two alternative gravels. Thus, regarding mineral dissolution and clogging affinity, both of the considered Quaternary gravels can without reservations be used as gravel pack material in dewatering wells.

Acknowledgements

The authors thank Andre Banning from the Institute of Hydrogeology of RWTH Aachen University for his help with processing of hydrogeochemical data. Stefanie Lorke from the Institute of Hydraulic Engineering and Water Resources Management is acknowledged for her organizational support in operating the clogging model. Christian Forkel, Wilhelm Schlegel, Morris Reich and Martin Back from RWE Power AG are acknowledged for their constructive collaboration and RWE Power AG for financial support.

References

DEBRIV (2012) Rheinisches Braunkohlenrevier. Website of the DEBRIV – Deutscher Braunkohlen-Industrieverein – Bundesverband Braunkohle. www.braunkohle.de/pages/grafiken.php?page=255, visited March, 9th 2013

Fliegel G (1910) Erläuterungen zur Geologischen Karte von Preußen und benachbarten Bundesstaaten, Blatt Sechtem, Gradabteilung 66(16). Königlich Preußische Geologische Landesanstalt, Berlin, 73 pp

German Institute of Standardization (1998) DIN 4924: Sande und Kiese für den Brunnenbau – Anforderungen und Prüfungen. Beuth, Berlin, 8 pp

Geroni JN, Sapsford DJ (2011) Kinetics of iron (II) oxidation determined in the field. Appl Geochem 26:1452—1457.

Henkel S, Weidner C, Roger S, Schüttrumpf H, Rüde TR, Klauder W, Vinzelberg G (2012) Untersuchung der Verockerungsneigung von Vertikalfilterbrunnen im Modellversuch – Ein Beitrag zum Prozessverständnis der chemischen Verockerung in der Tagebauentwässerung. Grundwasser 17(3):157—169

Houben GJ (2004) Modeling the buildup of Iron Oxide Encrustations in Wells. Groundwater 42(1):78—82

Kemna HA (2008) A Revised Stratigraphy for the Pliocene and Lower Pleistocene Deposits of the Lower Rhine Embayment. Neth J Geosci 87(1):91—105

Quaas A (1908) Erläuterungen zur Geologischen Karte von Preußen und benachbarten Bundesstaaten, Blatt Buir, Gradabteilung 66(8). Königlich Preußi sche Geologische Landesanstalt, Berlin, 49 pp

Tamura H, Goto K, Nagayama M (1976) The effect of ferric hydroxide on the oxygenation of ferrous ions in neutral solutions. Corros Sci 16:197—207

Weidner C, Henkel S, Lorke S, Rüde TR, Schüttrumpf H, Klauder W (2011) Investigation of clogging processes on vertical filter wells using an experimental model. In: Rüde TR, Freund A, Wolkersdorfer C (Eds) (2011) Mine Water – Managing the Challenges. 11th Congress of the International Mine Water Association, RWTH Aachen, Germany, p 79—83

Weidner C, Henkel S, Lorke S, Rüde TR, Schüttrumpf H, Klauder W (2012) Experimental modeling of chemical clogging processes on dewatering wells in lignite mining. Mine Water Environ 31:242—251

Wenzel WW, Kirchbaumer N, Prohaska T, Stingeder G, Lombi E, Adriano, DC (2001) Arsenic fractionation in soils using an improved sequential extraction procedure. Anal Chim Acta 436(2):309—323

Discrimination of bursting water source by hydrochemical and stable isotope method

Yazun Wu[1], Yun Lin[2], Guoying Pan[3]

Institute of Resources & Environment, Henan Polytechnic University, Jiaozuo, 454003, China,
[1]wuyazun@163.com, [2]ylzz5211@sina.com, [3]pan-gy@hpu.edu.cn

Abstract Take a typical coal field in north China as an example, the chemical characters of water in each aquifer were founded according to the standard water samples. Compared the chemical characters between bursting water and standard water, the source of water inrush can be judged. Some disputed sample results need judging again by the indexes of hydrogeological conditions and water burst characters. Based on this method, 491 samples were analyzed. The accuracy was 80 %. This method provides a way to identify the source of bursting water in the mine.

Keywords hydrochemical, piper diagram, stable isotope, water bursting source, karst water-filling coal field

Introduction

Hebi coal mine district is located in alluvial plain of the Taihang Mountain in Henan province. It is a typical karst water-filling coal field in North China coal basin, in which the coal deposits were mainly formed in the Carboniferous to Permian periods (Han and Yang 1984). In Hebi coal mine district, there were 392 times water burst in the history. The water source of the biggest water burst was the groundwater from the Middle Ordovician carbonate aquifer, the water yield was 13,507 m^3/h and the mine was flooded (Zhao 2007). Water disasters seriously threaten the safety of coal production. From bottom to top, the main aquifers in this coalfield are Middle Ordovician carbonate aquifer (O_2), the second thin-bedded limestone aquifer of Carboniferous Taiyuan group (L_2); the eighth thin-bedded limestone aquifer of Carboniferous Taiyuan group (L_8), the coal seam roof and floor sandstone aquifer of Permian Shanxi group (S) and the Neogene conglomerate aquifer (N). The groundwater occurrence in these aquifers is the main source of mine water bursting. Due to the difference of hydrogeochemical environment during groundwater formation process in different aquifer, the hydrochemical composition and stable isotopes content of groundwater are different. The hydrochemical composition and stable isotopes content of bursting water were sampled and assayed. Bases on the characters of hydrogeochemical, the source of water bursting cloud be ascertained (Wang 1990, Hu *et al.* 2010). It is the basis for rescue and water disaster control.

The Hydrogeological Background

In hebi coal mine district, the O_2 aquifer, which thickness is 400 m and the karst fissure is well-developed. According to pumping test data, the minimum value of water discharge rate per unit drawdown is 0.67 L/s/m and the maximum value is 83.91 L/s/m, the average value is 14.02 L/s/m. The middle Ordovician carbonate is widely outcropped in the Taihang Mountain area, and it accepts the recharge of precipitation infiltration. In addition, the river leakage recharges the groundwater through the karst fissure. After accepted the recharge in mountain area, the water runoff to the piedmont from west to east, and discharges by karst spring and mine drainage. Generally, if the mine water bursting which source is O_2 karst water, the water yield is greater than 100 m^3/h.

The L2 aquifer with an average thickness of 7 m has a stably distributed, but the karst fissure is poor-developed and inhomogeneous, and the water abundance is greatly different in spatial. According to the pumping test data, the water discharge rate per unit drawdown is about 0.012-2.619 L/s/m, the hydraulic conductivity is about 0.392-28.84 m/d. Because of the L_2 aquifer has limited outcrop area and no recharge source, the karst water is static reserves and easy to drainage. The water yield which comes from the L_2 aquifer is usually less than 100 m^3/h. Once O_2 water and L_2 water has hydraulic connection in some area by the faults, water yield can reach to hundreds of cubic meters per hour.

The L8 aquifer with an average thickness of 3–5 m has a stably distributed, but the karst fissure is poor-developed. It has little recharge source and the occurrence of water is limited. And water yield usually less than 50 m^3/h, it is 13.2–48.8 m^3/h.

The Shanxi group coal seam roof and floor is sandstone aquifer, in which the fracture is poor-developed and the groundwater is limited. During the mining, the fracture water in sandstone aquifer can discharge into the mine through natural fracture, mining fracture and fault, but the water yield is very small.

Neogene conglomerate aquifer is distributed in the southern part of hebi coal mine district with the thickness is 30 – 80 m. In this aquifer, the pore and fracture well developed, the precipitation and surface water are the main recharge sources. It is an important water-filling source of mining for the shallow coal seam.

Hydrochemical characteristics of the groundwater from each aquifer

In order to set up the hydrochemistry identification standard of each aquifer, multiple water quality surveys were carried out in Hebi coal mine district. The 491 groundwater were sampled for water quality analysis. The index include: HCO_3^-, Cl^-, SO_4^{2-}, K^+, Na^+, Ca^{2+}, Mg^{2+}, hardness, total dissolved solid (TDS), and pH. The groundwater hydrochemical characteristics of each aquifer are as follows (tab.1, fig. 1).

O_2 Karst water

The hydrochemical composition of Ordovician limestone karst water is controlled by water-

Groundwater type (Number of samples)		Major cation			Major anion			PH	Hardness	TDS
		Na^++K^+	Ca^{2+}	Mg^{2+}	Cl^-	HCO_3^-	SO_4^{2-}			
O_2 karst water (184)	average	12.34	79.69	20.99	13.19	298.79	31.71	7.78	281.56	330.16
	SD	4.14	22.36	5.59	5.58	53.96	17.28	0.25	61.33	87.88
L_2 karst water (54)	average	22.05	162.45	28.51	15.00	350.65	233.64	7.39	526.36	655.28
	SD	6.87	35.12	7.40	4.81	76.37	60.10	0.27	80.04	96.75
L_8 karst water (62)	average	117.93	73.77	25.90	25.20	467.73	76.62	8.20	290.84	533.52
	SD	37.67	22.49	8.05	11.34	89.04	26.51	0.39	60.47	125.60
Sandstone fissure water (106)	average	281.81	17.88	7.84	53.97	592.87	42.56	8.54	76.59	737.54
	SD	78.89	9.67	4.84	22.64	156.26	14.12	0.45	23.49	231.49
Conglomerate pore-fissure water(42)	average	35.21	83.49	22.00	31.78	289.84	44.99	7.98	299.04	442.37
	SD	12.36	25.01	5.33	8.42	35.95	15.20	0.30	86.95	94.08
Goaf water (43)	average	283.77	262.85	92.66	52.04	421.77	1101.95	7.98	1037.92	2066.85
	SD	58.08	64.00	24.09	13.69	107.58	244.29	0.40	243.60	428.55

***Table 1** The statistics characteristic of hydrochemical components*

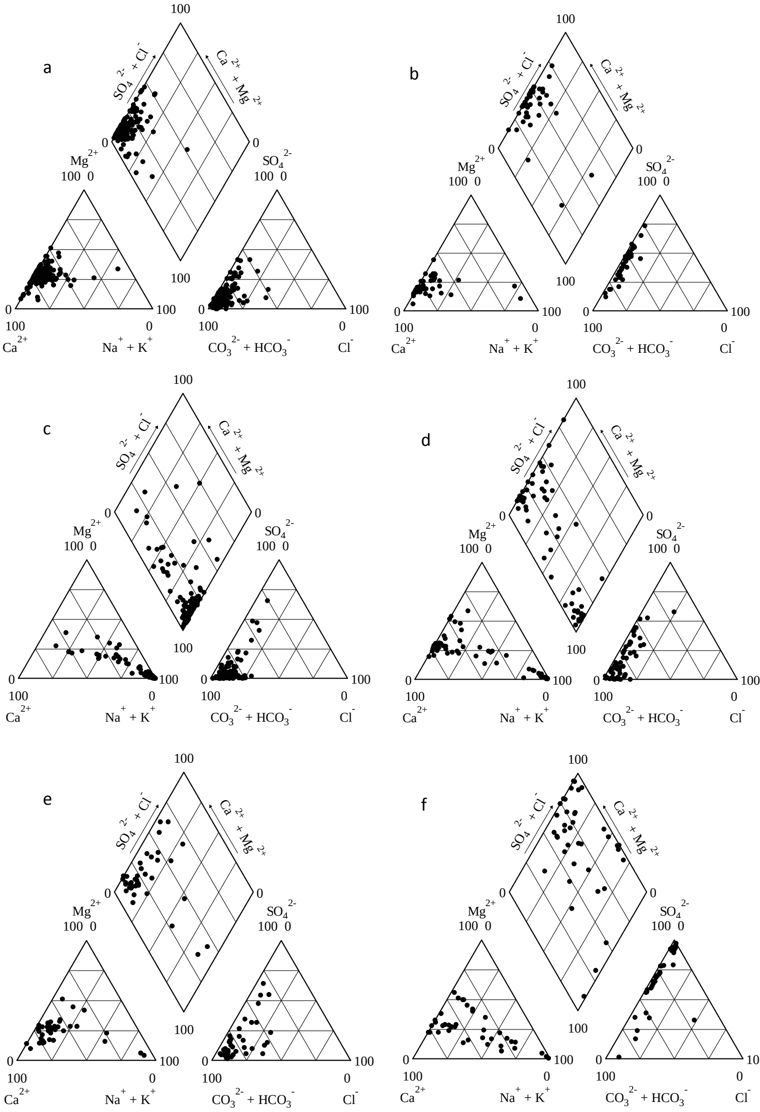

***Fig. 1** The piper diagram of groundwater a-O_2 karst water; b-L_2 karst water; c-L8 karst water; d-Sandstone fissure water; e-Conglomerate pore-fissure water; f-Goaf water*

rock interaction. In the groundwater, the cations are dominated by Ca^{2+} and Mg^{2+}, and the anion is HCO^{3-}. The O_2 karst water has some typical characters as follows. The hydrochemical type is $HCO_3^-Ca\cdot Mg$ (fig. 1-a). The TDS are at a low level, ranging from 200 to 400 mg/L. The total hardness is very low, ranging from 200 to 350 mg/L. The concentration of Cl^- is less than 25 mg/L. The concentrations of Ca^{2+} and Mg^{2+} vary from 60 to 90 and 15 to 30 mg/L. The percent meq/L of (Ca^{2+}+Mg^{2+}) is more than 90 %, and the percent meq/L of HCO_3^- is more than 80 %.

L_2 karst water

Affected by the natural in sediments and water-rock reaction, the ions of the water are dominated by HCO_3^-, SO_4^{2-}, Ca^{2+} and Mg^{2+} in L_2 aquifer. The hydrochemical type of L_2 water are $HCO_3\cdot SO_4$-$Ca\cdot Mg$ and $SO_4\cdot HCO_3$-$Ca\cdot Mg$ (fig. 1-b). The TDS are at a higher level, ranging from 500 to 700 mg/L, the average value is 655.28 mg/L. The concentration of SO_4^{2-} is range from 150 to 700 mg/L, the average value is 233.6 mg/L, and the percent meq/L is range from 30 % to 55 %. The concentrations of Ca^{2+} and Mg^{2+} in L_2 water are higher than O_2 water.

In L_2 water, the concentrations of Ca^{2+} and Mg^{2+} vary from 100 to 200 and 24 to 36 mg/L.

L_8 karst water

L8 aquifer is closed to sandstone aquifer and coal seam that the hydrochemical characters of L8 water are very complex. The concentration of SO_4^{2-} is higher when sulfide which comes from the coal seam dissolves into L8 aquifer. The mainly hydrochemical type of L8 water are HCO_3-Na•Ca•Mg, HCO_3•SO_4-Ca•Na•Mg and HCO_3-Ca•Mg. There also have a kind of water (HCO_3-Na) when lots of sandstone water flow in to L_8 aquifer (fig. 1-c).

Sandstone fissure water

The albite and potassium feldspar content are higher in sandstone stratum. Under the effect of weathering, hydrolysis and ion exchange function, Na+ and k+ are leached into the groundwater, while Ca^{2+}, Mg^{2+} in the groundwater precipitate with the forms of $CaCO_3$ and $MgCO_3$. This process leads to the cations are dominated by K+ and Na+ in the sandstone water. The hydrochemical characteristics of typical sandstone water are: (1) The hydrochemical type is HCO_3-Na, and the percent meq/L of ($Na^+ + K^+$) is more than 85 %, the percent meq/L of ($Ca^{2+} + Mg^{2+}$) is less than 15 %; (2) The total hardness is low, ranging from 40 to 90 mg/L; (3) The concentrations of HCO_3^-, CO_3^{2-} are high, ranging from 400 to 700 mg/L and 10 to 50 mg/L, respectively; (4) The percent meq/L of ($HCO_3^- + CO_3^{2-}$) which is higher than ($Ca^{2+} + Mg^{2+}$) is ranging from 75 % to 90 %; (5) The pH is 8.0-9.0, and the water is alkaline (fig. 1-d).

Conglomerate pore-fissure water

The hydrochemical type of conglomerate pore-fissure water are HCO_3-Ca•Mg, HCO_3•SO_4-Ca•Mg and HCO_3•Cl-Na•Ca•Mg (fig. 1-e). When the hydrochemical type is HCO_3-Ca•Mg, it is difficult to distinguish the conglomerate pore-fissure water and O_2 water. Because of the aquifer is shallow, the water quality is affect easily by human activity. In the conglomerate pore-fissure water, the concentrations of Na^+, Cl^-, SO_4^{2-} and TDS are higher than those in O_2 water.

Goaf water

The goaf water is the groundwater which exists in the worked-out section and the goaf. Because of the distribution and quantity are difficult to distinct, the goaf water bursting is emergency, unpredictability, and disaster. Generally, goaf water is well sealed, that the effect of water-rock interaction leads to the higher concentrations of SO_4^{2-} and TDS. And the concentration of SO_4^2 is greater than 400 mg/L. The TDS is range from 900 to 8000 mg/L. The hydrochemical type mainly are SO_4-Ca•Mg•Na and SO_4•HCO_3^--Ca•Mg•Na (fig. 1-f). It can be distinguishes with other groundwater according to the concentrations of SO_4^{2-} and TDS.

Distinguish the source of water burst by hydrochemical characters

The obvious differences of hydrochemical characters between different groundwater in different aquifers provide a way to distinguish the source of bursting water. For example, the hydrochemical type of groundwater in O_2 aquifer is HCO_3-Ca•Mg. The type in sandstone aquifer is HCO_3-Na, Na^+ and CO_3^{2-} are higher and the total hardness is low in this kind of water. The type in L_2 aquifer is HCO_3•SO_4-Ca•Mg or SO_4•HCO_3-Ca•Mg. The type in L_8 aquifer is the mixture of sandstone water and O_2 water. The goaf water is difference with other kinds of water because of the obviously higher in TDS and SO_4^{2-}. The source of burst water can be distinguished by the difference of hydrochemical composition and stable isotopes content of groundwater in different aquifer. However, when the difference is not apparent, this method is infeasible. For instance, conglomerate water has the same hydrochemical type with O_2 water that is HCO_3-Ca•Mg. Thus, it is difficult to make a distinction between these two kinds of water only by hydrochemical method. Under this circumstance, the effective way to solve this problem is combining with the formation condition and character of water burst. The implementation steps of distinguishing water source by hydrochemical are as follows.

Step one, the water source were analyzed according to the major ions or the hydrochemical type. For example, the percent meq/L of Na+ is more than 80 %, it must be sandstone water. If the percent meq/L of SO_4^{2-} is higher than HCO_3^-, which means this kind of groundwater is goaf water.

Step two, the water samples were identified in detail according to water quality index that are ion content, molar concentration, pH, hardness, alkalinity, TDS, the ratio between different ion and so on.

Step three, the results need revising and confirming by hydrogeological conditions, the location and characteristics of bursting water.

491 water samples were analyzed based on this method. The results show that 345 samples can be distinguished correctly by hydrochemical type and water quality index, and the accuracy rate is 70 %. 395 samples can be distinguished correctly combined with the hydrogeological condition, and the accuracy rate is 80 %. The remaining samples are L_8 water and O_2 water. Because of the two kinds of water has the similar hydrochemical type, and the water quality index are also the same, it is difficult to distinguish. But the water yield of L_8 and O_2 are different. It is abundant if the bursting water comes from O_2 aquifer, and the time of duration is long, the water yield is stable. On the contrary, it is L_8 water which instantaneous water yield is only 50 m^3/h, and the water yield reduced fast.

Distinguish the source of water burst by stable isotope

The altitude of karst water recharge area distribute within the scope of 500-1200m, which is 300-800m higher than piedmont plain. $\delta^{18}O$ of precipitation in mountainous area is -9.42 – -11.75 ‰, δD is -71.9 – -81.7 ‰. Meanwhile, $\delta^{18}O$ of precipitation in Hebi city is -8.40 – -8.95 ‰, δD is -59.5 – -65.2 ‰. The stable isotope in O_2 karst water has the relationship with the mountainous area precipitation and surface water caused by runoff process. $\delta^{18}O$ of O_2 water is -9.18 – -9.76‰, δD is -67.1 ‰ – -71.4 ‰. Conglomerate aquifer distributes at piedmont, and the groundwater accepts the recharge of precipitation that its stable isotope is similar with precipitation in plain terrain. $\delta^{18}O$ of conglomerate water is -8.53 – -8.76‰, δD is -63.9 – -71.4 ‰. Sandstone aquifer is occurrence in coal measure strata. Most of the sandstone water is paleogroundwater, which is due to their low velocities and long flow paths, and with a little bit modern precipitation. $\delta^{18}O$ of sandstone water is 9.8 –-10.4‰, δD is -70.1 –-73.1‰. The outcrop of L8 and L2 aquifers banded distribute at piedmont and the recharge source is local precipitation. It also has the relationship with O_2 water. $\delta^{18}O$ of L_8 water is -9.36 – -9.55‰, δD is -66.5 –-68.9 ‰. $\delta^{18}O$ of L_2 water is -9.25 –-9.98‰, δD is-65.9 –-72.1‰.

δD and $\delta^{18}O$ are different in different aquifer in Hebi mine. There have some obvious subareas in the Fig. 2. Different source of groundwater has its distribution area. We established a simple model based on the characters of isotope to analyze the source of water burst. The conglomerate water and sandstone water cloud be easy distinguish from karst water as shown the figure. The stable isotope method improves and complements the accuracy of hydrochemical method.

Conclusion

Due to the difference of hydrogeochemical environment in groundwater formation process in different aquifer, the hydrochemical composition and stable isotopes content are different. Once the mine water burst, the source of bursting water canbe ascertained by the hydrochemical composition and stable isotopes content. The results must be correct by the characteristics of water burst and geological conditions. Based on this method, 491 samples were analyzed. 395 identified results are accu-

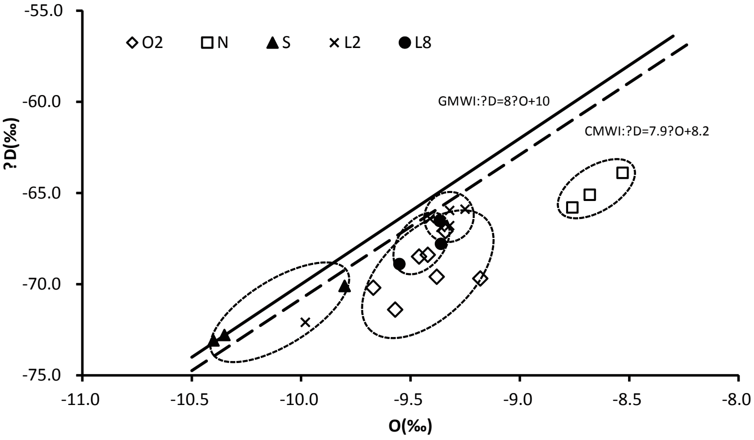

Fig. 2 *The relationship between δD and$\delta^{18}O$*

rate, and the accuracy is 80 %. In addition, the stable isotope of different groundwater has obvious distribution area, this method proved a way to distinguish the source of groundwater.

Acknowledgements

The data were from the reports that the author presided. This study was funded by the Doctor Foundation of Henan Polytechnic University (No: B2012-080).We also thank Guojun Chen for the useful suggestions.

References

Han D, Yang Q (1984) China Coal Geology, 2nd edn. Publishing House of Coal Industry, Beijing

Zhao T (2007) Comprehensive Prevention and Control Technology of Ordovician limestone water in North China. Publishing House of Coal Industry, Beijing

Wang Y (1990). The application of hydrochemistry method on the prevention of mine sudden flooding. Jo Shandong University of Science and Technology, (1):11-17

Hu W, Ma Z and Cao H (2010) Application of Isotope and Hydrogeochemical Methods in Distinguishing Mine Bursting Water Source. J Earth Sciences and Environ, 32(2), 268–271

6

RELIABLE MINE WATER CLOSURE

RELIABLE
MINE WATER CLOSURE

Innovative Mine Water Treatment in Post-Mining-Areas of Germany

Friedrich-Carl Benthaus, Beate Lucke

Lausitzer und Mitteldeutsche Bergbauverwaltungsgesellschaft mbH (LMBV), Knappenstr. 1, 01968 Senftenberg, fc.benthaus@lmbv.de, beate.lucke@lmbv.de

Abstract The lignite mining dominated landscape in the Lausitz and Leipzig district is characterized by a vast mined-out area which includes 240 km² pit lakes. The groundwater depression cone covers an area of about 2100 km² at the Lausitz, and 1200 km² in the Leipzig district. Water treatment is required either for the lake water bodies or the discharge waters. Besides conventional liming, development work is carried out on test implementation with soda ash. Alkalinity losses have been recognized due to sediment exchange. Innovative technologies are developed for *in situ* aquifer treatment by microbial sulfate reduction, resulting in a 40 % sulfate reduction as well as a 90 % iron reduction. Future development is to be carried out in the groundwater flow alongside a river bank.

Keywords Innovative treatment, soda ash, microbial sulfate reduction

Introduction

In the Lausitz and Leipzig mining areas lignite extraction resulted in about 50 large open mine pits as well as about 200 smaller residual openings. Open cast mining is actually the most efficient method of extracting lignite, which is located in shallow depth in tertiary and quartery layers of sand, clay and gravel. But this has a severe impact on the surface and on groundwater: the mining dominated landscape in the Lausitz area is for example characterized by 800 km² of mined-out area, followed by vast dump areas as well as 140 km² pit lakes (Fig. 1). The groundwater depression cone covers an area of about 2100 km².

Surface and groundwaters are affected by acid mine drainage (AMD). The generally accepted aim of remediation is the recovery of surface and groundwaters, balanced to a nearly stable level as well as reducing long lasting AMD.

In order to achieve a balanced system of end lakes, these lakes have been flooded with 3.8 Gm³ water diverted from nearby rivers, ongoing mines and groundwater inflow since 1995. The remediation aims to convert the water quality from pH values 2 or 3 to values between 6 and 8. A decrease of dissolved aluminum and iron as well as a decrease of sulphate concentration below the level of corrosion is important in order to eliminate the human threshold for health and ecological problems. In general, dissolved iron is not toxic to humans, but causes ochre precipitation along the outflow to surface streams and reduce biological life within these streams.

To optimize this flooding process, the forecast of water quality development is inevitable. Based on ground- and surface water modeling, hydro chemical calculations are carried out to predict the amount of acidity which has to be treated during the neutralization process as well as sulphate and iron reduction along the lifespan of the lake.

Mine water treatment

Flooding with surface waters from nearby rivers is considered the most effective way to stabilize the water household by means of quantity and quality. Adding alkaline substances is the traditional method of mine water treatment used in German pit lakes (Geller *et al.* 2012). The first time such treatment took place was at lake Senftenberg (1972–

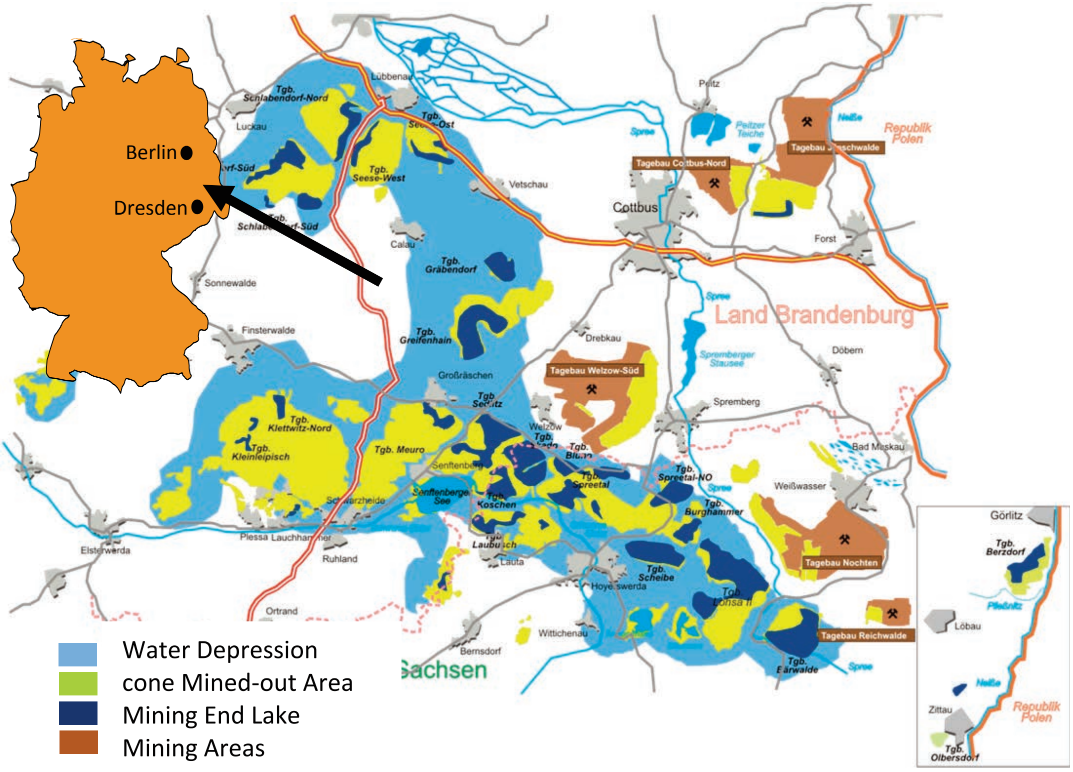

Fig. 1 *Impact on Groundwater in the Lausitz District due to Lignite Mining*

1975), followed by liming lake Koschen (2004–2005) and lake Burghammer (2009–2011).

In order to promote innovative techniques in water treatment of AMD, LMBV has launched a program called "Pilot- und Demo-Vorhaben". Within this program, new approaches derived from scientific research are tested full-scale and onsite. Based on basic research, application-oriented prototype testing proposals are evaluated according to feasibility, sustainability and economic results. After positive evaluation, these proposals are turned into testing projects either in dump areas, in the water bodies themselves or at the outflow of the lake. More than 80 proposals have been presented to and reviewed by LMBV over the past seven years out of which no more than twelve have been implemented. Few of these treatment techniques are ready to be implemented in remediation work.

The development of innovative liming technologies for in-lake treatment was focused on mobile treatment plants. Innovative neutralization technologies on mobile plants floating on the lake surface have been developed. Optimizing the liming process at Scheibe lake site, 380 mmol alkalinity were added in 16 weeks with effectiveness up to nearly 80 % on raw materials used. Further development work had been done in creating a hydrogen buffer by low suspension mixed in the lake waters. A specific technology developed underneath a special ship allows for high effectiveness during the distribution of the lime in the lake areas. Future development work is carried out on test implementation with hydro carbonate buffering with CO_2 gas injection. Further neutralization reagents are to be tested.

In-lake neutralization of Lake Bockwitz with soda ash

Lake Bockwitz consists of a number of smaller lakes within the former Leipzig mining area.

The Borna-Ost open pit was mined from 1961 to 1992. The open pit area is surrounded by dumps of tertiary und quartery materials to the south and west side, and by undisturbed terrain to the north and east. This area consists of glacial and fluvial sediments which are truncated by the bank slopes and laterally connected to the dump terrain. The flooding from 1993 to 2004 was realized by groundwater inflow originating from the tertiary fluvial aquifers. About 85 % of all inflow entered the lake's epilimnion laterally. The drainage area (3.1 km^2) is mainly comprised of bank slopes, of which about 30 % are uncovered (blank substrate and flutes), while 30 % are covered by scattered pioneer vegetation and grassland, 15 % by comprehensive grassland, and 25 % by young stands of trees (birch and pine). Surface runoffs and upstream interflow from the southern dump area enter Lake Bockwitz with low acidic load (Fig. 2).

From the beginning, the lake Bockwitz water was highly acidic (pH 2.7, Fe_{tot} 55 mg/L, Al_{tot} 19 mg/L) and did not meet the state authority criteria (pH >6, Fe_{tot} <3 mg/L, Al_{tot} <0.5 mg/L). Based on expert studies (Guderitz *et al.* 2003), in-lake treatment with soda ash was identified as the most reasonable treatment. Beginning in March 2004, light soda ash (99.4 % Na_2CO_3) was injected into the lake just below the surface through a floating pipeline located in the southern part of the lake. Within six years (2004–2011), a total of 17.2 kt of soda ash was supplied. Initial treatment shows a maximum efficiency of 62 %. It is estimated that 10 % of the added alkalinity neutralized the existing acid load from the surrounding overburden slopes and subsurface sources, 20 % were consumed by neutralization processes in the upper part of the lake sediment, and 5 % were consumed by losses through calcite precipitation. Considering the additional sinks of alkalinity, the soda treatment efficiency was between 90 and 95 %.

Even lake sediments have been identified by Boden- und Grundwasserlabor Dresden (BGD) as a source of net acidity through ion exchange processes, initially enhanced by soda treatments. However, the affected sediment depth will be limited (< 0.5 m), and residues of continued soda treatments may even provide a buffering capacity on the sediment surface.

Along with the soda additions, the acid inventory decreased and the sediment pH value increased from about pH 3 to 6.5. Later, the loss of acidity (*i.e.* H^+) in the sediment at this location was found to be in the same range as the increase of total sodium and calcium concentrations in the sediment bulk. Over 80 % of Na_2CO_3 in the sediment belonged to the exchangeable fraction. It can be assumed that about 10 % of the total Na+ supply with soda ash have been taken up by the sediment surface. The most consistent explanation for this phenomenon is cation exchange of Na+ and Ca^{2+} ions with protons absorbed into the sediment, thus enhancing the upward flux of acidity into the lake water (Fig. 3).

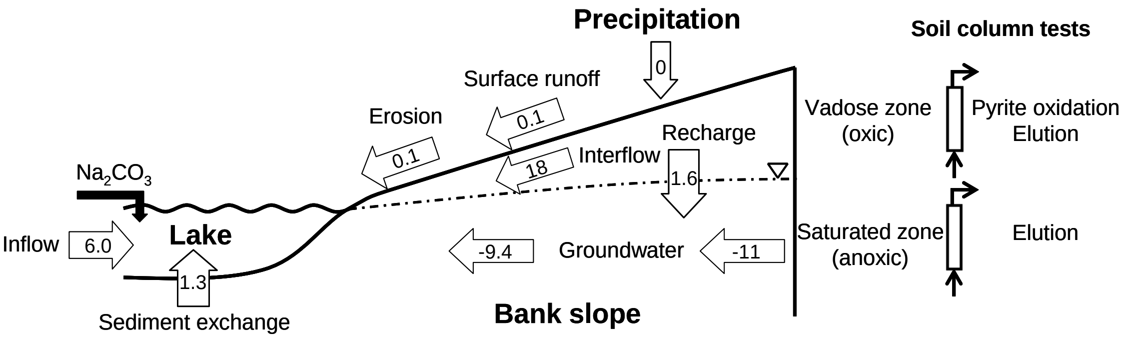

Fig. 2 *Major fluxes into lake Bockwitz, BNC and ANC fluxes in kmoL/d (Ulrich et al. 2012)*

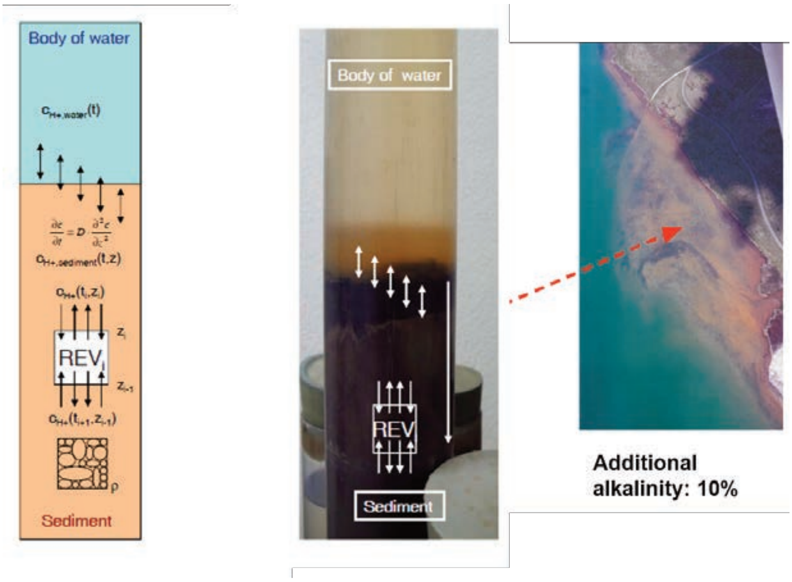

Fig. 3 *Exchange Process at lake sediments (Ulrich et al. 2012)*

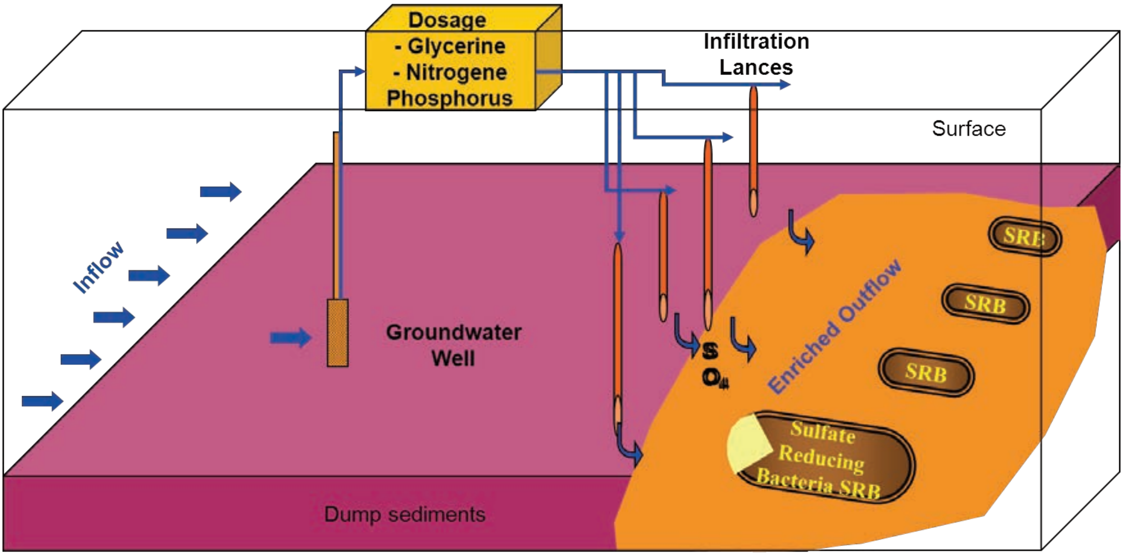

Fig. 4 In-situ *aquifer treatment plant for microbial sulfate reduction (Gast et al. 2010)*

Groundwater *in situ* aquifer treatment through microbial sulfate reduction

In order to reduce the acidic impact of groundwater inflow to the mining lakes, an innovative *in situ* aquifer treatment was developed.

Based on previous studies, the enhancement of the microbial sulfate reduction is considered to be the most promising method to improve groundwater quality in the upstream as well as in the downstream of lakes. Therefore, the Forschungsinstitut für Bergbaufolgelandschaft (FIB e.V.) and the Technische Universität Cottbus (BTU) designed an approach for *in situ* treatment of aquifers influenced by pyrite oxidation (Gast *et al.* 2010; Fig. 4). This approach aims to enhance the biochemical reduction of sulfate and iron in order to precipitate iron-sulfides in the aquifer. To enable the microbial-driven sulfate reduction, biodegradable organic nutrients are added to stipulate microbial catalyzed sulphate reduction. This was infiltrated by newly developed injection lances into the dump area. This led to the creation of a reactive zone in the aquifer that caused a significant reduction of sulfate, iron and potential acidity. The infiltrated glycerin was completely metabolized. This produced a carbon dioxide input to the water and generated an additional buffering capacity.

The quality of the groundwater is determined through infiltrated waters from Lake Partwitz as well as through the input of oxidized and acidic leachate from overlying sediments. The water that needs to be treated has a pH value of 4.9 – 5.1, concentrations of Fe^{2+} of about 230 – 320 mg/L and SO_4^{2-} concentrations of about 950 – 1150 mg/L.

The pilot plant was erected on "Skadodamm", an overburden dump between two mining end lakes. The hydraulic conductivities of this overburden are at about $k_f \approx 1 \cdot 10^{-5}$ m/s (light loamy sand), which are good conditions for *in situ* treatment.

In the middle of the pilot plant, a groundwater well hoists part of the water that passes through to the surface dosage station. At this stage, glycerin, nitrogen, and phosphorous fertilizer are added through an automatic dosage system. This mixture is directly infiltrated back into the aquifer by four injection lances (DSI-lances, Wils & Water GmbH, Germany) which are easy to install and highly economic. Infiltration takes place in depths of 15 m with rates between 0.8 to 1.8 m^3/h. The lances are charged individually with an automatic alternation every hour.

The dose of glycerin is based on the conditions mentioned above in order to allow 2.6 mmol/L in the infiltration water. In relation to the carbon input, nitrogen was added in a ratio of C/N = 25 and phosphorous in a ratio of C/P = 400. These ratios were derived from the estimated chemical structure of the microbial biomass. Within an operation period of 400 days, the groundwater in the downstream clearly shows an enhanced sulfate reduction (Fig. 5). Sulfate concentrations decreased by about 40 %; iron was removed completely. After a pause in the treatment of about 100 days, the sulphate and iron reduction immediately started after injection of nutrition. Meanwhile, the higher sulfide concentrations under special conditions allude to a lack of solute iron to be precipitated as FeS. This limitation requires a permanent monitoring and modulation of the input of organic matter. Otherwise, concentrations of solute sulfide may cause problems if outgassing of H_2S is conducted in a notable volume. In addition to the control of the organic matter input, an operation mode with pronounced breaks helps to mix iron-rich groundwater with the treated groundwater. The decomposition of glycerin is associated with an increase of TIC

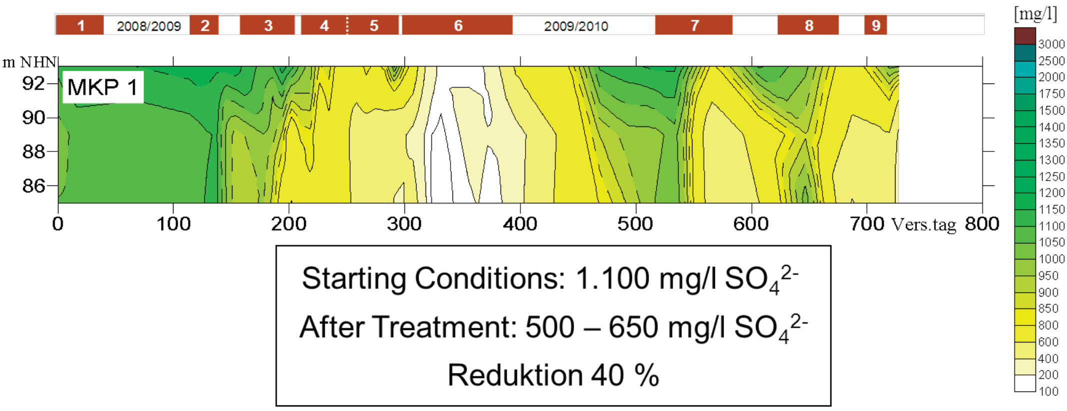

***Fig. 5** Sulfate reduction during treatment period*

that generates a considerable buffering capacity in the groundwater. This means that the groundwater was changed from an acidic quality to a significant buffering quality (Schöpke *et al.* 2013).

The operation of the aforementioned pilot plant was very successful. Furthermore, an adoption of this plant is projected to prevent groundwater inflow into nearby rivers banks.

References

Gast M, Schöpke R, Walko M, Benthaus F-C (2010) *In-Situ*-aquifer treatment by Microbial Sulfate reduction, in: Mine Water and Innovative Thinking, IMWA Sydney 2010, 119–122

Geller W, Schultze M, Kleinmann R, Wolkersdorfer C. (2013) Acidic Pit Lakes – The Legacy of Coal and Metal Surface Mines: Environmental Science and Engineering. – 525 p.; Heidelberg (Springer).

Guderitz I, Müller K, Bethge C, Neumann V, Nitsche C (2003) Limnological forecast on the pit lakes within the open-cast mining district Borna-Ost/Bockwitz (unpublished), LMBV mbH, Dresden, Dec., 2003

Schöpke R, Gast M, Walko M, Haubold Rosar M, Benthaus FC (2013) Entwicklung eines Sanierungsverfahrens für potentiell saure Kippengrundwässer im Lausitzer Braunkohlenrevier, gwf Wasser-Abwasser April 2013, 340–347

Ulrich K-U, Bethge Chr, Guderitz I, Heinrich B, Neumann, V, Nitsche C, Benthaus F-C (2012) In-Lake Neutralization: Quantification and Prognoses of the Acid Load into a Conditioned Pit Lake (Lake Bockwitz, Central Germany) in: Mine Water and the Environment (IMWA), 31(4), 320–338.

Impacts of Re-Rising Groundwater Levels in Rehabilitated Opencast Mining Areas – Prediction Tools and Potential Measures of Damage Limitation

Friedemann Brückner[1], Helena Ceranski[1], Holger Mansel[1], Christiane Uhlig[2]

[1]*Ingenieurbüro für Grundwasser GmbH, Nonnenstraße 9,*
04229 Leipzig, Germany, f.brueckner@ibgw-leipzig.de
[2]*Lausitzer und Mitteldeutsche Bergbau-Verwaltungsgesellschaft mbH, Walter-Köhn-Straße 2,*
04356 Leipzig, Germany, christiane.uhlig@lmbv.de

Abstract Post-mining sites in the Central German Lignite Mining Area are characterized by filled pit lakes. In this context the groundwater re-rose to its historical level with the result of potential damages on building basements. In details, a large-scale groundwater model based on the simulation software PCGEOFIM was used to predict the potential impact on the buildings of the city of Delitzsch as well as the effect of possible measures of damage limitation. According to the modeling results, the only reasonable measure to protect the large number of affected buildings was the improvement of the bed of the local river. The objective of the planned extension measures was the re-establishment of the connectivity between aquifer and river in order to ensure stable influent flow conditions and consequently declining groundwater levels.

Keywords lignite mining, rehabilitation, re-rising groundwater levels, groundwater model, PCGEOFIM, Central German Lignite Mining Area, riverbed extension measures

Introduction

Lignite mining has shaped the region between Leipzig and Bitterfeld with the city of Delitzsch in the center (Fig. 1) for more than a century. In this northern part of the "Central German Lignite Mining Area" large-scale transformation processes took place. The installation and operation of opencast mining led to land devastation, relocation of surface waters from the operating area, lowering groundwater level and changes of groundwater quality. Thus, mining had and is still having a profound impact on the water balance and water quality of this area.

Due to the location of Delitzsch between the two opencast mines "Delitzsch Southwest" and "Goitzsche/Holzweissig/Rösa" as well as the long term groundwater use for water supply the local groundwater level was lowered significantly. As a result, the former floodplains of river Lober dried up and parts were designated as residential areas.

The rehabilitation of the opencast mines started in 1993. At first, stable embankments were constructed. Afterwards, groundwater lowering wells were turned off and the flooding of the empty lignite pits began. Against this background defining the final water levels of the pit lakes as well as predicting the rate and impact of flooding processes were required. The groundwater flow of the whole region has been modeled with the large-scaled "Groundwater Model Leipzig North" (HGMN) based on the simulation software PCGEOFIM.

Final lake water levels were reached in 2005 (mining area "Goitzsche/Holzweissig/Rösa") respectively in 2010 (Lake Werbelin in the mining area "Delitzsch Southwest"). Consequently, groundwater level was re-rising up again to its historical level closely below the surface. As a result, potential damages to building basements were likely.

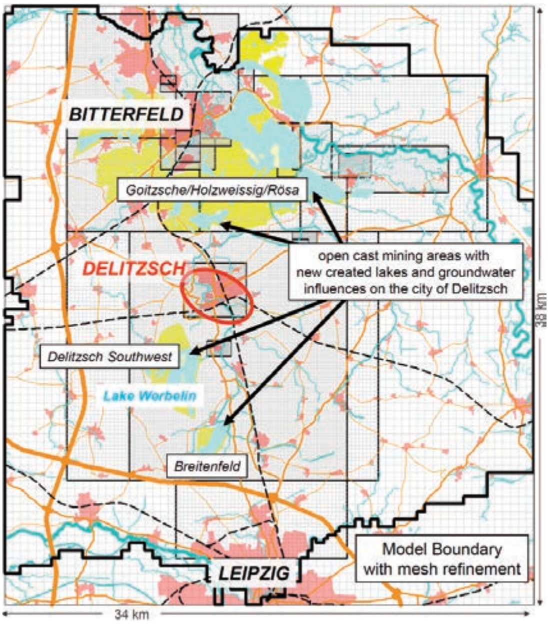

Fig. 1 *Location of study area within the “Groundwater Model Leipzig North”*

Prediction of the potential impact on buildings

Modeling system PCGEOFIM

PCGEOFIM (Sames *et al.* 2010) is a finite volume groundwater flow and transport model that is specifically designed for mining and post-mining areas. It provides some special features to be appropriate for the mining-specific conditions. The geological structure and subsurface parameters can be specified as time-dependent allowing for modeling the excavation of mine pits, deposition of mining dumps and creation of lakes all in one model run. The finite-volume method is characterized by a complete mass balance and provides unlimited telescopic mesh refinement. While working with a regular grid, multiple nested grid refinements that may overlap can be used to get higher resolution in areas of special interest.

The modeling system offers many ways to specify spatially varying groundwater recharge from constant in time as well as dependent on groundwater level below surface up to a sophisticate coupling with a rainfall-runoff-soil-water-budget model (Blankenburg *et al.* 2012).

PCGEOFIM provides a simple but very useful mechanism to reproduce the interactions between lakes and groundwater. The lake is represented as a water level – water volume relationship. In- and outflows such as groundwater and rivers are budgeted. Precipitation and evaporation yield a new lake water volume and hence a new water level. This water level is used as head for Cauchy boundary conditions that act jointly as “the lake”. Fig. 2 shows how groundwater model elements are either vertically or horizontally coupled to the lake.

Rivers can also be represented by several time changing Cauchy boundary conditions that act jointly while the surface water level is calculated with Manning’s formula based on the local discharge. Lots of special boundary conditions such as vertical and horizontal multi-level wells and defined outflow levels of lakes as well as sophisticated connections between rivers, lakes, and pipelines with control mechanisms provide a high level of representation of the natural system.

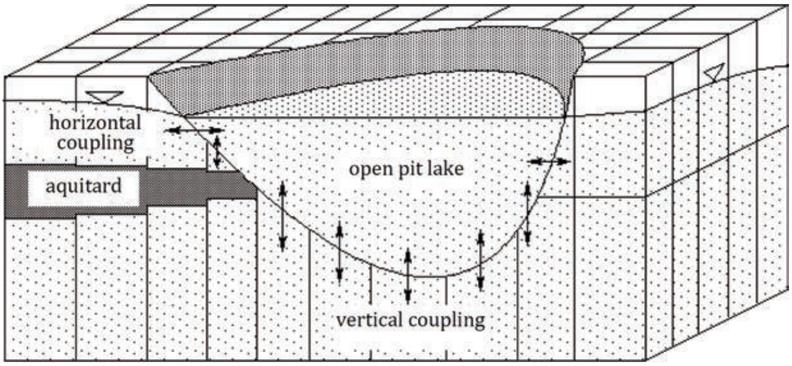

Fig. 2 *Representation of boundary condition “lake” in PCGEOFIM*

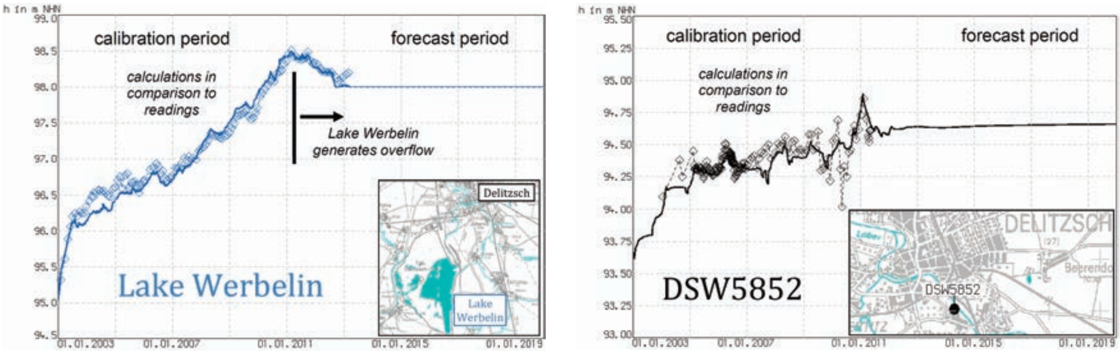

Fig. 3 Comparison of measured (rhombs) and simulated levels (solid line) at Lake Werbelin (left) and at a groundwater observation point in Delitzsch in the vicinity of river Lober (right)

Large-scale Groundwater Model Leipzig North (HGMN)

The large-scaled "Groundwater Model Leipzig North" (Mansel *et al.* 2011) covers 1079 km^2 with a maximum width of 38 km and a maximum length of 34 km (see Fig. 1). The telescopic nested mesh refinement uses widths from 500 m up to 30 m. The calculation of unsteady groundwater flow considers raising groundwater levels, emerging lakes and relocated rivers and creeks. The calibration period starts 2003 with variable groundwater recharge (monthly time step) and daily on-lake precipitation/evaporation. The main calibration parameters include soil saturated hydraulic conductivity as well as permeability of riverbed material. The forecast period begins 2012 with average climatic values corresponding to the time series 1980-2011.

Fig. 3 shows the measured and simulated rising water level at open pit lake "Werbelin" southwest of Delitzsch as well as the re-rising groundwater level at a groundwater observation point in Delitzsch with its unsteady flow conditions.

In details, the model "HGMN" was used to predict the potential impact on buildings. A building is considered, if the calculated differ-

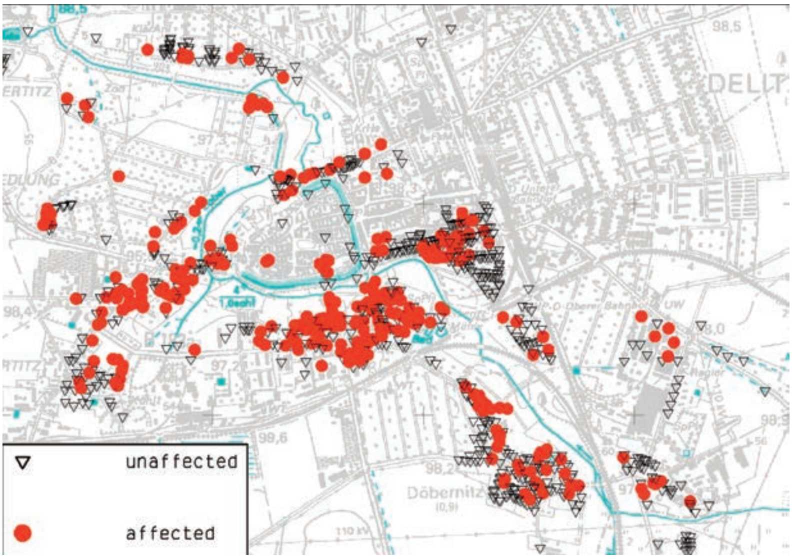

Fig. 4 *Potential affected buildings without measures according to modeling results*

ence between basement height and groundwater table is less than 0.5 m, assuming average climatic and steady flow conditions. The model predictions showed that without any limitation measures 436 buildings (by 1344) will be affected by high groundwater levels (Fig. 4).

Consequences and measures against damages on buildings

Individual measures such as sealing of basements, filling of basements with concrete or even house lifting are possible to protect buildings. If more than a few buildings are affected, large-scale measures such as horizontal filter wells, drainage systems or even improvements of conditions of water bodies may be considered as well.

According to the large number of affected buildings in Delitzsch, only integral measures appeared effective and sustainable. Due to low efficiency as well as high construction and operation costs, measures like wells and drainage systems were excluded.

In contrast, the extension of receiving waters appeared suitable. The muddy and clogged riverbed of river Lober led to a substantial reduction of the groundwater flow into the river resulting in increased groundwater levels up to the ground surface especially in the former floodplains. Differences of about 1 m were measured between ground and surface water levels in the vicinity of the river. Based on detailed hydrogeological investigations including pumping tests the permeability of the clogged riverbed material was found to be about $1{\times}10^{-7}$ m s^{-1}.

The objective of the measures to be planned was the re-establishment of the connectivity between aquifer and river in order to ensure stable influent flow conditions with a minimum of maintenance costs. As part of model studies, different variations of improved riverbed permeability and optimized levels of the riverbed were examined. Riverbed permeability in the range of $1{\times}10^{-5}$ m s^{-1} appeared attainable through extension measures.

In consequence of the riverbed improvement, groundwater levels will decline by approximately 0.5 to 1 m in the former floodplains and the number of buildings which are affected by high groundwater levels will decrease by 53 % (from 436 to 205 buildings), according to modeling forecasts.

Fig. 5 shows the sections with proposed riverbed improvements and the resulting affected buildings.

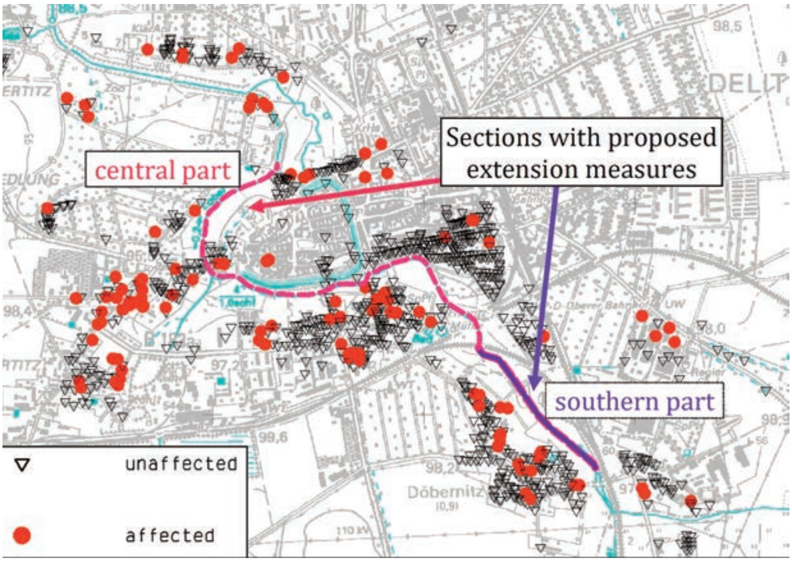

Fig. 5 *Sections with proposed riverbed improvements and resulting affected buildings according to model forecasts*

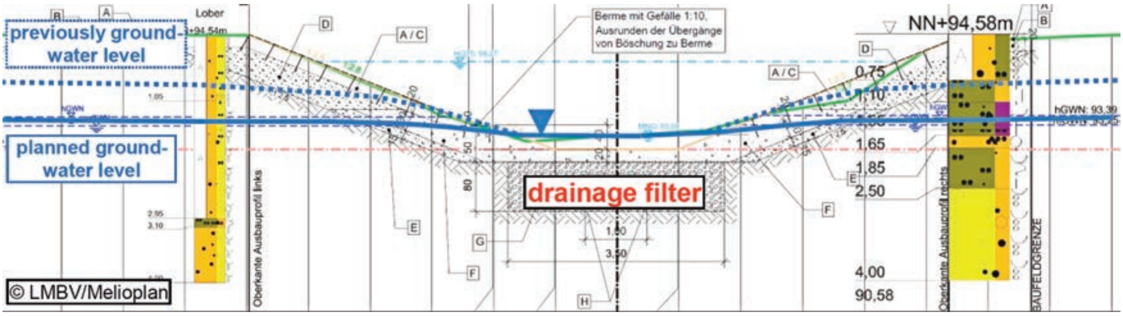

Fig. 6 An exemplary cross section

Fig. 7 Before (left) and during (right) the exchange of the riverbed material

Works carried out

Works began in 2011 with the southern section. Firstly mud deposits and the clogged riverbed were removed. Afterwards, a drainage filter was integrated and the riverbed was reshaped. The optimized riverbed shape was planned to ensure a minimum surface water flow velocity of 0.2 m s^{-1} (under average conditions) in order to prevent new mud deposits.

An exemplary cross section with the proposed drainage filter as well as the declined groundwater level (graphically-illustrated) is shown in the following Fig. 6 linked with views from the construction site in Fig. 7.

Results and future works

The groundwater monitoring showed that the predicted decline of groundwater levels occurred after completing the first construction stage. Fig. 8 shows the readings of the exemplary groundwater observation point "DSW5852" in comparison to the calculated levels with and without extension measures.

The decline of the groundwater level will remain on the basis of a regular maintenance. Hence, the protection of numerous buildings can be ensured permanently. So the construction of the second part in the center of Delitzsch started in 2013.

The most remaining affected buildings will be saved with special maintenance measures on small tributaries and trenches. The other few buildings can only be protected with individual measures in connection with special case examinations.

Conclusions

In consequence of the rehabilitation of the opencast mines in the vicinity of the city of Delitzsch, groundwater level rose up again to its historical level closely below the surface with the result of potential damages on buildings.

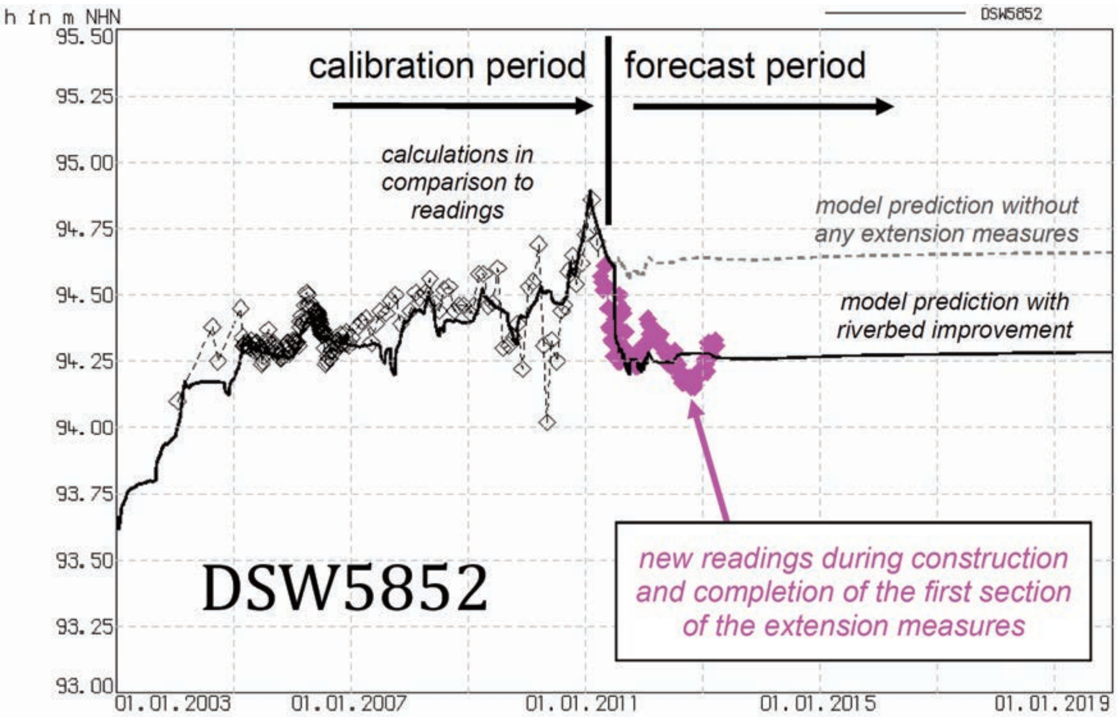

Fig. 8 *Comparison of measured (rhombs) and simulated groundwater levels (with and without riverbed improvement) at the groundwater observation point "DSW5852"*

According to the modeling results at average climatic conditions, the only reasonable measure to protect the large number of affected buildings was to improve the bed of the local river. The muddy and clogged riverbed led to a substantial reduction of the groundwater flow into the receiving waters resulting in increased groundwater levels up to the ground surface.

The objective of the river development was the re-establishment of the connectivity between aquifer and river in order to ensure stable influent flow conditions with a minimum of maintenance costs. The model prediction of the declined groundwater levels was confirmed by the groundwater monitoring during the first construction period.

References

Sames D, Blankenburg R, Brückner F, Müller M (2010) PCGEOFIM Anwenderdokumentation, Ingenieurbüro für Grundwasser GmbH, Leipzig/Germany

Mansel H, Büttcher H, Eulitz K, Bach F, Brückner F, Uhlig M, Blankenburg R (2011) PCGEOFIM als bewährtes Werkzeug zur Prognose des GW-Wiederanstiegs in den Bergbaufolgelandschaften Mitteldeutschlands und der Lausitz. In: Wirkungen des Grundwasserwiederanstiegs in den Bergbaufolgelandschaften auf die oberirdischen Gewässer, Kippen, Feuchtgebiete, Bauwerke und andere Rechtsgüter, Proceedings der Dresdner Grundwassertage 2011, DGFZ e.V., Dresden/Germany

Blankenburg R, Sames D, Mansel H, Pfützner B (2012) Modeling the impact of a possible climate change on the water balance in post-mining areas. In: International Mine Water Association Symposium, Proceedings of Symposium in Bunbury, Western Australia

Antimony and arsenic uptake by vegetation growing at abandoned mines

Rosa Cidu, Riccardo Biddau, Elisabetta Dore, Andrea Vacca

Cagliari University, Dipartimento di Scienze Chimiche e Geologiche, via Trentino 51, 09127 Cagliari, Italy, cidur@unica.it

Abstract This paper investigates antimony (Sb) and arsenic (As) occurrence in plants (Pistacia lentiscus), an evergreen shrub, collected at abandoned mines in Sardinia. Maximum concentrations observed in plants were 22 µg/g Sb and 0.35 µg/g As, with concentrations accumulated in roots being generally higher than those in leaves. The ranges of amounts washed out from leaves were 0.003-0.088 µg/g Sb and 0.002-0.024 µg/g As. Antimony and arsenic in vegetation samples collected in the mine area were much higher than concentrations observed in plants collected on the slopes upstream of the mine, although at levels much lower than observed in plants growing at mine sites elsewhere.

Keywords Antimony, arsenic, abandoned mine, vegetation

Introduction

Antimony (Sb) and arsenic (As) are categorized as non-essential elements for plants, animals and humans, while they have been listed as priority pollutants by the US Environmental Protection Agency and the World Health Organization.

Natural concentrations of arsenic in the soil typically range from 0.5 to 80 µg/g (Kabata-Pendias and Pendias 2001), and antimony in the soil is evaluated at few µg/g (Filella *et al.* 2002), although higher concentrations are frequently found in soils and sediments that have been affected by anthropogenic activities such as mining or agriculture, or where the soils are derived from As- and Sb-rich mineralized rocks. Both elements can be readily absorbed by plant roots when occurring in soluble form. The plant uptake of As may differ with respect to plant uptake of Sb depending on their dominant species (Tschan *et al.* 2008). Arsenic concentrations in plants growing on uncontaminated soils vary from 0.01 to 1.5 µg/g (Larios *et al.* 2012), and are in the range of 0.2 to 50 µg/g for Sb (Okkenhaug *et al.* 2011). Substantially higher As concentrations (up to 1400 µg/g; Larios *et al.* 2012) and Sb concentrations (up to 1600 µg/g; Murciego *et al.* 2007) have been found in vegetation growing in mining areas.

The Sardinia Regional Government has recognized relevant antimony contamination at the Su Suergiu mining site in SE Sardinia, Italy. Studies aimed at identifying the contaminant sources, and evaluate the extent of contamination have been carried out (IGEA 2009). This study aims to investigate the plant uptake of Sb and As in soils impacted by past mining at Su Suergiu. Assessing the capacity of plants in accumulating Sb and As is fundamental for evaluating the toxicity of these elements in the food chain. Taking into account that the Sardinia Region has established the need of remediation at Su Suergiu, the information derived from this study could be relevant for planning the best actions able to mitigate contamination.

Study area

The Su Suergiu study area is shown in Fig. 1. The Sb-As deposits were mined underground since 1880, with exploitation peaks in the 1920–1930, and mine closure in 1960. Afterwards, Sb-ore coming from Turkey and China was processed, a foundry being active from

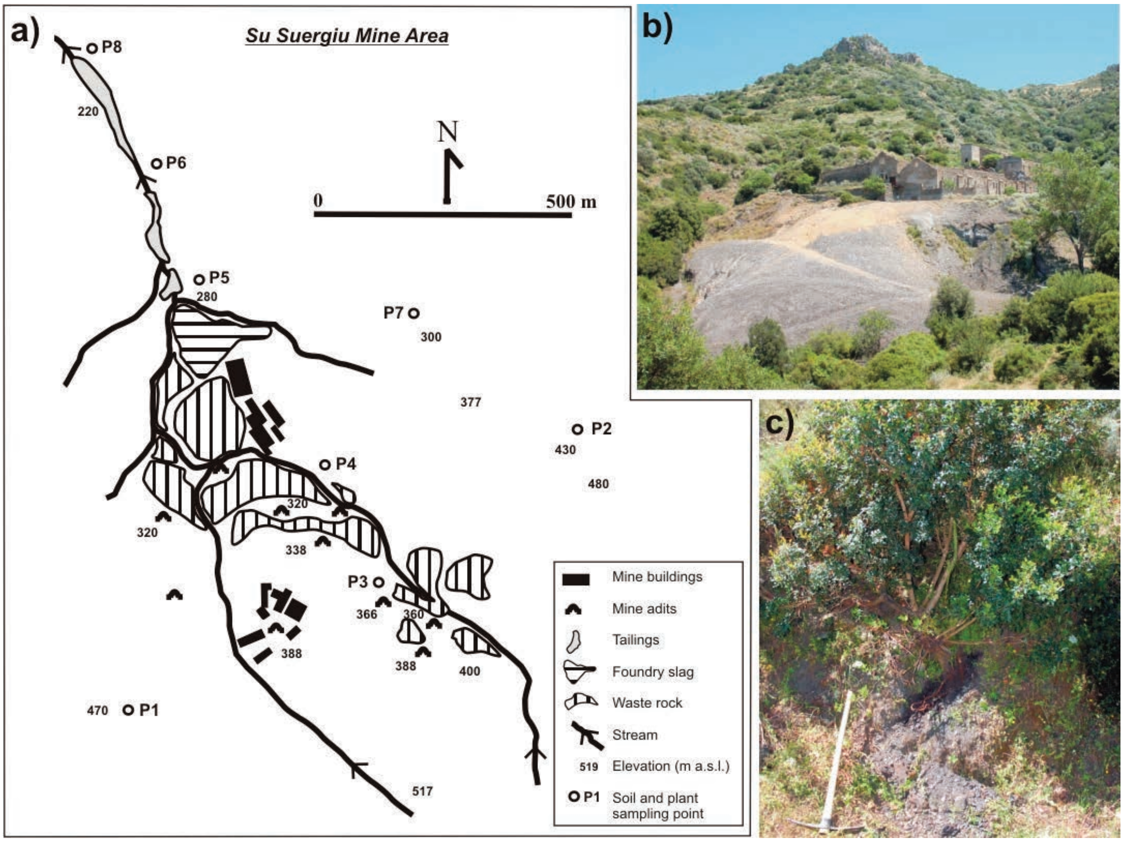

Fig. 1 *a) Schematic map of Su Suergiu and location of the vegetation samples; b) view of the slag heap and mine ruins; c) example of soil with Pistacia lentiscus.*

1882 to 1987. The mineralization is hosted in Paleozoic black schists and metalimestones, and consists of antimonite, scheelite, arsenopyrite and pyrite, with calcite and quartz in the gangue (Funedda *et al.* 2005). Slag and tailings (87 % of dumped materials), and waste rocks were left nearby the mine plant over a surface of 33,000 m^2. Mining residues are altogether estimated at about 66,000 m^3 (RAS 2003).

Climate in the study area is semi-humid, characterized by dry summer and rainfall variable from year to year, mostly occurring from October to April. Data collected from 1955 to 1992 at stations located in the area show mean annual precipitation of 670 mm and mean annual temperature of 16.2 °C (RAS 1998). Spring waters are scanty and usually have low flow (<0.1 L/s). The main river is the Flumendosa, only a few tributaries are large streams (flow > 100 L/S) while the other ones are intermittent streams. The flow of surface waters may vary dramatically depending on rainfall. The Rio Ciurixeda stream receives the untreated drainage from the Su Suergiu mine, and flows directly into the Flumendosa River, which supplies water for agricultural and domestic uses.

Methods

In June 2012, soil and vegetation samples were collected in the Su Suergiu Sb mining area and surroundings (Fig. 1). Eight soil profiles were opened down to 100 cm depth. Samples of each soil horizon were packed in polyethylene (PE) bags, air dried, hand-ground and dry-sieved with a 2 mm mesh sieve, and milled in agate vials and balls (Fritsch planetary ball milling pulverisette 5).

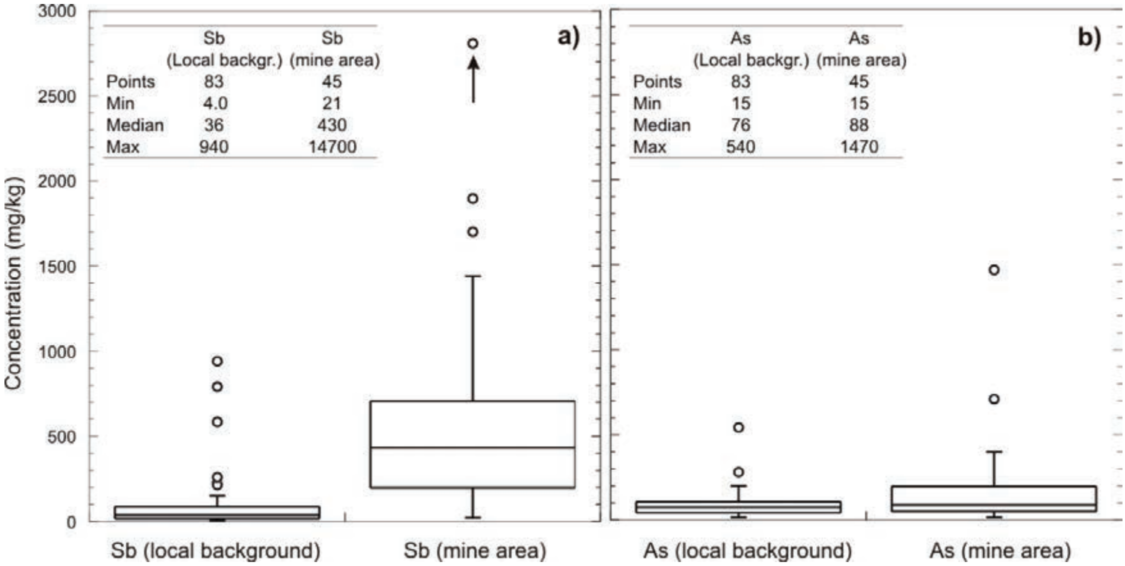

Fig. 2 *a) Antimony and arsenic concentrations in soil samples (data from IGEA 2009).*

Vegetation samples consist of Pistacia lentiscus, an ubiquitous plant in Mediterranean environments that also grows in the Su Suergiu abandoned mine area. Samples from three individual plants were collected at the same location as the soil samples. The plants were divided into roots and leaves (woody stems were not analysed), collected in separate PE bags, and stored at 4 °C until analysis. To evaluate the potential As and Sb dispersion in the atmosphere, 25 g of leaves were washed with 250 mL of 0.01 M hydrochloric acid (HCl), used as a proxy of rain water, and shaken for few minutes.

Arsenic and Sb in leaves and roots were determined by acid digestion; leaves and roots were washed with deionised water, dried at 60 °C until constant weight, and then ground to powder using a rotor mill (Retsch ZM1000). Acid digestion was carried out in a closed microwave digestion device (Milestone Ethos1) using 0.5 g of sample and 2 mL hydrogen peroxide (H_2O_2; 30 %), followed by the addition of 6 mL nitric acid (HNO_3; 67 %). Digestion of certified plant reference material was carried out for quality control (bush twigs and leaves GSV-2, and tea GSV-4; Madeddu and Rivoldini 1996).

The solutions derived from the wash of leaves, as well as those derived from acid digestion, were filtered at 0.4 µm, diluted to 50 mL with ultrapure water (>18 MΩ*cm), acidified with supra pure HNO_3 and analyzed by quadrupole inductively coupled mass spectrometry (ICP-MS) using rhodium (Rh) as the internal standard. The estimate errors of certified materials were about 9 % for As and Sb. Concentrations of As and Sb are reported in µg per g of plant dry weight.

Results and discussion

The main soils in the area are Leptosols, while Cambisols occur on slopes and colluvial deposits. Analyses on the soils samples are still in progress, but some information can be derived from previous studies at Su Suergiu (IGEA 2009). Fig. 2 shows the distribution of Sb and As in soil samples collected in the mine area and surroundings, the latter being used to estimate the local background. It can be observed that the median value of Sb in soils from the mine area is much higher than the local background median value, although a large variation in concentration occurs, *i.e.* 21 to 14700 µg/g Sb in the mine area (Fig. 2a). De-

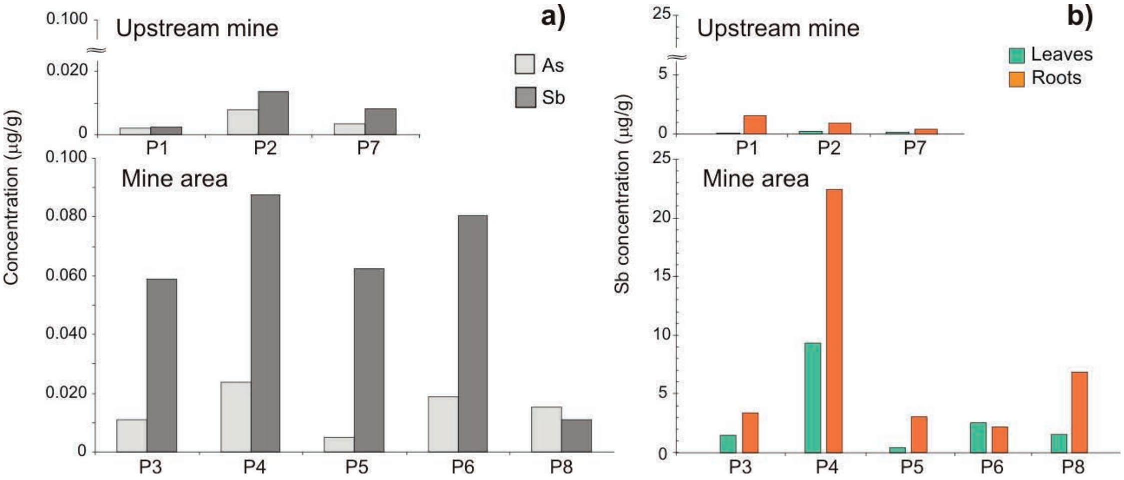

Fig. 3 *a) Sb and As concentrations leached by leaf samples. b) Sb concentrations in leaves and roots of Pistacia lentiscus*

spite the large range of As concentration too (15–1470 µg/g As), the median value of As in soils from the mine area is similar to the local background median value (Fig. 2b).

The Sb-bearing fine particles carried by the wind in the atmosphere can be deposited on vegetation, then fall again to the ground. Fig. 3a shows mean concentrations of As and Sb leached from the leaf samples collected in the study area (for sample locations see Fig. 1). Dust materials deposited on vegetation samples collected on the slopes upstream of the mine area (leaf samples P1, P2, P7) carry 0.007 µg/g Sb on average, while concentrations of Sb deposited on leaves collected in the mine area are much higher, mean 0.070 µg/g Sb (Cidu *et al.* 2013). A similar trend can be observed for arsenic with median value of 0.002 µg/g leached from samples collected on the slopes upstream of the mine area, and up to 0.024 µg/g As leached from samples collected in the mine area.

Fig. 3b shows concentrations of Sb hosted in the vegetation samples. It can be observed that the Sb uptake by the roots is higher than the leaf samples. The Pistacia lentiscus roots may accumulate up to 22 µg/g Sb. Arsenic in the Pistacia lentiscus roots was in the range of 0.08 to 0.35 µg/g, and was similar in the leaves 0.08 to 0.31 µg/g As.

In Sardinia, median concentrations in surface waters are estimated at 1 µg/L As and 0.25 Sb (Cidu and Frau 2009). Median concentrations in Sardinian groundwaters are estimated at 0.6 µg/L As and 0.5 Sb (Biddau 2012). Results on water samples at Su Suergiu show contamination peaks (up to 5900 µg/L As and 15000 µg/L Sb) in the waters flowing out of the slag heaps, clearly indicating that these materials are the main source of contamination at Su Suergiu. The contaminated water flows into the local streams. Dilution processes allow As concentrations to decrease to levels which are not of environmental concern, while the Sb contamination persists several km downstream of the mine till the Flumendosa river (Cidu 2011, Cidu *et al.* 2012, 2013).

Conclusions

Past mining at Su Suergiu affects the soil and the water system downstream of the mine. The soils may contain up to 14700 and 1470 µg/g Sb and As, respectively. Despite such high contents in the soils of the mine area, relatively low amounts of Sb and As (up to 32 and 0.5 µg/g Sb and As, respectively) are accumulated in the investigated plant Pistacia lentiscus growing nearby the mine. According to data available so far at Su Suergiu, the major effects of contamination were observed on the water bodies located downstream of the slag heap. Therefore, priorities of remediation actions should be focussed on addressing the environmental impacts of the slag heap.

Acknowledgements

Research funds were provided by the Italian MIUR (PRIN2009, Coordinator R Cidu), the University of Cagliari, and the Regione Autonoma della Sardegna.

References

Biddau R (2012) Approccio geochimico-statistico per la valutazione del background geochimico nelle acque sotterranee. Applicazioni agli acquiferi della Sardegna. FSE 2007–2013, L.R.7/2007, Regione Autonoma Sardegna, Cagliari, 123 pp

Cidu R (2011) Mobility of aqueous contaminants at abandoned mining sites: insights from case studies in Sardinia with implications for remediation. Environ Earth Science 64:503–512, DOI: 10.1007/s12665-010-0874-y

Cidu R, Biddau R, Dore E (2012) Antimony contamination of surface water at abandoned Sardinian mine sites. Proc IMWA 2012, Bunbury Australia (McCullough CD, Lund MA, Wyse L, Eds), pp 301–307, ISBN 978-0-7298-0707-4

Cidu R, Biddau R, Dore E., Vacca A (2013) Antimony dispersion at abandoned mines in Sardinia, Italy. Procedia Earth and Planetary Science, Water Rock Interaction [WRI 14]

Cidu R, Frau F (2009) Influence of the fine-particle load in Mediterranean rivers and streams on the distribution of trace elements in filtered and non filtered aqueous fractions. Applied Geochemistry, 24, 611–623. doi:10.1016/j.apgeochem.2008.12.013

Filella M, Belzile N, Chen Y-W (2002) Antimony in the environment: a review focused on natural waters I. Occurrence. Earth-Science Reviews 57, 125–176

Funedda A, Naitza S, Tocco S (2005) Caratteri giacimentologici *i.e.* controlli strutturali nelle mineralizzazioni idrotermali tardo-erciniche ad As-Sb-W-Au del basamento metamorfico paleozoico della Sardegna sud-orientale. Resoconti Associazione Mineraria Sarda CX: 25–46

IGEA (2009) Piano di investigazione iniziale dell'area mineraria di "Su Suergiu". IGEA S.p.A., Campo Pisano

Kabata-Pendias A, Pendias H (2001) Trace elements in soils and plants. Boca Raton London, New York, Washington.

Larios R, Fernández-Martínez R, LeHecho I, Rucandio I (2012) A methodological approach to evaluate arsenic speciation and bioaccumulation in different plant species from two highly polluted mining areas. Science of the Total Environment 414, 600–607

Madeddu B, Rivoldini S (1996) Analysis of plant tissues by ICP-OES and ICP-MS using an improved microwave oven acid digestion. Atomic Spectroscopy, 17 (4), 148–154

Murciego AM, Sanchez AG, Gonzalez MAR, Gil EP, Gordillo CT, Fernandez JC, Triguero TB (2007) Antimony distribution and mobility in topsoils and plants (Cytisus striatus, Cistus ladanifer and Dittrichia viscosa) from polluted Sb-mining areas in Extremadura (Spain). Environmental Pollution 145, 15–21

Okkenhaug G, Zhu Y-G., Luo L, Lei M, Li X, Mulder J (2011) Distribution, speciation and availability of antimony (Sb) in soils and terrestrial plants from an active Sb mining area. Environmental Pollution 159, 2427–2434

RAS (1998) Nuovo studio dell'idrologia superficiale della Sardegna. Regione Autonoma della Sardegna, Assessorato della Programmazione, Bilancio ed Assetto del Territorio, Ente Autonomo del Flumendosa, Cagliari (in Italian)

RAS (2003) Piano regionale di gestione dei rifiuti. Regione Autonoma della Sardegna (in Italian), 255 pp

Tschan M, Robinson B, Schulin R (2008) Antimony uptake by Zea mays (L.) and Helianthus annuus (L.) from nutrient solution. Environmental Geochemistry and Health 30, 187–191

Flooding of the underground mine workings of the Witwatersrand Gold Fields

Henk Coetzee

Council for Geoscience, Private Bag X112, Pretoria, 0001, South Africa, henkc@geoscience.org.za

Abstract South Africa's Witwatersrand Gold Field has produced almost 40 % of all the gold ever extracted, as well as being a significant source of uranium. The gold occurs in pyritic conglomerates located along the "Golden Arc" centred on the city of Johannesburg. Mining has led to the excavation of a series of large interconnected underground voids. In the oldest mining areas, underground mining has all but ceased and the workings have been allowed to flood. Since 2010, concerted efforts have been made to address the existing and potential impacts of AMD in this area.

Keywords Witwatersrand, acid mine drainage, legacies

Introduction

Gold occurs in the Witwatersrand Gold Fields in a number of conglomerate layers (locally known as reefs) within a large Archaean sedimentary basin. Resistant quartzite layers within this sedimentary pile define the ridge which gives the area its name, the "White Water Ridge". This ridge forms a continental water divide. Water falling to the north of the ridge flows north towards the Limpopo River, eventually flowing east to the Indian Ocean, while water falling south of the ridge flows south and west into the Vaal River and eventually to the Atlantic Ocean. The mineralised layers contain significant amounts of pyrite and elevated concentrations of uranium, which has been produced as a by-product of gold mining in some areas. Gold was discovered in Johannesburg in 1886, with a significant industry developing soon after. The initial gold discovery occurred in the Central Rand (largely located in the city of Johannesburg), with subsequent discoveries being made in the West Rand and East Rand (Fig. 1). Later discoveries were made in a number of areas where the Witwatersrand reefs are largely covered by younger rocks, with mining eventually developing along more than 300 km of strike length. In the years following the 2nd World War, significant amounts of uranium were also produced. Mines are developed within a number of more or less contiguous mining complexes, which define individual gold fields. Because of its location on the water divide, Johannesburg and the surrounding urban and industrialised areas are not located close to a significant water source, requiring water to be pumped to the city from the Vaal Dam some tens of kilometeres to the south.

Early mining was limited to the surface outcrops but it was soon realised that these were the surface expression of extensive southward-dipping sedimentary layers extending to great depths. The high costs of underground mining led to the consolidation of mines into large units which were interconnected at depth across the major goldfields. This interconnection allows water to flow relatively freely between the underground workings of mines within each of the gold fields (Pulles *et al.* 2005). Following the cessation of underground operations in many of the mines, water flowing into large areas of underground workings needed to be pumped by fewer and fewer operators. This became extremely costly for the remaining mines. Even-

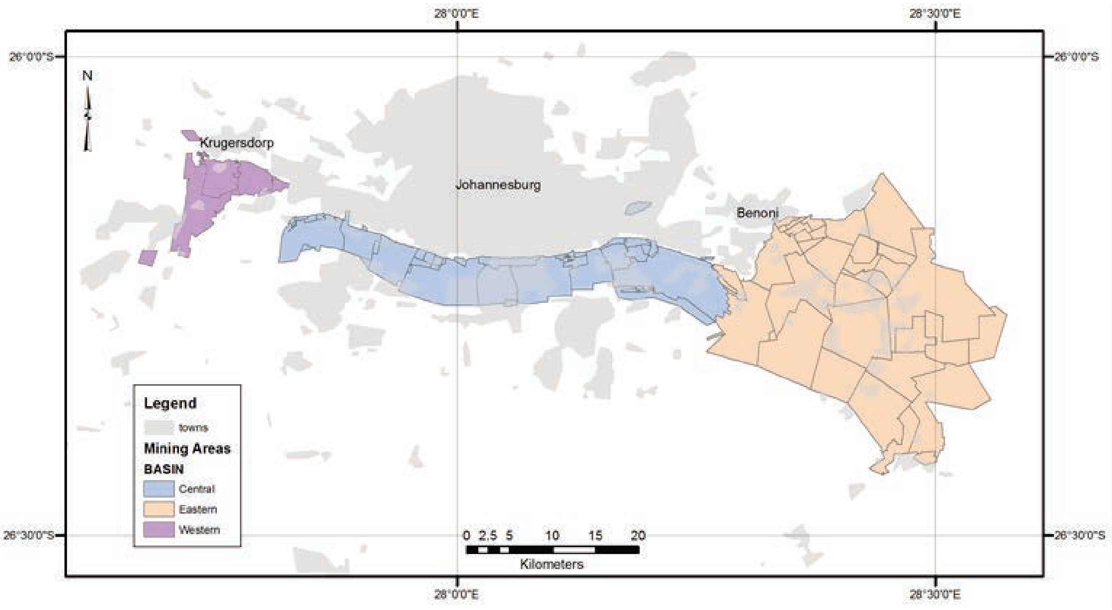

Fig. 1 *Location of the Western, Central and Eastern mining basins of the Witwatersrand Gold Field, relative to the populated urban areas of Johannesburg and its surrounds (Ramontja et al. 2011).*

tually these mines also ceased operations, stopped pumping and the interconnected mine voids began to flood.

Pumping ceased in the West Rand Gold Field in 1998. At the time, the mining company involved commissioned the development of a flooding model which predicted that water would decant from the underground workings to the surface in 2002. This prediction proved correct (Coetzee *et al.* 2005), with polluted water discharging into a stream to the north of the water divide (Fig. 2). Water polluted by Witwatersrand mining activities typically displays low pH, high TDS, high SO_4 (Ramontja *et al.* 2011) and may be contaminated with a range of metals, with uranium being among the contaminants of greatest environmental concern (Coetzee *et al.* 2006). Despite reports of acidity in this water as far back as the 1950s (Hocking 1986) no plans were put in place by either the mine owners or government agencies and the decanting water entered local aquifers and surface streams with serious negative effects (Hobbs and Cobbing 2007; Hobbs 2013).

In the Central and East Rand Gold Fields, single pump stations maintained the water at a level which permitted mining to continue, both of these discharging to the south of the water divide. These were operated by the last mines to operate within these areas and partially subsidised by the State in an effort to maintain gold production in these areas. Eventually these two operations also ceased pumping due to a fatal underground accident in the Central Rand in 2008 (Ramontja *et al.* 2011) and the liquidation of the last company pumping water in the East Rand in early 2011. The underground workings in these gold fields then also started to flood (Janse van Vuuren 2011).

Legislative environment

Mine closure and mine water management in South Africa are governed largely by the Mineral and Petroleum Resources Development Act (Act of No. 28 of 2002) and the National Water Act (Act No. 36 of 1998). These acts govern all aspects of the licensing, operation, environmental management and closure of mining operations as well as providing specific conditions on the use

Fig. 2 *Acid mine drainage discharging from an abandoned mine shaft in the West Rand Gold Field.*

and pollution of water. However historical legislation which governed mining was not as comprehensive, particularly with respect to environmental management and closure (Coetzee *et al.* 2008; van Tonder *et al.* 2008).

Regional considerations

A key concern is the discharge of acid mine drainage into rivers flowing to the south of the water divide. Before the cessation of pumping by the mines, water was neutralised and discharged to local streams which flowed south towards the Vaal River. Although this discharge entered the Vaal downstream of the point of abstraction for Johannesburg, it was known to affect downstream water quality. Historically this water quality impact has been mitigated with discharges of clean water from dams upstream of this discharge point. However this will not be sustainable in the long term, particularly as water is already transferred into the Vaal River System from other areas via expensive inter-basin transfer schemes (Department of Water Affairs and Forestry 2009).

Desalination of point sources of mine water is seen as an important component in the management of water quality at a regional level. This water will then be suitable for augmentation of local water supplies for domestic, agricultural or industrial use. However the often unseen benefit of removing the polluted water from river systems is that it makes water that would otherwise be required to dilute downstream saline discharges available for use, reducing the need for expensive augmentation schemes (Department of Water Affairs and Forestry 2009).

Proposal of solutions

The flooding of these mines and the risks posed by AMD discharges were identified before the flooding of mines commenced (Scott 1995; Rison Consulting (Pty) Ltd 2001). The interconnected nature of the underground workings also highlighted the need for integrated, regional solutions to be developed (Pulles *et al.* 2005; van Tonder *et al.* 2008). By and large, solutions have hinged on the eventual need to pump and treat water to maintain safe water levels within the underground workings and the longer-term aim of reducing the flow of water into the underground workings as a means to reduce the eventual costs of pumping and treatment (Krige 1999; Krige 2001; Strachan 2008).

During this period, the existing problems and threats due to the flooding of the underground workings rose to prominence in the public eye, often attracting sensationalist media reports of impending disaster. In the second half of 2010, the South African Government appointed an Inter-Ministerial Committee, representing the Ministries of Mineral Resources, Water Affairs, Environmental Affairs and Science and Technology and the National Planning Commission to investigate the issues surrounding acid mine drainage and make recommendations for a programme to manage it. This committee appointed a team of experts led by the Council for Geoscience combining the expertise within the relevant government institutions, science councils, the Water Research Commission and a number of universities. The Team of Experts produced an assessment of the situation and recommendations for a path forward.

The recommendations of this team (Ramontja *et al.* 2011), which were subsequently

Fig. 3 *Acid mine drainage generated in surface tailings deposits in the West Rand*

adopted by government combined the objectives of maintaining a safe water level by re-establishing the pumping of water from the underground workings and the reduction of volumes to be pumped via the control of surface water ingress. It was recommended that the pumped water be treated. Initially this would be by neutralisation, but it was recommended that desalination be investigated as a medium- to long-term measure. The importance of AMD sources over and above the underground mine voids, in particular diffuse sources such as surface mine residues (Steffen Robertson and Kirsten 1986; Fig. 3) was acknowledged, as was the long-term nature of the problem faced. A key gap identified is the long term funding of the process as many of the mines involved closed in the past when the legislative requirements for mine closure were not as strict as they are today. The need for enhanced water quality and flow monitoring was also recommended.

These recommendations were adopted by the South African Government in February 2011. Structures were put in place to oversee their implementation. The initial priorities were identified as the control of the discharge of AMD to the environment in the Western Basin and the prevention of the rise of the water levels to critical levels in the Central and Eastern Basins. During the months that followed, significant progress was made in the appointment of implementing agents and the commissioning of detailed feasibility studies. At the same time a process was initiated to undertake a feasibility study for a long-term solution to deal with AMD in the Witwatersrand (Department of Water Affairs 2012).

Implementation of solutions

Since 2011, South Africa's Department of Water Affairs has been overseeing the process of implementing measures aiming to prevent the rise of water above environmentally acceptable levels in the Central and Eastern Basins and to lower the level in the already flooded Western Basin. This programme incorporates measures to neutralise water pumped from the underground mine workings. An existing neutralisation plant in the Western Basin has been upgraded such that it has sufficient capacity for the volume of water required to control the water level, while infrastructure has been developed to pump this volume of water from the Basin.

As a consequence, no untreated water has been discharged to the environment in this area since mid-2012 (Hobbs 2013). A programme is in place for the installation of pumping and treatment infrastructure in the Central and Eastern Basins, although funding of this remains a challenge.

In parallel with this process, the Council for Geoscience (South Africa’s Geological Survey) and the Department of Mineral Resources are undertaking a programme to understand the ingress of water into the underground workings and implement measures to reduce these flows (Strachan 2008). This work comprises a programme of research into the hydrology and geohydrology of the gold fields as well as construction work aimed at reducing water ingress into the mine workings. A canal has been constructed in the west of Johannesburg, in an area where a surface stream crosses an area of historical surface mining and shallow undermining and feasibility studies are proceeding for the construction of additional canals.

Challenges

Despite significant progress, this process has not been without problems:

- Funding for the development and implementation of solutions is limited although significant funds have been forthcoming from the South African government. In addition, the DRDGold has made land available and Central Rand Gold has provided equipment for these interventions. The issue of who is liable for costs has also not been fully resolved (Nicolson 2013).
- Concerned citizens’ groups have complained that the level of public participation in these processes has not been adequate and that their concerns are not being taken into account, although comprehensive statements of concern (Pretorius and Liefferink 2011) have been submitted. Environmental activists also complain about government institutions not being forthcoming with information (pers. comm. M Liefferink 2013)
- The current interventions in largely-abandoned mining areas are hampered by a lack of monitoring data and other information and the fragmentation of information between different institutions. This has necessitated the adoption of conservative remedial interventions which may involve unnecessary costs being incurred.

Conclusions

More than a century of mining in the Witwatersrand has left a significant water legacy which will persist far into the future. However, concrete interventions are taking place to bring the situation under control and prevent serious environmental problems from developing. Existing environmental problems are also being managed to limit their impacts. Local and regional considerations will necessitate the upgrading of many of these interventions in the medium- to long-term.

Flooding mines and large point-source discharges of acid mine drainage have captured the attention of the South African media. It is important to realise that these are not the sole sources of polluted water entering the environment as a result of gold and uranium mining in the Witwatersrand region. These will also need to be addressed to address local and regional water pollution.

The processes undertaken to address acid mine drainage in the older gold fields of the Witwatersrand has been hampered by a shortage of reliable data on historical water flows and quality. While this cannot be remedied, it emphasises the need to ensure that sufficient data are collected to optimise the regional closure processes which will occur in the future in other related mining areas.

References

Coetzee, H., Croukamp, L., Venter, J. and de Wet, L. (2005) Contamination of the Tweelopiesspruit and environs by water from the Western Basin decant point on Harmony Gold’s property., Council for Geoscience, Report No. 2005–0148, Pretoria: 28p.

Coetzee, H., Nengobela, N. R., Vorster, C., Sebake, D. and Mudau, S. (2008) South Africa’s strategy for the management of derelict and ownerless mines. Mine Closure 2008: Proceedings of the third international seminar on mine closure. A. Fourie, M. Tibbett, I. Weiersbye and P. Dye. Johannesburg, Australian Centre for Geomechanics:113–124.

Coetzee, H., Winde, F. and Wade, P. (2006) An assessment of sources, pathways, mechanisms and risks of current and future pollution of water and sediments in the Wonderfonteinspruit Catchment, Water Research Commission, WRC Report No. 1214/1/06, Pretoria: 202p.

Department of Water Affairs. (2012) "Acid mine drainage: Long term solution feasibility study." Retrieved 11 April 2013, from www.dwaf.gov.za/ Projects/AMDFSLTS/default.aspx.

Department of Water Affairs and Forestry (2009) Vaal River System: Large bulk water supply reconciliation strategy: second stage reconciliation strategy (March 2009), Department of Water Affairs and Forestry, Report Number P RSA C000/00/4406/08, Pretoria: 130p.

Hobbs, P. J. (2013) Pilot implementation of a surface water and groundwater resources monitoring programme for the Cradle of Humankind World Heritage Site, Council for Scientific and Industrial Research, CSIR/NRE/WR/ER/2013/0023/B, Pretoria: 56p.

Hobbs, P. J. and Cobbing, J. E. (2007) A hydrogeological assessment of acid mine drainage impacts in the West Rand Basin, Gauteng Province, CSIR/THRIP, CSIR/NRE/WR/ER/2007/0097/C, Pretoria: 59p.

Hocking, A. (1986) Randfontein Estates: The first hundred years. Bethulie, Hollards, 280p.

Janse van Vuuren, A. (2011, 8 June 2011) "Acid drainage claims another shaft." MiningMX Retrieved 11 April 2011, from www.miningmx.com/news/ gold_and _silver/Acid-drainage-claims-another-shaft.htm.

Krige, W. G. (1999) An investigation into groundwater recharge derived from the upper Klip River tributaries where these cross the Main, Bird and Kimberley Reef outcrops and associated shallow mine workings, African Environmental Development: 14p.

Krige, W. G. (2001) A quantification of water volumes recharging the central rand mine void, associated with direct ingress from surface water sources, African Environmental Development.

Nicolson, G. (2013) "Joburg's acid mine drainage: Swapping sludge for salt." Retrieved 14 April 2013, from www.dailymaverick.co.za/article/2013-03-15-joburgs-acid-mine-drainage-swapping-sludge-for-salt/#.UWq597W7K9Q.

Pretorius, K. and Liefferink, M. (2011) Detailed Response to The Findings and Recommendations of Report to the Inter-Ministerial Committee on Acid Mine Drainage (December 2010), Federation for a Sustainable Environment: 64p.

Pulles, W., Bannister, S. and van Biljon, M. (2005) The development of appropriate procedures towards and after closure of underground gold mines from a water management perspective, Water Research Commission, WRC Report No. 1215/1/05, Pretoria: 138 p.

Ramontja, T., Coetzee, H., Hobbs, P. J., Burgess, J. E., Thomas, A., Keet, M., Yibas, B., van Tonder, D., Netili, F., Rust, U. A., Wade, P. and Maree, J. (2011) Mine Water Management in the Witwatersrand Gold Fields With Special Emphasis on Acid Mine Drainage Inter-Ministerial-Committee on Acid Mine Drainage, Pretoria: 146p.

Rison Consulting (Pty) Ltd (2001) Geological and Geohydrological control on the groundwater ingress into the central rand basin.

Scott, R. (1995) Flooding of Central and East Rand Gold Mines; An investigation into controls over the inflow rate, water quality and the predicted impacts of flooded mines, Water Research Commission, WRC Report no 486/1/95, Pretoria: 238p.

Steffen Robertson and Kirsten (1986) Report on the feasibility of emergency water supply from wells, Gemsbokfontein Compartment, prepared for Johannesburg Consolidated Investment Co. Ltd., SRK Report CI.5315/1.

Strachan, L. K. C. (2008) Strategy for the Management of Mine Water Ingress and Decant Problems in the Witwatersrand Gold Mining and KOSH Areas, South Africa, Council for Geoscience, unpublished, Pretoria.

van Tonder, D. M., Coetzee, H., Esterhuyse, S., Msezane, N., Strachan, L., Wade, P., Mafanya, T. and Mudau, S. (2008) South Africa's challenges pertaining to mine closure – The concept of regional mine closure strategy. Mine Closure 2008: Proceedings of the third international seminar on mine closure. A. Fourie, M. Tibbett, I. Weiersbye and P. Dye. Johannesburg, Australian Centre for Geomechanics:87–98.

Rapid field based analytical techniques for the environmental screening of abandoned mine sites

Henk Coetzee

Council for Geoscience, Private Bag X112, Pretoria, 0001, South Africa, henkc@geoscience.org.za

Abstract South Africa's long mining history has left a legacy of over six thousand abandoned mine sites, many of which are the results of the mining of materials which may have a negative impact on local surface streams and aquifers A field-based screening protocol for the assessment of water quality and the potential of solid materials to pollute has been assembled using commercially available consumable water tests and procedures requiring the minimum of specialised capital equipment and optimised for implementation by relatively unskilled field workers. Where needed this can be complemented with more sophisticated field and laboratory-based methods.

Keywords Field analysis, screening level assessment

Background

South Africa has a long history of mining, with formal records extending back to the 17th Century and archaeological evidence of mining extending further back into the past. This has left a legacy of over six thousand abandoned mine sites (Coetzee *et al.* 2008), many of which are the results of the mining of materials which may have a negative impact on local surface streams and aquifers. In order to manage these impacts, a programme has been initiated to assess the impacts of these sites on local communities and the surrounding environment and to identify high-priority sites for remedial action. As a water-stressed country the impacts on water need to be taken seriously.

Since 2005, the Council for Geoscience (South Africa's Geological Survey) has been undertaking research into the impact of these abandoned mines, with the aim of advising the country's Department of Mineral Resources – the government department legally responsible for addressing the impact of mines where no legally liable party can be identified – on the management of this problem. The primary activities have included the compilation of a detailed inventory of affected sites, the assessment of the hazards and risks posed by these sites to affected communities and the environment and the identification of priorities for remedial action and rehabilitation. More recently, this scope has expanded to include the implementation and management of rehabilitation projects.

Initial investigations undertaken on a number of sites have indicated that water contamination is not ubiquitous, even in cases where potentially polluting minerals such as sulphide hosted gold, copper, lead and other metals, uranium or sulphide-rich coal were mined. Pollution is not only a result of the commodity mined and mineralogy of the deposit but also depends on the local chemical and hydrological conditions which promote or inhibit immobilisation of pollutants and the rate of reactions.

Previous screening studies, based on simple models of the potential impacts of mineralised zones on the groundwater environment (Sami and Druzinski 2003) proved to be inadequate to predict water qualities (Tarras-Wahlberg *et al.* 2008) and identified the need for analysis of water samples and a suite of laboratory tests to characterise rock-water interactions.

Screening methods

The large number of sites to be assessed requires a screening protocol which will identify priority sites and areas rapidly, providing the necessary rigor to allow the identification of sites of minimal concern and lower priorities. In practice, the elimination of a site from the list of sites of concern is often more difficult than the identification of priority sites for remediation as it entails the elimination of concerns, rather than the identification of problems.

In screening large numbers of sites in a relatively short time, an approach is proposed which fulfills a number of criteria, based on the types of hazards posed by mining sites and the context of these sites within the South African environment.

- Field-based techniques provide which can rapidly provide sufficient information to allow the identification of problematic and non-problematic sites are preferable, as these allow field teams to focus on data collection in areas where data are required for potential future remediation actions.
- Rapid methods allow sufficient productivity to allow the assessment of several sites within a limited amount of time. In the screening phase it is preferable to screen more than one site per day.
- Field analyses need to be sufficiently comprehensive to cover key contaminants in the areas of interest. Existing knowledge of ore types and mineralogy and likely contaminant species can allow the selection of an analysis set for a specific mineral province.
- The analytical tools used need to have sufficient sensitivity to allow the identification of pollution. The detection limits of methods need to be of a similar order of magnitude to water quality targets or appropriate limits, while accuracy and precision should be adequate for at least a semi-quantitative analysis.
- Costs should be at best comparable with laboratory analyses.

South African organisations face a number of other challenges with respect to the analysis of large numbers of samples in screening studies. Laboratory facilities are relatively limited, leading to comparatively high analytical costs and long lead times for analyses. The lead times are a particular problem for the rapid screening needed in the assessment of large numbers of contaminated sites in a relatively short time.

Historical and recent factors have contributed to a situation where South Africa suffers an acute shortage of technically skilled personnel. Lawless (2008) reports that in the case of civil engineering professionals, South Africa scores poorly in a comparison of number of engineering professionals relative to the country's population. Many South Africans are not exposed to science laboratory work at all during their schooling. Tsipa *et al.* (2010) report that, in a sample of high school learners in Mpumalanga Province, 58 % of respondents had no laboratories in their schools and 75 % had no science equipment. A shortage of skilled teaching staff at schools level (Segar 2012) exacerbates this problem, and is likely to hamper the implementation of complex technical processes compound the relative lack of laboratory facilities on an extensive scale in South Africa into the future. Methods based on simple procedures which produce unambiguous results are therefore of great use in the South African context.

Complementary analytical methods

Often, the questions which require answering on a mine site go beyond a simple water analysis. In many areas, water quality will vary seasonally, much of South Africa being semi-arid, with large seasonal variations in precipitation. In many cases, sites are visited where no runoff is available for sampling, while physical evidence of seasonal as well as episodic runoff exists. Furthermore, determination of the pollution potential of a site is generally also critical. To this end, a suite of laboratory methods have been devised, starting from very basic

Analysis	Detection limit	Ranges
pH		2-9 (resolution 0.5)
Fe	2 mg/L	2-100 mg/L
	5 mg/L	5-1000 mg/L
SO_4	200 mg/L	200-1600 mg/L
Al (test strip with additional reagents)	5 mg/L	5-500 mg/L
Zn	2 mg/L	2-100 mg/L
Ni	10 mg/L	5-1000 mg/L

***Table 1** Analytical tests used in evaluation of the suitability of rapid tests for mine water screening*

batch methods to kinetic tests which are undertaken over a long term under controlled laboratory conditions (INAP 2013).

Rapid field screening can also be applied to samples collected in pollution prediction studies in the field. This adds detail to field screening methods. Methods where field analysis could be of value include field-based leach tests such as paste pH and the USGS Field Leach Test (Hageman 2007) and face washing (INAP 2013) as a means to predict leachate and runoff quality. Where possible, these tests should avoid the use of specialised equipment.

Where greater precision is required, more advanced colorimetric methods, requiring the use of a field-portable spectrophotometer may also be employed.

Assessment of preliminary testing

As a preliminary step, a number of test methods were identified and test kits (Macherey-Nagel 2012) purchased. The majority of these are based on a simple test strip which is dipped into a liquid sample and the concentration range within the sample determined by matching the colour(s) of one or more indicator patches to a standard chart, generally printed on the test strip container. For some elements test strips need to react with one or more reagents, typically supplied in powder form as part of a test kit. In the current study, only Al required additional reagents.

Assessments have been undertaken for analysis of pH, Fe(total), SO_4, Al, Zn and Ni on leachates generated from sulphide-rich rocks from the Witwatersrand Supergroup. These all have sufficient sensitivity to detect pollutant concentrations found in Witwatersrand mining environments (Coetzee *et al.* 2006; Hobbs *et al.* 2011) as well as having detection limits similar to typical regulatory limits for mining discharges (see Table 1). Furthermore, the different concentration ranges have been shown to be effective in ranking more or less polluted samples.

Applications

Field screening

The key application intended for these tests was for the rapid screening of sites in the field to allow field investigators to focus their attention on sites where preliminary studies demonstrate significant water contamination or contamination potential.

In-situ analyses

In other areas, *in situ* analysis provides the opportunity to recommend precautions based on water quality. This has specific application in areas where communities may be directly and immediately affected by contamination from mine sites. Rapid tests are also useful in the evaluation of passive treatment systems and natural attenuation in the field.

Laboratory applications

Rapid tests have direct application in laboratory studies and leach tests. Often rapid semi-quantitative results provide the necessary information to design lab testing programmes for a suite of samples without waiting for more precise laboratory data. In the process of demonstration of laboratory techniques and results, rapid analyses can often be used to illustrate processes in real-time.

Community-based monitoring programmes

In recent years, South African community and advocacy groups have shown progressively more and more interest in becoming actively involved in environmental monitoring programmes. Given the shortage of technically skilled personnel in regulatory and research institutions, this presents a real opportunity and rapid field tests have potential to enable meaningful monitoring. Conventional field instrumentation, despite simplicity of operation requires calibration and maintenance which may be beyond the level of available skills. Field equipment is also relatively expensive, limiting the number of sites where this can be deployed in communities.

The rapid methods explored in this study require no capital equipment and are relatively cheap. This makes it possible for kits to be deployed in communities, enabling them to perform at least rudimentary tests on local water and become involved in local water quality monitoring programmes.

Quality assurance and quality control

The field-based screening methods described rely largely on QA/QC procedures which form part of the production of the kit. Provided that proper training is provided to the operators and that the manufacturers' instructions are adhered to, most methods are relatively robust.

In preliminary testing, it has been found to be advantageous to photograph the test strips as a record of the laboratory results. If necessary, the standard colour scales can be included in this for comparison purposes. Digital cameras also record the time and date of the photograph and in many cases, the location, via a linked GPS receiver. In practice it has been found that a good quality mobile phone camera provides adequate image quality for this (Fig. 1).

Limitations

A number of limitations have been identified in the initial method testing phase.

1. Interpretation of some of the colour-based tests relies on identification of relatively subtle colour changes, although training and experience does permit a reduction in possible ambiguity. This may be of particular importance where test kits are provided to community groups. A photographic record of tests, as described

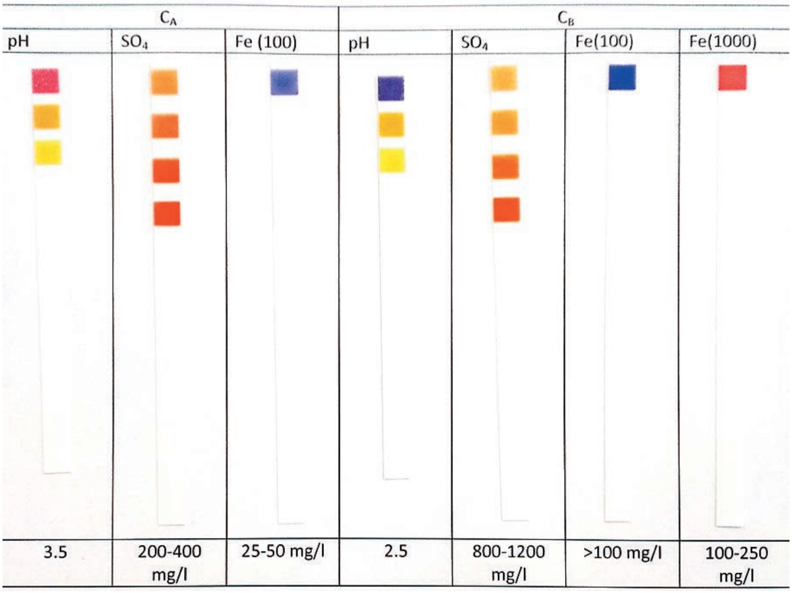

Fig. 1 *Photographic record of a test strip analysis of two leachate samples, C_A with relatively lower levels of contamination than C_B.*

above, may minimise possible ambiguities.

2. Obviously, this method does not provide a full suite of analyses for mine water. The most significant gap in the current analytical procedure is a proxy for total dissolved solids, although in many South African mining areas where water quality is well understood and characterised, the combination of SO_4, Fe and Ca may allow assessment of total salinity. Even where sufficient major elements are analysed, the relatively poor precision of each measurement will combine to provide poor data on total dissolved solids.
3. The ability to use field techniques to analyse trace elements at low levels is relatively limited, although arsenic test kits are available with detection limits as low as 0.005 mg/L.

Conclusions and recommendations

A field-based screening protocol for the assessment of water quality and the potential of solid materials to pollute has been assembled using commercially available consumable water tests and procedures requiring the minimum of specialised capital equipment. Where needed this can be complemented with more sophisticated field and laboratory-based methods. The method aims at the screening of sites to allow the identification of sites where little or no remediation is required to address water contamination, rather than the detailed characterisation of contaminated sites. The methods used do however need adequate detection accuracy and precision at concentrations appropriate for screening-level assessments.

An additional objective of this approach has been the identification of simple test procedures which can be implemented by non-specialist operators who may lack access to laboratory facilities and sophisticated equipment allowing qualitative to semi-quantitative water quality testing to be undertaken on a broader scale than would be possible given the shortage of skilled personnel in the country.

Over time, a suite of laboratory methods has been developed for the analysis of mine wastes and the prediction of water pollution (Sobek *et al.* 1978). Some of these may be undertaken in the field to expedite the screening of sites. Field screening is ideally suited to direct water analyses or the analysis of leachates produced during field tests which may be performed in relatively short times. This can be used to facilitate the rapid screening of sites where this is deemed necessary and the required test methods provide the necessary accuracy and precision.

Acknowledgements

The author thanks the Council for Geoscience for supporting the work which went into the production of this paper.

References

Coetzee, H., Nengobela, N. R., Vorster, C., Sebake, D. and Mudau, S. (2008) South Africa's strategy for the management of derelict and ownerless mines. Mine Closure 2008: Proceedings of the third international seminar on mine closure. A. Fourie, M. Tibbett, I. Weiersbye and P. Dye. Johannesburg, Australian Centre for Geomechanics:pp. 113-124.

Coetzee, H., Winde, F. and Wade, P. (2006) An assessment of sources, pathways, mechanisms and risks of current and future pollution of water and sediments in the Wonderfonteinspruit Catchment, Water Research Commission, WRC Report No. 1214/1/06, Pretoria: 202p.

Hageman, P. L. (2007) U.S. Geological Survey field leach test for assessing water reactivity and leaching potential of mine-wastes, soils, and other geologic and environmental materials., US Geological Survey.

Hobbs, P. J., Butler, M., Coetzee, H., Jamison, A., Leyland, R. and Venter, J. (2011) Situation assessment of the surface water and groundwater resource environments in the Cradle of Humankind World Heritage Site, Report Prepared for the Management Authority: Cradle of Humankind World Heritage Site & Dinokeng, Department of Economic Development, Gauteng Provincial Government, Johannesburg: 424 p.

INAP (2013) “The Global Acid Rock Drainage Guide.” Retrieved 10 April 2013, from www.gardguide.com

Lawless, A. (2008) The civil engineering skills development challenge in South Africa, South African Institute of Civil Engineers: 43 p.

Macherey-Nagel (2012) Rapid Tests. Germany, 162 p.

Sami, K. and Druzinski, A. L. (2003) Sami, K and Druzynski, AL. (2003). Predicted Spatial Distribution of Naturally occurring Arsenic, Selenium and Uranium in Groundwater in South Africa – Reconnaissance survey, Water Research Commission, Water Research Commission Report No. 1236/1/03, Pretoria.

Segar, S. (2012) “Crippling shortage of maths, science teachers.” Retrieved 10 April 2013, from www.iol.co.za/dailynews/news/crippling-shortage-of-maths-science-teachers-1.1305920#.UWUwM5O7K9Q.

Sobek, A. A., Schuller, W. A. and Freeman, J. R. (1978) Field and Laboratory Methods Applicable to Overburdens and Minesoils, United States Environmental Protection Agency, EPA-600/2-78-054: 203 p.

Tarras-Wahlberg, H., Wade, P., Coetzee, H., Chaplin, S., Holmstrom, P., Lundgren, T., Wyk, N. v., Ntsume, G., Venter, J. and Saml, K. (2008) To calibrate and verify a predictive model for the incidence of naturally occurring hazardous trace constituents in groundwater, Water Research Commission, WRC Project No. 1431/1/08, Pretoria: 193 p.

Tsipa, A., Sibiya, J. and Maubane, D. (2010) The impact of mobile science laboratories in the performance of Grade 12 learners in the Mpumalanga Province. 14th SAASTEC Conference. National Zoological Gardens, Pretoria, South Africa, South African Association of Science and Technology Centres.

Effects of CO_2 Degassing on pH and Fe(II) Oxidation Rates in Coal Mine Effluents

C. A. Cravotta III[1], J. N. Geroni[2]

[1]U.S. Geological Survey Pennsylvania Water Science Center, 215 Limekiln Road, New Cumberland, PA 17070, USA
[2]Cardiff School of Engineering, Cardiff University, Queen's Buildings, The Parade, Cardiff, CF24 3AA, UK

Abstract Elevated concentrations of dissolved CO_2 in groundwater from underground coal mines can depress pH and decrease the rate of removal of dissolved Fe(II) and associated metals within aerobic treatment ponds and wetlands. Mechanical aeration of the water can accelerate CO_2 removal (degassing), with consequent increases in pH and the rates of Fe(II) oxidation and Fe(III) precipitation. This paper uses kinetics modeling with the geochemical program, PHREEQC, to simulate interdependent changes in CO_2 degassing, pH, and Fe(II) oxidation rates that occur during aeration of waters discharged from abandoned coal mines.

Keywords abandoned mines; coal mine drainage; iron oxidation rate CO_2 degassing rate

Introduction

Concentrations of dissolved Fe(II) and CO_2 commonly are elevated in groundwater from coal mines (Kirby and Cravotta 2005). The elevated concentrations of dissolved CO_2 can be produced by reaction of acidic water with limestone or the oxidation of organic carbon (Langmuir 1997). Dissolved CO_2 will depress pH as indicated by the following reactions:

$$CO_2 + OH^- \rightarrow HCO_3^- \qquad (1)$$

$$CO_2 + H_2O \rightarrow HCO_3^- + H^+ \qquad (2)$$

Aeration of coal-mine effluent can promote CO_2 degassing and lead to an increase in pH (reverse of Eqs. 1 and 2) and an increase in Fe(II) oxidation rates (Cravotta 2007; Kirby *et al.* 2009; Geroni *et al.* 2012). This paper uses geochemical equilibrium and kinetics modeling with the geochemical program, PHREEQC (Parkhurst and Appelo 1999), to simulate interdependent changes in CO_2 degassing, pH, and Fe(II) oxidation rates during aeration of waters discharged from abandoned coal mines to treatment ponds or wetlands as reported in greater detail by Geroni *et al.* (2012).

Methods

Empirical time-series data on pH, temperature, dissolved oxygen (DO), and initial and final Fe(II) and alkalinity values during mechanical aeration experiments reported by Geroni *et al.* (2012) were used to estimate rates of Fe(II) oxidation and CO_2 degassing. Because the values for these unstable constituents changed rapidly, the mechanical aeration experiments were conducted for 2 hours or less. As previously described by Kirby *et al.* (2009), alkalinity was assumed to be consumed by the combined oxidation and hydrolysis of dissolved iron according to the stoichiometry:

$$Fe^{2+} + 2\,HCO_3^- + \tfrac{1}{2}\,H_2O + \tfrac{1}{4}\,O_2 \rightarrow Fe(OH)_3 + 2\,CO_2 \qquad (3)$$

Rates of Fe(II) oxidation were estimated to follow the abiotic homogeneous oxidation rate model presented by Stumm and Morgan (1996, 683–685):

$$-d[Fe(II)]/dt = k_1 \cdot [O_2] \cdot [OH^-]^2 \cdot [Fe(II)] \qquad (4)$$

where at pH > 5 and 20 °C, $k_1 = 8 \times 10^{13}\ M^{-2}\ atm^{-1}\ min^{-1}$ ($1.33 \times 10^{12}\ M^{-2}\ atm^{-1}\ s^{-1}$). The second-order dependence on $[OH^-]$ indicates a change in pH of 1 unit results in a 100-fold change in the oxidation rate. At a given pH, the rate increases by a factor of 10 for a 15 °C increase. By using the activation energy of 23 kcal/mol reported by Stumm and Morgan (1996, p. 684) with the Arrhenius equation (Langmuir 1997, p. 62), the rate can be adjusted to different temperatures.

A spreadsheet based 4th order Runge-Kutta (RK4) model was used to compute the concentration of residual Fe(II) with elapsed time based on Eq. (4). Values input into the model were initial Fe(II) concentration, along with the pH, temperature, and DO for each 10-second interval logged throughout the experiments. The apparent value for the homogeneous Fe(II) oxidation rate constant ($k_1^* = 1.33 \times 10^{12}$ to 1.33×10^{14} $M^{-2}atm^{-1}\ s^{-1}$) was chosen to yield the residual Fe(II) at the end of the experiment. These apparent rate constants were a factor of 1 to 100 times the reference value of 1.33×10^{12} $M^{-2}atm^{-1}\ s^{-1}$ at 20 °C (Stumm and Morgan 1996, p. 683).

To facilitate the evaluation of the interactions among the initial alkalinity, pH, and Fe(II) oxidation rate, the major carbonate speciation equations and thermodynamic constants from the PHREEQC data base (Parkhurst and Appelo 1999) were added to the spreadsheet RK4 model. The measured pH and temperature plus computed alkalinity (Eq. 3) were then used to estimate partial pressure of CO_2 ($p\text{CO}_2$) and the rate of CO_2 degassing during the aeration experiments considering asymptotic exponential models (Langmuir 1997; Geroni *et al.* 2012). The integrated form of the 2nd order asymptotic rate equation for CO_2 degassing is shown as Eq. (5),

$$t \cdot k_L a = [1/(C_S\text{-}C_t)+1/(C_S\text{-}C_O)] \qquad (5)$$

where C_S is the steady state (equilibrium) value, C_O is the initial value and C_t is the value at time t for the negative logarithm of $p\text{CO}_2$ in atmospheres (p_{CO_2}). Values for $-k_L a$ (the mass transfer coefficient) were calculated from the linear slope estimate of $[1/(C_S\text{-}C_t)+1/(C_S\text{-}C_O)]$ *vs.* t over the first 10 to 25 minutes of the experiments. The value of C_S was varied to yield $k_L a$ that approximated the trend for $p\text{CO}_2$ (C_t) during each experiment. The modeled values of C_S ($p\text{CO}_2 = 10^{-3.4}$ to $10^{-1.7}$ atm) and $k_L a$ for the batch aeration experiments were consistent with previous studies indicating initially rapid CO_2 degassing and approach to a steady state that can be at disequilibrium with atmospheric $p\text{CO}_2$ ($10^{-3.4}$ atm; Cravotta 2007; Kirby *et al.* 2009).

The PHREEQC aqueous speciation model (Parkhurst and Appelo 1999) was used to couple the rate equations for CO_2 degassing and Fe(II) oxidation and calculate the corresponding changes in pH and concentrations of Fe(II), dissolved CO_2 species, and other aqueous ions, assuming spontaneous equilibrium with atmospheric O_2 and considering thermodynamic feasibility for precipitation of $Fe(OH)_3$. Initial values for pH, alkalinity, DO, and Fe(II) concentration and the average temperature during each CO_2 stripping experiment were input along with estimated $k_L a$ (calculated for the 2nd order rate equation) and apparent k_1 values (as used in the RK4 model) estimated by multiplying the reference k_1 value of 1.33×10^{12} $M^{-2}atm^{-1}\ s^{-1}$ at 20 °C (Stumm and Morgan 1996, p. 683) by a factor ranging from 0.1 to 100. Model calibration was conducted by adjusting the apparent $k_L a$ and k_1 values to obtain the best fit of measured data for logged pH (paired values) and measured alkalinity and Fe(II) at the beginning and end of each experiment.

Results and Discussion

Initial pH of discharges at all four sites before aeration was circumneutral (5.6 to 6.7); however, the effluents were either net-acidic, with positive hot acidity (Blenkinsopp, Tan-y-Garn, and Ynysarwed; Table 1), or net-alkaline, with negative hot acidity (Six Bells). After 2 hours of aeration and CO_2 stripping from the net acidic waters, the Fe(II) concentration decreased from greater than 40 mg/L to less than 6 mg/L while pH remained within 0.1 unit of the initial

Site	Pre aeration					
	Hot Acidity (mg L^{-1} $CaCO_3$)	Cold Acidity (mg L^{-1} $CaCO_3$)	Alkalinity (mg L^{-1} $CaCO_3$)	pH	Fe(II) (mg L^{-1})	Temperature (°C)
Blenkinsop	33 to 55	423 to 476	264	5.6 to 6.0	137	13.4
Tan-y-Garn	16 to 22	177 to 186	57 to 58	5.6	41	12.2
Ynysarwed	29 to 33	259 to 280	143 to 146	5.8 to 5.9	93.7	13.9
Six Bells	-615	208 to 222	746 to 752	6.6 to 6.7	19	18.9
Site	Post aeration					
	Time elapsed (min)	Cold Acidity (mg L^{-1} $CaCO_3$)	Alkalinity (mg L^{-1} $CaCO_3$)	pH	Fe(II) (mg L^{-1})	Temperature (°C)
Blenkinsop	115	21 to 23	34 to 38	5.5 to 5.9	5.75	17.75
Tan-y-Garn	115	16 to 19	1	5.5 to 6.0	4.3	18.0
Ynysarwed	127	45 to 51	5 to 7	5.7 to 5.8	2.79	18.3
Six Bells	28	0	618 to 631	8.4	0.05	20.0

Table 1. *Comparison of measured hot acidity, cold acidity, alkalinity, pH, Fe(II) content, and temperature of water at the beginning and end of the batch-wise CO_2 stripping experiments*

Site	k_1 factor k_1= 1.33 × 10^{12}		k_{1*} × 10^{12} at 20 °C (M^{-2} atm^{-1} s^{-1})	Alk_0 (mg L^{-1})	C_o -log p_{CO_2}	C_s -log p_{CO_2}	k_La (log(atm)$^{-1}$ s^{-1})	Equilibrium assumption
	RK4	PHREEQCi models						
Blenkinsopp	64 to 70	40	94	250	0.40	2.0	0.001279	O_2; $Fe(OH)_3$
Tan-y-Garn	22 to 23	20	47	70	0.80	2.8	0.000426	O_2; $Fe(OH)_3$
Ynysarwed	90 to 100	50	107	165	0.64	2.8	0.000203	O_2; $Fe(OH)_3$
Six Bells	1 to 3.4	1	1.5	749	0.77	3.1	0.000933	O_2; $Fe(OH)_3$;$CaCO_3$

For PHREEQC models, initial pH, Fe(II), and alkalinity values and average temperature for batch aeration tests defined the starting solution. Apparent oxidation rate constant, k_1^*, for Eq. (4) indicated by k_1 factor multiplied by 1.33 × 10^{12} M^{-2} atm^{-1} s^{-1}. Apparent rate constant corrected to 20 °C using Arhhenius equation (Langmuir 1997, p. 62), with activation energy of 23 kcal/mol (Stumm and Morgan 1996). Exchange with atmospheric oxygen ($PO_2 = 10^{-0.27}$ atm) and precipitation of $Fe(OH)_3$ to SI< 0 were specified to maintain equilibrium. For calibrated Six Bells models, precipitation of calcite after supersaturation was considered to maintain $SI_{CALCITE} < 1.0$.

Table 2. *Values of constants and associated variables used in RK4 model of Fe(II) oxidation and calibrated PHREEQCi kinetics models of CO_2 degassing and Fe(II) oxidation*

value (Table 1). In contrast, after only 30 minutes of aeration of the net-alkaline water, Fe(II) decreased from 19 mg/L to less than 0.1 mg/L and pH increased by almost 2 units (Table 1). The pH of net acidic waters increased initially because of rapid CO_2 degassing and then decreased because of protons released by Fe(III) hydrolysis (Figs. 1a – 1c), whereas the pH of the net alkaline water increased progressively during aeration (Fig. 1d). The rapid increase in pH during early stages of aeration of all the waters coincided with an asymptotic decrease in the dissolved CO_2 from initial p_{CO_2} values of $10^{-0.4}$ to $10^{-0.8}$ atm to estimated steady-state values ranging from $10^{-1.7}$ to $10^{-3.4}$ atm (Figs. 1 and 2).

Figs. 1 and 2 show the measured pH, Fe(II), alkalinity, and p_{CO_2} and the PHREEQC simulated values produced by coupling the rate equations for CO_2 degassing and Fe(II) oxidation. Fig. 1 shows the paired values of measured pH as subparallel dotted curves and corresponding estimates of the pH by selected rate models as additional curves. The apparent Fe(II) oxidation rate corrected to 20 °C for the net acidic waters were 47 to 107 times the reference k_1 value at 20 °C, whereas that for the net alkaline water was 1.5 times the reference value (Table 2). Although these rates are within the range of reported homogeneous Fe(II) oxidation rates in mine waters (Geroni and Sapsford 2011), apparent k_1 factors greater than 1 may be attributed to heterogeneous oxidation by Fe(III) particles. We considered combined homogeneous and heterogeneous Fe(II) oxida-

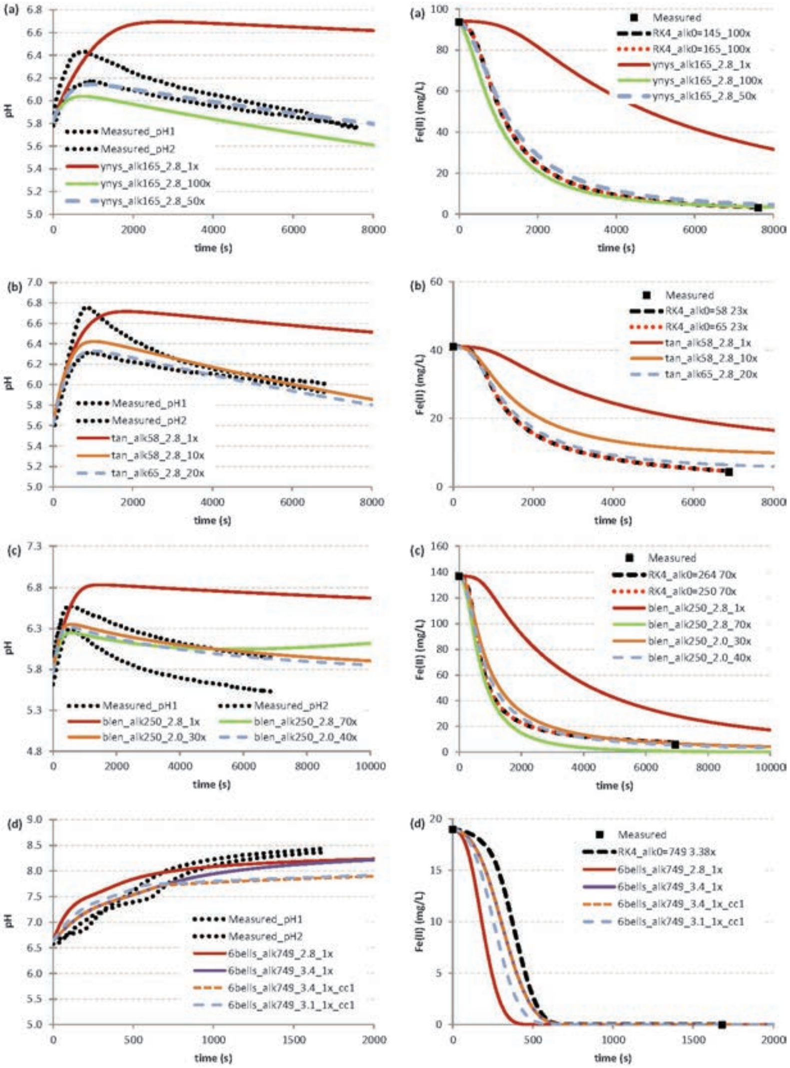

Fig. 1 *Comparison of measured pH and estimated Fe(II) concentrations from spreadsheet based RK4 model to simulated pH and Fe(II) from PHREEQC models (after Geroni et al. 2012): (a) Ynysarwed (ynys), (b) Tan-y-Garn (tan), (c) Blenkinsopp (blen), (d) Six Bells (6bells). Values for initial alkalinity and rate constants used for RK4 and PHREEQ models are summarized in Table 2. In legend, Alk$_0$ (58 to 749 mg/L CaCO$_3$ equivalent), steady-state pco$_2$ (2.0 to 3.4) and k$_1$ multiplication factor (1× to 90×) are given for each simulation. The unbroken red curve indicates the reference simulation for values of k$_1$ = 1.33×10^{12} $M^{-2}atm^{-1}s^{-1}$ and steady-state pco$_2$ = 2.8. Dashed curves show results for calibrated models; for Six Bells, calcite precipitation maintained SI$_{CALCITE}$ < 1 (cc1).*

tion rate equations (*e.g.* Dempsey *et al.* 2001) as an alternative model for the PHREEQC simulations. However, the inclusion of heterogeneous oxidation did not improve our ability to simulate the empirical results. By adjusting only the apparent rate constants for homogeneous Fe(II) oxidation and CO$_2$ degassing, the observed pH, Fe(II), and alkalinity data could be simulated. For refinement of the Tan-y-Garn and Ynysarwed models, the starting alkalinity values were increased from 58 to 70 mg/L and 148 to 165 mg/L, respectively, and for the Six Bells model, precipitation of calcite was simulated upon reaching supersaturation (SI$_{CALCITE}$ < 1.0). After calibration, simulated values for pH were within the range of measured values, and simulated values for Fe(II) and alkalinity were comparable to those at the beginning and end of the experiments (Figs. 1 and 2).

Conclusions

Elevated concentrations of dissolved CO$_2$ in effluent from underground coal mines can depress pH and decrease the rate of removal of dissolved Fe(II) within aerobic treatment ponds and wetlands. Aeration of the effluent can accelerate CO$_2$ removal (degassing) and increase pH, with a consequent increase in the rate of Fe(II) oxidation and Fe(III) precipitation.

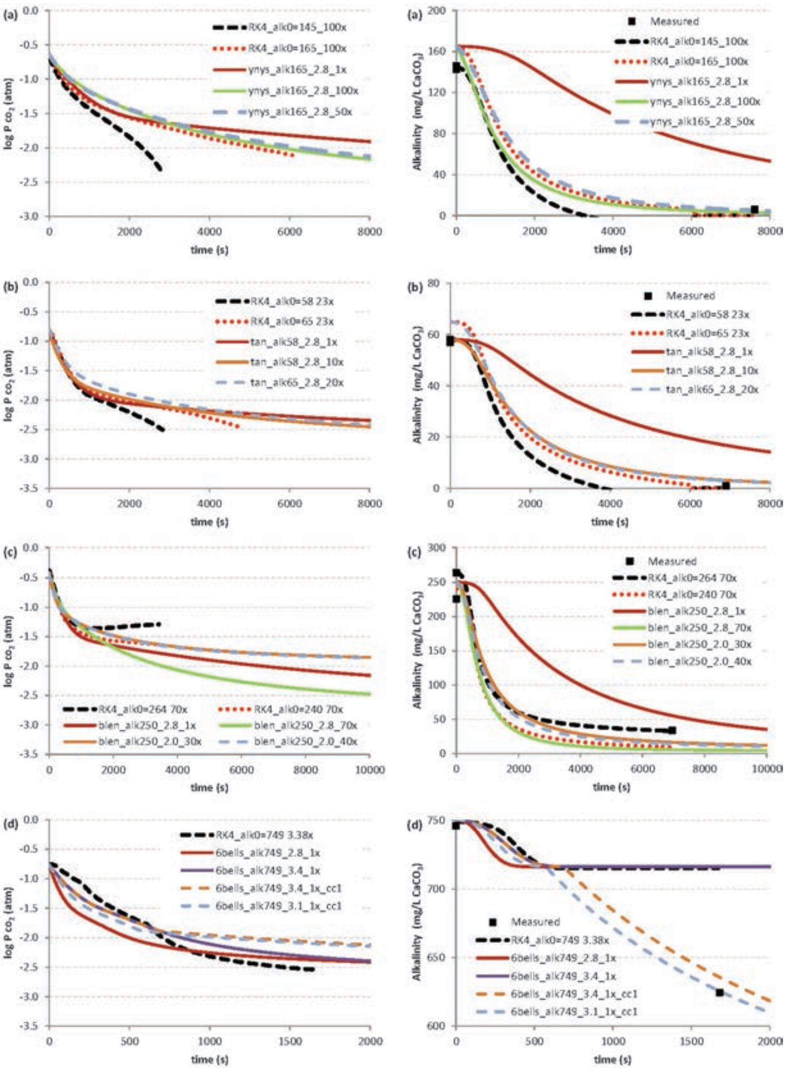

Fig. 2 *Comparison of estimated pco$_2$ and alkalinity concentrations from spreadsheet based RK4 model to simulated pco$_2$ and alkalinity from PHREEQC models: (a) Ynysarwed; (b) Tan-y-Garn; (c) Blenkinsopp; (d) Six Bells. Values for initial alkalinity and rate constants used for RK4 and PHREEQ models are summarized in Table 2. In legend, Alk$_0$ (58 to 749 mg/L CaCO$_3$ equivalent), steady-state pco$_2$ (2.0 to 3.4) and k_1 multiplication factor (1x to 90x) are given for each simulation. The unbroken red curve indicates the reference simulation for values of k_1 = 1.33 × 10^{12} M^{-2}atm^{-1}s^{-1} and steady-state pco$_2$ = 2.8. Dashed curves show results for calibrated models; for Six Bells, calcite precipitation maintained SI$_{\mathrm{CALCITE}}$ < 1 (cc1).*

The rate of CO$_2$ degassing during mechanical aeration experiments was successfully described using a 2nd order asymptotic exponential model and that for Fe(II) oxidation was described using a 1st order exponential rate model for homogeneous oxidation. Because the homogeneous rate model for Fe(II) oxidation is strongly dependent on the pH, the rate of CO$_2$ degassing was a major factor affecting the rate of Fe(II) oxidation. With the PHREEQC modeling approach, the pH was permitted to change with reaction progress and was controlled primarily by the rate of CO$_2$ degassing and secondarily by the extent of Fe(III) hydrolysis and the available alkalinity. The empirical data and associated simulations indicated that hydrolysis of Fe(III) depressed the pH of net acidic water to a greater extent than that of net alkaline water. Although the rates of Fe(II) oxidation for the net acidic effluents were 47 to 107 times the reference k_1 value at 20 °C, the Fe(II) oxidation and removal rates were slower for net acidic effluents than for the net alkaline effluent.

The measured trends in pH and Fe(II) concentrations during aeration experiments demonstrated potential for pH to affect Fe(II) oxidation rate in accordance with the homogeneous oxidation rate model. Despite limited availability and quality of the time-series data, kinetics modeling using the geochemical speciation program, PHREEQC, provided insight into the interactions among chemical processes and the relative importance of specific reactions, such as CO_2 degassing, Fe(III) hydrolysis, and calcite precipitation, on the pH of poorly buffered water. Empirical data on temperature, DO, pH, alkalinity, Fe(II) concentration, and associated solutes and solids generally are needed to estimate the kinetics of CO_2 degassing and Fe(II) oxidation during aeration tests or within treatment systems. With this information, treatment strategies can be evaluated to optimize the removal of Fe(II) while minimizing the use of chemicals for pH adjustment.

References

Cravotta CA III (2007) Passive aerobic treatment of net-alkaline, iron laden drainage from a flooded underground anthracite mine, Pennsylvania, USA. Mine Water Environ. 26, 128–149

Dempsey BA, Roscoe HC, Ames R, Hedin R, Jeon B-H (2001) Ferrous oxidation chemistry in passive abiotic systems for the treatment of mine drainage. Geochem. Explor. Environ. Anal. 1, 81–88

Geroni JN, Sapsford DJ (2011) Kinetics of iron (II) oxidation determined in the field. Appl. Geochem. 26, 1452–1457

Geroni JN, Cravotta CA III, Sapsford DJ (2012) Evolution of the chemistry of Fe bearing waters during CO_2 degassing. Appl. Geochem. 27, 2335–2347

Kirby, CS, Cravotta CA III (2005) Net alkalinity and net acidity 2: Practical considerations. Appl. Geochem. 20, 1941–1964

Kirby CS, Dennis A, Kahler A (2009) Aeration to degas CO_2, increase pH, and increase iron oxidation rates for efficient treatment of net alkaline mine drainage. Appl. Geochem. 24, 1175–1184

Langmuir D (1997) Aqueous environmental geochemistry. Prentice Hall, New Jersey, USA, 600 p

Parkhurst DL, Appelo CAJ (1999) User’s guide to PHREEQC (Version 2)—A computer program for speciation, batch-reaction, one-dimensional transport, and inverse geochemical calculations. U.S. Geol. Surv. Water-Resour. Inv. Re99–4259, 310 p

Stumm W, Morgan JJ (1996) Aquatic chemistry—chemical equilibria and rates in natural waters (3rd). New York, Wiley-Interscience 1022 p

New Insights on Factors Controlling Pit Lake Chemistry

Andy Davis, Maggy F. Lengke

Geomega Inc., 2525 28th Street, Boulder, Colorado 80301, USA, andy@geomega.com

Abstract Pit lake chemistry has not always been as predicted due to several issues For example, the pit lake surface at the rock/water interface has a ≈2 ft (0.6 m) capillary zone that enhances oxidation of available pyrite. If the redox boundary is above the pit lake surface accumulation of spall material on benches results in sulfides becoming reactive if the pit lake reaches that bench. From a remedial perspective, with initiation of deeper pit lakes, it is apparent that pit lake hydraulics, including is important. However, from an ecological risk perspective, a slightly acidic (pH 4.5) pit lake does not appear to result in an unacceptable ecological risk.

Keywords pit lake, ecological risk, pyrite, predictive modeling

Introduction

Cessation of dewatering activities at open pit mines results in the creation of a "pit lake" if the pre-mining groundwater table elevation is higher than the bottom of the pit after it is decommissioned. As part of the environmental assessment process, it is necessary to determine the environmental impacts of future pit lake chemistry on potential receptors including, 1) groundwater quality adjacent to the pit (in the case of a through-flow pit lake), and 2) the food web.

Pit lake chemistry is influenced by the nature of the wall rock, its mineralogy, alteration and the location of the redox boundary. Many gold deposits are rich in sulfides, commonly pyrite (FeS_2). When pyrite reacts with atmospheric oxygen and water, sulfuric acid is generated (Nordstrom and Alpers 1999), *i.e.*:

$$FeS_2 + 3.75\ O_2 + 3.5\ H_2O \rightarrow$$
$$Fe(OH)_3(s) + 2\ SO_4^{2-} + 4H^+ \qquad (1)$$

Coal deposits, except for those with very low sulfur contents, commonly contain substantial pyrite or its polymorph, marcasite. Organic-rich shales that are mined for phosphate fertilizer may also contain pyrite (Gammons *et al.* 2009). Uranium deposits may or may not contain significant pyrite, but the radionuclides from the ore can present their own problems. Pits producing metals, industrial minerals, and solid fuels may all generate acid pit lakes depending on the lithologic setting.

Consequently, environmental regulators require mining companies to estimate post-mining water quality predictions as part of the permitting process. Such analyses can also guide mine managers to develop site closure plans that minimize negative impacts and optimize the value of the pit lake as a future water resource.

Pit lake chemistry prediction for mine permits is usually based on site-specific groundwater hydrogeology, background groundwater chemistry, pit lake water balance, wall rock acid-base accounting and mineralogy, pit wall surface area, and wall rock kinetic humidity cell or column tests. Model verification may rely on laboratory or field analogs (Davis *et al.* 2006) and pre-existing pit lake data (*e.g.* Tempel *et al.* 2000) where it is available. Where such information has been collected during an interlude between mining eras, *e.g.* from the South and Center pit lakes at the Getchell mine (Davis *et al.* 2006) and the Liberty and Kimbley pit lakes at Robinson (Miller *et al.* 1996), it may shed light on pit lake chemogenesis subsequent to new pit expansion and then closure.

When mining ends, the resulting pit lake chemistry has not always been as predicted. The goals of this paper are to describe the pit lake modeling process and identify perceived data and conceptual gaps which are ripe for additional research to assist in developing more accurate predictive tools.

Modeling Pit Lake Chemogenesis

Pit lake water chemistry predictions typically combine the output from a groundwater flow model (*e.g.* MODFLOW), background groundwater chemistry, the extent of wall rock reaction, and solute releases based on kinetic humidity cell or column tests data for related formations exposed on the pit wall. (fig. 1).

Pit wall runoff of solutes into the pit lake during storm events may also affect the chemistry but is usually considered inconsequential compared to groundwater/wallrock interactions. Wall rock reactivity is a key component of the conceptual pit lake model, the extent of which is based on the pit wall surface area in contact with pit water and a reactivity factor. The pit wall surface area is usually calculated using geographic information system (GIS) software, by superimposing the geology on pit elevation contours.

Wallrock solute release to be well represented by humidity cell tests (HCTs) run on crushed rock representative of the exposed lithologies (ASTM 2007). HCTs appear representative of wall rock conditions due to the combination of moisture, air, heat and sulfides in the capillary zone. Curves fit to the effluent chemistry provide chemical release functions allowing cumulative mass of any parameter per surface area to be calculated as a function of time.

A finite difference groundwater model, *e.g.* MODFLOW (HydroGeoLogic 1996) is used to predict the infilling rate of the pit lake resulting in an estimate of the rate-of-rise of the pit lake with time. The same model is used to estimate the dewatering schedule to maintain a dry pit base during mining, any impacts to seeps and springs based on the extent of the ten-foot drawdown cone resulting from dewatering, and potential compaction due to withdrawal of water from the aquifer until recovery of the pre-mining groundwater elevation. The infilling rates from the groundwater model are correlated with the pore volumes passed through the HCTs as a function of the pit lake hydrograph, which describes the volume of water passing through any zone in the wall rock over time.

For non-reactive rock, standard equilibrium geochemical programs suffice to quantify mineral dissolution and precipitation reactions. However where there is substantial pyrite as well as other sulfides the kinetic dissolution rate becomes important, especially if these minerals are at higher elevations in the

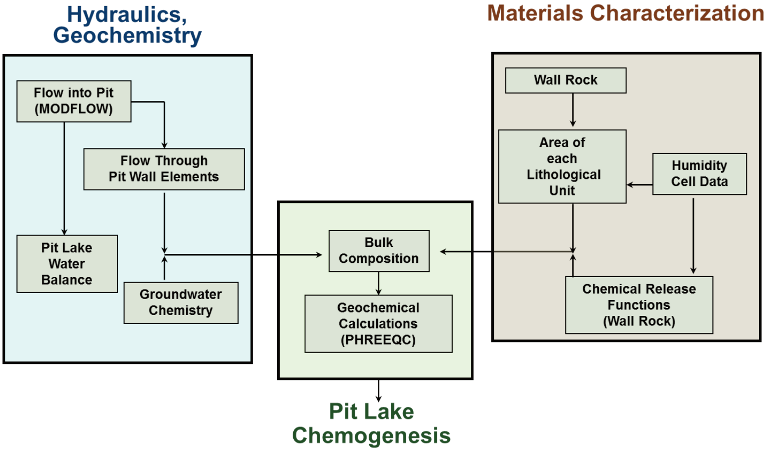

Fig. 1 *Typical pit lake chemistry modeling approach*

pit wall where infilling rates slow and there is a greater residence time for reactions prior to inundation by the rising pit lake. In these cases a reactivity factor has been used to predict pit lake chemistry (Geomega 2010). This factor acts as a calibration parameter (akin to variable hydraulic conductivity in the groundwater model) to incorporate factors such as increased surface area due to fracturing of wall rocks, slough material and the kinetics of sulfide oxidation.

Mechanisms Requiring Additional Attention

Rock Spalling

Open-pit mines result in benches that are usually 7 to 15 m high, depending on the size of the machinery in use and the stability of the high walls. The frequency and amount of spalling is a function of weathering rates, the type of rock, and inherent structural weakness. Benches collect rubble (fig. 2) resulting in an increase in reactive surface area as the infilling pit lake reaches this material. This factor is usually not incorporated into pit lake chemistry predictions. If the spall rocks are abundant and mostly acid-generating, then it may affect the pit lake pH.

Fig. 2 *Rock spall on pit benches.*

Land Slides

A land slide results in spalling of the pit wall (fig. 3) due to slope instability. Although designed with an allowable safety factor, slides do occur. For pit lake chemistry predictions, the land slide factor is usually not included, but depending on the acid-generating capacity of the wall rock it may be relevant in acute pit lake chemical evolution.

The Capillary Zone

At several pit lakes we have observed a 1–2 foot (0.3–0.6 m) capillary zone above the air/pit lake interface (fig. 4). When the pit lake infilling rate is rapid during early recovery of the drawdown cone, the oxidation of pit wall sulfides is limited due to, 1) inadequate time for oxidation before the sulfide is inundated, and 2) sufficient alkalinity to offset any acid generation from soluble acid salts. As pit infilling slows, there is increasing time for sulfide oxidation

Fig. 3 *A landslide covering several pit benches.*

Fig. 4 *Capillary zone during pit lake infilling.*

to be initiated in the capillary zone due to the availability of oxygen, heat, and moisture.

Sulfide oxidation (fig. 3) is indicated by the red iron oxide/hydroxide in the capillary zone. Abiotic pyrite oxidation rates increase over time (Lizama and Suzuki 1989) and under acidic conditions even more so if bacteria, *e.g. thiobacillus ferrooxidans* are present (Nordstrom 1982). This process indicates that reaction rate kinetics may be an important component of pit lake chemistry prediction in such settings, precluding the use of equilibrium geochemical programs (*e.g.* PHREEQC, MINTEQA2). The kinetic reactivity is usually not built into pit lake predictions, but it has been applied as part of pit lake predictions for the Getchel mine, Nevada, USA (Tempel *et al.* 2000) and the Martha mine, New Zealand (Castendyk and Webster-Brown 2007).

Mineralogy and Kinetic Reaction Rates

Pyrite is generally considered to be the sulfide engendering acidity. However, other iron sulfides such as pyrrhotite and marcasite can be equally or more problematic so that understanding wallrock mineralogy is an important geochemical variable. Pyrrhotite has a non-stoichiometric composition ($Fe_{n-1}S_n$ with n≥8), resulting in structures from Fe_7S_8 to $Fe_{11}S_{12}$. The oxidation reaction of aqueous pyrite or marcasite by dissolved oxygen is written in the above reaction (1) and the oxidation reaction of pyrrhotite is:

$$\begin{aligned} &Fe_{1-x}S + (2-0.5x)O_2 + xH_2O \rightarrow \\ &(1\text{-}x)Fe^{2+} + SO_4^{2-} + 2xH^+ \end{aligned} \qquad (2)$$

$$Fe^{2+} + 0.25O_2 + 2H^+ \rightarrow Fe(OH)_3(s) \qquad (3)$$

In addition, arsenic sulfides may have similar reactivity to iron sulfides depending on arsenic species in solution. For example, dissolution of realgar generates the same number of protons as pyrite, *e.g.*:

$$\begin{aligned} &AsS + 2.75\ O_2 + 2.5\ H_2O \rightarrow \\ &HAsO_4^{2-} + SO_4^{2-} + 4\ H^+ \end{aligned} \qquad (4)$$

as does each mole of arsenopyrite:

$$\begin{aligned} &FeAsS + 7\ O_2 + 8\ H_2O \rightarrow \\ &HAsO_4^{2-} + SO_4^{2-} + Fe(OH)_3(s) + 4\ H^+ \end{aligned} \qquad (5)$$

and orpiment :

$$\begin{aligned} &As_2S_3 + 8.5\ O_2 + 3\ H_2O \rightarrow \\ &2\ HAsO_4^{2-} + 3\ SO_4^{2-} + 4\ H^+ \end{aligned} \qquad (6)$$

The kinetic rate laws for oxidation of pyrite (Williamson and Rimstidt 1994), marcasite (Asta *et al.* 2010), and orpiment/realgar (Lengke and Tempel 2009) demonstrate that rates generally increase at higher pH values with increasing dissolved oxygen. However, the reaction of orpiment and realgar in the laboratory has not shown a complete oxidation reaction of arsenic and sulfur species (Lengke and Tempel 2009). The oxidation rate of pyrite by dissolved oxygen is much lower than marcasite at pH 2–3 and pyrrhotite at pH 2.8 while the pyrite oxidation rate is slightly higher than realgar and orpiment (fig. 5).

In a ferric iron-mediated system, the oxidation rate of pyrrhotite increases by one order magnitude at pH 2.8 (Janzen *et al.* 2000), while the oxidation and dissolution of arsenopyrite increases by approximately one to two orders of magnitude at pH 1.8 over non-ferric iron systems (Lengke and Tempel 2009).

Sulfide oxidation by iron- and sulfur-oxidizing bacteria facilitates oxidation of Fe^{2+} to Fe^{3+} or of elemental sulfur to sulfate, respec-

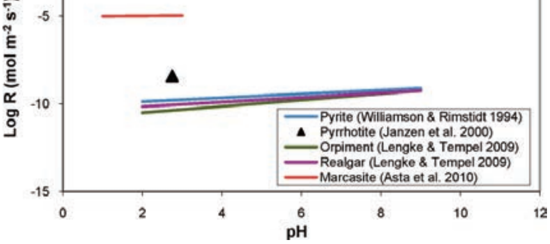

Fig. 5 *A comparison of Fe- and As-bearing sulfide oxidation as a function of pH.*

tively (Lengke and Tempel 2009). Because Fe^{3+} in solution can rapidly attack the sulfide surface, these minerals will be oxidized as rapidly as the bacteria can generate Fe^{3+}. In addition, increasing acidity as elemental sulfur is oxidized to sulfate may cause an increase in oxidation rates.

Pit Lake Hydrodynamics

An emerging field in pit lake chemistry is the evolution of the thermal (and chemical) profile as the pit lake fills. This phenomenon has been described previously in the Berkeley pit lake (Davis and Ashenburg 1989).

Where pit lakes are acidic and mitigation is necessary, this issue is consequential because of the need to manage liming over the course of yearly cycles of thermal stratification and breakdown. In addition, pits are often asymmetric in structure, such that evolving thermal and chemical conditions in deep portions of the pit lake can lag behind shallow areas.

Modeling pit lake hydrodynamics is complicated by these factors and also because the requisite data to calibrate the models is rarely available.

Integrating Ecological Risk with Pit Lake Predictions

A screening-level ecological risk assessment (SLERA) evaluates potential ecological risks associated with the actual range of pH and chemistry in a mine pit lake, specifically to wildlife attracted to the water. In the SLERA, a set of species representative of the food web is identified then the pit lake water concentration compared with different toxicity thresholds, *e.g.* the no- or the lowest-observed adverse effects threshold, the NOAEL or LOAEL, respectively, to ascertain the potential for risk.

A SLERA can also be used to develop a critical pH at which there should be no adverse impacts to biota. For example, the lowest pH at which Al is ≥ NOAEL (4.5 mg/L) is 4.0. Using a LOAEL (45 mg/L) the highest pH at which Al is ≥ LOAEL is 3.3 (fig. 6).

Conclusions

Predicting pit lake chemistry is not simple, and ultimately the accuracy of the prediction should be evaluated by comparing modeled pit lake chemistry to observed lake water chemistry during the post-mining period. Factors controlling pit lake chemistry such as rock spalling, land slides, and pyrite oxidation kinetics in the capillary zone may have significant impacts on pit lake chemistry that have not been incorporated into conceptual models. Ongoing monitoring of post-mining pit lakes is an important element of understanding pit lake chemogenesis that will improve our scientific understanding and lead to more

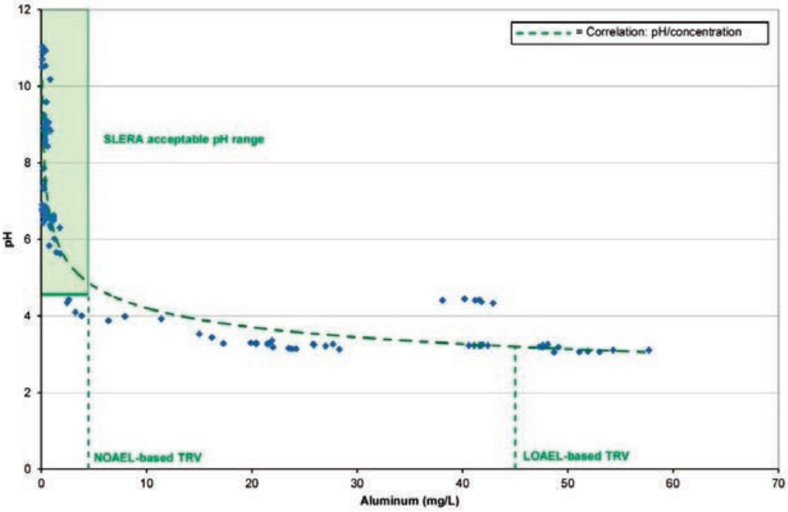

***Fig. 6** Determination of the relationship between Al concentrations in the pit lake over the period of record as a function of pH. The equivalent LOAEL Al values and the corresponding “safe” pH can be determined at the interception point with the dashed line.*

accurate predictions, and where necessary improve mitigation planning in the future.

Acknowledgements

The authors appreciate the comments of two anonymous reviewers which improved the quality of the original manuscript.

References

ASTM (2007) Standard Test Method for Accelerated Weathering of Solid Materials Using a Modified Humidity Cell, D 5744–07.

Asta MP, Cama J, Acero P (2010) Dissolution kinetics of marcasite at acidic pH. Eur. J. Mineral. 22:49–61.

Castendyk DN, Webster-Brown JG (2007) Sensitivity analyses in pit lake prediction, Martha mine, New Zealand 2: Geochemistry, water-rock reactions and surface adsorption. Chemical Geol. 244:56–73.

Davis A, Ashenburg GD (1989) The aqueous geochemistry of the Berkeley Pit, Butte, Montana, U.S.A. Appl. Geochem. 4: 23–36.

Davis A, Galloway JN, Nordstrom DK (1980) Lake acidification: its effect on lead in the sediment of two Adirondack lakes. Limnol. Oceanogr. 27:163–167.

Davis A, Bellehumeur T, Hunter P, Hanna B, Fennemore GG, Moomaw C, Schoen S (2006) The nexus between groundwater modeling, pit lake chemogenesis and ecological risk from arsenic in the Getchell Mine Pit, Nevada, U.S.A. Chemical Geol. 228:175–196.

Gammons CH, Harris LN, Castro JM, Cott PA, Hanna BW (2009) Creating lakes from open pit mines: processes and considerations, with emphasis on northern environments. Canadian Technical Report for Fisheries and Aquatic Sciences 2826, 105 pp.

HydroGeoLogic (1996) MODFLOW-SURFACT, Code documentation report: Herndon, VA., HydroGeoLogic, Inc.

Janzen MP, Nicholson RV, Scharer JM (2000) Pyrrhotite reaction kinetics: Reaction rates for oxidation by oxygen, ferric iron and for nonoxidative dissolution. Geochim. Cosmochim. Acta 64:1511–1522.

Lengke MF, Tempel RN (2009) The oxidation and dissolution of arsenic-bearing sulfides. Canadian Mineral. 47:593–613.

Lizama HM, Suzuki I (1989) Rate equations and kinetic parameters of the reactions involved in pyrite oxidation by *thiobacillus ferrooxidans.* Appl. Environ. Microbiol. 55, 2918

Miller GC, Lyons WB, Davis A (1996) Understanding the water quality of mining pit lakes. Environ. Sci. Technol. 30:118A-123A.

Nordstrom DK (1982) Aqueous pyrite oxidationand the consequent formation of secondary iron minerals. In Acid Sulphate Weathering (ed. D. K. Nordstrom), PP 37–56. Soil Sci. Soc. Amer. Spec. Publ. No. 10.

Nordstrom DK, Alpers CN (1999) Geochemistry of acid mine waters. Society of Economic Geologists, Reviews in Economic Geology 6A: 133–160.

Tempel RN, Shevenell LA, Lechler P, Price J (2000) Geochemical modeling approach to predicting arsenic concentrations in a mine pit lake. Applied Geochemistry 15:475–492.

Williamson MA, Rimstidt JD (1994) The kinetics and electrochemical rate-determining step of aqueous pyrite oxidation. Geochemica et Cosmochimica Acta 58:5443–5454.

Mine flooding prognosis making use of EPANET

Stefanus Rainier Dennis[1], Ingrid Dennis[2], Andrew Johnstone[3]

[1]*Centre for Water Sciences and Management, North-West University, 11 Hoffman Street, Potchefstroom, South Africa, 2531, rainier.dennis@nwu.ac.za*
[2]*Centre for Water Sciences and Management, North-West University, 11 Hoffman Street, Potchefstroom, South Africa, 2531, ingrid.dennis@nwu.ac.za*
[3]*Groundwater Consulting Services, 63 Wessel Road, Woodmead, South Africa, 2191, andrewj@gcs-sa.biz*

Abstract Flooding and associated decanting of many South African underground and opencast mines has been reported from a number of areas within South Africa. The South African government has stressed the urgency of implementing intervention measures as many of these mines are located close to densely populated areas. However before intervention actions can be taken, these systems have to be investigated and understood. This paper demonstrates that EPANET can be used to obtain a first estimate of the flooding prognosis before a detailed mine flooding model like the DMT BoxModel is implemented. A case study is used to compare model results.

Keywords Mine flooding prognosis, EPANET, DMT BoxModel

Introduction

Flooding and associated decanting of many South African underground and opencast mines has been reported from a number of areas within South Africa. Mine flooding needs to be managed and appropriate measures should be in place, in instances where mine decant can take place (Wolkersdorfer 2008). The South African government has stressed the urgency of implementing intervention measures. However before any intervention can be successful these flooding mine systems have to be understood.

There are numerous tools available to assist in this regard including numerical models. In fact some of the models have been specifically developed for the simulation of mine flooding. The BoxModel used by Deutsche Montan Technologie GmbH (DMT) is such an example.

Methodology

Linear interpolation of rising water levels can both lead to an over or under estimation of the date when a mine is 100 % flooded. This is due to the fact that this method cannot account for the variability and interconnection between different mine voids and also does not consider the change in the hydraulic gradient over time which is an important factor (Banks 2001). The use of porous flow models for mine flooding simulations are also incorrect under certain conditions due to the fact that the nature of the governing hydraulics are more related to pipe flow than porous medium flow.

Modelling has become a tool commonly used to analyze, estimate and predict associated impacts associated with mine flooding and decanting. Water inflow in the vicinity of open pits or underground mines is three-dimensional; consequently, 3-D numerical flow models must be based on 3-D hydrogeological data if they are to become reliable predictive tools for resolving issues listed above (Martinez and Ugorets 2010).

Two 3-D numerical models were applied in this study. The first model, namely the DMT BoxModel developed by Deutsche Montan

Technologie GmbH (DMT) has been employed as the numerical tool of choice and has been further developed to cope with the features of extensively exploited large coal fields (Eckart *et al.* 2004).

The BoxModel is a 3D finite volume program for modelling the flow of groundwater and mine water, heat transport and multicomponent mass transport including sorption, microbial degradation and the reactions with minerals. A special feature is the highly flexible discretization to model geological structures such as layers and faults as well as structural mining elements and mine excavations (DMT 2011).

The model supports multiple boxes in a free structure with multiple connections between boxes of various types. Turbulent, laminar and time dependent flow functions between boxes are supported, to name a few, as shown in Fig. 1.

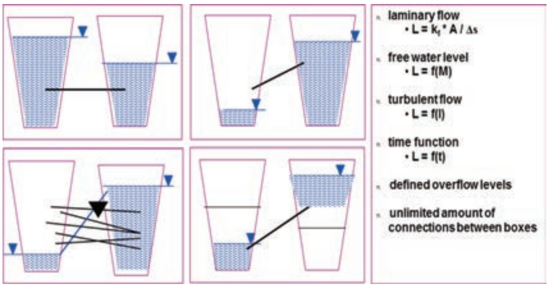

Fig. 1 *Various interconnection types between boxes (DMT 2011).*

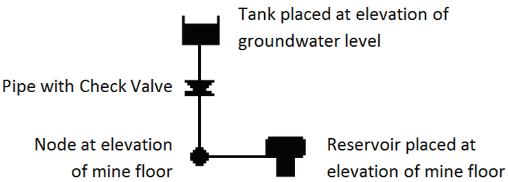

Fig. 2 *Head dependent inflow mine void configuration.*

The second model, namely EPANET (developed by the United States Environmental Protection Agency) was actually developed for the simulation of water distribution in piping systems. For the purpose of this paper, components of EPANET are used in a fixed configuration to represent the mine voids with head dependent inflows. The configuration is shown in Fig. 2. The purpose of the check valve is to ensure flow in only one direction and the

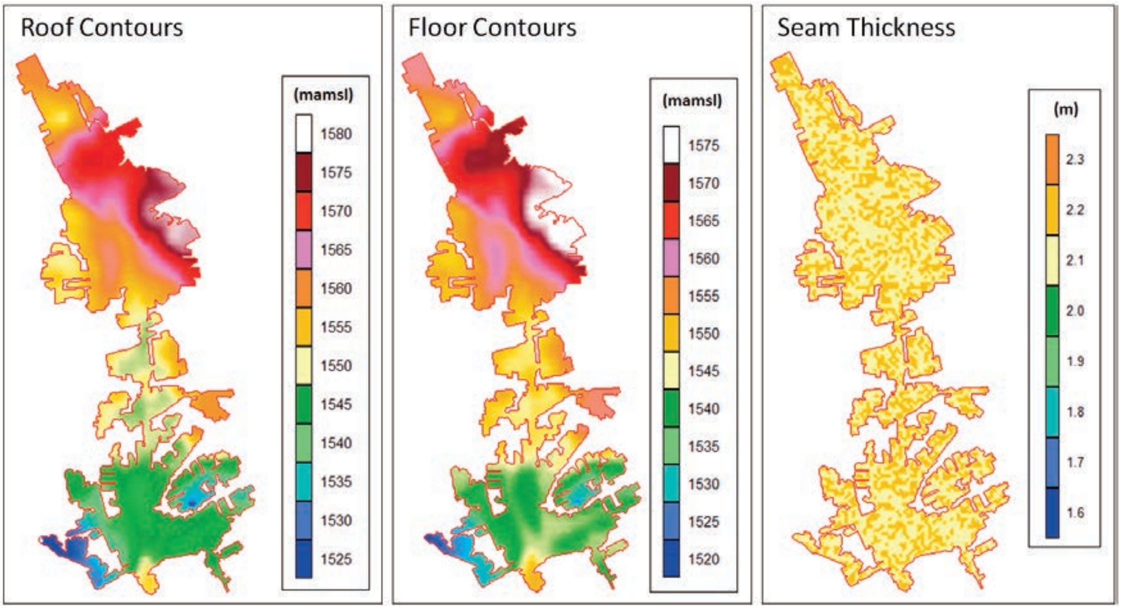

Fig. 3 *Roof, floor and seam thickness of coal mine.*

nodes are used to connect the various mine voids to a network.

Both models were used to simulate the same case thereby comparing the results and testing the hypothesis that EPANET can be used as a first approximation for mine flooding scenarios.

Case Study

An underground coal mine in the Mpumalanga province in South Africa is used in the case study. The mine closed in 1996 and since then water levels in the mine have been slowly rising. The roof and floor contours of the mine are shown in Fig. 3. A uniform seam thickness of 2.1 m was assumed for modelling purposes.

DMT Box Model Approach

In the DMT Box Model a box was created for each of the 668 mined-out areas and each of the boxes were connected with one another as shown in Fig. 4.

Recharge to the mine was applied based on the mining activity which resulted in 15 % recharge over fully stooped areas and 3 % recharge over the remainder of the area. Pumps were introduced into the model to sim-

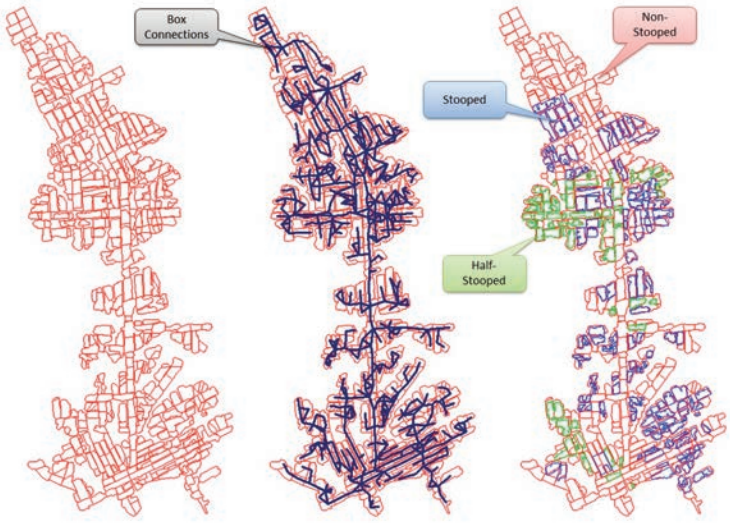

***Fig. 4** Mined-out and stooped areas.*

***Fig. 5** Virtual pumps and control points introduced into the model.*

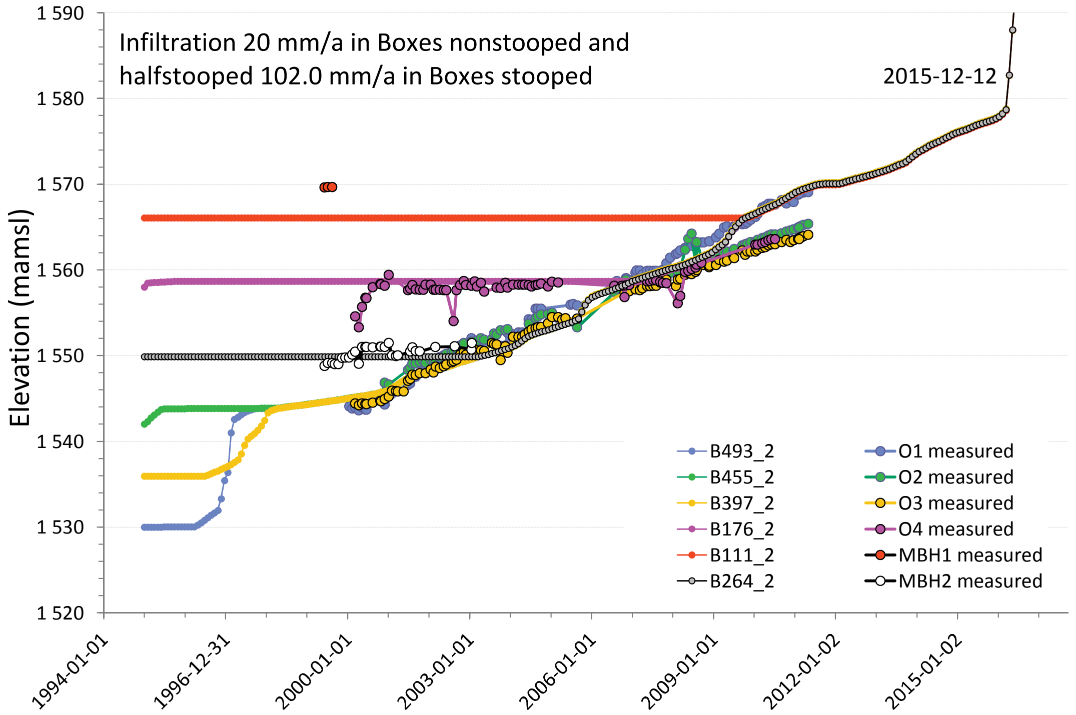

Fig. 6 *Simulated versus observed values of the DMT BoxModel*

ulate the hydrological conditions while the mine was in production. Control points were introduced in the model that coincides with monitoring boreholes intersecting the mine void as shown in Fig. 5.

Simulated versus observed values for the DMT BoxModel is shown in Fig. 6. Note the date of 100 % flooding is predicted to be December 2015.

EPANET Approach

The EPANET was used to setup an equivalent model to that of the DMT BoxModel. All parameters were kept exactly the same except for the delineation of the boxes. A coarse delineation based on floor elevations resulted in 43 mine voids (6 % of the total BoxModel voids) to be simulated with the EPANET configuration discussed earlier. The resultant floor elevations and equivalent EPANET model is shown in Fig. 7.

The comparison of the EPANET model versus the DMT BoxModel is shown in Fig. 8. The EPANET model is more conservative with the prediction of the flooding date which is 6 months earlier than that predicted by the DMT BoxModel. This behavior is contributed to the fact that the EPANET model assigns a fixed head condition to each defined void space which in turn is inter-connected through the node network. The step-wise nature of the EPANET curve is a result of the discretization of 668 boxes to 43.

Conclusions

Based on this information, and given the urgency of the situation of the mine flooding situation in South Africa, EPANET may be a solution to obtain a conservative mine flooding curve and expected time of decant. The advantage of EPANET is that it only takes a fraction of the time necessary for a complex 3-D model such as the BoxModel. However a word of caution is offered, in order to ensure accurate predictions on the sensitive mining areas, detailed field investigations are necessary,

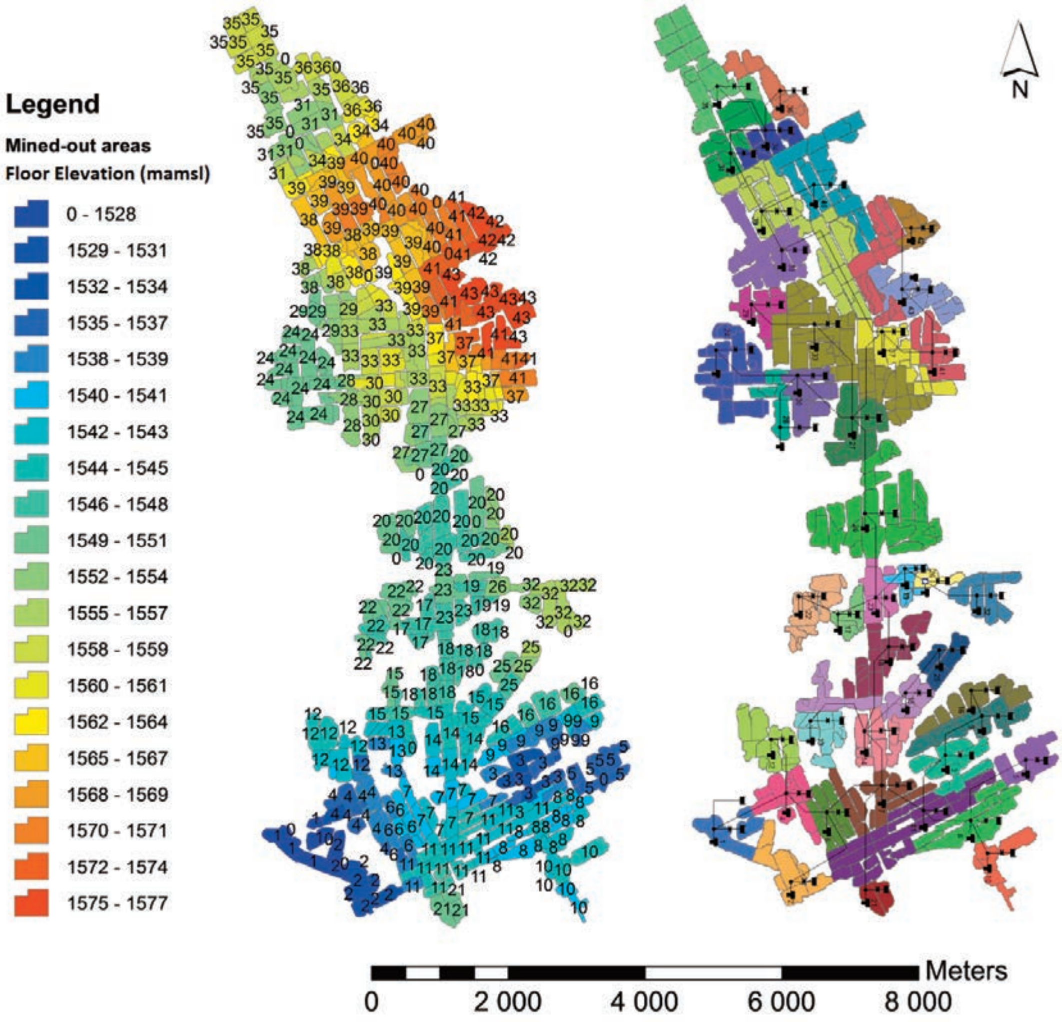

Fig. 7 *Equivalent EPANET model.*

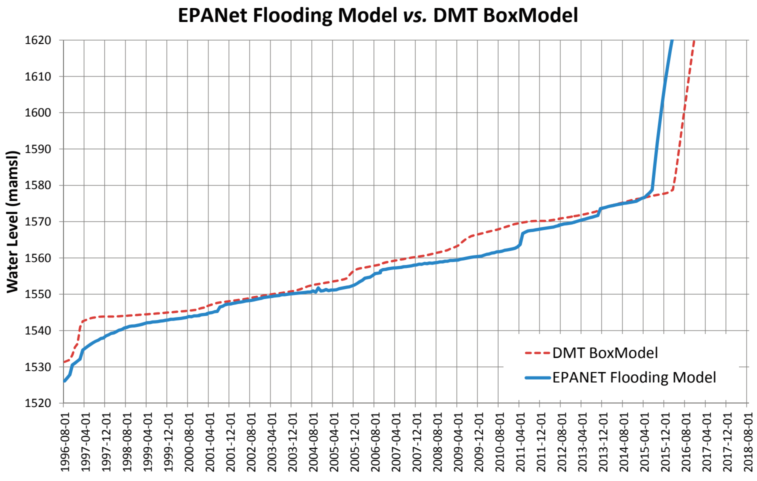

Fig. 8 *EPANET model results compared to the DMT Box-Model.*

including extensive data collection and monitoring to minimize uncertainty and to identify and investigate long-term solutions that would reduce the requirement for pumping and treating of poor quality water.

Acknowledgements

The authors thank Michael Eckhart from DMT for the results of the BoxModel for the selected case study.

References

Banks D (2001) A variable-volume, head-dependent mine water filling model. Ground Water – Vol 39, No3, p 362–365

DMT (2011) BoxModel Concept: ReacFlow3D. Program description accompanying BoxModel documentation

Eckart M, Kories H, Rengers R, Unland Werner (2004) Application of a numerical model to facilitate mine water management in large coal fields in Germany. IMWA 2004 Proceedings

Martinez C, Ugorets V (2010) Use of numerical groundwater modelling for mine dewatering assessment. Water In Mining 2nd International Congress, Santiago, Chile

Wolkersdorfer C (2008) Water management at abandoned flooded underground mines. Springer, Berlin Heidelberg

Tracer Testing to Evaluate Tailing Pile Hydrogeologic Characteristics to Support Closure and Reclamation

Craig Divine[1], Adam Griffin[2], Lee Christoffersen[3], Jeff Gillow[1],
Kelli Preston[1], Phil DeDycker[1]

[1]*ARCADIS U.S., Inc., 630 Plaza Drive, Highlands Ranch, Colorado, 80129, USA, Craig.Divine@arcadis-us.com, Jeff.Gillow@arcadis-us.com, Kelli.Preston@arcadis-us.com, Phil.DeDycker@arcadis-us.com*
[2]*ARCADIS U.S., Inc., 1100 Olive Way, Suite 800, Seattle, Washington, USA Adam.Griffin@arcadis-us.com*
[3]*OTEK Australia Pty Ltd, Level 1, 79 Hay St, Subiaco, WA, 6008, Australia, lchristoffersen@otek.com.au*

Abstract Applied tracers have been widely used for site characterization in natural hydrogeologic systems; here, we provide examples of their utility in elucidating complex flow patterns within heterogeneous tailings matrices and in the development of engineered approaches to mitigate tailing-water interactions and support reclamation. We present several examples where applied tracers, such as fluorescein, bromide, and sulfur hexafluoride (SF_6), were injected into legacy tailings and their transport behavior was characterized by arrival at nearby wells. These examples demonstrate the potential value of applied tracer studies in understanding, managing, and reclaiming mill tailings and reducing their potential to pollute groundwater.

Keywords water management, tailings, tracers, characterization, reclamation

Introduction

Mine and milling operations result in waste rock and tailings that require management throughout the life cycle of the mine. In the case of mill tailings, the materials have undergone significant physicochemical alteration relative to the natural ore. In addition, the deposition of tailings creates geologic heterogeneities and complex hydrogeologic conditions. Tailings are typically transported in a slurry form to a tailings impoundment. In subaerial disposal, tailings are then discharged into the impoundment through spigots or other discharge points. This process results in a succession of overlapping deltas (Vick 1990) and is similar to natural depositional settings. Coarser tailings (sands) settle from suspension close to the point of discharge, creating beaches, while finer tailings (slimes) are carried into the interior of the impoundment and tend to settle in the standing water of the decant pond. In some operations, tailings are cycloned prior to deposition to mechanically separate the sands and slimes, increasing the relative proportion of slimes tailings deposited in the impoundment. The separated sand tailings are often used to construct the embankment of the impoundment (*e.g.* USEPA 1994).

The deposition of tailings slurry creates significant vertical and horizontal heterogeneity in geotechnical and hydraulic properties throughout the impoundment. Sands and slimes tailings exhibit considerable variability in permeability (*i.e.* hydraulic conductivity), density, plasticity, compressibility, consolidation, shear strength, and stress parameters, which influence the design, stability, and drainage of the impoundment (Vick 1990). Vertical and horizontal variability in hydraulic conductivity is the primary consideration for the evaluation and management of seepage; layers of relatively high permeability sands are interbedded with relatively low permeability slimes, creating a complex hydrogeological regime (USEPA 1994). Ultimately, water flow and geochemical interactions are driven by the hydrogeological conditions in the tailings storage facility. The direction and quantity of seepage flow is controlled by the vertical and horizontal heterogeneity of hydraulic conductivity created by interbedded sands and slimes tailings. The movement of seepage is dominant in the relatively high permeability sands, which create preferential flow paths that may or may not be laterally as well as vertically continuous. Seepage flow can also be affected by hydraulic properties of the impoundment foundation and underlying aquifer, which determine the level of saturation and hydraulic connection between the impoundment and the aquifer (Vick 1990). Understanding both the hydraulics and geochemistry of tailings seepage is important for effective mitigation as well as management. For example, mitigation options for tailings sometimes include accelerating geochemical reactivity by manipulation of the water flow in a pile or decreasing reactivity of the tailings through introduction of chemical amendments.

Tracer testing techniques are well developed for characterizing natural hydrogeologic systems and are uniquely powerful for understanding flow characteristics and quantifying transport parameters and subsurface properties (*e.g.* Divine and McDonnell 2004). Applied tracers, which are defined as non-natural constituents that are intentionally introduced into the aquifer, are an especially powerful investigation tool for understanding the hydraulic behavior of an injected reagent at the remediation scale. Although tracers have frequently been used in hydrogeology for many decades, the application of tracers has only recently emerged as a best practice for understanding and characterizing solute transport to support groundwater remediation system design (Nelson and Divine 2005). In these applications, tracer testing, can reveal the heterogeneous nature of the aquifer, and support remediation system designs which maximize the efficiency of treatment areas. This paper illustrates the practical use of applied tracers to understand flow and hydrogeologic characteristics of tailings storage facilities, and to support the design and operation of seepage control and mitigation strategies.

Methods

Case Study 1: Tracer Tests to Support in situ Uranium Phosphate Precipitation Pilot Test Design

A pilot-scale field testing program (Pilot Test) was implemented in the tailings impoundment, targeting the dissolved uranium phases in the tailings porewater. Specifically, the pilot test was intended to evaluate the efficacy of sodium tripolyphosphate (STPP) as a phosphate source. STPP, which consists of linear chains of phosphate ions, has been evaluated by the Department of Energy (DOE) to treat uranium in groundwater through *in situ* application. Because STPP hydrolyzes over time, it can be transported in groundwater systems more widely than orthophosphate, which is immediately available to react. The primary objective of the Pilot Test was to evaluate the effectiveness of STPP at immobilizing uranium *in situ*. Tracer testing was conducted at two locations (the well network for Test Area 1 and Test Area 2 are shown in Fig. 1 below) prior to STPP injection to characterize the injection and hydraulic parameters of the impoundment in the Pilot Test area. Specifically, the tracers were intended to characterize the reagent distribution areas, flow directions and rates, and solute transport characteristics. Test Area 1 was located in an area of the tailings that is predominately fine material and slimes, while Test Area 2 was located in an area with a much greater sand content.

Conservative (*i.e.* non-reactive, non-sorbing) tracers were injected into the injection wells (*e.g.* wells labeled INJ1 ES10 in Fig. 1). Two tracers were used concurrently: bromide (as potassium bromide) as a quantitative tracer and the dye tracer fluorescein (as sodium fluorescein) as a visual tracer for field confirmation of tracer arrival. Approximate injected concentrations of bromide and fluorescein for both areas were 500 mg/L and 5 mg/L, respec-

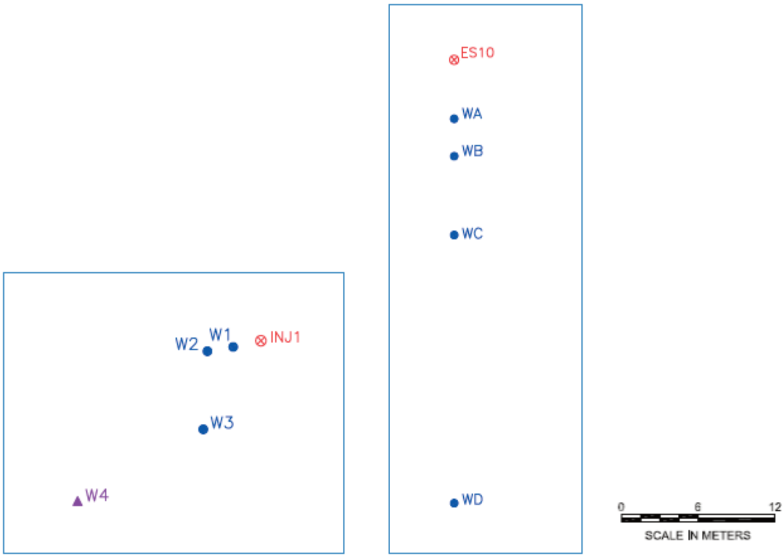

Fig. 1 *Well networks for Test Area 1 (left) and Test Area 2 (right). Red labels are the injection wells and blue labels are monitoring wells.*

tively. In Test Area 1, 17,000 L of tracer solution were injected at an approximate injection rate of 11.4 L/min, and in Test Area 2, a total of 83,000 L tracer solution were injected an approximate rate of 34.1 L/min. Post-injection monitoring extended after the tracer injections and continued for more than two months at Test Area 1 and more than seven months at Test Area 2.

Case Study 2: Tracer Test to Evaluate Performance of Tailings Flushing Program

A flushing and recovery approach has been applied to the tailings from a former uranium mill to reduce the long-term potential loading to the underlying aquifer. The flushing program involves the injection of clean water into the tailings and the subsequent extraction of pore water using a network of interconnected injection and extraction wells. In many areas, uranium areas have decreased substantially and therefore a tracer test was conducted to confirm treatment performance and better understand fluid flow behavior in the tailings. Specifically, the tracer test was designed to characterize the hydraulic connectivity and solute transport processes within tailings.

The study was designed to utilize a dissolved gas as a tracer, as opposed to more common tracer materials such as salts or dyes. A key advantage of using dissolved gas as a tracer is that it can be injected for an extended period of time with little field oversight, so a much larger volume of water can be dosed; additionally, many dissolved gas tracers have very low analytical detection limits resulting in a large “signal-to-noise” ratio. Sulfur hexafluoride, the selected tracer, is a non-toxic, inert gas and has been used for more than 20 years in applied studies (*e.g.* Wilson and Mackay 1993).

The well network for the dissolved gas tracer study and subsequent rebound monitoring is shown in Fig. 2. The injection wells for the tracer study were I1, I2, I3, I4, I5, and I6; these wells continued to inject clean water at total average flowrate of 75 L/min during the tracer test while being charged with SF_6. The gas was conveyed from compressed gas cylinders to approximately five feet from the bottom of each injection well. At the end of the piping, a microporous (6 micron pore size) diffusion stone discharged the gas to improve diffusion from the gas to the aqueous phase. A total of seven 53-kilogram-cylinders of SF_6 were injected from January 21 – 31 and from March 24 – May 9, 2011. In total, approximately 3.7 ML of water were dosed with SF_6 and injected into the tailings.

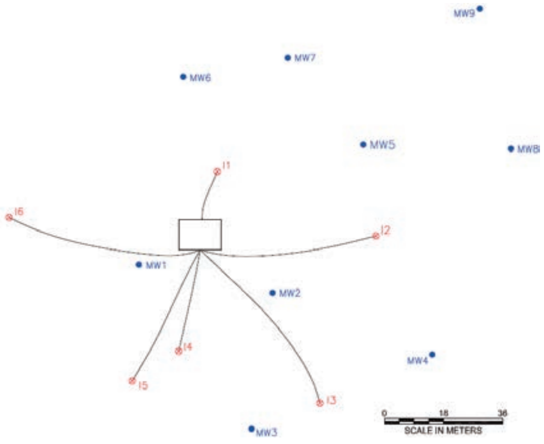

Fig. 2 *Well networks for Case Study 2. Red labels are the injection wells, blue labels are monitoring wells, and black lines depict above-ground gas conveyance piping.*

The monitoring wells were monitored for SF_6 during the tracer study to evaluate the distribution and transport of SF6 in the Rebound Evaluation area. Passive diffusion (PD) samplers, similar to those described in Divine and McCray (2004) were used to measure the concentration of dissolved gas in the pore water. PD samplers were deployed at different depths in the monitoring wells for a minimum of one week; SF_6 diffused through the membrane into the PD sampler to achieve equilibrium. The dimensionless Henry’s Law constant (the concentration in gas divided by the concentration in water under equilibrium) for SF_6 is 122 at 10 °C (Wilson and Mackay 1993). During the period of active injections (January through May 2011), the PD samplers were collected weekly for analysis; after collection, new PD samplers were deployed for the next monitoring event. Information about the injection system was also recorded weekly, and included tank pressure, header gas pressure for each injection well, totalizer readings from each injection well, and the measured water flow rate at each injection well. After SF_6 injections were discontinued on May 9, 2011, the PD samplers were analyzed through January 31, 2012.

Results

Case Study 1

Tracer breakthrough curves for Test Area 1 and Test Area 2 are included below as Figs. 3. The breakthrough curves illustrate bromide concentration data versus time (elapsed since injection), where the concentration data has been normalized to the injected concentration. The results of were very different in the two test areas due to the different hydrogeologic characteristics. In Test Area 1, (slimes-dominated), a relatively low maximum injection rate was achieved with a hydraulic and response only observed at W1. Tracer response at W1, which is approximately 1.7 m away from the injection well (INJ1), was observed after the injection of 6,800 L. Based on this response, the estimated mobile porosity (the pore space where the majority of flow occurs) was calculated assuming a cylindrical distribution to be approximately 4 % in this area. Based on the tracer washout rate from INJ1, flow velocities were estimated to be less than 0.5 m per day, based on water levels and the minimal tracer response in wells W1, W2, and W3, the flow direction was interpreted to be toward the north and northeast.

In Test Area 2 (sands), a much higher injection rate was observed, indicating much higher average hydraulic conductivity of the tailings. Based on the lack of observed tracer response at WA after the injection of 83,000 L, the estimated mobile porosity in this pilot test area is greater than 8 %. Post-injection tracer monitoring confirmed the arrival of tracer solution at monitoring wells WA, WB, and WC, all at normalized concentrations greater than 0.1. These results confirmed the southerly flow direction and implied relatively high flow velocities of about 1 m per day or greater. Based on these results, both areas were determined to be adequately permeable for the implementation of the STPP Pilot Test.

Ultimately, Test Area 1 was selected for the subsequent STPP Pilot Test because several factors including its close well spacing, significantly smaller target reagent injection volume

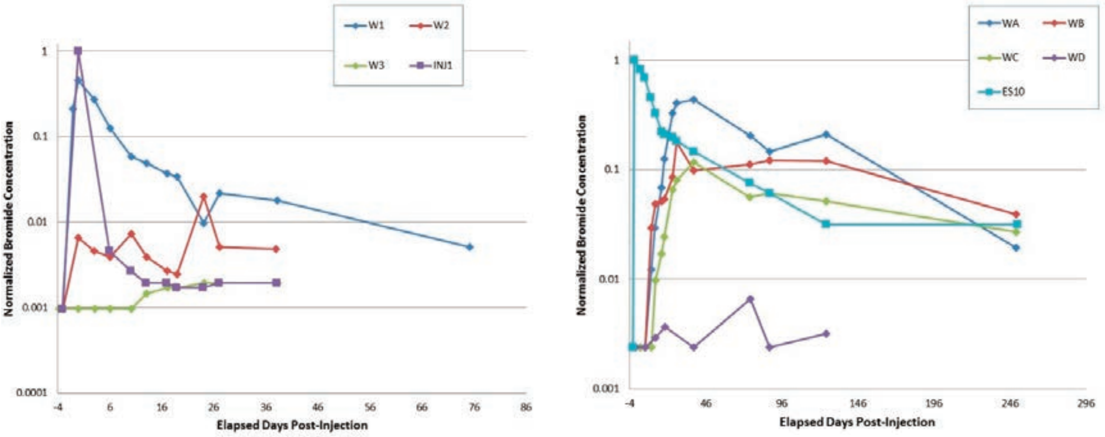

Fig. 3 *Normalized bromide tracer concentrations measured at injection and monitoring wells at Test area 1 (left) and Test Area 2(right).*

required, and lower flow velocity. Four additional monitoring wells were installed to the north and northeast of well INJ1 to further expand the monitoring well network.

Case Study 2

The SF6 tracer breakthrough curves for several monitoring wells are presented in Fig. 4. One of the most surprising observations is that the arrival of tracer was observed at four wells within 8 days of the initial tracer application and that the peak arrival of tracer occurred about 15 days after the start of the second tracer application period. These short arrival times indicate tracer transport rates were about 1–2 m per day. Based on the low average hydraulic conductivity of the tailings, and total pore space volume of the test area, the mobile porosity is very low, about 1 %. These interpretations are consistent with Cone Penetrometer Testing data collected from several nearby borings which identified thin continuous sand zones within the slimes matrix (Fig. 5). These observations imply that the flushing strategy

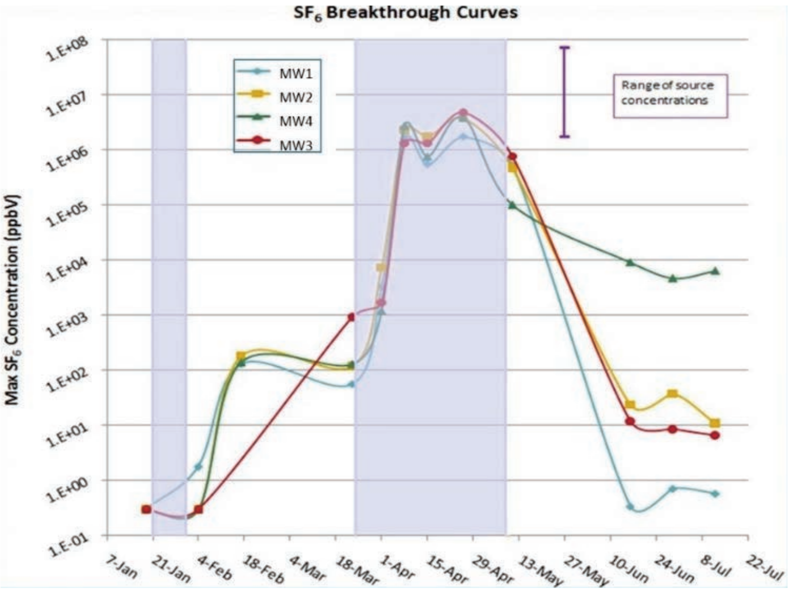

Fig. 4 *Uranium concentration and pH at downgradient monitoring wells. The shaded zones indicate time periods where tracer was continuously injected.*

can be very effective at accessing and recovering uranium and other constituents within the zones that contribute to flow and pose the most potential risk of mobilization and transport.

Another important observation is that the peak tracer concentrations were very similar to applied concentrations, even at wells located 10s of meters from the injection points. Additionally, tracer concentrations rapidly declined after the test. This behavior suggests that the diffusion-controlled solute exchange rates between the mobile porosity (flowing zones) and immobile porosity (low permeability non-flowing zones) is very low, back diffusion of uranium and other constituents after flushing may be limited.

Conclusions

The case studies presented in this paper clearly demonstrate that fluid flow in tailings materials is complex and governed by local-scale geologic structure and hydrogeologic conditions. Consequently tailings control and management strategies must be based on an appropriate understanding of fluid flow characteristics. Applied tracer testing, which is a well-developed technique for hydrogeologic investigations, is a practical and uniquely powerful for characterizing fluid flow behavior and permits direct quantification of transport parameters and other properties of tailings. This conceptual and quantitative information can be used to directly support tailings management system designs and long-term strategies.

References

Divine CE, McDonnell J (2005) The future of applied tracers in hydrogeology. Hydrogeology Journal, 13(1): 255–258

Divine CE, McCray JE (2004) Estimation of diffusion coefficients and equilibration times of VOC and dissolved gas solutes for LDPE passive diffusion samplers. Environmental Science and Technology, 38(6): 1849–1857

Nelson DK, Divine CE (2005) Tracers as tools for design of injection-based *in-situ* groundwater remediation systems. Environmental & Engineering Geoscience, 11(4): 383–394

U.S. Environmental Protection Agency (EPA) (1994) Design and Evaluation of Tailings Dams. Technical Report. EPA530-R-94-038/NTISPB94-201845. April

Vick SG (1990) Planning, Design and Analysis of Tailings Dams. BiTech Publishers Ltd

Wilson RD, Mackay DM (1993) SF6 as a conservative tracer is saturated media with high intragranular porosity or high organic carbon content. Ground Water, 34, 241–249

Wetland Photochemistry as a Major Control on the Transport of Metals in an Acid Mine Drainage Impacted Watershed

Sabre M. Duren[1], Diane M. McKnight[1]

[1]*Institute of Arctic and Alpine Research, University of Colorado at Boulder, Campus Box 450, Boulder, Colorado 80309–0450 USA*

Abstract A diel study was performed on October 14, 2011 in a wetland spanning about 20 acres located in Summit County, Colorado. The purpose was to quantify the concentrations and reaction rates of DOC, H_2O_2, Fe^{2+}/Fe^{3+}, and other metals based on photochemistry. The results of the experiment confirmed photochemistry is a major control on iron redox chemistry. The diel fluctuation of dissolved ferrous iron was associated with nearly identical trends in 23 different metal concentrations (Al, Cd, Ni, Mn, Pb, Zn, Dy, Er, Eu, Gd, Ge, Ho, La, Lu, Nd, Pr, Sc, Sm, Tb, Tm, U, Y, Yb).

Keywords photochemistry, hydrology, acid mine drainage, dissolved organic matter, rare earth metals

Extended Abstract

Throughout the state of Colorado, over 1,900 km of surface waters are affected by acid mine drainage (AMD; IMCC 1992). AMD is caused by the weathering of pyrite through a series of biogeochemical processes, which can also occur through natural weathering processes. AMD-degraded surface waters and streambeds cause deleterious effects to stream ecosystems, in many cases greatly reducing periphyton, benthic invertebrate, and fish populations for many kilometers. It is important to have an understanding of the role of the wetlands controlling the cycling of metals because of the potential major influence on the chemistry of receiving waters.

To date, few studies have focused on iron photochemistry in acid mine drainage impacted wetlands, although several studies have addressed iron photochemistry in acid mine drainage streams and lakes (McKnight *et al.* 1988; McKnight and Bencala 1988; Hrncir and McKnight 1998; McKnight and Duren 2004; Gammons *et al.* 2005; Parker *et al.* 2008; Nimick *et al.* 2011). Wetlands are “hot spots” for dissolved organic matter (DOM) photochemistry because the shallow waters are influenced by high light intensity and high DOM concentrations in slow moving waters with residence time for reactions to take place. DOM is key in understanding dominant diel processes on hydrogen peroxide, iron speciation, trace metals, and rare earth metals. The oxidation of Fe^{2+} and cycling of iron has been correlated to the cycling of DOM (Voelker and Sulzberger 1996; Hrncir and McKnight 1998). H_2O_2 can be produced through photolysis of DOM in the presence of ultraviolet light and O_2 (Voelker and Sulzberger 1996). The rates of superoxide radical (O_2^-), and H_2O_2 formation are functions of DOM concentration and reactivity and ultraviolet light intensity (Craig *et al.* 2009). While Fe^{2+} is produced by photoreduction, it is also consumed in the photo-Fenton reaction: $H_2O_2 + 2Fe^{2+} \rightarrow 2\,Fe^{3+} + OH^{\cdot} + OH^-$ (Voelker and Sulzberger 1996). If wetlands control the cycling of DOM and metals, photochemistry may have a major influence on the chemistry of receiving waters.

A diel study was performed on October, 2011 in a wetland system located downstream of Pennsylvania Mine in Summit County, Colorado to quantify the concentrations and reaction rates of DOC, H_2O_2, Fe^{2+}/Fe^{3+}, and other metals of interest. Ten hourly samples were collected during daylight hours and 5 samples were collected after dark. The pH throughout the experiment ranged from 3.41 – 3.97. The results confirmed that photochemistry is a major control on the oxidation and reduction of iron in AMD-impacted wetlands. At midday the H_2O_2 concentrations reached a maximum and then decreased in the afternoon (Fig. 1). The dissolved ferrous iron concentrations were a mirror image of the H_2O_2 concentrations due to consumption in the photo-Fenton reaction (Fig. 2). The corresponding ferrihydrite ($FeOH_3$) concentrations are a major variable for trace metal transport. The diel fluctuations of dissolved iron concentrations driven by changing light intensity were associated with nearly identical trends in the concentrations of 23 different metals, all of which increased as ferrous iron decreased (Fig. 3 shows an example; all 23 metals show a very similar trend). In addition to metals commonly found in AMD streams (Al, Cd, Ni, Mn, Pb, and Zn), these metals included a number of rare earth

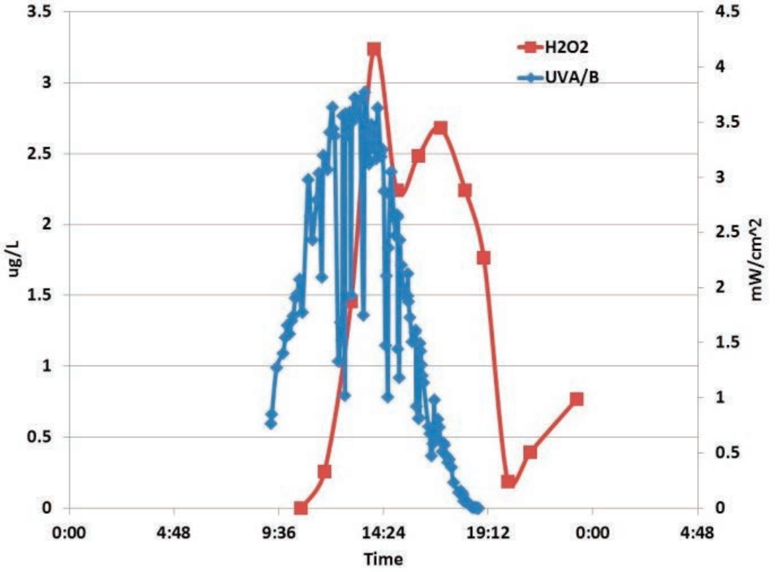

Fig. 1 *DOC photolysis produces hydrogen peroxide.*

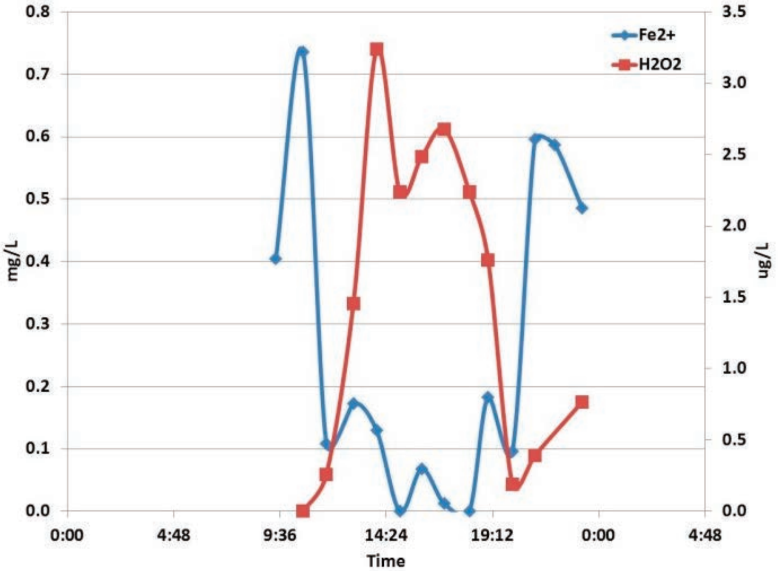

Fig. 2 *Ferrous iron is consumed in the photo-Fenton reaction.*

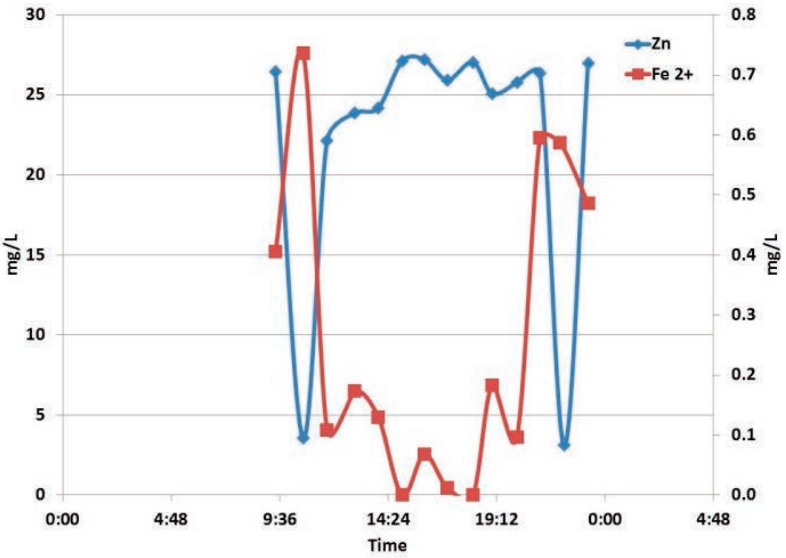

Fig. 3 *Representative diel metal trends: ferrous iron and zinc.*

metals (Dy, Er, Eu, Gd, Ge, Ho, La, Lu, Nd, Pr, Sc, Sm, Tb, Tm, U, Y, and Yb) some of which occurred in concentrations exceeding 200 µg/L. The data collected during the experiment confirmed the role of photochemistry in controlling the oxidation and reduction of iron, and the effect iron speciation has on other metal concentrations in a wetland.

References

Craig PS, Shaw TJ, Miller PL, Pellechia PJ, Ferry JL (2009) Use of multiparametric techniques to quantify the effects of naturally occurring ligands on the kinetics of Fe(II) oxidation. Environmental Science and Technology, 43:337–342

Gammons CH, Nimick DA, Parker SR, Cleasby TE, McClesky RB (2005) Diel behavior of iron and other heavy metals in a mountain stream with acidic to neutral pH: Fisher Creek, Montana, USA. Geochim. Cosmochim. Acta, 69: 2505–2516

Hrncir DC, McKnight DM (1998) Variation in photoreactivity of iron hydroxides taken from an acidic mountain stream. Environmental Science and Technology, 32: 2137–2141

Interstate Mining Compact Commission (IMCC) (1992) Inactive and abandoned non-coal mines: a scoping study. Prepared for IMCC of Herndon, VA by Resource Management Associates, Clancy, MT. Cooperative Agreement, X-817900-01-0

McKnight DM, Kimball BA, Bencala KE (1988) Iron photoreduction and oxidation in an acidic mountain stream. Science, 240: 637–640

McKnight DM, Bencala KE (1988) Diel variations in iron chemistry in an acidic mountain stream in the Colorado Rocky Mountains, USA. Arctic Alpine Research, 20: 492–500

McKnight DM, Duren SM (2004) Biogeochemical processes controlling midday ferrous iron maxima in stream waters affected by acid rock drainage. Applied Geochemistry, 19: 1075–1084

Nimick DA, Gammons CH, Parker SR (2011) Diel biogeochemical process and their effect on the aqueous chemistry of streams: A review. Chemical Geology, 283: 3–17

Parker SR, Gammons CH, Pedrozo FL, Wood SA (2008) Diel changes in metal concentrations in a geogenically acidic river: Rio Agrio, Argentina. Journal of Volcanology and Geothermal Research, 178: 213–223

Voelker B, Sulzberger B (1996) Effects of fulvic acid on Fe(II) oxidation by hydrogen peroxide. Environmental Science and Technology, 30: 1100–1114

Fabricated Soil Using Coal Mine Waste

Beatriz Alicia FIRPO VASQUEZ[1], Ivo André HOMRICH SCHNEIDER[1], Camila Maria TREIN[2],
Jean Carlo SALOMÉ DOS SANTOS MENEZES[2]

[1]*Universidade Federal do Rio Grande do Sul, LTM-DEMIN-PPGE3M, Av. Bento Gonçalves 9500, Porto Alegre, RS, 91501–970, Brazil, bia.firpo7@gmail.com, ivo.andre@ufrgs.br,*
[2]*Universidade do Oeste de Santa Catarina – Campus Videira, Rua Paese 198, Videira, SC, 89560–000, Brazil*

Abstract The objective of this work was to produce fabricated soil using coal mine waste as raw material. Coal mine waste from the Carboniferous region of Santa Catarina, Brazil, was ground and amended with steel slag powder and sewage sludge to, respectively, adjust acidity and provide organic matter as well as nutrients. Fabricated soils had pH, macro, and micronutrients analyzed while plant growth (*Sorgum bicolor*) was monitored. Balanced mixtures of coal waste, steel slag, and sludge can be used as a substitute for natural topsoil.

Keywords coal, waste, fabricated soil, sewage sludge

Introduction

Brazilian run-of-mine coals (ROM) contain high levels of impurities (rock minerals and pyrite), requiring concentration procedures (Kalkreuth 2010). It demands tailing deposits which occupy large physical areas, change topography, and generate acid mine drainage (AMD). Millions of tons of coal tailings cover 3,195.22 ha in the carboniferous region of Santa Catarina, generating environmental impacts and significant economic costs to avoid and treat AMD (Ministério Público 2012).

Amaral Filho *et al.* (2010), analyzing a typical coal waste tailing by a gravity concentration process, produced three output streams: (a) a low specific gravity material (relative density < 2.4) predominantly composed of shaley coal and carbonaceous shale; (b) an intermediated material (2.4 < relative density < 2.8) mainly composed of shale, siltstone and sandstone; and (c) a high specific gravity material (relative density > 2.8) rich in pyrite. The intermediate density material comprises 56.6 % of the total amount of waste and presents low sulfur content (from 1.8 to 2.8 %).

There have been some attempts, in Brazil, to reprocess coal waste deposits in order to recover valuable products such as carbonaceous materials for energy uses and, alternatively, concentrate pyrite for sulfuric acid production. However, the intermediate density material still remains, which is considered in this study as raw material to fabricate soils. Kefeli *et al.* (2008) defines "fabricated soil" as a mixture of substrates containing balanced amounts of carbon, nitrogen, phosphorus, potassium, and mineral elements that support plant growth.

Fabricated and mine soils have much in common. Soil developed from mine spoils depends greatly upon rock and soil mixes, soil amendments, geomorphology, hydrology, and the vegetation introduced (Wick *et al.* 2010). Studies from Sydnor and Redente (2002), Straken (2005), and Strzyszcz and Lukasik (2010) have shown that it is possible to establish new vegetation directly on spoils or waste once pH is adjusted and amendments (fertilizers as well as organic matter) are applied. Acid substrates are predominantly adjusted with calcium carbonate, but other alkaline amendments, *e.g.* steel slag, can be used (US EPA 2007). Biossolids (sewage sludge) are a source of nutrients and organic matter of much interest (Wick *et al.* 2010).

The aim of this work was to produce fabricated soil using coal mine waste, steel slag, and sewage sludge. The methods included materials characterization and fabrication of soil relating its fertility parameters to plant (*Sorghum bicolor*) growth. Results are discussed in terms of the possible use of fabricated soils in Brazilian coal mine degraded areas.

Methods

Three materials were selected: coal mine waste (CW – main material), steel slag (SLAG – alkalinity and micronutrients source), and sewage sludge (SLUDGE – nutrients and organic matter supply). Coal waste was obtained directly from a coal preparation plant which mines the Barro Branco seam (Santa Catarina State, Brazil). The material was submitted to a Fe-Si gravity separation process to obtain the fraction between the relative densities of 2.2 – 2.7, that are lower in sulfur and carbonaceous rock. Slag samples were obtained from a secondary refining furnace in special steel plant located in the state of Rio Grande do Sul, Brazil. Sewage sludge samples came from an UASB reactor operating on a local sewage water treatment plant in Criciúma, Santa Catarina State. In order to compare the fabricated soils behavior to native soils, a sample from the latter was collected. All samples were collected accordingly the Brazilian sampling standard NBR 10.007 (ABNT 2004). Coal waste and steel slag were ground in a jaw crusher followed by a roller mill crusher to particle size below 2 mm. Sewage sludge was dried at 100 °C and pounded to break up the clods.

All three materials were analyzed for ash and volatile matter (ABNT 1983a,b,c) and for C, H, N, and S concentrations (Elementar Vario Macro analyzer). Coal waste and steel slag had their crystalline material structure analyzed by X-ray diffraction (XRD). Acid–base accounting (ABA), as described by Sobek *et al.* (1978), was carried out to determine the net acidity generation potential.

In order to study for an isolated materials effect in the fabricated soils a factorial 2^{k-1} delineation experiment was implemented resulting in four different mixtures/fabricated soils shown in Table 1. Three repetitions of all fabricated soils and native soil were placed in plant growth trays. Each soil cell received seven *Sorghum bicolor* seeds whose growth was monitored for seven weeks. Fabricated soil samples and a control were analyzed for pH, P, K, Ca, Mg, S, Al, H+Al, organic matter, Zn, Cu, B, and Mn; cation exchange capacity (CEC); V % SMP index (EMBRAPA 1997). One repetition was kept for pH and SMP index analysis at 20 weeks. Environmentally available Cd, Co, Cr, Cu, Fe, Ni, Pb, and Zn (EPA 3050) were analyzed in the fabricated soils.

Results and Discussion

Coal waste (2.2 – 2.7) and steel slag have particles sizes between 0.1 – 2.0 mm (with a D50 approximately 0.9 mm), typical of a sandy soil. The XRD results reveal that main crystalline compounds are: (a) coal waste (2.2 – 2.7): quartz – SiO_2, plagioclase – $(Ca,Na)Al\,(Al,Si)Si_2O_8$, illite – $(K,H_3O)(Al,Mg,Fe)_2(Si,Al)_4O_{10}[(OH)_2,(H_2O)]$, alkaline feldspar – ($NaAlSi_3O_8$), gypsum – $CaSO_4.2H_2O$, and kaolinite – $Al_2Si_2O_5(OH)_4$; (b) steel slag: gehlenite – $Ca_2Al_2Si_2O_7$, merwinite – $Ca_3Mg(SiO_4)_2$, calcium oxide – CaO, magnetite – Fe_3O_4, wustite – FeO and periclase – MgO.

Table 2 summarizes results for elemental analysis, immediate analysis, and ABA. Total sulfur content in coal mine waste (1.1 %) implies an acid potential (AP) generation of 35 kg $CaCO_3.t^{-1}$. On the other hand, steel slag neutralization potential (NP) is equivalent to 353.1 kg $CaCO_3$ t^{-1}. Thus, acid base balance de-

	CW	CW+ SLUDGE	CW+ SLAG	CW+ SLUDGE+SLAG	Control
Coal mine waste – 170.0 g	X	X	X	X	-
Steel slag – 17.0 g	-	-	X	X	-
Sewage sludge – 27.5 g	-	X		X	-
Native soil – 170.0 g	-	-	-	-	X

Table 1 *Fabricated soils and their composition and native soil as control.*

	CW (2.2-2.7)	SLAG	SLUDGE
Elemental analysis			
C %	3.9	0.8	21.5
H %	1.1	0.1	5.2
N %	0.3	0.02	2.7
S %	1.1	0.7	8.4
Immediate analysis			
Ash %	88.3	100.0	-
Volatile matter %	8.4	0.0	-
Fixed carbon %	1.0	0.0	-
Acid Base Accounting			
AP kg $CaCO_3$ t^{-1}	35.0	0.0	-
NP kg $CaCO_3$ t^{-1}	0.0	353.1	-
NNP kg $CaCO_3$ t^{-1}	-35.0	353.1	-

Table 2 *Coal waste, steel slag, and sewage sludge elemental composition, immediate analysis and acid base accounting parameters.*

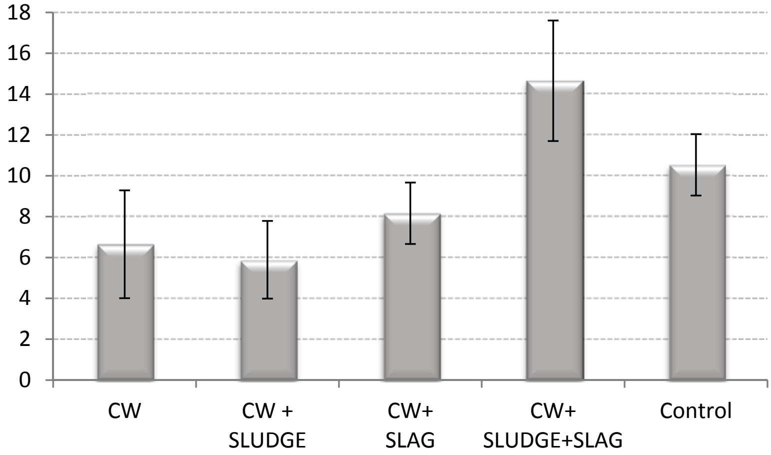

Fig. 1 *Fabricated soil and control* Sorghum bicolor*'s height at seven weeks (mean and standard deviation)*

termines a 10:1 ratio between coal waste and slag to establish neutrality.

Fig. 1 shows *Sorghum bicolor* height (mean and standard deviation) for each fabricated soil and control after seven weeks. Fabricated soils where steel slag was used had significantly higher heights than those without it (ANOVA – significance level $p \leq 5$ %). Also, sewage sludge promoted a significant contribution to *Sorghum bicolor* development where pH was neutralized by slag – seedlings grew about two times more than in other mixtures. CW+SLUDGE+SLAG treatment had heights even higher than control. Fig. 2 depicts *Sorghum bicolor* grown in native soil (control) and in a fabricated soil amended with sewage sludge and steel slag.

Analysis of the soil pH ($pH_{H_2O\ 1:1}$) at 7 and 20 weeks are presented in Table 3. The fabricated soils that received steel slag (CW+SLAG and CW+SLUDGE+SLAG) had pH values significantly higher (significance level $p \leq 5$ %) than those without steel slag (CW and CW+SLUDGE). A tendency of pH decrease, yet

Fig. 2 Sorghum bicolor *seven weeks old: (a, left) native soil – control and (b, right) CW+SLUDGE+SLAG fabricated soil.*

significant, was observed in all situations, but it was less expressive in the mixtures with steel slag.

Table 4 shows the fertility parameters – macro and micronutrients – of the fabricated soil and control (native soil) seven weeks after sowing *Sorghum bicolor* seeds. Clay content in all fabricated soils is 5 % while in the control it is 18 %.

The addition of steel slag significantly increased the values of calcium, magnesium, boron, cation exchange capacity (CEC), and base saturation percentage (V %), but decreased sulfur and manganese. Sewage sludge significantly increased phosphorus, organic matter (OM), sulfur, boron, and zinc. Potassium and copper were not influenced by any treatment. All results considered $p \leq 5$ %. Native soil shows very low quality in terms of fertility, especially when compared to the fabricated soil comprised of steel slag and sewage sludge. The native soil shows low pH and CEC is occupied mainly by aluminum and hydrogen, while there is low availability of nutrients.

Table 5 shows the concentration of the metals Cd, Co, Cr, Cu, Fe, Ni, Pb, and Zn (EPA 3050) in all fabricated soils as well the Brazilian standard values for prevention and intervention levels (CONAMA 420–2009). Among all metals analyzed, Cr is above prevention level when steel slag is applied, but still under agricultural intervention level. *Sorghum bicolor* growth has shown promising results, however, further research with Cr free steel slag as well as $CaCO_3$ as alkaline amendment will be taken.

Sheoran *et al.* (2010) considered that reclamation strategies must address soil structure, soil fertility, microbe populations, top soil management, and nutrient cycling in order to return the land as closely as possible to its undisturbed condition and continue as a self-sustaining ecosystem (Sheoran *et al.* 2010). The close relationship between soil and vegetation quality is clear. Yet, in Brazil it is common to reclaim degraded areas using soils from nearby deposits, which can mean additional environmental damage. Thus, the use of alternative soils and amendments mitigates not only the area to reclaim, but also avoids environmental impact in other sites and disposal costs of other wastes (slags and sewage). Using

	CW	CW+ SLUDGE	CW+ SLAG	CW+ SLUDGE+SLAG	Control
pH 7 weeks	3.5	4.3	7.7	6.8	4.6
pH 20 weeks	2.5	3.3	7.2	7.0	4.9
SMP 7 weeks	5.9	5.8	7.8	7.3	4.9
SMP 20 weeks	3.2	3.6	7.6	7.3	5.0

Table 3 *pH and SMP index for fabricated and native soil.*

Parameter		CW	CW+ SLUDGE	CW+ SLAG	CW+ SLUDGE+SLAG	Control
Al	mg dm^{-3}	1.9	1.8	0.0	0.0	3.7
H + Al	mg dm^{-3}	4.9	5.5	0.6	1.0	15.4
P	mg dm^{-3}	9.3	100.0	20.0	100.0	3.4
K	mg dm^{-3}	132	163	158	148	69
Ca	$cmol_c$ dm^{-3}	15.9	22.6	37.3	35.4	1.0
Mg	$cmol_c$ dm^{-3}	1.3	2.8	10.3	9.4	0.6
S	mg dm^{-3}	1455	2729	516	1997	24
Zn	mg dm^{-3}	9.4	71.0	9.1	51.0	1.7
Cu	mg dm^{-3}	8.5	6.7	5.0	4.0	1.6
B	mg dm^{-3}	0.9	1.1	1.3	1.8	0.7
Mn	mg dm^{-3}	72	103	7	24	94
CEC	$cmol_c$ dm^{-3}	22.6	31.5	48.6	46.2	17.4
V	%	78.0	82.0	99.0	98.0	10
OM	%	4.4	6.6	4.3	6.3	0.5

P e $K_{exch.\ Mehlich\ 1}$, $Ca_{exch.}$, $Al_{esch.}$, $Mg_{exch.}$ and $Mn_{exch.}$ KCl 1 mol L^{-1}, S $CaHPO_4$ 500 mg L^{-1}, Zn e Cu HCl 0.1 mol L^{-1}, $B_{hot\ water}$ e $OM_{humid\ digestion}$

Table 4 *Fabricated soils and native soil fertility parameters.*

	fabricated soils				prevention	intervention level		
	CW	CW+ SLUDGE	CW+ SLAG	CW+ SLUDGE+ SLAG	level	agricultural	residential	industrial
Cd mg kg^{-1}	0.15	0.16	0.17	0.17	1.3	3	8	20
Co mg kg^{-1}	8.83	9.74	9.51	10.42	-	-	-	-
Cr mg kg^{-1}	25.98	27.21	143.87	145.10	75	150	300	400
Cu mg kg^{-1}	27.04	28.94	37.23	39.13	60	200	400	600
Ni mg kg^{-1}	15.76	16.20	23.85	24.29	30	70	100	130
Pb mg kg^{-1}	19.97	20.74	20.99	21.76	74	180	300	900
Zn mg kg^{-1}	50.00	66.39	59.47	75.86	300	450	1000	2000

***Table 5** Concentration of Cd, Co, Cr, Cu, Ni, Pb, and Zn (accordingly method EPA 3050b) in fabricated soils and Brazilian standards values for prevention, and intervention for agricultural, residential and industrial uses.*

fabricated soil in mine reclamation projects is a part of this context.

Conclusion

Fabricated soil produced by the mixture of coal mine waste, steel slag and sewage sludge facilitated *Sorghum bicolor* development. Steel slag increased pH and levels of calcium, magnesium, and CEC in fabricated soils. On the other hand sewage sludge added organic matter, phosphorous, sulfur, and zinc. Results showed that ABA is an efficient methodology to achieve a neutral pH in fabricated soils when mixing coal mine waste (acidic) with steel slag (basic). Fabricated soils are a potential substitute for natural soils in mine reclamation projects. This study contributes to enhance environmental protection through mine waste management based on the concept of “zero waste production”.

Acknowledgements

The authors are also grateful for the financial support extended by CNPq and the Brazilian Coal Net for this research.

References

ABNT (1983a) NBR 8289 Carvão Mineral – Determinação do Teor de Cinza. Associação Brasileira de Normas Técnicas. Rio de Janeiro.

ABNT (1983b) NBR 8293 Carvão Mineral – Determinação de Umidade. Associação Brasileira de Normas Técnicas. Rio de Janeiro.

ABNT (1983c) NBR 8290 Carvão Mineral – Determinação do Teor de Matéria Volátil. Associação Brasileira de Normas Técnicas. Rio de Janeiro.

ABNT (2004) NBR 10.007 Amostragem de resíduos sólidos. Associação Brasileira de Normas Técnicas. Rio de Janeiro.

Amaral Filho JR, Schneider IAH, Tubino RMC, Brum IAS, Miltzarek G, Sampaio CH, Schneider CH (2010) Characterization of a coal tailing deposit for zero waste mine in the Brazilian coal field of Santa Catarina. In: Wolkersdorfer, Ch. and Freund, A.: Mine Water & Innovative Thinking. Sydney, Nova Scotia (CBU Press) p 639 – 643

EMBRAPA (1997) Manual de métodos de análise de solo. Empresa Brasileira de Pesquisa Agropecuária. Centro Nacional de Pesquisa de Solos. 2. ed. Rio de Janeiro.

Kalkreuth W *et al.* (2010) Depositional setting, petrology and chemistry of Permian coals from the Paraná Basin. 2. South Santa Catarina Coalfield, Brazil. International Journal of Coal Geology, v. 84, 213–236.

Kefeli V, Leininger C, Mastalski S, Pincin K (2008) Characteristics of fabricated soil for landscape rehabilitation: The four crop test for biological activity. Advances in Molecular Biology, 1(2): 79–85

Ministério Público (2012) Sexto relatório de monitoramento dos indicadores ambientais. Grupo Técnico de Assessoramento – GTA. Volume 1 Criciúma https://www.jfsc.jus.br/acpdocarvao/2012/GTA/GTA_6_2012_1_Sumario_Executivo.htm#IV

Sheoran V, Sheoran AS, Poonia P (2010) Soil Reclamation of Abandoned Mine Land by Revegetation: A Review. International Journal Of Soil, Sediment And Water, 3 (2): 1–21

Sobek A, Schuller W, Freeman J, Smith R (1978) Field and laboratory methods Applicable to overburdens and minesoils. U.S. Environmental Protection Agency, EPA-600/2-78-054, Cincinnati.

Straker J *et al.* (2005) Elk Valley coal waste as a growth medium: results of soil and vegetation analysis from Elk Valley Coal’s Fording River, Greenhills and Line Creek mines. In: The University Of British Columbia (Eds), 2005 British Columbia Mine Reclamation Symposium, Vancouver, p 1–6

Strzyszcz Z, Ukasik ŁA (2010) Initial forest ecosystem on hard coal mining waste dumps in the Upper Silesia. In: Myres (Eds), 4th Meeting of Young Researchers in Earth Sciences, Cottbus, p 117–119

Sydnor MEW, Redente EF (2002) Reclamation of High-Elevation, Acidic Mine Waste with Organic Amendments and Topsoil. Journal Environmental Quality 31(5): 1528–1537

US EPA (2007) The Use of Soil Amendments for Remediation, Revitalization and Reuse. U.S. Environmental Protection Agency. Washington, D.C. EPA EPA 542-R-07-013. http://nepis.epa.gov/Exe/ZyPURL.cgi?Dockey=60000LQ7.txt

Wick AF, Daniels WL, Nash WL, Burger JA (2010) Soil aggregate, organic matter and microbial dynamics under different amendments after 27 years of mine soil development. In: ASMR (Eds), 2010 National Meeting of the American Society of Mining and Reclamation, Pittsburgh, PA, p 1364–1386

Ziemkiewicz PF, Skousen J (1998) The use of steel slag in acid mine drainage treatment and control. In: 19th West Virginia Surface Mine Crainage Task Force Symposium 1998, Morgantown.

Arsenic contamination in the Baccu Locci mine watershed (Sardinia, Italy) after remediation

Franco Frau[1], Francesca Podda[1], Stefania Da Pelo[2], Carla Ardau[1]

[1] *Department of Chemical and Geological Sciences, University of Cagliari, Via Trentino 51, 09127 Cagliari, Italy; Frau F. – frauf@unica.it*
[2] *Via S. Alenixedda 111/E, 09128 Cagliari, Italy*

Abstract The old Pb-As Baccu Locci mine represents the first and only case of mine site remediation in Sardinia, Italy. This paper reports preliminary results on the level of contamination in the Baccu Locci stream after remediation. In particular, distribution of dissolved As has not substantially changed compared to pre-remediation situation, showing an increasing trend along the stream and a concentration of about 400 μg/L at a distance of 5 km from the mine. Future monitoring of the Baccu Locci system will provide fundamental information on the effectiveness of remediation measures adopted and their applicability to other mine sites in Sardinia.

Keywords Baccu Locci mine (Sardinia, Italy), arsenic contamination, remediation, environmental issues

Introduction

The sulfide deposit of Baccu Locci is located in south-east Sardinia, Italy. The extraction of galena [PbS] and arsenopyrite [FeAsS] for about a century (1873–1965) has left a significant environmental legacy, especially due to the unwise practice of discharging tailings from the flotation plant directly into the Baccu Locci stream (BLs), which drains the homonymous mine area, with consequent accumulation and wide scattering of highly contaminated materials over the whole watershed (Fig. 1) as far as the coastal plain located about 10 km downstream from the mine. The BLs is characterized by a typical torrential regime with alternation of low-flow periods, even in fall-winter, and recurrent, sometimes catastrophic, floods.

Arsenic represents the most relevant environmental concern in the Baccu Locci watershed, with concentrations in surface waters up to and sometimes over 1 mg/L (Frau and Ardau 2003; Frau *et al.* 2009, 2012). Previous studies (Frau and Ardau 2003, 2004; Frau *et al.* 2005, 2009), conducted before remediation, pointed out that waste-rock dumps and flotation tailings represent point and widespread contamination sources, respectively. The waste-rock dumps are located in the upper BLs course, where also the mining works occur; the flota-

Fig. 1 *Reddish-brown stain left by tailings on the rocks in the Baccu Locci stream at a height of about 1 meter from the bed, testifying that the tailings slurry discharged from the flotation plant for about 15 years (1949–1965) filled completely the watercourse even during drought periods.*

tion tailings are scattered in the medium-lower BLs valley and mostly represent a "hidden" contamination source because they are mixed with and buried under stream sediments. Arsenic is released to surface waters mainly by desorption from two-line ferrihydrite (HFO) contained in stream sediments/tailings along the medium-lower course of the BLs (Frau *et al.* 2008, 2010).

Remediation actions started in August 2008 and concluded in February 2012 with an all-in cost of 5.1 million euros. They were conducted according to regional guidelines (RAS 2009) and mainly consisted in: 1) creation of a "Storage Site" (Fig. 2), where materials from different waste-rock dumps and several tailings piles occurring along the BLs (Fig. 3) were placed; 2) permanent on-site safety measures on three waste-rock dumps; 3) treatment of leachate from the Storage Site and acidic water from the S. Riccardo adit (see Fig. 4) by passive adsorbent systems.

In previous studies, a prolonged persistence of As contamination was hypothesized (Frau and Ardau 2003) and the expected positive effects of remediation measures were evaluated at least as uncertain (Frau 2009), especially with regard to As contamination. For these reasons, this paper reports the first results on the BLs water chemistry after completion of remediation in order to immediately follow the geochemical evolution of the Baccu Locci system and understand how it will react with time to the remediation actions conducted.

Sampling and methods

The map of the BLs watershed (Fig. 4) shows the location of sampling stations, waste-rock dumps subjected to permanent on-site safety

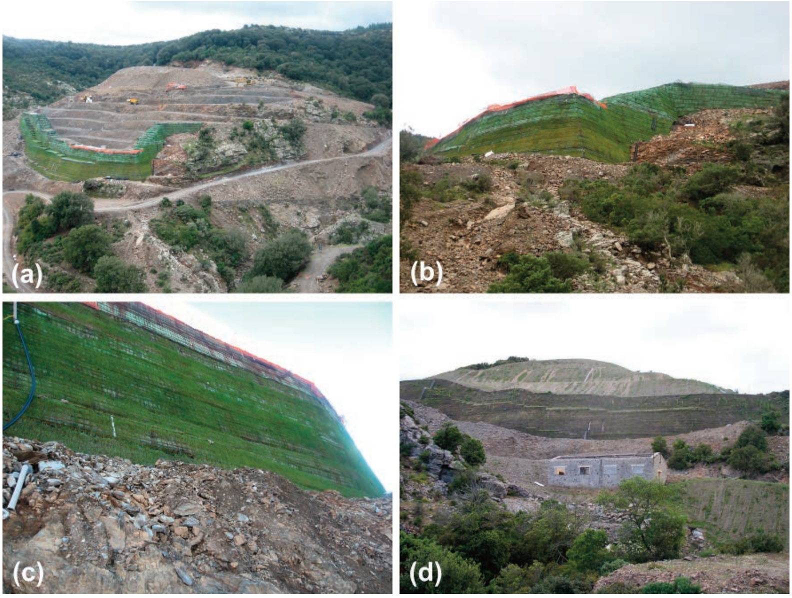

Fig. 2 *Some views of the Storage Site in February 2010 during its construction (a), (b) and (c), and in May 2012 after completion of remediation (d). The perimetric retaining wall is about 12 meters high.*

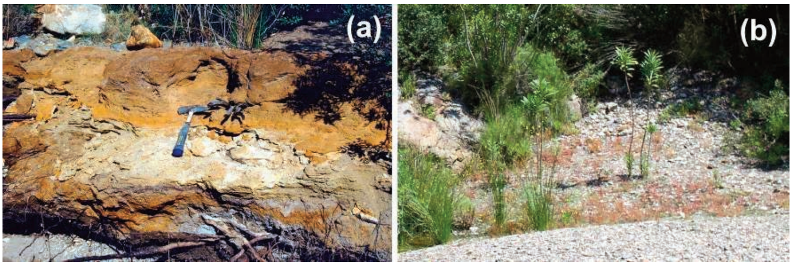

Fig. 3 *One of the sites along the Baccu Locci stream where the tailings deposits were more visible, photographed in January 2001 before remediation (a) and in May 2012 after remediation (b).*

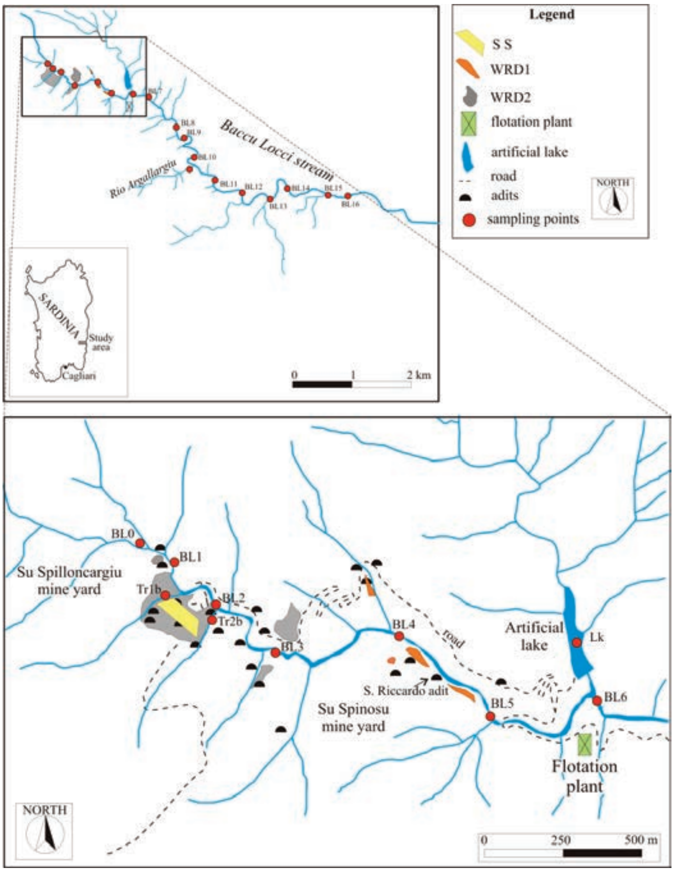

Fig. 4 *Schematic map of the Baccu Locci stream watershed showing the location of sampling stations (BL0-BL14, Tr1b, Tr2b, Lk), waste-rock dumps left in place (WRD1) and removed (WRD2), and the Storage Site (SS). The stations BL6, BL15 and BL16 were not sampled in May 2012.*

measures and those removed, and the Storage Site. The BLs was sampled in May 2012 at 14 different points from BL0, located upstream of the mine area, to BL14. The BLs was in a period of low flow; most of tributaries were dry (only the tributaries Tr1 and Tr2 were sampled), and the BLs water flow occurred in the hyporheic zone in some stretches and definitively downstream of the BL14 sampling station (Fig. 5). However, some water from the artificial lake (see Fig. 4) overflowed the dam and flowed into the BLs.

Temperature, pH, Eh, conductivity and alkalinity were measured at the sampling stations. Each water sample was filtered through 0.45 µm pore-size polypropylene filter into pre-cleaned high density polyethylene bottles. Filtered aliquots were acidified on site with 1 % v/v suprapure HNO_3 for analyses of major elements by ICP-OES, and minor and trace elements by ICP-MS. A filtered aliquot was acidified on site with 0.2 % v/v suprapure HCl for

Fig. 5 *The last sampling station BL14 in the Baccu Locci stream in May 2012, downstream of which the water flow definitively occurred in the hyporheic zone.*

the determination of As by on-line hydride generation ICP-MS. Major anions were determined by ion chromatography on filtered, unacidified aliquots. Estimated error of analytical data was <5 % for major components and <10 % for minor and trace elements.

Results and discussion

The BLs water is neutral to slightly alkaline (pH 7.2-8.0), oxidizing (Eh 0.44-0.52 V) and with low total dissolved solids (TDS 0.29-0.50 g/L). Major chemistry is dominated by Ca-Mg-HCO_3 or Ca-Mg-SO_4 composition. The chemical changes in the BLs water over a distance of about 7 km (Fig. 6) show strong similarities with pre-remediation samplings (Frau and Ardau 2003). Calcium, sulfate and TDS increase as soon as the BLs enters the mine area (BL0-BL3 stretch), a dilution occurs between BL3 and BL4 due to mixing with a tributary (not sampled), then bicarbonate rapidly becomes the dominant anion upon mixing with water from the lake (BL5-BL7 stretch) and this composition persists until the last sampling station, although with a progressive decrease of calcium, bicarbonate and TDS probably due to hyporheic flow from other tributaries.

Also trace elements distribution along the BLs shows strong similarity with pre-remediation samplings, in particular with low flow conditions (Frau and Ardau 2003). The metals Zn, Cd, Cu, Ni and Pb rapidly increase in the first km (BL0-BL3 stretch), then they decrease to very low concentrations (not shown).

Contrary to metals, the distribution of As along the BLs is characterized by a peculiar trend, with a gradual increase up to the maximum concentration of about 750 μg/L at BL10 (Fig. 7). Two drastic, significant decreases can be observed in the BL3-BL4 and BL10-BL11 stretches; the first one is probably due to both mixing with a tributary (not sampled) and co-precipitation/sorption with amorphous/low-crystallinity phases; the second one is due to hyporheic flow from the tributary Rio Argallargiu (just 10 μg/L As, when it was possible to sample it; Frau and Ardau 2003). Anyway, the dissolved concentration of As remains very high up to the last sampling station (about 400 μg/L at BL14).

Compared to previous samplings conducted in February 2000 (low flow conditions similar to those in May 2012) and January 2001 (flow higher than in May 2012; Frau and Ardau 2003), As generally exhibits higher concentrations, especially at BL2 and in the BL4-BL10 stretch (Fig. 8 and Fig. 9).

The behavior of As mainly depends on the peculiar feature of the widespread contamination source, represented by the flotation tailings, and its solid speciation. Although the visible tailings piles outcropping on the stream

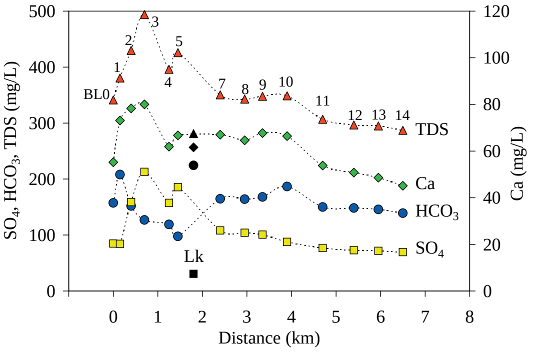

Fig. 6 *Major chemistry changes in the Baccu Locci stream (May 2012) over a distance of about 7 km; solid black symbols refer to lake water.*

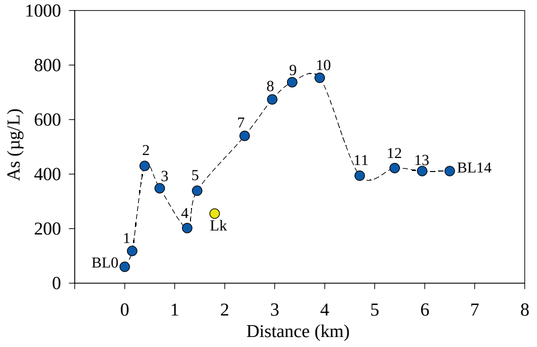

Fig. 7 *Arsenic distribution in the Baccu Locci stream in May 2012 over a distance of about 7 km.*

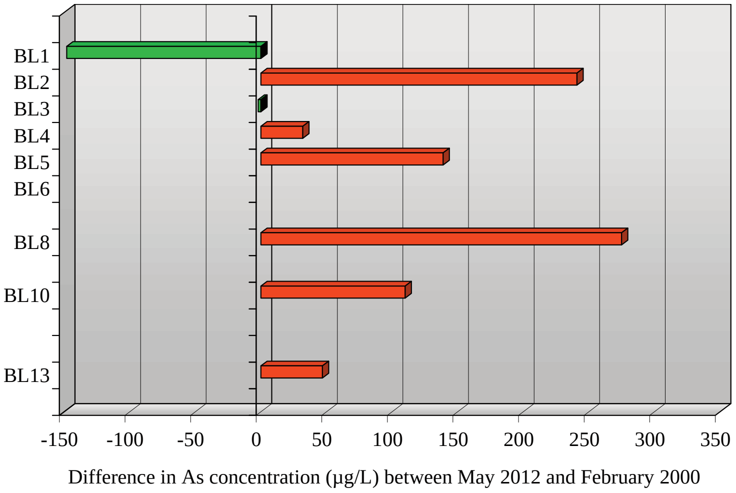

Fig. 8 *Difference in As concentration along the Baccu Locci stream between May 2012 and February 2000.*

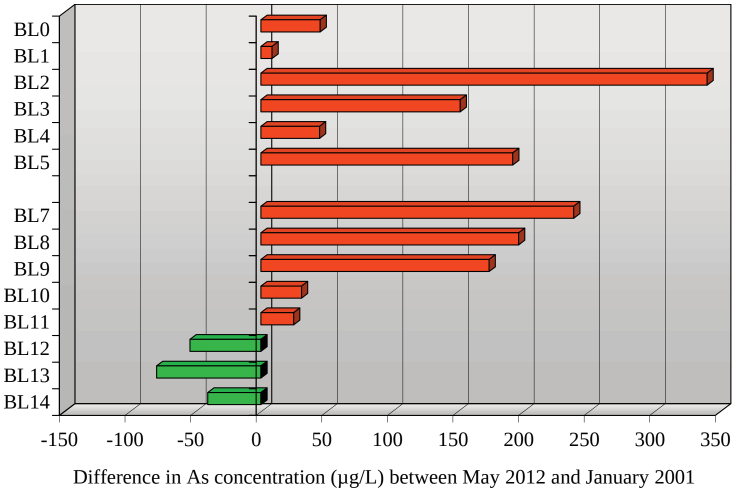

Fig. 9 *Difference in As concentration along the Baccu Locci stream between May 2012 and January 2001.*

banks have been removed according to the remediation measures adopted, they probably represented a small fraction of the total amount of tailings discharged into the BLs, scattered downstream, mixed with and buried under stream sediments down to at least 3 m deep. This widespread contamination source can not be completely removed and will probably continue to release As for a long time. In fact, the solid speciation of As in flotation tailings/stream sediments in the medium-lower BLs valley is dominated by arsenical ferrihydrite (HFO), and previous studies (Frau *et al.* 2008, 2010) have demonstrated that desorption of As from HFO in the Baccu Locci system is favored under neutral or slightly alkaline pH conditions and by the competitive effect of bicarbonate. Contrary to As, Pb is not released from the widespread contamination source in the medium-lower BLs valley because its solid speciation is dominated by plumbojarosite [$PbFe_6(SO_4)_4(OH)_{12}$] that is practically insoluble under the above-mentioned geochemical conditions (Frau *et al.* 2009), and therefore Pb is not at present an environmental concern.

Conclusions

Based on data currently available, the potential positive effects of remediation on water contamination in the Baccu Locci mine watershed are not yet visible. These first results are probably influenced by the short period of time elapsed from completion of remediation, and by climatic conditions, in particular rainfall and duration of dry and wet periods that can be highly variable in Sardinia, especially affecting a mountain stream like the BLs. Therefore, a prolonged monitoring for several years will be necessary in order to assess the real efficacy of remediation measures. However, post-remediation distribution of As in the BLs shows a trend very similar to pre-remediation conditions. Moreover, the in-depth knowledge of the mineralogical and geochemical processes responsible for contamination in the Baccu Locci system leads to hypothesize probable limited, beneficial effects of remediation on As contamination.

Acknowledgements

This study was supported by funds of F. Frau from the University of Cagliari (Italy) and the Consorzio AUSI (Consorzio per la Promozione delle Attività Universitarie del Sulcis-Iglesiente).

References

Frau F (2009) Point and diffuse contamination in relation to remediation actions: the case of the Baccu Locci mine in Sardinia. Rendiconti Online Società Geologica Italiana 6:249–250 (in Italian)

Frau F, Ardau C (2003) Geochemical controls on arsenic distribution in the Baccu Locci stream catchment (Sardinia, Italy) affected by past mining. Applied Geochemistry 18(9):1373-1386

Frau F, Ardau C (2004) Mineralogical controls on arsenic mobility in the Baccu Locci stream catchment (Sardinia, Italy) affected by past mining. Mineralogical Magazine 68(1):15-30

Frau F, Rossi A, Ardau C, Biddau R, Da Pelo S, Atzei D, Licheni C, Cannas C, Capitani GC (2005) Determination of arsenic speciation in complex environmental samples by the combined use of TEM and XPS. Microchimica Acta 151:189–201

Frau F, Biddau R, Fanfani L (2008) Effect of major anions on arsenate desorption from ferrihydrite-bearing natural samples. Applied Geochemistry 23(6):1451-1466

Frau F, Ardau C, Fanfani L (2009) Environmental geochemistry and mineralogy of lead at the old mine area of Baccu Locci (south-east Sardinia, Italy). Journal of Geochemical Exploration 100:105–115

Frau F, Addari D, Atzei D, Biddau R, Cidu R, Rossi A (2010) Influence of major anions on As(V) adsorption by synthetic 2-line ferrihydrite. Kinetic investigation and XPS study of the competitive effect of bicarbonate. Water, Air, and Soil Pollution 205:25–41

Frau F, Cidu R, Ardau C (2012) Short-term changes in water chemistry in the Baccu Locci stream (Sardinia, Italy) affected by past mining. Applied Geochemistry 27(9):1844-1853

RAS (2009) Linee guida per la caratterizzazione e la bonifica delle aree minerarie dismesse. Commissario delegato per l’emergenza ambientale relativamente alle aree minerarie del Sulcis-Iglesiente e del Guspinese della Regione Autonoma della Sardegna, D.P.C.M. 21.12.07, O.P.C.M. n.3640 15.01.2008, 220 pp

Monitoring the shallow subsurface for gas emission from abandoned underground mines

Christophe FRIPPIAT[1], Mathieu VESCHKENS[1], Daniel PACYNA[2]

[1]Institut Scientifique de Service Public, rue du Chéra 200, B-4000 Liège, Belgium, ch.frippiat@issep.be
[2]Service Public de Wallonie, Avenue Prince de Liège 15, B-5100 Jambes, Belgium

Abstract In this paper, a risk-based method is proposed for the design of networks of piezometers for the monitoring of near-surface gas emissions from abandoned underground coal mines. Risk is evaluated considering the location and extent of the mine and of the former underground mining infrastructures. Damage induced by the mining works on the upper geological formations and the associated increase in permeability is also taken into consideration, as well as potential impacts on humans. Damage is estimated using an empirical method based on the number of caved seams between the ground surface and a depth of 200 m.

Keywords surface gas emanation, GIS, risk assessment, damage function

Introduction

Underground storage of gas in natural or man-made cavities must be accompanied by appropriate monitoring measures to ensure that the gas is not leaking from the storage site, migrating upwards through the soil and reaching the soil surface. Properly designed monitoring networks include three types of monitoring points: (i) near all remaining surface mining installations, (ii) near potential accumulation zones in the underground sewer system or in housing basements, and (iii) near areas of the former mine where gas is likely to accumulate and migrate upward towards the ground surface. The appearance of near-surface gas emanations can be monitored using piezometers installed in geological layers overlying potential accumulation zones in the mined voids.

In this paper, we propose a method to design a network of piezometers aimed at monitoring potential gas emanations in shallow geological units. The method is based on an assessment of the risk to human population and is implemented within a GIS (Geographic Information System). It considers the location and extent of the mined areas, the ease of gas migration towards the ground surface, and the distance to the nearest housings.

The methodology is applied to two former gas storage sites installed in the abandoned coal mines of Péronnes-lez-Binche and Anderlues, in Belgium. When decommissioning the gas storage sites, it was recommended that the existing monitoring networks for surface gas emanations were complemented with additional piezometers. In this study, a preliminary assessment of the risk linked to surface gas emanations from the former storage sites is conducted and several suitable locations are identified for the installation of new piezometers.

Geographic and geological setting

The area of interest is located north and east of the city of Binche (Fig. 1) and takes to form of two imbricated areas framing the concessions of the coal mines in which natural gas was stored. The former gas storage site of Péronnes-lez-Binche fits within a rectangle of about 8 × 4 km^2, while that of Anderlues fits within a rectangle of about 4 × 4 km^2.

The average elevation of the zone is about +130 m a.s.l. In the western part of the zone (former storage site of Péronnes-lez-Binche), landscape is essentially marked by the valley of a small creek, flowing from South to North.

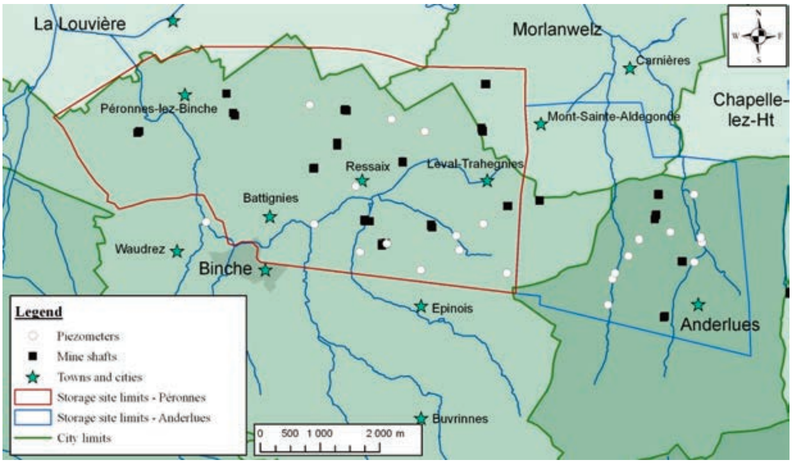

Fig. 1 *Geographic extent of the former storage sites.*

Surface elevations progressively increase from about +50 m a.s.l. in the northwest to about +180 m a.s.l. in the southwest of the zone.

In the eastern part of the zone (Anderlues), landscape is marked by two valleys with small creeks also running from South to North. Surface elevations range from about +110 m a.s.l. at the bottom of the valleys to about +220 m a.s.l. in the southern part of the zone.

Population density is highly variable. The city of Binche is an important urban nucleus (Fig. 1). A couple of smaller towns (Péronnes-lez-Binche, Battignies, Ressaix, and Leval-Trahegnies) also constitute more densely populated areas. Elsewhere, lands are mainly used for agriculture.

The stratigraphic sequence is characterized by a Carboniferous basement covered with Cretaceous and Tertiary sediments. Cretaceous units consist of marls of Turonian age and chalks. Turonian marls constitute a relatively continuous and impervious cover over the mined bedrock. Their average thickness is in the range of 20–30 m. They act as a hydraulic barrier and confine the gas that was stored in the former mines. The average thickness of the chalks is 60 m but can locally reach up to 100 m. The aquifer of the chalks is the main regional aquifer. It is an unconfined aquifer that is relatively heavily tapped for drinking-water production. Finally, tertiary sediments are mainly sands and clays. Kaufmann and Martin (2008) developed a full 3D geological model of the area that was used in this study.

Risk assessment

Risk assessment is conducted considering the simultaneous occurrence of (i) a source of danger, (ii) a pathway from the source to targets, and (iii) the presence of targets within distance of the source. Table 1 lists the variables that are used to quantify the components of risk. First, the source of danger is linked to the presence of exploited coal seams at a depth of less than

Component	Relevant element	Influence on the global level of risk
Source	Mined voids at a depth of less than about 200 m.	Risk is considered as negligible if no mined area can be found above a depth of about 200 m
Pathway	Minimum depth to mined voids	Risk increases where mined voids are closer to ground surface
	Geology / hydrogeology	Risk decreases in zones where low-permeability geological units are thicker (i.e. marl, clay, …)
	Damage to geological layers resulting from mining activities	Risk increases if damage to upper geological layers is important. Damage is directly linked to the distribution of mined voids.
Target	Distance to nearest habitations	Risk decreases in zones where the distance from the point of surface emanation to the nearest targets increases.

Table 1 *Relevant variables for risk assessment.*

about 200 m. While this value is relatively arbitrary, it is usually considered that significant ground damage will not occur at more than 150–170 m above a caved coal seam. It is considered that gas accumulating at larger depths is not likely to migrate towards the ground surface. Then, the pathway component is primarily evaluated based on the geology and on the damage linked to coal exploitation. Only vertical pathways are considered here: gas is assumed to migrate vertically. Finally, as the risk associated to surface gas emanations is primarily gas accumulation within a confined space and explosion, it is considered that any human being within distance of a zone where gas emanation could occur is at risk. The target component is quantified as the distance to the nearest housings. As the distance increases, the likelihood that gas accumulated in or near the housings decreases.

Source component

Regional-scale cross-sections of the mine were used to identify near-surface coal seams. Such cross-sections are three-kilometre-long North-South-oriented vertical cross-sections, generally available every 100 m along the West-East direction. They cover the whole territory and contain information from all existing mine concessions. Exploited coal seams are represented on the cross-sections, as well as the main access shafts and the connection tunnels. The ground surface and the limit between coal bearing units and upper non-Carboniferous units is also represented, with a limited precision considering that there is no vertical exaggeration.

A total of 267 cross-sections have been examined. If multiple copies of one cross-section were available, the most penalizing with respect to gas migration towards the surface was always kept. A 100 m × 100 m horizontal grid was adopted to analyze the cross-sections. The number of exploited coal seams between the ground surface and a depth of about 200 m was counted for each grid cell, as well as the depth to the shallowest exploitations, if there were any between the ground surface and a depth of about 200 m. Considering the vertical scale of the cross-sections and that the analysis was conducted manually and visually, depth measurement precision is estimated at about 10 m.

As an example, Fig. 2 shows the spatial distribution of the number of exploited coal seams. Most of the time, between 1 and 3 coal seams are identified per grid cell. There is however a relatively significant portion of the Péronnes-lez-Binche reservoir where the number of exploited coal seams increases up to 6. It only increases up to 9 in one area, and up to 12 in another area. In Anderlues, exploitations were generally much deeper than 200 m. Mined coal seams outside of the Péronnes-lez-Binche and Anderlues concession correspond to neighboring concessions.

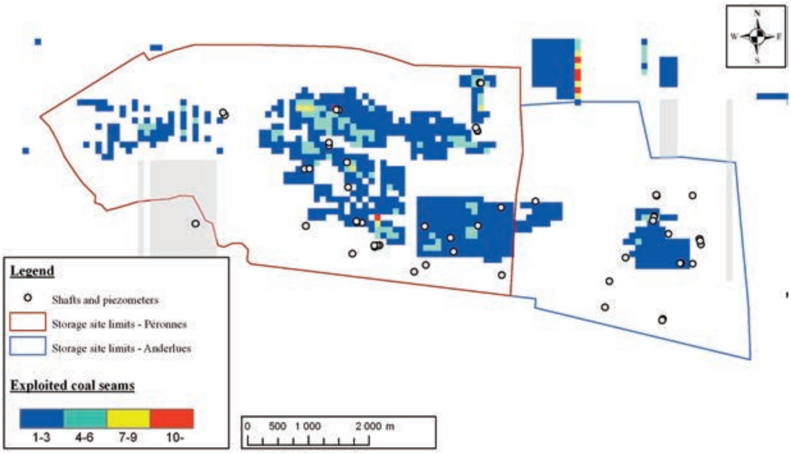

***Fig. 2** Number of exploited coal seams between the ground surface and a depth of about 200 m. Gray areas correspond to zones where no cross-section was available.*

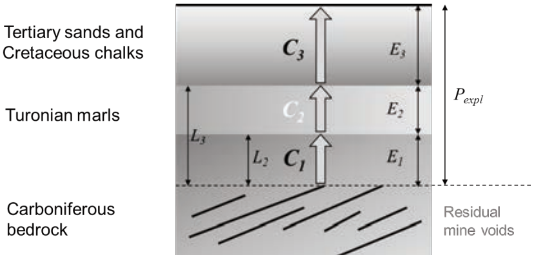

Fig. 3 *Definition of the variables needed to compute specific hydraulic conductance.*

Pathway component

The conceptual model used to quantify the pathway component uses the notion of specific hydraulic conductance (Harbaugh *et al.* 2000). Specific conductance is defined as the ratio of the permeability to the thickness of the geological layer. Based on Darcy's law for fluid flow in porous media, multiplying specific conductance by head difference and cross-sectional area for flow gives the total discharge. Hence, if permeability increases, gas will migrate towards the ground surface more easily. Similarly, for a given pressure difference, if thickness decreases, gradient and flow rate will increase.

The general model used for the storage sites of Péronnes-lez-Binche and Anderlues is depicted on Fig. 3. Three types of geological units are considered: the Carboniferous bedrock, the Turonian marls, and the upper chalk units and tertiary sands. Total specific conductance C_{tot} is computed using a serial model of the specific conductance of the Carboniferous bedrock (C_1), of the Turonian marls (C_2) and of the Tertiary sands and the Cretaceous chalks (C_3)

$$\frac{1}{C_{tot}} = \frac{1}{C_1} + \frac{1}{C_2} + \frac{1}{C_3} = \frac{E_1}{K_1} + \frac{E_2}{K_2} + \frac{E_3}{K_3} \tag{1}$$

Subscript indices 1, 2 and 3 will refer to the Carboniferous bedrock, to the Turonian marls, and to the Tertiary/Cretaceous cover, respectively. The thicknesses of the geological units (E_1, E_2, E_3) are directly obtained from the geological model of Kaufmann and Martin (2008). Permeabilities (K_1, K_2, K_3) depend on the geology and on the presence of nearby exploited coal seams. Indeed, mining activities can cause important ground fissuring and stress release in the bedrock and the upper geological units, sometimes resulting in important perturbations of subsurface permeabilities. In this paper, it is proposed to link the permeability of the damaged geological unit to its initial permeability using a mathematical model accounting for the damage caused by the underground exploitations.

The evaluation of the area impacted by the mining activities and the level of damage is relatively complex and depends on the nature and the geometry of mining works, on the nature and mechanical properties of the overlying rocks, on the method of roof control (caving or back-filling), on the local and regional tectonic contexts and on the local stress state of the rock. In this paper, it is proposed to adopt an empirical approach based on a damage function for the evaluation of the effect of underground mining activities on permeabilities. The damage function allows the determination of a dimensionless coefficient D [-], based on the density of mining works (*i.e.* number of coal seams exploited between 0 and -200 m, noted N_V [-]), and the distance L [m] to the mining works. The damage coefficient ranges from 0 to 1. The choice of the damage function is relatively arbitrary, provided that

- the function exhibits a maximum for a minimum distance and a maximum number of exploited coal seams;
- the function tends towards zero if the distance to the nearest exploitations increases, independently of the number of exploited coal seams;
- the function equals zero if the number of exploited coal seams is zero;
- the function increases with the number of exploited coal seams, for a given distance to the nearest exploitations.

The function proposed here is characterized by 4 parameters:

- a minimum distance L_{min}, under which damage is also maximum for a given number of exploited coal seams;
- a maximum distance L_{max}, beyond which damage is negligible;
- a maximum number of exploitation coal seams $N_{v,max}$, corresponding to a unit damage index D at short distance;
- a dimensionless shape factor $F > 1$ controlling the shape of the damage function.

The proposed damage function is best expressed using complex variables. One defines

$$x = \frac{N_v}{F \times N_{v,max}},$$
$$y = \frac{10(L - L_{min})}{(L_{max} - L_{min})}, \qquad (2a, b, c)$$
$$z = x + iy$$

where i is the complex number, with $i^2 = -1$. The damage index is given by

$$D = \log\left(\frac{1+z}{1-z}\right) \Big/ \log\left(\frac{1+F}{1-F}\right) \qquad (3)$$

Two example applications of the damage function corresponding to two different values of the shape parameter F are shown in Fig. 4. In the remaining part of the text, the values L_{min} = 15 m, L_{max} = 500 m, $N_{v,max}$ = 12 (corresponding to the maximum observed value) and F = 1.25 will be adopted. The distance to the nearest exploitation (*i.e.* L in Eq. 2b) is taken as the vertical distance from the bottom of the geologic layer of interest to the shallowest mined zone. It is noted L_2 when referring to the distance needed to compute the damage to Turonian marls and L_3 when referring to that relating to the tertiary sands and Cretaceous chalks (Fig. 3). These distances to the nearest exploitations can be computed from the geological model of Kaufmann and Martin (2008) and from the depth of the shallowest exploitations.

The permeability of the damaged geological unit is then computed from the damage index as

$$K = \exp\left((1-D)\log(K_{init}) + D\log(K_{max})\right) \qquad (4)$$

where K refers to K_1 when computing the permeability of the damaged Carboniferous bedrock, K refers to K_2 when computing that of the damaged Turonian marls, and K refers to K_3 when computing the permeability of the damaged Tertiary/Cretaceous cover. K_{init} [m/s] is the natural permeability of the geological layer and K_{max} [m/s] is its maximum permeability once it has been damaged. K_{max} is arbitrarily taken equal to 100 × K_{init}. Initial values of permeability were taken as 10^{-7} m/s, 10^{-10} m/s, and 10^{-9} m/s for the upper chalk

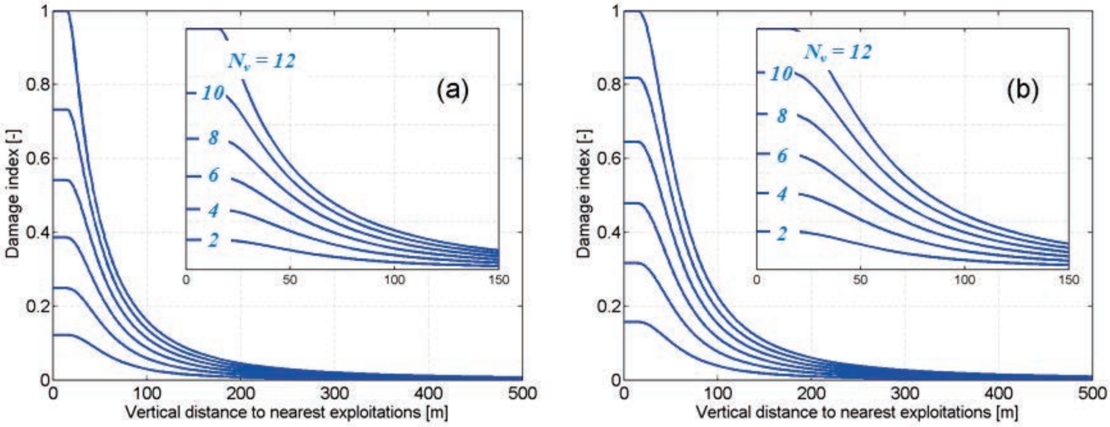

***Fig. 4** Damage function corresponding to L_{min} = 15 m, L_{max} = 500 m, $N_{v,max}$ =12. (a) F = 1.25. (b) F = 2.5.*

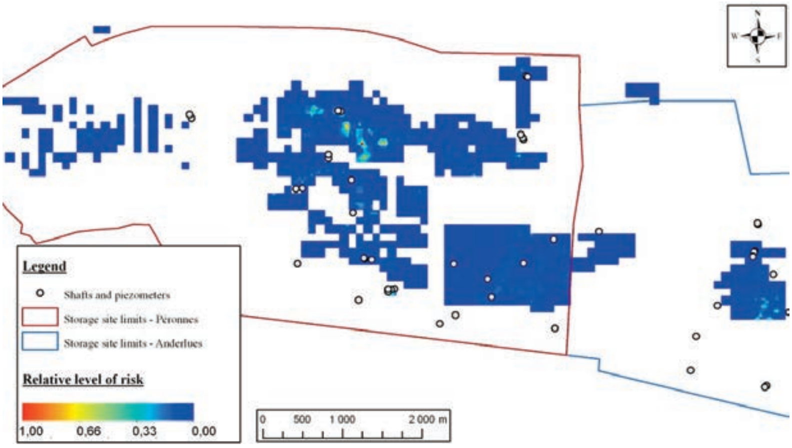

Fig. 5 *Relative level of risk of gas surface emanations*

and tertiary units, the Turonian marls, and the Carboniferous bedrock, respectively.

Target component

The target component is quantified as the distance to the nearest housings. It is directly computed within the GIS using a numerical version of the topographic map of the area.

Results

The global level of risk is directly computed as the ratio of the hydraulic conductance of the overburden C_{tot} to the distance to the nearest housings. Fig. 5 shows the results of the analysis. The pixel size is adjusted here on that of the geological model (30 × 30 m). The values are normalized so that they range from 0 to 1.

Several “hot spots” appear on the map. It can be seen that they do not directly correspond to heavily mined areas or to very shallow exploitations. Indeed, in Anderlues, while the exploitations are generally relatively deep, the overburden is usually much thinner and Turonian marls are not necessarily present over the whole storage site. As a result, zones of higher risk also appear in Anderlues. These hot-spots on the map could be selected as potential site for the installation of new piezometers.

Conclusions

A methodology has been developed in order to locate new piezometers to monitor surface gas emanations from former underground gas storage sites. The method uses regional-scale geological cross-sections to identify the number of exploited coal seams and estimate their depth. A damage index is computed in order to quantify the degradation of subsurface permeability. The methodology applied to the sites of Péronnes-lez-Binche and Anderlues, in Belgium. The sites are abandoned coal mines that have been used for gas storage for a period of about 20 years.

While the methodology has been applied to storage sites for natural gas, it is also largely applicable in the framework of carbon dioxide sequestration projects. The methodology is also applicable to abandoned mines undergoing flooding, the rising groundwater level pushing the residual gas towards upper mined voids and favouring gas migration towards the surface.

References

Harbaugh AW, Banta ER, Hill MC, McDonald MG (2000) MODFLOW-2000, the U.S. Geological Survey modular ground-water model – User guide to modularization concepts and the Ground-Water Flow Process. U.S. Geological Survey Open-File Report 00–92, 121 pp.

Kaufmann O, Martin T (2008) 3D geological modelling from boreholes, cross-sections and geological maps, application over former natural gas storages in coal mines. Computers and Geosciences 34(3): 278—290

Non-conclusive time series analyses – what can we learn on the behavior of the groundwater system? Understanding what caused the collapse of an abandoned drainage tunnel

Christophe Frippiat[1], Mathieu Veschkens[1], Daniel Pacyna[2], Luc Funcken[3]

[1]Institut Scientifique de Service Public, rue du Chéra 200, B-4000 Liège, Belgium, ch.frippiat@issep.be
[2]Service Public de Wallonie, Avenue Prince de Liège 15, B-5100 Jambes, Belgium
[3]Service Public de Wallonie, rue Côte d'Or 253, B-4000 Liège, Belgium

Abstract Time series analysis was used as an attempt to identify a potential accidental hydrogeological trigger to the collapse of an abandoned mine drainage tunnel in Belgium. Correlation, spectral and wavelet analyses were applied to piezometric data in order to characterize regional-scale hydraulic connections between groundwater bodies, but failed to provide direct insight into regional hydrogeology. No correlation between data collected in the hydrogeological unit of the collapsed area could be identified, showing that the piezometers were tapping isolated sand lenses. As a conclusion, the collapse was rather attributed to a slow increase in water pressure linked to a limited recharge.

Keywords correlation analysis, spectral analysis, wavelet analysis, barometric efficiency

Introduction

In February 2009, important ground subsidence suddenly occurred over an area of a diameter of about 50 m in the town of Saint-Vaast, near the city of La Louvière (Belgium; Fig. 1). Subsidence caused important cracks to several houses, to the sidewalks and to the road surface. A couple of days earlier, a torrent of mud erupted from the ground in a home garden near the Haine river, about 600 m south of the subsided area. It was rapidly found that an underground drainage tunnel ran at a depth of about 30 m under the subsided area and had its exit located near the eruption point of the mud torrent.

Historic documents report that the construction of the drainage tunnel started around 1747 and lasted for more than a century. Tunnel construction was heavily complicated as it had to cross wealden-facies sediments containing numerous pockets of quicksands. As tunnel construction progressed and reached such pockets, quicksands often burst into the tunnel, causing human losses and systematically filling the tunnel over significant distances. Eventually, tunnel construction was abandoned before it was connected to the mine works and used for drainage.

The likely scenario of the Saint-Vaast accident is that the drainage tunnel remained intact and water-filled over significant length portions but was plugged with debris materials near its exit. Water pressure acting on the plug eventually caused its failure, leading to a rapid emptying of the tunnel. This caused the collapse of the tunnel at one or several weak points, allowing the quicksands to flow into the tunnel and move towards its exit. The residual voids in the ground caused in turn surface subsidence.

The goal of the study is to improve the understanding of the causes of the collapse and, in particular, identify a potential accidental hydrogeological trigger to the increase in water pressure suspected in the likely scenario. The accident occurred in a region where natural groundwater flows are potentially affected by two important hydrogeological artifacts: the drawdowns at the boat lift of Strépy-Thieu and the groundwater rebound in the coal mine of

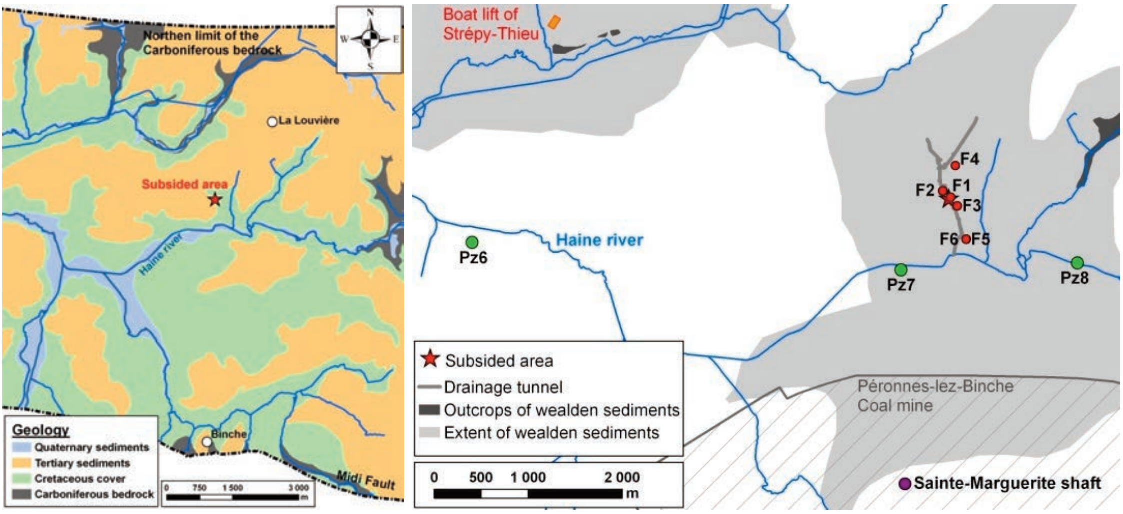

Fig. 1 *Geographic extent and geological setting of the zone of the accident. Extent of wealden-facies sediments as proposed by Marlière (1946)*

Péronnes-lez-Binche (Fig. 1). The boat lift of Strépy-Thieu is located 4.6 km northwest of Saint-Vaast. A permanent drawdown of about 28 m is maintained in the wealden-facies sediments in order to maintain the lower level of the lift dry. The coal mine of Péronnes-lez-Binche is located 3 km south of Saint-Vaast. At the time of the accident, groundwater level was rising at a rate of about 3 m/year in the Sainte-Marguerite shaft (Fig. 1) as a result of the flooding of the abandoned mine.

Considering the magnitude of these disruptions to natural groundwater flows, it was suspected that either one of those artifacts could be linked to the water pressure elevation in the wealden-facies sediments at Saint-Vaast that caused the failure of the plug in the abandoned tunnel.

Geological and hydrogeological setting

The study area is centered on the town of Saint-Vaast and extends from the Midi fault to the northern border of the Mons basin (Fig. 1). The mean surface elevation of the area is about +100 m a.s.l, ranging from about +130 m a.s.l. in the northwestern part of the zone down to about +80 m a.s.l. in its southeastern part. The regional topography is characterized by a number of small valleys and by the presence of numerous coal tips, some of them culminating at more than +200 m a.s.l.

The stratigraphic sequence is characterized by a Carboniferous basement covered with Cretaceous and Tertiary sediments. Cretaceous units consist of wealden-facies sediments, overlain by marls of Turonian age and chalks. The wealden-facies sediments are mainly distributed in kilometer-scale lenses preferentially located in local depressions of the basement. Their thickness can reach up to 50 m at Saint-Vaast. They are highly detritic sediments of various origins. They contain materials from gravel to thick clays, lignified wood debris and pockets of quicksands. Due to their high clay content, they globally behave as an aquiclude. However, the isolated pockets of sand and gravel contained in the weadlen-facies sediments are water-bearing. Turonian marls constitute a relatively continuous and impervious cover over the wealden-facies sediments. Their average thickness is in the range of 20–30 m. They act as a hydraulic barrier and confine the wealden-facies sediments. The average thickness of the chalks is 60 m but can locally reach up to 100 m. The aquifer of the chalks is the main regional aquifer. It is an unconfined aquifer that is relatively heavily tapped for drinking-water pro-

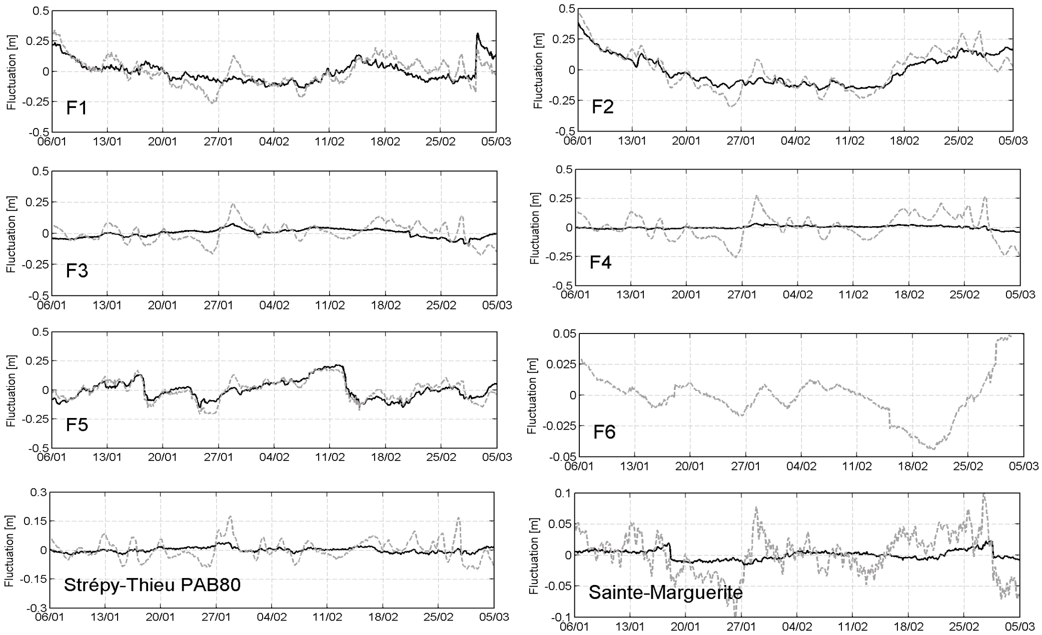

Fig. 2 *Example set of piezometric data (from January 6 to March 5, 2010). Raw data (dashed gray line) and data filtered for variations in atmospheric pressure and terrestrial attraction (black line).*

duction. Finally, tertiary sediments are mainly sands and clays.

The extent of the lenses of wealden-facies sediments at Saint-Vaast and near the boat lift of Strépy-Thieu was initially mapped by Marlière (1946; Fig. 1). Potential hydraulic connections could exist between the lens at Saint-Vaast and (i) the lens at Strépy-Thieu, as more recent log results seem to show that both lenses could be connected, (ii) the lower Carboniferous aquifer, and (iii) the upper unconfined chalk aquifer. As the wealden-facies sediment lens at Saint-Vaast is comprised between the upper clay-rich altered part of the bedrock and Turonian marls, it is expected that these hydraulic connections are of very limited magnitude. Moreover, the direct recharge area of the lens is of very limited extent (Fig. 1). All terms of the hydrogeological balance of the lens are thus expected to be relatively limited.

The initial goal of the study was to characterize hydraulic connections between aquifers at the regional scale and within the wealden-facies sediments lens at Saint-Vaast. Classical field methods based *e.g.* on pumping tests could only be used in a very limited fashion, in order to limit pressure variations in the wealden-facies sediments and avoid a new accident. Instead, correlation, spectral and wavelet analyses of piezometric data were used.

Piezometric data

Raw data

At the request of the authorities of the city of La Louvière, five piezometers (F1 to F5) were installed by the Service Public de Wallonie (the regional administration) in the wealden-facies sediments near the expected position of the abandoned tunnel (Fig. 1). Piezometric data were collected automatically using Level TROLL® probes on a 2-hour basis. As an example, detrended water levels measured between January 6 and March 5, 2010 are shown on Fig. 2. Significant correlations seem to be present, similar peaks in the raw data appearing for all five piezometers.

A sixth piezometer (F6) was installed in the shallower Cretaceous aquifer near F5 (Fig.

1), in order to gain insight into the vertical hydraulic gradient through the Turonian marls. Head difference is of the order of 9 m, yielding an ascending gradient of about 24 %. Data recorded during the example period from January 6 to March 5, 2010, are also shown on Fig. 2. Three existing piezometers tapping the chalk aquifer were identified in the vicinity of the subsided area and were also used in this study (Pz6, Pz7 and Pz8, reported on Fig. 1). Although correlation with F1 to F5 is less obvious, it seems that certain patterns also appear here.

The boat lift of Strépy-Thieu is a heavily instrumented engineering structure. Piezometric data are collected at a number of wells screened in the wealden-facies sediments, and the total discharge of the overflowing wells used to lower the water table around the basement of the lift is also continuously measured. A large number of datasets were used in this study. As an example, data recorded at well PAB80 between January 6 and March 5, 2010 is also shown on Fig. 2. A clear similarity appears with the raw data recorded at F1 to F5, seemingly supporting the assumption of a regional-scale influence of the boat lift.

Finally, a probe was also installed in the piezometer of the Sainte-Marguerite shaft, where the groundwater rebound in the mine of Péronnes-lez-Binche can be monitored. Data collected during the example time period of January 6 to March 5, 2010 are also reported on Fig. 2. Although exhibiting some high frequency fluctuation, similar peaks as in F1 to F5 also appear in the raw data collected here.

Filtering barometric and Earth tide effects

Variations in atmospheric pressure and terrestrial attraction act as distributed forces at the ground surface that can have various effects on groundwater levels, as a result of aquifer compressibility. While unconfined aquifers might not be significantly affected by such perturbations, confined aquifers will generally react to variations in atmospheric pressure and terrestrial attraction. Barometric efficiency is defined as the ratio of groundwater level fluctuations to the corresponding variations in atmospheric pressure (Batu 1998). A unit barometric efficiency expresses that the water level decreases by 1 cm when the atmospheric pressure increases by 0.98 mbar. It corresponds to a fully rigid rock matrix.

The water-bearing sand lenses in the wealden-facies sediments are confined. It was also suspected that piezometric data collected at Strépy-Thieu and in the former coal mine of Péronnes-lez-Binche could be partially influenced by such processes. The linear regression technique developed by Toll and Rasmussen (2007) was used to filter barometric and Earth tide effects. Barometric data was available at the Gosselies IRM station. Earth tide measurements were not available. Instead, a synthetic tide was generated using the software T-Soft (Van Camp and Vauterin 2005). It appears that piezometers F1 to F5 are heavily responsive to variations in atmospheric pressure. Barometric efficiencies range from 87 % for F4, 68 % for F3, 61 % for F2 and about 50 % for F1 and F5. Filtered data for the example time period of January-March 2010 are also shown on Fig. 2. There remains almost no visible fluctuation in F3 and F4. It also appears that most observed fluctuations at Strépy-Thieu are also linked to variations in atmospheric pressure. In the coal mine of Péronnes-lez-Binche, most observed mid-term fluctuations (6–24 hours) were linked to atmospheric pressure, while short-term (<6 hours) fluctuations were caused by Earth tides. The remaining jumps are of the order of one centimeter and are caused by human manipulation when performing manual checks of the measurements.

Correlation, spectral and wavelet analyses

While most visible peaks in groundwater levels were smoothed out when filtering for variations in atmospheric and terrestrial attraction, time-series analysis was conducted in order to attempt to identify correlations in the datasets. Theoretical considerations on the application of correlation, spectral and wavelet analyses to temporal data can be found *e.g.* in

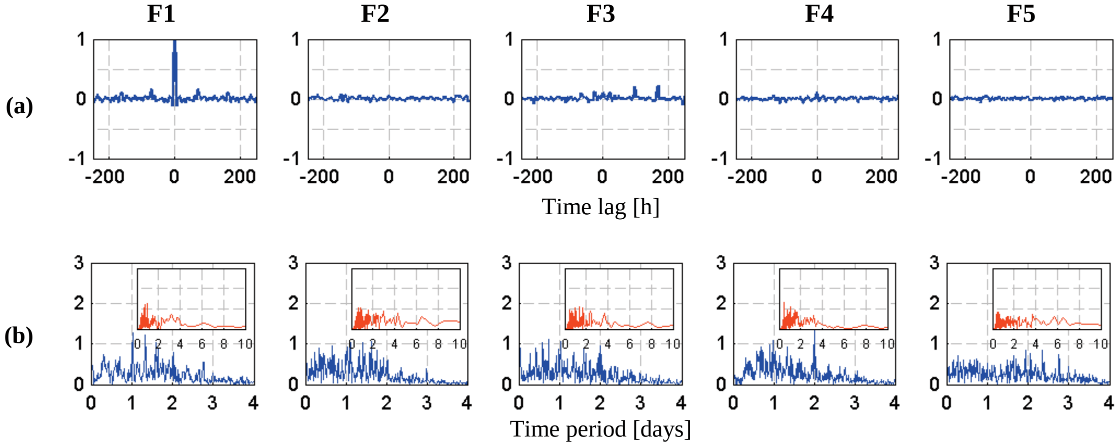

Fig. 3 *(a) Autocorrelation and cross-correlations of fluctuation rates of F1, with F1, F2, F3, F4 and F5. Data collected between November 28, 2009 and May 11, 2010. (b) Power spectral and cross-spectral densities of F1, with F1, F2, F3, F4 and F5. Densities are normalized. Densities are plotted as a function of the time period [days] (in blue) and as a function of frequency [cycle/day] (in red).*

Massei *et al.* (2006). Correlation and spectral analyses were conducted using standard Matlab® tools, and wavelet analysis was conducted using the Wavelab toolbox (Buckheit *et al.* 2005). Time series were not directly conducted on filtered piezometric data. In order to ensure data stationarity, analyses were conducted on data derivatives (*i.e.* fluctuation rates).

As an example, autocorrelation and cross-correlation functions between F1 and F2, F3, F4 and F5 are shown on Fig. 3.a. First, autocorrelation time is very small, of the order of measurement time. This indicates that fluctuations can be considered as random. Then, even though the piezometers are all screened in the wealden-facies sediments and located less than 800 m apart, no significant cross-correlation can be observed. A similar result is obtained when trying to establish correlations with data collected in the upper unconfined chalk aquifer, near the boat lift of Strépy-Thieu or in the former coal mine of Péronnes-lez-Binche. If a clear pattern appeared in the raw data, it was thus only linked to large-scale distributed forces of climatic origin simultaneously acting on all regional aquifers. Filtering for the effect of these forces removed any correlation between the time-series.

Similarly, power spectral and cross-spectral densities are shown on Fig. 3.b. The densities are plotted both as a function of the time period (in blue) and as a function of the time frequency (in red). Spectra are all relatively wide and do not exhibit any major peak. No cyclic pattern appears among the piezometer.

This led to the need to test wavelet analysis, in order to verify whether non cyclic pattern emerged in the data sets. The results are not shown here but follow the same lines: no similar type of behavior can be identified among the piezometers tapping the wealden-facies sediments and with the upper unconfined aquifer, with the aquifer at the boat lift of Strépy-Thieu or in the former coal mine of Péronnes-lez-Binche.

This is a rather disappointing result, as initial considerations and observation of raw unfiltered data led to make the assumption that regional perturbations to the groundwater system could have had an influence on water pressures within the wealden-facies sediments. Barometric effects were not directly suspected, as they affect in a much minor way unconfined aquifers and as measurements in the upper chalk aquifer (piezometer F6) seemed to show similar variations as the wealden-facies sediments aquifer. The corresponding peaks in the upper unconfined chalk aquifer were actually caused by direct recharge, a lowering of atmospheric pressure being usually accompanied by precipitations. The decreasing atmospheric pressure caused thus an increase in piezometric data in confined aquifers as a function of their barometric efficiencies, and the simultaneously-occurring precipitations caused a similar increase in the water table of the upper unconfined aquifer.

Discussion

A close examination of the boring logs of F1, F2, F3, F4 and F5 did not permit to identify any similar sequence of sand/clayey sand/sandy clay/clay. While the piezometers were all screened in sandy parts, there was thus no guarantee that they were tapping the same sand lens. Then, global trends in piezometric data (not shown here) are relatively different. Several piezometers have measured a significant decrease in water level after the accident and seem to have now stabilized. Piezometer F4 follows a very different pattern and seems to continuously increase. Piezometer F5 fluctuates much more than F1, F2, F3 and F4. A tracer test was also conducted in F1 and F2. While the flushing volume was as limited as possible (about 5 m^3), it caused a significant and persistent variation of the water level in the piezometer. The initial water level was only recovered after about 3 months. These elements allowed one to conclude that the five piezometers were tapping isolated lenses of sand, probably each of a relatively limited volume.

Hence, the wealden-facies sediments can be pictured as a series of conductive lenses embedded in a relatively impervious clay background. Recharge occurs through very limited areas and is probably extremely limited. Groundwater discharges very slowly and in very limited amounts towards the upper unconfined chalk aquifer through the Turonian marls and towards the Carboniferous aquifer and the former coal mine of Péronnes-lez-Binche through the upper altered part of the bedrock. There is no evidence of a hydraulic link with the groundwater bodies at the boat lift of Strépy-Thieu. All terms in the hydrogeological balance of the wealden-facies sediments are thus limited and it is not likely that a sudden variation in water pressure has occurred as a result of a variation in pressure in a neighbor aquifer.

Instead, the likely assumption is that water pressure slowly and gradually increased in the wealden-facies sediments, as a result of the slow and limited recharge. At some point, pressure was sufficient to overcome the mechanical resistance of the plug in the drainage tunnel, and caused its failure. This led to the sudden release of water, mud and sands. The residual voids in the wealden-facies sediments eventually resulted in the observed ground surface subsidence.

Conclusions

As an attempt to grasp a potential hydrogeological cause to the collapse of an abandoned mine drainage tunnel, time-series analysis was applied to piezometric data collected within different aquifers at a regional scale. The goal of the study was to highlight hydraulic links between aquifers and characterize the hydrogeological behavior of the wealden-facies sediments in which the tunnel was bored. Classical methods based on pumping tests or tracer tests could only be used to a limited extent in order to avoid a new accident caused by pressure variations.

The initial assumption was that either drawdowns at the boat lift of Strépy-Thieu or the groundwater rebound in a nearby abandoned coal mine caused a variation in the water pressure of the wealden-facies sediments. This hypothesis was further supported by significant correlations that were visually observed between water level fluctuations in the wealden-facies sediments and water level fluctuations in the neighbor aquifers. However, filtering barometric and Earth tide effects from piezometric data smoothed out most observed short-term fluctuations. The application of standard time series analysis techniques to filtered data failed to highlight any correlation in the data set. Correlation could not even be found between data collected in the different piezometers tapping the wealden-facies sediments at Saint-Vaast. A closer examination of available borehole logs revealed that the piezometers were probably tapping isolated more-conductive sand lenses in the wealden-facies sediments. This assumption was further supporter by the very long dissipation times that were observed after flushing one of the piezometer during a tracer test.

If a distant hydrogeological trigger was initially suspected, the final assumption is that of a very limited diffuse recharge that caused a slow and gradual increase in water pressure within the wealden-facies sediments. At some point, it is believed that the water pressure exceeded the resistance of a plug in the drainage tunnel, which failed.

References

Batu V (1998) Aquifers hydraulics: A comprehensive guide to hydrogeologic data analysis. John Wiley and sons, New York, 727 pp

Buckheit J, Chen S, Donoho D,Johnstone I, Scargle J (2005) About WaveLab. Ver. 0.850. Technical Report, Stanford University, 39 pp

Marlière R (1946) Deltas wealdiens du Hainaut : Sables et graviers de Thieu, argiles réfractaires d’Hautrage. Bull Soc belge Géol LV:69—101.

Massei N, Dupont J-P, Mahler BJ, Laignel B, Fournier M, Valdes D, Ogier S (2006) Investigating transport properties and turbidity dynamics of a karst aquifer using correlation, spectral, and wavelet analyses. J Hydrol 329:244—257

Toll NJ, Rasmussen TC (2007) Removal of barometric pressure effects and earth tides from observed water levels. Ground Water 45(1):101—105.

Van Camp M, Vauterin P (2005) Tsoft: Graphical and interactive software for the analysis of time series and earth tides. Computers & Geosciences 31(5): 631—640

Groundwater Stratification and Impact on Coal Mine Closure

Andrew Johnstone[1], Ingrid Dennis[2], Norman McGeorge[3]

[1] GCS (Pty) Ltd, PO Box 2597, Rivonia, 2128 South Africa. andrewj@gcs-sa.biz
[2]North West University, PO Box 19140, Noordbrug, 2522, South Africa. Ingrid.dennis@nwu.ac.za
[3]BHPBiliton Energy Coal South Africa. PO Box 6180, Marshalltown 2107 South Africa.
Noddy.mcgeorge@bhpbilliton.com

Abstract On closure of the Ermelo Mines in 1992, initial monitoring indicated that a water treatment would be required to treat the mine decant. The evolution of the water quality can be attributed to sulphate reducing bacteria, vertical recharge from the hanging aquifer and stratification. Water level and quality monitoring have shown that the water in the old mine void will not decant to surface due to the depth of the mine void, hydrogeological conditions, a "hanging aquifer" and the recharge mechanisms. As a result no water treatment will be required and the mine will not impact on the surface water.

Keywords monitoring, water, quality, stratification, decant

Introduction

The paper discussed a case study of the closure of the Ermelo Colliery (Pty) LTD, an underground board and pillar coal mine, situated in the Mpumalanga Province of South Africa and how the mine closure strategy changed with a better understanding of the hydrogeology and stratification of water in the mine.

Initial closure plans anticipated the construction of water treatment plant to treat possible poor quality decant water. As more scientific work was undertake by various people and organizations there emerged a clearer understanding of the rebound of water levels, the evolution of the groundwater chemistry and the stratification of water. This has significantly changed the mine closure strategy. Data shows that the mine will not decant poor quality water and it will not impact on the ambient hydrological regime (surface and groundwater).

The paper describes the hydrogeology of the mine, the mechanism of rebound of water levels, evolution of the groundwater quality and the new closure strategy. Groundwater flow and solute transport models were undertaken to predict the long term groundwater flow regime and water quality and to determine the potential for decant. Routine monitoring of groundwater quality and levels is undertaken to ensure that the hydrogeological predictions are correct. The also paper details the importance of correct monitoring and conceptual hydrogeological model and the influence this has on the mine closure planning

Location

Ermelo Mine is located in the eastern part of South Africa in the Mpumalanga province at an altitude of 1600 mamsl. The area is characterised by warm wet summers and cold dry winters. The average yearly rainfall is 650 mm/a which occurs in summer. The original vegetation was grassland but this has given way in areas to commercial cultivated agriculture, with the main crops being maize and pastures (Fig. 1).

The mine is the only mine situated in the Brakspruit (C11F) catchment, which is in the headwaters of the Vaal River catchment. The Vaal River, is one of the main rivers that drain the coal and gold mining areas of South Africa, and is under extreme pressure due to poor quality decant and seepage from the aban-

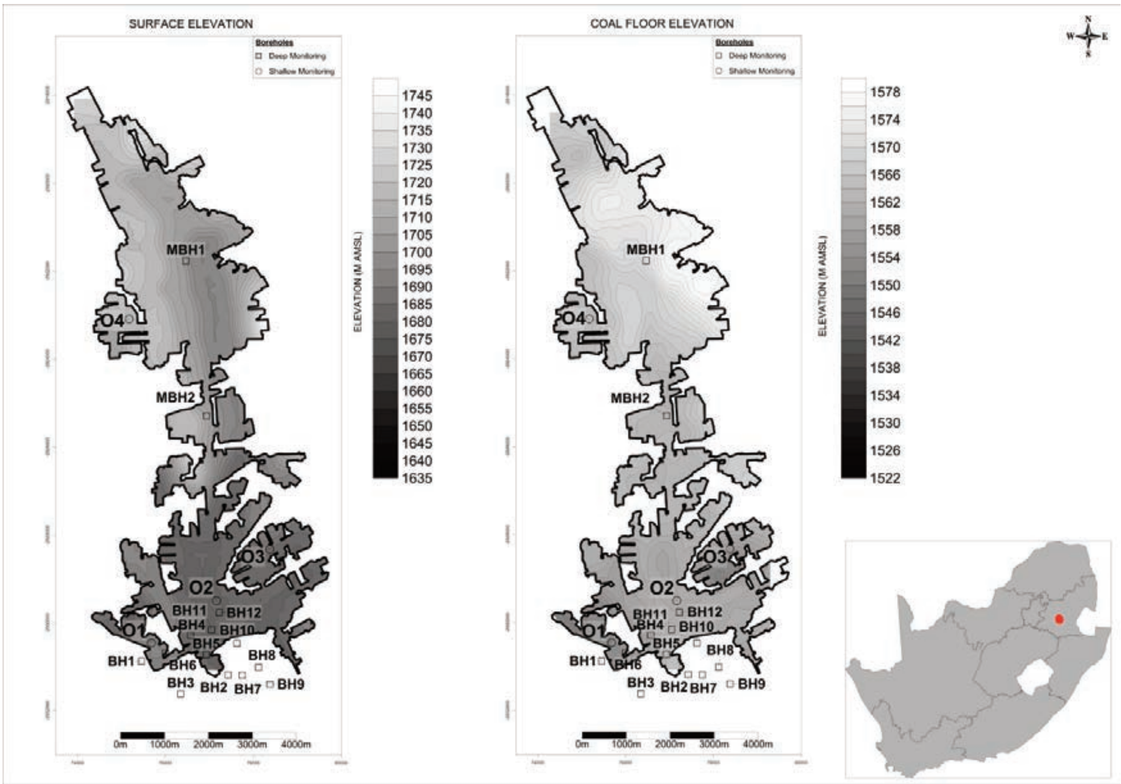

Fig. 1 *Locality plan*

doned, closed and operating mines. The Vaal River water quality is managed by strict control of decant, mine water treatment and dilution by means of intercatchment transfer from the Lesotho- Highlands scheme.

Farmers in the Brakspruit catchment rely on springs as well as boreholes that yield water from the shallow weathered aquifer. Most farmers boreholes are 40 m deep and do not intersect the coal measures. There are some small agricultural dams in the Brakspruit and theses are used for small scale crop irrigation.

Description of the Mine

Ermelo mine started in 1977 and was decommissioned in April 1997. The coal seam occurs between 90 and 180 meters below surface (mbs) and access to the coal was by means of shafts and declines. The mining method was board and pillar with limited pillar extraction (stooping). The mine was notorious for its high methane content which lead to some fatalities. The mine plan was largely controlled by faults, dolerite sills and dykes. The underground workings trend north-south, with the coal seam dipping 5 degrees to the south. The coal seam is the shallowest 90 mbs (1570 mamsl) in the north and the southern part being the deepest at 180 mbs (1520 mamsl). The surface elevation in the north is 1680 mamsl and the elevation at the south being 1600mamsl. As a result all rebound water flowing into the mine flowed down dip to the south (see Fig. 1).

Coal was processed on site in a washing plant and exported by rail. Discard were placed in a discard dump which has been shaped and vegetated. The dump is not discussed in this paper

On closure the envisaged logical places for the mine decant was in the southern area above the workings into the “Brakspruit” which flows into the Vaal River.

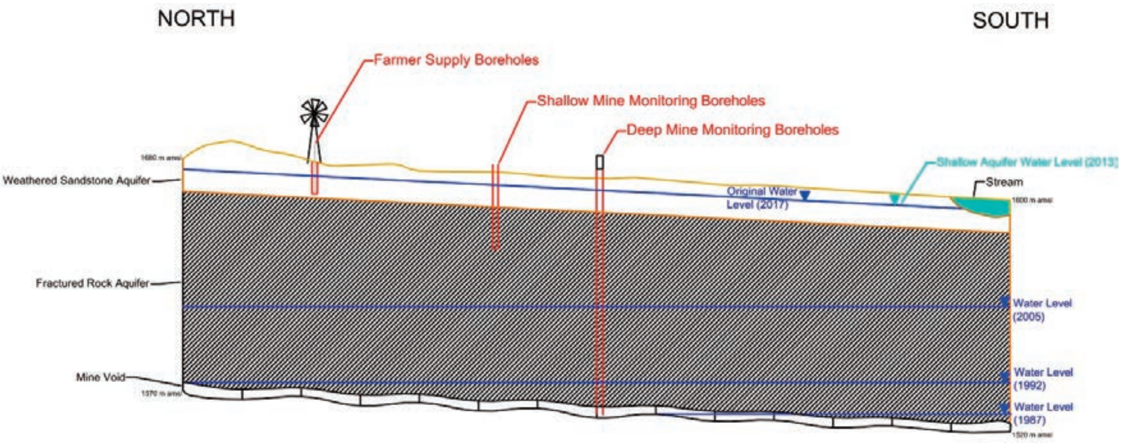

Fig. 2 *Conceptual Hydrogeological Model*

After decommissioning a number of deep boreholes were drilled into the mine void to monitor water quality and levels in the mined void. Shallow boreholes (0–60 m) were used to monitor water levels in the shallow “upper” aquifer. A very important hydrogeological observation was that only a few farmers’ water supply boreholes were affected by the underlying mining operations.

Hydrogeology

The mine hydrogeological regime is a typical sedimentary weathered and fractured aquifer. The geology consists of slightly dipping sedimentary units, varying from shales, carbonaceous shales, coal, silts and the roof being a thick, medium to fine grained sandstone. The sandstone roof is up to 80 m thick and is very competent. The area has been intruded by post depositional igneous intrusions in the form of dolerite dykes and sills. The contact zones of dykes and sills have resulted in post depositional zones of permeability. In certain areas the dolerite sills and dykes can act as permeable or no flow boundaries. The base of the aquifer for this study was taken as the tillite below the coal seam.

Recharge to the aquifer was modeled by mine stage curve analysis and numerical modelling is 5 % of mean annual precipitation (MAP) which is 32.5 mm/a. Water levels in the aquifer ranges from 0 (springs and seeps) to 10 m below surface (hills)

The shallow aquifer comprises weathered and fractured sandstone which is very important as it is the main water supply aquifer and has a significant contribution to the baseflow of the streams. Water quality in the aquifer is very good. The deeper aquifer comprises fractured sandstone & shales, bedding plane permeability and lithological contact zones. This aquifer was intersected during the mining operations and historical information indicated that the aquifer did not yield much water during mining. The conceptual hydrogeological model is shown in Fig. 2.

Pyrite is ubiquitous in all the South African coal mines and this leads to the formation of acid mine drainage in the mine. The formation of poor quality leachate is a function of the surrounding lithology’s that are disturbed during mining. At Ermelo there is pyrite in the coal seam as well as the roof and the floor.

Monitoring

On closure of the mine, a routine surface and groundwater monitoring program was instituted to determine the water quality and levels in the ground and surface water. The shallow aquifer was monitored by measuring water levels and water quality, in the farmers and dedicated mine monitoring boreholes

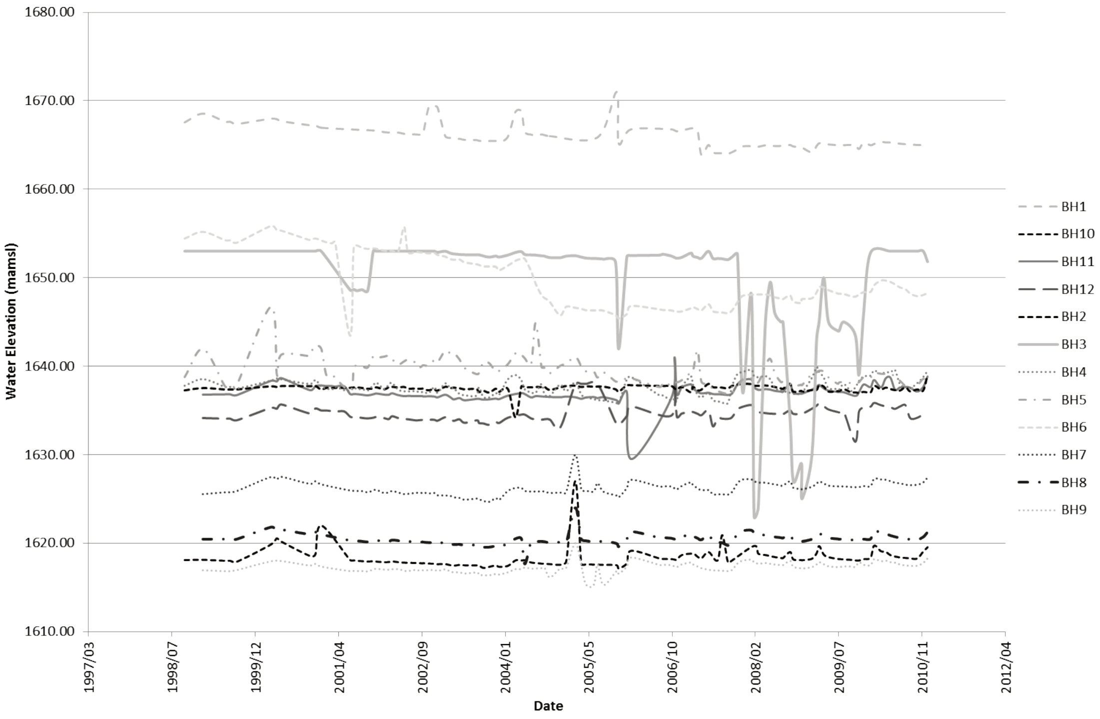

Fig. 3 Shallow monitoring borehole time series water levels

It is interesting to note that water levels in the shallow aquifer were not significantly impacted on during the mining operations and post mining, while water levels were recovering in the mine void. Groundwater level in the shallow boreholes is shown in Fig. 3. The majority of the boreholes are located above the mine void.

Dedicated deep boreholes were drilled into the mine void. These were used to monitor water quality and water levels in various areas in the mine (basins). The recovery of the water levels in various areas of the mine is shown in Fig. 4. The rebound of water levels indicates that the mine comprises of various

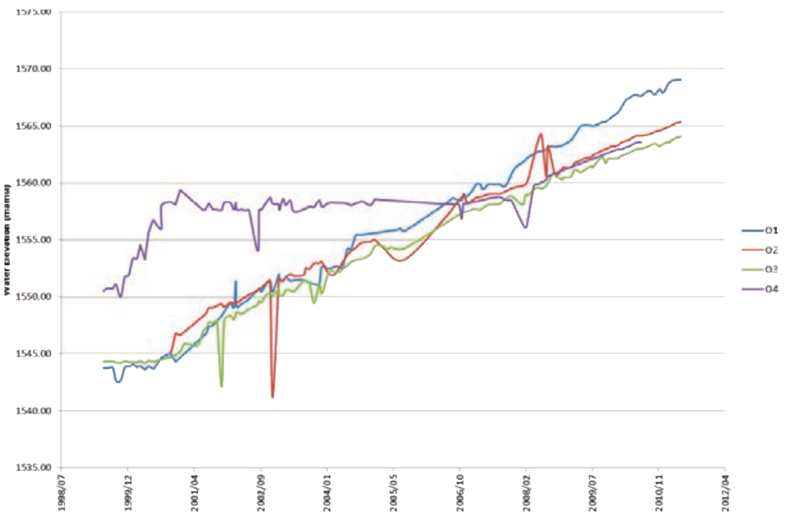

Fig. 4 *Deep Borehole in the mine void*

basins and these basins decanted into other basin depending on the coal floor contours and mine developments.

Groundwater Chemistry

The groundwater chemistry in the shallow aquifer is very different to the chemistry in the mine void. The water is low in dissolved solids and the chemistry shows it is recently recharged. The water quality on the Brakspruit is also good, despite its name.

The water quality in the mine void has proved very interesting. Initial water quality data indicated that the mine void water was very high in dissolve solids (5000 mg/L) mostly sulphate (3200 mg/L). This would be expected as all water in the void flowed to the southern area and was monitored in borehole 01 and 02. The water quality began to change and this lead to numerous disputes between practitioners working on the project. There were various theories from, "there is cascading water down the borehole which influences sampling, exchange with Na being substituted for SO4, incorrect sampling depths, impact of sulphate reducing bacteria".

During routine water sampling it was observed that there were hydrogen sulphides as well as a film in the deep holes. As a result it was decided to undertake a microbial investigation. Van Heerden and Botes (2012) undertook a study of the microbial activity at the mine. The recovering mine (methane filled void) and the flooded mine cavity presents an ideal environment for excluding oxygen from the system of acid rock drainage (ARD). Samples of the microbes were collected and the DNA was extracted and analysed. The result indicated that there were a high number of bacteria and numerous species and there is clearly an abundance of carbon sources, potential electron donors and most importantly a finite amount of terminal electron acceptors. At present there is sufficient buffering capacity to ensure neutral pH.

Stratification

There was difficulty in sampling the water quality in the mine boreholes and erratic re-

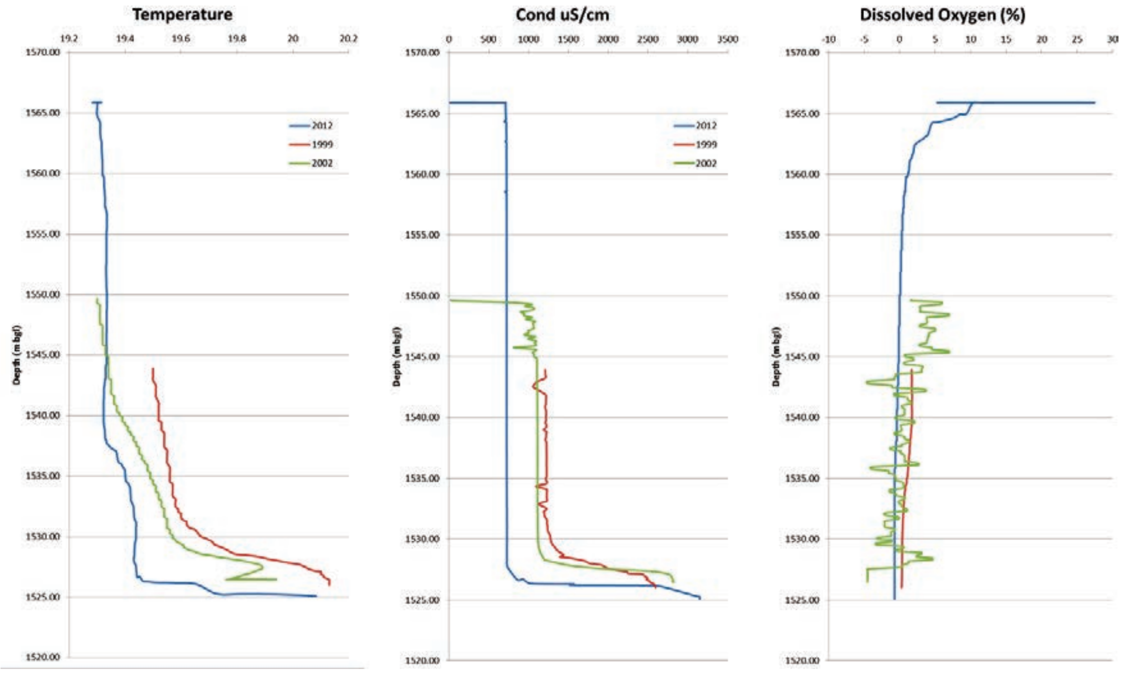

Fig. 5 *Borehole 04 Down hole profile*

sults were being received. In order to confirm the representativeness of the water quality that was collected from the mine void boreholes, a number of down hole profiles were undertaken in the deep mine monitoring boreholes. These were undertaken 1999, 2002 and 2012 and are shown in Fig. 5. The profiles clearly indicate the following:

- The water in the mine void is overlain by better quality water similar to the hanging aquifer
- There is stratification of water in the mine with better quality water above poorer quality water in the mine void
- The mine void water is essentially "trapped" in the mine void.
- In the unlikely event that the mine decants, the poor quality decant water will have to displace water in the upper aquifer. This is unlikely to occur as there is insufficient head and the roof is largely impermeable.

Conclusions

The closure plan for the mine has change considerable with a better understanding of the hydrogeology. It is clear that the mine will now not decant and the mine void water is confined to the old mine working and the water above the mine is ambient groundwater of good quality. There is not suffient head in the mine and the roof permeability is not suffcient to allow for large scale long term decant of poor quality water.

The paper shows the importance of hydrogelogical conditions in the deign of a mine in order to inhibit potential mine decant on closure. Factors that should be considered are shaft locations, aquifers, the importance of a "hanging aquifer" and the use of artificial recharge to flood mine voids on closure.

References

Ingwe, and BHP Billiton (2005) Closure Provisions: closure summary report

Ermelo Mines Services (2005) Mine Closure Cost Assessment Base, June 2005

Joseph D (2004) Closure Template Model Ermelo, Business Evaluation & Economics, Melbourne

Botes E, Ojo E, van Heerden E (2011) Microbial Diversity Fingerprinting. Ermelo Water Management Project. University of the Free State, South Africa.

Dennis I, Dennis R, Van Heerden E and Botes E (2012) Ermelo Colliery Assesmsent of the Underground Mine Decant. University of the Free State, South Africa.

GCS (Pty) Ltd (2006) Review of the Ermelo Mine Closure and Closure Cost. Rivonia, South Africa

Hodgeson F, Grobbelaar R (1999) Investigation into Long Term water quantity and quality trends at Ermelo Colliery. University of the Free State. South Africa.

Hodgson F (2004) Evaluation of the Mine Water Balance for Ermelo Colliery, Report no. 2004/13/FDIH, Institute for Groundwater Studies, University of the Free State, Bloemfontein, South Africa

Stemming Flow Using Hydraulic Adit Plug Closure – A Comparison: Glengarry Mine, New World District, Montana and World’s Fair Mine, Patagonia, Arizona

Allan Kirk[1], Henry Bogert[2], Mary Beth Marks[3], Eli Curiel[4]

[1] Geomin Resources, Inc., 227 East Olive St., Bozeman, MT 59715, USA, akirk@geominresources.com
[2] Consulting Mining Engineer, P. O. Box 3648, Hailey, ID 83333 USA, henrybogert@gmail.com
[3] Gallatin National Forest, 10 East Babcock, Bozeman, MT 59715 USA, mmarks@fs.fed.us
[4] Coronado National Forest, 300 Congress Street, Tucson, AZ 85705 USA, ecuriel@fs.fed.us

Extended Abstract Two historically mined, abandoned adits were closed using hydraulic plug methods to eliminate acidic, metal-laden groundwater point source discharges to surface water (Table 1). The Glengarry Mine, located near Cooke City in south-central Montana, consists of a 800 m long, 1.5 × 2.1 m adit, driven in a competent quartz monzonite intrusive where it exposes gold- and copper-bearing massive sulfide ore. The Glengarry Mine was closed under a contract with the USDA Forest Service, Gallatin National Forest (R1).

The World’s Fair adit, located in the Harshaw Mining District on the Coronado National Forest (R3), south of Patagonia, Arizona, was driven as a cross-cut structure in competent quartz diorite to serve as a main haulage from some 4,500 m of underground workings.

Following closure at the Glengarry Mine, groundwater behind the innermost adit plug rebounded over 120 meters, filling the cone of depression associated with the mine such that an underground monitoring well became artesian in just one month. In addition, two surface water tributaries overlying the mine transitioned from seasonal to perennial flow. Flow from the adit was reduced by 99 % with a reduction of metal loading to receiving waters of 99.9 %. Groundwater quality within the mine workings changed from pH 2.2 to 6.4, with reductions in Cu and Zn concentrations of about 2.5 and 1.5 orders of magnitude respectively. There has been no post

Parameter	Glengarry Mine, MT		World’s Fair Mine, AZ	
	Pre-Closure	Post-Closure	Pre-Closure	Post-Closure
pH	as low as 2.2	as high as 6.4	3.2	no flow
Exceedances of HH	As, Ba, Cd, Cu, Fe, Mn, Pb, Se, Zn			
Average flow	50 gpm (189 L/min)	<0.5 gpm (<2 L/min)	11 gpm (42 L/min)	no flow
Flow reduction		99%		100%
Load to receiving SW	30%	<0.1%	40%	0%
Load Reduction		99.9		100%
Closure Method	Complex Closure with Multiple Features	• Raise plug • fault grouting • 4 adit plugs • cement & mine waste backfill • free draining portal plug	Simple Closure	• 2 adit plugs, • mine waste backfill, • free draining portal plug
Cost		$2,900,000		$1,103,000
Project duration	2000 – 2005	5 years	06/09 to 02/11	17 months

***Table 1**. Comparison of Glengarry and World’s Fair Hydraulic Adit Plug Closure Projects*

closure flow from the World's Fair mine adit. These results indicate that stemming flow with hydraulic adit plug closures can create a reliable "walk-away" solution for point source discharges with significant potential to improve groundwater and down-gradient surface water quality.

Geochemistry of Improved Groundwater Quality Resulting from Adit Plugging, Glengarry Mine, New World District, Cooke City MT USA

Lisa B. Kirk[1], Lauren R. Bozeman[1], Allan R. Kirk[2], Mary Beth Marks[3]

[1]Enviromin, Inc., PO Box 1685, Bozeman MT 59771, USA, lkirk@montana.com
[2]Geomin Resources, Inc., PO Box 7005, Bozeman MT, 59771, USA, akirk@geominresources.com
[3]Gallatin National Forest, 10 East Babcock, Bozeman MT 59715 USA, mmarks@fs.fed.us

Abstract Construction of hydraulic adit plugs within the historically mined Glengarry Adit at Cooke City MT effectively reduced discharge by more than 95 % and resulted in groundwater rebound that flooded underground workings. This study evaluates geochemical controls of groundwater quality through comparison of changes in mineral saturation states and metal sorption potential, and shows that post-closure flooding resulted in increased alkalinity, which prompted precipitation of aluminum and iron-oxyhydroxide minerals followed by metal sorption, with associated increases in dissolved iron and sulfate primarily due to dissolution of jarosite. Improved water quality supports the use of this approach in other mine closure settings.

Keywords hydraulic adit plug, ARD, jarosite, geochemical modeling, Gallatin National Forest

Introduction

Discharge of contaminated water from historically mined underground workings at numerous locations indicates the need for effective methods of closure that address both geotechnical and hydrogeochemical concerns. Hydraulic adit plugs, together with grouting to control groundwater flow and backfilling, were used to close the Glengarry Adit in the New World Mining District located northeast of Yellowstone National Park, near Cooke City (fig. 1). In addition to limiting discharge to surface water, the closure design was intended to slow groundwater recharge enough to reduce the supply of oxygen available for continued sulfide oxidation and if possible, promote the development of reducing conditions within the flooded adit.

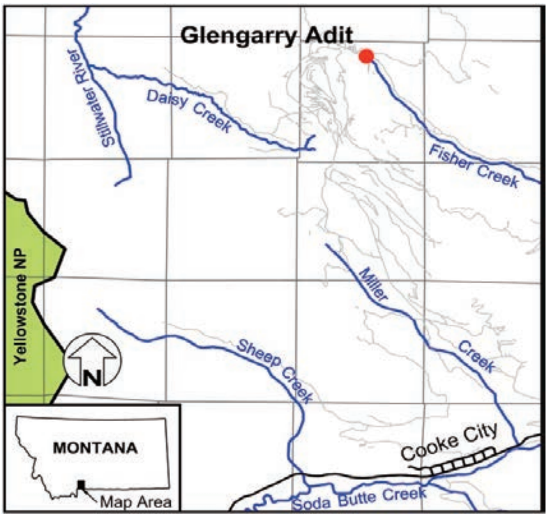

Fig. 1 Location of the Glengarry Adit, New World District, Cooke City, MT USA. Section grid: 1.6 km on a side.

In this study, probable geochemical controls of groundwater quality were identified based on comparison of changes in potential for mineral precipitation and metal sorption to ferrihydrite before and after the adit closure.

Background

The Glengarry Adit was driven beneath the Como Basin, located north of Cooke City MT (fig. 1), to access mineable copper and gold resources in the early 1900s. The adit intercepts sulfide mineralized Tertiary intrusive rock associated with massive sulfide and skarn mineralization hosted in the Paleozoic Meagher limestone (fig. 2).

Sulfide oxidation has historically produced acid rock drainage (ARD) in the adit, which when neutralized by carbonate mineralization downstream can be shown as Equation 1 below.

$$\mathrm{FeS_2 + 2\,CaCO_3 + \tfrac{3}{2}\,H_2O + \tfrac{15}{4}\,O_{2(g)} \rightarrow}$$
$$\mathrm{Fe^{III}(OH)_3 + 2\,CaSO_4{\cdot}2H_2O + 2\,CO_2(aq)} \qquad \text{(eq. 1)}$$

The primary oxidation reactions involved in this net reaction are influenced by pH, as shown,

$$\mathrm{FeS_2 + \tfrac{15}{4}O_{2(g)} + \tfrac{1}{2}H_2O \rightarrow}$$
$$\mathrm{Fe^{II+} + 2\,SO_4{}^{2-} + H^+} \qquad \text{(slow, abiotic, pH > 4.5, eq. 2)}$$
$$\mathrm{FeS_2 + 14\,Fe^{III+} + 8\,H_2O \rightarrow}$$
$$\mathrm{15Fe^{II+} + 2\,SO_4{}^{2-} + 16H^+} \qquad \text{(faster, biotic, pH < 4.5, eq. 3)}$$

Mean discharge from the adit prior to closure was strongly acidic, with pH as low as 2.7 and averaging 3.5, and high concentrations of metals that exceeded most relevant water quality standards (fig. 3). The pH and alkalinity of groundwater in the adit rose sharply at closure (fig 3), with associated decreases in concentrations of dissolved Al, Cd, Cu, Pb, and Zn (fig. 4). Elimination of discharge from the adit has greatly improved downgradient surface water quality, and has prompted significant interest in the use of hydraulic adit plug methods in other adit closure settings. In spite of improved groundwater quality, however, Fe, Ca, Mg, and SO_4 concentrations continued to increase significantly relative to pre-closure conditions (fig. 3), raising questions about post-closure geochemical processes influencing the evolution of water quality within the adit. Given the potential cost associated with the construction of hydraulic plugs, which typically requires underground adit rehabilitation prior to closure and can run costs into the millions of dollars, a thorough geochemical evaluation of post-closure changes in water quality is appropriate to determine the overall effectiveness of the closure method in shifting chemical equilibria from the strongly acid producing reaction described in Eq. 3 back to Eq. 2 and ultimately, Eq. 1.

Glengarry Adit Closure

In August of 1996, the US government acquired portions of the New World district from Crown Butte Mines, which ended proposed mineral development and initiated rehabilitation of historic mine lands (Maxim Technologies 2002). In 2004, Tetra Tech (on behalf of the USFS) initiated closure of the adit by constructing a raise collar grout curtain and a raise plug to prevent continued influx of water from the mineralized Como Basin bedrock and colluvium into the adit, as shown in fig 2. Grouting of several structures also served to limit groundwater flow into the adit. The adit was then backfilled behind each of four hydraulic plugs keyed to bedrock within the adit workings during the remainder of 2004 and 2005 (Kirk *et al.* 2013.). Monitoring well FCGW-100 was constructed immediately behind the innermost adit plug as shown in Fig 2. Groundwater rebounded rapidly, over a period of weeks, filling the adit and overlying fractures in bedrock.

Water Quality Sampling Methods

Monitoring of water quality in the adit has occurred since the 1980s via collection of samples from the discharge at the adit portal (site F-8A) prior to closure and from a monitoring well screened within the adit (FCGW-100) post-closure. Monitoring of the adit discharge at site F-8A pre-closure involved measurement of water flow and field parameters (pH; conductivity, redox potential; temperature; dissolved oxygen) and collection of samples for analysis major ion, and dissolved and total metals, as reported previously by Tetra Tech 2011. Following closure, discharge at F-8A largely ceased, but annual monitoring of groundwater chem-

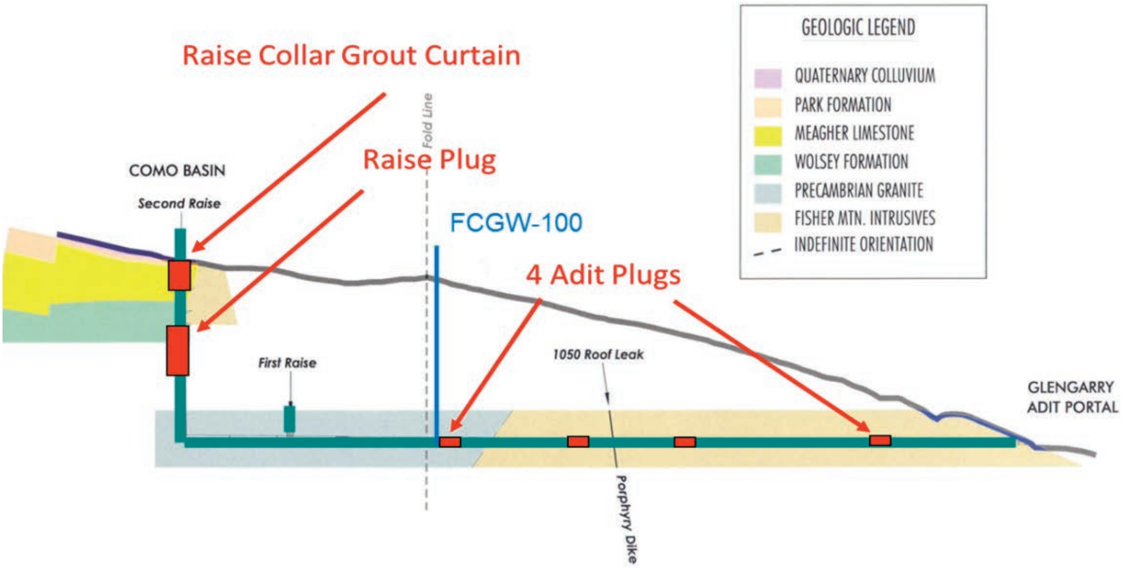

Fig. 2 *Glengarry Adit closure, showing FCGW-100 monitoring well. Sampling location F-8A was at portal. Fig. not to scale.*

istry in the adit has continued in the FCGW-100 well using a down-hole multi-probe to measure field parameters *in situ*. Major ion and dissolved metal groundwater samples have been collected with either a bailer or using a submersible pump (Tetra Tech 2011).

Glengarry Adit Water Quality Data

With the assistance of Crown Butte Mines, Noranda Minerals, Maxim Technologies and Tetra Tech, the USFS has assembled and maintained the public USDA New World Mining District Response & Restoration Project database that contains water quality data for the Glengarry Adit. The data used for this study were obtained from this public access database (USDA 2012).

Data for this study were selected from samples collected at the pre-closure adit portal (F-8A) and post-closure groundwater well (FCGW-100) sites for the period extending from 1990 to 2012. Samples were screened for completeness of the suite of dissolved major ions and metals as well as the calculated anion-cation charge balance for individual analyses reported over time. Samples with charge imbalances <15 % and a relatively complete list of major ions and dissolved metals were retained for initial analysis. Iron was speciated only at F-8A during the construction of the closure plugs in 2004. Changes in major ion chemistry including pH and dissolved Fe, Ca, Mg, and SO_4, and the dissolved metals Al, Cu, Zn, and Pb, were plotted for the selected data in fig. 3. Comparison of major ion ratios indicated that samples collected from site F-8A under low flow conditions were most similar to samples from FCGW-100 post-closure, so these samples were chosen for geochemical modeling to compare pre- and post-closure mineral precipitation, dissolution, and metal sorption processes. The complete data set was further constrained to select samples with charge imbalance smaller than 5 % for geochemical modeling of mineral equilibria and metal sorption relationships.

Geochemical Modeling Methods

The Geochemist Workbench SpecE8® and React® models were used to speciate the aqueous chemistry of the adit water, calculate changes in the relative equilibrium of the water with respect to Fe, Mn, and Al oxyhydroxide and sulfate minerals resulting from

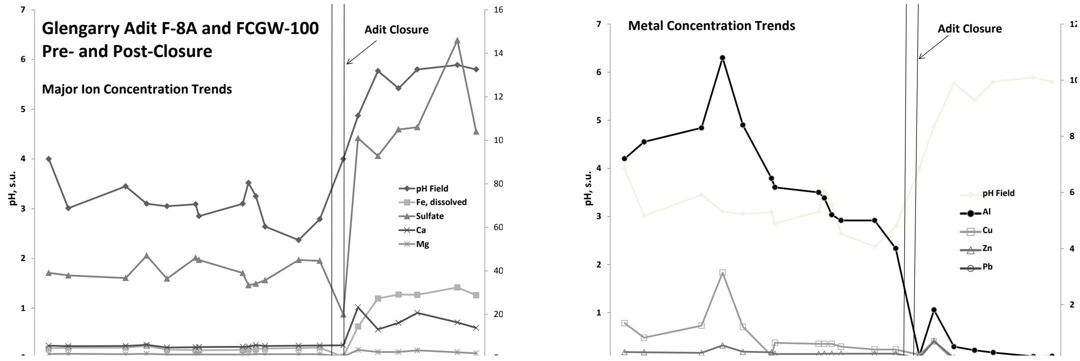

Fig. 3 *Change in (a: left) major ion and (b:right) metal chemistry with time, in the Glengarry Adit, as measured at stations F-8A pre-closure and FCGW-100 post-closure. Two stages of closure, in 2004 and 2005, are shown.*

the adit closure, and to calculate potential for sorption of metals to precipitated ferrihydrite (Rockware 2011). Calculations were made at pressure = 1 bar, using measured T, pH, Eh, HCO_3, SO_4, Cl, F, Ca, Mg, Na, K, and dissolved Al, Fe, Ag, Cr, Cu, Pb, Mn, Ni, Zn, and As concentrations. Dissolved oxygen concentration was calculated for modeling purposes based on the measured redox potential and dissolved carbon dioxide concentrations were calculated based on measured alkalinity. Charge was balanced prior to each calculation using the sulfate ion concentration. Changes in mineral saturation state were predicted using the SpecE8® software with the LLNL.dat database (Rockware 2011).

The precipitation and redissolution of minerals from the 2006 groundwater reacted with calcite, and subsequent sorption of metals to ferrihydrite, were calculated using the React® modeling utility of the Geochemist Workbench with a sliding fugacity model. Calcite (0.007 g) was reacted with the chemistry of water sampled at the time closest to closure, and the fugacity of carbon dioxide and oxygen were systematically swept to represent the increasing alkalinity (up to $p\mathrm{CO}_2$ = -2.2) and removal of oxygen (down to $p\mathrm{O}_2$ = -50) from the system under the flooded conditions. At each step, the minerals jarosite, alunite, gibbsite, boehmite, and ferrihydrite were allowed to precipitate. Dissolved metals were allowed to sorb to the precipitated ferrihydrite using the dataset FeOH+.dat provided with the Geochemist Workbench®, which assumes 600 m^2g^{-1} of sorbing surface area with site densities for the weakly and strongly binding sites, respectively, of 0.2 and 0.005 mole (mole $FeOOH)^{-1}$. The system was broadly constrained by the fugacity model and calcite addition to arrive at a final pH, TDS, and alkalinity roughly comparable to that measured *in situ* in 2008 (Table 1)

Although it is known from previous work that hematite and goethite are present in the adit, they are unlikely to precipitate directly from solution (Rockware 2011) and so were excluded from the calculations to avoid complicating iron redox equilibrium calculations. These Fe oxide minerals have been shown to form instead via recrystallization of the less ordered Fe-oxyhydroxide minerals (Liu *et al.* 2009). Although both redox and oxygen measurements were reported for most sampling events, Fe^{2+}/Fe^{3+} speciation was not uniformly reported in the database. Due to the strongly oxidizing characteristics of the acid, Fe^{3+}-rich acid mine drainage pre-closure, and based on the speciation measurements reported in 2004 at F-8A, iron was assumed to be Fe^{3+}

under pre-closure conditions. Modeling the transition to a geochemically closed system, as pH rose under increasingly reducing conditions, was challenging from an iron redox disequilibrium standpoint, however, because iron speciation data were not reported post-closure. For this reason, the post closure system was modeled with total iron input as Fe^{2+}, and the Fe^{2+}/Fe^{3+} redox couple enabled, so that the model speciated both the distribution of iron and calculated the dissolved oxygen based on the measured Eh value.

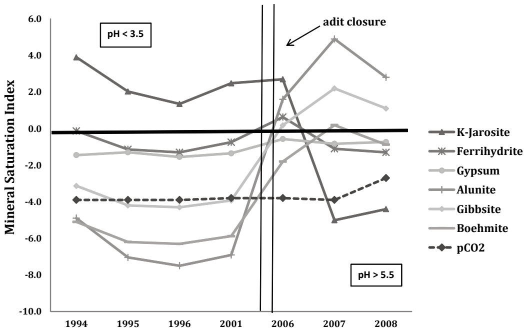

Fig. 4 Change in Mineral Saturation in Glengarry Adit Post-Closure.

Results

Alkalinity (dissolved HCO_3, and therefore, pCO_2) has steadily increased in the flooded adit, increasing the pH of groundwater (Fig. 3). Jarosite was the dominant stable phase prior to closure, which changed as increasing pH prompted precipitation of alunite, gibbsite, and ferrihydrite (fig. 4). Of the aluminum oxyhydroxide minerals, boehmite reached equilibrium last, and only briefly, after ferrihydrite saturation dropped in response to declining redox potential with decreased oxygen. Of particular interest is the undersaturation of jarosite under reducing conditions post-closure (fig. 4), as the dissolution of jarosite would explain the relatively large increase in dissolved iron and sulfate concentrations in spite of rising pH after 2006 (fig. 3). The precipitation of these aluminum minerals also explains the observed decrease in aluminum concentrations at closure.

Table 1 compares the model results with the speciated water quality samples for 2006 and 2008 These results show that the React® calculation based on the 2006 sample, using

Model Model input sample date	SpecE8® 2006	React® 2006	SpecE8® 2008
pE+pH	13.21	10.25	9.9
Alkalinity	0.01	1.13	0.58
pCO_2	-3.84	-2.2	-2.4
pO_2	-37.1	-49	-50
TDS	1399	1414	1494
Jarosite, $KFe^{3+}_3(OH)_6(SO_4)_2$	2.73	-3.53	-4.39
Ferrihydrite, $Fe(OH)_3$	0.62	-0.61	-1.27
Alunite, $KAl_3(SO_4)_2(OH)_6$	1.56	0.59	2.81
Gibbsite, $Al(OH)_3$	0.18	2.49	1.07
Boehmite, γ-AlO(OH)	-1.77	0.54	-0.88
Gypsum, $CaSO_4$-$2H_2O$	-0.57	-0.57	-0.72
Sorbed Cu, % removed	0	100	post closure
Sorbed Mn, % removed	0	100	post closure
Sorbed Pb, % removed	0	100	post closure
Sorbed Zn, % removed	0	100	post closure

***Table 1** Glengarry Adit Mineral Solubility and Metal Sorption Modeling Results.*

the fugacity slide model with a small amount of calcite to simulate carbon dioxide accumulation and oxygen depletion, reasonably simulates the observed chemistry in the post closure adit. The modeled 2006 React® results have a comparable chemistry to the 2008 SpecE8® results, which indicates that the ferrihydrite precipitation, and associated, Cu, Pb, Mn, and Zn sorption modeled in the React® calculations explain the observed changes in these constituents at closure. In these calculations, sorption to ferrihydrite was shown to potentially remove all of these metals from solution.

Conclusions

Following closure of the Glengarry adit CO_2 accumulated and alkalinity rose from below detection to almost 5 mg/L in 2012. As a result, pH rose from average of 3.5 to an over 5.5 post closure in the Glengarry adit. Total dissolved concentrations of Fe, Ca, Mg and SO_4 have also risen in the adit while Al, Cu, Pb, and Zn concentrations decreased (fig. 3). This is associated with precipitation of Fe and Al minerals including ferrihydrite ($Fe(OH)_3$), alunite ($KAl_3(SO_4)_2(OH)_6$), gibbsite ($Al(OH)_3$), and boehmite (γ-AlO(OH); fig. 4). The jarosite minerals $KFe^{3+}{}_3(OH)_6(SO_4)_2$ and $NaFe^{3+}{}_3(OH)_6(SO_4)_2$ were supersaturated within the acidic and oxidizing water of the adit pre-closure, but undersaturated in the more alkaline and reduced water post closure (fig. 4) and have likely re-dissolved, thus contributing to the observed increase in Fe and SO_4. Water in the adit post closure has slowly approached equilibrium with gypsum, but remains undersaturated with this mineral. The reason for the apparent decrease in ferrihydrite saturation post closure is unclear, but is probably due to increasingly reducing conditions. The rise in pH resulting from closure has succeeded in shifting the sulfide oxidation away from the strongly acidic reactions described in Eq. 3, to that of Eq. 2, with associated production of alkalinity as described in Eq.1. The closure design has thus successfully reduced sulfide oxidation substantially within the Glengarry adit, and increased the stability of iron oxyhydroxide minerals able to sorb the trace metals Cu, Pb, and Zn, thus improving both surface and groundwater quality.

Future Work

In the summer of 2013 the authors propose to complete additional sampling to improve understanding of redox conditions as well as to characterize the microbial community and mineralogy associated with the post-closure Glengarry adit.

Acknowledgements

The work of Shane Matolyak, Mark Pearson, Scott Colvin (1954–2006) and Mike Cormier (1955–2007) of Tetra Tech, and many others, in collecting the data used in this study is gratefully acknowledged.

References

Kirk, AR, Bogert, H, Marks, MB and Curiel, E (2013) Stemming flow using hydraulic adit plug closure, a comparison: Glengarry Mine, New World District, MT and Worlds Fair Mine, Patagonia, AZ. Proceedings of Reliable Mine Water Technology – 2013 International Mine Water Conference, August 5–9, 2013, Golden CO, this volume ##.

Maxim Technologies, Inc. (2002) Como Basin/Glengarry Adit/Fisher Creek Response Action Engineering Evaluation/Cost Analysis

Liu, H, Guo, H, Li, P, and Wei, Y (2009) Transformation from δ-FeOOH to hematite in the presence of trace Fe(II). Journal of Physics and Chemistry of Solids. 70: 182–191

Rockware, Inc. (2011) The Geochemist Workbench, version 8

Tetra Tech, Inc. (2012) 2011 Surface Water and Groundwater Monitoring Report New World Mining District Response and Restoration Project

USDA (2012) New World Mining District Response & Restoration Project database (http://206.127.65.86/newworld/NWtables.asp)

Passive Barriers for Long-Term Containment of Uranium and Vanadium

Christoph KÜLLS[1], Arnold BITTNER[2]

[1]*Albert Ludwigs University, Faculty for Environment and Natural Resources, Fahnenbergplatz, 79098 Freiburg, Germany, christoph.kuells@hydrology.uni-freiburg.de*
[2]*SLR, Windhoek, Namibia*

Abstract Mine closure plans require long term and stable strategies for containment of mined and associated metals and other pollutants. For several mining projects in the semi-arid Erongo Uranium Province, Namibia, an approach has been developed that combines containment and immobilization strategies based on geochemical processes. The approach is based on understanding and reconstructing *in situ* and geochemical conditions and processes that favored the enrichment and trapping of mined and associated substances. Hydraulic conditions that originally favored entrapment are included. Laboratory experiments on most suitable local material for passive barriers (sand, gypsum, crushed carbonate and iron hydroxides) as an environmental safety barrier were evaluated.

Keywords Mine closure, passive barriers, Uranium, Vanadium

Introduction

Concepts for passive barriers based on natural material for uranium and vanadium retention have been investigated within the framework of mine closure plans for carnotite-based mining operations (Dahlkamp 1993) in the Erongo Province of Namibia. The study area is characterized by semi-arid to arid climate with rainfall ranging from 150 to 100 mm per year and scarce flood events. Groundwater recharge in the study area is about 1–3 % of rainfall or 1–4 mm m^{-2} per year. Therefore groundwater flow is small and concentrates in shallow alluvial aquifers. The basement complex of the Erongo Region that is composed of granite, orthogneiss, amphibolite and schist is characterized by complex groundwater flow system with low fluxes and lithological and structural control. The low fracture volume, however, induces high groundwater levels in basement rock compared to porous aquifers resulting in subsurface discharge into alluvial aquifers that host the carnotite deposits. A mine closure plan and containment concept was developed taking into account these regional conditions of the Erongo Uranium Province.

Methods

The concept is based on several principles: Groundwater movement in alluvial aquifers is orders of magnitudes faster than groundwater movement in adjacent bedrock. Alluvial aquifers are subsurface drainage tubes for draining surrounding basement aquifers. Paleochannels are overlain by calcrete on which active sandy channels are episodically flooded. Hence, there is a system of four flow velocities: groundwater flow in bedrock (10^{-9} to 10^{-7} m/s), groundwater flow in buried paleochannels (10^{-8} to 10^{-7} m/s) and in recent alluvial aquifers (10^{-6} to 10^{-5} m/s) as well as episodic floods in ephemeral channels (10^{0} to 10^{-1} m/s). In the paleochannel and in the active channel transport velocity is further controlled by species-specific adsorption-desorption, precipitation and phase equilibrium reactions at the rock-water interface. For surface flow such controls are not effective. At all means a resurgence of polluted groundwater, subsequent evaporation and deposition of dissolved uranium or vanadium at channel surface of dry riverbeds need to be avoided as this would lead to a rapid transport of uranium and vanadium downstream by surface flow. The fact that uranium and vanadium concentrations in river sediments and channel groundwater downstream are very low (10–25 µg/L) indicates that there has been a natural mechanism of containment in place before mining and that these species have not entered surface flow transport path so far.

Groundwater flow in the basement aquifer is low but cannot be neglected in a long-term mine-closure and containment concept. All evidence from hydrochemical data, ^{14}C dating, tritium measurements, CFC residence time analysis and hydrochemical evolution along transects, as well as water level readings suggests that groundwater flow from the basement towards the alluvial aquifer system can be taken as a general feature of the region.

A first hydraulic principle of containment concepts for Uranium in the Erongo Uranium Province is the convergence of basement flow towards alluvial aquifers. A containment concept in this region therefore needs to assure that groundwater does not re-surface to avoid that evaporative crust or precipitates can be taken away by surface flow. Plumes need to be contained within the previously existing and Uranium-bearing paleochannels aquifers. This pre-condition can be achieved if hydraulic capacity of the reconstructed paleochannel (Fig. 1, L3) is sufficiently large to discharge groundwater recharge of the entire upstream catchment.

The dashed area contains carnotite and is mined. This part of the channel can be refilled with dried tailings material and waste rock. It is proposed to use waste rock as a scour protection on top of tailings material to prevent vertical erosion of the active alluvial channel. An important feature of the hydraulic concept is to maintain the lower part of the paleo-channel (L3) as a subsurface drainage for groundwater discharge from the upstream catchment. Re-filling this section with low-permeable ma-

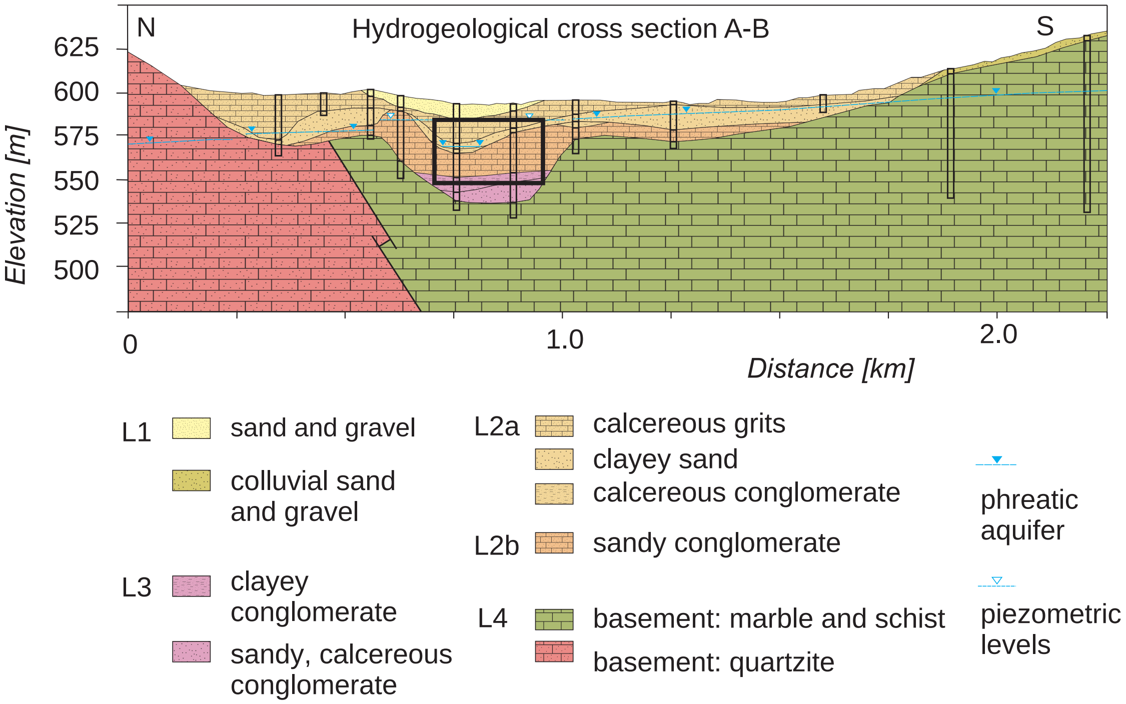

Fig. 1 *Schematic cross-section of a paleo-channel L2, L3 and ephemeral channel L1 containing a sequence of clayey conglomerate (L3) and carnotite bearing calcrete and calcereous grit, the dashed area is mined and refilled with tailings and waste rock (scouring)*

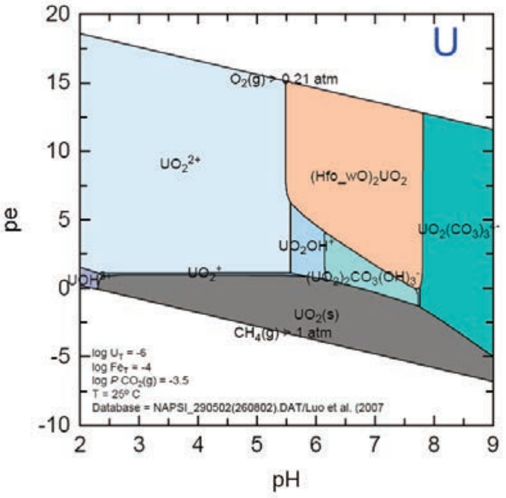

Fig. 2 *Mobility of uranium in a pH-pe diagram including surface complexation processes (Hfo_wO)$_2$UO$_2$. Mobility is constrained by solid UO$_2$ (grey) and by surface complexation on iron-hydroxide coatings or other complexing surfaces (beige/orange). Calculations are based on PhreeqC (Thortenson and Parkhurst 2002) and PhreePlot(Kinniburgh and Cooper 2011)*

terial could lead to a rise of groundwater level and connection with the active ephemeral channel. As tailings material is sufficiently fine it acts as a confining layer. Such a refilling sequence re-establishes the original hydraulic system that is knows to have provided hydrogeological conditions that contained uranium and vanadium before. The efficiency of these processes in trapping uranium and vanadium is such that downstream of shallow carnotite deposits of the Erongo Uranium Province uranium and vanadium concentrations in the alluvial aquifer and shallow groundwater are often below 10–25 µg/L.

A second key principle in long-term mine-closure and containment concept for this type of mine is to re-establish geochemical conditions that immobilize uranium and vanadium for good. Equilibrium thermodynamics of carnotite and of uranium and vanadium species in saline to fresh groundwater of carbonate rock have been analyzed and modeled (Pirlo *et al.* 1984; Pirlo and Giblin 2004). The occurrence of species and solubility of uranium and vanadium depends on pH, redox conditions and the activity of other complexing species in groundwater (Langford 1974). Uranium tends to form mobile species at $pH < 5.5$ and at $pH > 8.5$-9.0 and at positive pe values, mobility decreases in neutral and reducing conditions. Mobility of Vanadium increases with increasing pH and with the increasing activity of negatively charged Vanadium (V) species. In addition to pH and redox conditions, salinity, alkalinity and the presence of complexing agents affects transport and mobility (Mann and Deutscher 1978).

The second key principle of the mine closure and containment concept is to use thermodynamic controls on uranium and vanadium mobility and to try and keep ambient conditions around the re-filled tailings material and waste rock within a range that provides low mobility. All blue species have a certain degree of mobility: While mobility in the acidic ($pH < 5.5$) and basic domain($pH> 8.0$) is given at $pe \approx 0$, there is only a narrow bridge of mobility for pe-conditions near 0: at lower pe precipitation occurs and solid immobile UO$_2$ (s) is the prevailing thermodynamically stable species, at higher pe surface complexation imposes limits on uranium mobility, provided reactant surfaces for surface complexation such as iron hydroxides are available (Fig. 2).

The mobility of uranium and vanadium for typical groundwater chemistry in the Erongo Uranium province ranging from saline groundwater in basement rock to fresh groundwater stemming from flood recharge was investigated and modeled using PhreeqC (Thortenson and Parkhurst 2002) and Phree-

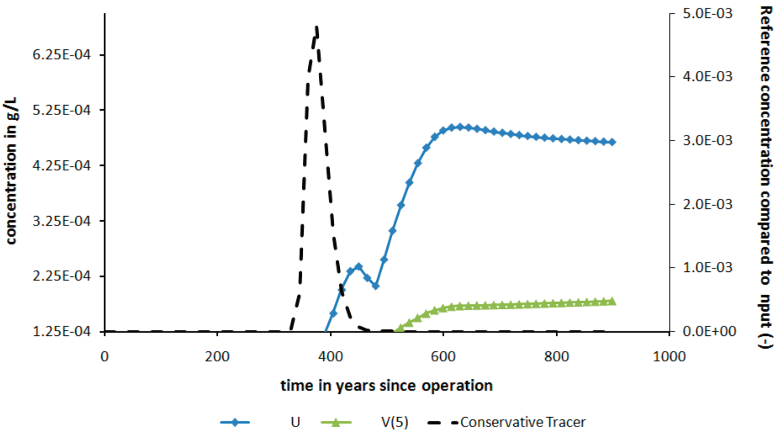

Fig. 3 *Modeled transport of a reference tracer (pulse of chloride at mine closure) and of uranium and vanadium released from tailings material*

Plot (Kinniburgh and Cooper 2011) at several sites. Thermodynamic calculations have been combined and coupled with advection dispersion transport for given and measured hydrochemical composition to account for species-specific transport stable species. Results of such calculations are given in Fig. 3. The transport of a pulse of conservative species (chloride) was always given as reference. However, the conservative tracer also fully accounts for dispersion effects during advective and dispersive transport. Retention and retardation of uranium and vanadium was found to depend on water chemistry (salinity, alkalinity, and pH) of other groundwater components from basement rock and on the composition of tailings (water content, alkalinity). A significant dispersion and retardation of uranium and vanadium was found.

Coupled reactive transport can be modeled for a range of initial conditions for a given groundwater chemistry and for a range of aquifer characteristics (hydraulic conductivity, porosity, geochemical composition of aquifer material). Sorption on exchange sites and surface complexation on iron hydroxide coatings were included. The surface of exchange sites and of surface complexants was determined from samples taken potential sites.

Finally, passive barriers were investigated as a third mechanism for containing uranium and vanadium within the mined area after mine closure. In the regional context of the Erongo Uranium Province, paleochannels and alluvial channels play a key role for retention. Due to the hydrogeological setting found, groundwater flow naturally converges in paleochannels and alluvial channels. Passive barriers in these channels can therefore be used as a third retention mechanism. If uranium and vanadium transport takes place passive barriers can retain these species. For economic reasons only materials available directly within the vicinity of the mine were investigated that can be transported easily and that just need to be separated mechanically on the site. Quartz sand, iron coated sediments (clays, mixed with sand), crushed gypsum and carbonate (not carnotite bearing) were investigated. Their retention capacity was tested using column experiments in the laboratory. To assure conditions similar to those found in the study area, transport calculations were carried out a) using a hydrochemical composition similar to that found in the study area (synthetic water hydrochemistry corresponding to major ion composition, electric conductivity, pH and alkalinity). Complexing agents such as fluoride and phosphate were not considered, they are also not relevant in the study area. Uranium and vanadium concentrations resembling to those found in the study area or expected in tailings materials were used. Experiments were carried out for several months, running several batches with 500 and 50 µg/L of uranium and vanadium.

Results

Results indicated that also natural materials such as quartz sand and iron hydroxide coated clays have a significant retention potential. Gypsum was found to have a specific retention capacity for vanadium but not for uranium. Carbonate was found to have the lowest retention capacity. The sorption capacity of quartz sand was found to be higher than that of iron hydroxide. As the desorption coefficient of iron hydroxide was by far the lowest the best material to be used in passive barriers is iron hydroxide coated clay mixed with quartz sand. Carbonate and gypsum, however play an indirect role in controlling transport by affecting pH and alkalinity as well as overall salinity of groundwater.

Conclusions

A mine closure and retention concept for the Erongo Uranium Province was investigated. The focus was on shallow carnotite-type associated uranium deposits associated with calcrete crusts and found in and on top of paleochannels, partially covered with ephemeral channels. A concept based on three mechanisms is proposed: Reconstruction of the hydraulic system, investigation of geochemical retention processes and modeling and finally a passive barrier system using natural materials as a backup. Functioning of passive barrier systems was investigated in the laboratory and found to be a safety option for uranium and vanadium retention.

References

Dahlkamp FJ (1993). Uranium ore deposits. Springer Verlag.

Giblin AM, Batts BD, Swaine DJ (1981). Laboratory simulation studies of uranium mobility in natural waters. Geochimica et Cosmochimica Acta, 45(5), 699–709.

Kinniburgh D, Cooper D (2011) PhreePlot. Center for Ecology & Hydrology, UK., 584 p.

Langford FF (1974). A supergene origin for vein-type uranium ores in the light of the Western Australian calcrete-carnotite deposits. Economic Geology, 69(4), 516–526.

Mann AW, Deutscher RL (1978). Genesis principles for the precipitation of carnotite in calcrete drainages in Western Australia. Economic Geology, 73(8), 1724–1737.

Pirlo MC, Giblin AM (2004). Application of groundwater–mineral equilibrium calculations to geochemical exploration for sediment-hosted uranium: observations from the Frome Embayment, South Australia. Geochemistry: Exploration, environment, analysis, 4(2), 113–127.

Thortenson, Parkhurst (2002) Calculation of individual isotope equilibrium constants for implementation in geochemical models. Water-Resources Investigations Report 2002–4172

Substrate and biogeochemical design considerations for sulfate reducing bioreactors

Lee LANDKAMER[1], Ilsu LEE[2], Dina DRENNAN[1], Jonathan O. SHARP[1], Linda A. FIGUEROA[1]

[1]*Colorado School of Mines, 1500 Illinois St. Golden, CO. 80401; e-mail: llandkam@mines.edu*
[2]*Freeport-McMoRan Copper and Gold, 1600 E. Hanley Blvd, Oro Valley, AZ. 85737*

Abstract This paper examines the effect of organic substrate on zinc removal, microbial community structure and geochemistry of sulfate reducing bioreactors. Eight columns supplemented with limestone have been receiving mining influenced water for 6 months. Columns containing Ponderosa Pine chips performed poorly (<50 % zinc removal) while columns containing alfalfa, walnut shells or Ponderosa Pine sawdust removed over 99 % of influent zinc. Phylogenetic characterization of microbial DNA showed significant differences in diversity with substrate. Geochemical modeling indicated that limestone dissolution should lead to $ZnCO_{3(s)}$ precipitation. Zinc removal in the eight columns appears to be a complex process of biotic and abiotic reactions.

Keywords sulfate reducing bioreactor mine water treatment

Introduction

Sulfate reducing bioreactors (SRBRs) are an inexpensive and simple, yet elegant way to remove metals from mining influenced water (MIW) via metal sulfide precipitation. An organic substrate mixture such as wood and hay is used as a carbon and energy source by a complex microbial community responsible for the reduction of sulfate to sulfide. This sulfide then complexes with metal ions forming insoluble precipitates. However, the apparent simplicity of SRBRs belies the complexity of the biogeochemistry that is responsible for metal removal. Design of SRBRs must incorporate organic and inorganic substrate selection and, geochemical considerations, along with physical design parameters. While pine chips are a common and inexpensive component of SRBR’s, terpenes found in pine resin can inhibit microbial activity. Ponderosa Pine in particular has been associated with inhibitory concentrations of terpenes (Himejima *et al.* 1992). Field experience has shown that SRBRs often fail to efficiently remove metals or experience premature failure, indicating that improved design guidelines are needed.

The goal of this paper is to present our preliminary evaluation of substrate and biogeochemical considerations relative to the performance of 8 large-scale columns operated under field conditions by Freeport-McMoRan (FCX). Results to date support multiple concurrent mechanisms of zinc removal and varied extent of zinc removal.

Methods

MIW

The columns were fed mining influenced water (MIW) collected from a FCX mine site and stored in a large tank. The MIW had a pH ≈ 6.5 with the following major constituents: sulfate, 5200 mg/L; chloride, 30 mg/L; calcium, 520 mg/L; magnesium, 720 mg/L; sodium, 180 mg/L and zinc, 160 mg/L. The alkalinity of the MIW was essentially zero.

Column Construction and Operation

The columns were constructed from 6″ (0.15 m) I.D. plastic pipe with an active substrate containing length of 40″ (1 m). Five liquid phase and three solid phase sampling ports were installed along the length of the col-

Column	Woodchip %	Sawdust %	Alfalfa %	Walnut Shells %	Limestone %	Total Mass (kg)	Pore Volume (L)
C1	50	10	10	-	30	3.9	14.3
C2	-	35	35	-	30	3.7	14.2
C3	35	-	35	-	30	3.6	13.9
C4	35	35	-	-	30	5.2	13.7
C5	-	-	70	-	30	3.5	12[a]
C6	-	70	-	-	30	6.2	13.1
C7	70	-	-	-	30	3.9	15.1
C8	-	-	-	70	30	14.4	12.7

[a] Approximate. Column began to leak while filling.

***Table 1**. Column content by mass fraction and approximate pore volume of each column.*

umn. The columns were packed with various combinations of Ponderosa Pine woodchips, Ponderosa Pine sawdust, alfalfa hay or crushed walnut shells (Table 1). All of the columns contained 30 % limestone by mass with a particle size between 4.8 and 6.3 mm. The columns were then filled with MIW and the inoculum mixture described below. The initial MIW and inoculum mixture was then recirculated through the columns for circa 2 months. The columns were then switched to down-flow mode with a flow rate of 0.4 L/d (hydraulic residence time between 30 to 38 days). The flow rate for columns C2, C5, C6 and C8 was increased to 0.8 L/d 92 days after flow was initiated.

Organic Substrate

The Ponderosa Pine woodchips and sawdust were both sourced from a lumber mill in Santa Clara, NM. The woodchips were collected about 5 years ago. For the last 4 years, the woodchips were stored outside in a plastic 55-gallon (208 L) drum. The sawdust was procured in early 2012 where it had been sitting for a few months at the sawmill in an area that was outside and partially exposed. Trees for both materials were sourced from the same geographical region with no major changes in material or location in the last 10 years as part of a thinning operation that only cuts younger trees. The alfalfa was grown near Safford, AZ. The origin of the crushed walnut shells is unknown, other than being grown in the United States of America. No attempt was made to sterilize the organic substrates.

Inoculum

A sulfate reducing enrichment culture grown on sulfate and ethanol obtained from the University of Arizona was used to inoculate five separate microcosms, each containing one of the organic substrates used in the columns. Because the organic materials were not sterilized, they likely contained additional microorganisms beyond the inoculum. These microcosms were then incubated under sulfate reducing conditions. A mixture of the liquid phase from these five microcosms was then used to inoculate the columns.

Sampling

Liquid samples for DNA extraction were collected from the middle liquid sampling ports 41 days after pumping was initiated. These samples were collected under a flow of nitrogen to maintain anaerobic conditions. Liquid effluent samples were collected periodically for metals analysis.

Analytical

Metals were analyzed by inductively coupled plasma emission atomic spectroscopy (ICP-AES) using a Perkin Elmer Optima Model 3000. Alkalinity was measured in the field by titration. Sulfide was measured using a HACH test kit (part number 223801). Oxidation-reduction potential (ORP) and pH were measured on-site using potentiometric probes.

DNA Processing

DNA was extracted from aqueous phase samples collected from the middle sampling port of each column. Ten mL of effluent was filtered with 0.2 micron polycarbonate filters and bead beaten for 1.5 minutes, DNA was extracted using a phenol chloroform protocol, reducing the contaminants such as humics and other PCR inhibitors. The DNA was then processed by high-throughput pyrosequencing by a commercial laboratory (Engencore) and analyzed using the quantitative inferences into microbial ecology pipeline (QIIME) and the Greengenes database.

Results

Metal Removal and Effluent Chemistry

The major contaminant of concern in the selected MIW is zinc. Fig. 1 displays the effluent zinc concentration in each column as a function of elapsed time after pumping was initiated. No data was presented until after one pore volume of water had been pumped through the columns. The zinc concentration in columns containing pine chips increased to above 100 mg/L by day 118. The rest of the columns achieved zinc effluent concentrations of less than 1 mg/L by day 118. Fig. 2 presents alkalinity data for the same time period. The decreasing trend in alkalinity for columns C2, C5, C6 and C8 after day 90 corresponds with the increased pump-rate that occurred at that time. Other factors may also be affecting alkalinity.

Microbiology

Based on the liquid phase DNA samples collected on day 40 of column operation, species diversity as measured by the number of species per number of sequences per sample, was greatest in C6 (sawdust only) and lowest in C7 (woodchips only). The species diversity in C6 was 4 – 5 times greater in C6 relative to C7. No clear trend has been identified between the microbial species present and zinc removal efficiency. No microbial density measurements have been performed.

Geochemical Modeling of Metal Removal Mechanisms

Geochemical modeling (Visual MINTEQ, Gustafsson 2011) indicates that the influent MIW is slightly over-saturated with respect to gypsum ($CaSO_4(s)$) at 25 °C. Modeling predicts that at equilibrium, 58 mg/L calcium and 138 mg/L sulfate should precipitate to form 196 mg/L gypsum. In fact, several MIW samples that were not diluted or acidified before transport to CSM contained precipitate. This

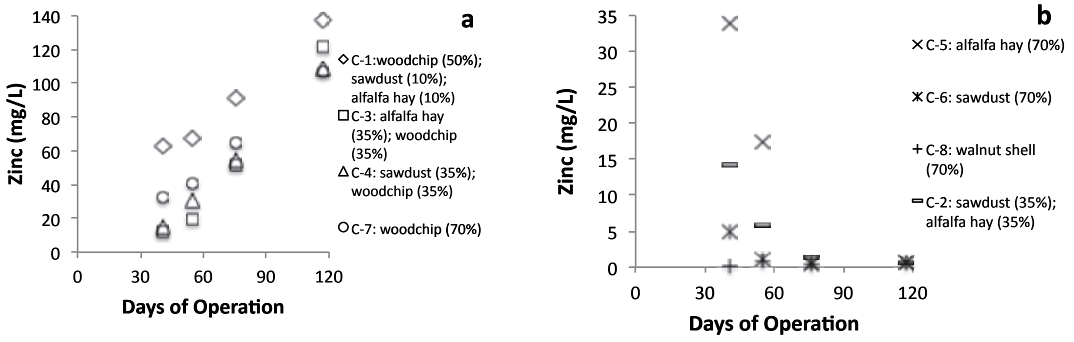

Fig. 1 *Zinc concentration in column effluent as a function of time elapsed after pumping commenced. a) displays data from columns that contained pinewood chips. b) has only the columns that contained no pine woodchips.*

Column Number and Contents	Zn (mg/L)	pH	DO[1] (mg/L)	ORP[2] (mV)	Alkalinity[3] (mg/L)	Ca^{2+} (mg/L)	S^{2-} (mg/L)
C-1: woodchip (50%); sawdust (10%); alfalfa (10%)	137	6.6	2.3	87	150	670	0
C-2: sawdust (35%); alfalfa hay (35%)	0.7	6.8	0.3	-258	470	740	55
C-3: alfalfa hay (35%); woodchip (35%)	122	6.5	1.7	84	330	770	0
C-4: sawdust (35%); woodchip (35%)	109	6.5	1.8	82	160	670	0
C-5: alfalfa hay (70%)	0.6	6.5	0.6	-181	520	840	59
C-6: sawdust (70%)	0.6	6.9	1.8	30	200	740	1
C-7: woodchip (70%)	107	6.7	2.5	79	120	600	0
C-8: walnut shell (70%)	0.5	6.8	0.5	-181	480	740	33

[1]Dissolved Oxygen, [2]Oxidation-reduction potential, [3]Measured as mg/L $CaCO_3$

***Table 2**. Column effluent chemistry on day 118 of column operation.*

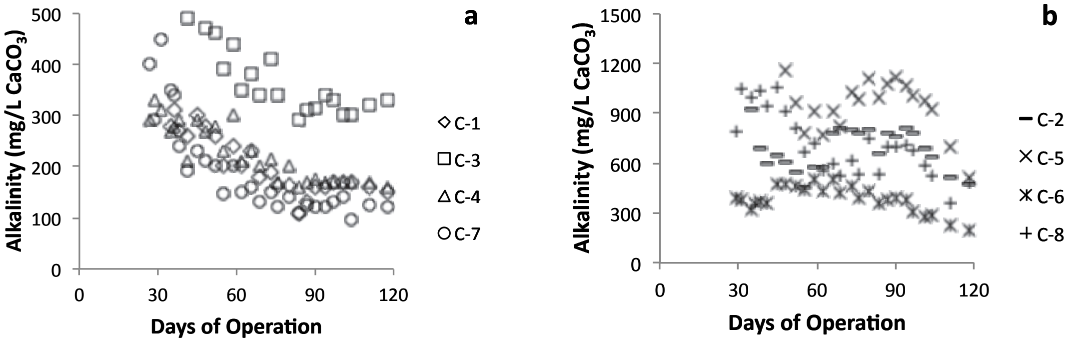

***Fig. 2** Alkalinity in column effluent as a function of time elapsed after pumping commenced. Fig. 2a displays data from columns that contained pinewood chips. Fig. 2b has only the columns that contained no pine woodchips.*

also occurred in some column effluent samples that were not diluted upon collection.

Analysis of ICP data from the supernatant of a sample containing precipitate before and after the precipitate was dissolved by acid showed both calcium and sulfur mass decreasing by 33 % when precipitation occurred. Interestingly, the concentrations of zinc, magnesium and sodium also decreased (circa 30 % by mass), indicating that these ions had co-precipitated with the gypsum. It is likely that these elements were co-precipitated because geochemical modeling indicated that none of these three ions (Na, Zn and Mg) were over-saturated.

As the MIW contacts limestone in the columns, the limestone will dissolve releasing calcium and carbonate. Substantial limestone dissolution is occurring in all of the columns except C7 as indicated by increased calcium concentration in the effluent. Additionally, the process of sulfate reduction produces carbonate. The increased calcium causes the system to be even more over saturated with respect to gypsum, increasing the likelihood of gypsum precipitation in the column and presumably co-precipitation of other cations. Gypsum has been observed in water samples taken from the column side-ports. In addition, the increased CO_3^{-2} concentration may lead to the over-saturation as well as precipitation of zinc carbonate ($ZnCO_{3(S)}$). The solubility of zinc carbonate is strongly dependent on total carbonate concentration and pH (higher pH leads to lower solubility because more of the total carbonate is in the form CO_3^{2-}).

To model $ZnCO_{3(s)}$ precipitation, the amount of carbonate produced in the columns must be estimated. The following two methods were used. Alkalinity titrations were used assuming that all of the alkalinity in the water samples is due to carbonate and that the titration captures all of the carbonate. There are two major sources of error in this assumption: 1) other sources of alkalinity are likely present, notably, organic acids, leading to over-estimation and 2) the starting pH of the titrations is near the first pK_a of carbonic acid so not all of the carbonate will be captured in the titration, leading to under estimation of total carbonate. Another estimate of carbonate was made by looking at the amount of calcium produced in the column, using the assumption that all of the calcium is coming from the dissolution of limestone (1 mole CO_3^{-2} for each mole Ca). This method could lead to under-estimation due to: 1) any carbonate produced via microbial metabolism will be missed because no calcium is produced and 2) precipitation of gypsum in the column will cause under-estimation of calcium produced.

The modeling predictions in Table 3 were made assuming the total carbonate produced in the columns ranged from 120 to 800 mg/L (as $CaCO_3$) as indicated by the two methods described in the above paragraph. Zinc and sulfate concentrations of 160 mg/L and 5200 mg/L, respectively, were used. The sulfate affects the precipitation of zinc carbonate by forming soluble zinc-sulfate complexes that act to increase zinc solubility. The effluent pH of the columns ranged from 6.5 to 6.9 on day 118, which would result in between 21 to 97 % of the zinc being removed by zinc-carbonate precipitation (assuming equilibrium), depending on the carbonate concentration.

pH	Carbonate (mg/L $CaCO_3$)	Zinc Precipitated (%)
6.0	120	0
6.0	800	56
6.5	120	21
6.5	800	91
7.0	120	55
7.0	800	98

Table 3. *Zinc precipitation ($ZnCO_{3(s)}$) predicted by Visual MINTEQ with 160 mg/L zinc and 5200 mg/L sulfate.*

The production of organic acids in the column could increase zinc solubility by forming soluble zinc organic-acid complexes. However, Visual MINTEQ predicts this effect to be small. If 200 mg/L of both acetic acid and propionic acid were present, this would decrease the precipitation of zinc at pH 6 when 716 mg/L carbonate is present by approximately 1 %.

If sulfide is present, geochemical modeling predicts that essentially all of the sulfide produced will form zinc-sulfide precipitate (spharelite, $ZnS_{(s)}$) until all of the zinc is consumed. Because zinc sulfide is over 10 orders of magnitude less soluble than zinc carbonate, as long as excess dissolved sulfide is present, any zinc carbonate present should be converted to zinc sulfide.

Discussion

The Ponderosa Pine woodchips used in these columns appeared to affect initial microbial diversity as indicated by the microbial DNA data. Zinc removal after 4 months of operation is also low in the columns containing woodchips, although it is not entirely clear if this is due to reduced sulfide production (less zinc sulfide precipitation) or because the pH and alkalinity are lower in these columns, which would result in less zinc carbonate precipitation. The temporally increasing zinc concentration in columns C1, C3, C4 and C7 corresponds with the decreasing alkalinity in these columns. These trends and the modeling results in Table 3 suggest that zinc carbonate precipitation may be the primary zinc removal mechanism in the woodchip containing columns; the decreasing alkalinity may explain the increasing zinc concentration. However, zinc sulfide production in these columns cannot be discounted with the available data. The decreasing alkalinity may be due either to less limestone dissolution as well as decreasing sulfate reduction. It is difficult to estimate limestone dissolution from the calcium concentration because of gypsum precipitation in the columns. It is possible that both zinc removal mechanisms are occurring simultaneously.

The higher alkalinity in the columns without woodchips suggests that microbial activity is higher in these columns relative to the woodchip containing columns. This is also supported by the detection of sulfide in the non-woodchip containing columns; as mentioned previously, sulfate reduction results in the production of alkalinity. The enhanced zinc removal in columns C2, C5, C6 and C8 would most likely be due to zinc sulfide precipitation due to the lower solubility of zinc sulfide relative to zinc carbonate. The higher alkalinity in these columns would, however, make zinc carbonate formation more likely in the case that sulfide is completely consumed.

Interestingly, the Ponderosa Pine sawdust does not seem to have the same inhibitory effect as pine-chips. It is possible that the inhibitory compounds have leached out of the sawdust due to increase mass transfer rates resulting from the much greater specific surface area of the sawdust. Sealed methanogenic batch incubations performed by CSM with these two materials both exhibited relatively low biodegradability (data not shown), suggesting that the sawdust is also inhibitory in a sealed system where potentially inhibitory compounds cannot be flushed away.

Geochemical equilibrium modeling suggests potential zinc removal mechanisms but the predictions must be interpreted judiciously. One reason is that the modeling assumes equilibrium when predicting the formation of precipitates. However, the kinetics of precipitation can be slow and real systems are often not in equilibrium. Another reason is that, prediction of the quantity of precipitates relies on knowing the total amounts of the constituent reactants present. If precipitation is occurring in the columns, the measured aqueous concentrations of the relevant elements may not reflect the total concentrations in the system. Regardless, geochemical modeling provides valuable insight as demonstrated by the potential for zinc carbonate precipitation in the columns.

A more complete story on the substrate and biogeochemical considerations for sulfate reducing bioreactor design is forthcoming. Future plans include additional collection of liquid phase and solid phase samples from the still operating columns. This will allow comparison between liquid phase and biofilm microbial community structure. The identity of mineral precipitates on the solid phase substrate will be examined by scanning electron microscopy – energy dispersive x-ray spectroscopy (SEM-EDS) and presumed metal forms based on sequential extractions (*e.g.* Tessier *et al.* 1979). The relative amount of solid phase organic matter degradation will also be evaluated. The relationship of the microbial community with geochemistry and organic matter changes are expected to allow us to improve our design procedure for SRBRs treatment mining influenced water.

References

Himejima Masaki, Kenneth R Hobson, Toshikazu Otsuka, David L Wood, Isao Kubo (1992) Antimicrobial Terpenes from Oleoresin of Ponderosa Pine Tree Pinus Ponderosa : A defense mechanism against microbial invasion. Journal of Chemical Ecology 18 (10): 1809–1818.

Gustafsson, J. P. (2011). Visual MINTEQ. Chemical equilibrium modeling software for the calculation of metal speciation, solubility equilibria, sorption etc. http://www2.lwr.kth.se/English/OurSoftware/vminteq/

Tessier A., Campbell P.G.C., Bisson M. (1979) Sequential extraction procedure for the speciation of particulate trace metals. Analytical Chemistry 51, 844–851

Importance of catchment vegetation and design to long-term rehabilitation of acidic pit lakes

Mark A. Lund[1], Eddie J.B. van Etten[1], Clint D. McCullough[1,2]

[1]*Mine Water and Environment Research Centre (MiWER), School of Natural Sciences, Edith Cowan University, 270 Joondalup Drive, WA 6027, Australia; m.lund@ecu.edu.au*
[2]*Golder Associates, West Perth, Western Australia 6005, Australia*

Abstract Lakes are an extension of their catchment and neither should be considered in isolation. However, pit lakes have typically small catchments that have rarely been designed for their ecological significance to the lake. This paper discusses a preliminary assessment of the vegetation of catchments around selected pit lakes of the Collie Lake District. We examine how effectively modern and historical catchment revegetation techniques contribute organic matter to the pit lakes. Overall, there appear to be a number of areas where modified rehabilitation and revegetation in pit lake catchment design at closure could lead to enhanced ecological values in the lakes.

Keywords Water quality, catchment, ecology, pit lake, end-uses, mine closure.

Introduction

A lake is a product of its catchment. Natural lakes connected to drainage lines often have large catchments relative to the lake surface area. Catchments provide lakes with sources of water (surface and subsurface), nutrients and allochthonous (external to the lake) carbon. Natural catchments also show a gradient of vegetation into the lake, moving from terrestrial communities, through riparian to fringing vegetation assemblages (Van Etten *et al.* 2012). In many regions, shallow areas connected (fully or partially) to the lake (wetlands) provide a range of ecosystem services including nutrient retention as well as transformation, and sources of biological diversity and propagules (see Mitsch and Gosselink 2007). In contrast, pit lakes which are formed upon cessation of mining, when open-cut voids that extend below the water table fill with groundwater and surface runoff, are rarely rehabilitated to incorporate all these natural features (Van Etten *et al.* 2011).

For many mine pit lakes, the catchment area to lake area ratio is relatively low at <4:1. Surface inflows may bring high quality rainwater into the lake which can help maintain water quality against evapo-transpiration and solute inputs. However surface runoff, from the catchment is often deliberately minimised to reduce the potential inflow of acid and metalliferous drainage (AMD) from the mine waste in the catchment (Müller *et al.* 2011). Oxidation of sulphidic minerals in exposed mining waste in the presence of water and bacteria can lead to AMD when there is limited neutralisation capacity in the pit lake catchment.

Prior to relinquishment, catchments are often shaped to geotechnically stable slopes and revegetated to or below the waterline. However, many pit lakes fail to attain riparian (water influenced terrestrial vegetation) or fringing (located in the lake water) vegetation, even many years following closure (Lund and McCullough 2012). This is mainly due to a lack of planting of riparian species, unstable pit lake margins, low nutrient concentrations in the soils and rapidly changing pit lake water levels during filling (van Etten 2012). The contribution of organic carbon (C) by riparian and catchment vegetation was recognised many years ago as a primary causative factor in water quality improvements in AMD pit lakes (King *et al.* 1974). Riparian vegetation will also contribute physically to bank stabilisation, facilitating further littoral and bank vegetation establishment.

In this study, we aimed to quantify the organic matter generated by pit lake catchments and investigated the transfer of this material into the pit lakes in the Collie Lake District (Western Australia).

Methods

Study Site

The town of Collie (population over 10,000) is located on the north western rim of the Collie Coal Basin within the Collie River catchment. Collie lies nearly 160 km south-southeast of Perth and is the centre of coal mining in Western Australia (Fig. 1). The major land uses in the catchment are coal mining, timber production, power generation and agriculture. Approximately 79 % of the catchment is production forest. The Collie Coal Basin covers an area of approximately 225 km^2. It is 27 km long by 13 km wide and elongated in a north-west to south-east direction. The basin consists of two lobe-shaped sub-basins, the Cardiff sub-basin (151 km^2) to the west and the Premier sub-basin (74 km^2) to the east, in part separated by a faulted basement high, known as the Stockton Ridge (Moncrieff 1993). Collie coal is a sub-bituminous coal with a relatively low sulfur content (0.3 – 0.9 %), and low caking and low ash (4–9 %) properties (Le Blanc Smith 1993). Low amounts of acidity are generated through pyrite oxidation, ferrolysis and secondary mineralization. This acidity is still sufficient to generate low pH in the pit lakes due to the low buffering capacity of the surrounding rock.

Collie is situated in an area of Mediterranean climate, with hot, dry summers (range 12–29 °C) and cool, wet winters (range 4–15 °C; Commonwealth of Australia Bureau of Meteorology, 25/02/2009). 75 % of the rainfall occurs during the five months from May to September. The 100 year mean annual rainfall for the Collie Basin is 939 mm (Commonwealth of Australia Bureau of Meteorology, 25/02/2009), although this has decreased to an average of 690–840 mm over the past 20 years (Craven 2003).

Several pit lakes of various sizes have created a Lakes District within the Collie Coal Basin. Four pit lakes (Stockton, WON9, Lake Kepwari and Black Diamond) and a sumpland formed around an overburden pile adjacent to

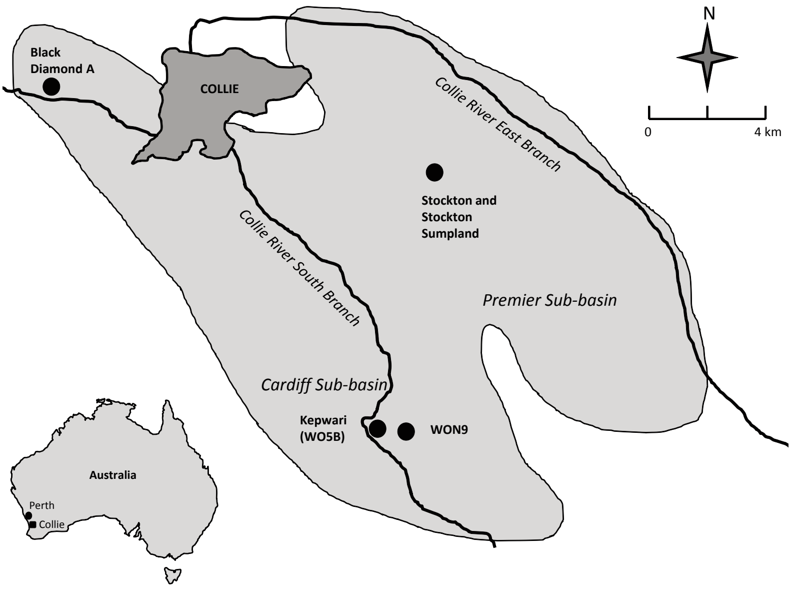

Fig. 1 *Map showing location of the Collie Coal Basin and pit lakes sampled.*

Stockton Lake were sampled. More details of the pit lakes can be found in Lund and McCullough (2012).

Sampling Methods

Five sites including four pit lakes and a nearby sumpland were sampled in June 2013. At each site, a 5 m wide belt transect was run perpendicular to the shore to the top of the catchment through each vegetation community. The transect extended into the lake, with samples taken at 5 m in from the shore. Between two to five transects were taken at each site, with at least one transect placed in each vegetation cover type. Every tree in the belt transect was identified and its diameter at breast height measured. At least at 5 m intervals, in the middle of the transect, % litter cover and depth were assessed. Within 2 m of the lake shore and in the middle of the transect a 0.25 × 0.25 m quadrat was used to collect all surface leaf litter, and soils 0–50 mm deep. Google Earth and ground-truthing were used to determine catchment areas and areal extent of vegetation communities. Litter and soils were air dried, then dried at 80 °C to constant weight. Loss on ignition (LOI) was used as an assessment of organic matter, following burning at 550 °C to constant weight.

Results and Discussion

Stockton Sumpland and WON9 had catchment to lake area ratios that were just above 4, while Black Diamond A was approximately 3 and Stockton and Kepwari <2 (Table 1). All the lakes had no major surface inflows other than runoff, although Kepwari was rapidly filled by the Collie River (Salmon *et al.* 2008). Stockton has received dewatering water from the nearby Ewington mine via a small stream in the past, although this is not currently occurring and so has been excluded from the estimate of the catchment area. The catchments of WON9 and Kepwari were revegetated using a typical upland jarrah (*Eucalyptus marginata*) forest seed mix (jarrah forest is the dominant forest ecosystem in the area). WON9 had no riparian or fringing vegetation, the older (50+ years) lakes of Stockton and Black Diamond all had small patches of fringing vegetation (<20 % of perimeter) but no true riparian, Stockton Sumpland (50+ years) was almost completely surrounded by fringing vegetation but no riparian. Lake Kepwari is starting to show development of patches of both riparian and fringing vegetation believed to be due to entry of propagules during a river breach (see McCullough *et al.* 2012).

The two Lake Stockton catchments are covered in relatively few jarrah trees (self-established, after ≈ 50 years without formal rehabilitation), but these trees are large and overall these catchments resemble old growth jarrah forest in terms of stocking rates (Table 2).

The Lake Kepwari catchment is almost entirely covered in ≈ 10-15 y.o. rehabilitation and in terms of tree density resembles 50–80 y.o. regrowth jarrah forest (McCaw 2011), although

Lake	Lake Area	Catchment Area	Lake: Catchment Area Ratio	Revegetation	Jarrah Forest	Plantation	Sparse
Stockton	15	23	1.5				7.3
Stockton Sumpland	1.9	75	4.0				5.6
WON9	7.8	31-	4.0	23			
Black Diamond A	4.9	15	3.0		4.5	1.7	3.9
Kepwari	99	150	1.5	50			

Table 1 *Area (ha) of the pit lakes, catchments and major vegetation communities*

Lake	Tree Density		Tree Basal Area		Surface Litter	
	trees ha-1	trees catchment-1	m^2 ha-1	m^2 per catchment	t ha-1	t catchment-1
Stockton	330	2400	27.0	197	7.6	55
Stockton Sumpland	310	1800	14.8	84	1.9	11
WON9	166	3900	0.4	9	0.9	21
Black Diamond A	660	6700	12.7	128	12.8	129
Kepwari	702	35000	8.3	417	9.5	480
Old Growth & Long Unburnt Jarrah Forest#	200-500		30-50		15-25	
Regrowth & Prescribed Burned Jarrah Forest#	500-1000		20-30		5-10	

data based on (Abbott and Loneragan 1986; Stoneman et al. 1997; McCaw 2011)

Table 2 *Tree density, basal area and surface little coverage for the pit lake catchments compared to natural and revegetated jarrah forest.*

stocking in terms of basal area per hectare is lower than regrowth at this early stage. The WON9 catchment is also post-mine rehabilitation but is only a few years old and trees are all less than 100 mm in diameter. The low density of these small trees suggests mature tree density will be very low in this catchment (*e.g.* compared to Kepwari catchment). The Black Diamond A catchment is covered in a variety of distinct vegetation types (regrowth jarrah forest, dense plantations and sparse/disturbed jarrah forest). On average, it is similar to jarrah regrowth in terms of tree density, but has substantially lower basal area per hectare than jarrah forest.

When scaled up to whole catchments, there are thousands of trees in the pit lake catchments, with around thirty five thousand trees in the largest Kepwari catchment (Table 2). This is however several orders of magnitude lower than might be expected in natural jarrah forest catchments. The size of jarrah forest catchments varies widely depending on stream and catchment position, in the range of 1000 to several 100,000 ha (Borg *et al.* 1987), but are typically much larger than the Collie pit lake catchments.

Surface leaf litter quantities per hectare in mine pit catchments are generally similar to that found in regularly burned jarrah forest, with the exception of WON9 (yet to see much litter build up) and the Stockton sumpland catchment (which has a lot of bare ground). They are lower than long unburnt jarrah forest however (Table 2). Litter per hectare is typically less near lake edge compared to interior of vegetation. For instance, 18 t ha^{-1} of surface litter is found inside Kepwari rehabilitation, on average, whereas in rehabilitation closest to the edge of lake it only averages 1.1 t ha^{-1}. This suggests that litter either doesn't make its way down to the lake edge (via surface water flows as well as gravity), doesn't accumulate here because of low tree density, or is readily lost from this zone.

The relatively young age of the pit lakes is reflected in the low carbon contents (Loss on Ignition) of the sediments near the shore (Table 3). The only exception was Stockton which had levels starting to approach those of natural sediments in the local area (>30 %).

Lake	Soil	Water
Black Diamond A	3.4±1.0	4.1±1.6
Lake Kepwari	1.8±0.6	2.2±0.2
WON9	5.4±1.8	5.4±1.6
Stockton	3.9 (*n*=2)	24.1±10.9
Stockton Sumpland	-	4.3 (*n*=2)

Table 3 *Loss on Ignition in soil and sediment collected within 5 m of the shoreline at 0–50 mm depth for soil and 0–10 mm depth for sediment at the pit lakes.*

This however may not truly reflect organic matter inputs as loss on ignition also includes coal particles which occur in some samples. Equally poor organic matter concentrations were found in the catchments, despite some being of reasonable age and both WON9 and Lake Kepwari being rehabilitated with stored topsoil.

Conclusions

Rehabilitation of pit lake catchments achieves values of trees, biomass and litter that approximate those of natural forest within 10–15 years compared to 50 years at unrehabiliatated sites. Pit lake catchments are very small compared to comparable natural systems, typically at least 10 times smaller. Therefore despite the relatively high production of leaf litter and other plant debris, the total quantity available will be similarly smaller. Observations at the pit lakes studied, noted that horizontal ripping created potential barriers to litter transport to the lakes. This was overcome partially by the steep slope of pit lake catchments and that surface runoff utilises the contour rips as drainage lines. As no defined flow paths have been engineered into the pit lake catchment, surface flow collects along the rip lines it eventually overtops and creates an erosional gully into the lake. This gully cuts through all the carefully layered overburden and potentially exposes acid generating materials. We recommend that hydrological studies be made and that drainage lines be engineered into the catchment prior to revegetation; ideally with detailed erosion considerations such as bio erosion modelling with SIBERIA or similar model (Willgoose 2005). There is little evidence that the leaf litter produced in the catchment enters the lake, although this could be simply be due to the low quantities produced. Riparian species need to be included in seed mixes around the lakes edge to stimulate the growth of this important aquatic community, which after 50 years is still absent around the pit lakes studied (McCullough and Van Etten 2011; Van Etten *et al.* 2012). Connection to natural waterways, where this can be achieved safely, has the advantage of introducing a range of propagules that stimulate the development of riparian and fringing communities. This study highlights that current practices of minimising catchment areas around pit lakes may work against their long term natural remediation.

Acknowledgements

This study was jointly funded by Australian Coal Association Research Program (Project C21038) and Premier Coal Yancoal Ltd. The authors are grateful to Dr Digby Short at Premier Coal and the Department of Environment and Conservation for access to the lakes. Thanks to Mark Bannister (ECU) for chemical analysis.

References

Abbott I, Loneragan OW (1986) Ecology of Jarrah (*Eucalyptus marginata*) in the northern Jarrah forest of Western Australia. Dept. of Conservation and Land Management., Perth.

Borg H, Stoneman GL, Ward CG (1987) Stream and Ground Water Response to Logging and Subsequent Regeneration in the Southern Forest of Western Australia: Results from Four Catchments. Dept of Conservation and Land Management, Perth.

Craven E (2003) Acid Production in the Overburden of Lake WO5B, Collie. Environmental Engineering Project 640.406, Thesis, University of Western Australia, Australia, Perth.

King DL, Simmler JJ, Decker CS and Ogg CW (1974) Acid strip mine lake recovery. Journal of the Water Pollution Control Federation 46: 2301–2315

Le Blanc Smith G (1993) The geology and Permian coal resources of the Collie Basin, Western Australia. Western Australian Geological Survey Report 38. 86 p

Lund MA, McCullough CD (2012) Meeting environmental goals for pit lake restoration – factoring in the biology. In: Mine Pit Lakes: Closure and Management, McCullough CD (ed) Australian Centre for Geomechanics, Perth, 83–90 pp

Lund MA, McCullough CD, Kumar RN (2012) The Collie Pit Lake District, Western Australia: An Overview. In: McCullough CDL, M.A.; Wyse, L. (Ed.) International Mine Water Association Symposium. Bunbury, Australia, IMWA, p 287 – 294

McCaw WL (2011) Characteristics of jarrah (*Eucalyptus marginata*) forest at FORESTCHECK monitoring sites in south-west Western Australia: stand structure, litter, woody debris, soil and foliar nutrients. Australian Forestry 74: 254–265

McCullough CD, Kumar RN, Lund MA, Newport M, Ballot E and Short D (2012) Riverine breach and subsequent decant of an acidic pit lake: evaluating the effects of riverine flow-through on lake stratification and chemistry. In: International Mine Water Conference. Bunbury, Western Australia, IMWA, p 533–540

McCullough CD, Van Etten EJB (2011) Ecological restoration of novel lake districts: new approaches for new landscapes. Mine Water and the Environment 30: 312–319

Mitsch WJ, Gosselink JG (2007) Wetlands. 4th edn, John Wiley & Sons Inc, Hoboken, NJ.

Moncrieff JS (1993) Hydrogeology of the Collie Basin, Western Australia: Western Australia Geological Survey. 129–153 p

Müller M, Eulitz K, McCullough CD and Lund MA (2011) Model-based investigations of acidity sinks and sources of a pit lake in Western Australia. In: Rüde TR; Freund A and Wolkersdorfer C (Eds.), Proceedings of the International Mine Water Association (IMWA) Congress. Aachen, Germany, p 41–45

Salmon SU, Oldham CE, Ivey GN (2008) Assessing internal and external controls on lake water quality: Limitations on organic carbon-driven alkalinity generation in acidic pit lakes. Water Resources Research 44: W10414

Stoneman GL, D. S. Crombie, K. Whitford, F. J. Hingston, R. Giles, C. C. Portlock, J. H. Galbraith and Dimmock. GM (1997) Growth and water relations of *Eucalyptus marginata* (Jarrah) stands in response to thinning and fertilization. Tree Physiology 17: 267–274

Van Etten EJB (2012) The role and value of riparian vegetation for mine pit lakes. In: Mine Pit Lakes: Closure and Management, McCullough CD (ed) Australian Centre for Geomechanics, Perth, 91–106 pp

Van Etten EJB, McCullough CD, Lund MA (2011) Setting restoration goals for restoring pit lakes as aquatic ecosystems: a case study from south west Australia. In: Proceedings of the Heavy Minerals 2012 Conference. Perth, Australia, p 339–350

Van Etten EJB, McCullough CD, Lund MA (2012) Importance of topography and topsoil selection and storage in successfully rehabilitating post-closure sand mines featuring pit lakes. Mining Technology 121: 139–150

Modeling potential impact of geothermal energy extraction from the 1B Hydraulic System of the Sydney Coalfield, Nova Scotia, Canada

Jessica MacSween, Chandra Raman, Rajendran Kaliaperumal, Ken Oakes,
Martin Mkandawire

Verschuren Centre for Sustainability in Energy and the Environment, Cape Breton University, P.O. Box 5300, 1250 Grand Lake Road, Sydney, Nova Scotia, Canada B1P 6L2, Jessica_MacSween@cbu.ca

Abstract To predict the hydrogeochemical stability of the 1B Hydraulic System of the Sydney Coalfield in Nova Scotia, we are simulating the behavior of groundwater flow and pollution transport using FEFLOW. In order to utilize mine water for geothermal energy extraction, predicating alterations in thermal dynamics is of concern. The simulation considered effects of pumping water from a lower depth and re-injecting into higher depths as well as the change in temperature of the water after energy extraction. This paper presents our preliminary results simulating the potential impact of the geothermal energy extraction on the behavior of groundwater flow and pollution transport.

Keywords groundwater, FEFLOW, finite element analysis, 3D Models, coal seams, geothermal extraction

Introduction

Geothermal energy extraction from mine water is a strategy that makes mine water management economically appealing. In conventional geothermal systems, natural heat from the Earth is extracted to generate electricity and heat buildings; in this case the mine water is used as the heat source. The efficient use of this natural resource can turn mine water management from a burden to an economic opportunity. Consequently, this strategy is among others that is being advocated in the management of the massive mine water legacy left by coal mining that spans close to four centuries in the Sydney Coalfield of Cape Breton, Nova Scotia (Shea 2009). When mining ceased in 2001, the flooding process began and over time the interconnected collieries filled with mine water. In order to counteract this, the upper areas of the major mine pool, the 1B Hydraulic System, are controlled -18 ft (-5.49 m) below sea level (Shea 2008). The 1B Hydraulic System contains 76.7 Mm^3 of water, making it the single largest mine pool within Cape Breton (Shea 2009). The mine water has been geothermally warmed overtime through contact with the rock strata causing the temperature of the water to increase, leaving a high potential for geothermal heat extraction.

Therefore, a geothermal project has been initiated at the 1B Hydraulic System, utilizing the 10 inter-connected and abandoned collieries located in 3 different coal seams. The project will use mine water as a geothermal energy source to provide heating in the winter and cooling in the summer to a senior citizens complex located in New Aberdeen, Glace Bay. The mine workings involved are those of the No. 2 colliery (extraction well) which worked the Phalen Seam between 1899 and 1949 and the No. 9 colliery (injection well) which worked the Harbour Seam between 1899 and 1924 (Shea 2009). The geothermal system in place is an open loop in which the mine water from the No. 2 colliery is pumped from a 253 m deep well into a building, where it runs through a heat pump that either removes or adds heat, it is then injected into a 124 m deep well that is aligned with a depillared area of the No. 9 colliery located 43 m away (Fig. 1). The effects of

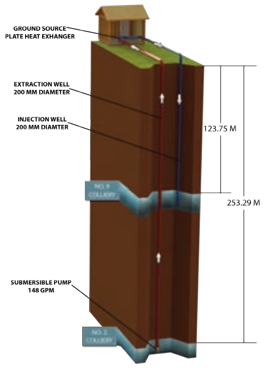

Fig. 1 *Open- loop geothermal system showing the extraction well into the No. 2 colliery and injection well into the No. 9 colliery.*

differences in well depths and change in temperature of the water after energy extraction on the behavior of groundwater flow and pollution transport is unknown.

In light of this, a numerical heat-transport model has been initiated at Cape Breton University using FEFLOW® (Finite Element subsurface FLOW system) developed by DHI-WASY GmbH. The FEFLOW model simulates three-dimensional groundwater flows using finite-element techniques and contamination concentration trends. For our simulation, the model domain is divided into approximately 5000 nodes, creating cells in each layer and covering 20 km^2 of the 1B Hydraulic System. Hypothetical temperature changes and pumping rates based on the capacity of the heat exchanger were utilized. This paper presents our preliminary results simulating the potential impact of the geothermal energy extraction within the 1B System. The flow and pollution transport between these two collieries was not taken into account during this simulation.

Geography and geology of study area

The modeled study area delimits the mine waters of the 1B Hydraulic System, located beneath the communities of Glace Bay, Reserve Mines and Dominion in eastern Cape Breton. The 1B System is one of the three major mine pools within the Sydney Coalfield, consisting of ten abandoned and interconnected underground collieries (No. 1A, No. 1B, No. 2, No. 5, No. 9, No. 10, No. 20, No. 26, Lingan, and Phalen). The No. 1A, No. 5, and No. 10 collieries do not extend under the ocean, while No. 1B, No. 20, No. 26, Lingan and Phalen are entirely submarine. The No.2 and No.9 collieries straddle both the land and the submarine environments. This preliminary study will examine the potential influence of establishing geothermal energy extraction operations at the No.2 colliery, as well as the effect on the No. 9 colliery of which the geothermally extracted water will be injected. Additional collieries situated in the 1B Hydraulic System will be included as the work progresses.

The 1B Hydraulic System was formed following the cessation of mining activities within the Glace Bay Syncline and along the northward flanks of the Bridgeport Anticline (Shea 2009). The mining occurred within the three major coal seams (Emery, Phalen, and Harbour), each occurring at different depths, with Emery being the deepest and Harbour the shallowest (Shea 2008). The coal strata are of Carboniferous age, with the seams separated by sequences of sedimentary material with inter-seam strata generally consisting of mudstone, shale, siltstone, sandstone, and minor carbonaceous limestone (Shea 2009). Probably the inter-seam strata are the result of deposition activity which occurred within fluvial as well as lacustrine environments (Shea 2009).

Mine Connections

The collieries associated with this geothermal project are Nos. 2, 9 and 20 which are part of the larger 1B Mine Pool (1B Hydraulic System). The collieries are located in the New Aberdeen district in the community of Glace Bay. No. 9 colliery was opened in 1899 and was accessed by three deep (approximately 125 m) shafts sunk to the Harbour Seam. That same year, No. 2 Colliery was developed by extending two of the former No. 9 Colliery shafts, and later a third in 1946, down 135 m to the Phalen Seam. In 1939, No. 20 colliery was developed by driving two cross measures tunnels from No. 2 Colliery to the Harbour Seam to access the coal that lay down the dip of No. 9 Colliery (Frost 1962). No. 2 Colliery closed in 1949, however, No. 20 remained open until 1971. During the operation of No. 20 Colliery, No. 9 Colliery had to be kept dry through pumping to avoid overflow into the No. 2, which was directly connected to No. 20. In 1965, to avoid having to maintain No. 9 Colliery, cross measure borehole B-133 was drilled which allowed No. 9 Colliery water to drain into No. 2 Colliery where the water from both collieries was collected and pumped to surface. When No. 20 Colliery ceased operation and pumping terminated, flooding of these collieries began, starting with No. 20, then No. 2 and finally No. 9 Colliery.

The current understanding is that these 3 collieries are hydraulically connected to each other by this main borehole connection (B-133) and it is assumed that the borehole is open. In addition, the collieries could be hydraulically connected through their shafts, however, the connections are likely weak because the shafts were backfilled . The method of water flow through these collieries is not well understood and more time is needed to comprehensively analyze the mine workings and potential hydraulic connections so that they can be included in the model. For this preliminary study, only No. 2 and No. 9 Collieries have been taken into account.

No. 9, No. 2 and No. 20 Collieries are connected to the 1B Mine Pool of the Sydney Coalfield however the connection is not well known. The 1B Mine Pool water is kept at -5.5 metres below sea level by pumping at Neville Street Wellfield (Shea 2008, 2009). In 2010, a drilling program investigated the mine waters of No. 2 and No. 9 Collieries and the average mine water elevation for the collieries over a 2 month period (CRA 2010) was measured as -8.87 and -4.47 metres respectively. Because of the different hydraulic heads, it is suspected that the mine water in these two collieries is not significantly influenced by the pumping at Neville Street Wellfield. There is a tunnel connection between No. 2 and No. 1B Colliery to the west however, this connection is documented to be blocked by a constructed dam, though the current theory suggests there is probably some leakage around the outside of the dam.

Modeling and simulation conditions

The geometry of the model was created using the mine maps of the No. 9 and No. 2 collieries (Fig. 2). Thereon a super mesh was created that contained a definition of the outer model boundary, followed by the creation of the finite element mesh. Subsequently, the model was extended into three dimensions (3D) with the 3D layer configuration adjusted so the layers corresponded to actual layers found underneath the study area, including the Harbour and Phalen Seams. Four layers were selected which automatically lead to five slices. The thickness of the layers was obtained from ECBC 2010 Drilling Program. The thickness of the layers is as follows: 121.31 m for the first rock layer, 2.13 m for the Harbour Seam, 129.85 m for the subsequent rock layers and 2.20 m for the Phalen Seam. The data regionalization was done using Akima interpolation procedure. The model has approximately 7000 triangular prismatic elements and approximately 5000 nodes.

The flow simulation was set as a standard saturated groundwater flow equation based on Darcy's model with the state set as transient. For this simulation, the boundaries of the model are confined within the No. 2 and No.9 collieries, therefore, no flow is assumed between these collieries and the nearby collieries of the 1B mine pool. Two wells, B-218 (injection) and B-219 (extraction), will be used in this model for the geothermal heat exchange. For these two multi-layer wells, several parameters were assigned. The well radius was set as 0.10 m and top elevations were set at 19.52 and 19.42 m while bottom elevations were set at -237.13 and -104.33 m for wells B-219 and B-218, respectively. The state of the thermal energy transport was set to transient and a time series

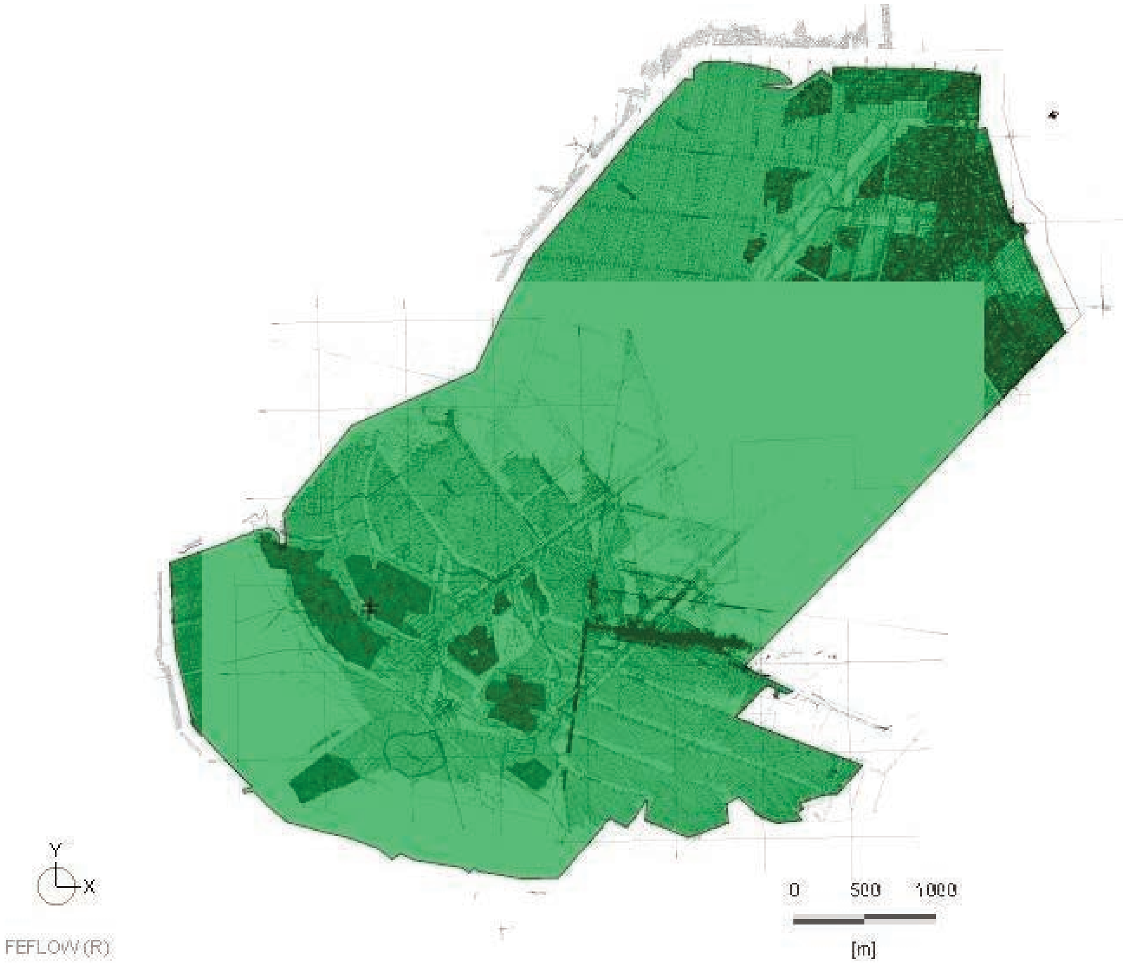

Fig. 2 *Model area – The area encompasses the No. 9 and the No. 2 collieries of the 1B Hydraulic System of the Sydney Coalfield, Cape Breton, Nova Scotia (during the interlaying, part of the No. 2 colliery has been blanked out).*

with linear interpolation was set for the wells detailing the hypothetical pumping rates throughout the year.

Next several parameters for the hydraulic flow were set. The groundwater recharge data was obtained from the Environment of Canada National Climate Data and Information Archive for Sydney A from 1999–2013 and is 1492.2 mm/a. The hydraulic conductivity was approximated using lithological data from Conestoga-Rovers and Associates (2010) and Baechler (1986). The first and third layers in the model represent the layers of rock above and below the coal seams in question. This area contains about 140 m of siltstones and sandstones, with interbedded mudstones, shale, occasional limestones, and two thin coal seams (Cain *et al.* 1994). Therefore, a hydraulic conductivity average was created for these layers using the hydrostratigraphic unit for siltstone and sandstone. The lower range values are 4.2×10^{-7} and 1.0×10^{-5} cm/s for siltstone and sandstone respectively (Bachelor 1986), the mean value of 5.2×10^{-5} cm/s was used as the hydraulic conductivity. The conductivity of the subsequent layers was set at 8.2×10^{-5} cm/s for the Harbour and Phalen Coal Seams. The values obtained from Baechler (1986) state that the coal seams of the Upper Morien range from 1.6×10^{-5} to 4.1×10^{-7} cm/s. For this study, the mean value was used as the hydraulic conductivity for the Harbour and Phalen Seams. The author acknowledges that these values will vary over the landscape and are not constant values; the averages are used for the preliminary study until more information can be pooled to get a comprehensive portrayal of the lithology.

Lastly, the open loop system was incorporated into the model. Open loops systems are treated as multi-layer wells in FEFLOW, containing both injection and extraction wells. The initial temperature of the model was set to 15.7 °C, which is the temperature of the extraction well recorded by ECBC 2010 Drilling Program. A time series with linear interpolation for the open loop was also set and the nodes belonging to the injection/pumping nodes were assigned a value equal to the number of the time-varying power function which contains the corresponding temperature differential for the model. The temperature differential for the model utilizes Δ T +3 K for heating and -3 K for cooling. The varying pumping/infiltration rate is based on a similar demand model and includes the maximum pumping capacity of 148 US.liq.gal/min (560 L/min) indicated in the heat schematics of the proposed system. In each time step, the module will calculate the average extraction temperature and averaging will be based on the contribution to total energy extraction by pumping from each extraction node (DHI-WASY Support, personal communication April 19th, 2013).

3D Heat Transport Model

The temperature difference between the extraction and injection wells can be seen in Fig. 3. The result of the simulation shows that the temperature at the point of injection after 7300 days is 10.2 °C, while the extraction temperature is 13.2 °C. This verifies that the system is working properly as the average temperature over the course of 7300 days shows the prescribed temperature differential between the inlet and outlet of 3 °C. The Fig. depicts a heating period with a maximum pumping rate 806.7 m³/d.

The final Fig. displays the injection and extraction temperatures over the period of 7300 days (Fig. 4). The injection temperature appears to be stable throughout the time period, as well as the extraction temperature. However, there is a slight decrease in the extraction temperature over the course of 7300 days. Most notably, at 4205 days where the temperature changes to 13.9 °C and at 7262 days it changes further to 12.9 °C. This is a possible indication of a short circuit situation which could affect the longevity of the system. In addition, it should be noted that the two wells are located at 43 m away from each other. The wells have different extraction and injection points, separated by approximately 130 m of rock strata. However, the cooling of the geothermal reservoir is a possibility and should not be overlooked during production. For this preliminary study, however, due to the fact that the connections of the two mines were not taken into account this result is not conclusive and requires further investigation.

Discussion

The preliminary results suggest the impact of a geothermal energy extraction scheme on mine water temperature is dependent on many variables, those of which have yet to be interpreted. The modeled scenarios did not take into account the important connections between these two collieries, namely the main connection borehole B-133 that connects the

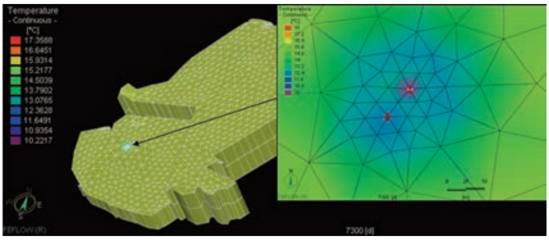

Fig. 3 *3D model of the temperature differences between the injection and extraction wells at the final time series of 7300 days.*

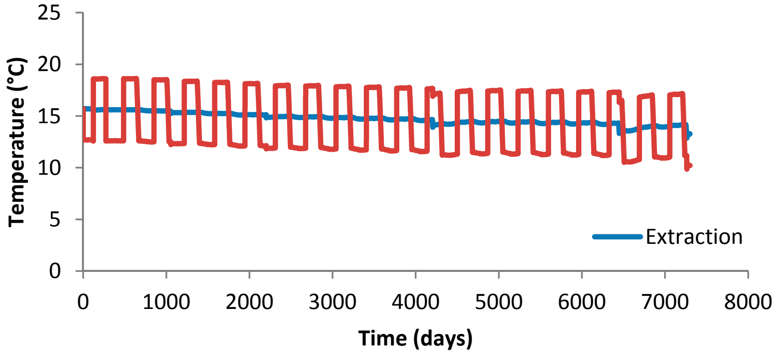

Fig. 4 *Extraction and injection temperature results showing the oscillations of the temperature differential, as well as the slight decrease in the extraction temperature.*

No. 9 and No. 2 collieries. However, this model is a step in the right direction. Further investigations are needed to properly calibrate and take into account the mine workings, so that a predicted flow regime can be applied to the model.

Acknowledgements

The authors thank Profs. Bob Bailey, and Deanne von Rooyen; Ben Pickles, Kevin Driscoll – all of Cape Breton University – and Glenn Macleod of CBCL Ltd. for assistance with the project, including mine data, geological issues and mapping services. Also, thanks to the technical support staff at DHI-WASY GmbH and to Trevor Arsenault from Lynk Electric Ltd., whom helped conceptualize the geothermal system. The study is funded though support received from Enterprise Cape Breton Corporation.

References

Baechler FE (1986) Regional Water Resources Sydney Coalfield, Nova Scotia. Province of Nova Scotia: Department of the Environment.

Cain P, Forrester DJ, Cooper R (1996) Water Inflows at Phalen Colliery in the Sydney Coalfield and their Relation to Interaction of Workings. In International Mine Water Proceedings, Nottingham, U.K., p 83–95.

Conestoga-Rovers and Associates (CRA) (2010) ECBC Drilling Program Investigate Mine Water at No. 2 and No. 9 Collieries, Glace Bay, Cape Breton County, Nova Scotia. Ref No. 059546.

Frost L (1962) The Louis Frost Notes 1685 to 1962. Retrieved June 13, 2013 from www.mininghistory.ns.ca/lfrost/lfdn2.htm.

Shea J (2008) Innovative Mine Water Management Techniques for Submarine Coal Mines of the Sydney Coalfield, Nova Scotia. Presented at West Virginia Mine Drainage Task Force Symposium, Morgantown, West Virginia, April 22, 2008.

Shea J (2009) Mine Water Management of Flooded Coal Mines in the Sydney Coal Fields, Nova Scotia, Canada. In: International Mine Water Proceedings, Pretoria, South Africa, p 289–297.

Aqueous geochemistry of the "other" pit lake in Butte, Montana, USA

Amber L. McGivern[1], Christopher H. Gammons[1], Terence E. Duaime[2]

[1]*Montana Tech, Dept. of Geological Engineering, 1300 W. Park Street, Butte, Montana, 59701, USA,, cgammons@mtech.edu, almcgivern@mtech.edu*
[2]*Montana Bureau of Mines and Geology, Butte, Montana, 59701, USA, tduaime@mtech.edu*

Abstract The Continental porphyry Cu-Mo mine, located 2 km east of the famous Berkeley Pit lake of Butte, Montana, contains two small lakes that vary in size depending on mining activity. In contrast to the acidic Berkeley Pit lake, the Continental Pit waters have near-neutral pH and relatively low metal concentrations. The main reason is geological: whereas the Berkeley Pit mined highly-altered granite rich in pyrite with no neutralizing potential, the Continental Pit is mining weakly-altered granite with lower pyrite concentrations and up to 1–2 % hydrothermal calcite. The Continental Pit waters are near equilibrium with a number of carbonate, sulfate, and molybdate minerals.

Keywords neutral mine drainage, trace metals, pit lake, geochemistry, mineral solubility

Introduction

Just east of the famous Berkeley Pit lake in Butte, Montana (Davis and Ashenberg 1989), there is a lesser known active open pit mine, the Continental Pit. The Continental Pit contains a large but low-grade Cu-Mo porphyry deposit (Czehura 2006). Two small water bodies exist on the property, here called the North Pond and the South Pond (Fig. 1). Presently, the elevations of these lakes are maintained at a low level by the Sarsfield pumping well, located near the north shore of the North Pond. Pumping ceased in 2001–2003 after the mine temporarily shut down in 2000 due to unfavorable economics. Dewatering resumed in 2003 when the mine reopened, and continues to the present day, at a typical rate of 800 to 1200 liters per minute (S. Czehura, pers. commun. March 2013).

During the mine-closure period of 2000–2003, samples of groundwater from the Sarsfield Well as well as samples of surface water from the North Pond (Fig. 2A) were collected monthly by the MBMG. Since 2006, the active mine has been collecting water samples twice a year from several locations on their property,

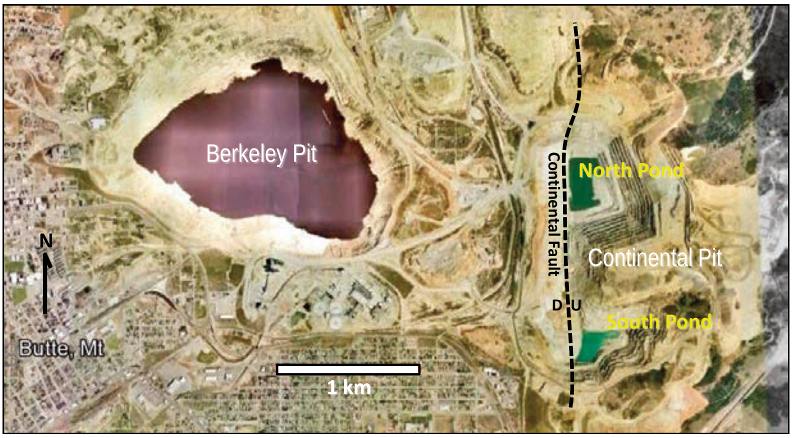

Fig. 1 *Google Earth image showing the location of the North and South Ponds in the Continental Pit, with the nearby Berkeley Pit lake for comparison. Image taken July 16, 2002.*

including the North and South Ponds, the Sarsfield Well (sampled instead of the North Pond when the latter is dry or frozen), and the Pavilion Seep. The water quality results are sent to the Montana Department of Environmental Quality (MDEQ), and are publically available upon request. The Pavilion Seep is a relatively small volume of acidic groundwater that enters the Continental Pit from a bench on the southeast highwall. At the time of this writing, Pavilion Seep water is collected and pumped to a site outside of the pit where it is mixed with Sarsfield Well water and used in the mill.

Because the active mining company intends to continue open-pit mining for decades, no formal plans for closure of the Continental Pit exist. The final closure scenario may well not include a pit lake. Nonetheless, it is interesting to look at the data in hand to predict the water quality of a hypothetical lake formed from flooding of the Continental Pit, and to compare this result to the nearby Berkeley Pit lake (Fig. 2B).

Methods

Water chemistry data for the North Pond from 2001 to 2003 were downloaded from the MBMG's Groundwater Information Center website (GWIC 2013). In June of 2003, shortly before dewatering resumed, a vertical profile of field parameters in the North Pond was collected by MBMG from a boat, and water samples were taken at near-surface and at a depth of 11 m. Additional data for the North Pond, the South Pond, and the Pavilion Seep collected between 2006 and 2012 were provided by MDEQ. All of the water quality analyses were conducted by certified labs following strict quality assurance protocols. In March 2013, the authors sampled the discharges from the Sarsfield Well and the Pavilion Seep. Samples were submitted for chemical analysis, as well as determination of $\delta^{18}O$ and δD of water, $\delta^{34}S$ and $\delta^{18}O$ of dissolved sulfate, and $\delta^{13}C$ of dissolved inorganic carbon. Results from the March 2013 sampling were not available at the time of this writing, but will be presented at the 2013 IMWA meeting.

Data for each chemical analysis of the North Pond between 2001 and 2003 (n = 17) were input into the program Visual Minteq, v. 3.0 (a recent adaptation of the original MINTEQA2 program of Allison *et al.* 1991), and saturation indices (S.I.) were determined for a number of minerals and amorphous solid phases. In this paper, the S.I. values for each solid were adjusted to one metal ion per formula unit. For example, amongst the common secondary Cu minerals, the S.I. value for malachite ($Cu_2CO_3(OH)_2$) was divided by two and the S.I. value for azurite ($Cu_3(CO_3)_2(OH)_2$) was divided by three. This was done so that S.I. values could be more equally compared between a set of minerals that contain a common element of interest. For modeling purposes, dis-

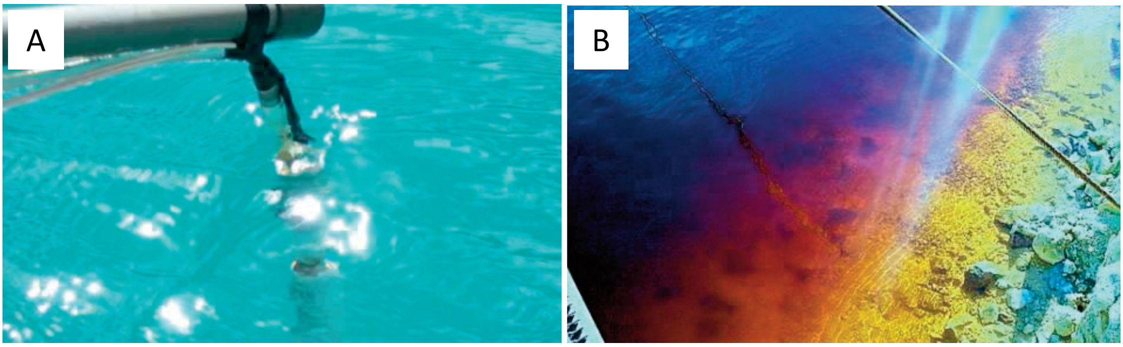

Fig. 2 *Close-up photographs comparing the appearance of water in the North Pond of the Continental Pit (left, with a submersible pump) and the Berkeley Pit lake (right).*

solved Cu and Mn were assumed to be in the +2 valence, Fe was assumed to be +3, and Mo and U were assumed to be +6. These redox assignments are consistent with the presence of > 5 mg/L dissolved oxygen throughout the water column of the lake in June 2003 (see below).

Results

The chemical compositions of the North and South Ponds in the Continental Pit are very similar (see Table 1). Both water bodies have a pH near 7, with a significant amount of bicarbonate alkalinity (> 100 mg/L as $CaCO_3$). The concentrations of most metals of concern, such as Cu and Zn, are quite low when compared to the Berkeley Pit lake, but are nonetheless well above regulatory standards for surface water. However, it is emphasized that these standards are not relevant as long as the mine is in operation. Unlike some pit lakes with neutral or alkaline pH, the concentration of arsenic in both of the Continental ponds is not particularly high (< 10 µg/L). This is not due to a lack of As in the ore body, since the Butte deposits are locally rich in the Cu-As-sulfide minerals enargite and tennantite (Meyer *et al.* 1968). It is possible that As is being adsorbed onto secondary Fe-oxy-hydroxide minerals on weathered bedrock surfaces. In contrast to the Berkeley Pit, which has undetectable quantities of dissolved Mo (Table 1), concentrations of Mo in the North Pond are elevated (in the 0.5 to 0.7 mg/L range). This difference is geological, as the Berkeley deposit produced no Mo, whereas molybdenite is an important ore mineral at the Continental deposit (Czehura 2006). Between 2006 and 2012, the Pavilion seep had an average pH of 3.31, and concentrations of dissolved metals and metalloids were much higher than in the North and South Ponds, but still considerably lower than the Berkeley Pit lake (Table 1).

Fig. 3 summarizes long-term trends in the concentrations of Cd, Cu and Zn in the North Pond as well as Sarsfield Well between 2001 and 2012. During the period of mine closure (2001–2003), concentrations of these metals steadily increased. The North Pond was seasonally stratified during this time (Fig. 4), with a chemocline situated at a depth of 4.2 m in June 2003. A single water sample collected at 11 m depth had slightly lower pH and significantly higher concentrations of Cd, Cu and Zn compared to a near-surface sample (Table 1). Dissolved oxygen concentrations were > 5 mg/L at all depths, which is in contrast to the Berkeley Pit lake, which typically has undetectable DO concentrations below the top 1–3 m (Pellicori *et al.* 2005). Although the moni-

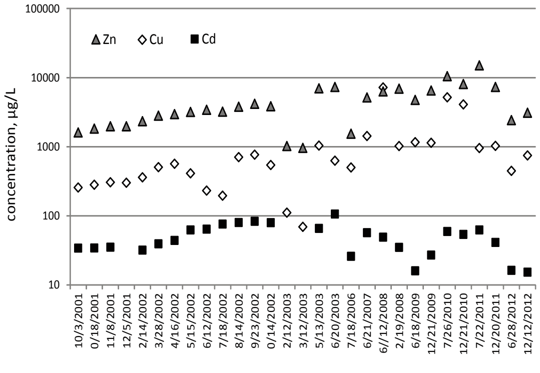

Fig. 3 *Concentrations of Cu, Cd, and Zn in the North Pond from 2001 through 2003 (GWIC 2013) and from 2006 through 2012 (MDEQ 2013). Some of the latter data are from the Sarsfield Well.*

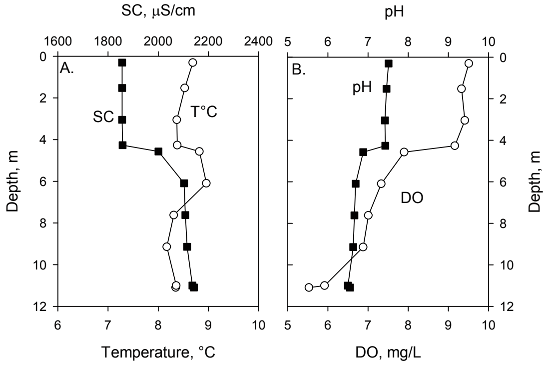

Fig. 4 *Vertical profiles in water temperature, specific conductance (SC), pH, and dissolved oxygen (DO) for the North Pond of the Continental Pit, collected on June 12, 2003.*

Location	pH	SC[1]	Ca	Mg	Na	K	SO_4^{2-}	Cl^-	F^-	HCO_3^-	NO_3-N	PO_4-P
CP-N surface[2]	7.34	2050	433	37	38	10	1241	9.1	3.3	146	1.3	<0.5
CP-N surface[3]	7.05		502	43	36	8	1310	8.9	4.2	123	0.6	0.04
CP-N 11 m[4]	6.55	2140	477	46	41	11	1440	8.6	4.3	92	1.7	<0.5
CP-S surface[5]	7.33	1860	397	38	32	6.1	1070	8.9	4.1	115	0.23	0.08
Pavilion [6]	3.31	2360	225	86	24	4.6	2060	5.3	4.7	< 1	0.57	0.14
BPit surface[7]	2.75	7340	475	534	74	9.6	8170	<50	30	< 1	<5	<5
BPit 210 m[7]	2.53	8160	442	515	74	7.6	9090	<50	30	< 1	<5	<5
	Al	As	Cd	Cu	Fe	Mn	Mo	Ni	Si	Sr	U	Zn
CP-N surface[2]	0.98	0.001	0.05	0.43	0.05	3.1	0.69	0.031	5.5	4.07	0.29	3.14
CP-N surface[3]	1.01	0.005	0.04	1.61	4.0	5.5	n/a	0.043	9.3	2.94	n/a	6.46
CP-N 11 m[4]	0.18	<.005	0.17	3.71	0.04	5.5	0.55	0.039	5.4	5.27	0.22	8.92
CP-S surface[5]	0.24	0.003	0.06	1.05	0.23	8.6	n/a	0.047	8.7	1.75	n/a	6.76
Pavilion [6]	41	0.02	0.43	58.6	76.7	22	n/a	0.15	28	0.66	n/a	46.2
BPit surface[7]	275	0.135	2.26	79	564	261	<0.02	2.4	38	1.55	1.97	627
BPit 210 m[7]	268	0.097	2.27	153	1007	248	<0.02	1.6	36	1.43	1.45	638

[1]Specific conductance in μS/cm; n/a = not analyzed; [2]Continental Pit North Pond, average of 17 samples collected in 2001–2003 (GWIC 2013); [3]Continental Pit North Pond or Sarsfield pumping well, average of 11 samples collected in 2005–2012 (MDEQ 2013); [4]Lake sample collected at depth of 11 m (GWIC 2013); [5]Continental Pit South Pond, average of 10 samples collected between 2005 and 2012 (MDEQ 2013); [6]Pavilion Seep, average of 11 samples collected between 2005 and 2012 (MDEQ 2013); [7]Berkeley Pit lake samples collected on Nov. 6, 2007 (GWIC 2013).

Table 1 *Chemical composition of selected water bodies of interest in the vicinity of the Continental Pit; Solute concentrations are in mg/L.*

toring data became more scattered after resumption of mining operations in 2003, average values for most water quality parameters in the North Pond from 2001–2003 are similar to those from 2006–2012, suggesting that water quality trends have been fairly stable in the last decade.

Based on the computed saturation indices (Fig. 5), water in the North Pond in 2001–2003 was close to equilibrium with gypsum ($CaSO_4{\cdot}2H_2O$) and fluorite (CaF_2), as well as a number of carbonate minerals, including calcite, dolomite, smithsonite ($ZnCO_3$), hydrozincite ($Zn_5(CO_3)_2(OH)_6$), and rhodochrosite ($MnCO_3$). On average, the lake waters were undersaturated with otavite ($CdCO_3$). It is possible that Cd resides as an impurity in calcite or another carbonate phase. A large number of Cu(II) minerals were also near equilibrium, including malachite ($Cu_2CO_3(OH)_2$), azurite ($Cu_3(CO_3)_2(OH)_2$), antlerite ($Cu_3(SO_4)(OH)_4$), brochantite ($Cu_4SO_4(OH)_6$), langite ($Cu_4SO_4(OH)_6{\cdot}2H_2O$), and possibly atacamite ($Cu_2Cl(OH)_3$). Both the North and South Ponds have a distinctive greenish blue color (Fig. 1, Fig. 2A), which could be partly caused by precipitation of one or more of these sparingly soluble secondary copper minerals. It is significant that metal concentrations in the North Pond appear to be controlled by mineral solubility limits, as this means that the concentrations of elements such as Cd, Cu, Mn, and Zn cannot increase without a simultaneous decrease in pH as well as bicarbonate concentration. Amongst the various silica polymorphs, the lake waters were closest to equilibrium with chalcedony (micro-crystalline quartz). Finally, it is interesting that the lake waters were found to be near equilibrium or supersaturated with several molybdate minerals, including $CaMoO_4$, $CdMoO_4$, $CuMoO_4$, and $ZnMoO_4$.

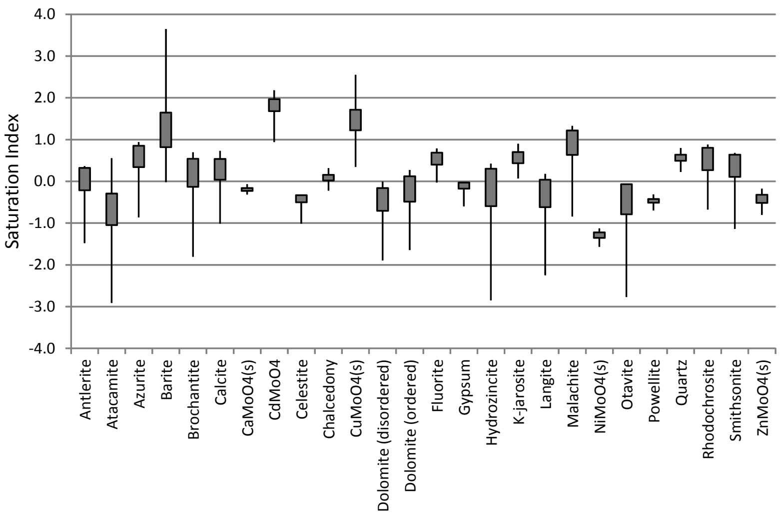

***Fig. 5** Saturation indices of various minerals based on 17 chemical analyses of the North Pond of the Continental Pit. Rectangles represent one standard deviation. Lines show total range.*

Discussion

The data presented above show a stark contrast between the highly acidic and metal-rich Berkeley Pit lake and the nearby Continental Pit lakes which have neutral pH and relatively low metal concentrations. The main reason for this difference is geological. The two open pit mines are separated by the Continental Fault (Fig. 1), a large normal fault with > 1 km of vertical displacement (Czehura 2006; Rusk *et al.* 2008), down-dropped to the west. The Berkeley deposit is rich in pyrite (> 5 wt %) with highly altered granitic bedrock (all feldspar and mafic minerals converted to muscovite as well as clay + quartz) that has no acid-neutralizing potential. In contrast, the Continental deposit, which represents a deeper and more peripheral mineral assemblage within the Butte District, contains weakly-altered granite wallrock (fresh feldspars with abundant primary and secondary biotite) with lower pyrite content (1 to 2 wt %) and a small but significant quantity of hydrothermal calcite. The latter occurs as thin veins and disseminations throughout the ore body (Newbrough and Gammons 2002; Lamsma 2012). In addition, whereas the Berkeley Pit is surrounded and underlain by 1000’s of km of underground mine workings (Duaime *et al.* 2004; Gammons *et al.* 2009), very few underground workings extend into the Continental Pit area. Thus, the hydrology of groundwater flow is dominated by open or backfilled/collapsed voids in the vicinity of the Berkeley Pit, as opposed to fractured bedrock in the vicinity of the Continental Pit.

Newbrough and Gammons (2002) used long-term humidity cell tests to compare leachate from crushed bedrock exposed in the Berkeley and Continental Pits, and found very similar water chemistry results to the data presented in this paper. However, Newbrough and Gammons observed that calcite was being dissolved from the crushed Continental Pit samples faster than pyrite was oxidized. Extrapolation of these results suggested that the Continental Pit leachates could become acidic at a future time, when the neutralizing potential was completely depleted. Due to the small number of samples in the Newbrough and Gammons study, and the inherent difficulty of scaling humidity cell tests to field settings, it is difficult to say if or when the small ponds in the Continental Pit might become acidic. The Pavilion Seep shows that some acidic drainage already exists in the Continental Pit, although the volume of this acidic water is presently much less than the pH-neutral, alkaline water that resides in the ponds, or that is being pumped from the Sarsfield Well. Over time, these conditions could change with continued weathering of the ore body.

Conclusions

The Continental Pit contains two small lakes that have near neutral pH and relatively low metal concentrations compared to the Berkeley Pit lake, which is highly acidic. Mining activity is expected to continue for decades, and closure plans for the Continental Pit may not include a pit lake. Based on Visual Minteq modeling, the existing ponds in the Continental Pit are close to equilibrium saturation with a number of carbonate, sulfate, and molybdate minerals. For metals whose solubility is limited by carbonate minerals (*e.g.* Zn, Cu), dissolved concentrations can only increase if pH or HCO_3^- concentrations decrease. No clear trend in this direction is apparent from the past 10 years of water quality monitoring. Some acid mine drainage does exist within the boundaries of the Continental Pit, and it is possible that the volume as well as severity of this AMD could increase in the future with continued weathering of the ore body. Nonetheless, the weight of evidence presented in this paper suggests that any hypothetical pit lake formed by flooding of the Continental Pit would have substantially different chemistry than that of the Berkeley Pit lake, with higher pH and lower dissolved metal concentrations.

Acknowledgements

We thank Montana Resources for access to data and also permission to sample on the property. We appreciate the help from Nick Tucci of MBMG with sampling and James Castro of Montana DEQ for help tracking down data.

References

Allison JD, Brown DS, Novo-Gradac KJ (1991) MINTEQA2/PRODEFA2, a geochemical assessment model for environmental systems. US Environ Protection Agency, EPA/600/3-91/021

Czehura SJ (2006) Butte: a world class ore deposit. Mining Eng 58(9):14-18

Davis A, Ashenberg D (1989) The aqueous geochemistry of the Berkeley Pit, Butte, Montana, USA. Appl Geochem 44:23–36

Duaime T, Kennelly P, Thale P (2004) Butte, Montana: Richest Hill on Earth: 100 Years of Underground Mining. Mont Bur Mines Geol, Misc Contribution 19: unpaginated poster

Gammons CH, Snyder DM, Poulson SR, Petritz K (2009) Geochemistry and stable isotopes of the flooded underground mine workings of Butte, Montana. Econ Geol 104:1213–1234

GWIC (2013) Montana Bureau of Mines and Geology, Groundwater Information Center. http://mbmggwic.mtech.edu/

Lamsma J (2012) Economic geology of the eastern margin of the Continental Cu-Mo porphyry deposit. M.S. Thesis, Montana Tech, Butte, Montana. http://gradworks.umi.com/15/12/1512987.html

MDEQ (2013) Montana Department of Environmental Quality, Helena, MT: unpublished data provided upon request.

Meyer C, Shea EP, Goddard CC Jr (1968) Ore deposits at Butte, Montana. in Ridge JD ed, Ore Deposits of the United States 1933–1967. Amer Inst Mining Metall Petrol Eng, 1373–1416

Newbrough P, Gammons CH (2002) Experimental investigation of water-rock interaction and acid mine drainage at Butte, Montana. Environ Geol 41(6): 705–719

Pellicori DA, Gammons CH, Poulson SR (2005) Geochemistry and stable isotope composition of the Berkeley pit lake and surrounding mine waters, Butte, Montana. Appl Geochem 20: 2116–2137

Rusk BG, Reed MH, Dilles JH (2008) Fluid inclusion evidence for magmatic-hydrothermal fluid evolution in the porphyry copper-molybdenum deposit at Butte, Montana. Econ Geol 103: 307–334

Management of water collection and treatment in the remediation of an uranium mill tailings site

Thomas Metschies, Jan Laubrich, Jürgen Müller, Michael Paul, Ulf Barnekow

WISMUT GmbH, Jagdschänkenstraße 29, 09117 Chemnitz, Germany

Abstract As of the-Mid 1990s remediation of former uranium mining and milling sites is under way including the geotechnical stabilisation of tailings storage facilities at Seelingstädt (Germany). With advancing remediation water management requirements evolve facing new challenges: changing chemical water composition, more restrictive concentration limits and shrinking water storage space while the treated water volume just slowly decreases. The paper outlines ways to adapt water collection and treatment strategies to the new challenges and points out the influence of water management on the physical remediation works. Lessons learned for similar remediation projects are presented to allow considering relevant aspects at an early stage of a mining legacy remediation planning.

Keywords Mine water management, mill tailings, remediation, case study

Introduction

Uranium mining and milling in Eastern Germany took place between 1946 and 1990. A significant portion of the mined ore was processed at the Seelingstädt milling site leaving behind the two major tailings storage facilities (TSF) of Trünzig and Culmitzsch with a total volume of about 105 Mm^3 of stored tailings material. Each of the TSF consists of two individual ponds separated by a dividing dam and store the residuals of the alkaline and the acidic leaching process respectively. The storage facilities were developed in mined out open cast uranium mines operated between 1949 and 1967. Additional rock-fill dams were erected to contain the deposited tailings material. These dams were sealed by discharging fine slimes (auto-stable dams). Tailings material was disposed into the Trünzig TSF from 1960 until 1967 and the Culmitzsch TSF between 1967 and 1990. According to the historic discharge pattern, sandy tailings settled out near the discharge points while fine tailings more distantly below the water table usually in the centre of the ponds (Barnekow *et al.* 2012).

By the end of uranium production in 1990 only the Culmitzsch TSF was in use while the Trünzig TSF was already inoperative and remained in a managed but unremediated condition with supernatant pond water covering most of the deposited material.

A dry *in situ* stabilisation technology was selected as the most appropriate general remediation option under the given local conditions requiring the removal of supernatant pond water as a first step. Concurrently with this, the exposed tailings surfaces were immediately covered with an interim cover layer of 1 m thickness to reduce radiological impacts. Before covering and contouring the tailings material had to be geotechnically stabilised using various technologies. During this process highly contaminated pore waters were released from the tailings material which had to be treated. For the covering of the tailings preference was given to locally available materials from adjacent mine dumps.

Site characterization

The conditions at the four separate ponds of the Trünzig and Culmitzsch TSF are summarised in Table 1. In terms of area covered and stored material volume the Culmitzsch TSF clearly exceeds the Trünzig TSF. Because of the earlier end of deposition and the consequently more advanced process of consolidation, contouring and final covering of the Trünzig TSF started already in 1992 and is nearly complete now.

Remediation of the Culmitzsch TSF will last until 2022. The present status with contouring work in progress on pond B is shown in Fig. 1. Pond A still contains supernatant water on top of the fine slimes.

Pore and seepage water composition is strongly determined by the chemical processing applied (Table 1). While pore water from the acidic process deposited in the A ponds contains very high concentrations of iron and magnesia thus resulting in elevated hardness, the main characteristics of the pore waters at the B ponds are high uranium concentrations. Sulphate and chloride concentrations are generally high in both ponds. Table 2 shows the average as well as a representative range of the concentrations of major water constituents based on samples from sampling wells in the sandy and transition zones. Pore water of the fine slime tailings stored in major parts of the TSF contains even higher concentrations (Table 3).

In 2001 a treatment plant was put into operation close to the TSF with a design capacity of 300 m^3/h, replacing the water treatment unit of the former mill. The main treatment of collected water is done by lime addition thus reducing the concentration of metals and semi-metals as well as of uranium below the discharge limits but not decreasing the salt and hardness content. Uranium complexes have to be removed prior to the lime treatment. Therefore the water is acidified and fed into stripping columns where free CO_2 is removed by an air stream to reduce the carbonate content of the water as a first step.

Seepage water collecting drains and pumping wells are installed downstream of the TSF to contain the flow of contaminated waters. These actively collected waters and any other surface water or contaminated seepage

***Fig. 1** Aerial photograph of the Culmitzsch TSF with pond A (left, with supernatant water) and pond B (right) and the Lokhalde waste rock dump (centre foreground) during remediation (2012).*

Tailings Impoundment	Culmitzsch Pond A	Culmitzsch Pond B	Trünzig Pond A	Trünzig Pond B
Residues of processing type	Acidic	alkaline	acidic	alkaline
Tailings surface area (ha)	159	84	67	48
Tailings volume (Mm^3)	61	24	11	6
Solid mass (Mt)	64	27	13	6
Max. tailings thickness (m)	72	63	30	28
U_{nat} in solids (t)	4,800	2,200	1,500	7,00
U_{nat} in pore water (mg/L)	0.3 ... 3.9	1.0 ... 16.5	1...19	1...20

***Table 1** General characterization of the TSF at the Seelingstädt site.*

2000 – 2013	pH	U mg/L	Mg mg/L	Ca mg/L	SO_4 mg/L	Cl mg/L	Fe mg/L	Ni µg/L
Pond A								
Median	8.0	0.9	1,300	380	12,000	1,500	0.67	28
10th percentile	7.2	0.2	590	340	7,200	860	<0.08	<15
90th percentile	8.3	2.2	2,300	420	15,000	2,200	104	470
Pond B								
Median	8.3	6.2	110	27	8,200	1,100	0.18	<20
10th percentile	7.8	0.9	66	11	6,200	750	<0.04	<10
90th percentile	8.7	11.2	650	380	9,500	1,500	1.15	40

***Table 2** Concentration levels in sampling wells at the beach and transition zones of the Culmitzsch TSF.*

2000 – 2013	pH	U mg/L	Mg mg/L	Ca mg/L	SO_4 mg/L	Cl mg/L	Fe mg/L	Ni µg/L
Median	6.7	0.3	1,400	380	11,000	1,300	75	410
10th percentile	5.9	0.1	700	360	6,600	770	14	68
90th percentile	8.0	1.9	2,800	460	15,000	2,400	220	1400

***Table 3** Concentration levels in pore water of fine slime tailings of the Culmitzsch TSF pond A (sampling points CA 90A, CA91A, CA 93A).*

and pore waters pumped from the TSF are treated. Standards for waste water discharge into the receiving streams were set by the regulatory authorities of Thuringia for metals, semi-metals and uranium. Limits for the salt concentrations and water hardness are given for a sampling point in the receiving Culmitzsch creek downstream of the tailings site as well as further downstream in the Weiße Elster river. At least temporarily these limits restrict the discharge volume of treated waters and therefore curtail the water management operations at the Seelingstädt site (Metschies *et al.* 2012). As a result the full technical capacity of the water treatment plant might not be available throughout the year depending on the discharge conditions in the respective water bodies as well as additional sources of salts and hardness in the watershed.

During the ongoing remediation of the Culmitzsch TSF additional major challenges for the water management are (1) the treatment and release of supernatant waters from the pond A in order to allow sufficient work to progress on the surface areas, (2) the collection and treatment of the released, pumped or expelled pore waters and as a consequence (3) the continuous adaptation of the water treatment to the changing water composition to ensure the full treatment capacity is available throughout the year.

Water quantity aspects

On average about 40 to 50 % of the treated waters are seepage and contaminated groundwaters which continuously emerge. The Trünzig and Culmitzsch TSF, as well as the adjacent operational areas such as waste rock dumps and the former milling and processing site, cover a total area of about 650 ha. The collected surface run-off from this area requiring treatment strongly depends on the climatic conditions. The annual average precipitation varied between 450 and 800 mm during the past 10 years dramatically influencing the collected water volumes. Even with the existing water treatment plant running close to the design capacity (Fig. 2, left diagram) such variations of the collected water quantities are not easily to cope with. Therefore especially during past wet years the storage of surplus waters in pond A (Fig. 2, right diagram) was necessary to ensure the safe operation of the treatment facility and as consequence to meet the limit values for the discharge.

With the progress of geotechnical stabilisation and covering of the Culmitzsch TSF the large water storage potential of pond A will not be available for water storage in the future. Consequently the need for additional storage volumes at the site or alternative management measures arises. Construction of a water storage facility to accommodate the surplus water of up to 1 Mm³ (Fig. 2) in case of extended periods of precipitation is not feasible. Apart from the cost aspect and a lengthy permitting process any reservoir of such size within the TSF would interfere with the remediation goal while due to the contamination of the collected waters (*e.g.* U) a storage pond outside of the existing radiation protection area will not be permitted.

Therefore the further water management at the site requires a combination of (1) reduction of contaminant water formation and (2) the installation of a reasonable storage volume for the time till the end of physical remediation works.

Separate collection of uncontaminated surface waters from already remediated areas and their direct discharge into the receiving creeks is pursued. This however requires agreements with the permitting authorities regarding additional discharge points and quality criteria for waters to be discharged. Therefore, priority is given to selecting such discharge points where surface waters will be permanently discharged due to the final contour of the facilities. Nevertheless it has to be proven that the discharge limits are met and that no additional risks for floods are generated by these discharges in case of high waters. Following this concept it was possible to already reduce the surface water inflow to the treatment system from a total area of nearly 150 ha till now decreasing the total drained area by about 20 %.

The storage capacity in engineered basins at the site is presently extended to about 100,000 m³ which in combination with other management measures will allow to cope with most of the expected rainfall scenarios (compare Fig. 2) based on the conditions of previous years. Nevertheless the contaminated overflow of these storage reservoirs is directed into the pond A and thereby remaining safely contained within the existing depression of the pond surface. Therefore the technical planning and implementation of the stabilisation and contouring work on pond A have to make sure that in case of such extreme precipitation events only separated areas of the pond are reflooded and that work could safely proceed without disruption on the remaining un-

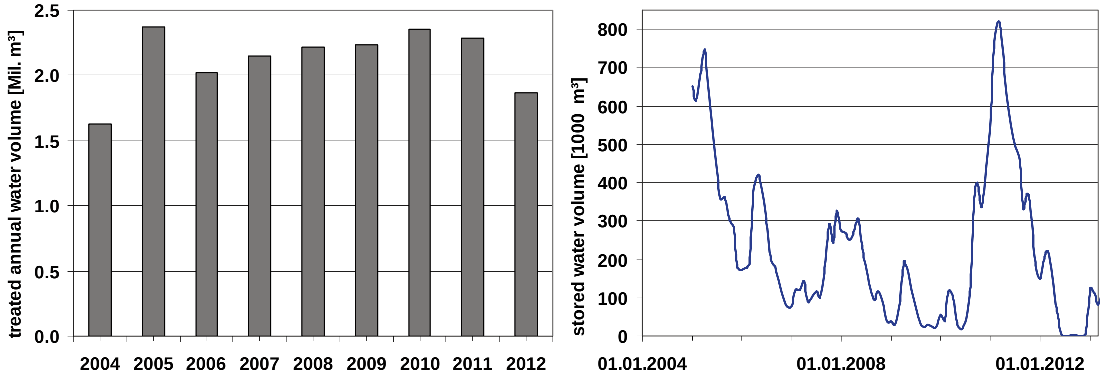

Fig. 2 *Treated annual water volumes (left) and water volume of the supernatant water body stored on top of pond A of the Culmitzsch TSF.*

flooded part. This requires adapting continuously the contour of the pond surface during remediation to account for the temporary storage of the surplus water. On the other hand it has to be ensured that in such cases the water is removed from the re-flooded areas as soon as possible and sufficient storage volume is generated again in the available reservoirs to minimise the impact on the already stabilised, contoured and covered areas.

Water quality aspects

Short term fluctuations in concentration levels in the collected waters result from the meteorological conditions showing a clear seasonal variation (Fig. 3), but also from operational conditions such as the emergence of pore waters during the consolidation of the fine slime tailings. These fluctuations were smaller in case of high volumes stored in pond A resulting in a homogenisation of the feed flow to the treatment plant.

Long-term concentration trends as shown for sulphate and uranium in Fig. 3 are influenced by two partly opposing processes: (1) a continuous dilution of the outflow from the contaminant source and (2) the initiated additional water release in the progress of the remediation works. As a consequence of the temporary covering and contouring of the tailings material considerable volumes of highly concentrated pore waters are collected for treatment. On the other hand seepage water flow from the tailings is reduced resulting in a reduction of contaminant release in the mid- and long-term.

The geotechnical stabilisation and contouring of the Culmitzsch TSF pond B commenced already in 2009 contributed 15 to 25 % to the total uranium load in the flow to the water treatment plant in the past years. In addition to other effects uranium concentration of the waters increased making higher demands to the treatment operation to meet the discharge limits. The influence of expelled pore waters from the pond B will decline in the future but reduced dilution will nevertheless lead to higher uranium concentrations in the feed water to the treatment plant. In addition uranium removal from the waters depends on the effectiveness of the stripping process which itself is sensible to air and water temperatures. To adapt the existing treatment technology to this future development an optimisation of the acid dosage and additional air sparging prior to the stripping columns is presently implemented.

Starting in 2014, the geotechnical stabilisation of pond A will again lead to significant changes in the composition of the collected water by the additional release of an expected 3 Mm^3 of pore water as result of the consolida-

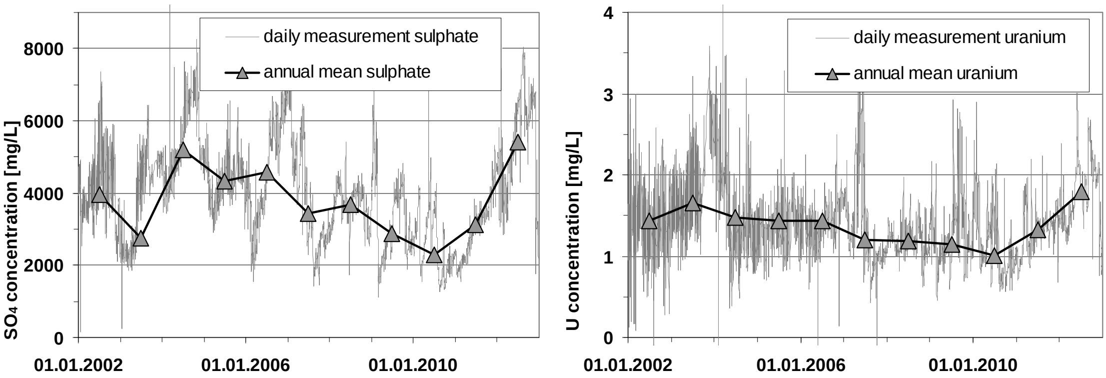

Fig. 3 *Long-term trend of concentrations in the feed water to the treatment facility versus daily fluctuations.*

tion of fine tailings mainly over a period of about 5 years. Based on sampling of pore waters in the fine slime tailings, iron concentrations of up to 250 mg/L (Table 3) are expected in these waters having tremendous influence on the operational stability of the treatment process. Presently technical measures are planned and implemented to cope with these waters to ensure a stable operation of the treatment facility.

Discharge limits apply to sulphate and chloride as well as hardness given as concentrations in the receiving creek downstream of the tailings site. Especially under low flow conditions this constrains the discharge from the treatment plant requiring to temporarily halt the water treatment as it happened in 2012 when the treated volume was significantly reduced (fig. 2). During that time no significant accumulation of water in the pond A occurred due to the similarly reduced surface run-off. At the same time additional pore water pumping from sandy beaches in order to reduce the mobile contaminant inventory was not possible although sufficient treatment capacity would have been available. To optimise the remediation and allow additional water discharge even under low flow conditions it was agreed with the authorities as a temporary measure to additionally discharge water pumped from the Weiße Elster river via a pipeline formerly used to pump processing water for the milling operation. This increases the flow rate in the Culmitzsch creek and allows to continuously discharge waters from the remediation site.

Conclusions

Management of surface, seepage, pore and groundwaters in terms of water quantity and quality is a crucial part of any tailings remediation project. Progress of physical remediation works and the operation of the water collection and treatment closely depend on each other. These interactions have to be seriously taken into account in planning the remediation works already at an early stage especially in extensive remediation projects.

It is one of the main scopes of the remediation to achieve a reduction of water contamination. Therefore the management of uncontaminated and contaminated waters is a relevant aspect under the remediation project. With remediation in progress the amount of surface waters meeting the discharge limits should continuously increase. A minimisation of the hydraulic load onto the water collection and treatment system could be required to ensure necessary technical resources for the water management. Separation of uncontaminated precipitation and surface runoff and their direct discharge or reuse could be achieved by a continuous management of the respective catchment areas during the ongoing remediation but requires a close coordination between the construction activities and water management on the site. However, separation of clean water should be done at reasonable costs because additional effort might be required in terms of construction work to provide the necessary pipes or channels as well as to contain the respective catchment areas. On the other hand isolation and discharge of clean fractions of water also influence the operation of other parts of the site water management. It could have an effect on the remaining water composition which itself directly influences the treatment operation possibly requiring a necessary revision or even extension of the treatment process.

Changes in the water quantity and quality may occur over the entire project period and have to be monitored thoroughly. A prediction of these changes is necessary to adapt the water collection and treatment in due time. This requires a thorough understanding not only of the remediation object but also of the interaction with the surroundings in terms of hydrogeological and hydrological conditions as well as the relevant sources and sinks for the geochemical components but also the transport pathways of the waters to be handled. In addition the possible effects of the future remediation works on the composition of the collected water have to be taken into account in these predictions.

Providing sufficient water storage capacity on the site is essential to ensure a stable operation of the water treatment unit in terms of cutting peaks of water discharge as well as to ensure a constant rate and composition of flow to the treatment facility. The storage basin or ponds need to be located on the site properly avoiding an interference with the future remediation progress. Planning of these storage facilities should already take into account any relevant needs for the removal of the installations or any contaminated precipitates at the end of the remediation operation.

Release limits for the water discharge into the receiving stream might impose significant constraints on the water management at the site. Especially concentration limits set for the receiving stream which depend on the flow rate within these streams could influence the possible discharges depending on the seasonal variations. The applied treatment technology should therefore assure that the limits are met even under unfavourable conditions with low flow rates in the watercourse and high concentrations of the collected waters to be treated.

In planning such type of remediation projects provisions in terms of costs and effort have to be made for a continuous monitoring, evaluation, optimisation and adaptation of water collection and treatment at the remediation site. As far as possible the choice of treatment technology applied should provide for a safe operation during the entire remediation period taking into account the expected variance of the relevant parameters.

References

Barnekow U, Müller J, Metschies T, Paul M (2012) Experiences gained and major challenges for the remediation of Wismut's Culmitzsch tailings pond. In: Fourie AB and Tibbett M (Eds), Conference Mine Closure 2012, Australian Centre for Geomechanics, p 209 – 222

Metschies T, Paul M (2012) Management of mine and tailings seepage water discharge in an intensively used watershed. In: McCullough CD, Lund MA, Wyse, L (Eds), International Mine Water Association Symposium, Bunbury Australia, p 409 – 416

Modeling Pit Lake Water Quality – How Do We Solve Multi-Disciplinary Problems?

Mike Müller

hydrocomputing GmbH & Co. KG, Zur Schule 20, 04158 Leipzig, Germany

Abstract Pit lakes are complex systems and their modeling requires an interdisciplinary approach. Coupled models for pit lake water quality modeling can often give convincing results. Further insight can be achieved by adapting the model to site-specific conditions. However, the communication in carrying out such a modeling project may prove less effective than should be. The paper provides suggestions on how to improve this communication process through information technology protocols. Finally, unifying the technical process of modeling and model development with the human interactions is proposed.

Keywords pit lakes, water quality modeling, multidisciplinary, collaboration

Introduction

Pit lakes belong to some of the most complex hydrological systems in terms of modeling, because important processes often involve several disciplines, such as hydrodynamics in the lake and the groundwater, hydro-geochemistry, and limnology. In addition, these systems are artificial and may be considerably different from natural conditions, and engineering measures often manipulate the lake to regulate the lake water level or to improve water quality.

This multidisciplinarity needs to be addressed in modeling approaches. While there is a considerable body of knowledge in modeling of single domains such as natural lakes, groundwater, erosion, and hydrogeochemisity, the interactions between these domains are much less understood. This may be attributed to two main reasons: (1) the technical difficulties to appropriately connect computational models of different domains, and (2) the different approach required when experts from different domains need to communicate and collaborate to solve a common problem. The technical difficulties, although not trivial, can be overcome by coupling established models from different domains.

There are several programs for modeling hydrodynamic processes in lakes such as DYRESM (Imerito 2013) for one-dimensional, CE-QUAL-W2 (Cole and Buchak 1995) for two-dimensional and ELCOM (Hodges, Dallimore 2013) for three-dimensional representation of lakes. Codes for modeling limnological water quality include AQUASIM (Reichert 1994), CAEDYM (Hipsey *et al.* 2007), and CE-QUAL-W2 (coupled hydrodymanics and water quality). Common models for hydro-chemical calculations are EQ3/6 (Wolery and Daveler 1992), PHREEQC (Parkhurst and Appelo 1999), and CORE2D V4 (Samper *et al.* 2012).

Salmon *et al.* (2008) describe a coupling of DYRESM and CAEDYM. Hipsey *et al.* (2006) used a coupling of ELCOM and CAEDYM for lake modeling. Another coupling is that of DYCD-CORE (Moreira 2010; Moreira *et al.* 2011). This paper uses PITLAKQ (Müller 2013) as an example. PITLAKQ is open source and freely available for further development. It couples CE-QUAL-W2 and PHREEQC as well as a few other models and additional algorithms to provide a comprehensive representation of important processes and their interactions. Modern software development techniques and powerful hardware facilitate the development and application of this type of model.

The second problem, the collaboration of experts from different, sometimes rather remote, fields is harder to solve. Setting-up, running and especially interpreting the result of such a model require in-depth knowledge in different domains. While experts know a lot about their fields, they may be novices in the field of their collaborators. This is compounded by ambiguous terminology definitions. The same technical term may describe something different in different technical disciplines, leading to potential miscommunication.

Important processes in pit lakes

There are many processes in a pit lake that can influence the water quality. Depending on the location and size of the lake, the sinks and sources of water and their water quality, and the intended use of the lake, emphasis on specific processes may vary. Processes thought to have a strong impact on the system may turn out not to be as significant as other processes that were not considered at all in the beginning. While some generalizations are possible, it seems that each lake is slightly or sometimes totally different and requires a modification in the modeling approach. The problem is that the need for these modifications often becomes clear only after some modeling has been done that shows problems in representing the system. Which process needs to be modeled in detail, which process can be simplified, and which process can be ignored can often only be determined by running sensitivity analyses with different processes included or excluded.

The challenge

Science and engineering are subdivided into subjects. Typically, people specialize in one subject and spend most of their professional life deepening their knowledge in it. While it is important to really know one subject and keep up with newest development in this field, it can become problematic when it comes to pit lake modeling. As can be seen from the above listed important processes, these processes cross over different disciplines such as hydrology, geochemistry, limnology, soil mechanics, groundwater hydrology, computational fluid dynamics and software engineering. These specialities may have overlaps but may come from different schools like natural science and engineering.

From the author's experience, frequently knowledge from people with diverse backgrounds, as indicated above, is needed to adequately tackle pit lake modeling problems. People from different disciplines tend to use different approaches to solve problems and often put emphasis on different tasks such as field sampling, laboratory experiments, data analyses or model building. While this is useful to cover aspects necessary to capture the nature of a pit lake, it can also cause new problems for solving the task at hand.

Miscommunications among specialists may arise because:

- They have different assumptions about the problem.
- They use slightly different terminology for the same thing.
- They use the same terminology for different things.
- They see the task from their domain and give it the most weight.
- They don't always fully understand what the other team members do.

We need diversity in backgrounds and approaches but at the same time a communication between team members that allows for working together towards one goal rather than working side-by-side focusing on individual specialties.

The software engineering approach – Example PITLAKQ

One attempt to model processes controlling pit lake water quality comprehensively is PITLAKQ. This modeling software is a new implementation of the work by Müller (2004) and continuous modifications and applications to different sites (Müller *et al.* 2008, 2011; Werner *et al.* 2008; Müller and Eulitz 2010). The idea here is not to implement a fully new model but rather to reuse existing modeling tools from different domains and to combine them to a new, integrated tool.

This approach has the advantage that many person years of programming, evaluating and improving of these tools can be uti-

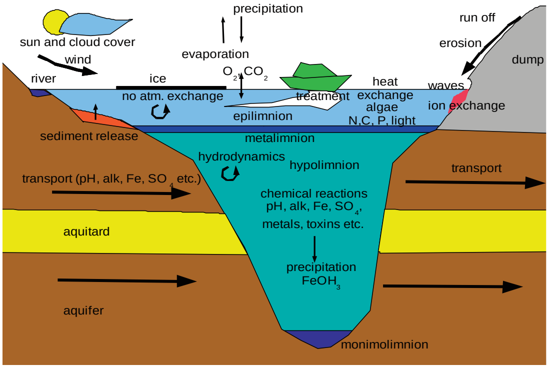

Fig. 1 *Schematic of processes in PITLAKQ.*

lized. Combining CE-QUAL-W2 and PHREEQC allows building upon the power of these public domain and well established tools.

One disadvantage of combining existing tools is that each comes with its own assumptions. Often this is not a substantial problem as along as the programmer and user of PITLAKQ takes this into account. But there are surprising cases that only become obvious after modeling results show unexpected effects. While some of these effects can be accommodated by catching potential errors with sanity checks, in the end the user needs to be sufficiently familiar with how both of these basic models work to successfully apply PITLAKQ.

Fig. 1 shows the processes implemented in PITLAKQ schematically. About 22 major process groups can be distinguished. This is sufficient for various pit lakes, focusing on acidic lakes. Often, a new site requires some modification of processes by adding a configuration option or adding a new process or variation of a process. While CE-QUAL-W2 is written in Fortran and PHREEQC in C, PITLAKQ is implemented in Python (Python Developers Team 2013). Very important is the interfacing of codes with Python to access the data structures from each individual model that allows for a fast implementation and testing process. Furthermore, all pre- and post-processing tools are written in Python. This allows working efficiently with large datasets which would be difficult or laborious to do with traditional tools such as spreadsheets. For many tasks the user needs only very basic Python knowledge to successfully modify pre- or post-processing scripts. This provides great flexibility to adapt to new types of problems.

Applications of PITLAKQ show that due to the dynamic nature of coupling, the coupled model often yields significantly different results to those obtained from uncoupled models that use pre-set boundary condition to represent the coupling partner. The models often show surprising results and trigger deeper investigations. These investigations often give a good indication of which data would need to be measured in more detail and which are not as important.

The human communication approach – interdisciplinary cooperation

While the implementation and the use of PITLAKQ are not trivial, it is a useful tool that can be applied and adapted to a variety of pit lake modeling problems. However, it does not do away with the need for expert knowledge from different domains outlined above.

As simple as it sounds, communication is paramount. Two types of communication should be included:

1. There should be regular physical meetings of all team members.
2. There should be a common document stating the objective of the modeling.

The common document should be continuously updated during the project and it should answer these questions:

- Is the objective still valid?
- Does the objective need modifications?
- What are the likely important processes for the objective?
- What measured values are needed and how are they turned into parameters?
- How sensitive are the parameters?

The document should contain a glossary explaining the used terminology. Even those seemingly simple terms like model, parameter, measured value or system should be defined. The definition should preferably be formulated using wording that can be understood by all team members while avoiding too much jargon.

The unified approach – effective communication supported at the technical level

Principles

Technical communication needs to be combined with the software engineering approach. One way of doing this would be through programming. Programming, as it is used here, can be defined as the expression of ideas in a formalized way that is restricted or guided by the programming languages. A program should primarily be useful for human communication and only secondly be executable by a computer. Programming can be done at various levels. For example, there is the distinction between systems programmers, library programmers and application programmers. Each type of programmer works with a different level of abstraction and with different objectives targeting different users of the software.

Why not add the "special domain programmer", a specialist in a domain who has sufficient programming knowledge to write his own, simple, programs and use libraries supplied by other programmers with deeper software engineering knowledge. While this does not sound like a viable way using languages such as C or Fortran, the advent of programming languages that allow a much higher level of abstraction changes the situation. Python is a general purpose programming language but has turned out to be useful for people who spend a minor proportion of their time programming, such as many scientists and engineers. They can learn enough programming in a rather limited time and can apply their knowledge to solve problems that otherwise would be very tedious or impossible to solve.

What would be the advantages of such an approach?

- Everybody in the team would use the same language, the programming language, to express their ideas.
- All ideas can be verified by running the resulting program.
- Outputs can be evaluated and automatically compared to expected values.
- The distinction between modeler and non-modeler in the team would become much weaker.
- Potentially all participating team members would get a much better understanding of the whole project.
- New ideas can be implemented in an unprecedented way.
- Of course there are disadvantages:
- This would be very new to many people and might not be accepted.
- Everybody who wants to participate has to learn the programming language.

Partial models

A partial model represents only a small part of a model focusing on one process or a few interrelated processes. Instead of interacting with the rest of the complex model, it receives predefined values the user has specified. This approach allows testing the behavior of individual parts of the model without all the complexity of the coupled model.

For example, the release of substances from the lake bottom sediment may depend on the water quality of the lake water right at the sediment-water interface. PITLAKQ can represent this process but needs parameters that have to be obtained through laboratory experiments. Naturally, the experimenter doing the laboratory study has the most expertise in measuring parameters. Now, instead of handing the parameters over to a modeler, the experimenter can use them in the partial model and see first hand what effect different parameters have on the release from the sediment.

Those partial models typically have very short run times in the order of seconds or a few minutes. Therefore, several model runs can be done as a parameter study. Using a few simple programming constructs such as loops and if-statements, many of these studies can be semi-automated. When the application programmer provides a good and simple programming interface, experimenters, who might not program otherwise, can perform parameter studies and adapt them flexibly to their needs.

There are several outcomes of this approach. (1) The experimenter better understands the impact of the parameter they measure. (2) The experimenter can better estimate the impact of the inherent variability in the measurement on the modeling results. (3) The coupled model will receive better parameters and their effects on the whole system can be better understood.

Of course, the extraction of partial models from a large model has one big disadvantage: it removes the feedback otherwise received from the other parts of the model. Therefore, the results from a partial model must be interpreted with caution. Despite this drawback, partial models can be useful and can help to better integrate the project team.

Interface definition between models

Another way where some basic programming techniques can help improve the communication are interface definitions between processes. Let us assume that there are biological processes in the lake that impact the hydro-geo-chemistry and vice versa. Two experts, one from the field of limnology and one from hydro-geo-chemistry describe what happens from their individual point of view. Naturally they will focus on their own domain, stressing either the limnological or chemical processes. Furthermore, both describe environmental factors that account for the "outside world" of the process from their point of view.

In addition to writing down their assumptions about the environment, both experts specify an interface in a programming language. That is essentially a list of environmental parameters with allowed ranges. When formalized in a programming language, the application programmer can write a small control program that checks for potential inconsistencies. This can be the basis for further discussions and adjustments of these interfaces. This is different from actually running the model because only the data flow between units representing different processes is checked and no process is modeled. The effort and therefore the turnaround times are much smaller than running a process model.

Conclusions

Pit lake modeling is a complex task that needs an interdisciplinary solution. Furthermore, sites and objectives are often so different that they require an adapted modeling solution. The coupling of existing models in combination with adding new model processes has proven to give new insight into pit lake behavior. The technical solution alone is not enough and a clear communication between all participants needs to be established, making objectives and meanings clear, as well as eliminating ambiguities in the terminology. This paper suggests that both the technical and the human communication part can be combined using programming. While this seems to be a highly technical solution, the use of a modern programming language such as Python, which is relatively simple yet powerful and widely used by occasional programmers, can actually facilitate communication among scientists. The restrictiveness of a programming language can help to achieve clearer problem definitions, resulting in better mutual understanding.

Acknowledgement

The author thanks Thomas Cole for CE-QUAL-W2 and giving valuable advice on details of its source code. Many thanks go to David Parkhurst for providing PHREEQC and long discussions on programming details. Furthermore, the author thanks Katja Eulitz for her valuable feedback on how to improve the handling and the process representation in PITLAKQ.

References

Castendyk and Eary (eds) (2009) Mine pit lakes: Characteristics, predictive modelling, and sustainability. Society for Mining, Metallurgy and Exploration, Littleton.

Cole, TM, Buchak, EM (1995) CE-QUAL-W2: A two-dimensional, laterally averaged, hydrodynamic and water quality model 2.0, US Army Corps of Engineers, Waterways Experiment Station, USA.

Hipsey, MR., Alexander, RA, Dallimore, CJ (2006) Simulation model of Lake Coeur d'Alene: Volume 2 –

Water quality modelling using ELCOM-CAEDYM, CWR Report.

Hipsey, MR, Romero, JR, Antenucci, JP, Imberger, J (2007) The Computational Aquatic Ecosystem Dynamics Model (CAEDYM): a versatile water quality model for coupling with hydrodynamic drivers, Pro. of the 7th Int. Conference on Hydroinformatics, Nice, France, 03–08 Sept. 2006, Vol 1., 526–533.

Hodges B, Dallimore C (2013) Estuary, Lake and Coastal Ocean Model: ELCOM, v2.2 Science Manual, Centre for Water Research University of Western Australia.

Imerito, A (2013) Dynamic Reservoir Simulation Model DYRESM, v4.0 Science Manual, Centre for Water Research University of Western Australia.

Müller, M (2004) Modellierung von Stofftransport und Reaktionen mit einem neuentwickelten, gekoppelten Grund und Oberflächenwassermodell am Beispiel eines Tagebaurestsees, Ph.D. Thesis, Dresden.

Müller M, Eulitz K (2010) Characterizing Water Quality of Pit Lake through Modeling, in Proceedings Mine Water & Innovatiev Thinking, C. Wolkersdorfer and A. Freund (eds), International Mine Water Symposium, 5–9 September 2010, Sydney, Nova Scotia, Canada, Cape Breton University Press, Sydney, Nova Scotia, Canada, pp. 375–378.

Müller M, Eulitz K, McCullough CD, Lund MA (2011) Model-based Investigations of acidity sources and sinks of a pit Lake in Western Australia, in Proceedings Mine Water – Managing Challenges, T.R. Rüde, A. Freund and C. Wolkersdorfer (eds), International Mine Water Congress, 4–11 September 2011, Aachen, Germany, RWTH Aachen, Germany, pp. 41–45.

Müller M, Werner F, Eulitz K, Graupner B (2008) Water Quality Modeling of Pit Lakes: Development of a Multiply-Coupled Groundwater Lake Circulation and Chemical Model, in Proceedings 10th International Mine Water Association Congress – Mine Water and the Environment, N. Rapantova, H. Zbynek and J. Zeman (eds), 10th International Mine Water Association Congress, 2–5 June 2008, Karlovy Vary, Czech Republic, Ostrava (VSB – Technical University of Ostrava), pp. 547–549.

Parkhurst DL, Appelo CAJ (1999) User’s guide to PHREEQC (Version 2) – A computer program for speciation, batch-reaction, one-dimensional transport, and inverse geochemical calculations, Water-Resources Investigations Report 99–4259, U.S. Geological Survey, 310 p.

McCullough CD (ed) (2011) Mine pit lakes: Closure and Management. Australian Centre for Geomecanics, Perth

Moreira S (2010) Coupled hydrodynamic and geochemical models for open pit lakes: application to the as pontes pit lake. Ph.D: thesis. Universidad a Coruña, Spain.

Moreira *et al.* (2011) Coupled hydrodynamic and geochemical model of the meromictic Waldsee in East Germany. Aquatic Geochemistry 17, 265–280.

Müller M (2013) PITLAKQ Documentation, viewed April 10, 2013. www..pitlakq.com.

Python Developers Team (2013) Python viewed April 10, 2013. www.python.org.

Reichert P (1994) AQUASIM – A tool for simulation and data analysis of aquatic systems, Water Sci. Tech., 30(2), 21–30.

Salmon SU, Oldham CE, Ivey GN (2008) Assessing internal and external controls on lake water quality: Limitations on organic carbon-driven alkalinity generation in acidic pit lakes. Water Resources Research 44, W10414, doi:10.1029/2007WR005959

Samper J, Yang C, Zheng L, Montenegro L, Xu T., Dai Z, Zhang G, Lu C, Moreira S (2012) CORE2D V4: A Code for Water Flow, Heat and Solute Transport, Geochemical Reactions, and Microbial Processes. In: Zhang F, Yeh GT, Parker J (2012) Groundwater Reactive Transport Models, 160–185.

Werner F, Eulitz K, Graupner B, Müller M (2008) Pit Lake Baerwalde Revisited: Comparing Predictions to Reality, in Proceedings 10th International Mine Water Association Congress – Mine Water and the Environment, N. Rapantova, H. Zbynek and J. Zeman (eds), 10th International Mine Water Association Congress, 2–5 June 2008, Karlovy Vary, Czech Republic, Ostrava, pp. 623–626.

Wolery TJ, Daveler SA (1992) EQ6, A computer program for reaction pat modeling of aqueous geochemical systems: theoretical manual, user’s guide, and related documentation (version 7.0). Lawrence Livermore National Laboratory, UCRL-MA-110662.

Some problems concerning determination of barium in mine waters of Upper Silesia (Poland)

Aleksandra MUSIOLIK[1], Irena PLUTA[2]

[1]*Central Laboratory of Investigation and Research, Jastrzębie Zdrój, Poland, e-mail abmusiolik@wp.pl*
[2] *Central Mining Institute, Department of Water Protection, Plac Gwarków 1 40–166 Katowice, Poland e-mail i.pluta@gig.katowice.pl*

Abstract Insoluble precipitates in mine waters of coal mines in Upper Silesia (Poland) contain mostly barium sulphate and are characterized by varying granulation. These solid-phase deposits precipitate under intensive flowing and mixing conditions in mine workings and pipes pumping mine waters to the surface. They contain up to 10–15 % of small granulation less than 0.45 mm. Using recommended procedure to analyze barium in mine waters, both the soluble barium ion and the insoluble forms with grains from 0.1 to 0.45 mm are determined. We recommend using membrane filters with pore size less than 0.1 mm.

Keywords Mine waters, Upper Silesia, Barium Sulphate, Mine deposits, solid phases

Introduction

Natural mine waters of various origin and chemical composition flow into coal mines of Upper Silesia in Poland. Chemical composition of these waters results from natural (geogenic) hydrogeochemical processes and anthropogenic activities linked to the mining industry, causing differences in the content of barium and sulphate (VI) ions. In natural mine waters of the Upper Silesian Coal Basin concentrations of barium reach up to 2910 mg/dm^3 and of sulphate (VI) up to 8170 mg/dm^3 (*e.g.* Pluta 2005, 2011). In some coal mines waters with different contents of these compounds are mixed in the mine workings and insoluble precipitates, suspensions, colloids or mineral deposits are formed.

Analysis of barium and other micro-components in mine water consists of determination of the soluble form, *i.e.* barium ions (Nielsen 1991; Standard Methods 1989; Ordinance of the Minister of Environment 2006). According to Polish Law, analytical methods appropriate for groundwater and for mine water drained into surface waters can be used for this purpose. All mandatory analytical methods require water samples to be filtered with membrane filters with pore size 0.45 mm.

This paper presents results of the studies of the barium insoluble forms (mineral deposits, solid phases) precipitated in mine waters and pipes of mine-water transporting systems in coal mines of Upper Silesia.

Analytical methodology

Water samples were taken from mine workings of the Krupiński and Zofiówka coal mines, in which precipitation of barium takes place. Samples of mine water from Krupiński mine were taken and barium precipitated with sodium sulphate in the laboratory. The precipitation was variously conducted with the stirrer operating at 120 rotations per minute, by shaker, by hand mixing and without stirring.

Solid-phase deposits precipitated in mine waters and transportation systems were analyzed for granulation and chemical composition. Granulation measurements were performed employing a laser granulometer. The method allows determination of grains with size varying from 0.05 to 900 mm. Chemical composition of the insoluble forms was determined by sequential X-ray fluorescence (WD XRF) with wavelength dispersion using the

PRIMUS II spectrophotometer. Photographs of solid-phase deposits precipitated from mine waters were taken using the microscope at 10 and 110 times enlargements.

Results

Chemical composition of mineral deposits and solid phases precipitated in mine waters

Solid-phase deposits occur during mixing of the barium-containing natural mine waters flowing out of the Carboniferous strata, waters containing sulphate (VI)), waters removed from various mining technologies and the added sodium sulphate. These insoluble forms containing up to 53 % of barium occur mainly in mine waters flowing in mine workings, galleries and in pipes through mining floors up into the surface. They contain: $BaSO_4$, $CaSO_4$, $MgSO_4$, $SrSO_4$; or $BaSO_4$, $CaSO_4$, $SrSO_4$; or $BaSO_4$, $SrSO_4$; but mostly barium sulphate. For example, a typical deposit consists of $BaSO_4$ (94.1 %), $CaSO_4$ (3.3 %) and $SrSO_4$ (1.6 %) or $BaSO_4$ (86.4 %) and $SrSO_4$ (7.8 %). The varying chemical composition of insoluble forms results from different chemical compositions and origins of natural mine waters of the Carboniferous strata (*e.g.* Różkowski *et al.* 2004; Pluta 2005, 2011).

Granulation of solid phases precipitated in mine waters flowing in the mine workings

The histogram of granulation of the solid phase in mine water of the Krupiński coal mine is shown in Fig. 1. Like others, these insoluble forms have precipitated in mine waters flowing in the mine workings. They consist of two fractions: one with the size ranging from about 0.1 to 1.0 mm and the other with sizes from about 5 to 300 mm. The dominant fraction has the higher granulation. The solid phase also contains grains with size less than 0.45 mm.

In order to explain the differences in granulation the process of barium precipitation in mine water from Krupiński coal mine was studied under various types of mixing in the laboratory.

Granulation and appearance of the deposit precipitated in mine water under intensive mixing with sodium sulphate (stirrer)

Precipitation of barium and other ions in mine water using sodium sulphate was conducted with a stirrer operating at 120 rotations per minute. The size of grains of the resulting deposit was measured. The histogram of the granulation and appearance of the deposit are depicted in Fig. 2. It is evident that two fractions dominate: one with grain size from 0.1 to 1.0 mm and the other from a few to about 30 mm. The latter fraction is more abundant.

The deposit contains about 15 % grains smaller than 0.45 mm in diameter.

Granulation and appearance of the deposit precipitated in mine water under intensive mixing with sodium sulphate (shaker)

Fig. 3 displays the histogram of granulation of the deposit precipitated in mine water under intensive mixing with sodium sulphate in the shaker. Similar to the previous case, the histogram shows two fractions, with granulation in the range from 0.1 to 1.0 mm and from a few to about 30 mm. The external appearance

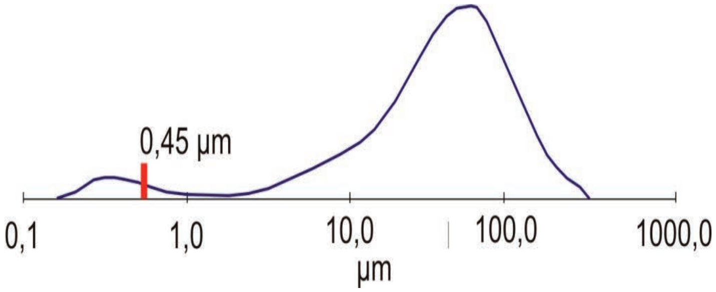

Fig. 1 *Histogram of granulation of the solid phase precipitated in mine water flowing in mine workings*

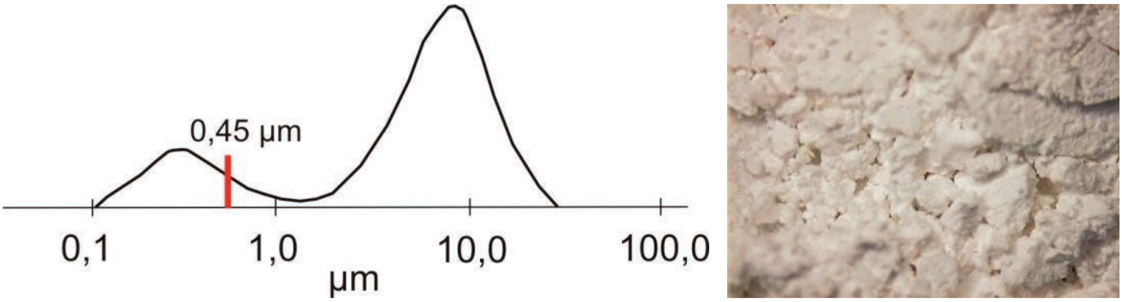

Fig. 2 *Histogram of granulation and appearance of the deposit precipitated in mine water under intensive mixing with sodium sulphate (stirrer)*

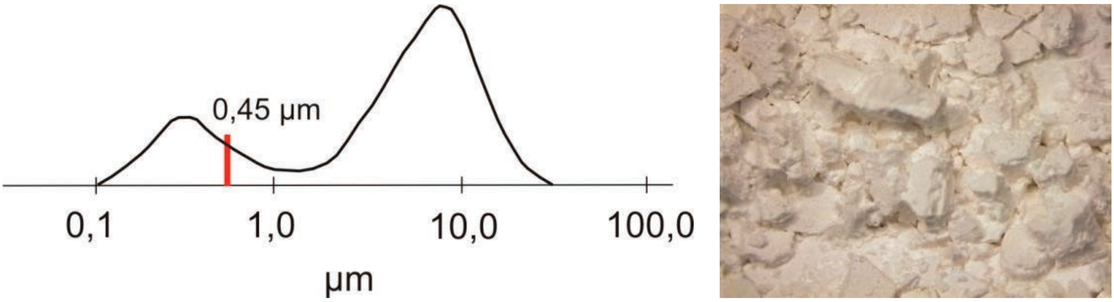

Fig. 3 *Histogram of granulation and appearance of the deposit precipitated in mine water under intensive mixing with sodium sulphate (shaker)*

of this deposit is also similar to the previous one.

Granulation of the deposit precipitated from mine water under gentle mixing with sodium sulphate (manual mixing)

The deposit precipitated under a few minutes of gentle, manual mixing shows the granulation without any dominant fraction (Fig. 4). The fraction of grains less than 0.45 mm is small. Granulation reaches up to approximately 800 mm.

Granulation and appearance of the deposit precipitated in mine water after adding sodium sulphate without mixing

The deposit obtained without mixing shows granulation in the range from about 50 to 1000 mm (Fig. 5), with the majority of the deposit in the range above 100 mm. This deposit does not contain grains with size less than 0.45 mm.

Granulation and appearance of the solid phase precipitated in the pipe filled with mine waters

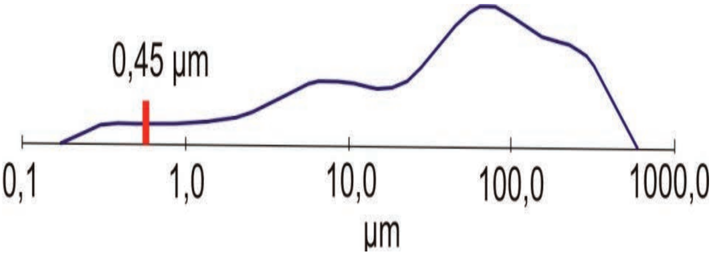

Fig. 4 *Histogram of granulation of the deposit precipitated from mine water under gentle mixing with sodium sulphate (manual mixing)*

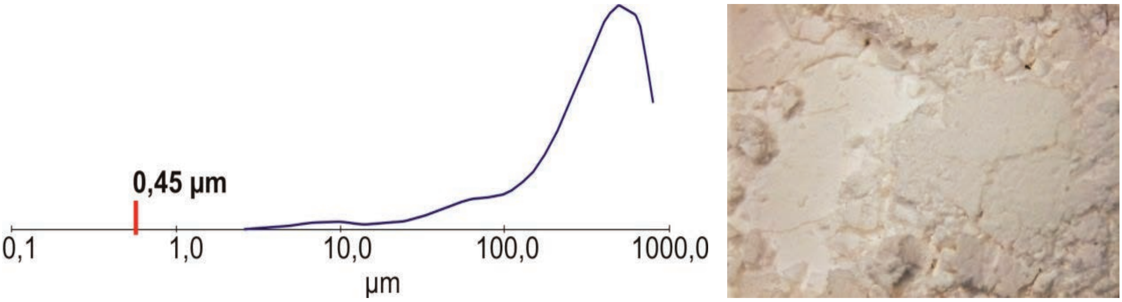

Fig. 5 *Histogram of granulation and appearance of the deposit precipitated in mine water after adding sodium sulphate without mixing*

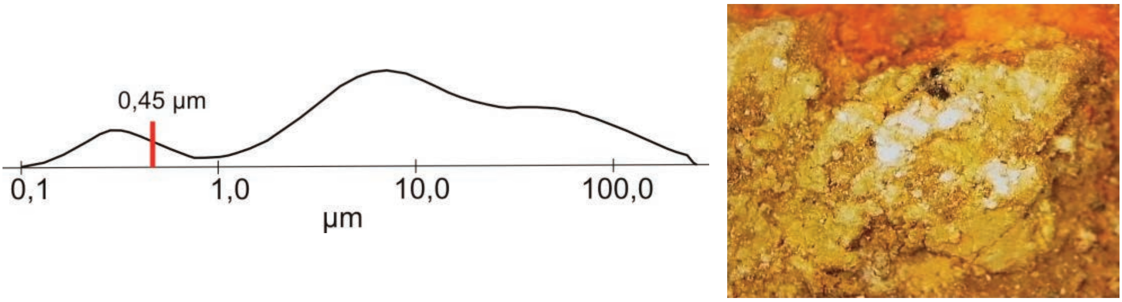

Fig. 6 *Histogram of granulation and appearance of the solid phase precipitated in the pipe filled with mine waters flowing from the underground sedimentation tank*

flowing from the underground sedimentation tank

Granulation of the solid phase precipitated in the pipe filled with mine waters flowing from the underground sedimentation tank toward the pump moving water to the surface is characterized by three ranges: from 0.1 to 1.0 mm; from a few to about 30 mm; and above 30 mm (Fig. 6). The fraction from few to 30 mm is the majority. The contribution of grains less than 0.45 mm is about 10 %.

Granulation of the solid phase precipitated in the pipe with water pumped out into the surface

Solid phases precipitated in the pipe in which mine water was pumped out into the sedimentation tank on the surface are characterized by granulation similar to the deposits formed in the laboratory under intensive mixing. Two fractions are present: from 0.1 to 1.0 mm and from a few to approximately 40 mm (Fig. 7). The solid phase contains about 10 % grains with the size less than 0.45 mm.

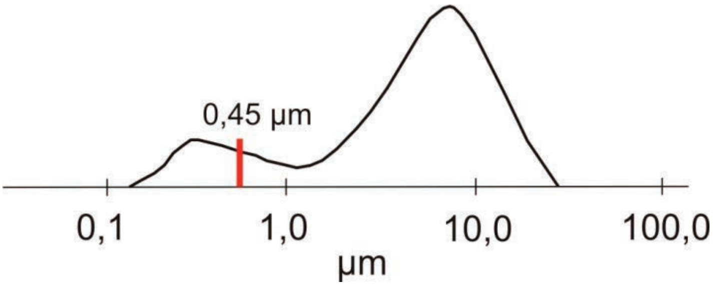

Fig. 7 *Histogram of granulation of the solid phase precipitated in the pipe with water pumped out into the surface*

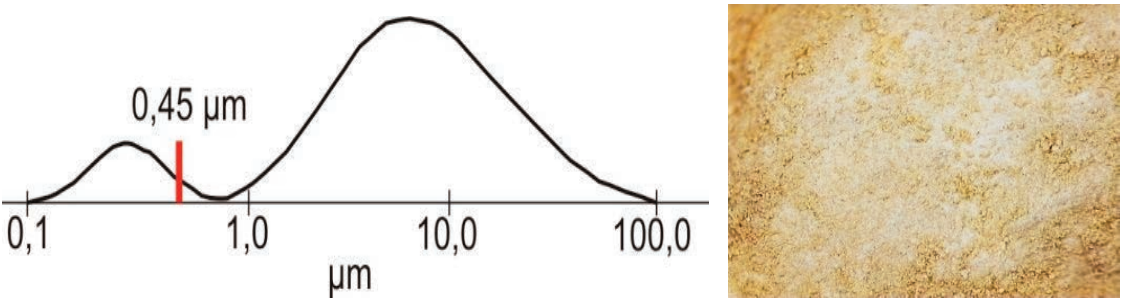

Fig. 8 *Histogram of granulation of the deposit precipitated in the pipeline of the Olza Collector*

Granulation and appearance of the solid phase precipitated in the pipeline of the Olza Collector

Water pumped up out of the mine flows into the sedimentation tank on the surface, from which after a few days (about 3–5) it is pumped into the Olza Collector pipeline carrying mine water into the Oder river. The histogram of the granulation and the appearance of the solid phase precipitated in the pipeline of the Olza Collector are depicted in Fig. 8. This solid phase contains two fractions of granulation: from 0.1 to 1.0 mm and from 1.0 to almost 100 mm. The contribution of grains less than 0.45 mm is about 15 %.

Interpretation and summary

Studies of solid phases and mineral deposits precipitated in mine waters of coal mines in the Upper Silesia (Poland) show variability of their composition and granulation. They contain mostly barium sulphate and are characterized by varying granulation. Two fractions of the deposits precipitated in mine waters mixed with sodium sulphate – one from 0.1 to 1.0 mm, and the other from a few to approximately 100 mm – are formed under intensive mixing of mine waters. Similarly, two ranges of granulation have been found in the solid phases precipitated in mine waters flowing in mine workings, in pipes with mine waters being pumped out into the surface, and in the Olza Collector pipeline. Lower mixing speed favors the deposit with larger grains and sometimes continuous granulation up to several hundreds of mm.

All solid phases and deposits in coal mine waters are characterized by up to 20 % small granulation from about 0.1 to 1.0 mm. This fraction also contains particles of less than 0.45 mm diameter. Solid phases from intensively flowing mine waters contain about 15 % of grains less than 0.45 mm. Using the recommended procedure to analyze barium in mine waters, both the soluble barium ion and the insoluble forms with grains from 0.1 to 0.45 mm are determined. Changes of the granulation of deposits and solid phases depend on the speed of the flowing waters. Therefore, it is highly recommended to use membrane filters with pore sizes less than 0.1 mm when barium in mine waters is to be determined.

References

Bojakowska J, Sokołowska G (1998) Influence of mining and metallurgy on pollutants in sediments of Oder river (in Polish). Przegląd Geologiczny, 7:603–608

Nielsen DM (1991) Practical handbook of groundwater monitoring. Chelsea, Lewis Pub., 1991, p.717.

Ordinance of Minister of Environment 2006 in Poland (w sprawie warunków jakie należy spełniać przy wprowadzaniu ścieków do wód lub do ziemi oraz w sprawie substancji szczególnie szkodliwych dla środowiska wodnego, Dz. U. 2006, Nr 137, poz. 984 z późniejszymi zmianami).

Pluta I (2005) Wody kopalń Górnośląskiego Zagłębia Węglowego – geneza, zanieczyszczenia i metody oczyszczania, Prace Naukowe GIG, No 865, 169 pp (in Polish).

Pluta I (2011): Hydrogeochemia utworów karbonu obszarów górniczych południowej części

Górnośląskiego Zagłębia Węglowego. Wyd. GIG, 171 pp (in Polish).

Różkowski A *et al.* (2004) Hydrochemical environment of Carboniferous coal-bearing formations of the Upper Silesian Coal Basin (in Polish), SU, Katowice 2004, p 174

Standards Methods for the Examination of Water and Wastewater, Pub. APHA Public Heath Ass., AWWA and WPCF, 17th Ed, 198

Metal pollution sources and transport in mined watershed: an insight from Ermelo Coalfield, South Africa

N. O. Novhe[1], R. Netshitungulwana[2], B. Yibas[3], T. Motlakeng[4], E. Sakala[5]

Council for Geoscience, 280 Pretoria Rd, Silverton, 0184, South Africa,
[1]onovhe@geoscience.org.za,[2]robertn@geoscience.org.za;
[3]byibas@geoscience.org.za;[4]tmotlakeng@geoscience.org.za; [5]esakala@geoscience.org.za

Abstract Metal pollution of water resources is a widespread environmental problem facing a supply of drinking water in South Africa. An investigation has been conducted in respect of a mined watershed in the Ermelo coalfield to identify metal pollution sources and associated pathways. Pollution is derived primarily from both abandoned and operational coal mines, in a form of acid mine drainage characterised by low pH and high concentration of Fe, Al, Mn and SO_4^{2-}. Streams are the major pollutants pathways. Ground geophysical surveys also revealed potential shallow pollution plume. The work conducted has enabled proper prioritization of the identified pollution hotspots and selection of appropriate cost-effective pollution management plan at point sources.

Keywords Coal mines, acid mine drainage, metal pollution, Ermelo Coal Field,

Introduction

Most of the coal mines in South Africa are affected by acid mine drainage, and over years this has led to a deterioration in the water quality in many surface streams (Geldenhuis and Bell 1998). The environmental impacts of AMD have been reported in the coal mine sites (Bell *et al.* 2001, McCarthy and Pretorius 2009, McCarthy 2011). Acid mine drainage, owing to its high content of dissolved solids, suspended solids and iron, low pH value and its possible toxicity, can render the water in the receiving water bodies unfit for many applications, unless costly treatment is applied. Concerns have been raised relating to pollution of domestic water supplies. More spectacular metal pollution incidents have occurred recently, such as the pollution of the Boesmanspruit dam in the Ermelo coalfield situated south of Carolina in the Mpumalanga Province (Fig.1). The dam is an abstraction point that feeds the municipal water treatment works for domestic water supply, and its contamination with elevated metal contaminants has resulted in failure to meet the required water quality standard for domestic use and disruption of water supply to the surrounding communities. This work focus on the investigations conducted in the area around the Boesmanspruit dam, to identify and characterise pollution sources, pathways/ transport and to propose suitable management measures.

The area falls within the quaternary drainage region 11XB, which forms part of the Komati West sub-catchment in the Inkomati Water Management Area. The X11B sub-catchments form a watershed between two larger catchments feeding two non-perennial tributaries of the Boesmanspruit. Geologically, the area forms part of the Ermelo Coalfield, situated south of Carolina. The northern and eastern boundaries are defined by the sub-outcrop of the coal-bearing strata against pre-Karoo rocks. All of the coal Seams occur within the Vryheid Formation of the Ecca Group, Karoo Supergroup. Sandstones with subordinate shales represent the bulk of the Vryheid formation (Bell and Jermy 2002). Currently, the area is comprised of both abandoned and operational coal mines, most of which are situ-

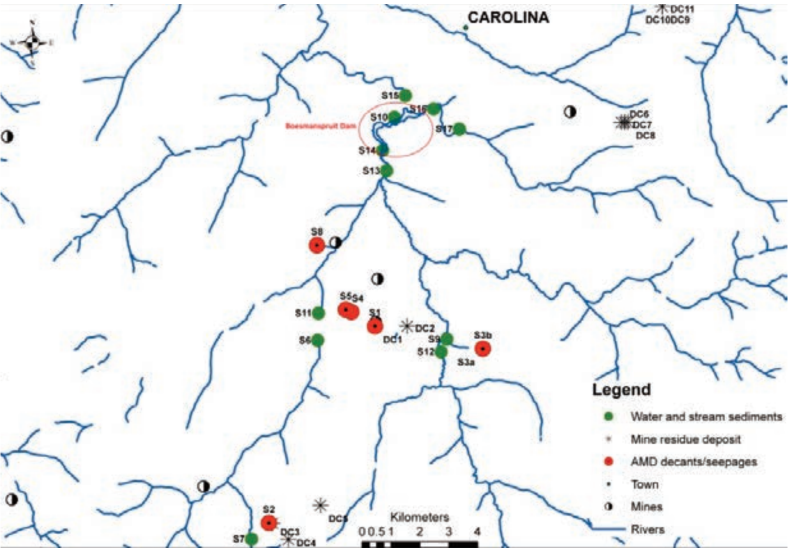

Fig. 1 *Location of Boesmanspruit dam and associated tributaries*

ated upstream of the Boesmanspruit dam (on the southern portion of the area). Of the total saleable production of 222.551 Mt in 2001, the Ermelo Coalfield contributed about 7.2 Mt (Jeffrey 2005).

Material and methods

Fieldwork observation and sampling have been conducted to identify and characterise pollution sources in the area. Both water (discharges from flooded underground mines, leachate from mine residues and stream water) and solid (mine residue deposits and stream sediments) samples have been collected and analysed. Water samples were analysed by means of ICP-MS and IC analytical techniques and the elements concentrations were compared to the South African domestic water quality standard. Solid samples were analysed by means of XRF, XRD and ICP-MS analytical techniques for metal loadings and mineralogical compositions. Acid base accounting (ABA) was also conducted on the mine residues samples to determine the potential of acid generation. Two geophysical methods namely Frequency Domain Electromagnetic (FDEM) profiling and electrical resistivity tomography (ERT) were applied in order to identify depth and lateral extent of any possible pollution plume. The 20 m horizontal coil separation of EM34 FDEM unit used has depth of investigation of about 15 m while IRIS Syscal Pro ERT system can probe up to around 40 m depth.

Results and discussions

The pollution manifest itself in a form of acid mine drainage seepages as well as run-off from mine residue deposits, such as discard coal dumps and slimes; decants from flooded abandoned underground coal mines; and seepages of acid mine drainage from abandoned backfilled open cast mines. Most of the identified pollution sources are situated upstream of the Boesmanspruit dam, and in some areas there is direct discharges/seepages into the tributaries of the Boesmanspruit (Fig. 1). Onsite and laboratory analyses of the water parameters, such pH, Electrical conductivity (Ec), and metal composition have been conducted in respect of the identified pollution sources and the adjacent streams.

All the sampling points are indicated in Fig. 1 and the results are summarised under Table 1 and 2. The analytical data is compared with the limit for human consumption, as per the Department of Water Affairs (DWAF) guideline. These problem areas are generally characterised by low pH, with elevated concentration as much as two and even three orders of mag-

Sample ID	pH	Ec mS/m	Fe (mg/L)	Al (mg/L)	Mn (mg/L)	SO_4^{2-} (mg/L)	As(mg/L)
	6-9*	N/A	0-0.1*	0 - 0.15*	0-0.05*	0-200*	0-0.01*
S1	2.4	1,017	3,307.23	820	264.62	21,492.52	0.98
S2	3	710	2,091	261.35	14.4	4,404.09	0.05
S3a	3.1	235	308	37.24	23.7	2,067	0.06
S3b	3.2	280	128	26	32	1,889	0.05
S4	3	170	2.67	3.31	42.32	1,243	0.05
S5	3	157.2	4.9	1.16	20.52	952	0.05
S8	6.9	11.64	4.0	0.3	1.16	10	0.04

*Department of Water Affairs limit for Human consumption

Table 1 Analytical data for acid mine drainage sources in the study area

Sample ID	pH	Ec mS/m	Fe (mg/L)	Al (mg/L)	Mn (mg/L)	SO_4^{2-} (mg/L)	As(mg/L)
	6-9*	N/A	0-0.1*	0 - 0.15*	0-0.05*	0-200*	0-0.01*
S6	3.8	145	<0.1	6.77	36.04	929	0.04
S7	4.6	16.07	0.28	275	0.04	31	0.05
S9	7.4	9.02	< 0.1	0.3	0.24	7	0.04
S10	4.3	65.5	<0.1	2.41	10.43	361	0.04
S11	7.3	8.84	<0.1	0.28	0.08	7	0.04
S12	7.2	111	<0.1	0.27	1.45	622	0.04
S13	6.8	9.63	< 0.1	0.34	0.05	4	0.04
S14	7	32	< 0.1	0.31	0.15	69	0.04
S15	7	56.7	< 0.1	0.4	0.28	265	0.04

*Department of Water Affairs limit for Human consumption

Table 2 Water quality data for the Boesmanspruit dam and associated tributaries

nitude of Fe, Al, Mn and Sulphate most and slightly elevated As than the acceptable limit. The analytical data is summarised in Table 1.

Mine residue deposits

Mine residue deposits (MRDs), such as discard coal and slimes, are denoted as DC1 to DC11. Based on acid base accounting results, Ermelo coalfield MRDs are classified as potential acid generating. Fig. 2 shows subdivision according to the ration of AP and NP (NPR). Majority of the samples plot at NPR>1. The acid potential of all the samples exceeds the neutralization potential. The acid potential (AP) ranges from 11 kg $CaCO_3$/ton to 250 kg $CaCO_3$/ton, whereas neutralization potential (NP) ranges from - 11 kg/ton $CaCO_3$ to 24 kg $CaCO_3$/ton. The sulphur percentage ranges from 0.9 to 8 %, averaging at 2 %. Based on XRD results, pyrite is the important acid producing mineral, whereas kalionite, mica and plagioclase are the potential acid consuming minerals. XRF results identified Al, Mn and Fe as potential pollutants that may affect the quality of water, provided the physico-chemical conditions prevailing at the MRDs site allow leaching of these metals in significant amounts. In addition, As, Ni, Co are intermediate in concentration. Analyses in respect of seepages from mine residues samples (DC1 and DC2) also revealed low pH and high concentration of Fe, Al, Mn and SO_4^{2-} (ranges from 2,091–3,307; 261–820; 14-264 and 4,404–21,492 in mg/L respectively). It was also observed during the time of investigation that in

Samples ID	Fe (57)	Al (27)	Mn (55)	V (51)	Cr (52)	As (75)
S6	25,985.5	35,696.6	302.6	47.2	78.0	4.9
S8	7,626.1	12,937.9	61.2	18.1	25.9	<2
S7	63,541.0	43,193.5	1,780.3	153.6	304.6	11.4
S10	6,003.8	9,484.7	69.1	11.2	25.3	<2
S11	126,209.0	66,954.8	1,151.6	107.2	126.3	19.3
S12	49,967.4	46,057.5	762.5	88.3	217.6	6.6
S13	14,897.0	19,160.1	166.9	21.4	34.5	<2
S14	12,357.0	19,266.2	129.9	25.1	75.3	<2
S15	7,272.1	12,725.8	99.3	14.7	38.2	<2
S16	16,215.0	13,655.4	120.4	31.6	118.6	2.1
S17	18,141.2	22,977.3	218.0	40.4	56.7	2.5

Table 3 *stream sediments geochemistry of the study area (as ppm)*

some areas the river, dam and ponds were filled with coal fines, especially in the central tributary. As indicated by ABA results, the coal fines also have a potential to contribute to the generation of AMD, and the possible sources are the adjacent mining activities through runoff associated with poor storm water management measures or poorly designed mine dump residues.

Geophysical surveys were done across two streams to investigate the lateral and depth extents of a possible contaminant plume from coal mine tailings. FDEM and ERT surveys were carried out a south-north line (Fig. 3). FDEM method identified high conductivity zone with readings of the order of 250 mS/m at depth of 15m. ERT survey identified a sub-vertical low resistivity zone which extends to depth at station 50 m. The bedrock is deepest within this zone. An abrupt break in the bedrock topography at station 200 m could be due to a saturated dipping fault zone as evidenced by very low resistivity values of about 20 Ωm. Visible traces of mine residue (AMD) in water were noted on surface at this point corresponding to water sample number S7. The interpreted fault zone extends to depths greater than 40 m could be a potential plume or pathway to groundwater resources.

Underground flooded and Backfilled open cast mines

Decants from abandoned underground mines have been identified in the area, denoted as S3 and S8. Field tests, in respect of decant point S3 revealed that the water quality is very poor (pH = 3.1, EC = 235 mS/m) with elevated concentration of Al, Mn, Fe and sulphate (37.24, 308.0, 23.70 and 2067 in mg/L respectively). The flow/discharge rate was determined using the bucket and stop watch method, and was found to be 50.3 m^3/day). The analyses conducted in respect of decant S8 show that the water quality is not as poor as S3. The pH is near neutral (pH = 6.9) but with elevated Fe, Al, Mn than the acceptable limit (4.0, 0.3 and 1.16 in mg/L respectively). Several subsidence areas and sinkholes have been identified in areas around the

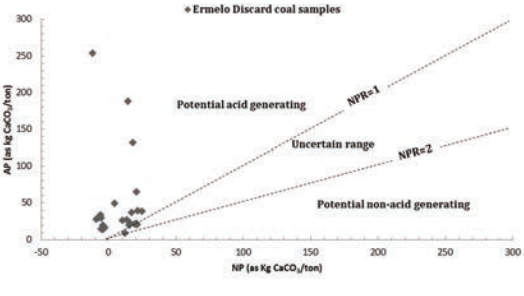

Fig. 2 *Acid Potential vs. Neutralisation potential graph indicating areas of likely acid generation and unlikely acid generation*

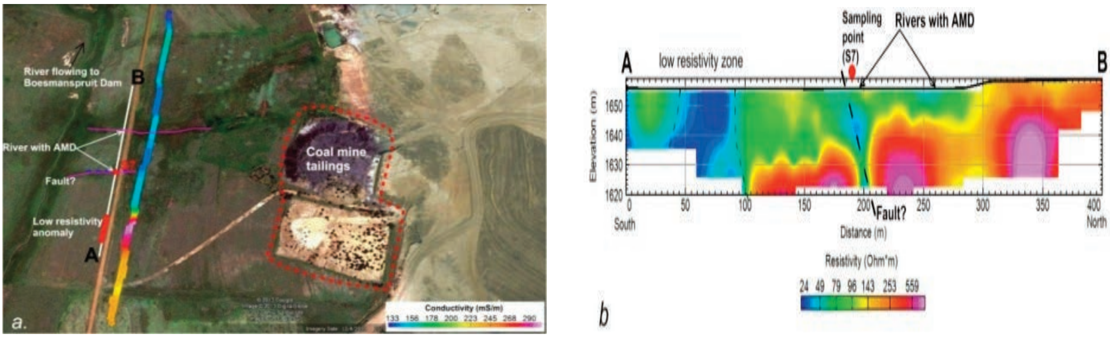

Fig. 3 *Geophysical survey results showing (a) elevated earth conductivity values above 250 mS/m and (b) interpreted fault zone where AMD flows on surface at one coal mine south of Boesmanspruit dam*

decant points, indicating failures in respect of the remaining mine workings (such pillars). Investigation done by Vermeulen and Usher (2006) concerning recharge in South African underground collieries, revealed subsidence areas and sinkholes as potential water ingress points. AMD also emanates from old opencast workings which have been backfilled (S4 and S5).

Pollutants pathway and metal fate

Streams are considered as major pollutants pathways/transport. The analytical data for the water quality and stream sediments geochemistry are summarised in Table 2 and 3. For the water quality, comparison was made with the targeted limit for human consumption as per DWAF guideline showed that the quality of water is generally poor, especially in the vicinity of pollution sources. Water sample number S7 and S6 generally show extremely poor water quality, comparing to other points that are situated downstream of the Boesmanspruit tributaries. Stream sample S6 is situated in close proximity of the old backfilled open cast mine area (hot spots number S4 and S5) which seeps AMD into the central tributary. Sample S7 is situated in immediate proximity of an old mine residues dump (DC2, DC3 and DC4), which also discharge acid leachate into the central tributary. However, the water quality improves downstream or away from the AMD sources. The general downstream improvement in water quality could be attributed to natural attenuation associated with the existence of extensive wetlands in the area. The wetlands serve as a sink for pollution where polluting metals are trapped in sediments and peatlands (Tutu *et al.* 2008). The dam (S10) was acidic during the time of investigation, with a pH of 4 and is comprised of high levels of Al, Mn, and sulphate and As (2.4, 10.43, 361 and 0.04 mg/L respectively). The high concentration of the metals in the dam as compared to the stream tributaries could be attributed to the low pH.

The stream sediments results also show that the major contaminants in the area include Fe, Al, Mn, whereas minor contaminants include As, V and Cr. The metal fate in the stream follow similar pattern as the water samples, in that the concentration decreases away from the pollution sources. Sample number S6, S7, S11 and S12 that are situated upstream, in close proximity of the pollution sources, are comprised of high concentration of the major contaminants Fe, Al and Mn (in a range of 25,985–126,209; 35,696–66,954 and 302–17,80 in mg/kg respectively). The downstream samples also show decreased concentration of Fe, Al and Mn (in a range of 7,272–18,141; 12,725–22,977 and 99–218 in mg/kg respectively). The dam (S10) also shows decreased concentration of the major contaminants Fe, Al and Mn (7,626; 9,484 and 69 in mg/kg respectively).

Conclusions and Recommendations

The metal pollution of the Boesmanspruit dam is associated with the coal mining activities (both active and abandoned), and might continue for a long period unless proper management measures are developed and implemented. However, the extent in which individual mines contribute towards the problem is not yet known due to the lack of long-term flow data in the catchment.

Major pollutants in the surrounding surface water include Al, Mn, Fe and sulphate which are the major environmental signatures of the Ermelo Coalfield and are associated with acid mine drainage. Major pollution sources relate to decant of acid mine drainage from flooded underground coal mines and seepages associated with backfilled open cast mines and mine residue deposits. Streams are the major pollutants pathways/transport into the domestic water supply dam. The concentration of contaminants decreased downstream and away from the pollution sources. Ground geophysical surveys revealed elevated electrical conductivity readings above 250 mS/m at 15 m depth and an interpreted fault zone could be a possible conduit of pollution from the old coal mine dump.

It is recommended that the identified pollution sources such as decants and seepages from the back filled opencast mines be treated at point source. Suitable passive treatment can be implemented based on the quality of the water to be treated and the required water quality standard. Measures to reduce ingress of water into the backfilled open cast area and the abandoned underground must also be investigated.

Proper storm water management measures must be put in place in respect of the mine residue deposits sites, to contain the seepages and prevent further runoff. An extensive mapping of the areas contaminated with coal fines/carbonaceous sediments and development of appropriate cleaning measures must be conducted.

Acknowledgements

The authors thank the Department of Mineral Resources for financial support. Lusunzi Rudzani, Modiba Moleboeng, Madikizela Khaya, Kwata Maphuthi, Scasamba Sisanda and Mchunu Philani are also thanked for their assistant in the field.

References

Bell FG, Bullock SET, Hälbich TFJ, Lindsay P (2001) Environmental impacts associated with an abandoned mine in the Witbank Coalfield, South Africa. International Journal of Coal Geology 45:195–217

Bell FG, Jermy CA (2002) An investigation of primary permeability in strata from a mine in the Eastern Transvaal Coalfield, South Africa. Quarterly Journal of Engineering Geology and Hydrogeology 35: 391–402

Department of Water Affairs and Forestry (1996a) South African Water Quality. Guidelines (second edition), Volume 3: Industrial Use.

Geldenhuis S, Bell FG (1998) Acid mine drainage at a coal mine in the eastern Tranvaal, South Africa. Environ Geology 34:234–242

Jeffrey LS (2005) Characterization of the coal resources of South Africa. Jornal of South African Institute of Mining and Metallurgy 106: 453–458

McCarthy TS, Pretorius K (2009) Coal mining on the Highveld and its implications for future water quality in the Vaal River system. International Mine Water Conference 19th – 23rd October 2009. Proceedings ISBN Number: 978-0-9802623-5-3 Pretoria, South Africa.

McCarthy, TS (2011). The impact of acid mine drainage in South Africa. South African Journal of Science, 107(5/6): 1 – 7

Tutu H, McCarthy TS, Cukrowska E (2008) The chemical characteristics of acid mine drainage with particular reference to sources, distribution and remediation: The Witwatersrand Basin, South Africa as a case study. Applied Geochemistry 23: 3666–3684

Reclamation of a Pit Lake at a Coal Mine in the Pacific Northwest

Arthur O’Hayre[1], Paul Kos[1], Dennis Morr[2]

[1]Norwest Corporation, 950 S. Cherry St., #800, Denver, CO, 80246 USA, aohayre@norwestcorp.com
[2]TransAlta Centralia Mining, LLC., 913 Big Hanaford Rd, Centralia, WA USA, Dennis_Morr@transalta.com

Abstract TransAlta Centralia Mining, LLC (TCM) developed reclamation plans for the Central Packwood Pit at its Centralia Mine in Washington that included a pit lake. Models of pit lake hydrology and water quality were developed to guide the reclamation plans and to support the probable hydrologic consequences assessment. The modeling relied on the extensive water quantity and quality data collected at the site. The model predictions were then coupled with relevant water quality and limnological information from near neutral pit lakes and natural lake analogues in order to assess the likely biochemical and limnological conditions for the lake.

Keywords pit lake, mine reclamation, probable hydrologic consequences

Introduction

TCM is currently conducting reclamation at the Centralia Mine located about 6 mi (9.7 km) northeast of the town of Centralia, Washington. Plans for reclamation of the Central Packwood Pit were revised after mining was discontinued following a slope failure in the pit footwall. The revised plans addressed reclamation of approximately 460 ha of disturbed land, including designs for a pit lake of approximately 87.7 ha, referred to as the Central Packwood Lake.

This paper describes the development of the water balance and water quality models that were used to support the design of the pit lake and for the probable hydrologic consequences assessment (PHC) of the reclamation plan. The PHC assessment included the expected range in lake filling times, the expected fluctuations in lake levels and lake outflows, the expected water quality in lake outflows, and the expected water quality and limnological conditions within the lake. The lake water balance and the mass balance water quality model were supported by considerable site data. Results from geochemical modeling and from natural lakes and pit lake analogues were also used in the assessment.

Climate data, including precipitation, evaporation, temperature and wind speed, have been collected at the Centralia Mine since 1981. The site has a predominately marine climate, characterized by mild temperatures. A dry season extends from late spring to midsummer, with precipitation frequently limited to a few light showers. Winter storms are common with strong winds and heavy precipitation during the months from October through March. These storms are frequent and may continue for several days. TCM has also obtained periodic measurements of groundwater elevations and water quality sampling from a network of monitoring wells and has conducted aquifer tests at these wells. Water quality samples have also been collected from surface runoff from active mine areas and reclaimed areas. These data have been used to develop the pit lake water balance and water quality predictive models. Furthermore, TCM has obtained water balance measurements at Pit 7, a flooded mine pit, and water quality samples at selected depths from partially flooded mine pits. These data have been used to assess the reliability of the predictive models and assessments.

Water Balance Modeling

The water balance model is fundamental to the design of the pit lake and for predicting solute loads to the lake. A pit lake daily water balance simulation model was constructed using the pit lake bathymetry, groundwater inflows (GWin) using simplified groundwater flow equations, and estimates of daily surface water inflows (SWin), direct precipitation on the surface of lake (P), the evaporation from the surface of the lake (E), and surface water outflows (SWout). The daily change in pit lake water volume ΔS was simulated using the general water balance equation:

$$\Delta S = P + SW_{in} + GW_{in} - E + - SW_{out}$$

P and E in the water balance are determined from the daily precipitation and evaporation records from the eleven year record and the lake surface area corresponding with the water elevation in the lake in the water balance simulation. The daily change in the pit lake water elevation in the water balance simulation is calculated from the daily change in water volume (ΔS) divided by the lake surface area at the simulated water elevation in the lake. The surface water outflow (SW_{out}) is the lake outflow calculated using the outlet rating curve and the water elevation in the lake. Models for simulating surface water inflows (SW_{in}) and groundwater inflows (GW_{in}) are required to complete the lake water balance simulation. The lake water balance analysis was simulated on a daily basis to provide information on the expected fluctuations in lake levels and lake outflows.

The groundwater inflow to the pit has been negligible during mining and pumping was required only for pit inflows from surface runoff during and immediately following precipitation events. The Dupuit-Forchheimer radial flow discharge formula (Bear 1979) was used to estimate groundwater inflow from the mine spoils along the east of the lake and from the undifferentiated bedrock and coals around the south and west sides of the lake. The one dimensional form of the steady-state analytical equation was used to estimate groundwater inflow from the alluvium and underlying bedrock on the north side of the lake. The hydrogeological characteristics and the boundary conditions for the analytical models were derived from site monitoring wells, well tests and site groundwater investigations provided in the mine permit application. The approach modeled groundwater inflow as a series of steady state solutions. The empirical data and modeling results indicate that the overall rate of groundwater flow toward the pit is quite low relative to inflows from precipitation and surface water due to the low permeability and steeply dipping geologic strata.

Several rainfall-runoff models were evaluated in a water balance analysis of the flooded Pit 7 performed using records on daily rainfall and evaporation, pit pumping and periodic pit water level measurements. A seasonal curve number model using a curve number of 89 for the period from April 1 through October 31 and a curve number of 98 for the period from November 1 through March 31 was found to provide the best results for the Pit 7 water balance. These seasonal curve number estimates bracket the curve number estimate obtained from the empirical tables for bare soil at the site (Natural Resource Conservation Service 2004). These "calibrated" seasonal curve numbers were used to model the rainfall-runoff relationship during reclamation when the lake is filling.

The seasonal runoff curve numbers were adjusted to model the rainfall-runoff relationship for the lake water balance after final reclamation when the lake is full. The rainfall runoff response during the period from April 1 through October 31 is expected to decline considerably following reclamation because of the higher infiltration rates and higher evapotranspiration loss from the forest cover during this period. A seasonal curve number of 70 is specified in the Mine Permit Application for forest cover conditions at the site and was selected to represent the seasonal curve number for the low antecedent moisture conditions during the dry period from April 1 through Oct 31. A seasonal curve number of 96 was used to model the surface runoff and delayed interflow response to rainfall for the high antecedent moisture conditions during the wet period from November 1 through March 31. The reduction in the winter season curve number from 98 to 96 was selected based on the relatively low water loss during the winter by interception and evapotranspiration of the forest cover following reclamation.

While these seasonal curve number adjustments were initially based on professional judgment, the reliability of the estimates were evaluated by comparing the surface runoff volume estimated by applying the seasonal curve number model to a nearby 538 ha watershed with forest cover comparable to the reclamation cover planned for the Central Packwood Lake drainage. The surface runoff from this drainage was collected in a pond where it was pumped around mining operations. The pumped volume measured over a 19 month period was within 5 % of the net runoff volume estimated for this drainage using the seasonal curve number model and the daily precipitation and evaporation records.

Surface water runoff from the surrounding watershed provides about 65 % of the lake inflow when the lake is full. The remaining inflow is mostly from direct precipitation on the lake surface while groundwater inflows average only about 1.2 % of the total lake inflow. The simulation results show that the lake water elevations are below the outlet control elevation during the months of July through October, although the duration of the period of no outflow from the lake varies with the seasonal patterns of precipitation and evaporation. The annual lake outflows averaged 2.27 Mm^3 based on the 11-year simulation period. With a total lake capacity of 16.529 Mm^3, the mean residence time for water in the lake is estimated to be approximately 7.3 years.

Water Quality Modeling and Assessment

The evolution of water quality in the Central Packwood Lake will be controlled largely by the quality of water entering the lake during and after reclamation. Pit wall mineralogy is also cited as a control of pit lake water quality (Boehrer and Schultze 2006). However, the spoil material and the bulk of the overburden at the pit is not acid forming and the exposed coal seams and any acid forming overburden material will be covered with neutralizing spoil material. Thus, pit wall mineralogy is not expected to adversely impact lake water quality or pH levels.

The water balance modeling and representative concentrations for the various water sources were used to construct a mass balance model to simulate the evolution of water quality in the lake during lake filling and after reclamation. The water quality of the surface water draining the east spoil pile was used to represent the surface water quality entering the lake during reclamation operations. The water quality of surface water entering the lake following reclamation was based on the average concentrations in samples collected in runoff from reclaimed areas at the Centralia Mine. The median concentrations in samples from groundwater wells were used to represent the water quality in lake inflows from each of the groundwater sources around the lake.

The water quality modeling results for the lake during filling and after the lake is full are summarized in Table 1. These results show that sulphate and sodium are the dominant ions in lake water. The TDS and most of the major ions and trace constituents are predicted to decline over time due to the reductions in the concentrations in surface water inflows and the larger contribution of essentially pure water from precipitation when the lake is full. Nitrate concentrations are predicted to increase due to the site data indicating higher nitrate in surface water from areas following reclamation.

The pH of water entering the lake is projected to be near neutral based on samples of surface runoff from active mine areas and reclaimed areas. Although a mass balance of hydrogen ions could be used to model pH in the lake, pH was not modeled because it will be affected by biogeochemical processes within the

Constituent	Units	Lake Filling	Final
Total Alkalinity	mg/L ($CaCO_3$)	107	55
Calcium	mg/L	81.6	62.5
Chloride	mg/L	4.0	4.0
Iron	mg/L	1.378	0.380
Magnesium	mg/L	25.0	20.5
Manganese	mg/L	1.923	0.921
Nitrate/Nitrite	mg/L	0.195	0.423
Potassium	mg/L	4.9	3.2
Selenium	mg/L	0.0001	0.0004
Sodium	mg/L	197	75
Sulphate	mg/L	595	317
Total Dissolved Solids	mg/L	1033	579
Total Phosphorus	mg/L	0.713	0.175

Table 1 *Water Quality Modeling Results.*

lake and will vary with depth when the lake stratifies. The mass balance modeling approach treats all lake water quality parameters as conservative constituents. Concentrations of water quality constituents in the lake will deviate from the model predictions, depending upon the actual mass loading rates for various water sources and the influence of physical and biogeochemical processes within the lake. Iron and manganese can precipitate in the oxygenated waters of near neutral pit lakes and be removed by settling. Furthermore, a constructed wetland at the inlet to the lake is expected to result in reduced the iron and manganese loadings to the lake. Likewise, the chemical characteristics of the water entering the lake together with the climate of the site and the physical characteristics of the lake will influence biological processes, lake temperature, pH and chemical stratification. These processes will result in lake water chemistry that deviates to some degree from the mass balance modeling results. Nevertheless, the mass balance modeling results are still useful for geochemical modeling, for predicting trophic condition, and for assessment of likely biogeochemical processes within the lake and lake sediments.

The mass balance modeling indicates that total phosphorus loadings should stabilize at a level of approximately 0.0181 g/m^2 of lake surface per year. The phosphorus loading versus mean depth divided by residence time relationship in Vollenweider and Dillon (1974) indicates that lake will be oligotrophic. The trophic level and photosynthesis will have a significant influence on lake water quality. Calcium precipitation can be triggered by high pH levels corresponding with high rates of photosynthesis (Flite 2006). Biomass and calcium, iron, and manganese precipitates settle to the lake bottom along with the nutrients and the metals that adsorb to the settled organic and inorganic material. Likewise, sulphate reduction under anoxic conditions in deep water and lake sediment can remove sulfate. However, sulphate reduction is generally not significant under oligotrophic conditions, where the supply of organic matter limits the rate of sulphate reduction in the anoxic portions of lake sediments (Holmer and Storkholm 2001). These constituents may be sequestered in the lake sediments or some or all may be recycled depending upon geochemical conditions in the lake sediments. The fate of these constituents and the dissolved oxygen conditions will depend on the biological productivity of the lake and whether seasonal or sustained stratification develops within the lake.

Lake Stratification, Water Chemistry and Dissolved Oxygen

Most natural lakes in temperate zones exhibit thermal stratification during the summer but mix in the fall as the water near the surface cools and mixes with the deeper water in the lake. The lowland lakes in western Washington will mix throughout the winter and are referred to as monomictic (Bortleson *et al.* 1974). Many pit lakes and a few natural lakes do not mix throughout the water column but remain stratified over sustained periods and are referred to as meromictic (Boehrer and Schultze 2006). Dissolved solids become concentrated in the deep water in a meromictic pit lake resulting in a water density difference between the shallow and deep water that is sufficient to withstand the destabilizing forces of wind. Reduced metals, hydrogen sulfide, carbon dioxide and anoxic conditions are usually found within the deep water in a meromictic pit lake (Boehrer and Schultz 2006). While the density stratification in meromictic lakes isolates the metals and hydrogen sulfide in the deep water from mixing with the rest of the lake, there is a risk that an event such as a slope failure or extreme wind storm that could release metals, nutrients and hydrogen sulphide to the water in the upper portion of the lake. The Central Packwood Lake is not expected to become meromictic based on the physical characteristics of the lake, the expected chemical and biological conditions in the lake and a comparison with natural and pit lake analogues.

Meromictic lakes are usually deep compared to their surface area. This morphometric feature is quantified by Walker and Likens (1975) by the relative depth ratio (Zr) defined as the ratio of a lake's maximum depth to its mean diameter expressed as a percent. The relative depth ratio for the Central Packwood Lake is 3.4 %. This ratio is low compared to the pit lakes surveyed by Doyle and Runnells (1997), which typically have a Zr of 10 % or more.

Roesiger Lake (North Arm), an oligotrophic lake in western Washington, provides a good natural analogue for the Central Packwood Lake as the surface area, capacity, average depth, maximum depth and relative depth ratio are nearly the same. Based on this natural analogue, the Central Packwood Lake should be seasonally stratified and mix throughout the water column during the winter. However, the water in Roesiger Lake (North Arm) has very low concentrations of dissolved solids in comparison with the estimates for Central Packwood Lake. Thus, the comparison with this natural analogue is not alone sufficient to conclude that the lake will not become meromictic.

Inflow of iron rich or saline groundwater was the cause for meromixis in many pit lakes (Boehrer and Schultze 2006). In addition, calcite precipitation, iron cycle, and manganese cycle may add solute density to the lower water sufficient to establish meromixis (Boehrer and Schultze 2008). Analogues of near neutral pit lakes and geochemical modeling were used to assess whether meromictic conditions might develop in the Central Packwood Lake.

Flite (2006) studied the South Pit Lake, a near neutral meromictic pit lake in South Carolina with a relative depth ratio of 9.18 %. A phytoplankton bloom resulting from high phosphorus loads increased pH levels, which led to calcite precipitation. Calcite dissolved in the lower portions of the lake water column when it encountered water with higher CO_2 and lower pH. This cycling of calcium along with intrusion of iron rich groundwater induced a strong enough density difference for the lake to become meromictic. Analysis of the predicted Central Packwood Lake water chemistry using PHREEQC (Parkhurst and Appelo 1999) shows the water to be undersaturated with respect to calcite at near neutral pH. Calcite saturated occurs when pH increases above 8. However, calcite precipitation in surface water and lakes requires high levels of supersaturation for nucleation to take place (Suarez 1983, Kosamu and Obst 2009). Given the expected lake water chemistry from mass balance simulations, the level of supersaturation required for calcite precipitation is unlikely to occur in the oligotrophic Central Packwood Lake.

Hatfield Consultants (2011) studied nine near neutral coal mine pit lakes in western Alberta. These pit lakes may be better analogues as all are classified as oligotrophic. The relative depth ratio appears to have some influence on meromixis in these pit lakes. The lakes that fully mixed during the spring and fall featured relative depth ratios ranging from 2.4 % to 5.4 % while the lakes with relative depth ratios ranging from 4.7 % to 9.4 % were meromictic. However, Hatfield Consultants (2011) identified the inflow of higher salinity groundwater as the most significant factor contributing to meromixis. They also found that the anoxic water in five of the six meromictic lakes was confined to the very deep portion of the lake well and had little impact on the relative amount of suitable habitat for aquatic life. Groundwater inflows are only 1.2 % of the total Central Packwood Lake inflow, which is unlikely to cause meromixis.

Finally, two flooded mine pits at the Centralia Mine are useful analogues for the Central Packwood Lake. Results of monitoring performed at various depths within the flooded pits are summarized in Table 2. These results indicate that the water in the flooded pits does not change much with depth and the entire water column remains oxygenated during sampling in the fall and winter. From these pit analogues we can expect that the Central Packwood Lake will mix throughout the water column during the fall and winter and that entire water column should remain oxygenated.

Conclusions

Based on the physical characteristics of the Central Packwood Lake, the modeling results and the comparison with natural and pit lake analogues, the Central Packwood Lake is expected to stratify during the summer but mix throughout the water column during the fall and winter similar to natural lakes in western Washington. Phosphorus loading results indicate that the Central Packwood Lake will be oligotrophic. The concentrations of major ions in the lake are expected to be similar to the concentrations in Table 1 as predicted by mass balance modeling. Calcium precipitation is not expected to have a significant influence on calcium concentrations within the lake water column. Iron and manganese and other metals are expected to be at lower concentrations than predicted by the modeling results in Table 1 due to the removal by a constructed wetland at the inlet to the lake and by settling of organic and inorganic sediments within the lake.

Pit	Date	Depth (m)	Temp (°C)	Specific Conductance (mS/cm)	pH	DO (mg/L)	note
3E	11-Nov-10	1.5	11.4	1800	6.87	na	
3E	11-Nov-10	3	11.4	1800	6.91	na	
3E	11-Nov-10	27.5	11.3	1800	7.35	na	
3E	11-Nov-10	32	11.3	1900	7.3	na	
3E	11-Nov-10	41	11.3	1900	7.53	na	bottom +1.5m
Pit 7	30-Nov-07	1.5	8	2000	7.5	13.8	
Pit 7	30-Nov-07	3	7.9	2000	7.59	13.8	
Pit 7	30-Nov-07	12.2	7.9	2000	7.75	12.8	
Pit 7	30-Nov-07	15.25	8.3	2000	7.76	13.0	bottom +1.5m
Pit 7	30-Nov-07	16.75	8	2000	6.76	0.7	at bottom
Pit 7	7-Feb-08	1.5	3.6	1800	7.89	12.9	
Pit 7	7-Feb-08	19.5	3.6	1900	7.96	12.1	bottom +1.5m
Pit 7	11-Mar-09	1.5	5.6	2000	8.32	14.4	
Pit 7	11-Mar-09	18.7	5.6	2100	7.75	7	bottom +1.5m

Table 2 *–Flooded Pit Water Sampling Results, Centralia Mine.*

The results of the study demonstrate the importance of collecting adequate site data to support the development of predictive models and to evaluate the reliability of the predictions. Predictive models alone cannot account for all of the geochemical and limnological processes that are important considerations for end pit lake design. Therefore, the model predictions should be coupled with relevant water quality and limnological information from pit lakes and natural lake analogues in order to assess the likely physical, chemical and limnological conditions for the pit lake.

Acknowledgements

The authors thank TransAlta Centralia Mining, LLC for permission to publish the results of the Central Packwood Lake reclamation plan. The authors also thank Colorado School of Mines for hosting the IMWA 2013 Conference and the reviewers for critical comments on this paper.

References

Bear, J. 1979. Hydraulics of Groundwater. McGraw-Hill. 567p.

Boehrer, B. and M. Schultze 2006. On the Relevance of Meromixis in Mine Pit Lakes. Intern. Conf. on Acid Rock Drainage, March 26–30, 2006. St Louis, MO

Boehrer, B. and M. Schultze 2008. Stratification of Lakes. Rev. Geophys 46. American Geophysical Union.

Bortleson, G.C., G.T. Higgins, and G.W. Hill. 1974. Data on Selected Lakes in Washington, Part II. USGS Water Supply Bulletin 42.

Doyle, G.A. and D.D. Runnells 1997. Physical limnology of existing mine pit lakes. Mining Engineering 49, 76–80.

Flite, O.P., 2006. Onset and Persistence of Biogenic Meromixis in a Filling Pit Lake –A Limnological Perspective. PhD Dissertation, Clemson University,

Hatfield Consultants 2011. An Evaluation of Water Quality in Existing End-Pit Lakes in the Coal Valley Mine Area-Final Report. Prepared for Coal Valley Resources, Edson, Alberta.

Holmer, M. and P Storkholm, (2001). Sulphate Reduction and Sulphur Cycling in Lake Sediments: A Review. Freshwater Biology, Volume 46, Number 4, April 2001, 431–451(21)

Kosamu, I.B.M and M Obst. 2009. The influence of picocyanobacterial photosynthesis on calcite precipitation. Int. J. Environ. Sci. Tech. vol. 6(4), p 557–562.

Natural Resource Conservation Service. 2004. Chapter 9, Hydrologic Soil-Cover Complexes. Part 630 Hydrology, National engineering Handbook. U.S. Department of Agriculture.

Parkhurst, D.L. and C.A.J. Appelo (1999) User’s Guide to PHREEQC (Version 2). U.S. Geological Survey Water-Resources Investigations Report 99–4259, 312p.

Suarez, D.L. 1983. Calcite supersaturation and precipitation kinetics in the Lower Colorado River, All-American Canal and East Highline Canal. Water Res. Research, Vol. 12(3), pp653–661, Jan. 1983.

Vollenweider, R.A. and P.J. Dillon (1974). The application of the phosphorus loading concept to eutrophication research. National Research Council of Canada, Ottawa, Ontario: Technical Report 13690.

Walker, K.F. and G.E. Likens 1975. Meromixis and a reconsidered typology of lake circulation patterns. Verh. Int. Verein. Limnol. 19, 442–458.

Mine Flooding and Water Management at Underground Uranium Mines two Decades after Decommissioning

Michael Paul, Jürgen Meyer, Ulf Jenk, Delf Baacke, Andrea Schramm, Thomas Metschies

WISMUT GmbH, Jagdschänkenstraße 29, 09117 Chemnitz, Germany

Abstract Closure and flooding of five underground uranium mines represent a key component of the Wismut Environmental Remediation Program. By 2013, all mines are abandoned and flooded to a large extent. In order to avoid adverse effects of groundwater rebound, water collection and treatment systems had to be installed at all sites. Monitoring data recorded during more than 20 years allow comparison with earlier model predictions. Evolution of mine water quality suggests that the operation of treatment systems will remain an ultimate requirement over the next decades at most sites. Opportunities and constraints to use and enhance natural attenuation processes in mine water bodies are delineated.

Keywords uranium, arsenic, underground mines, mine flooding, water management, environmental impacts

Introduction

Germany still ranks No. 4 amongst the historical uranium producing countries, as SDAG Wismut had been one of the world's major uranium suppliers from 1946 through 1990. Upon cessation of uranium mining in 1991, Wismut GmbH was commissioned as a government-owned enterprise to establish and run the decommissioning and rehabilitation of the legacy production sites. Roughly 90 % of Wismut's total production of almost 220 kt of uranium came from underground mining. After termination of uranium production, the mines were decommissioned and prepared for flooding which included underground remedial work, removal of materials with the potential to pollute the incoming groundwater, stabilization of shallow mine galleries, and physical closure of shafts and adits. Differences in geology, hydrogeology, and mining technology necessitated site-specific flooding strategies and technological arrangements. First experiences made with flooding the Wismut mines were summarized by Gatzweiler *et al.* (2002), reflecting mainly the conceptual and preparation phases. By 2013, all mines are closed, and more than 97 % of the underground workings are flooded. Hands-on experience and comprehensive monitoring programs, implemented and operated for more than 20 years, deliver insight into the real behaviour of the systems allowing comparison with earlier model predictions. The paper presents a selection of most recent findings regarding mine flooding and post-flooding water management.

Mine characterization

The Wismut Remediation Program comprises, inter alia, the closure of five huge to medium-size underground mines located in the German Saxothuringian uranium province. Deposit types range from "veins in crystalline host rock" (Schlema, Pöhla), to "black shale associated" (Ronneburg), "roll-front sandstone" (Königstein) and "uraniferous coal" (Dresden-Gittersee). Average uranium grades were low (approximately 0.1 % U), and mining methods mainly conventional (room and pillar with backfill, overhand stoping with self-fill, caving, seam mining). The most important production centres were those at Ronneburg and Schlema. The Ronneburg mine field consisted of six interconnected mines with 40 shafts and 3,000 km of mine workings, complemented by a huge, meanwhile completely backfilled open cast mine. The Schlema mine included 80 day and blind shafts with 4,200 km of headings on 62 levels down to a maximum depth of almost 2,000 m. The smaller Pöhla-Tellerhäuser mine close to the Czech border was exclusively accessed by a main adit hosting 2 blind shafts, so that the mine voids were shielded from ground surface by undeveloped overlying country rock. Uranium mining at Gittersee represented the last episode of underground mining in the Döhlen coal basin, which had been ongoing since the 16th century. The activities were dedicated to uraniferous hard coal in three separate mine fields using longwall caving. The only mine with a deviating production scheme was Königstein, where in 1984, as a response to decreasing uranium grades, conventional room and pillar mining was completely replaced by an underground block leach technology using dilute sulphuric acid as leaching agent. Key features of the five mines are summarized in Table 1.

Mine water rebound and water level control

Given the prevailing climatic conditions (annual average precipitation 700...1150 mm, average annual temperature 6...9 °C), the mines were largely flooded due to natural groundwater inflow following cessation or throttling of mine water pumping. With the exception of Pöhla, groundwater rebound was allowed to proceed stepwise and in a controlled manner, in order to ensure proper mine abandonment, but also to gain hands-on experience with the flooding process. Since mine flooding was strongly interrelated with other remedial measures and initially characterized by significant uncertainties, flooding strategies had to be laid out with flexibility including back-up options. Although mine flooding aims for a wide restoration of close-to-nature groundwater conditions in general, in case of the Wismut mine sites the installation and perpetuation of emission barriers, *i.e.* water collection and treatment systems, was and still is inevitable to avoid adverse effects of groundwater rebound. Of the complete list of potential problems known from the literature (*e.g.* Younger and Robins 2002), the following are the most relevant, in descending order: (a) surface water pollution (all sites except Gittersee), (b) pollution of overlying aquifers (Königstein, Ronneburg), (c) localized flooding of agricultural or residential areas (Ronneburg, Gittersee), (d) surface subsidence (Schlema, Gittersee), and (e) mine gas emission, namely radon-222, into residential buildings (Schlema). With the exception of the Pöhla mine, which is dewatered gravitationally through its access tunnel, mine water level control is basically performed using submersible pumps, installed in shafts or extraction wells.

Forecasts of the flooding process and its impact on the local ground and surface water regimes proved to be difficult. Despite the fact, that state-of-the-art modelling techniques were used and highly qualified mine water

Mine	Mine voids subject to flooding, Mm^3	Mean annual mine water Inflow, Mm^3	Operating Life	Mine flooded From – to	Recent water abstraction method
Schlema	36.5	6.0	1946–1990	1991–2000	Submersible pumps
Ronneburg	25	4.3	1951–1990	1997–2007	Collection drains and submersible pumps
Königstein	4.1	1.0	1967–1990	2001–2013	Submersible pumps
Pöhla	1.0	0.12	1967–1990	1992–1995	Dewatering adit
Gittersee	0.5	1.0	1949–1954 1968–1989	1995–2003	Submersible pumps

Table 1 *Characteristics of Wismut's flooded Uranium Mines and recent water management regime.*

professionals were involved, some of the predictions failed. The reasons for that are manifold, but chiefly comply with those discussed by Brown (2010) and Younger and Robins (2002): (i) highly variable and poorly defined systems parameters including problems of scale, (ii) analytical complexity and insufficient knowledge of key processes, (iii) inadequate data base, especially poor quality of pre-mining data, (iv) limited possibilities for model calibration prior to flooding, and finally (v) diverging interests of the parties involved when it comes to interpretation and decision-making (stakeholder pressure). Appearance, relevance and consequences of such erroneous predictions shall be illustrated by three examples:

(1) Flooding of the Schlema mine was initiated in 1991, flood water emerged quicker than expected. The volume of mine water at post-flooding state had been originally predicted to be around 450 m^3/h, based on measured mine inflow data prior to flooding, but assuming a head-dependent inflow reduction. When flooding was in progress the actual volume, however, levelled off at an average of about 800 m^3/h, since significant inflow reduction did not occur. In consequence, construction of the planned water treatment plant had to be sped up and its capacity augmented to accommodate a recent maximum rate of 1,150 m^3/h, with regard to storm water events.

(2) In 2003, the Gittersee mine had been allowed to flood up to the natural water level. Contrary to all expert predictions, sufficient subsurface runoff to the local receiving stream as well as an historic dewatering adit, draining a neighbouring abandoned mine field, did not materialise, obviously due to an overestimation of the hydraulic conductivity of the mined ground/goaf. Instead of that, water logging occurred in the Freital urban area. Following repeated hydrogeological investigations, the original dewatering concept had to be discarded, and preference was given to extend the historic Elbstolln drainage gallery by some 3 kilometres, to ensure long-term runoff while safely precluding any surface water emergence.

(3) At Ronneburg, water discharge from the underground mine started in 2006 in line with original plans, feeding a near-surface collection system installed in a local valley. The collection system had been placed and instrumented according to model predictions (Unland *et al.* 2002). The installations, however, proved not to be sufficient in their effectiveness, causing substantial reworking measures. Further rise of mine water heads up to a maximum of some 20 m above the valley bottom did finally cause significant uncontrolled discharges to the local creek, leading to a pollution of downstream water courses in 2010/11. The problems were initially caused by an insufficient hydraulic range of the basic system in high yield areas, but also by water creeping at old boreholes and backfilled raise drifts, due to their insufficient state of preservation. More seriously, pumping and treatment capacities proved to be undersized to cope with the increasing quantities of escaping groundwater and contaminated surface waters during the wet year of 2010. A back-up extraction well, although installed in time, could not be fully used due to the shortage in treatment capacity. In consequence, water treatment and pumping capabilities had to be augmented, and water management strategy is recently under major revision.

Mine water quality and water treatment

The well-known "first flush" phenomenon (Younger *et al.* 2002), characterized by an increase of dissolved matter concentrations in the mine water as water table rises, followed by a steady decline after flooding is complete, was observed at all Wismut mines. Its occurrence, however, differed from mine to mine, was element specific, but also modified by contaminant's discharge from other sources into the mine water, such as above ground objects (*e.g.* waste dumps), mine sections above the water table, or re-flooded host rock. Moreover, temporal variations in mine inflow, water table fluctuations and changes in the water management regime were complicating the picture. With respect to environmental aspects, the monitoring of mine water quality was focussed on U, ^{226}Ra, Fe, Mn, As, Ni, Zn, Cu, Cd, SO_4^{2-} and total hardness, complemented by components with relevance to treatment issues and process understanding, including temperature, pH, redox potential, electric conductivity, O_2, HCO_3^- and others. Table 2 summarizes the recent mine water quality at Wismut's different mine sites.

In order to outline some typical phenomena, Fig. 1 is illustrating the uranium and arsenic concentrations in the Schlema and Pöhla mine waters over a 15 or 20 years time span, respectively. Both mines are characterized by a wide homogeneity within the mine water column, mainly due to thermal convection. Mine waters are circum-neutral in pH and show intermediate to reducing redox potential. Related to low sulfide and high carbonate contents, acidification can be ruled out. Under these conditions mine water is only moderately mineralized, and mobilization of pollutants is limited to U, ^{226}Ra, As, Fe and Mn (Table 2). After flooding at Schlema was chiefly complete in 2000, the following decline of uranium concentrations could be satisfactorily explained by dilution over a period of about 7 years. This finding is indicated by the reasonable fit between the measured uranium concentrations and those deduced by an ideal dilution estimate based on a mean hydraulic residence time of 6.1 years and a uranium concentration of 0.3 mg/L in the mine inflow (Paul *et al.* 2011). However, a change of the mine water abstraction point back in 2006 and, even with a bigger response, a temporary water table drawdown/re-inundation cycle in 2011 triggered a noticeable deviation from the ideal dilution curve. This observation and the most recent quasi-stagnant uranium values are a clear indication of uranium mobilization from a mine internal source, probably sludges which were precipitated earlier at upper mine levels. At Pöhla, by contrast, uranium showed a rapid decrease even before the mine reached steady-state flow conditions, most likely driven by microbiologically catalysed sulphate reduction leading to uranium precipitation as immobile uranium (IV), since sulphate levels dropped also rapidly with a distinct lead time compared to uranium. Arsenic concentrations, on the other hand, reveal for both Schlema and Pöhla a significant arsenic mobilization within the flooded mines, clearly over-compensating the dilution by meteoric waters. There is

		Schlema	Pöhla	Königstein	Ronneburg	Gittersee
pH		7.0	7.2	3.1	5.7	6.8
Ca	mg/L	180	50	110	470	240
Mg	mg/L	120	20	10	485	45
HCO_3^-	mg/L	590	330	<5	75	530
SO_4^{2-}	mg/L	660	<5	760	3,530	1,010
Fe	mg/L	4.2	5.5	100	230	18
Mn	mg/L	2.5	0.2	2.9	11	1.8
U	mg/L	1.8	<0.02	10.1	<0.2	0.07
Ra-226	Bq/L	1.7	4.2	10.0	0.1	0.025
As	mg/L	1.0	2.1	0.3	<0.04	0.02
Cu	µg/L	<5	<5	32	810	<20
Cd	µg/L	<1	<1	49	32	<1
Ni	µg/L	<7	<5	330	1,580	<10
Zn	µg/L	<5	15	4,370	1,100	35

***Table 2** Mine water qualities at Wismut's flooded underground mines, 2011 mean values*

strong evidence, that native arsenic which is very common in both deposits and contains elevated levels of arsenolite As_2O_3 due to partial oxidation during mine operation, is the key driver of this process, similarly under oxidising or reducing conditions (Paul *et al.* 2010).

In consequence of what was stated above, water treatment units had to be commissioned at any mine site. Key target parameters include radionuclides (U, ^{226}Ra), Fe and Mn, As (most relevant at Schlema and Pöhla), and base metals like Zn, Cd, Cu, and Ni (crucial at Ronneburg and Königstein). Against this background, all facilities are currently operated as modified or HDS-lime precipitation plants, with capacities ranging from 60 m^3/h (Pöhla, under construction) to 1,150 m^3/h (Schlema). The new Pöhla unit will replace a semi-passive treatment facility, being in full-scale trial operation since 2005, which could not achieve the design expectations regarding performance, maintenance efforts and, hence, operational cost. At Königstein, an ion-exchange process step prior to HDS-lime treatment is being operated, recovering uranium as a saleable concentrate to gain revenue partially covering treatment expenditures. At any site, treatment residues have to be immobilized and disposed of into engineered disposal cells, mainly situated on top of waste dumps.

Specifics of the Königstein mine

Amongst Wismut's former production sites the Königstein mine is exceedingly special due to the underground acid leach technology applied, namely in an ecologically very sensitive area close to the Elbe river. The ore body located in the lowest of four sandstone aquifers had been dewatered during mine operation over an area of some 6 km^2, and about 100

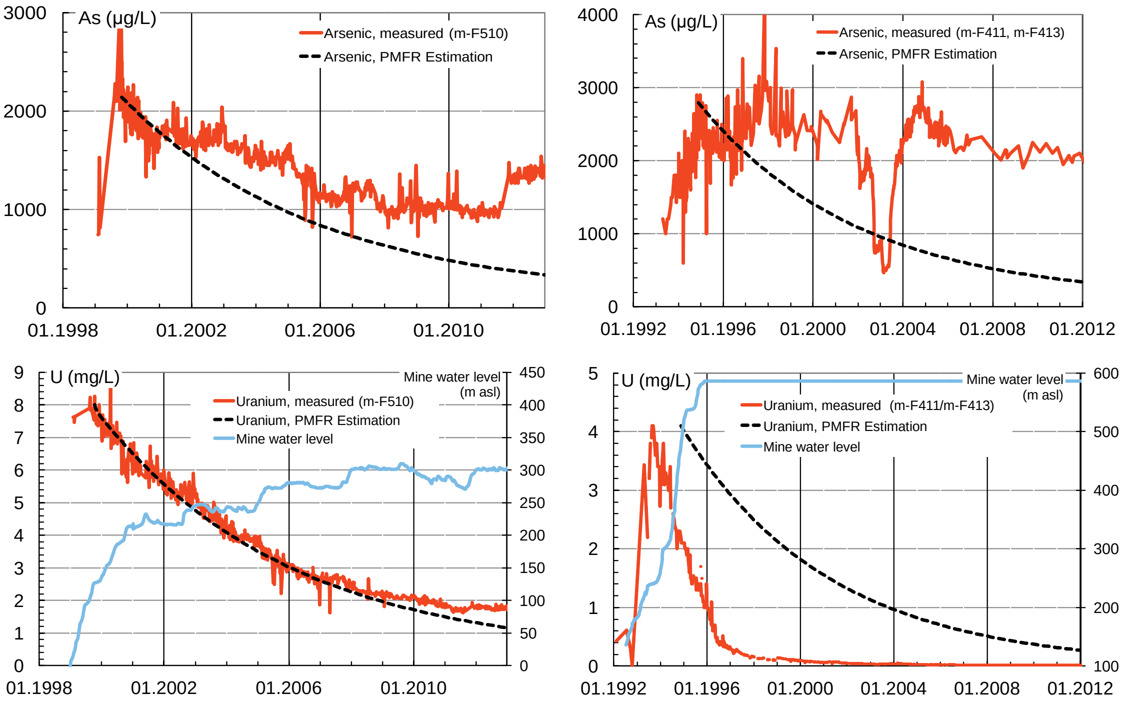

Fig. 1 *Uranium and arsenic concentrations in the Schlema (left) and Pöhla (right) mine waters, in relation to the mine water level. Comparison of measured vs. estimated (Perfectly Mixed Flow Reactor approach, Paul et al. 2011) values after First Flush Peak concentrations. Arsenic values for Pöhla between 2002 and 2004 were influenced by a field test with temporary change in mine water management (see Paul et al. 2006).*

sandstone blocks with volumes of 0.1...1 Mm^3 each were leached with solutions containing 2 to 3 g/L of H_2SO_4. In consequence, the geochemical status of the rock was substantially modified, with high levels of acidity, sulphate, radionuclides, and (semi)-metals remaining within the deposit after the stop of production. The mine closure and rehabilitation plan involves flooding of the mine workings up to the natural level of groundwater rise. Following comprehensive preparation, stepwise controlled flooding was initiated in 2001, resulting in a significant flush with maximum uranium concentrations of more than 200 mg/L in the mine water. Contrary to any other Wismut mine, remediation of the contaminated mine water pool is actively accelerated by additional injection of groundwater and treated discharge of the water treatment facility, respectively. Recent mine water quality is also shown in Table 2. While flooding proceeded, the general challenge consists in maintaining control of water-soluble contaminants in the context of restoring natural groundwater conditions. By the end of 2012, the mine was completely abandoned. Water level control to ensure hydraulic isolation of the mine from the surrounding and overlying groundwater resources is implemented by means of two pumping wells, which are connected to the northernmost and deepest mine workings known as control drifts. Mine water is completely captured and treated. Predictions point to probable flood water qualities that will require water treatment to continue for decades to come.

Towards a walk-away status – natural attenuation potential and *in situ* treatment

Wismut’s general approach for a sustainable remediation aims for reduction of present and future environmental impacts with reasonable spending to a socially accepted level, preparing the former mine sites for a value-added re-use. Insofar, achievement of a walk-away status should be the ultimate goal for any remediated object. With regard to most flooded underground mines this seems, however, unattainable at least in the short run, mainly for two reasons: (i) the necessity for long term maintenance of drainage installations, to safely preclude any surface water emergence, and, even more importantly (ii) the insufficient water quality. In order to comply with maximum concentration limits for mine water discharge as defined by the regulatory bodies, the operation of active systems to collect and treat contaminated mine water will remain an ultimate requirement over the next decades. The only exception is the Gittersee mine, where with the new drainage tunnel being complete, flood water quality will allow direct discharge into the Elbe River (see Table 2), since residual iron is assumed to precipitate along the 9 km passage along the tunnel.

Apart from that, mine water treatment will be the most cost-intensive long-term task related to the entire Wismut Remediation Program. Besides uranium, iron and (semi)-metals, the most challenging contaminants are radium and arsenic. A lot of research has been conducted to understand, use and enhance possible natural attenuation processes in flooded mine water reservoirs. First experiences with the investigation and testing of supporting *in situ* technologies to improve the mine water quality have been outlined earlier (Paul *et al.* 2006). As a key result, an immobilization technology for non-flooded leach blocks was developed and implemented at Königstein, as long as those mine areas were still accessible (Jenk *et al.* 2004). Full scale applications of in-situ-approaches can, however, only be conceived as supporting measures to conventional technologies, since they are hampered by a multitude of difficulties. The most serious are: (i) incomplete knowledge regarding the overall systems’ behaviour, (ii) restricted accessibility of the mine system for reagent input, monitoring and process control, (iii) insufficient or uncertain efficiency, uncertainties regarding potential reversibility of target processes, (iv) reverse reactions of contaminants with diverging geochemical behaviour, and resulting from all that (v) limited acceptance by the regulatory bodies.

Most recently, R&D work was carried out with the objective to improve mine water quality by injecting reactive substances via boreholes. To this end, two alternative approaches were considered: (1) Stimulation of natural sulphate reduction, taking the Pöhla case as a natural analogue, and (2) Neutralisation of acid flood waters by injection of buffer substances (Wismut 2010, Jenk *et al.* 2013). Based on the discoveries made during a field experiment carried out at Königstein, a technology applicable to the Königstein mine as a whole was designed and conceived as a supportive measure to enhance further mine flooding.

Conclusions

Real data from five flooded underground mines revealed, that flooding predictions have not been matched by reality in any case. Therefore, technological arrangements must be flexible and robust to cope with deviations from what was expected. In the context of the lessons learned and with regard to the predicted further mine water quality evolution under the site situations described above, mine water treatment will remain indispensable at the Königstein, Schlema, Pöhla, and Ronneburg mine sites for the foreseeable future. Key contaminants include U, ^{226}Ra, As, Fe, Ni, Zn and Cd. In the context of European Water Legislation and its further implementation at national level it is to be assumed that even stricter environmental standards will come into force in the longer term. In order to avoid burdens in perpetuity, however, careful balancing of ecological, economic and social interests will be necessary.

References

Brown A (2010) Reliable Mine Water technology. Mine Water Environ (2010) 29:85–91

Gatzweiler R, Jakubick AT, Meyer J, Paul M, Schreyer J (2002) Flooding the WISMUT mines – Learning by doing or applying a comprehensive systematic approach? Proc. Int. Conf. Uranium Mining and Hydrogeology III, Springer, 745–754

Jenk U, Paul M, Ziegenbalg G, Klinger C. (2004) Alternative methods of mine water treatment – Feasibility and technical limitations for a full-scale application at WISMUT's Königstein mine site (Germany). Proc. 8th Int. Mine Water Association Congress, Newcastle, UK, Vol. 1, 245–251

Jenk U, Zimmermann U, Uhlig U, Schöpke R, Paul M (2013) *In situ* Mine Water Treatment – Field Experiment at the Flooded Königstein Uranium Mine (Germany). Mine Water Environ (in press)

Paul M, Metschies T, Frenzel M, Meyer J (2011) The Mean Hydraulic Residence Time and its Use for Assessing the Longevity of Mine Water Pollution from Flooded Underground Mines. Proc. 6th Conf. Uranium Mining and Hydrogeology, Freiberg, 689–699

Paul M, Meyer J, Jenk U, Gengnagel M (2006) Source manipulation in water bodies of flooded underground mines – Experiences from the WISMUT Remediation Program. Proc. 7th ICARD, St. Louis, 1514–1530

Paul M, Meyer J, Jenk U, Jahn S, Klemm W (2010) Investigation of arsenic emissions from flooded ore mines of the Westerzgebirge region, Saxony, Germany. In: Proc. IMWA Sympos. Sydney, Nova Scotia, Canada, September 5–9, 2010, 387–390

Unland W, Eckart M, Paul M, Kuhn W, Ostermann R (2002) Groundwater rebound compatible with the aquatic environment – technical solutions at WISMUT's Ronneburg mine. Proc. Int. Conf. Uranium Mining and Hydrogeology III, Springer, 667–676

Wismut (2010) Nachhaltige Minimierung des langzeitlichen Stoffaustrags aus unterirdischen anorganischen Schadensherden am Beispiel der gefluteten Uranerzgrube Königstein. Projektförderung BMBF, Förderkennzeichen 02WN0755

Younger PL, Banwart SA, Hedin RS (2002) Mine water – Hydrology, Pollution, Remediation. Kluwer, 422 pp.

Younger PL, Robins NS (2002) Challenges in the characterization and prediction of the hydrogeology and geochemistry of mined ground. Geol. Society, London, Special publications, v. 198, 1–16

The challenges of re-opening historical Canadian mine sites with respect to water quality

Tania Perzoff[1], Jessica Banning[2], Scott Kingston[3], Rick Hoos[4]

EBA, A Tetra Tech Company, 9th Floor – 1066 West Hastings Street, Vancouver, British Columbia,
[1]tperzoff@eba.ca, [2]jbanning@eba.ca, [3]skingston@eba.ca, [4]rhoos@eba.ca

Abstract Bringing historical Canadian mines back into production following a period of closure is discussed in the context of mine site water quality management and evaluation. Navigating the regulatory process for such projects can be challenging, particularly given stricter environmental expectations, guidelines and requirements for site water quality management and evaluation. Incorporating historical data into modernized water quality programs is sometimes difficult and often poses additional challenges. Examples are drawn from the experiences of the Cantung Mine, currently in operation in the Northwest Territories, Canada. Re-opening a historic mine can be challenging but can also provide numerous economic and environmental benefits.

Keywords water quality, historic operations, water licence requirements and expectations

Introduction

Increasingly rigorous environmental regulations and expectations pose a challenge to developers looking to permit mines, including those that are inactive or abandoned. Historical mines are often attractive targets as they once hosted, and still potentially host, economically viable mineral resources. Advances in mining technologies, higher resource prices, and changing demand for raw materials can all work to shift prospects that were previously considered un-economic back into an economically viable project. Historic mine sites with economically viable mineral resources can provide effective use of a previously disturbed area that often reduces the overall environmental impact of past and proposed projects. In many cases, when historic mines were abandoned or closed they were left in conditions that do not meet present day standards for reclamation. By reopening historic mines under the current regulatory and permitting processes in Canada, there is some assurance that the mine site will be left in better condition than when it was first abandoned or closed.

Regulations at both the Federal and Provincial/Territorial level push mines to operate at globally recognized standards. Although important in the context of protecting the natural environment, satisfying certain environmental regulatory and permitting requirements can pose a challenge for companies attempting to bring a historic mine back into production. Some of these challenges will be illustrated using extensive experience at the Cantung Mine, located in the Northwest Territories.

Challenges

Many of the challenges associated with re-opening historic mines result from legacy issues that remain from past operations. When re-opening a historic mine there will almost always be a requirement to improve site conditions to fit updated and more rigorous regulatory, permitting, and environmental management expectations. Additionally, more comprehensive data sets, particularly those characterizing site water quality, are often required as part of the regulatory and permitting process. Data that were collected and managed inconsistently during previous operations are typically more difficult to incorporate into modernized water quality programs than designing and implementing a program from scratch.

New mines are also being designed more consistently with closure in mind; however, historic mines often contain infrastructure components that were never intended to be remediated to the extent that reclamation activities are carried out today.

Water Quality Guidelines

Legislation regulating the quality of mine effluent in Canada has evolved over the years to become some of the most rigorous in the world. The primary Federal legislation governing mine effluent was enacted in 1977 as the Metal Mining Liquid Effluent Regulations (MMLER) under the Fisheries Act. These regulations have been amended over the years and are now known as the Metal Mining Effluent Regulations (MMER; Department of Fisheries and Oceans Canada 2013; Environment Canada 2012).

National Water Quality Guidelines (WQG) were also developed by the Canadian Council of Ministers of the Environment (CCME) in 1987 and serve as the benchmark for the protection of water quality and aquatic life in Canada.

In addition to conforming with established national water quality standards and guidelines, many Canadian provincial and territorial regulatory agencies are moving towards the establishment of site specific water quality objectives (SSWQOs) for contaminants of potential concern (COPCs). These objectives are being relied upon more and more to maintain site-specific conditions as a means of supporting and protecting the most sensitive identified use of water.

Defining Background Concentrations

The establishment of SSWQOs and identification of COPCs often relies on background or pre-mining water quality conditions which are commonly derived from data collected during baseline studies, as well as from established water quality guidelines such as CCME (CCME 2003). Baseline data collection is often implemented early in the regulatory process, and for many historical mines these data may not exist or be suitable for use.

Determining appropriate SSWQOs can be a challenge for many prospective mine sites, particularly those with a previous development history. Sites that are being evaluated for their mining potential often exhibit water quality conditions that do not conform to established guidelines, largely because of naturally occurring mineralization (Nordstrom 2008). Historical sites displaying water quality concentrations above established guidelines have the added challenge of determining whether these conditions are the result of naturally occurring mineralization or past operations and site disturbance (or both).

Meeting Data Expectations

Historical data, where they exist, may contribute to the process of determining background concentrations of COPCs for a particular site as they may provide an indication of water quality conditions prior to any disturbance. Alternatively, they may simply highlight water quality trends over the years.

However, prior to the incorporation of historic data into more contemporary water quality programs, consideration must be given to the quality of the data collected. Over time, improvements to sampling equipment, collection methodologies, and QA/QC procedures have generally resulted in the generation of higher quality data.

Additionally, changes to sampling requirements such as an increase in the sampling frequency, the number of sampling locations, or the number of parameters analyzed can result in datasets that contain gaps or that are unbalanced. Such datasets may limit the ease of which direct comparisons can be made, particularly during statistical analyses.

Changes in project ownership and prolonged periods of mine closure can also result in data gaps.

Improvements in laboratory techniques and equipment have contributed to higher quality data over time. Standardized analysis techniques and lower detection limits allow water quality samples to be analyzed more accurately than was once historically possible.

The drawback to these advances, both in terms of data requirements and more sensitive analysis techniques, is that it can invalidate or make more challenging the comparison of data collected under these differing conditions. For mines that have maintained a long-term water quality program, these changes can unintentionally obscure data trends and interpretation.

Case Study

Some of the challenges described above are being experienced at the Cantung Mine, located at Tungsten in the Northwest Territories (NWT), just east of the Yukon border. The mine has operated on and off since 1962, for a total of 33 of the past 51 years, and has held a valid water licence since 1975. The water licence has been renewed a total of nine times to date, and is up for renewal in 2016.

Canada Tungsten Mining Corporation Ltd. owned and operated the mine from 1962 to 1997, and following a long period of closure from 1986–2001, sold it to North American Tungsten Corporation (NATC). Since being purchased by NATC, the Mine has operated more or less consistently since December 2001, with short term closures from 2003–2005 and 2009–2010. A relatively recent photo of the Cantung Mine site is presented in Fig. 1.

The Cantung Mine is not without its legacy issues. During the initial years of operations in the early 1960s, approximately 172,000 t of tailings were deposited directly into the Flat River floodplain behind a causeway (which has since been removed) designed to partially contain the tailings. Additional tailings were likely introduced to the Flat River from accidental spills from the tailings ponds and untreated sewage was also historically discharged directly into the Flat River just upstream of the causeway.

The first Conditional Water Licence was issued to the Cantung Mine by the Northwest Territories Water Board (NWTWB) in 1975. Since this time, the mine has been responsible for the execution of monitoring programs, particularly those that focus on the aquatic environment. Initial monitoring in 1975 was in

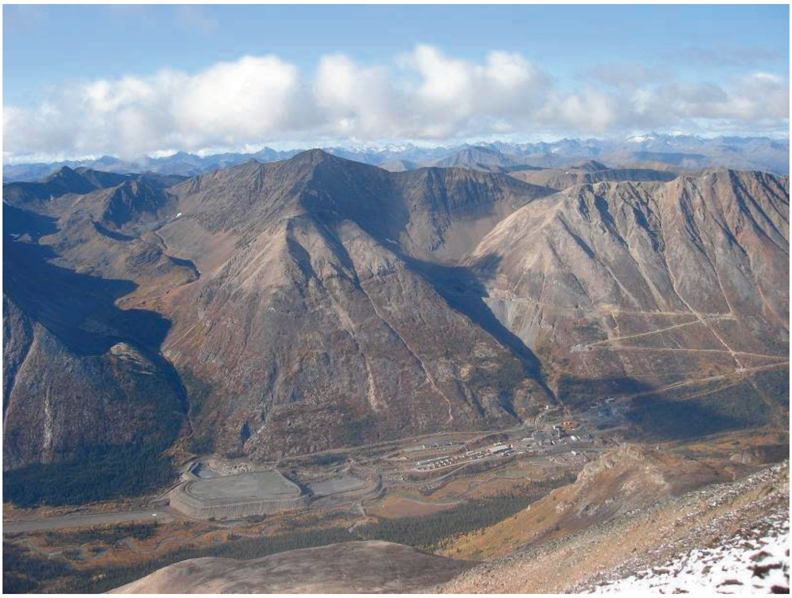

Fig. 1 *Cantung Mine Site*

the form of a Surveillance Program and involved the regular monitoring of several fixed stations and parameters (the exact number and parameters assessed by this program are unknown). With successive Water Licence renewals, this program has gradually evolved into a Surveillance Network Program (SNP), which is a program commonly implemented at mines throughout the NWT, and remains a key component of the Cantung Mine Water Licence to this day. Available records indicate that the number of stations comprising the SNP has varied since NATC's involvement in mine operations, with stations being added and abandoned throughout the years.

The current SNP includes 19 surface water monitoring stations that are located upstream and downstream of the mine infrastructure as well as throughout the mine site area. There are six stations sampled monthly, and alternative sampling locations that can be sampled if the primary stations are inaccessible. Five stations are sampled when seepage is visible, one station is sampled bi-weekly, and another station is sampled weekly. All water quality samples are analyzed for a standard suite of parameters which includes ICP metal scan (total and dissolved), total suspended and dissolved solids, total ammonia, nitrite and nitrate nitrogen, chloride, fluoride, sulphate, alkalinity, hardness, and pH. Select stations, dependant on location, require additional analyses which may include total organic carbon, total Kjeldhal nitrogen, ortho-phosphorous, biochemical oxygen demand (BOD), extractable petroleum hydrocarbons (EPH)/benzene, toluene, ethylbenzene, and xylene (BTEX), and faecal coliforms.

In 2002, following the enactment of the MMER, effluent sampling and quarterly reporting were required of the mine, in addition to the established SNP. Furthermore, periodic Environment Effects Monitoring (EEM) biological studies were also required under the MMER to determine whether discharges from mine operations have resulted in downstream effects to aquatic biota. Three EEM studies have been conducted to date (in 2006, 2009, and 2012) which analyzed fish, benthic invertebrates, water quality, and sediment quality for potential contaminants of concern.

Other studies of the Flat River environment that have been commissioned by NATC include an aquatic study to characterize fish presence in the Flat River (EBA 2002); a Flat River Plume Study to delineate the exfiltration plume emanating from the tailings pond adjacent to the Flat River (NATC 2008); a Comparative Qualitative Ecological Risk Assessment (QERA) to evaluate two primary management options for the historic tailings located within the Flat River floodplain (EBA 2009); and a report that summarized available water quality data for the Cantung Mine (which spanned from the 1980s to present) and compared results to limits established in the current Water Licence and CCME guidelines (EBA 2013b).

Additionally, the University of Saskatchewan carried out a multi-trophic level effects monitoring program on two tributaries of the Nahanni River, which included the Flat River downstream of the Cantung Mine and the Prairie Creek Mine (Spencer *et al.* 2008).

Discussion – Ongoing Permitting Issues

Findings from the various environmental monitoring programs, studies, and reports carried out to date have concluded that there is no evidence of adverse effects to water quality, fish, or aquatic life in the Flat River downstream of the mine (EBA 2013a). Some measurable differences in the Flat River ecosystem downstream of the mine are present, and these differences, in terms of invertebrate community indices and sediment chemistry can be attributed in part to past, discontinued practices.

Despite the increasing rigour and breadth of the various monitoring programs that have been carried out at the Cantung Mine over the years, the overall conclusions have remained fairly consistent in that no significant adverse effects to the receiving aquatic environment have been identified. All water quality parameters currently regulated under the Water Licence, with a few limited exceptions, are at or below CCME guidelines, and the EEM program continues to show benign results where aquatic organisms are concerned.

These encouraging results aside, regulatory expectations continue to increase for the Cantung Mine. Discussions with various agencies allude to future commitments to SSWQOs as part of the upcoming Water Licence renewal process even though downstream water quality remains unaffected. SSWQOs established for several new mines have, in some instances, been set below accepted CCME values, making for even more stringent levels than the accepted national guidelines. Similarly, although the Cantung EEM program continues to show negligible results to aquatic organisms, further studies continue to be required under the MMER.

Conclusion

There are multiple challenges associated with re-opening and operating historic mines in Canada including meeting increasingly more stringent environmental regulations and expectations, establishing backgroundwater quality concentrations when pre-mine water quality data is either non-existent or not sufficient, and working with historic data, should they exist. Further to these challenges, re-opening historic mines often involves assuming responsibility for environmental issues caused during past ownerships.

Experience at the Cantung Mine has shown an increase in the number and extent of environmental studies geared towards the characterization of effects to the aquatic environment, all of which have demonstrated that adverse effects are minimal to negligible. Determining with certainty whether any differences detected in the downstream receiving environment are attributable to legacy issues or current operations remains a challenge. Even with these results, regulatory expectations continue to increase.

Despite these challenges there are many benefits to re-opening a historical mine site when economically viable. Historical mines coming back into operation will contribute to both local and provincial/territorial economies while maintaining a smaller environmental footprint than opening a new mine. During current operations, mines will comply with the current environmental standards and at closure the mine will be reclaimed to a higher standard than it had been historically.

Acknowledgments

The authors thank North American Tungsten Corporation Ltd. for allowing the use of the Cantung Mine as a case study for this paper. They also acknowledge the International Mine Water Association for providing an opportunity to present on this topic.

References

Canadian Council of Ministers of the Environment. 2003. Guidance on the Site-Specific Application of Water Quality Guidelines in Canada: Procedures for Deriving Numercial Water Quality Objectives.

EBA Engineering Consultants Limited. 2002. Fish and benthos inventory for the Flat River at Tungsten, NT-Fall 2002. EBA Engineering Consultants Ltd., prepared for the North American Tungsten Corporation Ltd.

EBA Engineering Consultants Limited. 2009. Comparative Qualitative Ecological Risk Assessment for the Cantung Mine Site, NWT. Report prepared for North American Tungsten Corporation Ltd., March 2009.

EBA Engineering Consultants Limited. 2013a. Cantung Mine Metal Mining Effluent Regulations Third Interpretive Report for Environmental Effects Monitoring Studies. Report prepared for North American Tungsten Corporation Ltd., March 2013.

EBA Engineering Consultants Limited. 2013b. Historical Data and Interpretation Report of Water Quality at the Cantung Mine, NWT. Report prepared for North American Tungsten Corporation Ltd., Revised January 2013.

Environment Canada. 2012. Assessment of the Aquatic Effects of Mining in Canada. Environment Canada. Retrieved March 16, 2013, from www.ec.gc.ca/eseeeem/default.asp?lang=En&n=8AF5467D-1&offset=1&toc=hide

Fisheries and Oceans Canada. 2013. Metal Mining Effluent Regulations. Fisheries and Oceans Canada. Retrieved March 16, 2013, from www.dfo-mpo.gc.ca/index-eng.htm

NATC. 2008. 2008 Flat River Plume Survey, Results Summary Report. North American Tungsten Corporation. Watson Lake, NT.

Nordstrom, D. K. 2008. Questa Baseline and Pre-mining Ground-water Quality Investigation 25. Summary of Results and Baseline and Pre-mining Ground-water Geochemistry, Red River Valley, Taos County, New Mexico 2001–2005. US Geological Survey.

Sigma Resources Consultants Ltd. and John A. Jemmett Associates Ltd. (Sigma and Jemmett). 1978. The Effects of Heavy Metals and Sewage on the Biota of the Flat River, NWT. Report prepared for Canada Tungsten Mining Corporation Ltd., January 1978.

Spencer P., Bowman, M.F., and M.G. Dubé. 2008. A multitrophic approach to monitoring the effects of metal mining in otherwise pristine and ecologically sensitive river in Northern Canada. Integr. Environ. Assess. Manag. 4(3): 327–343.

Baseline geochemical characterization of trace elements in stream sediments in mineralized watersheds of the Duluth Complex, northeastern Minnesota

Nadine M. PIATAK[1], Laurel G. WOODRUFF[2], Robert R. SEAL II[1], Perry M. JONES[2]

[1] *U.S. Geological Survey, 954 National Center, Reston, Virginia, USA, npiatak@usgs.gov, rseal@usgs.gov*
[2] *U.S. Geological Survey, 2280 Woodale Avenue, Mounds View, Minnesota, USA, woodruff@usgs.gov, pmjones@usgs.gov*

Abstract Characterizing baseline conditions in mineralized watersheds of the Mesoproterozoic Duluth Complex, northeastern Minnesota, is essential to establishing the scientific context needed to responsibly extract minerals in one of the most prospective mining areas in the United States. Future mining could potentially release metals into watersheds that already naturally contain significant amounts of some elements.

Stream-sediment samples were collected from 19 sites in three watersheds that span a diversity of geologic settings and mineralization styles in the Duluth Complex to help characterize baseline stream sediment geochemistry prior to mining. The geochemistry of the sediments reflects underlying rock types, glacially transported unconsolidated materials, and the mineralization style within each watershed. The watersheds are located: 1) where Cu-Ni-PGM mineralization occurs in near-surface boulders and outcrops along the basal Duluth Complex (Filson Creek); 2) where Cu-Ni-PGM mineralization occurs only at great depth (Keeley Creek), and 3) in the vicinity of Fe-Ti oxide ultramafic intrusions that occur at the subcrop beneath glacial cover (St. Louis River).

In Filson Creek, with mineralization near the surface, stream sediments generally contain higher Cu than where mineralization occurs only in the deep subsurface (Keeley Creek). In the St. Louis River, concentrations of Fe Cr, Mg, and Ti increase downstream near the basal section of the Duluth Complex, and Cr, Cu, Ni, and Pb are highest where the river flows across exposed rocks of the Virginia Formation, a Paleoproterozoic shale/greywacke unit. The influence of trace element concentrations on the aquatic ecosystem also was evaluated. Total Cr concentrations in stream sediments in the lower part of the St. Louis River and total Cu and Ni concentrations at some sites in Filson Creek exceed concentrations at which harmful effects to sediment-dwelling organisms are likely to be observed (probable effects concentrations). Nearly all of the Cd, Cu, Pb, and Zn, and most of the As, likely occur in bioaccessible forms, based on an extraction method that solubilizes metals not tightly bound to silicates and sulfides. In addition, an excess of labile metals that are not bound to metal sulfides (based on AVS/SEM) suggest potential toxicity; however, the high organic carbon of some sediments (up to 5 wt. %) could sequester significant amounts of trace elements.

Characterizing sediment trace element content and bioaccessiblity, and assessing impacts on the current ecosystem health in these watersheds, may help to develop successful strategies that can minimize and mitigate future impacts of mining and develop appropriate restoration goals.

Keywords Cu-Ni-PGE deposits, Fe-Ti oxide deposits, St. Louis River, organic carbon, AVS/SEM

Mine Water Quality at Abandoned Uranium Mining Sites in the Czech Republic

Nada Rapantova[1], Monika Licbinska[1], Arnost Grmela[1], Karel Lusk[2]

[1] *VSB – Technical University of Ostrava, Institute of clean technologies for mining and utilization of raw materials for energy use, 17. listopadu 15, 708 33 Ostrava, Czech Republic, nada.rapantova@vsb.cz*
[2] *DIAMO, s.p. – Straz pod Ralskem, Machova 201, 471 27 Straz pod Ralskem, Czech Republic, lusk@diamo.cz*

Abstract The aim of study is to assess the evolving water quality of uranium mines abandoned between 1958 and 1992 in the Czech Republic. Monitoring of mine water quality was performed at all locations of previous uranium exploitation. Multivariate analyses were applied in order to identify groups of samples based on their similarity. Evaluation of hydrogeochemical evolution of waters was done using Geochemist’s Workbench. The sampling proved that uranium concentrations in waters did not predominantly exceed 0.45 mg/L. In case of discharges from adits abandoned more than 40 years ago uranium concentrations were below MCL of US EPA for drinking water.

Keywords uranium, radium, mine closure, mine water, environmental impact, geochemical modelling, the first flush

Introduction

From 1945 to the mid 1990’s, uranium mining was an important industrial branch in the Czech Republic, and the Czech Republic occupied a prominent global position in the production of uranium concentrate. A marked phase-out of the industry in the first half of the 1990’s, especially due to a marked reduction in possibilities of sales as a result of the economic-political changes taking place at the turn of the 90’s of the last century, led to the closure of many underground uranium mines. At present they are closed and flooded (Michalek *et al.* 2005). Mining operations are only performed in one underground mine in the Rozna deposit.

In the recent past, the vast majority of underground uranium mines in the Czech Republic were decommissioned by naturally flooding the mines after underground mining operations and the necessary preparations in connection with mine decommissioning were complete. Mine water levels at recently abandoned deposits are kept by pumping or gravitationally below the level of natural drainage from deposit (decant point). This mine water level is determined for each deposit by considering the terrain morphology and man-made decant points (*e.g.* old adits) and is crucial for avoiding the uncontrollable release of contaminated mine waters that could endanger the ambient environment. The absolutely fundamental task of uranium mining in relation to the environment, both in the course of mining the deposit and subsequently during mine decommissioning and mitigating the impact of mining, is to minimize the negative effects of released radionuclides on the environment and health of the population.

In the course of development and exploitation of individual uranium deposits, the chemistry of mine water changes depending upon the extent of the drawdown area, the total surface area of exposed mine workings, the mineralogical composition of the rock environment (including residues of unmined uranium and other radioactive minerals in these mine workings), and also the depth of mining. During the flooding of underground mines as part of decommissioning, other sig-

Fig. 1 *Main mining and treatment sites of uranium mining in the Czech Republic.*

nificant changes occur in the content of dissolved matter in the waters. This involves a several-fold increase in content of dissolved matters (uranium, radium, iron, and others) due to the previous oxidation of minerals when the deposit was being exploited. With reference to the high concentrations of dissolved matter in mine water (above the limits determined for discharge), it is necessary to treat the water drained from the flooded mines before discharging to surface water.

Uranium deposits and their exploitation in czech republic

Altogether about 110 000 t of uranium have been mined in the Czech Republic since 1945. Six main mining areas have participated in this production; a small amount has also been extracted as part of geological exploration in other regions. Uranium deposits in the Czech Republic (fig. 1) occur in the Bohemian Massif, which represents a denudation relict of the Variscan mountains and one of the greatest uranium-bearing provinces in Europe. Uranium mineralisation is represented here by endogenous and exogenous deposits: the endogenous deposits being confined predominantly to basement series and granitoid masses, and the younger, exogenous deposits confined to Permian-Carboniferous, Cretaceous and Tertiary platform formations.

The endogenous deposits are situated in the areas of Pribram, West Moravia and West Bohemia and are formed by highly dipping ore bodies of zone, vein and metasomatic types situated in compact rocks. The prevailing thickness of ore mineralisation ranges from 1.5 to 2.0 m, and less frequently up to 10.0 m. The depth range of mining was usually from the surface to a depth of 600–700 m. The deposits of Zadni Chodov (1250 m) and above all Pribram (1550 m) were mined at great depth and the deposit of Rozna (1200 m) is still being exploited. Exogenous deposits are found in the Cretaceous sediments of North Bohemia. They are represented in places of uranium mineralisation by sandstones and siltstones. Here we find subhorizontal ore bodies of great thickness at a depth of about 250 metres. Straz pod Ralskem and Hamr are two such deposits that were exploited in the Czech Republic. The deposit of Hamr was exploited by underground mining with backfilling the worked-out stopes with a consolidated material, and the deposit of Straz pod Ralskem was exploited by the acid leaching of uranium from the ore directly in ore bodies (*in situ* leaching). With regard to the specific hydrogeological conditions and their different methods of decommissioning, this paper will not deal with the deposits of Hamr and Straz pod Ralskem.

Impact of uranium mine closure on groundwater in czech republic

Czech uranium deposits were abandoned, with the exception of Rozna deposit between 1958 and 1992. When uranium ore exploitation was finished and the mine dewatering stopped the process of spontaneous mine flooding started. Depending on excavated volumes, the depression cone area and the hydrogeological conditions of the deposit, this process took several years for each mine. In the case of deposits abandoned in the 1990's, conditions for proper mine water management were created in advance. Groundwater is pumped from the shafts, in order to preserve groundwater level below the decant level, to surface water. After treatment it is discharged to surface streams. This ensures that shallow groundwater and surface water is not threatened by uncontrolled discharges of contaminated water from flooded mines. All these deposits are systematically monitored and as soon as water quality corresponds with the limits approved by the Czech Inspectorate of Environment (CIZP) for mining site under closure the groundwater pumping can be stopped (Hajek *et al.* 2006).

Monitoring of uranium mine waters' chemical composition in the Czech Republic has been carried out systematically since the beginning of their opening and exploitation. Part of the information is currently archived in the state-owned enterprise DIAMO in Straz pod Ralskem which has been managing all abandoned uranium mines in the Czech Republic since 1990's, *i.e.* it also bears the responsibility for consequences of former uranium exploitation and processing. DIAMO, s.p. carries out systematic monitoring of abandoned mines' selected locations. Due to the tradition of uranium mining in the Czech Republic and the existence of uranium deposits abandoned from 1958 to 1992, the studies of uranium mining impacts on hydrosphere constitute valuable experience for countries with developing uranium mining. The aim of this article is to assess impacts of uranium mines closure and abandonment on groundwater in the Czech Republic including the evolution of mine water quality after the deposit is abandoned.

Studying the natural processes that take place in mine water on flooded deep mines is very difficult due to the inaccessibility of the remote parts of the mine after flooding. More information is known about the regime of shallow circulation water chemistry, whose regular monitoring is possible. However, we still do not know exactly all of the processes in quasi-stagnant water accumulated in deeper parts of former mines. In a majority of cases it is not technically possible to monitor this water and describe the evolution of its physical-chemical properties and natural processes that affect them. Experience tells us that the quality of mine water on flooded deposits stratifies (Zeman *et al.* 2009; Nuttall and Younger 2004).

Water management of abandoned mines requires a combination of theoretic model studies and long-term monitoring of abandoned uranium mining sites that can bring empirical experience usable for validation of conceptual and numerical geochemical and transport models. The issue of water management of abandoned mines was dealt with in detail in monographs by Wolkersdorfer (2008); Younger *et al.* (2004).

In literature, we can find a number of experiences with detailed (sometimes even systematic) monitoring of individual abandoned uranium mining sites. The monitoring is very often connected to remediation activities on site. Carvalho *et al.* (2007) published an extensive regional study focused on detection of radionuclides concentrations in soils in 60 areas of former radium and uranium mining in Portugal. Nevertheless, systematic regional study focused on uranium mining impact on groundwater has not been found.

Methodology of study

The mine waters of all available sites of previous uranium exploitation with special focus on endogenous deposits were sampled in 2010. Several from these deposits are systematically monitored, but regularly analyzed chemical parameters of mine waters are highly limited (generally just TDS, U, Ra and sporadically sulphate, Fe, Mn, physical parameters).

Non-filtered water samples were analyzed in the laboratories of VSB-TU Ostrava (major ions and As, Cd, Co, Cu, Ni, Fe, Pb, Zn), Zdravotni ustav Ostrava (Ag, Al, Ba, Sb and Sr) and DIAMO, s. p., o. z. TUU Straz pod Ralskem (U and Ra). Uranium was analyzed by photometric analyses with Arsenazo III after separation of uranylic ions on silicagel (CSN 75 7614). Radium was determined by scintillation determination of ^{226}Ra after co-precipitation with $BaSO_4$ and $PbSO_4$ (PP-LAB-35-02). Ag, Al, Ba, Sb and Sr were analyzed by ICP-MS (CSN EN ISO 17294–2), other metals by AAS. In the field, conductivity, Eh, pH and temperature were measured by GREISINGER GMH 3430 (conductivity with precision ± 0.5 % of measured value), by WTW pH315i with pH electrode SenTix 21 (pH with precision of ± 0.01 pH), and by GREISINGER GmbH 3530 using the electrode GREISINGER GE 105 BNC (Eh). Alkalinity was also determined in the field using HCL titration.

The sampling method always reflected the specific conditions of each location. In some cases (mine adits, uncontrolled discharges) gravity-flow discharges were sampled (fig. 2). In the case of stagnating shafts, shallow-water samples were taken using a peristaltic pump. In the case of shafts in a dynamic state (pumped to maintain water level), pumped water was taken.

Since traditional methods (Piper diagram) failed in differentiating among water samples described by multiple parameters, multivariate methods have been applied. We applied Principal Component Analyses PCA (Jolliffe 1986) in order to transform the original set of variables to a new set of uncorrelated variables and visualize the distribution of samples based on two main components. Cluster analysis was conducted with MATLAB using Ward-Wishard clustering strategy (Manly 1994). The code generates dendrogram with similarity/dissimilarity values for samples and a computation log with information on the individual clusters (Cressie 1993).

The Geochemist’s Workbench® (Bethke 2007) and PHREEQC for Windows (Parkhurst and Appelo 1999) software were used for geochemical modelling.

Results and discussion

Apart from the uranium, radium and basic chemical and physical parameters of mine waters, Al, Ag, As, Ba, Cd, Co, Cu, Ni, Pb, Sb, Sr and Zn were also determined. With small exceptions, they correspond to the natural background and do not exceed legal limits given by Decree No. 369/2004 Sb. Concentration limits of Al, Co and Ni (Al ≈ 14.2 mg/L *vs.* 0.25 mg/L limit) were exceeded in the Licomerice site and in the Dylen site (below mine dump). In both cases, the enhanced metal concentrations are related to low pH (5.30 Licomerice site, 4.24 Dylen site), which increases metal mobility.

With respect to the goal of this work, our attention focused on radionuclide concentration in mine waters. The uranium mobility in mine water is controlled by a number of factors, among which pH, Eh and concentration of major ions are the most important.

Uranium concentration in most cases ranges up to 0.45 mg/L. Water discharges from adits of mines abandoned more than 40 years ago showed values below or slightly above the Maximum Contaminant Level (MCL) of US EPA (2011) for uranium in drinking water (0.03 mg/L) given by the Safe Drinking Water Act. These discharges also mostly met the provisional guideline value of U in drinking water 0.03 mg/L (WHO 2011). Limits for uranium in drinking water are, in Czech Republic, regulated by the State Office for Nuclear Safety concerning radiotoxicity and by Head Health Officer directives. Radiotoxicity reference and limit values are given by the Decree of State Office for Nuclear Safety 499/2005 Sb, appendix 10. Toxicity limits for uranium concentrations in drinking water are given by the Directive of Head Health Officer CR OVZ-32.4-19.4.2007 (0,015 mg/L since 1.1.2010).

Concentrations of U between 0.45 and 1.23 mg/L were only detected at remediation stations of Rozna and Olsi Mine. Rozna is an active dewatered mine, and on the Olsi Mine is the mine where uranium is exploited by pumping from a deep well. Only three samples showed anomalously high uranium concentrations. These samples were taken from the pumped Pribram shafts J-19 and J-11A – No. 1 (5.61 mg/L) and No. 2 (5.44 mg/L) and the sample from a deep well at the Olsi Mine (6.43 mg/L). All these samples quite clearly represent waters of deeper circulation. Increased values of uranium content in these waters correspond well with the conclusions regarding mine water stratification.

Activity concentration of ^{226}Ra on most sampled locations range between 0.03 and 1.85 Bq/L, and elevated values (max. 17.1 Bq/L) were detected at two mining sites: Vitkov and Okrouhla Radoun. These values relate to a naturally increased background where radium is a product of uranium decay in uranium-bearing granitic rocks. In the case of radium content in mine waters, complicated and indeterminable trends depending on the time passed from the mine flooding are manifested. At a majority of deposits, increases with a low correlation coefficient appear.

In order to study natural relations among samples multiparametric analyses were conducted. The cluster analysis with use of non-standardized samples by the Ward-Wishard cluster strategy resulted in separation of 6 clusters. The analysis shows that clusters are separated on the basis of sample membership to a geological environment: type of deposit, except for actively pumped shafts. The geological environment differentiates mine water chemistry especially in view of major ion content. The time after mine flooding did not manifest at cluster separation. That is why principal component analyses were elaborated. The components are linear combinations of data file parameters; in our case two first components accounts for 55 % variability of the 30-dimensional data file (metals were included into analyses). Interpretation of the PCA analysis brought a number of interesting conclusions, including the hypothesis regarding mine water evolution on abandoned uranium deposits.

Based on the results of PCA the evolution of mine water chemistry was described. In combination with the information on weights of parameters we can deduce which parameters most rapidly change over time after mine flooding. Those are especially TDS, and mainly the sulphate and some other major ion concentrations, as well as U concentration. Component 2 is rather significantly affected by pH-Eh conditions change and metal content in waters.

The mine water evolution seems to have obvious logical relation to the time from the site flooding and the origin of water sample in the respective depth level. Mine water chemistry systematically evolves from dewatered

Fig. 2 *Mine water discharge from Barbora adit – Horni Slavkov*

shafts and boreholes (samples correspond to a mixture of mine waters from various depth horizons with prevailing waters pumped from deeper levels) through shafts with a maintained water level up to the shafts with stagnated waters (sampled by peristaltic pump) and finally to gravity-flow discharges from old adits, shafts and uncontrolled discharges (abandoned more than 40 years ago).

Results of PCA are supported by natural relations observed at mines from the period of flooding through maintaining the water level under the decant level (preventing contamination of surface water) up to natural decant of waters either via adits or uncontrolled discharges. In course of mine water flooding, hydrochemical stratification (with solutes concentrations in mine water growing with depth) gradually develops due to groundwater inflows from various aquifers and depth levels.

Though the hydrochemical stratification in flooded deep mines is a generally accepted fact and has been recognised since 1970’s (Cairney and Frost 1975; Younger and La Pierre 2000; Johnson and Younger 2002) it is not always appropriately respected when assessing mine water sampling. Water samples taken from shallow parts of shafts or mine water discharges are often assumed to represent mine water quality for the whole flooded mine.

Mine water samples, though they often represent gravity-flow discharges, represent groundwater circulations of various depths. If mine shafts are sampled, the sampling method also has to be taken into account.

The evaluation of mine water geochemical development was done using geochemical modelling (Geochemist Workbench and PHREEQC). Uranium mobility was assessed in relation to all hydrodynamic processes at site.

As indicated by results of physical-chemical parameters of monitored mine waters, individual types of mine water at uranium deposits can be differed just upon the standard measurements of pH, Eh and temperature. These parameters also affect total composition of water.

Upon the results of geochemical models, three time phases of deposit evolution can be identified. In the first phase in active mines or shortly after their closure, uranium in waters is relatively immobile depending on concentration of other compounds, especially sulphate, hydrogencarbonate and on Eh-pH condition. In the second phase uranium is dissolved out of the deposit. In the third phase more than 40 years after the deposit was abandoned, uranium no longer leaches from the deposit and poses no hazard to surface water courses. It is a typical description of deposit maturation. Geochemical behaviour of radium has not yet been reliably described, but its mobility in both oxidation-reduction and acid-base conditions is high. Crystallization (with Ba, Ca), precipitation (with Mn, Fe) and adsorption to Fe-Mn oxides, clay minerals and organic matter are considered to be the main geochemical barriers.

Acknowledgments

The article has been made in connection with project ICT CZ.1.05/2.1.00/03.0082 (Institute of clean technologies for mining and utilization of raw materials for energy use) supported by European Union and from the means of state budget by Ministry of Education, Youth and Sports. This research was also financially supported by the Czech Science Foundation (research project No. 105/09/0808).

References

Cairney T, Frost RC (1975) A case study of mine water quality deterioration. Mainsforth Colliery. County Durham. J Hydr 25(3–4): p 275–293

Carvalho FP, Madruga MJ, Reis MC, Alves JG, Oliveira JM, Gouveia J, Silva L (2007) Radioactivity in the environment around past radium and uranium mining sites of Portugal. J Env Rad 96 (1–3): p 39–46

Cressie NAC (1993) Statistics for Spatial Data – Revised Edition. John Wiley & Sons. New York

Hajek A, Lusk K, Vsetecka M, Vesely P (2006) Analysis of flooding the uranium mines in the Czech Republic. Archives of Diamo s. p., 171pp and suppls. (in Czech), MS

Jolliffe IT (1986) Principal Component Analysis. Springer-Verlag, New York

Manly BFJ (1994) Multivariate Statistical Methods. A Primer. Chapman & Hall, London

Michalek B, Hajek A, Grmela A (2005) Closure of Uranium Mines in the Czech Republic. In: Proceedings of the Conference Mine Planning and Equipment Selection 2005, Singhal (ed.), Banff, Canada, p 805–826

Johnson KL, Younger PL (2002) Hydrogeological and geochemical consequences of the abandonment of Frazer's Grove carbonate hosted Pb/Zn fluorspar mine, North Pennines, UK. In: Younger PL. Robins NS. (Eds.), Mine Water Hydr and Geoch. Geological Society, London, Spec. Publ. 198: p 347 – 364

Nuttall CA, Younger PL (2004) Hydrochemical stratification in flooded underground mines: an overlooked pitfall. J Cont Hydr 69 (1–2): p 101–114

Parkhurst DL, Appelo CAJ (1999) User`s guide to PHREEQC – a computer program for speciation. batch – reaction. one dimensional transport. and inverse geochemical calculations. U. S. Geol. Surv. Denver. Colorado. USA. [online] available on: http://water.usgs.gov/software. [cited 1. 3. 2012]

Wolkersdorfer Ch (2008) Water Management at Abandoned Flooded Underground Mines. Springer-Verlag, Berlin

Younger PL, La Pierre AB (2000) 'Uisge Me`inne': mine water hydrogeology in the Celtic lands, from Kernow (Cornwall, UK) to Ceap Breattain (Cape Breton, Canada). In: Robins NS. Misstear BDR. (Eds.), Groundwater in the Celtic Regions: Studies in Hard Rock and Quaternary Hydrogeology. Geological Society, London, Spec. Publ. 182: p 35–52

Younger PL, Wolkersdorfer Ch, ERMITE-Consortium (2004) Mining Impacts on the FreshWater Environment: Technical and Managerial Guidelines for Catchment Scale Management 23. Supplement 1: p 2–80

Zeman J, Cernik M, Supikova I (2009) Dynamic model of long term geochemical evolution of mine water after mine closure and flooding. Water Institute of Southern Africa & International Mine Water Association: Proceedings. International Mine Water Conference. Pretoria (Document Transformation Technologies) p 828-836

A Rational Approach to Pit Lake Chemistry Modeling

Dave Richers[1], C. Doc Richardson[1], Amy L. Hudson[2]

[1]*Tetra Tech, 350 Indiana Street, Suite 500, Golden, Colorado 80401, USA, dave.richers@tetratech.com; doc.richardson@tetratech.com*
[2]*Tetra Tech, One Monarch Drive, Suite 202, Littleton, Massachusetts 01460, USA, amy.hudson@tetratech.com*

Abstract Pit lake modeling can be complex due to the need to consider the water/rock interactions with the lithology exposed on the final pit walls and with any backfill material. Taking a systematic and iterative approach to pit lake modeling will ensure the proper level of detail and more accurate predictive results are generated. Developing a pit lake model in a stepwise method (conceptual model to "general" system representation to a detailed spatially representative statistically based model) allows for the model to be aligned with the level of detail of the data and the complexity of the scenario.

Keywords Pit Lake, PHREEQC, Geochemistry, POSTGRES, Groundwater, Mine Closure

Introduction

Several approaches to pit lake modeling have been utilized, that while yielding generally grossly comparative results, can result in subtle differences in the final pit lake chemistry. These differences are due either to considering or ignoring spatial chemical variability in wall rock materials, runoff solutions, groundwater solutions, and pit lake waters. For a sound, representative model water chemistries, pit wall, and backfill material need to be consider material type, spatial parameters, and overall chemical (particularly ARD/ML) parameters. These are used to develop the probable pit lake chemical behavior and composition from inception through post-closure, as well as provide source term inputs for numerical models. For many projects, the quantity and quality of data available may be such that the model of the pit lake cannot be developed beyond the conceptual model phase. Even at this stage, the model can provide some information about the potential for geochemical risk. Whenever possible, the GIS component should be applied and averaging, or lumping parameters should be avoided.

Developing a sound pit lake model requires significant amounts of data, often more than what most investigators utilize. In most cases, the model only utilizes the "average or generalized" groundwater chemistry and the zonal leachate chemistry of each rock type, along with the effective area (volume) of rock exposed on the pit wall as well as backfill within the pit. Such aqueous calculations are carried out using geochemical modeling packages such as the United States Geological Survey (USGS) PHREEQC software (Parkhurst and Appelo 1999). This type of model results in a simplified pit lake chemistry that can be a good approximation of the system, especially where limited data exists. For many projects, such a model will provide enough detail to develop water management and permitting strategies. However, the complex nature of these systems may require additional detail to fully characterize the long-term behavior of a pit lake. Using detailed spatial information to model groundwater/wall rock interactions, along with localized differences in the chemistry of the wall rock and backfill materials, results in a more detailed picture. Additionally, by taking into account chemical processes such as dissolution, precipitation, and colloidal formation, as well as utilizing a statistical representative number of static and kinetic samples that also spatially representative, a more defensible and accurate pit lake model will ensue. Application of GIS then becomes a preferred and necessary step in fine tuning the overall model.

Conceptual Model Method

Regardless of the complexity of the system and the data available, the first step in understanding the long-term behavior of a post closure pit lake is the development of a conceptual model of the system, including all water and chemistry inputs and outputs. Prior to mining, groundwater is generally in equilibrium with the country rock. As the groundwater passes through the ore body, natural concentration gradients might exist in the pre-mining stage. Once mining commences, the normal flow of groundwater is disrupted often resulting in changes in flow dynamics. After the completion of mining and cessation of dewatering the rate of pit filling and stage of the pit lake will be controlled by the post-closure water balance. Conceptually, the post-closure water balance can be expressed as:

$$\Delta_{\text{pit lake volume}} = I_{\text{precip}} + I_{\text{run-off}} + I_{\text{pit run-off}} + \mathrm{GW}_{\text{inflo}} - E_{\text{pit}} - \mathrm{GW}_{\text{outflow}} - \mathrm{SW}_{\text{outflow}}$$

Where:

I_{precip} inflow from direct precipitation falling on the lake surface;

$I_{\text{run-off}}$ inflow from run-off from up-gradient drainages;

$I_{\text{pit run-off}}$ inflow from pit wall run-off (the fraction of precipitation falling on the pit walls that ultimately reaches the pit lake);

$\mathrm{GW}_{\text{inflow}}$ groundwater inflow to the pit lake;

E_{pit} open water evaporation from the pit lake surface based on a pan or estimated evaporation rate;

$\mathrm{GW}_{\text{outflow}}$ outflow of groundwater from the pit lake; and

$\mathrm{SW}_{\text{outflow}}$ outflow from surface water from the pit lake.

The interaction between these parameters is presented schematically in Fig. 1.

Understanding the geochemical reactions of mined rock and water interactions is critical in assessing the potential for mining projects to adversely affect the quality of the surrounding environment. There are two different classes of mine drainage that might impact water quality:

- Alkaline drainage (basic pH water that may contain elevated total dissolved solids (TDS), oxy-anions such as arsenic and selenium);
- Neutral pH (that may contain elevated TDS and metals that remain soluble at neutral pH such as zinc, nickel, and sometimes copper); and

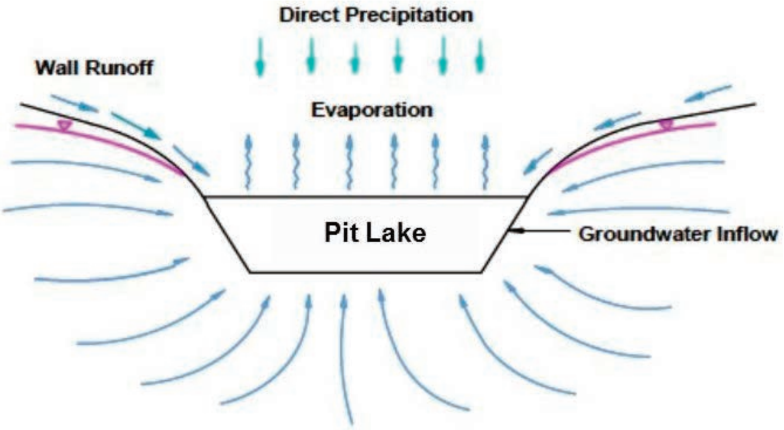

Fig. 1 *Post Closure Pit Lake Water Balance.*

- Acid drainage (acidic pH water that usually contains elevated aluminum, iron, manganese, copper, and other metals).

During the mining stage atmospheric oxygen, humid air, run-off, and precipitation can impinge on the wall rock and produce local zones of ARD/ML allowing for the buildup of metal salts on and in the wall rock surfaces. As the pores within the wall rock are resaturated they can react with the pit wall runoff or lake water at alter the chemistry. The hydration of stored salts and acids in the pore rock can be significant, with near instant additions of acidity as well as metals to groundwater as well as pit lake waters. Similarly carbonate dissolution with an increase in alkalinity may occur depending upon the particular litho-chemical environment.

Simple Numeric Modeling Method

Numeric modeling can act as a useful tool in addressing potential future impacts of mining facilities (Zhu and Anderson 2002). The use of computer modeling codes provides a way to quickly test a variety of scenarios for a particular system. The results are a quantitative estimate of the system that can be used to identify key parameters and understanding of the system.

Mining facilities are complex systems that need to be addressed with a multidisciplinary approach. Therefore, numerical modeling of a post closure pit lake development can require multiple modeling platforms and methods to be utilized. Hydrologic modeling can be used to establish a water balance of this system, which provides information about the quantities, as well as the interactions, of the water inflows and outflows in the affected areas. Hydrogeologic models can be applied to simulate dewatering systems, pit filling, facility/groundwater interactions, and fate and transport of any impacts to the groundwater. Limnological modeling can be a key component in a predictive modeling study to define the lake's physical behavior or temporal. Finally, the geochemical modeling is used to determine the overall water chemistry of the pit lake's life.

By integrating different modeling disciplines into a site-wide model, the system can be tuned to generate a more realistic characterization. This type of a modeling approach by its nature is extremely data intensive and one often resorts to some simplifying assumptions and data averages.

Such simplification should be avoided if at all possible as the use of a highly integrated approach can provide a complete understanding of the pit lake system over time as well as better predict potential environmental issues that may arise.

Spatially Distributed Data Modeling Method

In larger mining projects and more complex systems modelers may have access to large quantities of data, which if spatially distributed, results in a more detailed model. As with the previous numerical modeling discussed, spatially distributed data modeling relies on multiple disciplines to provide a more detailed pit lake model. For this type of modeling, several components are required. First, an accurate mapping of differences and character of groundwater chemistry spatially around the pit is paramount. As mining ceases, the cone of depression that was generated during dewatering around the pit will rebound. Initially, at least, this water will encroach on the pit from all directions. Fig. 2 illustrates two of the many possible variations that may be encountered in the geologic settings and thus the groundwater chemistry near an ore body. By utilizing the models such as those shown in Fig. 2, it can be seen that infilling water may exhibit differing chemistries depending on whether it is migrating from upgradient or down gradient areas.

In that the chemistries of the groundwater may be different depending on the local character of country rock adjacent to the pit, using an averaged groundwater composition, as is commonly done in traditional pit lake

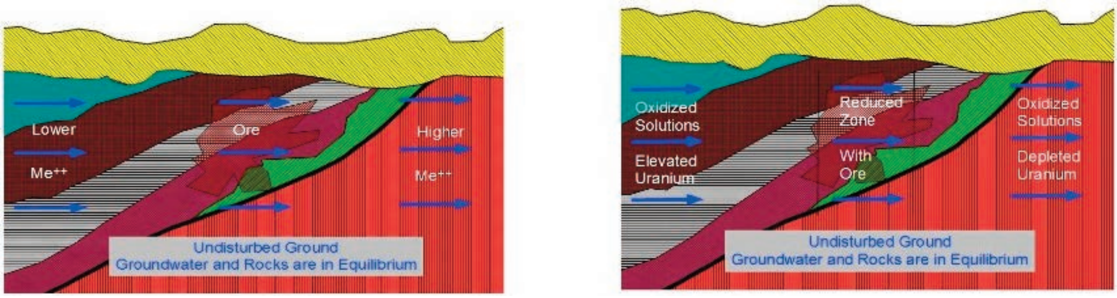

Fig. 2 *Groundwater Character Prior to Mining*

models will result in an inaccurate model. Rather, using spatially distributed modeling methods to define the groundwater chemistry, based on well data and the proximity to those wells to the wall rock (Richers *et al.* 2012a) is a better approach. Utilizing lake filling models such as those derived from the MODFLOW LAK2 or LAK3 packages will allow groundwater nodes to be defined to relate sources of flow relative to wall rock geology. By coupling these models with Geographic Information Systems (GIS) the spatially defined wall rock interactions with the groundwater regime can be utilized (Richers *et al.* 2012b). This flow can then be partitioned among its nearest wall rock cells using some spatial weighing method such as a simple inverse square distance function. In effect, this allows one to assign a measured influence between groundwater nodes and a wall rock geologic cell; those closer would have influence than would more distal groundwater cells (Fig. 3). By defining the chemistry of the groundwater to specific model nodes, spatial differences can be better accounted for and possible localized chemical reactions and processes that otherwise might be overlooked can be included in chemical management considerations.

By carefully integrating the localized groundwater chemistry interaction with the pit walls, reactions that might otherwise be ignored or misrepresented in an averaging approaches to modeling may be realized. Also, depending upon the detail in the groundwater model, areas of localized higher flow, such as along fracture systems or higher porosity zones can be identified. Additionally, areas of preferentially higher chemical reactivity, as well as the inverse, may be identified and exhibit can be simulated to allow prediction of the expected chemical interactions between groundwater and wall rock.

The wall rock composition of the Ultimate Pit Surface (UPS) is also an important data requirement for spatially distributed data models (Moran and Richers 2011). Generally, a geologic block model of the lithology is merged through a GIS application to show the geology on the UPS. This provides a means to ascertain

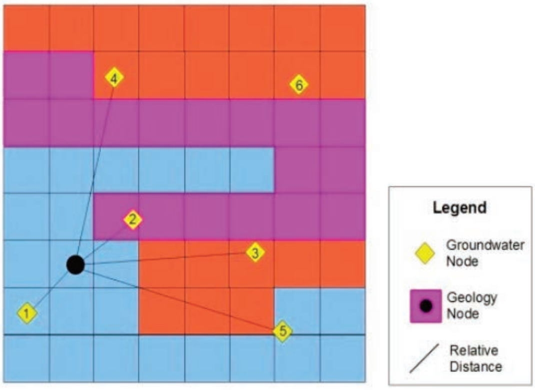

Weighted Distance (Wi) Is Determined as:

$$W_i = \frac{\left[\frac{R-h_i}{Rh_i}\right]^2}{\sum_{j=1}^{n}\left[\frac{R-h_j}{Rh_j}\right]^2}$$

Fig. 3 *Inverse Square Distance Weighing Example.*

relative proportions of rock types on the UPS and allows for calculating exposed areas of each rock cell. The accurate definition of the spatial extent of the UPS is an essential step in the process and should be made with great care. Generally a slope correction is applied to this surface to adjust the exposed area to represent actual areas of the horizontal or vertical exposures. Similarly, rather than utilizing an average wall rock chemistry, lithologically defined source terms are spatially applied to the UPS. This allows detailed groundwater-wall rock interactions potentially resulting in the dissolution/precipitation of species from the solution to be evaluated spatially throughout the pit. When averaging rock types, these local reactions are often missed resulting in a subtle, but distinctly different chemical outcome of the model, as well as potentially overlooked mitigation strategies.

Fig. 4 depicts what a typical groundwater node location map might look like relative to the UPS. Each node is defined over all time steps of the model to determine the flux of the groundwater into (or out of) the pit lake. This will vary over time and will help to define the geochemical inputs and mixing requirements of subsequent geochemical modeling. Geostatistical modeling software is used to derive the geologic input from evaluating many thousands of lithologic data points in 3D space and applying an appropriate 3D Kriging model. The resulting map is then used to correlate the chemical results of representative samples to the static chemical tests, kinetic tests, or both. It should be noted that the assignment of the chemical results of the formation sample that most closely matches the UPS geology node is required. It is not unusual for a given formation to exhibit acid generating character at one location and show a completely different character at another location. Having sufficient geochemical samples to track this reduces the overall uncertainty related to the simulated model predictions.

As with more traditional pit lake modeling approaches, the water chemistry conditions over time are predicted using PHREEQC (Parkhurst and Appelo 1999) or a similar geochemical modeling program. Utilizing software specific to geochemical simulations allows for a robust evaluation of the expected geochemical process, such as dissolution/precipitation adsorption, and speciation, to be applied to the spatially defined water-rock interactions. In that such an approach often is data

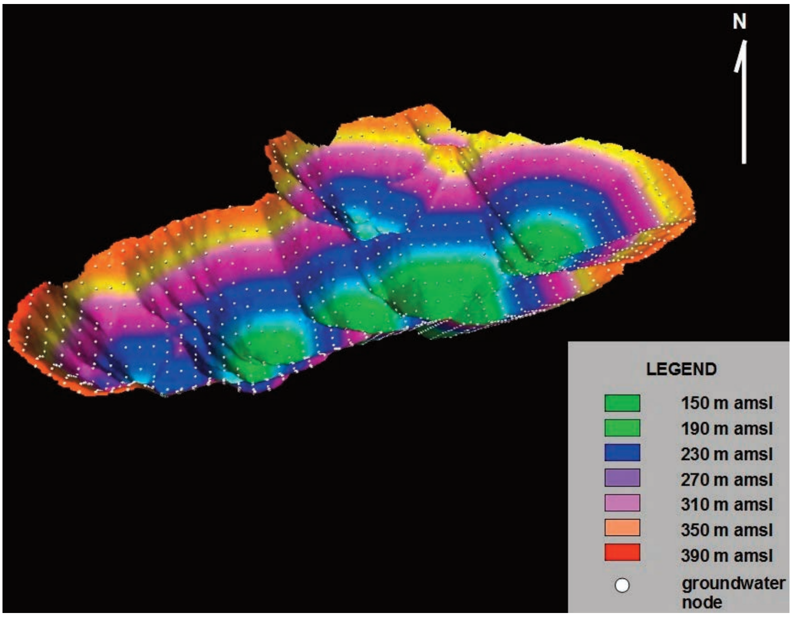

Fig. 4 *Mapping Groundwater Nodes to UPS*

intensive, input and output data from the geochemical modeling program, as well as all pertinent GIS data relationships are stored in a POSTGRES database and extracted utilizing customized scripts. Depending upon the complexity of the groundwater model and the size and nature of individual geologic cells, the model may involve several hundreds of thousands to millions of calculations that are better suited in customized computer programs rather than traditional chemical accounting techniques.

Conclusions

Pit lake systems can have a significant amount of complexity, but understanding the limitations of the quality and quantity of the site data that is available and developing appropriate pit lake models is critical to properly managing these post closure features. Applying a stepwise approach to the modeling allows for the model to be aligned with the level of detail of the data and the complexity of the scenario. For early phase projects and sites with limited data, pit lake modeling may be limited to a conceptual model defining the expected water balance components and general geochemical character of the geologic setting. This can provide a basic understanding of the geochemical risk, but will not allow for development of management strategies.

More traditional numeric models can be powerful tools used to develop and understanding of the level of geochemical risk, as well as to develop mitigation and management solutions. Numerical modeling can be very data intensive, forcing most post closure pit lake models to be based on a limited data set and many simplifying assumptions. However, by carefully integrating the spatial distribution of the information, the pit lake model can be used to evaluate localized, but often important chemical reactions that might otherwise be overlooked. Utilizing geologic block models and integrating the UPS with the geochemical characterization provides for a means to develop a more detailed and spatially distributed model of the long-term conditions of a post closure pit lake.

References

Moran P, Richers D (2011) Mapping Wall Rock Chemistry on the Ultimate Pit Surface of an Open Pit Mine Utilizing GIS, Proceedings Tailings and Mine Waste, Vancouver, BC, November 6–9, 2011.

Parkhurst DL, Appelo CAJ (1999) User's Guide to PHREEQC (Version 2) – A Computer Program for Speciation, Batch-Reaction, One-Dimensional Transport, and Inverse Geochemical Calculations, USGS WRIR 99–4259.

Richers DM, Richardson CD, Moran P (2012a) Impact of Groundwater Chemistry on Wall Rock Chemical Leaching and Pit lake Character, SME Proceedings, Seattle, WA.

Richers D, Richardson CD, Edington D, Bijold B, Roemer G (2012b) Pit Lake Modelling – The Total System Approach, IMWA 2012 Conference, Bunbury, Western Australia, 6p.

Zhu C, Anderson G (2002) Environmental Applications of Geochemical Modeling. Cambridge University Press: Cambridge, United Kingdom.

Innovative Systems for Mine Closure at the Haile Gold Mine

Jerry Rowe

Hatch Consultants, 198 Union Blvd, Suite 200, Lakewood, Colorado, USA, jrowe@hatch.ca

Abstract Mine closure is an important part of the mine life cycle. The management of acid rock drainage (ARD) is a major consideration for closure at mining properties that contain sulfide-bearing materials. The use of innovative engineering designs that include passive systems for prevention and long-term management of ARD is often a good option. The Haile Gold Mine closure project implemented in about 2000 to 2005 used several innovative engineering solutions that incorporated passive systems. The goals of the closure systems were to minimize the potential for ARD generation, eliminate the need for long-term active treatment, and require minimal long-term maintenance.

Keywords mine closure, mine water management, water balance, passive treatment, ARD

Introduction

The best options for mine closure systems vary depending on the mine facilities, ore body, site conditions, and climate. Selecting the right closure system involves defining closure goals and criteria, assessing viable options for the mine site, defining a strategy to meet regulatory requirement, and balancing costs and benefits with risks and feasibility. The following items should be considered when developing the criteria for closure systems at a mine site:

- Understanding the site conditions that will affect the closure system including environmental and social constraints
- Defining the corporate goals and expectations of the mining company for closure
- Defining what performance measures will be used to determine success
- Evaluating the technical feasibility of the closure system
- Evaluating the regulatory feasibility of the closure system
- Understanding prior experience, including failures and successes
- Incorporating industry standards (*e.g.* MEND guidelines for ARD (Gilles and Hogan 2001))

At the Haile Mine, a careful evaluation of potential closure options was conducted that considered the following elements that are generally applicable to all mines:

- Maximize the use of natural conditions
  - In arid climates consider dry disposal and evaporative systems
  - In wet climates submergence is commonly used
  - Consider options for natural attenuation
  - Consider options for passive treatment systems
- Minimize long-term water treatment
- Utilize passive treatment measures to reduce long-term costs
- Evaluate cost/benefit of up-front closure work versus long-term operation and maintenance
- Educate regulators and other stakeholders to achieve buy-in to the innovative concepts in the closure plan
- Provide flexibility in design, construction, and operation
- Manage financial assurance and bond release
- Evaluate costs based on water quality goals and criteria
  - Focus on activities that will reduce or

eliminate active water treatment
    - Minimize contact water volumes that require treatment
    - Segregate waters to keep clean water clean
- Build closure systems that can be sustained with low operation and maintenance costs
- Understand public and regulatory perceptions and limitations

Haile Gold Mine

The Haile Gold Mine is located at the eastern edge of the Piedmont Province in South Carolina, USA. The mine property is in the Haile Gold Mine Creek (HGMC) watershed, which is characterized by moderate topography and is mostly covered with pine forest. Climate is sub-tropical with high rainfall (mean annual total of about 122 cm) and relatively high evaporation (mean annual total open water evaporation of about 107 cm).

The property is located within the Carolina Slate Belt. Metasedimentary bedrock units in the HGMC watershed include Pre-Cambrian argillites, subgreywackes, and felsic volcanics. All bedrock units have undergone extensive hydrothermal alteration and mineralization. The altered rocks are naturally enriched in sulfides. Mineralization and alteration extends upgradient within the HGMC drainage a considerable distance beyond the mined areas. The Tertiary Coastal Plain Sand (CPS) unit overlies bedrock on the higher areas of the HGMC watershed but has been eroded away along the stream valleys. This unit is predominantly comprised of bedded sand and silty sand.

The site-wide groundwater movement generally reflects topography, with gradients and flow directions towards the HGMC and tributary drainages. The CPS groundwater moves downslope relatively quickly, with a fairly short residence time. It enters into the lower-lying areas and contributes to surface water flow in the creek. Groundwater movement in the bedrock is much more limited because of the overall low permeability of the rock units, and also because of geologic structures which form barriers to groundwater flow. Thus, the bedrock groundwater is a very minor component of stream flow in the HGMC.

Gold was first discovered in stream placer deposits in 1827. Subsequently, lode deposits were developed into hillsides and eventually into glory hole and underground mining. The early mine facilities were destroyed during the Civil War but mining resumed at the site after the war and significant production occurred from 1888 to 1908. Mining was discontinued after this time until 1936, and then shut down again during World War II. Several mine shafts to depths greater than 35 m were constructed and the historic Blauvelt and Bequelin pits were used for tailing disposal during the 1930's and 1940's.

Modern mining operations at the site started in 1985 and produced gold through 1991. Operations consisted of mining ore from four small open pits and processing it using cyanide heap leaching technology. The modern mine features include the Champion, Snake, Red Hill, and Haile open pits, waste dumps, heap leach pads, and other associated mine facilities. In 2001, the Champion Pit was successfully closed and reclaimed as a pit lake and in 2003 the Snake Pit was closed as a shallow pit lake that incorporated an organic layer comprised of a 50/50 mix of inert soil and organic matter (woodchips, manure) with small amounts of crushed limestone (Rowe and Turner 2005). Both closures have performed very well to date. The Red Hill and Haile pits were closed as evaporative wetlands and the Blauvelt/Bequelin pits containing historic tailings were closed as a passive treatment wetland system in about 2005.

Red Hill Pit

The Red Hi1ll Pit was mined to a depth of about 40 m, which exposed sulfides in the pit walls. The closure approach selected for the Red Hill Pit included partial backfilling of the pit and creation of an evaporative sink/wetland on the surface of the backfill. Groundwater is man-

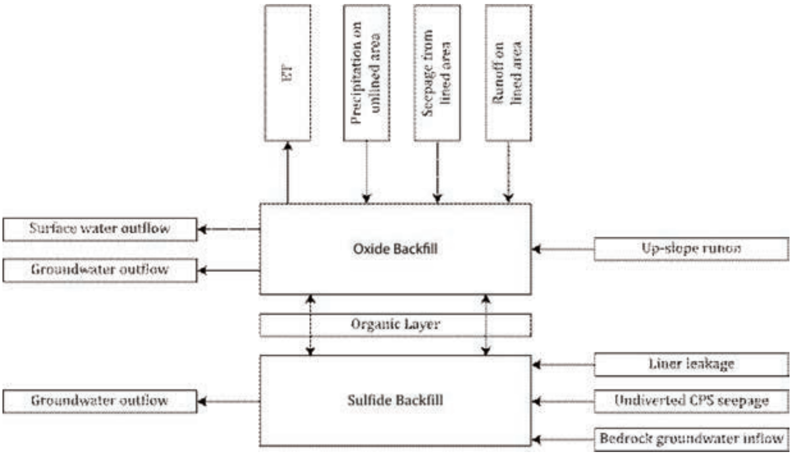

Fig. 1 *Red Hill Pit Closure Water Balance Components*

aged such that the groundwater table is maintained at or near the land surface.

Prior to designing a closure system, the hydrogeological, hydrological and climatic conditions for the pit were incorporated into a water balance model illustrated in Fig. 1. The model incorporated the key components of the closure system, including a sulfide backfill layer, an organic layer, and an inert oxide backfill layer.

Fig. 2 is a schematic section illustrating the cover system that was constructed in the central portion of the pit where the evaporative sink/wetland was formed. It consists of the following elements:

- Limestone-amended backfill consisting of sulfide waste rock. The alkalinity added to the backfill was sufficient to offset the existing acidity of the sulfide backfill material. Potential future ARD generation from the sulfide backfill is minimized by permanently submerging the material.
- An organic soil layer consisting of inert soil material mixed with organic media and limestone placed above the backfilled sulfides. This layer promotes reducing conditions that help stabilize the pore water chemistry and strip oxygen from waters that may from migrate from surface into the sulfide backfill.
- A top layer consisting of inert borrow material mixed with crushed limestone to provide a vegetative soil cover. The groundwater level in the pit was stabilized within the upper soil cover to provide permanent submergence of the sulfide backfill.
- A central swale across the cover surface to collect and control runoff of non-contact

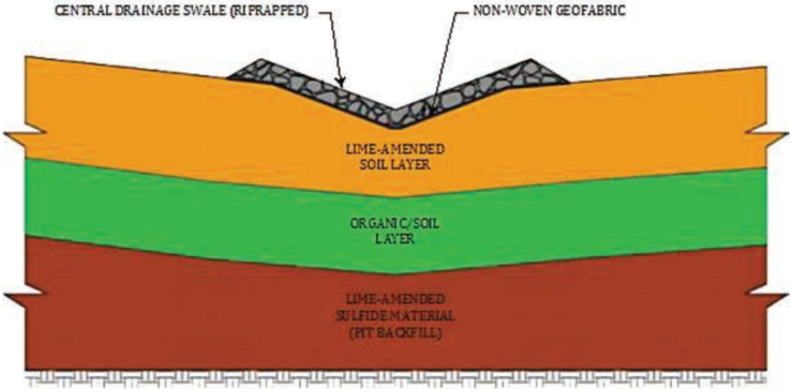

Fig. 2 *Organic System for Central Area of Red Hill Pit*

stormwater falling on the pit area. This channel keeps water from ponding on the cover.

Other elements of the closure system included:

- Engineered fill slopes on the pit walls with some areas covered by an impermeable synthetic liner and vegetative soil layer to isolate potentially reactive wall rocks from infiltrating precipitation and to minimize exposure of the wall rock to air. Precipitation falling on the cover will be shed as non-contact stormwater.
- Crushed limestone amendment along portions of the base of the pit wall to neutralize acidity that has built up over time in the pit walls. This zone may be saturated with groundwater or subject to periodic perched groundwater flows after closure.
- A collection drain at the top of the liner along some sections of the pit wall to intercept seepage from perched groundwater flowing in the CPS unit overlying bedrock to direct it out of the pit area before it can contact sulfide rocks.
- An interceptor ditch at the top of the liner along sections of the pit wall to intercept surface runoff from upslope areas and direct it out of the pit area. This ditch was designed with rip rap to prevent erosion and is intended to require minimal maintenance.

Fig. 3 is a photograph of the Red Hill pit shortly after the closure systems were implemented. It shows the diversion channel located near the bedrock/CPS contact on the pit slope, the lined and covered pit slopes below the channel, and the central portion of the pit. Stormwater originating below the diversion channel was retained by a temporary embankment at the outlet to the pit and sent to the treatment facility until it was demonstrated that the closure system was functioning as designed. It is now released as non-contact stormwater.

Blauvelt/Bequelin Pits

The Blauvelt and Bequelin pits were historic mine features dating back to about 1935. They were filled with tailing material from a nearby historic mill. The Blauvelt Pit was about 40 m deep and the Bequelin Pit was about 30 m deep. Historic mine maps indicated that underground workings also intersected the pits. The tailings area was very wet, being fed by both upstream surface water and groundwater sources. Fig. 4 shows a photograph of the tailings located in the Blauvelt Pit prior to closure. Water from the tailings area was collected and treated.

***Fig. 3** Red Hill Pit after Closure*

***Fig. 4** Blauvelt Pit Tailings Area*

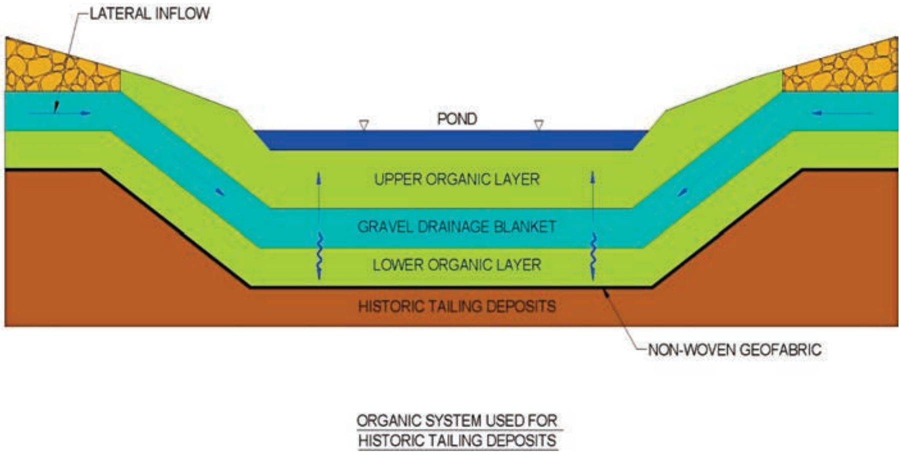

Fig. 5 *Conceptual Design of Wetland Area over Historic Tailings*

The closure and reclamation plan for the Blauvelt/Bequelin focused on capping and managing the historic tailing deposits contained in the area. The closure concepts used were similar to those being used elsewhere at the Haile Mine. They consisted of several key components that incorporated passive measures and a number of contingency measures to improve overall long-term performance.

Scattered tailing deposits in the Blauvelt/Bequelin area were consolidated into the pit areas and covered to prevent contact with stormwater. Sulfide materials that may exist in the historic tailings were submerged, stabilized, and permanently isolated to minimize the generation of acid drainage. The historic tailing deposits in the old pits were either covered with soil or a wetland area to minimize contact with stormwater. The cover system over the tailing deposits consisted of an organic layer to help stabilize the tailings and a gravel-drainage layer. Clean soil was placed over the top of the cover to reach final contours and then revegetated.

An upper wetland was established in the historic pit area to provide a source of water to keep the tailing material permanently submerged. The upper wetland included a gravel drainage layer sandwiched between organic layers. The gravel layer provides a subsurface pathway for shallow seepage to reach the wetland area, where most of it passes through the upper organic layer into a shallow pond. A schematic of the cover system is shown in Fig. 5. The upper wetland was designed to meet Best Management Practices for stormwater and shallow seepage occurring in the Blauvelt/Bequelin area.

All upgradient surface water flow was intercepted, diverted out of the Blauvelt/Bequelin area and released to the North Fork of Haile Gold Mine Creek. A significant portion of the subsurface flow in the upgradient CPS deposits was also intercepted and diverted out of the Blauvelt/Bequelin area by this feature. This significantly reduced the subsurface seepage to the Blauvelt/Bequelin area. A photograph of the construction of the central wetland is shown in Fig. 6 and the wetland area shortly after construction is shown in Fig. 7.

The North Fork of Haile Gold Mine Creek was diverted away from the existing channel that ran adjacent to the historic pits and a lower wetland was established in the old channel area to provide a contingency collection area for potential subsurface seepage from the historic pits. The lower wetland included a gravel drainage layer overlain by an organic layer and was designed to meet Best Management Practices for any shallow seepage flow from the historic Blauvelt/Bequelin area that may occur along the North Fork.

The Blauvelt/Bequelin closure system has functioned well since it construction in about 2005. Water from the wetland area meets applicable standards and is released to HGMC.

Fig. 6 *Wetland Closure System for Tailing Area*

Fig. 7 *Wetland Area After Construction*

Conclusions

The prevention and management of ARD is a key element for the successful closure of many mines. Often, the need for long-term active treatment of mine waters can be minimized or eliminated by effective closure designs that utilize passive systems for managing ARD. Permanent submergence of sulfide material limits exposure to oxygen and has been used successfully to manage ARD at many sites. Similarly, the use of organic materials to promote reducing conditions that result in the removal of metals and improvement of water quality is becoming increasingly common. The successful implementation of passive systems requires a good understanding of the overall site water balance to take advantage of the favorable site-specific hydrologic conditions. The Haile Mine implemented a number of closure systems that incorporated passive measures. These systems were constructed in the early to mid 2000s. Although detailed monitoring data are not publically available, the systems have functioned well to date.

References

Ford KL (2003) Passive Treatment Systems for Acid Mine Drainage. Technical Note 409, BLM/ST/ST-02/001+3596, Bureau of Land Management Web based report available online at www.blm.gov/nstc/library/techno2.htm

Rowe J, Turner T (2005) Innovative Systems for ARD. Mining Environmental Management, March 2005

Tremblay G, Hogan C (Eds) (2001) MEND Manual Report 5.4.2. Natural Resources Canada

Implications of high dissolved organic carbon concentrations on potential copper toxicity in surface waters in the vicinity of Cu-Ni-PGM deposits of the Duluth Complex, northeastern Minnesota

Robert R. Seal, II[1], Perry M. Jones[2], Nadine M. Piatak[1], Laurel G. Woodruff[2]

[1]*U.S. Geological Survey, 954 National Center, 12201 Sunrise Valley Drive, Reston, VA 20192*
[2]*U.S. Geological Survey, 2280 Woodale Drive, Mounds View, MN 55112*

Abstract Regional baseline surface-water sampling was conducted in northeastern Minnesota to understand the potential effect of high dissolved organic carbon (DOC) concentrations on copper toxicity to aquatic organisms in the context of proposed new mining in the area. The low-sulfide magmatic Cu-Ni-platinum group metal (PGM) deposits of the Duluth Complex have significant potential for future mining. The four main deposits that currently represent advanced exploration targets are Spruce Road, Maturi, Birch Lake, and NorthMet. They are distributed along a 40 km strike length trending NE—SW. These deposits are dominated by disseminated Cu-Ni-Fe sulfide minerals and occur near the base of troctolitic intrusions that comprise the complex. The surface-water hydrology of the area consists of lakes and wetlands connected by streams and rivers. The average annual precipitation is 71 cm, the average low temperature in January is –23 °C and the average high temperature in July is 9 °C.

Nineteen sites along streams that transect the complex were sampled in September 2012 near base-flow conditions to document pre-mining baseline water-quality conditions. The samples were neutral (pH 6.9 ± 0.4), dilute (EC 59 ± 20 µS/cm), and oxic (dissolved oxygen 7.6 ± 1.8 mg/L). The dissolved cations were dominated by Ca (5.1 ± 2.2 mg/L) and Mg (4.2 ± 1.6 mg/L) with lesser Na (1.8 ± 0.9 mg/L) and K (0.3 ± 0.1 mg/L). Bicarbonate, as reflected by the alkalinity values (19.8 ± 8.7 mg/L $CaCO_3$), and sulfate (2.2 ± 0.7 mg/L) were the dominant anions. Water hardness ranged from 18.1 to 49.6 mg/L $CaCO_3$ and DOC concentrations were substantial, ranging from 17.7 to 46.7 mg/L. Substantial dissolved trace elements were Fe (472 – 3,950 µg/L), Al (54.4 – 228 µg/L), Cu (0.8 – 7.7 µg/L), Ni (1 – 4.8 µg/L), and Co (0.4 – 2.5 µg/L).

The toxicity of Cu and other trace elements to aquatic organisms commonly associated with mining is known to vary with water chemistry. Site-specific water-quality criteria for Cu were calculated for these samples using both the U.S. Environmental Protection Agency hardness-base equation and the Biotic Ligand Model (BLM) to evaluate the potential role of local water chemistry on the toxicity of dissolved Cu. Results using the hardness-based equation suggest acute toxicity can be expected from dissolved Cu concentrations beginning at 3.5 to 9.2 µg/L. Based on this model, six samples exceeded acute criteria. In contrast, results from the BLM, which uses a broader range of water-quality parameters including DOC concentrations, suggest that acute toxicity can be expected from significantly higher concentrations beginning at 4.3 to 130.5 µg/L. All samples were below the BLM-based criteria. Thus, results from the BLM suggest that complexation with DOC should significantly mitigate the toxicity of Cu in the watersheds in the vicinity of the Duluth Complex.

Keywords platinum-group metals, copper, surface water, biotic ligand model, Minnesota

Vegetation of historical mine waste from the Ljusnarsberg deposit with *Agrostis capillaris* – Impact on leaching of copper

Viktor Sjöberg[1], Stefan Karlsson[1], Anna Grandin[1], Bert Allard[1]

[1]Man-Technology-Environment Research Centre, Örebro University, 701 82 Örebro, Sweden
viktor.sjoberg@oru.se

Abstract In Sweden there are hundreds of sites that need to be remediated due to high release of metals such as Cu. In order to minimize costs the methods should involve cheap materials and technical solutions. This study focuses on the possibility to establish *Agrostis capillaris* on sulfidic mine waste, after mixing with 30 % bark compost, and the subsequent release of Cu. Initially the substrate produced leachates with pH 3.5 containing approximately 1 mg/L Cu. After 4 months the pH had increased to 4.5 and up to 80 % of the Cu was retained.

Keywords *Agrostis capillaris*, bark compost, mine waste, copper, Cu

Introduction

In Sweden hundreds of historical mine waste sites exceed national standards for the release of toxic metals to the environment (SEPA 2013). Most of the sites are relatively small and often located in remote areas. At many sites the metal content in the waste exceeds what is today classified as ore and the waste material is often rich in elements that had no value at the time of mining. Since many of the mines were closed more than 100 years ago there is rarely an identifiable owner. Instead, the ownership of the sites is transferred to the local municipality, which then becomes responsible for the remediation. Therefore the remediation strategy for such sites must be cost efficient (*i.e.* low initial and maintenance costs). Hence, traditional techniques, such as dry or wet covers and water treatment plants, are not feasible solutions at the majority of the sites. Several passive techniques are attractive options for stabilization and water treatment. By establishing a vegetation cover it is possible to lower the erosion from wind, rain and frost as well as reducing the volume of infiltrating rain water (Yang *et al.* 2010). In the case of mine waste this may decrease the release of metals. However, physical and chemical properties of many historical mine waste materials do not promote plant growth due to low nutrient content, coarse structure, low pH and high content of soluble phytotoxic elements (*e.g.* Cu). To overcome these growth-limiting factors, different kinds of additives can be used that either specifically affect one factor (*e.g.* addition of fertilizers to provide more nutrients) or a combination of them (*e.g.* addition of alkali to increase the pH and precipitate metals as insoluble hydroxides). To decrease the cost of the remediation it is of interest to find cheap materials that preferably combine these properties. One candidate material is bark compost since it increases the water holding capacity and also acts as a buffering agent for acid generated during sulfide weathering. The bark also serves as an effective adsorbent for many different metals, including Cd, Cu and Zn, within quite a wide pH range (Reddy *et al.* 1997, Seki *et al.* 1997, Gichangi *et al.* 2012). It is also very essential that the chosen plant species are suitable for these harsh environments. One species that has shown good tolerance against drought, low pH and high metal concentrations is *Agrostis capillaris* (Common bent; Cotter-Howells and Caporn 1996, Banásová *et al.* 2006, Bech *et al.* 2012). In order to improve the establishment of the plants as well as their long term survival addition of species specific mycorrhiza is beneficial or even necessary (Turnau *et al.* 2008).

Here we report some results on the release of phytotoxic Cu when historic sulfidic mine waste is mixed with bark compost (30 %, volume) in order to improve the growth conditions for A. capillaris. The study includes data from two seasons with outdoor pot experiments as well as a general characterization of the materials. The effects on Cu mobilization by addition of mycorrhiza, alkaline material and an easily accessible carbon source are also included.

Materials & Methods

Weathered sulfidic mine waste older than 150 years was collected at the Ljusnarsberg mine site in south central Sweden in late June 2011. Eighteen month before, the mine waste was sieved and material larger than 5 mm was discarded. To enhance the water holding capacity, commercially available bark compost (< 20 mm in size) was added (30 % volume). To estimate the water-soluble fraction of Cu in the mine waste and the bark compost, respectively, a conventional leaching with 18.2 MΩ water was performed at a liquid to solid ratio (L/S) of 10 in an overhead shaker for 24 h at room temperature.

Before filling of the pots, the mine waste and bark compost were thoroughly mixed with garden forks to a test substrate. After mixing, 1.8 L of the substrate was put on top of a 3 cm layer of granite gravel, 10 mm in diameter, in 2 L plastic pots (diam. 180 mm, height 160 mm) and they were gently tapped to compact the mixture. The treatments that were evaluated, according to table 1, were prepared in triplicates. The mycorrhiza culture was kindly provided by Prof. K Turnau (Jagiellonian University in Krakow, Poland). For reference purposes dead mycorrhiza was prepared by heating a sub-volume of the mycorrhiza culture. Water works granules (WWG) were used as an alkaline additive. They are a spherical (diam. 1–4 mm) refuse from softening of potable water and consist of a calcium/magnesium carbonate matrix with varying concentrations of other carbonate forming elements. As an easily accessible carbon source for heterotrophic microorganisms, aspen (*Populus tremula*) wood shavings (AWS) were added to one series. Mycorrhiza (living or dead) as well as WWG were mixed into the top 50 mm whilst AWS was mixed into the entire volume of the substrate. Mycorrhiza, WWG and AWS equivalent to 0.3 L m^{-2}, 0.5 kg m^{-2} and 50 L m^{-3}, respectively, were added.

After preparation of the pots, 40 mL m^{-2} of *A. capillaris* seeds was spread on top of the substrate. No seed cover was used and the pots were immediately sprayed with collected rainwater, equivalent to 10 mm rainfall. After 3 weeks of growth, 2 of the pots from T7 received a single dose of commercial inorganic fertilizer. After hibernation 40 mL m^{-2} of new seeds were spread on each pot to compensate for any loss of plants due to an unusually long period with repeated freezing and thawing during the early part of the winter.

During the first season the pots were watered with rainwater (collected as well as as

Treatment	*Mycorrhiza*		WWG	AWS
	living	dead		
T1	—	—	—	—
T2	—	—	Yes	—
T3	—	Yes	—	—
T4	Yes	—	—	—
T5	—	Yes	Yes	—
T6	Yes	—	Yes	—
T7	—	—	—	Yes

Table 1 *Design of the treatments with living and dead mycorrhiza, water works granules (WWG) and aspen wood shavings (AWS).*

rainfall), equivalent to 10 mm rainfall, every week and samples of the percolation water were collected. During the second season only natural rain falls were used to generate leachates, and sampling took place less frequently. After sampling were the solutions immediately frozen (-20 °C) to maintain their composition. After thawing, pH and electrical conductivity were measured in unfiltered samples. Solutions for Cu and total organic carbon (TOC) analysis were, prior to analysis, filtered through 0.20 µm polypropylene filter disks. Copper was measured by ICP-MS (Agilent 7500 cx) with 10 µg/L Rh as an internal standard and TOC analysis was performed with a Shimadzu TOC-VPH analyzer. For modeling of the aqueous phase Visual Minteq (ver. 3.0) was used.

Results & Discussion

No significant (p 0.05) difference in germination was found between the treatments and approximately 90 % of the seeds gave seedlings. After 2 weeks of growth there was no significant (p 0.05) difference in shoot length between the treatments. After the snowmelt and in the beginning of the second season the length of the shoots were re-measured and it was found that addition of WWG (T2, T5 and T6) promoted growth, or at least sustained it, (p 0.05). Among these treatments, addition of WWG and living mycorrhiza (T6) gave the longest shoots (p 0.05). Even longer shoots (p 0.05) were found in the two pots from T7 that received inorganic fertilizer which is clear evidence that the concentration of available nutrients limited the growth in the other treatments.

After leaching of the mine waste with 18.2 MΩ water, an average of 8900 µg/L Cu was found in the solutions ($n = 3$). The corresponding concentration for the bark compost was 9 µg/L. Compared with the CCME (Canadian Council of Ministers for the Environment) "water quality guidelines for the protection of aquatic life" (CCME 2013) the leachates from the mine waste exceeded the guidelines by more than tree orders of magnitude. The results clearly show that the mine waste is a severe environmental threat. They also indicate that the contribution of Cu from the bark compost in the substrate is of minor importance, even negligibly. In the pot experiments the systems reached an L/S of approximately 5 after the first season and by the end of the second season it had increased to almost 10. During this period the Cu concentration in all leachates (table 2) was only some 20 % of those in the L/S 10 leaching of mine waste which indicates retaining properties of the bark compost as well as the additives. All treatments followed the same decreasing trend during the first season, illustrated in Fig. 1 with data from T1 (reference system). At the end of the first season, reduction factors of 2 to 5 were obtained for Cu in the leachates from the different treatments (table 2). During the second season all treatments produced leachates with slightly increased Cu concentrations.

In T2 and T7 the highest initial concentrations of Cu were observed and also the highest reduction with time (table 2). Over the two seasons the total reduction was as for the first season highest in the treatments that gave the highest initial concentrations (table 2). Addition of WWG (T2) or AWS (T7) resulted in a

Sampling	T1	T2	T3	T4	T5	T6	T7
Initial 07/02/11	933	1321	663	939	1108	823	1919
Final 11/20/11	371	330	327	440	362	248	408
Season 2 average	416	567	488	673	689	418	787
Reduction season 1	2.5	4.0	2.0	2.1	3.1	3.3	4.7
Reduction season 1+2	2.2	2.3	1.4	1.4	1.6	2.0	2.4

Table 2 *Initial and final Cu-concentrations (µg/L) in leachates from all treatments and calculated reduction factors.*

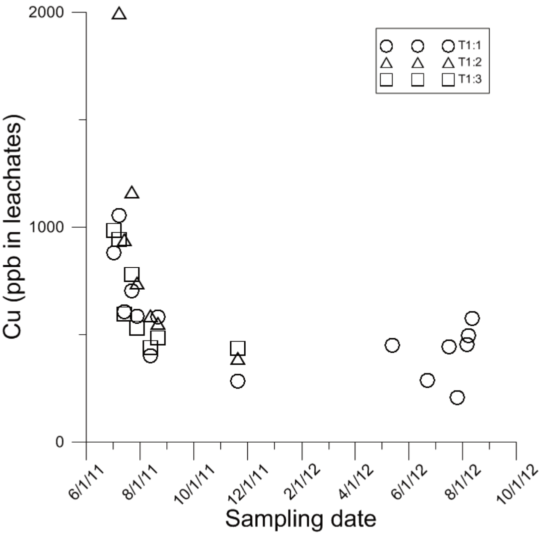

Fig. 1 *Cu-concentration in leachates from T1 during the first and second growth season.*

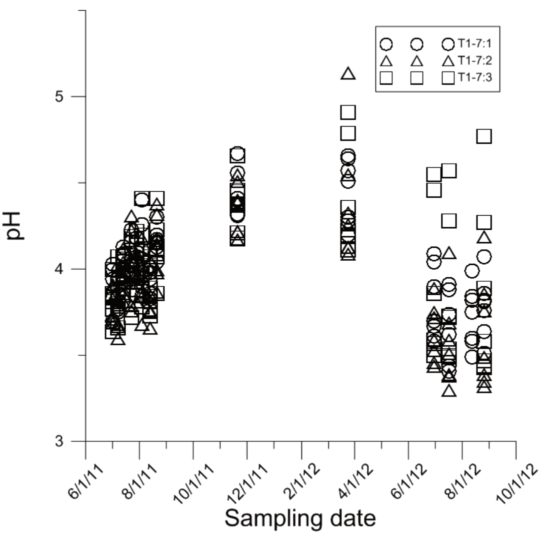

Fig. 2 *Variation of pH in leachates from T1 to T7 during the first and second growth season.*

higher initial release of Cu but the total removal was highest for those two treatments over two seasons (table 2).

During the first season pH increased with 0.5 to 1 unit in all systems. Initially a minimum of approximately 3.5 was observed which increased to a maximum of approximately 4.5 (Fig. 2). Apparently this was related to the high release of humic substances (Karlsson *et al.* 2013) from the bark compost and their collective buffering capacity. As the concentrations of DOC went down during the second season there was an increased variation of the pH for all treatments (Fig. 2). There was also a general decrease in pH with final readings close to or below their initial values. At this point, the readily available humic substances had been leached from the substrate and the DOC concentrations were lowered to some 10 mg L^{-1} of non-humic carbon compounds (Karlsson *et al.* 2013). Hence, the increase in pH during the first season might also have been influenced by heterotrophic production of alkalinity by the microbial community.

A clear decreasing trend in the electrical conductivity was found during the first season in all treatments, from approximately 2 – 0.8 mS cm^{-1}. The concentrations of Cu followed the development of electrical conductivity (r^2 0.82), although this ion is not a dominating constituent. As the electrical conductivity increased to some 1.5 mS cm^{-1} by the end of the second season its correlation with Cu became weaker (r^2 0.61). Hence, it appears as if different mechanisms controlled the concentrations of dissolved Cu. Equilibrium modeling indicated three major (> 5 %) Cu-species in the solution phase. Both initially and after two seasons Cu^{2+} accounted for some 75 %. Aqueous Cu-sulfate and Cu bound to organic carbon made up the remaining 25 %. The initial distribution was approximately 15 % and 10 % of Cu-sulfate and Cu bound to organic carbon, respectively, while the final distribution had changed to approximately 5 % and 20 %. The calculated saturation indices for predicted Cu-minerals were all below -5 why it is unlikely that any precipitation of stoichiometric Cu-phases occurred. Co-precipitation with Fe was also an unlikely redistribution mechanism since the only predicted mineral was cupric ferrite which had a saturation index below -13. The increase of organic Cu-complexes in solution suggests that a similar mechanism might explain the increased sorption of Cu. Hence, it can be concluded that the immobilization of Cu-ions at low pH, was caused by adsorption either directly to the surface of the bark compost or by adsorption of the Cu-organic complexes. It is not clear if the organic ligands originate from a physical release from the bark compost or if they were excreted from the microbial community.

Conclusions

By adding bark compost, WWG and living mycorrhiza to weathered sulfidic mine waste the growth of A. capillaris was promoted. Probably three factors were involved: i) adsorption of Cu to the bark compost or macromolecules from the same, ii) adsorption of Cu to macromolecules released from the mycorrhiza, and iii) neutralization of generated acid in the root zone. Hence, the growth was promoted due to detoxification of the pore water.

By adding bark compost to the sulfidic mine waste up to 80 % of the available phytotoxic Cu was retained in the solid phase. In combination with the surface stabilizing effect of A. capillaris it seems like addition of bark compost and A. capillaris can be a successful first action to minimize the environmental impact of phytotoxic Cu from sulfidic mine waste. However, it may be necessary to combine it with other additives such as mycorrhiza and alkaline material to promote the growth of A. capillaris. Before performing large scale operations the adsorption of Cu to bark compost or immobilization by root exudates must be better understood, in order to avoid secondary release of immobilized Cu-species in a longer time frame than in these experiments.

Acknowledgements

We thank the UMBRELLA-project for financing the study and its participants for valuable discussions. We also thank prof. Katarzyna Turnau and her staff, Jagiellonian University in Krakow, Poland, for providing us with seeds and mycorrhiza. The study was by financed by FP7 contract 226870.

References

Banásová V, Horak O, Čiamporová M, Nadubinská M, Lichtscheidl I (2006) The vegetation of metalliferous and non-metalliferous grassland in two former mine regions in central Slovakia. Biologia, Bratislava 61(4):433-439

Bech J, Corrales I, Tume P, Barceló J, Duran P, Roca N, Poschenrieder C (2012) Accumulation of antimony and other potentially toxic elements in plants around a former antimony mine located in the Ribes Valley (Eastern Pyrenees). Journal of Geochemical Exploration 113:100–105

CCME (2013) Canadian Council of Ministers of the Environment; Water quality guidelines for the protection of aquatic life. http://st-ts.ccme.ca Accessed 7 March 2013

Cotter-Howells J, Caporn S (1996) Remediation of contaminated land by formation of heavy metal phosphates. Applied Geochemistry 11:335–342

Gichangi EM, Mnkeni PNS, Muchaonyerwa P (2012) Evaluation of the heavy metal immobilization potential of pine bark-based composts. Journal of Plant Nutrition 35:1853–1865

Karlsson S, Sjöberg V, Grandin A, Allard B (2013) Bark compost as amendment to historic sulphidic mine waste – Release of dissolved organic substances. Environmental Science and Pollution Research Subm.

Reddy BR, Mirghaffari N, Gaballah I (1997) Removal and recycling of copper from aqueous solutions using treated Indian barks. Resources, Conservation and recycling 21:227–245

Seki K, Saito N, Aoyama M (1997) Removal of heavy metal ion from solutions by coniferous barks. Wood Science and Technology 31:441–447

SEPA (2013) Swedish Environmental Protection Agency www.naturvardsverket.se/upload/sa-mar-miljon/mark/avfall/Inventering-av-gruvor/Forteckning-nedlagda-anlggningar-120427.pdf (2013-02-25)

Turnau K, Anielska T, Ryszka P, Gawro´nski S, Ostachowicz B, Jurkiewicz A (2008) Establishment of arbuscular mycorrhizal plants originating from xerothermic grassland on heavy metal rich industrial wastes – new solutions for waste revegetation. Plant Soil 305:267–280

Yang SX, Liao B, Li JT, Guo T, Shu WS (2010) Acidification, heavy metal mobility and nutrient accumulation in the soil-plant system of a revegetated acid mine wasteland. Chemosphere 80:852–859

Enhanced 3-D Visualization as a Powerful Data Analysis and Stakeholder Communication Tool During Mine Closure

Matthew S. Spurlin [1], Eric Rogoff [2], Daniel M. Cichy[3], Craig E. Divine[3]

[1]ARCADIS US, Inc., 4999 Pearl East Circle, Suite 200, Boulder, Colorado, USA, Matt.Spurlin@arcadis-us.com
[2]ARCADIS US, Inc., 14201 North 87th Street, Suite 135, Scottsdale, Arizona, 85260, USA, Eric.Rogoff@arcadis-us.com
[3]ARCADIS US, Inc.,630 Plaza Drive, Suite 100, Highlands Ranch, Colorado, 80129, USA, Dan.Cichy@arcadis-us.com, Craig.Divine@arcadis-us.com

Abstract Three-dimensional (3-D) subsurface geologic modeling and visualization techniques are well developed and have proven to be powerful data analysis tools for many geosciences problems, including site investigation and mine water management applications. However, they are currently underutilized by environmental practitioners to analyze geologic and hydrogeologic data and effectively communicate findings to non-technical stakeholders. This presentation highlights several examples of where MVS, a leading 3-D visualization software, was effectively applied at mine sites to more thoroughly understand and convey information on hydrogeologic and environmental conditions. These examples support our recommendation that 3-D analyses should be more widely applied.

Keywords 3-D visualization, modeling, data analysis, planning, design, groundwater investigation, discharge, treatment, site investigation, mine water management

Introduction

Three-dimensional (3-D) geologic modeling and subsurface visualization techniques are proven and powerful data analysis tools for many geoscience applications, and have been used in mine planning and design for many years (Armstrong 2012; Rogoff 2012; Rogoff 2009; Spurlin 2010). However, they are currently underutilized by environmental practitioners to analyze geologic, hydrologic, and contaminant data, and to effectively communicate the results to non-technical stakeholders. Empowered by advancements in computer technology, software with specialized capabilities for environmental applications, and increased use of high-resolution investigation methods, practitioners are in a better position than ever before to drive innovation and develop opportunities by leveraging these tools. While conventional two-dimensional (2-D) methods are commonly employed, only a full 3-D analysis can integrate all geologic data and reveal the spatial correlations critical for accurate conceptual site model development. The 3-D analysis can then be utilized for remedial evaluation and selection of designs that minimize costs while achieving remediation objectives, and ultimately enable mine site closure. This paper describes how 3-D visualization tools can be cost-effectively applied at mine sites to dramatically improve the understanding of site conditions and perform remedial evaluations.

Methods

The use of 3-D modeling and visualization software to integrate geologic, hydrologic and geochemical data into a comprehensive, 3-D framework, provides a unique opportunity to gather important information about the spatial variability in site conditions. The Mining Visualization System (MVS) is a state-of-the-art 3-D software package that integrates geology, hydrology, geochemistry, and site features and is designed specifically for this application. These extensive capabilities allow analysis of complex, large datasets, yielding insights into the spatial variability in site conditions, which would otherwise remain hidden. Specifically, the package was used to combine analytical results from soil and water analyses with lithologic data obtained during visual core logging, cone penetrometer testing (CPT), hydraulic profiling testing (HPT), and geophysical logging (*e.g.* gamma, resistivity, spontaneous potential, neutron), to develop a comprehensive conceptual site model (Fig. 1). Output from quantitative flow and transport models (*e.g.* MODFLOW and MT3-D) can be readily displayed alongside site geology and other site data. Modeling of hydrogeologic data in MVS can also be performed as a precursor to groundwater numerical modeling in order to provide more accurate spatial representations of hydrogeologic conditions (Fig. 2). Additional subsurface conditions, such as the orientations of bedding and major fracture sets and faults, hydraulic head and gradient, mobile and immobile porosity, soil bulk density and moisture content, can be utilized in combination with lithologic and contaminant data to identify preferred groundwater migration pathways and zones of high contaminant mass flux. Using MVS, practitioners can produce animations that show changes in contaminant plumes or groundwater levels through time. MVS can maximize the value of information stored in large databases generated over decades of site management by developing a visible record that is more readily accessible and utilized, and facilitates data quality review. Furthermore, MVS also allows incorporation of GIS information, high-resolution topography and aerial imagery, as well as drawings from external sources (eg. CADD), so that all information can be placed within visual contexts that are familiar and easily understood.

The primary advantage of this 3-D modeling approach is the preservation of spatial integrity through the development of truly quantitative models. Unlike traditional conceptual visualization, this approach honors site data and can incorporate expert interpretations based on fundamental geologic, hydrogeologic, and geochemical processes. This approach consistently provides deeper insights into site conditions that are often overlooked

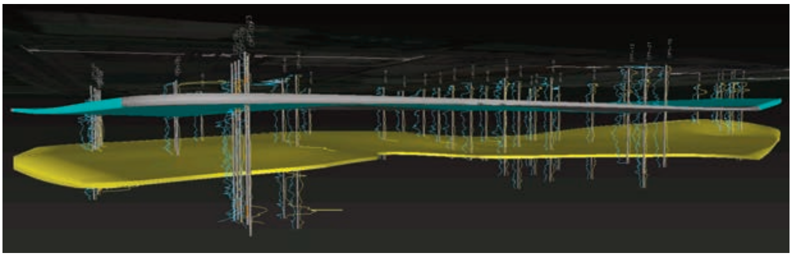

Fig. 1 *MVS can readily display and correlate characterization data obtained from CPT, geophysical and other high-resolution subsurface investigation techniques.*

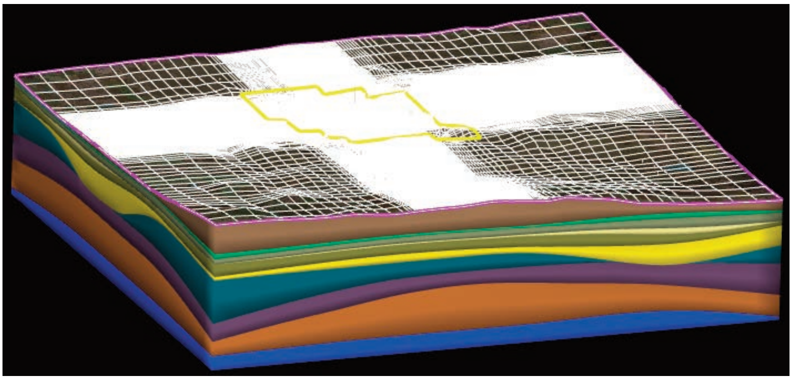

Fig. 2 *Modeling of hydrogeologic data in MVS can be performed as a precursor to groundwater numerical modeling in order to provide more accurate spatial representations of hydrogeologic conditions.*

with conventional 2-D analyses. Furthermore, a 3-D geologic model not only provides better insight into site conditions, but also serves as an effective communication tool for all stakeholders.

MVS model output is most commonly distributed using the Four-Dimensional Interactive Model (4DIM) Player, which is a free, standalone viewer. 4DIM Player files are fully interactive, and can contain multiple frames customized for data evaluation or communication of a focused message. Each frame can be zoomed, panned and rotated as a static 3-D model, allowing an astounding degree of flexibility and control to view results from any angle or magnification. The 4DIM Player can also run animations that allow full interaction by the viewer, which is a very effective way to illustrate groundwater or vapor flow, or movement of plumes through time. 4DIM modeling output is analogous to the portable document format (.pdf) file type; files are distributable and viewable by anyone with a viewer, and the content is controlled and locked from editing.

3-D geologic modeling is useful in many mining applications during the permitting, operation, and closure phases of the mine lifecycle. For example, MVS has been used to support baseline hydrogeologic characterization, ore body delineation, open pit operation, shaft and tunnel mining, solution mining, mineral exploration and extraction, and remediation design and performance assessment. Fig. 3 shows two examples where 3-D geologic modeling was used to understand complex bedrock structure and overall site geology. The first example provided an improved understanding of the spatial extent of vertical hydraulic communication between faulted and dipping water-bearing bedrock aquifer units and an overlying alluvial aquifer that is impacted with dissolved constituents sourced

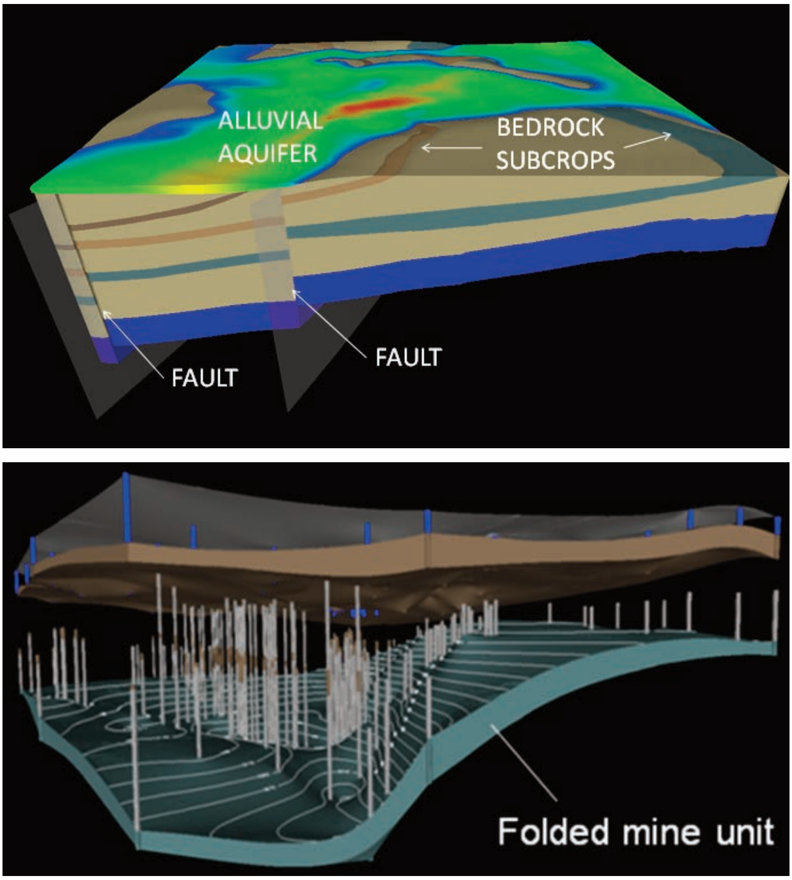

Fig. 3 *Two examples depicting the use of 3D geologic modeling at mine sites to understand and communicate complex bedrock structure and overall site geology.*

from an unlined mine tailings impoundment produced by milling operations. The second example was the basis for approval of an aquifer exemption petition where previous interpretations of a structurally folded, deep uranium ore mine unit was inaccurately characterized initially as a faulted and structurally offset feature acting as a potential source of dissolved radionuclides at an *in situ* leachate mine operation.

Fig. 4 further illustrates geologic modeling used to delineate the extent and saturated thickness of an impacted alluvial aquifer. The extent of the saturated alluvium was modeled as the intersection between the undulating eroded bedrock surface and the water table, which produced a highly accurate channelized geometry as a result of the high density of pertinent borehole locations.

Due to the data-driven nature of MVS, the modeling approach also serves as a quality control measure for available site information. Unlike conventional methods of data reporting (*e.g.* data tables or plan view location maps), this tool builds a "visual database" where missing data, discrepancies, and errors are readily identifiable. When coupled with expert interpretations by qualified practitioners, this intrinsic characteristic to 3-D modeling ensures the quality of all site data while permitting the seamless integration of various data sources.

Fig. 5 highlights several quantitative aspects of the MVS tool. In this example, 3-D modeling was utilized to assist with excavation planning for a former smelter site. A LiDAR (Light Detection And Ranging) mission was flown over the site to obtain a precise "point cloud" of surface elevations. The point cloud was converted into a TIN (triangular irregular network) surface and draped with an aerial image, producing an exceptionally accurate ground surface for subsequent quantitative assessment. The results of soil quality analyses from borings advanced within the slag pile were integrated into the model and iso-surfaces were generated at various potential target cleanup levels. MVS was then used to calculate impacted soil volumes and the total contaminant mass exceeding several environmental risk thresholds. These spatial results were then used as the basis for excavation planning. The value in this modeling approach was the high-degree of spatial accuracy and rapid visualization (within a single day), which were then used to assist with decision making, project planning and budgeting.

The costs associated with developing MVS models for mining applications depend on the project objectives, the volume and types of data to be incorporated, and the complexity of the site. Costs range from less than $5,000 for relatively simple tasks (*e.g.* posting analytical data), to more than $100,000 for comprehensive models with large historical databases and complex hydrogeology. Prior to commencing MVS modeling, a customized, well-defined scope should always be developed with buy-in from the project manager and the client to control costs while focusing on high-quality

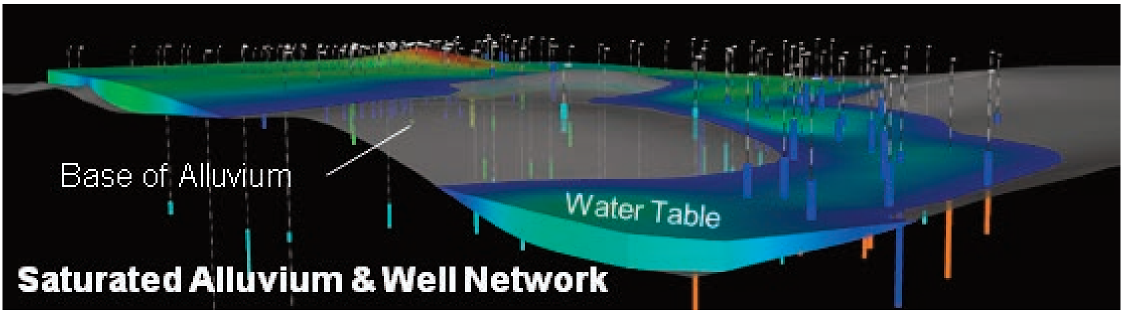

Fig. 4 *Geologic modeling of the extent and thickness of an alluvial aquifer.*

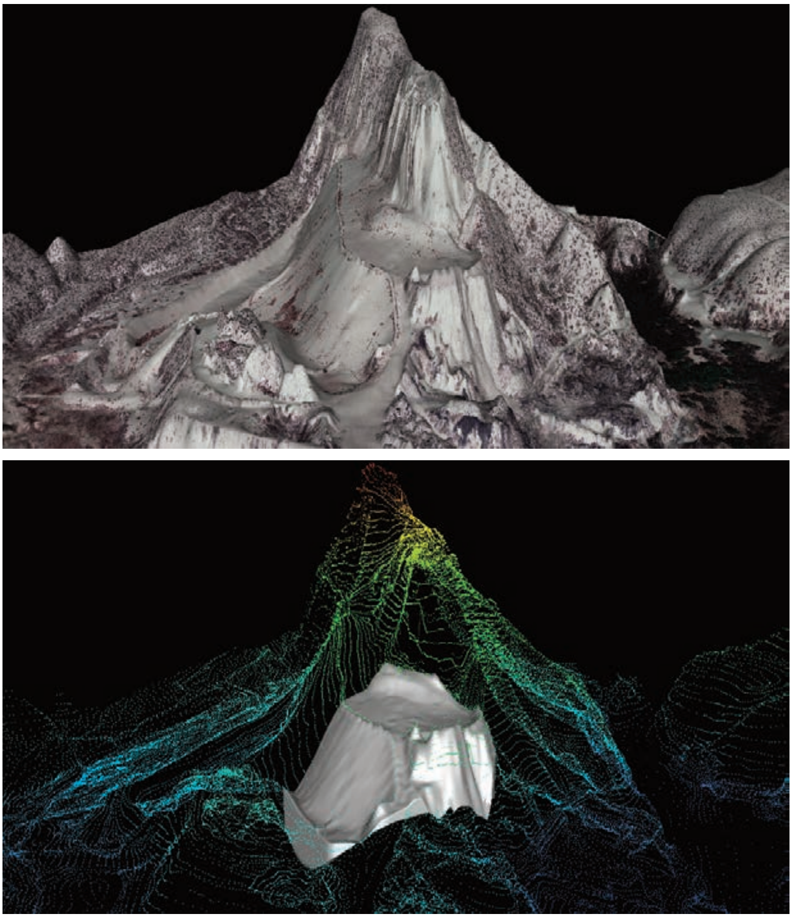

Fig. 5 *High-resolution LiDAR and soil quality data were integrated to calculate the soil volume and mass exceeding environmental risk thresholds within a slag pile.*

results. In this capacity, incorporating MVS into a project can be the most cost effective way to analyze and report site data, particularly in preparation for remedial planning and design ultimately focused on mine site closure. This is due to the ability of MVS to quickly incorporate data from sources that are typically already prepared (*e.g.* spreadsheets, databases, GIS shapefiles, CAD drawings). Integrating an MVS task into the project scope and budget at the early stages of project planning will typically reduce overall project costs over the lifecycle of the project.

Conclusions

In summary, 3-D geologic modeling can be powerfully applied at mine sites to more thoroughly understand hydrogeologic and environmental conditions, ensure the quality of all site data, and effectively communicate key elements of site conditions to all project stakeholders. MVS is a sophisticated tool for environmental practitioners and is a cost-effective, data-driven approach to integrate site data and maximize value for mining-related applications. This paper highlighted several examples of where 3-D modeling using MVS was effectively applied at mine sites and supports our recommendation that 3-D analyses should be more widely applied.

Acknowledgements

The authors thank Colorado School of Mines for hosting the IMWA 2013 Conference.

References

Armstrong M, Divine CE, Spurlin M, Burnell S, Griffin A, Potter S (2012) Use of Next-Generation Characterization Tools and Three-Dimensional Visualization to Enhance Remedy Performance. 8th International

Conference on Remediation of Chlorinated and Recalcitrant Compounds, Monterey, California. May

Rogoff E, Fisher T, Shifano V, Thompson W (2012) High Resolution TarGOST/CPT Characterization of DNAPL and Evaluation of Remediation Trenches using MVS. Poster and paper in proceedings of the Battelle 8th International Conference – Remediation of Chlorinated and Recalcitrant Compounds, Monterey, California. May 21 – 24

Rogoff E, Kivett J, Hickman C (2009) Three-Dimensional Analysis of Lithology and Groundwater Basin Flow, West Salt River Sub-Basin, Arizona. Presentation and paper in proceedings of the Arizona Hydrological Society/American Institute of Hydrology 2009 Annual Water Symposium. Scottsdale, Arizona. August 30 – September 2

Spurlin MS, Divine CE (2010) Enhanced 3D Visualization as a Data Analysis Tool in Remediation Hydrogeology. National Ground Water Association. Proceedings of the 2010 NGWA Ground Water Summit, Denver, Colorado. April

Assessment of Legacy Contaminant Remediation at the Phoenix Mine, Nevada

Robert M. St. Louis

Newmont Mining Corporation, 1655 Mountain City Highway, Elko, NV 89801

Abstract Groundwater underlying a pre-regulatory gold tailings storage facility (TSF) was impacted when a previous mine operator utilized calcium hypochlorite to neutralize cyanide in the tailings. In anticipation of a planned expansion of the current copper TSF, a desk top study was conducted which examined the effectiveness of on-going chloride remediation, currently being effected through the use of extraction wells. An integrated approach utilizing hydrogeology, water chemistry, geology and geophysics was employed to complete the study, and achieved reduction in the chloride mass is consistent with earlier numerical predictions. Replacement remediation well locations have been selected. Clarification of misconceptions regarding processing limitations with respect to chloride content of make-up water has resulted in a water management plan that allows for better utilization of impacted water in on-going processing operations.

Keywords Gold tailings, groundwater, remediation, hydrogeology, chloride contamination

Introduction

This paper reviews the findings of an integrated study that analyzed the progress made in remediating legacy chloride-impacted groundwater underlying a tailings storage facility (TSF) at Newmont Mining Corporation's (Newmont) Phoenix mine in Lander county, Nevada U.S.A. In addition, with a planned expansion to the TSF being considered, an evaluation of the optimal locations of new remediation well sites has been made and a revised water management plan has been developed that will allow for better utilization of chloride-impacted water in processing operations.

The Phoenix mine is approximately 20 mi (33 km) southwest of Battle Mountain, Nevada (fig. 1). In 1978 a previous mine operator transitioned from copper to gold recovery, utilizing carbon-in-leach recovery technology. The tailings were stored in an un-lined TSF; at the time the facility was constructed, regulations governing construction standards and operating requirements for tailings impoundments had not been promulgated. Furthermore cyanide neutralization, using calcium hypochlorite as the neutralization agent, was commissioned in 1979. Groundwater approximately 75 ft (23 m) beneath the TSF (fig. 1) was soon found to be impacted by chloride, and shortly afterwards a groundwater remediation plan was filed with Nevada environmental regulators. To-date elevated chloride concentrations have not been detected in groundwater deeper than 400 ft (122 m) below ground surface.

Three wells (CM-2, CM-3, and CM-4 on fig. 2) were installed at the downslope toe of the tailings embankment in 1979 to intercept and extract chloride-impacted groundwater that had percolated through the vadose zone from the unlined TSF. An older water supply well (CM-1) near the southwest corner of the TSF (fig. 2) was also dedicated to the remediation effort. Gold processing operations were terminated in March 1993, and the gold tailings were covered and vegetated. A number of hydrogeologic studies were conducted between 1991 and 1996 to assess the extent of the impacted groundwater, and to provide guidance for remediation.

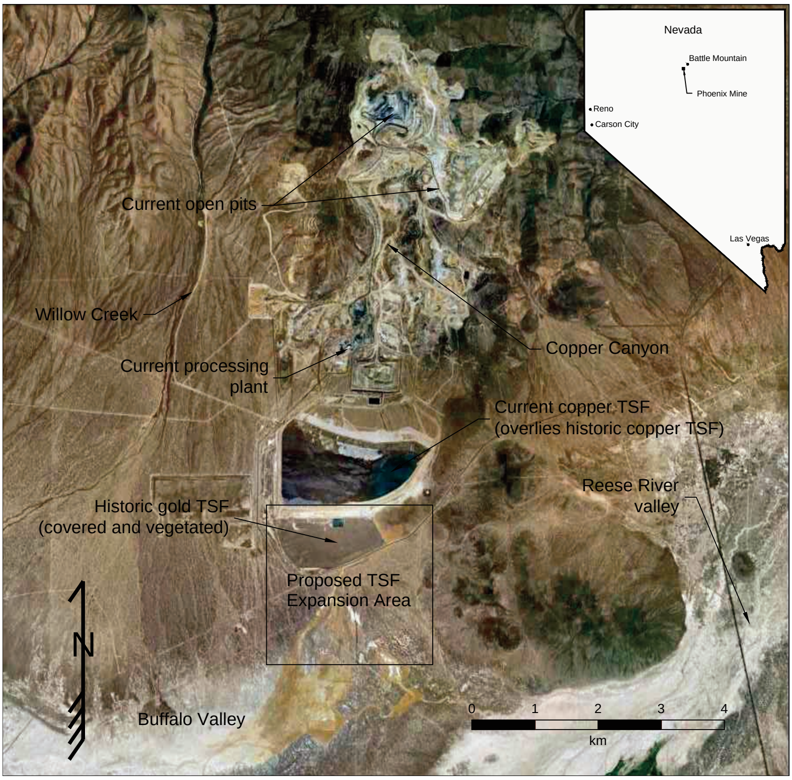

Fig. 1 *Location map and 2010 Google Earth image of the Phoenix operations with key points of reference.*

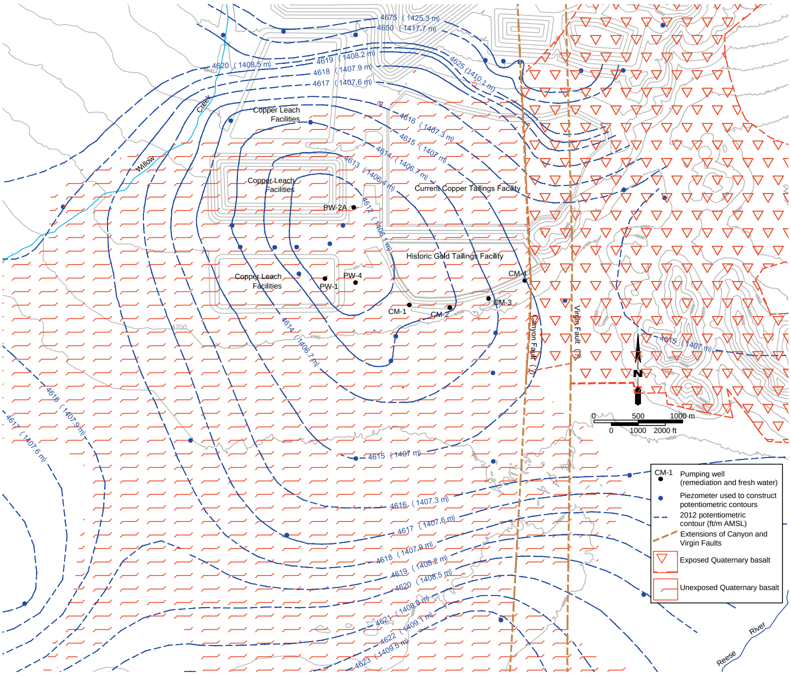

Fig. 2 *Potentiometric contours (based on end of 2012 water levels), extent of exposed and unexposed Quaternary basalt, and aeromagnetically-inferred extensions of the Canyon and Virgin Faults. Note that the contour interval changes in the northern portion of the area shown.*

Newmont acquired the property in the year 2000 and plans to expand the existing TSF over and to the south of the historic gold tailings. The expanded TSF will employ a synthetic liner with under-drainage leachate collection, which should eliminate future meteoric infiltration through the historic gold tailings. The planned expansion will require the abandonment of the existing remediation wells, and hence the construction of new wells to continue remediation efforts is required.

Hydrogeology

The TSF overlies a broad alluvial fan about 3 mi (5 km) south of the mouth of Copper Canyon, within the Buffalo Valley hydrologic basin (fig. 1). Copper Canyon trends north-south, with its head in the uplands of the Battle Mountain Range, and contains the bulk of the current and historic mines in the district. The hydrologic basin boundary between the Lower Reese River Valley and Buffalo Valley basins is just east of the TSF.

Buffalo Valley basin is a closed desert basin with no surface-water outlet. Lower Reese River Valley basin is open with both surface and subsurface water flow directed northward to the Humboldt River. The climate in the Phoenix mine area is arid, with annual average precipitation of 7 to 12 in (180 to 300 mm), depending on elevation. Pan evaporation exceeds 60 in (1,500 mm) per year in the vicinity of the TSF (JBR Environmental Consultants 2011).

The alluvial sequence beneath the TSF is typical of Nevada’s Basin and Range physiographic province, comprising sand, silt, clay and gravel (ranging from very fine to boulders in size). Porosity within the alluvial sequence is generally 30 %. Contained within the alluvial sequence is a Quaternary-aged volcanic sequence consisting primarily of basalts and basaltic tuffs. Basalt is exposed just east of the TSF (fig. 2), but this sequence is covered by 150 to 500 ft (46 to 152 m) of alluvium in the vicinity of the TSF. Depth to groundwater ranges from 18 ft (6 m) down-gradient of the TSF to 160 ft (50 m) in the up-gradient direction. In the immediate vicinity of the TSF, groundwater is 75 ft (23 m) below the original ground surface. Potentiometric contours for water elevations (AMSL) at the end of 2012 are shown in fig. 2.

Simon Hydro-Search (1993) determined that the horizontal groundwater gradient within the alluvial sequence beneath the TSF was 1.6×10^{-4} to the southwest, with an estimated hydraulic conductivity of 55 ft/d (17 m/d). Even though the hydraulic conductivity was determined to be high, the very low hydraulic gradient resulted in extremely slow movement of the chloride plume, estimated to be about 20 ft/a (6 m/a) under steady-state conditions (Simon Hydro-Search 1993).

Sources of data

In addition to reports prepared by and for the previous operator, a significant database of water-level measurements and chloride analyses is available for a number of wells and piezometers. However, gaps in these data sets have resulted from

- inconsistent sampling and water-level measurements,
- abandoned or damaged monitoring points, and
- the lack of any monitoring within the TSF footprint.

In addition, pumping data were available only as monthly averages derived from totalizer readings, and comprehensive pumping data were only available after 2001.

Three of the remediation wells (CM-2, CM-3, and CM-4) produced relatively low volumes of water, ranging from 27 to 60 gpm (2 to 4 L/s). Furthermore these three wells have discharge lines that are exposed and relatively small diameter that could quickly freeze during cold weather if pumping were interrupted. As power bumps are fairly common at Phoenix, these wells are often turned off during the winter months to prevent freezing of discharge lines. In the past, remediation wells had also been turned off during times of high chloride production, because it was then incorrectly believed that the copper flotation circuit could not tolerate the high chloride water.

Geologic logs of borings for the remediation wells, three fresh water wells, two piezometers and five boreholes were used to interpret the upper surface of the unexposed

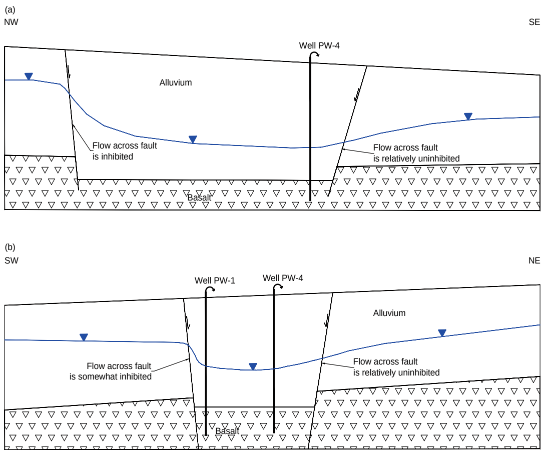

Fig. 3 *Conceptual cross-sections parallel to groundwater flow resulting from the pumping wells (a) and perpendicular to flow (b). Note how fabric developed in alluvium during faulting as well as juxtaposition of different facies across faults creates slightly lower K zones along some faults, but not others. Vertical scale is exaggerated.*

Quaternary basalts. Aeromagnetic data (reduced to pole, with second vertical derivative, rendered in gray) were used to identify the extent of unexposed Quaternary volcanic units, and to identify the presence of probable unmapped faults.

The conceptual hydrogeologic model is shown in schematic cross-sections in fig. 3. Fig. 3a is oriented northwest-southeast through the center of the composite cone of depression (shown in fig. 2), and fig. 3b is oriented northeast-southwest. The two lines of section intersect at fresh water well PW-4. Note that the potentiometric surface in these sections is vertically exaggerated to better illustrate the conceptual model.

The asymmetry in the composite cone of depression (fig. 2) indicates lateral anisotropy. Faulting is inferred to have produced fabrics within the alluvial sequence, and has presumably juxtaposed facies with different K across some faults. These fabrics/juxtaposed facies create preferred flow directions as a result of slightly decreased K across some of the faults.

Methods

Groundwater sampling wells, which included both fresh water and remediation wells, were grouped according to their baseline geometric mean chloride concentrations. Baseline was defined as the period 1993 to 1998 because work performed by Simon Hydro-Search (1993) demonstrated that this represented the time required for residual percolation of chloride-impacted water through the vadose zone beneath the TSF. Five distinct groupings were determined from the baseline data (Table 1). The Well Group High consisted of three remediation wells (CM-2, CM-3, and CM-4). The Well Group Medium included CM-4 and three monitor wells; the Well Group Medium-low contained one monitoring well and a fresh water well PW-4; the Well Group Low included fresh water wells PW-1 and PW-2A and eight monitoring wells. The Well Group Low-low consisted of 14 monitoring wells. In order to minimize the effects of outliers within the data, largely resulting from the sporadic pumping of the remediation wells, chloride analyses were composited for each group over multiple-year increments (1993–1998, 1999–2004, 2005–2009 and 2010–2012).

Chloride-concentration data were contoured for the baseline period, the recent period (2010–2012), and the change in chloride concentrations between the two periods. Change in chloride concentration contours are illustrated in fig. 4. Note that many sampling wells have been constructed after the baseline

Well Group	Wells (n)	1993 – 1998 Composite Max.	Min.	Geo. Mean	2010 – 2012 Composite Max.	Min.	Geo. Mean	Δ Geo. Mean (%)
High	3	4,630	314	3,425	3,110	649	1,631	-48
Medium	4	2,540	835	1,632	1,570	107	326	-80
Medium-low	2	1,550	166	562	538	75	166	-70
Low	10	300	67	158	217	71	106	-33
Low-low	14	196	17	42	66	13	31	-25

Table 1 *Well groupings by chloride concentration (mg/L)*

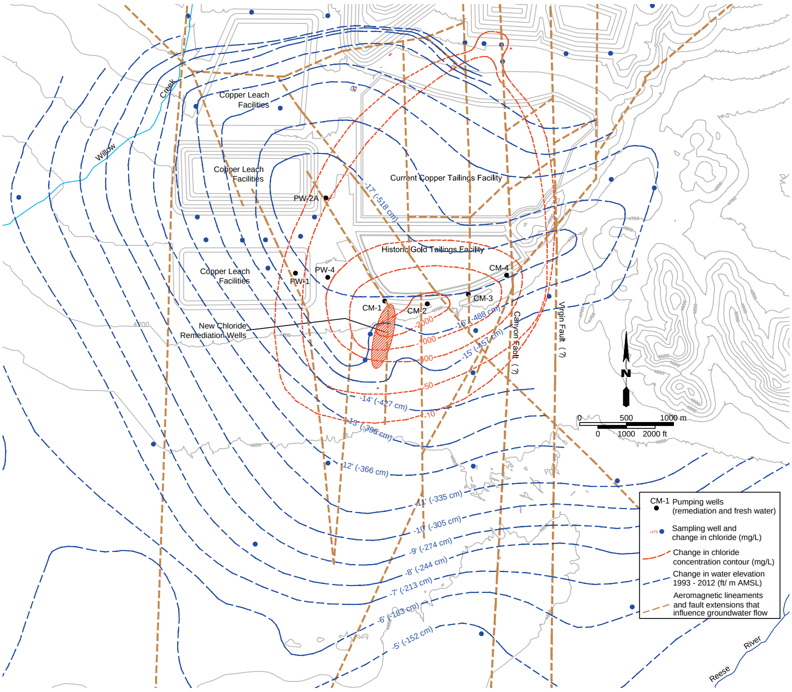

Fig. 4 *Change in water elevation contours from 1993 to end of 2012, and change in chloride concentration contours (1993–1998 vs. 2010–2012 [mg/L]). Key aeromagnetic lineaments that are interpreted to represent faults that have created zones of varying conductivity, and geophysically-inferred extensions of mapped faults that also act as hydrologic boundaries are shown, along with the area selected for replacement remediation wells.*

period, so data from these wells were not used in the change in chloride contours that appear on fig. 4. Contours of the change in water-elevations between 1993 and 2012 are shown in fig. 4. These contour maps provide insight into groundwater flowpaths as well as the propagation of cones of depression over time.

A network of monitoring wells constructed by the previous mine operator and Newmont are distributed over approximately 36 mi^2 (≈ 100 km^2), and were used to establish the background chloride concentration in groundwater within the study area. The previous owner estimated background chloride concentration at approximately 70 mg/L, but a recent reassessment of the data from an expanded groundwater monitoring well network indicates that a concentration of 100 mg/L was a more accurate estimate. This elevated background level was attributed to both the exposed and unexposed Quaternary volcanic rocks in the study area. Sampling wells near the Willow Creek drainage, approximately 1 mi (1.7 km) west of the TSF, showed very low chloride concentrations ranging from 16 to 40 mg/L. within the subsurface flow regime associated with this drainage. This is to be expected, because the bulk of this drainage is within an area dominated by Paleozoic sedimentary rocks. Basalts are interpreted beneath the alluvial fan at the mouth of Willow Creek drainage, at an undetermined depth.

Aeromagnetic interpretations of probable faults were confirmed by comparison with mapped geology wherever possible. Structure contours of the top of the unexposed Quaternary basalt were constructed from somewhat limited, widely-spaced borehole data. Structure contours showed that the top of the Quaternary basalt dips about 2° to the southwest. When overlaid on the aeromagnetic image, the structure contours were judged to be reasonable. The geophysics support the hypothesis that the exposed and unexposed Quaternary volcanic rocks are spatially related to the areas with 100 mg/L background chloride concentrations.

Results and discussion

Examination of chloride concentration data indicated that the centroid of impacted water was beneath the TSF, in the vicinity of CM-1, CM-2 and CM-3 (fig. 4). The baseline chloride contours expressed themselves as concentric ellipses, with their long axes oriented east-west, suggesting that pumping from the chloride remediation and fresh water wells influenced groundwater flow. Contours of the recent chloride concentrations indicated that the three fresh water wells (PW-1, PW-2A, and PW-4), located immediately west of the TSF, have apparently captured chloride-impacted water, although chloride has been decreasing in these wells since 1997. Over time, the three fresh-water wells clearly exhibit an inverse relationship between pumping rate and chloride concentration of the water that they produce. Recent chloride-concentration contours exhibited the east-west elongation observed in the baseline data, and comparison of the baseline and recent chloride concentration contours indicates that the areal extent of the plume of impacted water has not expanded noticeably over time.

Given that chloride impacted water has not been observed deeper than 400 ft (120 m) below the ground surface, that lower boundary and the current static water level were used to determine a saturated thickness of the impacted zone of 238 ft (73 m). Using the area within each of the baseline chloride contours, background chloride concentration of 100 mg/L, the saturated thickness, and the assumed porosity (30 %), the initial chloride mass was estimated to be 1.08×10^8 kg, similar to an estimate provided by Hydro-Search (1996) of 1.16×10^8 kg. The 2010–2012 average chloride contours were then used to calculate a remaining chloride mass of 6.3×10^7 kg of chloride. This indicates a 42 % reduction in the chloride mass with the original remediation goal of 82 % reduction.

Water-elevation contours of 1996 data showed a composite cone of depression around the fresh water and mitigation wells that was elongated northeast-southwest, with a secondary elongation to the south. Contours of 2012 water elevations (fig. 2) exhibited an enlarged composite cone of depression, with a pronounced northwest-southeast elongation, and a maximum drawdown of 17 ft (5.2 m). Drawdown resulting from pumping has propagated into the Lower Reese River Valley southeast of the TSF, and into the Willow Creek drainage to the northwest.

Contours of the change in water elevation from 1993 to 2012 recorded pronounced lateral anisotropy, suggesting the presence of several high and low K areas within the overall area impacted by the remediation pumping (fig. 4). Lineaments defined following aeromagnetic survey evaluation coincide with the apparent limits of these high and low K areas, indicating that the anisotropy is likely related to faulting (fig. 4). Using this interpretation the area selected for replacement remediation wells (fig. 4) was viewed as having minimal impact on the TSF expansion while allowing for continued capture of the chloride impacted groundwater. The potential locations for replacement mitigation wells would target an area downgradient of the centroid of chloride concentration within an area of apparently higher K. This higher K zone has been interpreted from the shape of the change in water elevation contours in the target area shown in fig. 4.

An additional and unexpected outcome of the study occurred when discussions with Phoenix process operations leadership revealed that the previous assumptions regarding operational limits on chloride concentration in make-up water for the existing copper flotation plant were overly conservative. In practice, higher chloride concentrations can be tolerated in the process than had been previously assumed and furthermore, process operations have also planned to implement changes that will result in reducing and may even eliminate the need to use any fresh water from non-remediation wells. Given that the inconsistent pumping of the remediation wells has had the effect of slowing remediation efforts in the past, plans have now been made to prepare these wells for year around pumping. Reducing demand on the fresh water wells for process water coupled with increased utilization of water from the remediation wells is expected to help further reduce the footprint of the impacted groundwater.

To help validate the sites chosen for replacement remediation wells, the conceptual hydrogeologic model developed during this study will be used to construct a numerical groundwater flow model. Once calibrated and accepted as representative, the numerical model will be utilized to determine the optimum locations for the replacement remediation wells as well as the likely volume of groundwater required to be pumped in order to achieve the remediation goal. While the currently-planned life of mine at Phoenix extends well into the 2030s, and it is currently anticipated that remediation will be completed long before the operation is shut down this outcome will be confirmed utilising predictive runs of the numerical model.

Conclusions

By expanding the groundwater monitoring well network, the background chloride concentrations in the groundwater underlying the Phoenix Mine Gold Tailing Storage Facility have been revised up to 100 mg/L from the previous 70 mg/L estimate. Besides the revision of the background chloride concentration, predictions made during previous investigations have been confirmed by the current study. Remediation efforts conducted to-date are estimated to have resulted in the removal of approximately 42 % of the chloride that was introduced to groundwater as a result of historic gold recovery at Phoenix. Due to the groundwater pumping efforts conducted since the commissioning of the original capture system in 1979, the plume of chloride-impacted water has not expanded from its baseline extents. The recent study indicates that more efficient remediation efforts can be achieved by:

1. modification of the copper flotation plant water balance,
2. enhancing emphasis on utilization of water produced from remediation wells instead of fresh water wells,
3. taking steps to allow the low volume remediation wells to pump year around.

New remediation well locations have been selected, and will be assessed by use of a numerical groundwater flow model. The numerical groundwater model will also be used to estimate volumes of pumped water required to meet the remediation target (originally set at 82 % mass removal, but subject to revision based on numerical modeling results). The currently-planned life of the Phoenix operation is currently expected to be more than sufficient to achieve substantial remediation of chloride-impacted groundwater, however this finding will also be confirmed via a pending numerical modeling program.

Acknowledgements

The author thanks Kimra Page for her efforts in gathering the chloride data, Heather Skeen for insights into the aeromagnetics, and Bryce Vorwaller for the Newmont pumping records. Discussions with Karen Tempel and Clayton Prothro were instrumental in arriving at a better approach to utilization of remediation water in process operations. Comments by Bob Sterrett, Tom Byers, Chris Cottingham, Jeff White, Matthew McGann and IMWA reviewers greatly improved this manuscript.

References

Hydro-Search, Inc. (1996) Addendum to Battle Mountain Gold Company Technical Memorandum Fortitude Tailings Disposal Area: Additional Modeling Scenarios, 15 pp plus tables and appendices

JBR Environmental Consultants, Inc. (2011) Closure Options Evaluation Phoenix Copper Leach Project, 15 pp plus appendices

Simon Hydro-Search (1993) Battle Mountain Gold Technical Memorandum Fortitude Tailings Disposal Area, prepared for Battle Mountain Gold Company, 75 pp plus appendices

Hydrogeochemistry of the Mine Water from “Rudna” mine (Lubin Region, South Poland)

Bernadetta Stochel[1], Mariusz Czop[2], Zenon Krzywański[3], Magdalena Worsa-Kozak[1]

[1]KGHM Cuprum R&D Centre, ul. Gen. Wl. Sikorskiego 2–8, 53–659 Wroclaw, Poland,
bstochel@cuprum.wroc.pl, mworsa@cuprum.wroc.pl
[2]AGH University of Science and Technology, al. Mickiewicza 30, 30–059 Krakow, Poland,
mariucz@agh.edu.pl
[3]KGHM Polska Miedź S.A., “Rudna” Mine, ul. Henryka Dąbrowskiego50, 59–100 Polkowice, Poland,
z.krzywanski@kghm.pl

Abstract “Rudna” is one of the mines in Legnica-Głogów Copper Basin (LGOM) – which is the main copper industry center in Poland and one of the world biggest copper extraction sites. “Rudna” is known as a mine with relatively small inflow of groundwater into the dewatering system which ranges from 1.8 to 2.0 m^3/min. TDS of water from Basalkalk ranges from 17.6 g/dm^3 to 328 g/dm^3. Mineralization of Rotliegendes groundwater varies between the minimum value equal to 92.4 g/dm^3 and the maximum one equal to 186.5 g/dm^3. The hydrochemical type of Na-Cl dominates in the mine water samples and Na-Ca-Cl type also occurs sometimes.

Keywords hydrogeochemistry, mine water, copper mine, Rudna mine, Lubin region, Poland

Introduction

“Rudna” is one of the mines in Legnica-Głogów Copper Basin (LGOM) – the main copper industry center in Poland and one of world biggest copper extraction sites. It is located in south-west part of Poland in Lower Silesia Province, about 100 km north–west from Wrocław (fig. 1).

Mining activity in “Rudna” copper mine has been carried out since 1970. The deposits occur at the depth from 690 m in south part of the mine to 1090 m in its north part. Groundwater inflowing to the mine workings located in a deeper part of ground is generally highly mineralized with TDS ranging from 17.6 – 328.8 g/L. Chemistry of mine water is an important factor of the environmental impact induced by mining activity. Mine water from all mines in LGOM area (Rudna, Polkowice-Sieroszowice and Lubin) is mixed and used in the copper ore treatment process. Water excess is drained to the Odra river, near Głogów and is responsible for soluble constituent load to surface water environment. Hydrogeochemistry of mine water in “Rudna” mine is also an important factor for determination of the origin of particular inflows and also for identification of processes responsible for the formation of the specific water type.

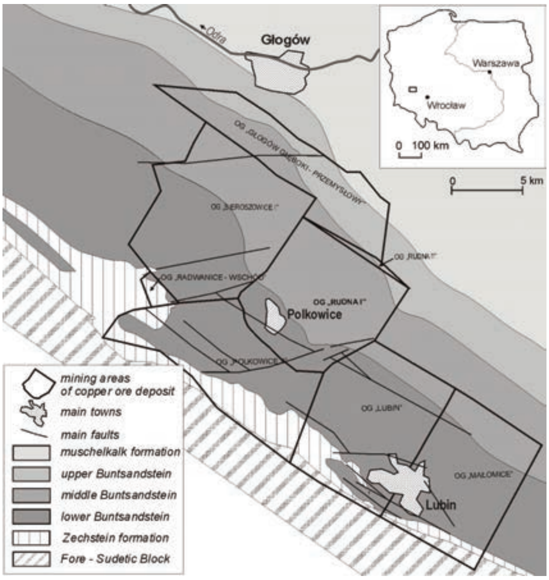

Fig. 1 *Map of the copper deposit occurrence in the Legnica-Głogów Copper Basin (LGOM)*

Geology and Hydrogeology

Copper deposit extracted in "Rudna" mine occurs in Permian limestones and Zechstein dolomites as well as in Rotliegendes sandstones (fig. 1). Permian formation with covering Triassic rocks occurs within the Fore-sudetic Monocline, dipping north-west at small angle, from 3 to 6°(Bochenska *et al.* 2003; fig. 2).

"Rudna" mine has a relatively low inflow of groundwater water into the mine workings ranging from 1.8 to 2.0 m³/min. This inflow comes from two aquifers occurring within the Permian formation *i.e.* from carbonate rocks of Basalkalk and sandstones of Rotliegendes. The carbonate Basalkalk aquifer is connected with the Permian dolomite and limestone of average thickness about 52.7 m (7–106 m), with relatively low conductivity range from 1×10^{-9} – 1×10^{-6} m/s (geometric mean 1×10^{-7} m/s). The Rotliegendes aquifer is built of Permian sandstones with summary thickness of about 300 m. Conductivity of this formation is very low from 1×10^{-9} – 1×10^{-6} m/s (geometric mean 1×10^{-8} m/s; Worsa-Kozak and Stochel 2013).

During the "Rudna" mine history the main source of water inflows was the Basalkalk aquifer. Since 2003 the inflow from Rotliegendes has increased to 1 m³/min and thus, it is equal to the value of inflows from the Basalkalk recorded since the beginning of the copper deposit exploitation (fig. 3).

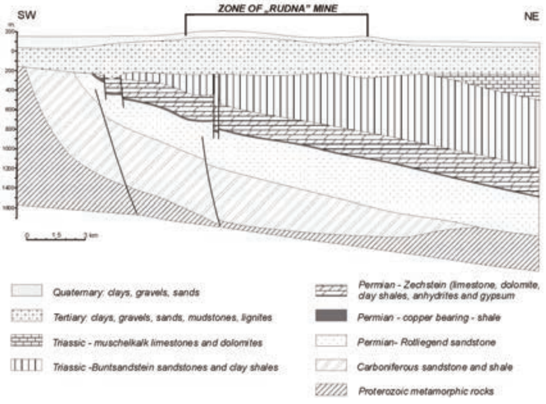

***Fig. 2** Geological cross-section of the "Rudna" mine*

Mine Water Chemistry

Most of groundwater both from the Basalkalk and the Rotliegendes formations are brines. Average mineralization of water from the Basalkalk is about 126 g/dm³, ranging from 17.6 – 328 g/dm³. The average mineralization of the Rotliegendes water is 147 g/dm³ with the minimum value 92.4 g/dm³ and the maximum one equal to 186.5 g/dm³ (Worsa-Kozak and Stochel 2013).

Descriptive statistics of the all measured constituents has indicated similarity of the groundwater samples from both Permian aquifer. Average and median values of all parameters have practically the same values with only small difference. Due to the highest amount of analysis of groundwater from the Basalkalk aquifer the observed range of particular constituents of the data is wider then for Rotliegendes (Table 1).

The main fraction in total dissolved solid is forming by concentration of chlorides (Cl) and sodium (Na) ions which is connected with dominance of Na-Cl type groundwater. Average concentrations of other main ions *e.g.* sulfate (SO_4), calcium (Ca) and magnesium (Mg) are much more lesser, only about 1–5 g/L. Especially calcium is observed with concentration values between 0.2–9.4 g/L, and in a few cases forming the groundwater with Na-Ca-Cl type.

Increase of the depth of the mining exploitation in the "Rudna" mine is also connected with the increase of the groundwater sample mineralization (TDS) in both Muschelkal and Rotliegendes aquifers. Chloride concentration in groundwater sample on the co-ordinate about -700 m a.s.l reached the value of about 50–60 g/L. Successive deepening of the "Rudna" mine exploitation level influenced strongly the groundwater TDS. Below the co-ordinate -1000 m a.s.l the groundwater TDS has increased twice to value of about 110–140 g/L (fig. 4). It's obvious that future deepen-

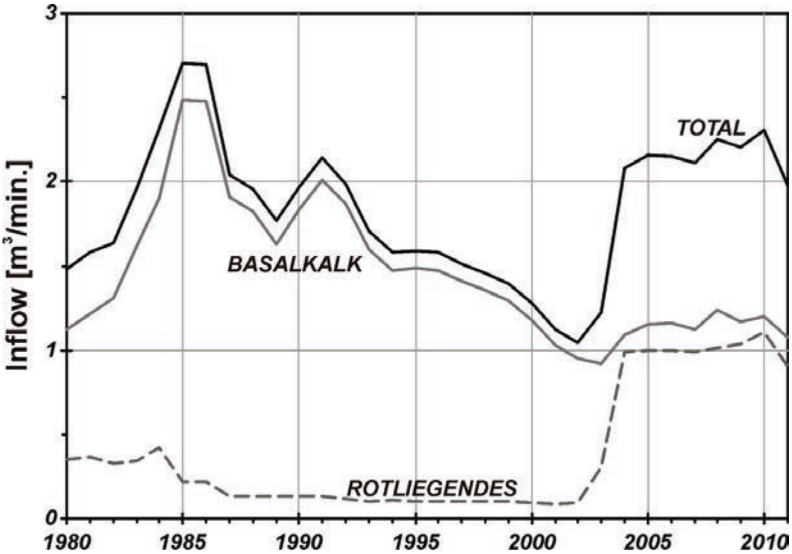

Fig. 3 *Groundwater inflows to the "Rudna" mine from Basalkalk and Rotliegendes aquifers*

ing of the mining workings will be connected with continuation of this evident trend.

Trace elements, connected with the sulfide copper ore, are also occurring in the groundwater inflows to the "Rudna" mine. Unfortunately the significant number of chemical analysis of mine water is without any information concerning concentration of the trace elements. Single analysis of mine water inflows from both Basalkalk and Rotliegendes aquifers have indicated that trace elements concentrations (As, Cr, Cu, Fe, Mn, Pb, Rb, Se, V and Zn) usually range from 0.1 mg/L to a few mg/L. The amount of accessible analysis including trace elements concentration and measurements of mine water pH and redox potential (Eh) is not sufficient to obtain representative characteristics of the concentration range, speciation and mobility. The research project aiming to investigate trace elements occurrence in the mine water from LGOM copper mines is currently at the initial stage. Pre-

Parameter	*Minimum*	*Maximum*	*Average*	*St. dev.*	*25th quantile*	*Median*	*75th quantile*	*n*
				BASALKALK				
pH	3.77	8.01	6.77	0.53	6.42	6.75	7.12	1149
TDS	17600.0	328800.0	125740.1	42435.5	117942.5	132140.0	146047.5	1204
Na	3850.0	119800	40044.1	13331.5	36500.0	40700.0	46650.0	1153
K	10.0	2480.0	509.0	204.1	420.0	520.0	600.0	1153
Ca	268.0	9398.0	4608.3	931.9	4501.4	4711.4	5002.1	1154
Mg	122.4	2138.0	903.4	223.3	838.9	912.8	1001.1	1153
HCO_3	1.2	372.1	142.4	35.5	128.1	140.3	155.6	1177
SO_4	758.0	3481.7	2423.9	255.4	2334.0	2450.1	2535.1	1204
Cl	8376.0	194304.0	69705.3	24527.7	65479.9	72284.4	82000.0	1207
NH_4	0.0	320.0	3.1	9.8	2.1	2.7	3.4	1105
Fe^{2+}	0.0	98.3	1.9	6.1	0.2	0.4	1.1	1117
				ROTLIEGENDES				
pH	5.23	7.30	6.38	0.46	6.12	6.31	6.60	44
TDS	92400.0	186480.0	147073.0	23230.0	132765.0	148260.0	163151.0	44
Na	22600.0	52600.0	46832.7	7358.8	44540.0	47800.0	50250.0	43
K	225.0	855.0	477.4	170.8	332.5	440.0	602.5	43
Ca	3716.4	6572.0	4791.1	641.1	4314.6	4738.2	5252.9	44
Mg	554.5	2497.6	1001.4	406.3	817.2	906.7	970.7	44
HCO_3	61.0	189.1	96.8	24.5	82.4	91.5	115.9	43
SO_4	1952.4	3097.2	2544.9	314.5	2305.6	2587.5	2748.1	44
Cl	48030.5	106734.4	81223.0	13551.0	75875.0	83416.0	89208.4	46
NH_4	0.5	10.95	3.1	1.9	2.0	2.7	4.0	39
Fe^{2+}	0.03	168.0	7.5	25.8	0.2	1.1	3.3	45

Table 1 *Descriptive statistics of mine water chemistry for the Permian aquifers in the "Rudna" mine (concentrations of chemical constituents in mg/L); n: number of samples*

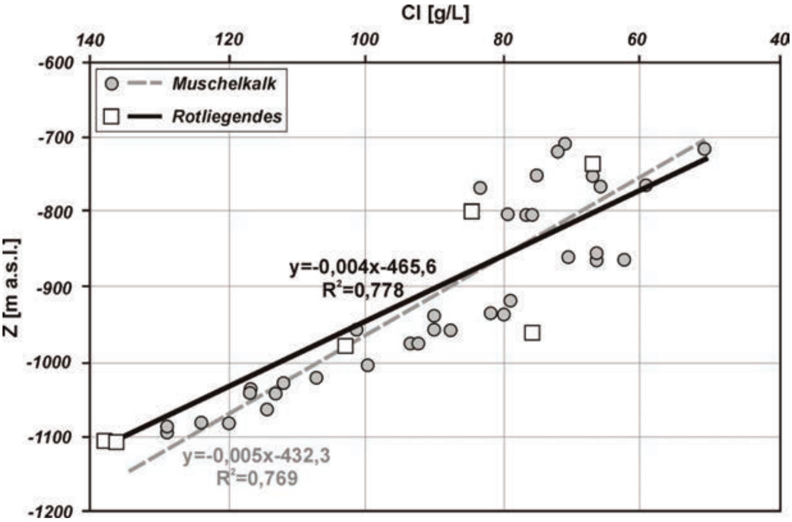

Fig. 4 *Chlorides increasing trend with depth of mining exploitation for both Permian aquifers*

liminary results of this research indicate that in the water inflows to the mine workings both aerobic and anaerobic conditions occurs.

Conclusions

Chemical composition of groundwater in the Basalkalk and the Rotliegendes aquifers is formed mainly by the processes of halite (NaCl) and anhydrite ($CaSO_4$) dissolving. The salts occur in great amounts in the profile of Permian evaporates formation of Zechstein, and their dissolving decides the level of chloride (Cl) and sulfate(SO_4) ions content found in the mine waters. Additionally the process of ion exchange is of basic importance in regard to the concentration of main cations (Na, K, Ca and Mg) in the water under examination.

Copper ore extraction development towards the north is connected with the evident increase of total dissolved solids in the groundwater inflows into the “Rudna” mine workings. It is reason for both much bigger depth of rocks being drained, due to dip of monocline orientation of Permian formation, and with the larger distance from the outcrop zone. The outcrop zone of the Permian formation is covered by a rock mantle and it is the supply area for the Permian (Basalkalk and Rotliegendes) aquifers. In the past, the water inflowing there had the lowest mineralization of all water samples being tested. In connection with the increasing distance from the Permian formation outcrops, the brines with relatively very high mineralization are observed now. With the deeper and deeper extraction, also in the neighboring area of “Głogów-Głęboki Przemysłowy”, the further increase of mine waters mineralization, towards the fully saturated brines, is predicted.

Acknowledgements

This work was supported by research program no. 501-02-0006-0-08-B/07/0657.001 of the KGHM Cuprum R&D Centre. We thank an anonymous reviewer for useful suggestions and editorial changes, which improved the manuscript.

References

Bochenska T, Downorowicz S, Kalisz M (2003) Fore-sudetic Monocline. Hydrogeological conditions. In: Wilk Z, Bochenska T, (ed) (2003) Hydrogeology of the mineral ores of Poland and water hazards in mining. Vol. 2 – Hydrogeology of metallic elements ores. AGH Krakow (in Polish).

Worsa-Kozak M, Stochel B *et al.* (2013) Hydrogeological conditions documentation of the “Rudna” Copper Mine. Report (in Polish).

Cerro Rico de Potosí, Bolivia – Broader Impacts from Unabated Acid Mine Drainage

W. H. J. Strosnider[1], F. S. Llanos López[2], J. A. LaBar[3], K. J. Palmer[1], R. A. M. Peer[1], R. W. Nairn[3]

[1]Saint Francis University, Loretto, PA, USA; [2]Universidad Autónoma Tomás Frías, Potosi, Bolivia;
[3]University of Oklahoma, Norman, OK, USA;

Abstract Intensive mining and processing of the polymetallic sulfide ore body of Cerro Rico de Potosí (Bolivia) has occurred since 1545 and likely less intensively in pre-Colombian times from the 10th to 15th centuries. Mining for Ag, Sn, Pb, and Zn with no or minimal environmental controls has led to severe degradation of surface and subsurface waters, stream sediments, and soils at the headwaters of the economically vital, yet highly impacted, Rio Pilcomayo. Human populations are at risk as elevated concentrations of ecotoxic metals have been noted in local produce irrigated with impacted waters. Previous studies documented extremely elevated concentrations of a relatively limited suite of metals (*e.g.* Al, As, Cd, Cr, Cu, Fe, Mn, Pb, Zn) in local waterways from acid mine drainage (AMD), terrestrial and in-stream tailings, and ore processing plant discharges. However, contamination from a wider assortment of ecotoxic metals was considered likely due to the highly mineralized polymetallic nature of the ore body. To further investigate AMD discharges and their link to downstream contamination, data were gathered during two sampling events in the most extreme periods of the dry and wet seasons of one water-year. Concentrations of Ag, B, Ba, Mo, Sb, Se, Sn and V in AMD and receiving streams were greater than Bolivian discharge limits and receiving water body guidelines as well as international agricultural use standards. Results indicate that contamination from mining has a larger scope than previously understood and underscore the importance of remediation.

Keywords Acid mine drainage, tailings, historic, acid rock drainage

Radiological effect of mine dumps on surrounding water resources

Victor Tshivhase, Manny Mathuthu

North-West University (Mafikeng), Centre for Applied Radiation Science and Technology, Cnr Dr Albert Luthuli drive and University drive, Mmabatho, 2375; victor.tshivhase@nwu.ac.za

Abstract A study was performed to identify the radionuclides in the tailings from the Princess Mine dump in Roodepoort, South Africa and to determine their corresponding concentrations. Radiation levels were monitored on site using the Electra, Radiagem and Teletector equipment. The samples were collected at different heights above sea level and different positions of the mine dump. The collected soil, leaves and seeds samples were analysed with EDXRF and HPGe detector to identify the trace, toxic, radiotoxic and radionuclides as well as their activity. The presence of the similar radionuclides was detected in water in the area around the mine dump.

Keywords toxic, radionuclide and specific activity

Introduction

South Africa is rich in mineral resources (Wendel 1998). The history of minerals extraction dates back to the discovery of diamonds at Kimberley in 1871 and the discovery of gold-bearing conglomerate on Langlaagte Farm near Johannesburg in 1886 (South Africa – Mining History). In the process of sorting out extracted minerals like Gold, Uranium is recovered as a by-product and also as the main product in Uranium mines. Uranium is naturally occurring element that emits radiation with a half life of 4.5×10^9 years. It undergoes radioactive decay into a long series of 13 different radionuclides before finally reaching a stable state in ^{206}Pb (Canada Nuclear Association). These radionuclides emit alpha or beta radiation and some also emit gamma radiation of widely varying energies. The mineral by-products and unwanted minerals are stored in the tailings storage facilities (TSF) during the period of the operation of the mine until rehabilitation or reclamation of the TSF (Hossner and Hons 1992). Unfortunately the mining industry, in South Africa left behind huge number of unrehabilitated mines and TSF (Audit Report 2009). The TSF are rich in Uranium as a common element in nature and other radioactive elements. Human beings in search of accommodation in the cities have build houses in close proximity to the TSF (Winde 2002; Winde and Walt 2004) and therefore use water from the streams, dams and boreholes dug in close proximity to the mine dumps. This study presents the specific activity levels in and around the mine dumps to the water system.

Materials and Methods

Thirty soil, water, leaves and seeds samples were collected from Princess mine dump, Roodepoort in South Africa shown in Fig. 1. The GPS sample positions are listed in table 1. Six samples were collected from the top 15 cm layer of the tailings (A, C, D, H, K and L1). Six different depth tailings samples were collected and (L1, L2, L3, L4, L5 and L6). Water, seeds and leaves samples were collected (E, F, H).

Soil and leaf samples were placed in the 1 kg plastic bags for the further processing in the laboratory. Water samples were collected in the sealable bottles. During the sample collection process radiation levels were constantly monitored with the Electra, Radiagem, Inspector 2000 and Teletector, and only the background radiation could be detected.

Sample preparations

The collected tailings samples were fine soil

Fig. 1 *Location of the Princess mine dump, in Roodepoort, South Africa. (Ngigi 2009).*

Sample	latitude	longitude	elevation
A	-26.15783	27.853915	1697
B	-26.15814	27.854521	1700
C	-26.16037	27.855434	1710
D	-26.16129	27.854728	1716
E	-26.15738	27.851937	1692
F	-26.15788	27.851987	1692
G	-26.15862	27.855237	1706
H	-26.15883	27.85535	1706
I	-26.16031	27.855468	1711
J	-26.16033	27.855419	1711
K	-26.16037	27.85546	1713
L	-26.1609	27.856088	1724
M	-26.16132	27.855983	1732

Table 1 *GPS sample positions on the Princess mine dump, in Roodepoort South Africa.*

and there was no need for them to be ground. The powdered samples were packed in glass vial and sealing cap, with a diameter and height of 22mm and 50mm, respectively. Each container accommodated the sample with an average mass of 16 g and the samples were given enough time, 24 days, to allow radium daughters to come into circular equilibrium.

The portable gamma spectrometer based on high-purity germanium coaxial detector GCD-35190 Spectrometric device MCA 527 with basic spectroscopy software WinSPEC was used to acquire the data. The detector and sample were placed inside the Lead shield during data acquisition process. The same samples were divided for analaysis with the Energy dispersive XRF.

Results and discussion

Results from the HPGe detector are shown in Table 2 to Table 5. From Table 2, samples L1 of ^{214}Pb, K of ^{232}Th, L1 of ^{214}Bi, C of ^{228}Ac and L1 of ^{226}Ra show the highest concentrations in composite tailings of 767.8±16.0 $Bq.kg^{-1}$, 13±0.3 $Bq.kg^{-1}$, 356.1±13.0 $Bq.kg^{-1}$, 44.6±2.9 $Bq.kg^{-1}$ and 403.9±4.4 $Bq.kg^{-1}$, respectively. The samples D of ^{214}Pb, D of ^{232}Th, D of ^{214}Bi, D of ^{228}Ac and D of ^{226}Ra show the lowest concentrations in composite tailings of 94.6±25.1 $Bq.kg^{-1}$, 0.4±0.1 $Bq.kg^{-1}$, 58.4±17.2 $Bq.kg^{-1}$, 1.3±0.3 $Bq.kg^{-1}$ and 43.7±5.7 $Bq.kg^{-1}$, respectively. Sample A shows that ^{223}Ra dissolved in the water from the dump whereas samples L1 to L6 indicate that ^{226}Ra is not detected (ND) as the depth increases. ^{226}Ra shows highest specific activity at

Sample Positions	^{214}Pb (Bq/kg)	^{232}Th (Bq/kg)	^{214}Bi (Bq/kg)	^{228}Ac (Bq/kg)	^{223}Ra (Bq/kg)	^{226}Ra (Bq/kg)
A	ND	ND	ND	ND	78.89±31.19	ND
C	282.3±14.9	ND	347.8±20.8	44.6±2.9	ND	58.0±2.2
D	94.6±25.1	0.4±0.1	58.4±17.2	1.3±0.3	ND	43.7±5.7
H	478.0±4.1	ND	161.6±1.6	ND	ND	ND
K	767.8±16.0	13.1±0.3	300.6±3.3	ND	ND	403.9±4.4
L1	490.9±6.8	ND	356.1±13.0	ND	ND	284.3±1.6

Table 2 *Specific activity of ^{214}Pb, ^{232}Th, ^{214}Bi, ^{228}Ac ^{223}Ra and ^{226}Ra from A, C, D, H, K and L1 of tailings sample from Princess Mine dump.*

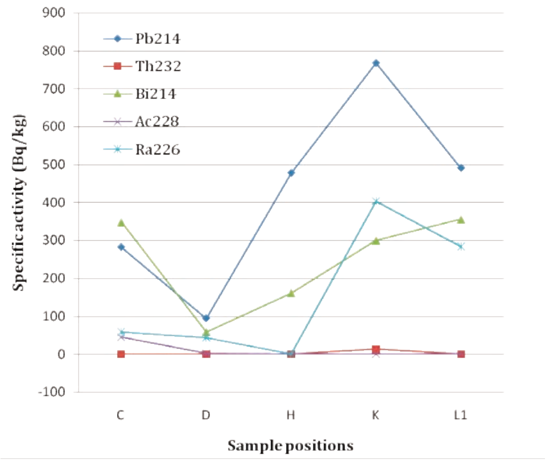

***Fig. 2** Graph of Concentrations of Radionuclides ^{214}Pb, ^{232}Th, ^{214}Bi, ^{228}Ac and ^{226}Ra from the top 15 cm layer at points C, D, H, K and L1 of the Princess Mine dump.*

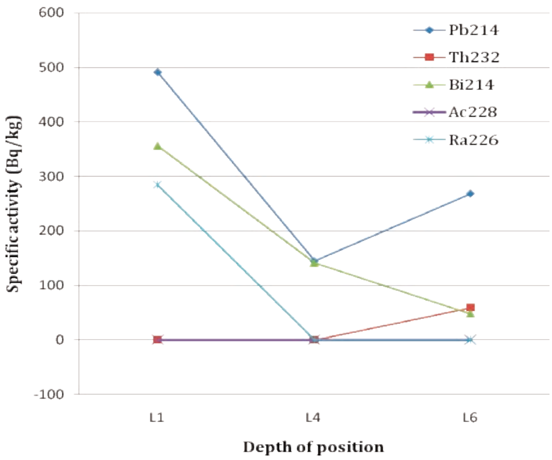

***Fig. 3** Concentrations of Radionuclides ^{214}Pb, ^{232}Th, ^{214}Bi, ^{228}Ac and ^{226}Ra as a function of depth of position L of the Princess Mine dump.*

the depth of L1=15cm. ^{214}Pb and ^{214}Bi are detectable everywhere on the dump except in water (sample A).

From Table 4, Leaves of ^{228}Th, Leaves of ^{7}Be, Blue gum seeds of ^{140}Ba and Blue gum seeds of ^{228}Ac show the concentrations of 143±58 Bq.kg^{-1}, 247±128 Bq.kg^{-1}, 169±77 Bq.kg^{-1} and 105±56 Bq.kg^{-1}, respectively. These results from the leaves on the dump show concentrations of Thorium which indicate that there should be a production of certain amount of ^{220}Rn and ^{222}Rn in the area.

From Table 5, samples K of ^{144}Pr and H of ^{7}Be show the concentrations of 1610±868 Bq.kg^{-1} and 19±5 Bq.kg^{-1}, respectively.

The Table 6 shows the spread of metals at different depth as measured by the Energy dispersive XRF detector. Only a few metals were detected at single level.

From Table 6 the concentrations of toxic elements; Sr, Fe, Si and Cr are relatively constant with depth through the tailing. This might mean that these elements do not leach easily through the sandy mine dump. However Pb concentration increased with depth suggesting relative ease of leaching to the environment due to dissolved nitrates and sul-

Sample depth	^{214}Pb(Bq/kg)	^{232}Th(Bq/kg)	^{214}Bi(Bq/kg)	^{228}Ac(Bq/kg)	^{226}Ra(Bq/kg)
L1	490.9±6.8	ND	356.1±13.0	ND	284.3±1.6
L4	144.5±25.3	ND	141.1±1.5	ND	ND
L6	268.4±4.4	58.9±0.3	47.8±0.4	ND	ND

***Table 3** Specific activity of ^{214}Pb, ^{232}Th, ^{214}Bi, ^{228}Ac and ^{226}Ra from the depth L1, L4 and L6 .*

Sample	^{228}Th(Bq/kg)	^{7}Be(Bq/kg)	^{140}Ba(Bq/kg)	^{228}Ac(Bq/kg)	^{207}Bi(Bq/kg)
G seeds	ND	ND	169±77	105±56	
Leaves	143±58	247±128	ND	ND	
K	ND	ND	ND	ND	
M6	62±27	ND	ND	ND	
W1					39±16

***Table 4** Concentrations of Radionuclides ^{228}Th, ^{7}Be, ^{140}Ba, ^{207}Bi and ^{228}Ac from Princess Mine dump.*

Sample	^{144}Pr(Bq/kg)	^{208}Tl(Bq/kg)	^{7}Be(Bq/kg)	^{228}Ac(Bq/kg)	^{228}Ac(Bq/kg)
Seeds	ND		ND	Double escape	Single escape
H	ND	11±5	19±5	ND	ND
K	1610±868		ND	ND	ND

Table 5 *Concentrations of* ^{144}*Pr,* ^{208}*Tl,* ^{7}*Be and* ^{228}*Ac from Princess Mine dump.*

	0cm	30cm	60cm	90cm	120cm
Si	87.59	93.59	93.72	94.61	91.21
Fe	8.67	4.68	5.56	4.78	5.49
K	2.63	1.13			2.44
Ti	0.57	0.46	0.41	0.37	0.55
Zr				0.04	
Cr	0.1	0.07	0.07	0.04	0.08
V		0.02			0.02
Sr		0.02	0.02	0.01	0.02
Cu		0.02			
Rb	0.02		0.01		
Pb	0.1		0.06		0.09
As	0.09				
Tm	0.17		0.13	0.12	0.1
V	0.03		0.02	0.02	
Ac				0.02	

Table 6 *The percentage concentration of elements in Sample L at different depth.*

	Leaves	Seeds
Si		
Fe	1.51	2.53
K	24.48	50.71
S	8.84	
Ca	41.77	30.89
Mn	22.64	13.66
Cu		2.19
Ni	0.75	

Table 7 *Concentration of elements in the Leaves and Seeds samples*

phates from mining activities.

The Table 7 and 8 show that some metals were absorbed by the trees and dissolved into the water from the mine dump.

The seeds and leaves contained very small concentrations of the essential elements: Si, Fe, Cu, S, Ca, Mn, Ni and K.

The Table 8 shows that some metals have dissolved into the water from the mine dump. Columns A, E and F show the percentage concentrations of elements in water draining from the mine dump compared to the percentage concentrations of the same elements from the soil sample of the mine dump (columns C and D). In the samples Fe and S dominate in the percentage concentration. These two elements could be a result of mining processing that included use of sulphuric acid and wear and tear of the machinery.

Conclusions

The specific activity concentrations of the radionuclides have to be monitored against the general limits of all nuclides to avoid environmental exposure (Muazu 2004).

The samples L1 of ^{214}Pb, K of ^{232}Th, L1 of ^{214}Bi, C of ^{228}Ac and L1 of ^{226}Ra show the highest concentrations in composite tailings of 767.8±16.0 Bq.kg^{-1}, 13±0.3 Bq.kg^{-1}, 356.1±13.0 Bq.kg^{-1}, 44.6±2.9 Bq.kg^{-1} and 403.9±4.4 Bq.kg^{-1}, respectively. The samples D of ^{214}Pb, D of ^{232}Th, D of ^{214}Bi, D of ^{228}Ac and D of ^{226}Ra show the lowest concentrations in composite tailings of 94.6±25.1 Bq.kg^{-1}, 0.4±0.1 Bq.kg^{-1}, 58.4±17.2 Bq.kg^{-1}, 1.3±0.3 Bq.kg^{-1} and 43.7±5.7 Bq.kg^{-1}, respectively. The ^{228}Th, ^{7}Be, ^{140}Ba and ^{228}Ac show the concentrations of 143±58 Bq.kg^{-1}, 247±128 Bq.kg^{-1}, 169±77 Bq.kg^{-1} and 105±56 Bq.kg^{-1}, respectively.

The concentration of ^{228}Th was detected in leaves and concentration ^{223}Ra was also detected in water from the mine dump. The ^{228}Th and ^{223}Ra as well as the metals in the leaves, seeds and the water presents the possibility of the pathway of the radionuclide and metals to the environment and the water system. Our investigations shows that toxic elements like Sr, Fe, Si and Cr are relatively constant with depth through the tailing but Pb concentration are less at the top surface probably due to ease of leaching from the tailing. The highest concentration of ^{226}Ra, 403.9±4.4 Bq.kg^{-1}, was found

	A water	C	D	E water	F Water
Si		96.3	49.03		
Fe	55.8	1.55	32.99	50.21	69.61
K		0.71	0.92		
S	44.23	0.67	14.26	38.64	
Ti		0.45			
Sm		0.07			
Zr		0.05	0.02		
Ta		0.04			
Cr		0.04			
W		0.02			
Ca		0.02	1.57	11.15	16.34
V		0.02			
Ge		0.02			
Mn		0.01	0.06		
Zn		0.01	0.05		
Sr		0.01	0.02		
Cu		0.01	0.05		14.05
Fr		0.01			
Ni		0.004	0.03		
Th		0.004			
Rb		0.004			
Pb		0.003			
Y		0.003	0.003		
Nb		0.002	0.002		
P			0.44		
As			0.38		
Tm			0.18		
V			0.03		
Se			0.002		

Table 8 *Concentration of elements in the water samples around the mine dump*

in sample K. This value is below the reference level of 800 Bq.kg^{-1} for normal operations of the mine for which regulation is not required (Mobbs 2007).

Acknowledgements

The authors thank the Council for Geoscience for the financial support towards this research work.

References

Audit Report (2009) Report of the Auditor-General to Parliament on a performance audit of the rehabilitation of abandoned mines at the Department of Minerals and Energy

Canada Nuclear Association. http://curriculum.cna.ca/curriculum/cna_radiation/uranium^{2}38-eng.asp?, cited 15 April 2013

Hossner LR, Hons FM (1992) Reclamation of mine tailings, Springer-Verlag New York Inc. Advances in soil Sciences, Vol 17.

Mangset WE, Sheyin AT (2009) Measurement of radionulides in processed mine tailings Jos, Plateau State. Bajopas Vol 2. No 2: 56–60.

Mobbs S, (2007) Establishment of Reference Levels for regulatory control of workplaces where materials are processed which contain enhanced levels of naturally-occurring radionuclides. Health protection agency.

Muazu I, Umar IM, Akpa TC, Mallam SP (2004) Natural

Radioactivity in soils from Sokoto Basic Area, Nigeria. Zuma Journal of Pure and Applied Sciences. Vol. 6. No. 2, pp. 71 – 74.

Ngigi SM, (2009) Establishing effective, appropriate and applicable technologies in treating contaminated surface water as part of a rehabilitation strategy for the Princess dump in Roodepoort, west of Johannesburg. MSc research project, University of the Witwatersrand.

South Africa – Mining History. http://info.goldavenue.com/info_site/in_mine/in_min_sa_his.htm, cited 15 April 2013.

Wendel G (1998) Radioactivity in mines and mine water—sources and mechanisms The Journal of The South African Institute of Mining and Metallurgy.

Winde F (2002) Uranium contamination of fluvial systems-mechanisms and processes. Part I. Geochemical mobility of uranium along the water-path: The Koekemoerspruit (South Africa) as a case study.

Winde F, van der Walt IJ (2004) The significance of stream chemistry on waterborne uranium contamination of streams-a case study from a gold mining site in South Africa. J. Hydrol., 287:178–196.

Development of a 3-D electrical conductivity image for a colliery in South Africa to determine post-closure management options

Danie Vermeulen[1], Lize Wessels[1], E. Lukas[1]

[1]*Institute for Groundwater Studies, University of the Free State, Bloemfontein, 9301, South Africa*

Abstract The colliery is situated in the Vereeniging-Sasolburg Coalfield, immediately southwest of Sasolburg in the Republic of South Africa. The colliery is in the fortunate position that it has a very complete and concise monitoring program in place and over 200 boreholes were drilled throughout the life of mine. Down-the-hole chemical profiles of over 90 boreholes were created with a multi-parameter probe. From the data collected a three-dimensional image was created from the electrical conductivity values at different depths. This image is very helpful in aiding the decision making process in the future management of the colliery.

Keywords Colliery, electrical conductivity, three-dimensional image, management

Introduction

The stratigraphy of this coal field is typical of the coal-bearing strata of the Karoo Sequence. The succession consists of pre-Karoo rocks (dolomites of the Chuniespoort Group of the Transvaal Sequence) overlain by the Dwyka Formation, followed by the Ecca Group sediments, of which the Vryheid Formation is the coal-bearing horizon. Mainly the lava of the Ventersdorp and Hekpoort Groups underlie the coal. The Karoo Formation is present over the whole area and consists mainly of sandstone, shale and coal of varying thickness.

Mining at the colliery ceased in 2004 and the underground mine was flooded. An ash-filling project was undertaken by the colliery from 1999 to stabilize mine workings located beneath the main roads in the vicinity. A key issue is: if the mine eventually decants what the quality of the water will be? This information is important for the future planning of the company, as this will determine if a water treatment plant is necessary, and what the specifications for such a plant would be, if required.

It was therefore decided to do a down-the-hole chemical profile of each available and accessible borehole with a multi-parameter probe with the aim of observing any visible stratification. It was possible to create chemical profiles of over 90 boreholes. From the data collected a three-dimensional image was created from the electrical conductivity values at different depths to see if any stratification was visible in the shallow aquifer. Due to the ash-filling operations the normal aquifer conditions were disturbed, creating different pressures than normally expected at a deeper underground colliery. According to the Mineral and Petroleum Resources development Act (RSA 2002:49) no closure certificate may be issued unless it has been confirmed by the Inspector of Mines and the Department of Water Affairs that the management of pollution to water resources has been addressed. It is for this reason that the three-dimensional image may prove to be very helpful in the aiding in the decision making process in the future management of the colliery and eventually obtaining a closure certificate, and also to determine whether ash-filling is a viable option in discarding the ash.

Materials and Methods

The down-the-hole chemical profiling was carried out using a multi-parameter probe which measured the temperature, the specific conductivity, the dissolved oxygen concentration, the depth, the pH and the oxidation reduction potential. The data recorded by the probe was immediately downloaded onto a laptop computer. Fig. 1 indicates the position of the 94 boreholes that the down-the-hole chemical profiling was done on, the #2 coal seam as well as the #3 coal seam, Wonderwater open-pit mine, Mohlolo underground mine and the ashfill areas indicated in yellow.

After the chemical profiling was completed the downloaded data was entered into a WISH (Windows Interpretation System for

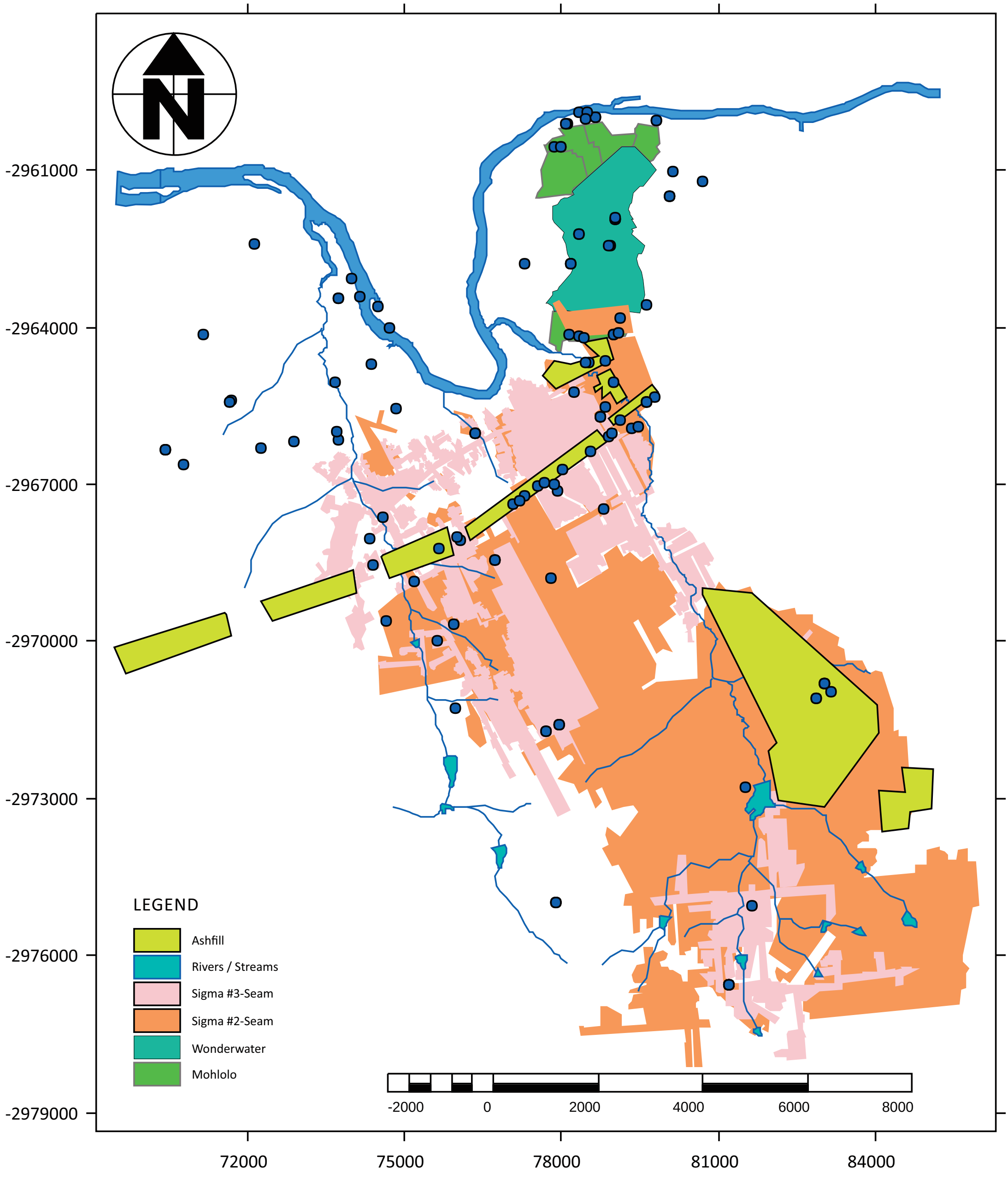

Fig. 1 *The boreholes profiled with the down-the-hole chemical profiling with the ashfill areas indicated in yellow.*

the Hydrogeologist) database. WISH was developed especially for the Hydrogeologist and is a hybrid between a CAD system, a Geographical Information System, Chemical analysis package and pumping test programs. It was decided to use the electrical conductivity values to create a three-dimensional image since electrical conductivity is a measure of the ability of water to conduct an electric current and this is dependent on the concentration of the ions, such as Ca^{2+}, Mg^{2+}, K^{+}, Na^{+}, HCO_3-, Cl-, SO_4^{2-} and NO_3-, present in the water. WISH was then used to create the three dimensional image of the electrical conductivity of the boreholes in relation to the local topography.

To get a more concise image of whether decant will occur and what the water quality will be in the event that decant does occur, sections of water level versus topography were also created with WISH where the water level was very shallow. The three dimensional image of the electrical conductivities of the boreholes in close vicinity to these shallow water levels was then also used to determine the water quality of the possibly decanting water.

Results and discussion

The three-dimensional image of the electrical conductivity profiles in relation to the local topography and the underground mining area can be viewed in Fig. 2. From this image the high electrical conductivity areas (in red and yellow) are clearly visible and these areas can be focused on by creating sections in these specific areas.

Four sections were created in areas of shallow water levels where possible decant might occur. These sections are section A –AA, section B – BB, section C – CC and section D – DD.

The locality of section A – AA, section A – AA and the three dimensional image of the electrical conductivities of the boreholes in close vicinity to section A – AA can be viewed in Fig. 3.

The areas on Section A – AA (Fig. 3) encircled with red, are areas where the water level appears to be very shallow, and could thus be possible decant positions. The second area where the water level appears to be shallow is close to a river. Boreholes close to these areas are identified on the locality map in Fig. 3. From the EC logs it is evident that the EC of these boreholes varies between 1.7 mS/m and a 99 mS/m. This is well within the ideal to acceptable range for electrical conductivity values according to SANS241:2006 drinking water standards which is between 0 and 150 mS/m. It can be assumed that in the event that decant would occur, the water quality of the decanting water will be within the acceptable range.

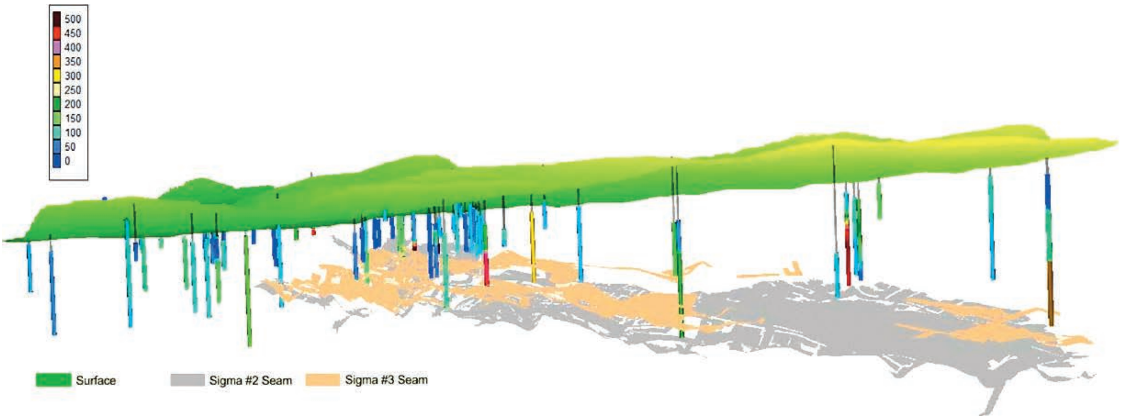

***Fig. 2** Electrical conductivity profiles of boreholes in relation to the local topography with a topographic high where the red contours are displayed.*

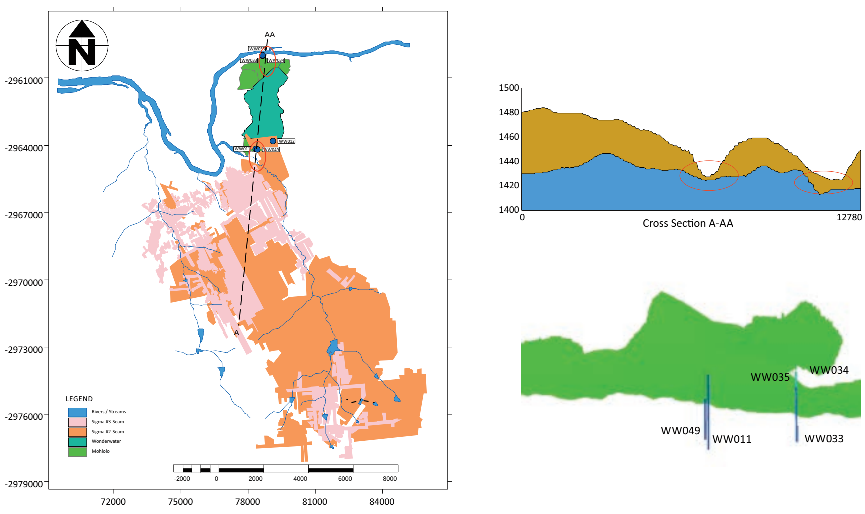

Fig. 3 *The locality map of section A – AA with the section A – AA and the 3D-image of the electrical conductivity values in relation to topography in close vicinity to section A – AA.*

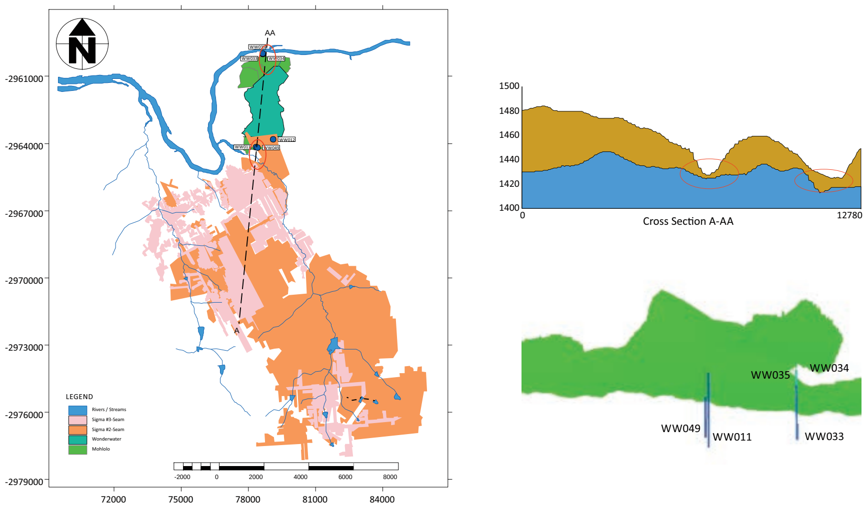

Fig. 4 *The locality map of section B – BB with the section B – BB and the 3D-image of the electrical conductivity values in relation to topography in close vicinity to section B – BB.*

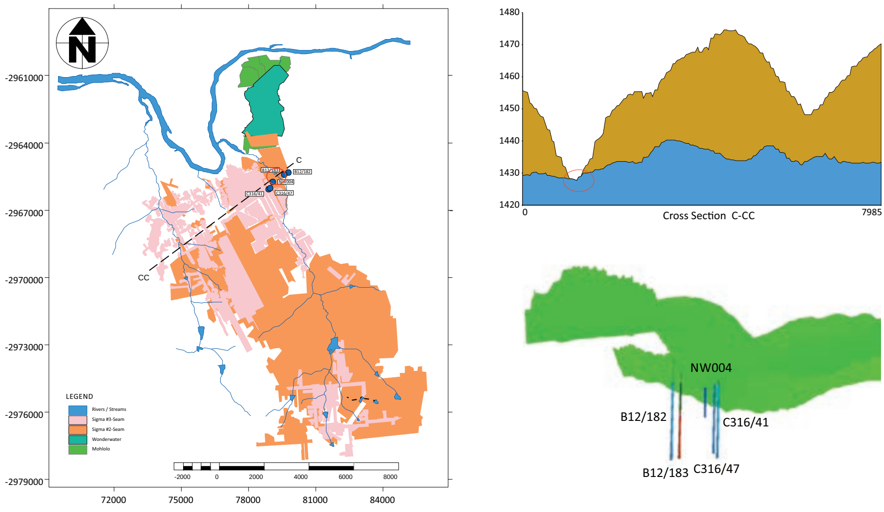

Fig. 5 *The locality map of section C – CC with the section C – CC and the 3D-image of the electrical conductivity values in relation to topography in close vicinity to section C – CC.*

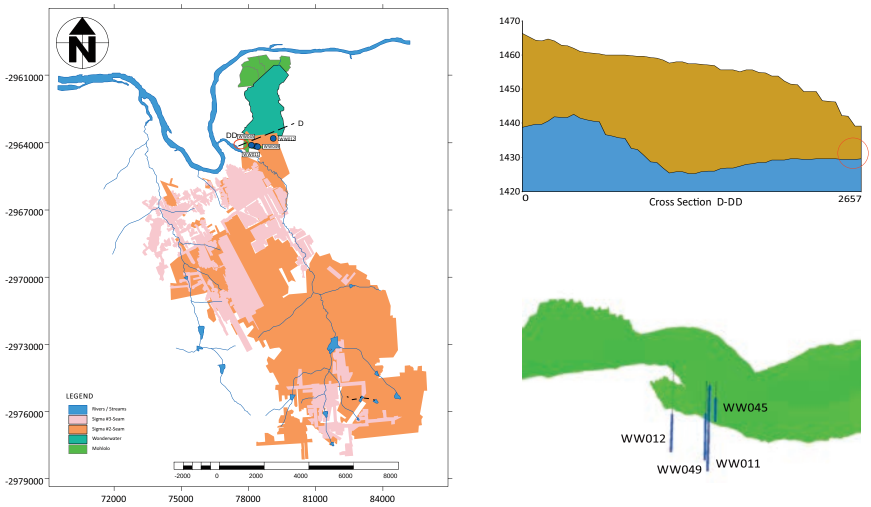

Fig. 6 *The locality map of section D – DD with the section D – DD and the 3D-image of the electrical conductivity values in relation to topography in close vicinity to section D – DD.*

The locality of Section B – BB, section B – BB, and the three-dimensional image of the electrical conductivities of boreholes in close vicinity to section B – BB can be viewed in Fig. 4.

The areas encircled in red (Fig. 4) again are areas where the water level appears to be very shallow and could be possible decant positions. The first two areas where the water levels appear to be shallow are close to rivers. Boreholes nearby to these areas are visible on the locality map in Fig. 4. From the three-dimensional image of the electrical conductivity logs it is evident that the EC of these boreholes range between 70 mS/m and 132 mS/m. These values are still within the acceptable range according to SANS241:2006 drinking water standards, which is between 0 and 150 mS/m. It can be assumed that should decant occur in the areas encircled in red (Fig. 4) the decanting water will still be within the acceptable range according to SANS241:2006 drinking water standards and will not be polluted water.

The locality of section C – CC, section C – CC and the three-dimensional image of the electrical conductivities of the boreholes in closse vicinity to section C – CC can be viewed in Fig. 5.

The area encircled in red (Fig. 5) is an area where the water level appears to be very shallow and could indicate a possible decant position. Boreholes close to this area are identified on the locality map in Fig. 5. The EC values for the boreholes range between 12 mS/m and 450 mS/m. The high EC values are found in borehole B12/183 and could be attributed to the fact that this borehole is an ashfill borehole. Water decant from ashfill boreholes would be due to artificial pressure caused by the ashfill that was pumped into the boreholes. If decant should occur from this borehole the water quality of the decanting water would be in the “not allowable” range according to SANS241: 2006 drinking water standards. If any of the other boreholes discussed, or the area surrounding these boreholes, should decant the water quality of the decanting water will be within the acceptable range according to SANS214:2006 drinking water standards.

The locality of Section D – DD, section D – DD and the three-dimensional image of the electrical conductivities of boreholes in close vicinity to section D – DD can be viewed in Fig. 6.

The area encircled in red (Fig. 6) is an area where the water level appears to be fairly shallow and could be a possible area of decant. The boreholes in nearby this area are visible on the locality map in Fig. 6. From the EC logs it is evident that the EC of these boreholes varies between 1.7 mS/m and a 99 mS/m. This is well within the “ideal to acceptable” range for electrical conductivity values according to SANS241:2006 drinking water standards. It can be assumed that in the event that decant would occur, the water quality of the decanting water will be within the acceptable range.

Conclusions

Once the mine has filled up with water, the piesometric level of the mine will rise with the storage coefficient value of the mine as conditions have changed from unconfined to confined. The flux from the overlying aquifers into the mine aquifer will decrease as the two water levels approach each other. The flux from the underlying dolomitic aquifer towards the mine will also decrease as the mine level increases. Once the level of the mine aquifer is higher than that of the dolomite aquifer, water from the mine will flow towards the dolomite aquifer. It is only if the mine level increases above that of the level of the top weathered aquifer, that decant could occur. The chance that the water level of the mine would increase above the water level of the top aquifer is very small because the dolomite has a much higher transmissivity value than the top aquifer. Thus the chance of decant occurring is very unlikely. No stratification was visible in the top aquifer and it was only when ash filling of the mining voids was introduced that problems were created and stratification of the top aquifer became visible. The only place where decant and pollution of the shallow aquifer is evident is where ash filling has been done. Thus if the company then chooses to continue with the ash filling a water treatment plant will become necessary which will incur more costs.

Acknowledgements

The authors are grateful to the colliery for providing the site for investigation.

References

RSA (Republic of South Africa) (2002) Mineral and Petroleum Resources Development Act 2002 (Act No. 28 of 2002). Pretoria: Government Printer

South African National Standards 241:2006. SA Drinking Water Standards.

The Water-Quality Effects of a Bulkhead Installed in the Dinero Mine Tunnel, near Leadville, Colorado

Katherine Walton-Day[1], Taylor J. Mills[1], Adolph Amundson[2], Kato T. Dee[3],
Melissa R. Relego[3], Caitlin Borbely[3]

[1]U.S. Geological Survey, Box 25046, MS 415, Denver, Colorado, USA, kwaltond@usgs.gov, tmills@usgs.gov
[2]Colorado Division of Reclamation, Mining, and Safety, 1313 Sherman St., Room 215, Denver, Colorado, USA, al.amundson@state.co.us
[3]Natural Resources Management Institute, Colorado Mountain College, 901 S. Highway 24, Leadville, Colorado, USA, kdee@coloradomtn.edu, melissarwolfe@gmail.com, cborbely@maulfoster.com

Abstract In 2009, a bulkhead was installed in Dinero tunnel to reduce drainage and improve water quality and aquatic habitat downstream in Lake Fork Creek. Monitoring during 2006 and 2010 to 2012 indicated water-quality improvement in Lake Fork Creek (zinc concentrations and loads decreased). However, water quality degraded in areas adjacent to Dinero tunnel (pH decreased and zinc concentrations increased) due to increased water-table elevation behind the bulkhead. Continued monitoring will help assess if water-quality degradation continues adjacent to Dinero tunnel, and if low pH, zinc-rich water breaks through the Dinero wetland area and negates water-quality improvement in Lake Fork Creek.

Keywords mine drainage, bulkhead, water quality, monitoring

Introduction

The Dinero tunnel is a historic mine adit in the Sugar Loaf Mining District near Leadville, Colorado (fig. 1). The mining district produced silver, some gold, lead, and zinc primarily from 1880 until 1893, and then operated sporadically until the 1920s (Singewald 1955). Mine drainage from Dinero tunnel is the primary source of manganese and zinc loading to Lake Fork Creek (Walton-Day and others 2005). Water-quality data for 2002–2009 indicate that cadmium, manganese, and zinc chronic aquatic-life water-quality criteria were periodically exceeded in portions of Lake Fork Creek downstream from Dinero tunnel (Lake Fork Watershed Working Group 2010). Benthic macro-invertebrate surveys indicated macroinvertebrate abundance and diversity decrease downstream from Dinero tunnel (Barrack 2001, Lake Fork Watershed Working Group 2010). In 2009, a bulkhead was installed in Dinero tunnel to reduce water flow from the tunnel and help improve downstream water quality and aquatic habitat (fig. 1). Hydrostatic pressure recorded behind the bulkhead has been relatively steady since late in 2010, and indicates that groundwater elevation rose to approximately 115 m above the bulkhead after installation and closure; mine pool elevation is approximately 3,097 m.

The U.S. Geological Survey, in cooperation with the Colorado Division of Reclamation, Mining, and Safety, the Bureau of Land Management, and Colorado Mountain College conducted a monitoring program to assess the water-quality effects of bulkhead emplacement. Monitoring of water quality and discharge in surface water, springs, and seeps within about a 3 km radius of the tunnel was conducted prior to and for three years following bulkhead closure. Samples were collected from between 22 to 50 of the 70 sites shown on Fig. 1 four times (June, July, August, and October) in 2006 before bulkhead installation and closure, and during high and low flow periods (generally June and September) in 2010, 2011,

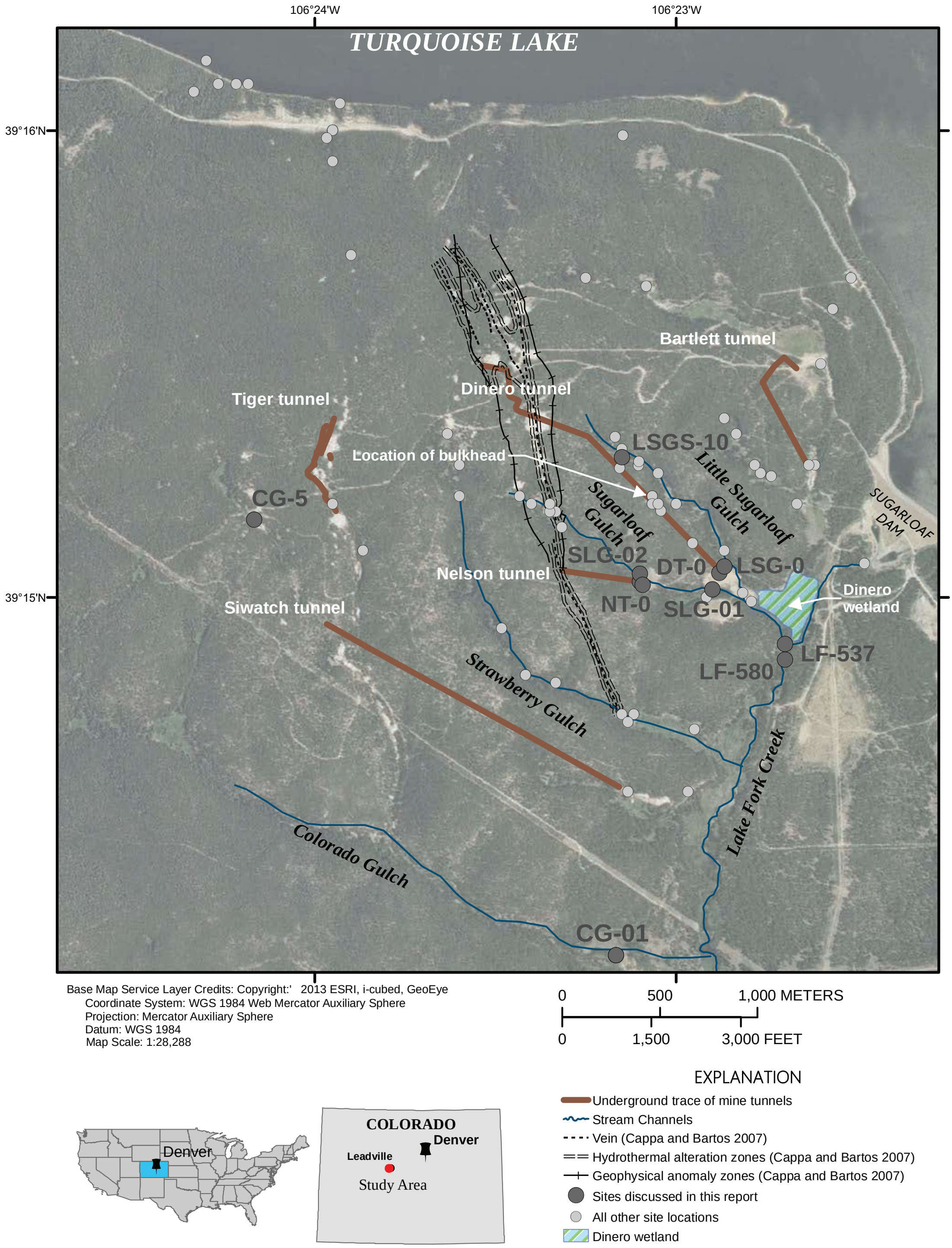

Fig. 1 *Sugar Loaf Mining District showing sample sites, mine tunnels, and a vein system with associated hydrothermal alteration.*

and 2012 after bulkhead installation and closure. The objective of this paper is to present results for sites adjacent to the Dinero tunnel and in Lake Fork Creek downstream from

[DT-0: Dinero tunnel portal; LF-537: channel draining Dinero area; LF-580: Lake Fork Creek downstream from Dinero area; Q: discharge; Total refers to concentrations and loads in unfiltered samples; Zn_{tot}: total Zn concentration; M_{Zn}: total Zn load; J: June; M: May, O: October; S: September]

	DT-0				LF-537				LF-580			
Month ‘year	Q (L/s)	pH (–)	Zn_{tot} (µg/L)	M_{Zn} (kg/d)	Q (L/s)	pH (–)	Zn_{tot} (µg/L)	M_{Zn} (kg/d)	Q (L/s)	pH (–)	Zn_{tot} (µg/L)	M_{Zn} (kg/d)
J ‘06	7.4	5.2	19,200	12.3	1.9	3.7	9,790	1.61	408	7.0	232	8.18
J ‘10	0.51	6.7	3,230	0.14	4.0	4.5	1,890	0.65	235	7.0	49	0.99
J ‘11	1.3	6.7	4,520	0.51	17.3	4.5	4,170	6.2	487	6.5	711	29.9
M ‘12	0.82	6.5	5,100	0.36	0.59	4.7	4,320	0.22	484	7.2	25	1.05
O ‘06	4.8	6.3	10,100	4.19	2.7	4.2	6,820	1.59	549	6.9	61	2.89
S ‘10	0.57	6.4	4,700	0.23	0.06	4.9	2,520	0.01	84.1	6.4	70	0.51
S ‘11	1.1	6.2	6,050	0.57	0.85	4.5	1,720	0.13	84.7	6.6	49	0.36
S ’12	0.82	6.9	5,390	0.38	0.51	4.4	1,300	0.06	490	7.5	34	1.44

Table 1 *Discharge, pH, and unfiltered zinc concentration and load, Sugar Loaf Mining District study area*

Dinero tunnel (fig. 1) to highlight changes in water quality (pH and zinc) that occurred after bulkhead emplacement.

Study Area

The study area lies on the eastern flanks of the Sawatch mountain range, west of Leadville Colorado. Elevations range from 2,926 m at site CG-01 (fig. 1) to 3,008 m at full pool elevation in Turquoise Lake, to 3,260 m at the highest sampling site (CG-5, fig. 1). Most of the Sugar Loaf Mining District is forested and contains abandoned, draining mine tunnels such as the Dinero, Bartlett, Nelson, Siwatch, and Tiger tunnels (fig. 1) and numerous mine waste and tailing piles. Precambrian granitic and metamorphic rocks underlie the study area (Singewald 1955). The area drains to Turquoise Lake, Colorado Gulch, and Lake Fork Creek, which is tributary to the Arkansas River. Average annual precipitation of 45 cm per year (1948–2006) occurs primarily as snow in the winter, with summer thunderstorms sometimes contributing substantial rainfall (Sugarloaf Reservoir climate station; Western Regional Climate Center, www.wrcc.dri.edu, accessed April 2013). Surface-water and some groundwater hydrographs are dominated by a broad peak related to snowmelt runoff and recharge of groundwater systems that generally occurs between April and July with peak flow occurring between late May and early June (Walton-Day and Poeter 2009).

Methods

Water-quality samples were collected using modifications of standard sampling protocols (U.S. Geological Survey variously dated) to facilitate sampling in remote locations where sites were accessed by hiking. Modifications included use of a portable filtering apparatus, acidification at a central location (rather than at the sampling site), and use of smaller sample bottles. Quality-control samples indicated the modified sampling methods did not adversely affect the quality of the data (K. Walton-Day unpublished data). Data and sample collection at each site included the following: (1) Measurement and documentation of the field parameters (water temperature, specific conductance, pH, and dissolved oxygen) *in situ* using individual (2006) or multiparameter (2010 to 2012) field meters that were calibrated at the beginning of each field day and received calibration checks at mid-day and at the end of the day. If calibration problems were noted, those measurements were flagged in the database, and the instrument was recalibrated before collecting more samples. (2) Measurement of flow rate in each flowing spring, draining mine feature (tunnels and seeps associated with mine waste and tailing piles), and stream site using volumetric techniques, flumes, or velocity cross-section techniques depending on the flow rate and channel configuration at each site (Rantz and others 1982; Turnipseed and Sauer 2010). (3) Collection of composited water-quality samples using equal-width increment techniques (U.S. Geological Survey variously dated), where stream channel width and depth allowed, or grab samples in smaller channels, seeps, and springs. One large composite sample (1 to 2 L) was divided into separate 125 mL unfiltered and filtered (0.45 µm) acidified aliquots (ultrapure HNO_3) for analysis of major and trace elements by high resolution- inductively coupled plasma mass spectrometry at the University of Southern Mississippi Center for Trace Analysis using procedures similar to Shiller (2003). Replicate and blank samples were collected at approximately 10 % of sample sites to assess data quality. Results indicate no adverse effects to the quality of results presented herein (K. Walton-Day unpublished data). This paper presents streamflow, pH, zinc, and iron results for a subset of all samples collected. Results from all environmental samples are publicly available through the U.S. Geological Survey National Water Information System (http://maps.waterdata.usgs.gov/mapper/index.html).

Results and Discussion

Bulkhead emplacement in Dinero tunnel in 2009 greatly reduced discharge, total zinc concentration, and instantaneous zinc mass load (total load on table 1) from Dinero tunnel drainage collected at the portal (DT-0) as evidenced by lower values in 2010–2012 relative to 2006 (table 1). Similarly, zinc concentrations and instantaneous mass loads generally decreased at site LF-537 which drains most of the area that includes the Dinero tunnel, Sugarloaf Gulch, and Little Sugarloaf Gulch, and at site LF-580, located on Lake Fork Creek, downstream from LF-537 (fig. 1, table 1). In addition, pH at LF-537 generally increased by almost 1 unit during high flow. One exception to these water-quality improvements was June 2011 at LF-537 and LF-580 when snowmelt runoff was at near-record levels due to a larger than average snowpack. The large snowmelt-related runoff likely increased runoff from draining mines and abandoned mine features leading to decreased water quality at these two sites.

In contrast to these general water-quality improvements, after bulkhead emplacement, zinc concentrations increased or pH decreased (or both) at sites adjacent to Dinero tunnel (DT-0) including SLG-01 (the mouth of Sugarloaf Gulch), LSG-0 (the mouth of Little Sugarloaf Gulch), and NT-0 (the Nelson mine drainage tunnel; fig. 2). Results at CG-01 (fig. 2) indicate that decreasing pH and increasing zinc concentrations after bulkhead emplacement were not a regional phenomenon but were limited to sites near Dinero tunnel. The low pH at CG-01 during June 2011 is due to the large snowmelt-related runoff at that time, which increased runoff from mine waste in the Colorado Gulch watershed, between Tiger Tunnel and Colorado Gulch (fig. 1), causing low pH and elevated zinc concentrations. The generally decreasing water quality at SLG-01, LSG-0, and NT-0 suggests that the elevated water table and mine pool created by emplacement of the bulkhead in Dinero tunnel increases groundwater discharge into the gulches and Nelson mine tunnel and degrades water quality at these sites.

In addition to these changes in water quality, there were coincident increases in flow at some of these sites. During October 2006, low to no flow in both Sugarloaf and Little Sugarloaf Gulches prevented sampling at most sites. In contrast, in 2010 to 2012, flow in both gulches was sufficient to collect samples at almost all sites during the "low flow" sampling trips. Although 2011 was a high-flow year, flow during two years (2006, 2010) was not unusually high or low. In contrast, 2012 was a fairly low-flow year, yet most sites in these gulches had flowing water in September 2010, 2011, and 2012. The increased amount of flow observed in Sugarloaf and Little Sugarloaf Gulches during low-flow sampling after bulk-

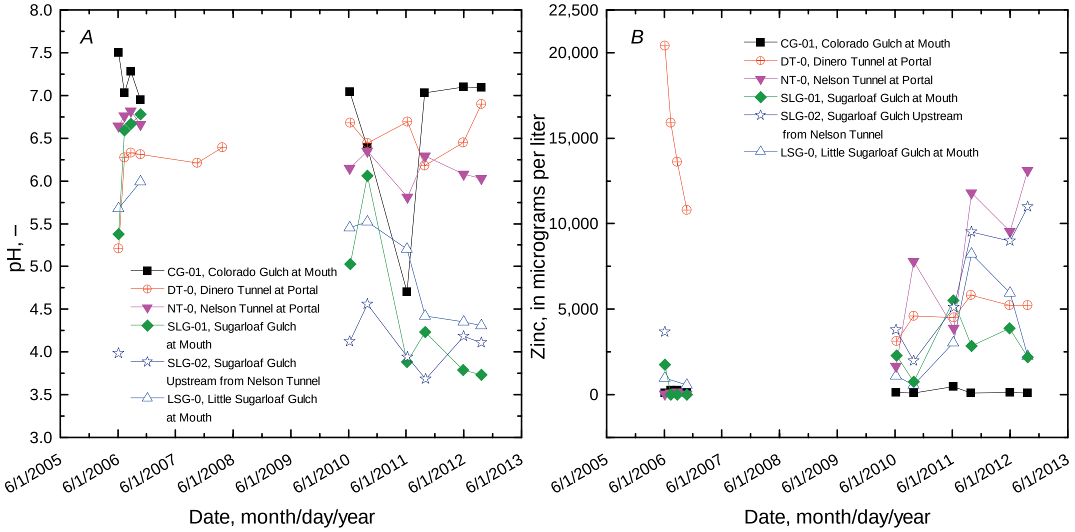

Fig. 2 *Graphs of (A) pH and (B) zinc concentrations through time at selected sample sites.*

head emplacement is additional evidence that the mine pool created by the bulkhead increased groundwater discharge to the gulches.

Water-quality changes at SLG-01 (Sugarloaf Gulch at the mouth) are related to changes at NT-0 (Nelson tunnel at the mouth) and SLG-02 (Sugarloaf gulch upstream from Nelson tunnel) because flow from the two sites combines to form most of the flow at SLG-01. At all three sites, zinc concentrations increased after bulkhead emplacement (fig. 2). Before the bulkhead (2006), NT-0 and SLG-01 had near neutral pH and SLG-02 had lower pH (fig. 2). After bulkhead emplacement, the pH at SLG-02 did not change appreciably and pH at NT-0 decreased slightly. These small pH changes do not explain the substantial reduction in pH that occurred at SLG-01. The likely cause of the low pH at the mouth of Sugarloaf Gulch (SLG-01) is the precipitation of iron oxyhydroxides associated with increasing discharge of iron from NT-0 following bulkhead emplacement. At NT-0, concentrations of filtered iron and instantaneous mass loads of filtered iron increased from median values of about 0.9 mg/L and 0.01 kg/d during 2006 to median values of 38 mg/L and 1.1 kg/d during 2010 to 2012, an increase in iron mass load of almost 2 orders of magnitude. At SLG-01, concentrations and instantaneous mass loads of filtered iron changed from median values of about 17 mg/L and 0.2 kg/d during 2006 to median values of 1.4 mg/L and 0.09 kg/d during 2010 to 2012. These comparisons indicate that there were sources of iron mass load to SLG-01 other than Nelson tunnel in 2006 (primarily SLG-02). However, more importantly, the much larger iron mass load contributed from Nelson tunnel during 2010 to 2012 was largely removed from solution by the time the water reached the mouth of Sugarloaf Gulch (SLG-01). This simplified reaction

$$\mathrm{Fe^{3+}} + 3\,\mathrm{H_2O} \longleftrightarrow \mathrm{Fe(OH)_3} + 3\,\mathrm{H^+} \qquad (1)$$

illustrates how precipitation of iron hydroxides (and by analogy, iron oxyhydroxides) increases acidity (lowers the pH) in solution. This reaction is likely responsible for the loss of iron load and the decrease in pH observed between NT-0 and SLG-01 during 2010 to 2012.

After bulkhead emplacement, zinc concentrations in Nelson tunnel (NT-0) have been increasing and are generally greater than those in Dinero tunnel (fig. 2). The Dinero tunnel lies within the ridge between Sugarloaf and Little

Sugarloaf Gulches (fig. 1). The Nelson tunnel is driven into the next ridge to the south, in a west/northwest direction, generally away from the Dinero tunnel (fig. 1). It is not readily apparent how water from the mine pool in the ridge between Sugarloaf and Little Sugarloaf Gulches could move into Nelson tunnel without also causing drastically increased flow in Sugarloaf Gulch. However, Fig. 1 illustrates the configuration of mineral-bearing veins relative to Nelson and Dinero tunnels. The vein at the west end of Nelson tunnel runs directly to Dinero tunnel. We hypothesize that this vein facilitates water flow between the Dinero mine pool and the Nelson tunnel. The decreased water quality at Nelson tunnel could be due to increased groundwater flow along this vein after bulkhead emplacement and subsequent raising of the water table.

If Dinero tunnel water is causing the increased zinc concentrations at Nelson tunnel, we might expect the concentrations to be similar to, or less than, those in Dinero. For example, a new seep that emerged in Little Sugarloaf Gulch starting in September 2011 (LSGS-10, fig. 1) is fairly close to Dinero tunnel and has water quality almost identical to Dinero water collected at the same time. It is likely that water flowing to Nelson tunnel encounters soluble, metal-rich salts within the mineralized vein, or that the introduction of water to parts of the vein that previously were dry is fueling acid-mine drainage reactions, dissolving more minerals, and increasing zinc concentrations relative to those at Dinero tunnel. Similarly, at other sites showing greater zinc concentrations than Dinero (LSG-0, SLG-02, fig. 2) it is likely that the elevated water table dissolves soluble, acidic salts or fuels acid-mine drainage reactions in newly wetted, previously dry portions of the aquifer.

Implications

These findings suggest that although the Dinero bulkhead has improved downstream water quality in Lake Fork Creek, water quality has degraded in the gulches adjacent to the ridge containing Dinero tunnel, and in Nelson tunnel. The low pH, zinc-rich water that now occurs at the mouth of Sugarloaf Gulch is flowing into a wetland that exists between Dinero tunnel and Lake Fork Creek (fig. 1). This wetland is mitigating the effects of the poor-quality water, but it is not known if this poor-quality water will eventually break through to Lake Fork Creek. The elevated zinc loads at LF-580 in June 2011 (table 1) may indicate that breakthrough occurs during unusual high-flow periods. Continued monitoring may indicate if the increasing zinc concentrations observed at several locations (fig. 2) eventually level off, or even decrease. Continued monitoring would also indicate whether water-quality improvement in Lake Fork Creek continues, or if the low-pH, zinc-rich water eventually breaks through to the creek causing renewed water-quality degradation.

Summary and Conclusions

Bulkhead emplacement in Dinero tunnel in 2009 generally resulted in improved water-quality from 2010 to 2012 at the portal of Dinero tunnel (DT-0), in the main source of water draining the area near Dinero tunnel into Lake Fork Creek (site LF-537), and in Lake Fork Creek downstream from the Dinero tunnel area (site LF-580). Although water quality improved at these sites, water quality has degraded (increasing zinc concentrations or decreasing pH, or both) at the mouths of Sugarloaf Gulch (SLG-01) and Little Sugarloaf Gulch (LSG-0), which are adjacent to Dinero tunnel, and in Nelson tunnel (NT-0). In addition, after bulkhead emplacement, increased flow was noted during low-flow periods in Sugarloaf Gulch and Little Sugarloaf Gulch, indicating increased groundwater discharge to the gulches. These post-bulkhead changes suggest that the mine pool formed by emplacement of the Dinero tunnel is discharging into the two gulches and degrading water quality. Decreased pH at the mouth of Sugarloaf Gulch is likely caused by precipitation of iron oxyhydroxides associated with increasing discharge of iron from Nelson tunnel following bulkhead emplacement. Water-quality degradation in Nelson tunnel is likely due to transport of mine-pool water along mineralized veins that directly link Dinero and Nelson tunnels. Additional monitoring will help assess if water quality continues to degrade in the areas adjacent to Dinero tunnel, and if the water-quality improvements in Lake Fork Creek downstream from the Dinero area continue or are negated by the breakthrough of low pH, zinc-rich water through the Dinero wetland area.

Acknowledgements

The authors thank the myriad of students at Colorado Mountain College who assisted with sample collection. In addition, Stephanie Ashley, Julianne Brown, Andrea Fleming, Jennifer Moore, Rodney Richards, Susan Hartley, Sarah Gonzalez, and Christine Dowling from U.S. Geological Survey contributed to sample collection, sample processing, data management, and Fig. preparation. Alan Shiller at the University of Southern Mississippi Center for Trace Analysis provided all major and trace element analyses. Helpful comments from Michael Rupert and an anonymous reviewer improved this manuscript.

References

Barrack, J (2001) Baseline water quality and macro-invertebrate study of the Lake Fork Watershed. www.coloradomtn.edu/UserFiles/Servers/Server_2935393/File/lfwwg/Final_Baseline_LF_Rev_718.pdf

Cappa JA, Bartos PJ (2007) Geology and Mineral Resources of Lake County, Colorado. Colorado Geological Survey, Resource Series 42, 59 pp

Lake Fork Watershed Working Group (2010) The Lake Fork of the Arkansas River Watershed Plan. Online document, 61 pp, www.coloradomtn.edu/c/document_library/get_file?uuid=252f50a7-58e7-41db-a5f8-845ef6cf66c4&groupId=1461862

Rantz SE and others (1982) Measurement and computation of streamflow v.1. Measurement of stage and discharge. U.S. Geological Survey Water-Supply Paper 275, 284 pp

Shiller AM (2003) Syringe filtration methods for examining dissolved and colloidal trace element distributions in remote field locations. Environ Sci Technol 37(17), p 3953–3957

Singewald QD (1955) Sugar Loaf and St. Kevin mining districts, Lake County, Colorado. U.S. Geological Survey Bulletin 1027-E, p 25–297

Turnipseed EP, Sauer VB (2010) Discharge measurements at gaging stations. U.S. Geological Survey Techniques and Methods, book 3, chap. A8, 87 pp

U.S. Geological Survey (variously dated) National field manual for the collection of water-quality data. U.S. Geological Survey Techniques of Water-Resources Investigations, book 9, chaps. A1-A9

Walton-Day, Katherine, Flynn JL, Kimball BA, Runkel RL (2005) Mass loading of selected major and trace elements in Lake Fork Creek near Leadville, Colorado, September—October 2001. U.S. Geological Survey Scientific Investigations Report 2005–5151, 45 pp

Walton-Day Katherine, Poeter, Eileen (2009) Investigating hydraulic connections and the origin of water in a mine tunnel using stable isotopes and hydrographs. App Geochem 24, p 2266–2282

Hydrodynamics in a flooded underground limestone mine

Christian WOLKERSDORFER[1,2], Holger KOMISCHKE[2,3], Sandra PESTER[2,4],
Andrea HASCHE-BERGER[2]

[1]*International Mine Water Association, Ginsterweg 4, 90530 Wendelstein, Germany, Christian@Wolkersdorfer.info*
[2]*TU Bergakademie Freiberg, Lehrstuhl für Hydrogeologie, 09599 Freiberg/Sachsen, Germany (at the time of conducting the site investigations)*
[3]*Bayerisches Landesamt für Umwelt, Hans-Högn-Str. 12, 95030 Hof, Germany*
[4]*Landesamt für Bergbau, Energie und Geologie, Stilleweg 2, 30655 Hannover, Germany*

Abstract This paper describes a mine water tracer test in a flooded Germany underground limestone mine. Uranine was injected at two locations and the tracer concentration measured with an on-line fluorimeter. The breakthrough curve shows two peaks, relating to the two injection sites. Background values were reached after 24 months making this tracer test the longest mine water tracer test ever. Mean effective velocities range between 0.1 and 0.5 m d^{-1} indicating a slow water circulation. The paper concludes that low effective velocities are an indication for mines with a simple geometry and that simple mine geometries facilitate stratification and a lower pollution potential.

Keywords tracer test; *Felsendome Rabenstein*; Saxony; hydrodynamics, abandoned mine

Introduction

In contrast to hydrogeochemical investigations related to mine water, the number of hydrodynamic investigations of the water flow within a mine is rather restricted. One reason might be that taking samples and conducting physico-chemical investigations of mine water is relatively simple compared to conducting hydrodynamic investigations in mines. Hydrodynamic investigations usually require access to the mine water at more than one location which is not always possible, unless bore holes are drilled, shafts reopened or discharge adits made accessible. In addition, the injection of tracer substances and their analysis is not a standard method and therefore does not belong to the investigations carried out as often as physico-chemical analyses. Another reason might be that mining operators, researchers, and authorities consider the quality of mine water draining out of a mine as “given” and consequently focus on the chemistry rather the flow of the water through the mine. But, as we will show, the flow of water in mines depends on the mine’s geometry and this knowledge might be used to plan remediation strategies for underground mines before their flooding.

Mine operators or researchers initiate relatively few investigations relating to the flow of the mine water itself (Semmler 1937; Merritt & Angerman 1972; Wolkersdorfer & Hasche 2001). In those cases, where a tracer test is conducted the key question is usually if two or more locations are hydraulically connected rather than identifying the hydrodynamics within the mine itself. First investigations of the hydrodynamics of flooded mines were conducted by Wolkersdorfer *et al.* (1997) and optimised thereafter (Wolkersdorfer 2008). The potential for stratification in flooded underground mines was investigated by several researchers based on the hydrogeochemistry or physico-chemical parameters of the mine water (*e.g.* Wolkersdorfer 1996; Kories *et al.* 2004; Nuttall & Younger 2004; Wolkersdorfer & Merkel 2005; Rapantova *et al.* 2009; Reichart *et al.* 2011).

Our own tracer investigations and the investigations of others revealed three facts:

- the mean effective velocity of water in flooded underground mines is in a relatively narrow range of 0.3…1.6 m min^{-1} (95 % confidence interval of 42 tracer tests; Wolkersdorfer 2008)
- several mines have a relatively fast effective velocity of the mine water (6…11 m min^{-1})
- some mines have a very slow effective velocity of the mine water (10^{-4}…10^{-2} m min^{-1})

The hypothesis resulting from those facts was that mines where the shafts are hydraulically well connected with each other show faster velocities (‘multiple shaft mines’), while mines with only one or two poorly connected shafts show slower effective velocities (‘single shaft mines’). To prove this hypothesis we conducted two tracer tests in mines with only one or two shafts that we assumed are poorly connected with each other. One of those mines was the Austrian *Georgi Unterbau* and the other one the German *Felsendome Rabenstein*. In this paper we are presenting the results of the latter tracer test. Preliminary results of the first one are published elsewhere (Wolkersdorfer *et al.* 2002, Wolkersdorfer 2008).

A quasi-stagnant situation is typical for ‘single shaft mines’ where the geothermal gradient is not high enough to start free convection, nor does a major regional forced convection exist. Water in the shaft flows very slowly and it can be assumed that there is a laminar Poiseuille flow situation in the upper part of the shaft and diffusive flow in the lower part of the shaft. Therefore, this shaft was selected for a tracer test in a mine with a low vertical flow characteristic and a simple mine geometry.

Location and mining history of the *Felsendome Rabenstein*

The *Felsendome Rabenstein* is a former underground limestone mine located in Rabenstein/Germany, a suburb of Chemnitz/Saxony consisting of four worked mine levels (Fig. 1). Since the beginning of the 20th century the two lowermost levels have been flooded and the mine started to become a local tourist attraction in 1936 (Geißler *et al.* 1984). During the

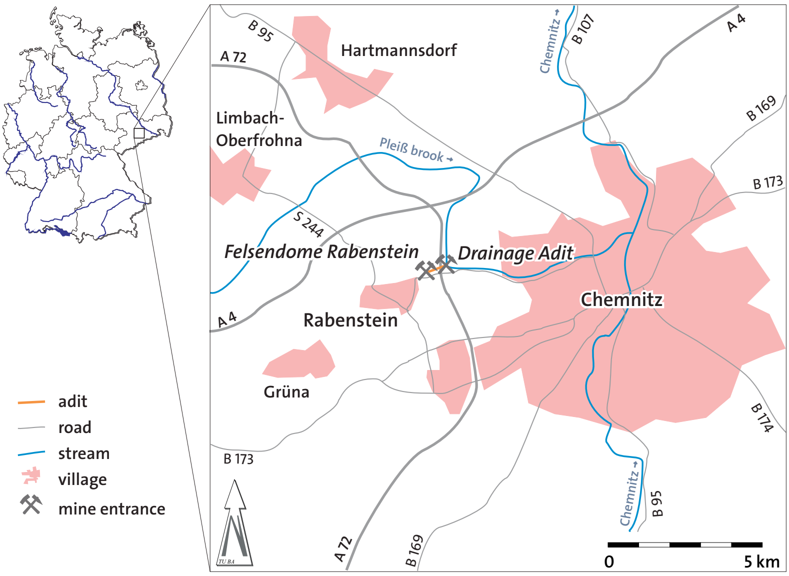

Fig. 1 *Location of the Felsendome Rabenstein abandoned underground limestone mine.*

last two decades, the site was converted into an attractive recreation area, and the underwater part is now extensively used by divers (Meier & Meier 2007).

First underground limestone mining in the area began in medieval times (Riedel 1993). In 1834, the Rabenstein underground mine opened and 40 years later, the 35 m deep *Maschinenschacht* (machine shaft) was sunk, connecting the three lowermost levels with each other (15, 22, and 27 m below the surface; Fig. 2). At the end of the mine’s lifetime, four levels existed: the upper and lower level as well as the 1st and 2nd deep levels (level 3 and 4), extending over an area of 250 × 100 m with caverns ranging from 6–8 m in height. An underground drift adit in the *Grüne Grotte* (green grotto) and the *Maschinenschacht* connected the two deeper levels with the lowest level. To dewater the mine, a 220 m long drainage adit to the Pleiß brook was constructed in 1855, which still dewaters the mine from the lower level, with daily mean discharges between 3 and 40 $^{-1}$. Extreme precipitation can induce total discharges up to 120 $m^3\ d^{-1}$. During active mining, the water from the 1st and 2nd deep levels was pumped into the adit. In 1902, six years before the closure of the mine, the two deepest levels were allowed to flood and since then the connecting shaft has been filled with a 15.8 m high water column. Based on available data, the volume of the *Maschinenschacht*, the *Grüne Grotte* incline, and the flooded 1st and 2nd deep levels is 124, 120, and 2,100 m^3, respectively. Only the parts that were thought to be relevant for the tracer test were used in the calculation. The total volume of each level must be another 20–30,000 m^3. Using that data, a total flooding time of several years can be estimated. However, Dietrich (1965) calculated a flooding time of 12 weeks for the two underground levels, which seems to be rather low considering a mean flow of 12 $m^3\ d^{-1}$.

At two locations the flooded part of the mine is accessible: the *Grüne Grotte* and the *Maschinenschacht*, which are 140 m apart from each other. Between 2002 and 2005, when the tracer test was conducted, the electrical conductivity of the mine water was relatively constant at 1,190…1,260 µS cm^{-1}, with a pH of 6.5…8.9, an E_H of 350…510 mV, and a temperature of 7.5…8.7 °C. Slightly different values prevailed at the *Grüne Grotte*: electrical conductivity 800…1,000 µS cm^{-1}, pH 7.1…8.7, E_H 340…510 mV, and a temperature of 4.8…6.8 °C.

According to the known records of the *Felsendome Rabenstein* mine and the reports of divers, the flooded and partly backfilled *Maschinenschacht* (machine shaft) is con-

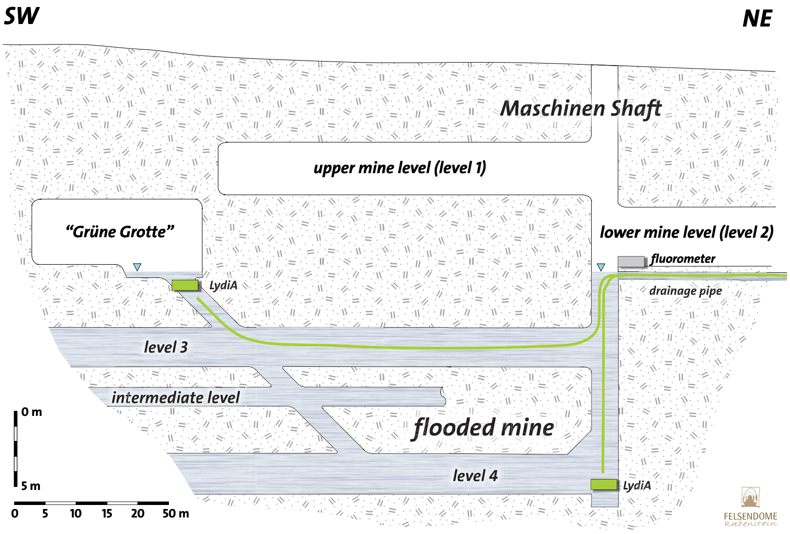

Fig. 2 *Cross section through the partly flooded Felsendome Rabenstein limestone mine showing the injection and sampling sites as well as the proposed flow path of the uranine tracer. Scales only correct for the flooded mine parts. Not to scale above the water table.*

nected to the 1st and 2nd deep levels at depths of 6 and 12 m below the mine water surface. Several small blind shafts and the incline within the *Grüne Grotte* connect the 1st deep level with the 2nd deep level. No precise data are available about the shaft’s outflow, but it was estimated with an area velocity measurement to be in the range of 1…2 L min^{-1}. Only a poorly developed thermal stratification can be found in the *Maschinenschacht*. The temperature in the shaft is relatively constant at 7.9 °C and small temperature fluctuations can be observed at the two onsetting stations (Fig. 3).

Outline of the Geological Situation

Geologically, the mine is located in the Rabenstein-Formation within the Schist Cover of the Saxonian Granulite Massiv and the rocks are assumed to belong to the Cambrian Series 2…3. Primarily, the mined strata comprise metamorphosed limestone, a coloured calcite marble in combination with phyllites, alum shale-like black phyllites, and amphibolites. Pyrite occurs frequently in the limestone and especially in the phyllites, and copper pyrite (chalcopyrite), often oxidised to malachite, can be found in vugs. The whole formation is slightly folded with northwest striking folding axes, and faults in a northeastern direction with offsets in the range of 5 m are common (Dietrich 1965; Freyer *et al.* 1982; Geißler *et al.* 1986). Some of the faults are hydraulically active, as water penetrates from the surface to the mine during high precipitation periods (*e.g.* a fault between the *Blauer Salon* and the *Gnomengang*). Divers have reported that they can regularly see bead-like air bubbles moving in straight lines from the 2nd deep level through the rock into the 1st deep level.

Methods and Investigations

In 2002, the flooded part of the mine was investigated hydrogeologically and the potential for a mine water tracer test was evaluated. The water analysis did not indicate potential problems for a tracer test and the pH was circumneutral, suggesting that no decomposition of the tracer, uranine (sodium fluoresceïn), would be expected. A discontinuous temperature log in the *Maschinenschacht* showed a small temperature variation at the two flooded onsetting stations with no temperature shift. Later, continuous temperature logs revealed a small positive temperature shift of about 0.05 K/10 m (Fig. 3).

Between 2002 and 2005, the mine was visited 16 times and the physico-chemical on-site parameters were measured regularly. One full analysis of the mine water was conducted, showing that the water is of the Ca-Mg-SO_4-

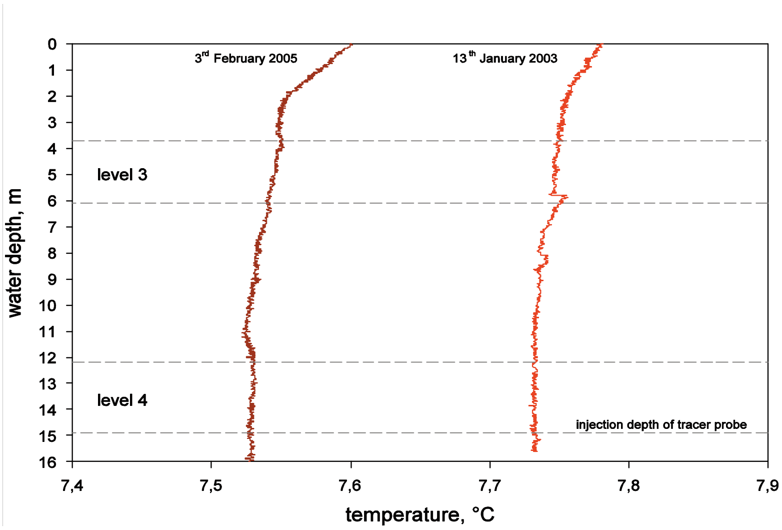

Fig. 3 *Temperature–depth profile in the Felsendome Rabenstein Machinenschacht before and after the tracer test.*

HCO_3-type. Five temperature and electrical conductivity logs were conducted in early 2003 and 2005 before and after the tracer test with uranine.

On 21 March 2003, the tracer test with uranine, scheduled for a duration of about 3 months, was started. With a tracer probe (LydiA; Wolkersdorfer *et al.* 1997), 15 g of uranine were lowered to a depth of 15 m into the *Maschinenschacht* and 250 g at a depth of 2…3 m within the incline of the *Grüne Grotte* (Fig. 2, 4). The recommendations about the use of tracer amounts summarised in a later paper by Wolkersdorfer & LeBlanc (2012) were followed. After 96 weeks, the tracer concentration came down to background values and was therefore brought to an end. Thus, the *Felsendome Rabenstein* Tracer test has the unique distinction of being the longest lasting tracer test ever conducted in an underground mine (Fig. 5). Due to a malfunction of the piezometer that measured the total flow of the mine water no recovery rates can be given at this stage of the investigation.

To clarify which of the two peaks belongs to which injection place, the vertical distribution of the tracer in the shaft was measured four times in the *Maschinenschacht* and once in the *Grüne Grotte* incline.

Results and Interpretation

Our investigations in the *Felsendome Rabenstein* showed that there is only a minor stratification of 0.1 K which is not strong enough to prevent the flow from the lowest mine level to the shaft's drainage point. Furthermore, the mine has only two main shafts which are connecting the two flooded levels. Based on the flow measurements in summer 2002 and assuming a mean flow of 0.3…1.6 m min^{-1} a duration of 1…2 months was calculated for the concentration of the tracer to return to background levels. Yet, the tracer concentrations did not decrease to the background values even after 19 months into the test period. From the tracer's maximum at about 3 months after the tracer test's beginning it can be calculated that the effective velocities between the injection and sampling points are about 0.1–0.4 m d^{-1} (Wolkersdorfer 2005, 2008).

No relevant stratification could be observed in the *Felsendome Rabenstein* mine. Neither the temperature nor the electrical conductivity plots show signs of stratification, though small fluctuations in the area of the onsetting stations were observed. While the temperature slightly increases (by about 1.5 K) from bottom to top, the electrical conductivity decreases by about 100 µS cm^{-1}, proving a

Fig. 4 *Tracer probe in the Grüne Grotte incline. The green colour of the water is from the uranine still in the mine water.*

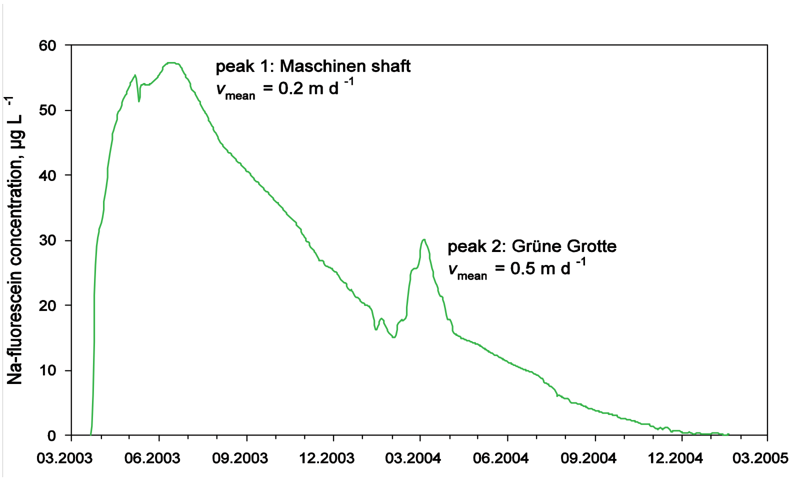

Fig. 5 *Breakthrough curve of the 2003–2005 Felsendome Rabenstein tracer test with uranine.*

mainly diffusion-based flow scenario in the *Maschinenschacht*, with only a small advective component.

In the breakthrough curve, two tracer peaks could be observed, the first one after 65 days, the second one 350 days after the tracer injection (Fig. 5, Table 1). Our hypothesis is that the first peak results from the tracer injected at a depth of 15 m in the *Maschinenschacht*; the second one from tracer injected 171 m away in the *Grüne Grotte* incline. From that data, an effective velocity v_{eff} of 0.10^{-1} was calculated for peak 1 and 0.48 m d^{-1} for peak 2. The smaller peak after peak 2 might have been induced by divers training in the flooded underground mine.

In contrast to the first peak, which has an extremely long tail of about 620 days, the second one has a tail of only 120 days, indicating a larger calculated longitudinal dispersion coefficient of 7.1 · 10-6 m^2 s^{-1} for peak 1 and a smaller one of 1.3 · 10^{-6} m^2 s-1 for peak 2. From the vertical tracer distribution in the *Maschinenschacht*, it became clear that the first peak results from the tracer injected into the *Maschinenschacht* and the second one from the tracer in the *Grüne Grotte*. The long tail of the first peak shows that the mass transport from the 2nd deep level to the surface is possibly diffusion-based and the flow from the *Grüne Grotte* must be via the connecting adit between the incline and the *Maschinenschacht* on the 1st level. If the water had followed the connecting adit at the 2nd level, a tailing similar to peak 1 would have been observed. It can be concluded that the transport from the 2nd level

	Effective velocity v_{eff}			Mean velocity v_{mean}		
Peak	Time d	Distance m	Velocity m d^{-1}	Time d	Distance m	Velocity m d^{-1}
1	149	15	0.10	65	15	0.23
2	356	171	0.48	350	171	0.49
2’	320	165	0.53	314	165	0.52

Table 1 *Results of the Rabenstein tracer test. Peak 2’ is the reconstruction of the travel times for the* Grüne Grotte *tracer from the* Grüne Grotte *to the onsetting station of the 1st deep level at the* Maschinenschacht. *It has been calculated from the travel times and distances of Peak 2 less the distance to the onsetting station and the mean travel times calculated from peak one and the mean of the effective and mean velocities of peak 1. Velocities are based on the data given in this table. No extensive modelling has been used.*

into the region of the 1st deep level is probably diffusion-dominated whereas the shaft above the 1st deep level shows Poiseuille-dominated flow.

Conclusions

The *Felsendome Rabenstein* tracer test proved our hypothesis that slow effective velocities in flooded underground mines are a result of restricted hydrodynamic connections of the mine workings. Only one larger diameter shaft and an incline as well as two minor shafts are connecting the two flooded levels with each other which does not induce an overall convective flow regime in the mine. The effective velocities in the mine water range between 0.1 and 0.5 m d^{-1} and are therefore in the lowest range of effective velocities ever measured in a flooded underground mine. Obviously, the mine is not very deep, but in conjunction with the *Georgi Unterbau* tracer test results, where a 100 m deep shaft is connecting the levels, we cannot reject our hypothesis that a simple mine geometry prevents convective flow in flooded underground mines.

In combination with the results of previous tracer tests we therefore draw the following conclusions:

- simple mine layouts abet slow effective mine water velocities
- modifications of the mine layout prevent an overall convective flow in the mine
- modifications of the mine layout before a mine is flooded reduce the effective velocity of the mine water
- a reduced effective velocity and convective flow regime hamper the spreading of the potential contaminants throughout the mine

Because the higher contaminated parts of a mine can usually be found in the deeper parts of the mine (*e.g.* Frost *et al.* 1977; Kories *et al.* 2004; Wolkersdorfer 2008) we therefore recommend to prevent an overall convective flow by modifying the mine layout before flooding starts. This might induce a stratification in the mine and the contaminant load draining out of the mine will be reduced.

Acknowledgements

We thank the *Felsendome Rabenstein*, and especially Eyke Tomek for providing us this interesting research object. Part of this text follows an earlier publication of one of the authors (Wolkersdorfer 2008).

References

Dietrich P (1965) Zur Geologie des Kalksteinvorkommens von Niederrabenstein. Unveröff. Studienarbeit Bergakademie Freiberg, Freiberg, 17

Freyer G, Geißler E, Hoth K, Tran TN (1982) Die Altersstellung des Karbonatgesteinshorizonts Rabenstein-Auerswalde und ihre Bedeutung für die Geologie des südöstlichen Schiefermantels des sächsischen Granulitgebirges. Z geol Wiss 10:1403–1424

Frost RC, Bernascone TF, Cairney T (1977) A light-weight and cheap depth sampler. J Hydrol 33(1–2):173-178

Geißler E, Nhuan TT, Strauss R (1984) Die Rabensteiner unterirdischen Felsendome – zur Geologie und Geschichte des Schaubergwerkes, 4th edn. Städtische Museen, Karl-Marx-Stadt [Chemnitz], 38

Kories H, Rüterkamp P, Sippel M (2004) Field and numerical studies of water stratification in flooded shafts. In: Jarvis A. P., Dudgeon B. A., Younger P. L. mine water 2004 – Proceedings International Mine Water Association Symposium, vol. 1. University of Newcastle, Newcastle upon Tyne, 149–159

Meier J, Meier G (2007) Sächsische Besucherbergwerke – eine Form der Nachnutzung von Altbergbau. In: Meier G. 7. Altbergbau-Kolloquium. Glückauf, Essen, 333–341

Merritt GL, Angerman TW (1972) The use of ionic tracers in determining the subsurface flow of mine drainage – A case study. Papers Presented Before the Symposium on Coal Mine Drainage Research 4:340–343

Nuttall CA, Younger PL (2004) Hydrochemical stratification in flooded underground mines: an overlooked pitfall. J Contam Hydrol 69(1–2):101-114

Rapantova N, Zeman J, Vojtek D, Grmela A, Michálek B (2009) Mathematical Modelling Application for Optimisation of Utilisation of Mine Waters with High

Uranium Concentrations from Flooded Mines. In: Water Institute of Southern Africa, International Mine Water Association. Proceedings, International Mine Water Conference. Document Transformation Technologies, Pretoria, 89–94

Reichart G, Vaute L, Collon-Drouaillet P, Buès MA (2011) Modelling heat and salinity related convective processes in deep mining flooded wells. In: Rüde T. R., Freund A., Wolkersdorfer C. Mine Water – Managing the Challenges – 11th International Mine Water Association Congress. RWTH Aachen University, Aachen, 183–188

Riedel L (1993) Zur Geschichte des Bergbaues um Chemnitz. Veröff Mus Naturk Chemnitz 16:1–88

Semmler W (1937) Untersuchungen, Wassermessungen und Färbungsversuche zur Ermittelung der Herkunft der Wasserzuflüsse im Felde der Grube Victoria, Püttlingen-Saar. Der Bergbau 50(6):87-93

Wolkersdorfer C (1996) Hydrogeochemische Verhältnisse im Flutungswasser eines Uranbergwerks – Die Lagerstätte Niederschlema/Alberoda. Clausthaler Geowissenschaftliche Dissertationen 50:1–216

Wolkersdorfer C (2005) Mine water tracer tests as a basis for remediation strategies. Chem Erde 65(Supp 1):65-74

Wolkersdorfer C (2008) Water Management at Abandoned Flooded Underground Mines – Fundamentals, Tracer Tests, Modelling, Water Treatment. Springer, Heidelberg, 466

Wolkersdorfer C, Hasche A (2001) Tracer Test in the abandoned Fluorspar Mine Straßberg/Harz Mountains, Germany. Wissenschaftliche Mitteilungen 16:57–67

Wolkersdorfer C, LeBlanc J (2012) Regulations, Legislation, and Guidelines for Artificial Surface Water and Groundwater Tracer Tests in Canada. Water Quality Research Journal of Canada 47(1):42-55

Wolkersdorfer C, Merkel B (2005) The flooded Freiberg/Sachsen Mining District – Hydrogeochemistry, Hydrodynamics and Environmental Impacts. In: Loredo J., Pendás F. Mine Water 2005 – Mine Closure. University of Oviedo, Oviedo, 185–187

Wolkersdorfer C, Feldtner N, Trebušak I (1997) LydiA – A new Method for tracing Mine Water. Proceedings, 6th International Mine Water Association Congress, Bled, Slovenia 1:43–55

Wolkersdorfer C, Trebušak I, Feldtner N (1997) Development of a Tracer Test in a flooded Uranium Mine using *Lycopodium clavatum*. In: Kranjc A. Tracer Hydrology 97, vol. 7. Balkema, Rotterdam, 377–385

Wolkersdorfer C, Hasche A, Unger K, Wackwitz T (2002) Tracer Techniken im Bergbau – Georgi-Unterbau bei Brixlegg/Tirol. Wissenschaftliche Mitteilungen 19:37–43

Electronic attachements can be found at:
http://bitly.com/IMWA2013_429

Methodology for assessing water pollution and risks associated with abandoned lead-zinc mining at Wanlockhead and Leadhills, southwest Scotland, UK

Lee M Wyatt, Arabella M L Moorhouse, Ian A Watson, Steven Kershaw

The Coal Authority, 200 Lichfield Lane, Mansfield, Nottinghamshire NG18 4RG, UK
leewyatt@coal.gov.uk

Abstract Within the UK, no organisation is currently responsible for pre-2000 abandoned non-coal mines. Commonly, following cessation of mining, limited work was undertaken to remediate these mine sites and associated mineral processing areas. Consequently these landscapes are often dominated by disused mine entries, spoil mounds, smelting mills and other associated features. Due to the unmaintained nature of these locations, there are often numerous risks present including blockages, collapses and contaminated ground. The Coal Authority has investigated metal contamination in two water-bodies in southwest Scotland, employing a dynamic, flexible sampling strategy enabling the prompt identification of possible sources in a changing environment.

Keywords metal mine water, abandoned mines, mining legacy, risk of abandoned mines, dynamic methodology of water investigation

Introduction

The villages of Leadhills and Wanlockhead are two former lead (and zinc) mining villages located in southwest Scotland, situated towards the headwaters on the Glengonnar Water and Wanlock Water respectively. Mining in the area dates back to the 13th Century (Rowan *et al.* 1995), however the most intensive period of activity occurred between the 17th Century and mid 20th Century. The Scottish Environmental Protection Agency (SEPA) have monitored these two water-bodies and determined that both are failing the Environmental Quality Standards (EQS) defined for these rivers (SEPA 2011). In 2010 and 2012 the Coal Authority were commissioned to undertake two studies to determine the sources of pollution and identify any 'blow-out' risks associated with a blocked mine drainage adit. Due to the restriction in timescales and expenditure, the Coal Authority implemented a dynamic and adaptable approach to assess these study areas. This paper outlines the methodology used for these studies, and highlights a number of the key risks and findings identified from the investigations.

Methodology of assessments

Methodologies employed for undertaking a study investigating the sources of pollution are typically based on a fixed monitoring and sampling regime, over a minimum time period of one year; with sample locations usually determined through a 'desk-top' study and 'walk-over' survey. However, for the studies described in this paper, the time-scales were limited to 5 and 11 months, and included a strict sampling budget. In order to obtain instructive results and provide sufficient data for an informative assessment to be made, the Coal Authority had to adapt and use an alternative strategy.

The first stage of each study followed the typical approach, where a desk-top study of each area was undertaken to identify the extent of the mining area, the mining zones, any potential point sources (*i.e.* mine adits) and sites of diffuse pollution (*i.e.* ore processing areas; see Fig. 1), in conjunction with a review of any relevant studies and reports. The desk-studies were subsequently followed by a walk-over survey of the study areas. The walk-over survey assists with the assessment of any point sources identified in the desk-top study, in addition to providing valuable information relating to the nature of the possible sources of contamination, and highlighting possible pollution pathways to the principal receptors (*e.g.* freshwater streams and rivers). Furthermore, the walk-over survey also identifies other features, which may benefit the study such as extra potential monitoring points (see Fig. 1) in addition to detecting other unforeseen risks (*i.e.* blowouts). The walk-over is restricted to a single ‘one-off’ visit to the study area, and any observations made during the inspection, combined with the climatic conditions on the day, can have an influence on all subsequent visits and assessments. As the two studies commissioned by SEPA were constrained by both time and expenditure, it was determined that a more adaptable approach was required to fully assess the study areas.

Leadhills (Glengonnar Water) Study This study had a restricted time-scale of 5 months, which is usually regarded as insufficient to undertake a complete study, as the full extent of any seasonal variations are not represented in the reporting period. However, some historical data for the area were available, which combined with the 5 month study, allowed an assessment of the pollution sources and some blowout risks to be determined. The key concerns addressed by the study included determining the extent of the environmental pollution of lead (Pb), zinc (Zn) and cadmium (Cd; *i.e.* SEPA 2011) and their sources, combined with an appraisal of the risk of a sudden outburst (blowout) of mine water from the blocked Gripps Drainage Level (Fig. 2; Schmolke 1998, Coal Authority 2011). The initial desk-top study and walk-over survey identified 12 key monitoring points along the Glengonnar Water, which defined the point sources of pollution (Fig. 3), in addition to locating three shafts, which would allow the level of the water in the mine workings and the pressure acting on the blockage to be determined. For the duration of the study, a continual assessment of the data and observations obtained in the field resulted in an additional 15 sites being identified and tested (Fig. 2). These included an overflow pipe relating to the Horse Level Adit, a number of seepages from the base of two air shafts along the Gripps level, a number of ‘springs’, which on site testing suggested may

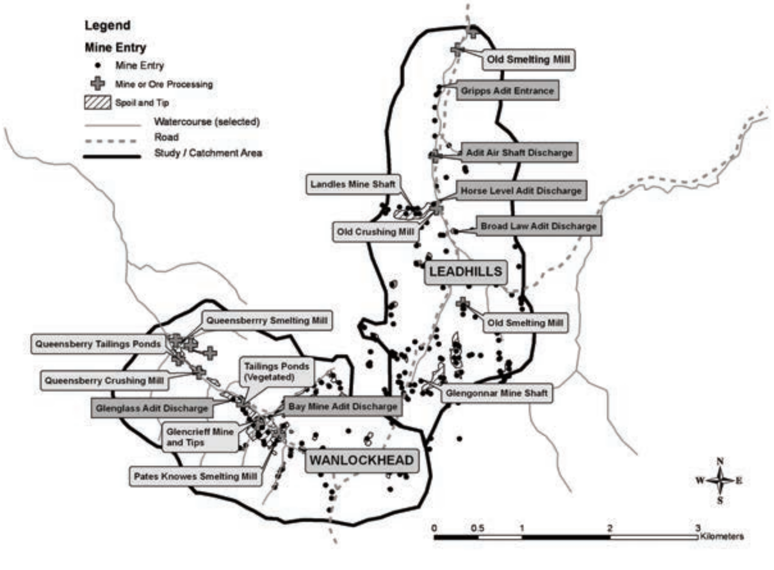

Fig. 1 *Map of the main mining features for both study areas.*

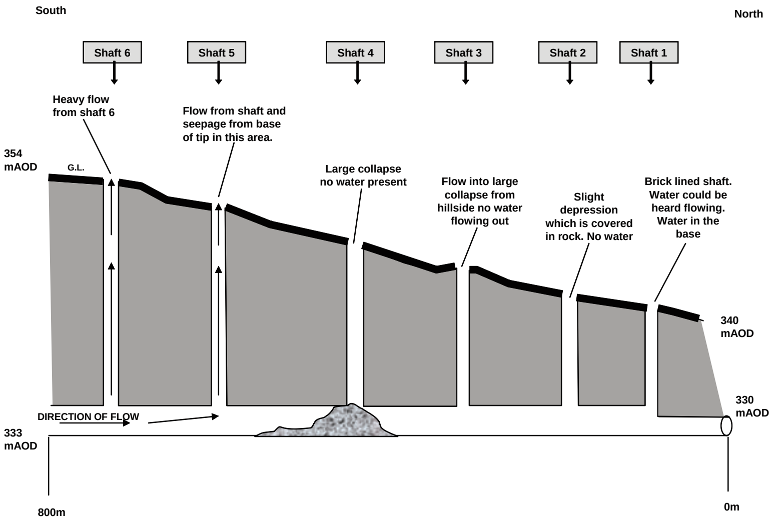

Fig. 2 *Diagrammatic section of the Gripps Drainage Adit and blockage.*

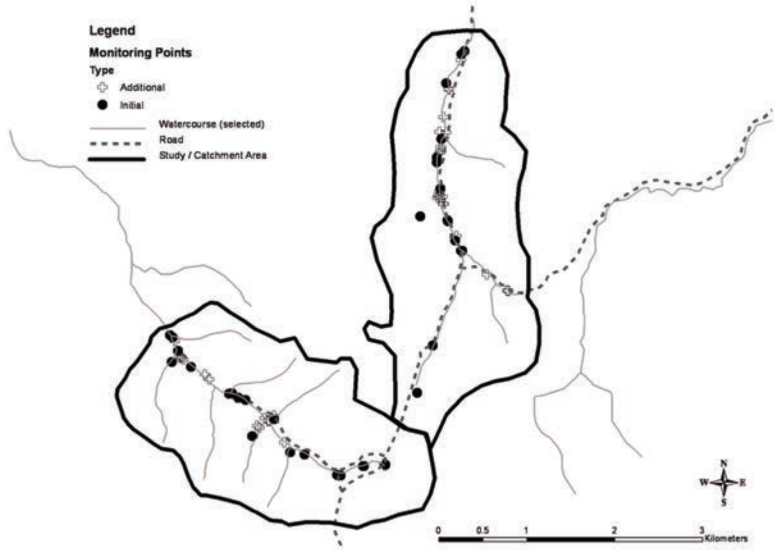

Fig. 3 *Map of the initial and additional monitoring points for both study areas.*

be mine water, and a selection of specific sampling sites, which related directly to the specific weather conditions (*i.e.* high rainfall) on the day of the visit.

Wanlockhead (Wanlock Water) Study This study had a limited time-scale period of 11 months to undertake a complete study of the Wanlock Water and assess the sources of the environmental pollution caused by Pb, Zn and Cd (SEPA 2011). The initial desk-top study and walk-over survey initially identified 22 individual monitoring sites along the Wanlock Water (Fig. 1), which included two mine adit discharges, two possible mine adit discharges, and numerous locations to assess the impact from diffuse sources. With a continual assessment of the new data and observations made, combined with conditions relating to the changeable weather conditions, a total of 25 additional sites (Fig. 3) were also identified. These included for example, ephemeral or intermittent streams, springs and seepages from the tips and ore processing material.

Throughout both studies the general strategy employed was to identify the key monitoring locations, which were sampled throughout the duration of the study. These included upstream and downstream river samples of the study area; upstream and downstream of the known point sources; and upstream and downstream of any large areas of potential diffuse, and possible point, sources. Weather conditions varied considerably between each visit, therefore instantaneous assessments were made on site to determine any additional sampling requirements, for example transient runoff from tailings ponds or intermittently flowing adit discharges. Throughout both of these studies, extra sampling was also used to assess any new water sources found post the initial walkover survey.

Upon receipt of the results from the laboratory after each visit, the sampling requirements for future site visits were re-appraised to ensure that any previously unknown sources of contamination were tested for. This ensured that over the 11 month period, sufficient analyses were obtained to allow a representative view of the chemistry of these samples to be acquired. This dynamic approach allowed the sample points identified in the study to be re-classified so that sites could be either removed, or added to the programme as judged necessary. Overall, the fixed sampling points enable the identification of the key pollution sources in the study area. Furthermore, comparisons of the ad-hoc samples can also be made against these fixed sites where necessary, to elucidate the possible effects of any temporal sources of contamination. Both the study sites are located in upland areas, where there is typically a high annual precipitation in excess of 1,500 mm/a (Rowen *et al.* 1995) which are likely to vary greatly; throughout the study period, the annual rainfall was approximately 1,750 mm/a.

Changes made to initial sampling

Leadhills (Glengonnar Water) Initially the routine sampling was designed to assess impacts from the known mine water discharges from the Horse Level Adit, the Gripps Drainage Adit and the associated shaft 6 discharge (Fig. 2). Prior to the study, it was believed these mine water discharges were the main contributors to the elevated concentrations of Pb, Zn and Cd determined in the river. After studying the first set of results from the river water and adit discharges, it became evident that the mine water discharges were not the main source of Pb and Cd contaminants (*i.e.* concentrations of these metals were low in the mine water). During the first visit, and subsequent visits, it was concluded there was no, or very little flow, in the Glengonnar Water at its confluence with the Dead Burn tributary, therefore, one of the intermediate sample points was removed from the programme. In addition to this, two ephemeral mine water sources were found (Coal Authority 2011); one source originated from an overflow pipe associated with the Horse Level Adit, the other source is a low flow, high concentration discharge from the Broad Law Adit. In wet weather conditions seepages and upwellings were observed to occur from the base of air shaft mounds 4 and 5, and water was also seen emerging from a tension crack along the top of the Gripps Drainage Adit (Coal Authority 2011). With low Pb and Cd concentrations in the mine water, an increased effort was made to determine the source(s) of the Pb pollution. This was achieved by undertaking soil/sediment samples of the flood plain and surrounding area, in conjunction with additional water samples from the Glengonnar Water, to aid with identifying the primary sources. It was concluded that the principal source of the Pb and Cd was from the alluvial floodplain material (*i.e.* up to 10 % Pb wt/wt; Coal Authority 2011) which contained sediment from historical mining and ore processing waste in the form of particulate lead.

Wanlockhead (Wanlock Water) This study began with a programme to assess the impacts from the known mine water discharges from the Glenglass Adit, Bay Mine Adit and two unnamed adits upstream of the mining museum in Wanlockhead. Prior to the study, the source of the Pb, Zn and Cd were uncertain but were believed to originate from the mine water and possibly other "unknown" sources. Following the initial three sampling visits it was concluded that the two unnamed adit discharges were predominantly "clean" water with little, or no, detectable Pb, Zn or Cd concentrations (Coal Authority 2013); these samples were therefore removed from the routine sampling programme. Furthermore, after reviewing the initial set of results it was evident there was also very little, or no Pb, Zn or Cd contamination entering into the Wanlock Water upstream of Straitsteps Mine (Coal Authority 2013). It should also be noted that the Wanlock Water is a losing stream between Straitsteps Mine and the Bay Mine Adit discharge (and probable resurgence) and is often dry before reaching Bay Mine Adit. In a similar scenario to Leadhills, it was found that the Pb and Cd pollution does not originate primarily from the mine water (Coal Authority 2013) but from an alternative source. Assessment of the river water samples showed a stepped increase in the river concentrations of Pb and Cd downstream of Glencrieff Mine and the final downstream sample. Water flows originating from an old crushing mill and un-vegetated tailings pond associated with Queensberry Smelting Mill (Fig. 4), first observed after 3 months of monitoring, were scheduled for additional, regular monitoring in order to determine whether these areas were the principal sources of the pollution. Although the seepages and flows from these ore processing areas are small, they contain elevated concentrations of Pb, Zn and Cd (Coal Authority 2013) when compared to the mine water discharges (*i.e.* a factor of 5 to 10 times greater).

Conclusions

Although the time-scales and budgets for undertaking idealised sampling programmes were restricted, the Authority were successfully able to identify and provide an estimate of the contaminant loadings of Pb, Zn and Cd affecting both the Glengonnar Water and Wanlock Water as required by SEPA. The process of using a set number of fixed routine sample points combined with ad-hoc or flexible sampling points can be used to determine and target metal contamination in a relatively limited timeframe. However, this process requires a continual and comprehensive assessment of the entire study area, only achieved by making detailed observations at each locality and checking the whole area on each visit for any

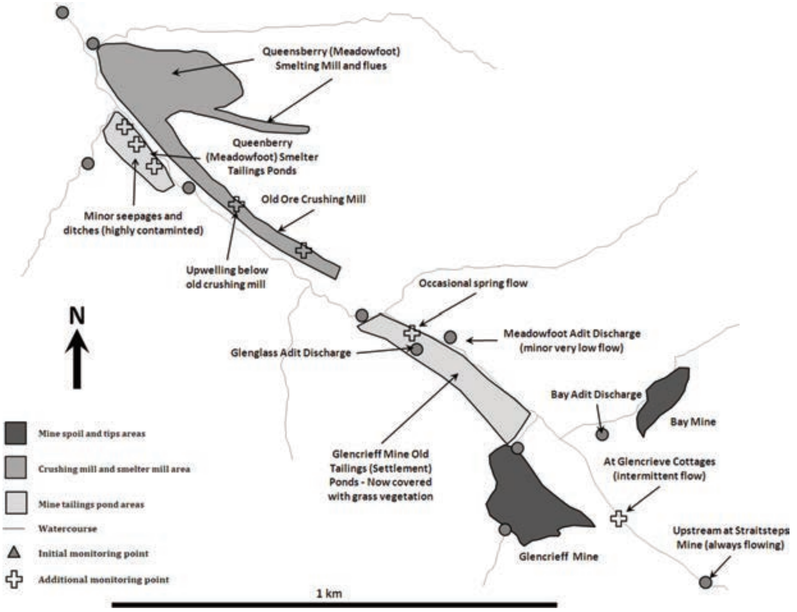

Fig. 4 *Diagrammatic plan of part of the Wanlock Water study area.*

changes. For this reason it is important the samples are collected by a small pool of individuals who are very familiar with the site. Some approximate estimates can be made using the limited data, (if it is assumed the study is undertaken during a typical 'normal' year for rainfall) to give an idea of the sizing criteria required to remediate any pollution. It also allows for a programme of more detailed future works and strategies to be undertaken whilst still gathering key parameters such as chemistry and flow data. However, due to limited time-scales and, in particular, the limited number spot flow measurements, this method should be used with care, especially if attempting to undertake a more detailed design and sizing investigation for any remedial works. Despite this limitation however, on occasions when prompt remediative measures are required this type of sampling methodology can provide invaluable information in a reasonably short timeframe.

Acknowledgements

The authors thank Integrated Water Services for their assistance with the sampling at Wanlockhead.

References

Coal Authority (2011) The impacts of mining on the Glengonnar Water Leadhills South Lanarkshire, Scoping Study, 116 pp. Prepared for SEPA. SEPA Restoration Fund project number RF006-012

Coal Authority (2013) The impacts of mining on the Wanlock Water Wanlockhead Dumfries & Galloway Scoping Study, In preparation. SEPA Restoration Fund project number RF007-010

Rowan JS, Barnes SJA, Hetherington SL, Lambert B (1995) Geomorphology and pollution: the environmental impacts of lead mining Leadhills Scotland, Journal of Geochemical Exploration 52: 57–65

Schmolke CMP (1998) Leadhills, Scotland – Flood and pollution threat from disused lead workings. In: Fox HR, Moore HM, McIntosh AD (Eds) Land Reclamation: Achieving Sustainable Benefits, Balkema, Rotterdam, p 517–523

SEPA (2011) Review of metal concentrations data held for Glengonnar Water and Wanlock Water, South Central Scotland

A holistic approach towards best management practices of mine pollution impacts using a catchment area strategy, South Africa

Bisrat Yibas[1], Robert Netshitungulwana[2], Obed Novhe[3], Haile Mengistu[4],
Emmanuel Sakala[5], Abraham Thomas[6], Peter Nyabeze[7]

Council for Geoscience, 280 Pretoria Rd, Silverton, 0184, South Africa
[1] byibas@geoscience.org.za, [2] robertn@geoscience.org.za, [3] onovhe@geoscience.org.za,
[4]hmengistu@geoscience.org.za, [5]esakala@geoscience.org.za, [6]athomas@geoscience.org.za,
[7]pnyabeze@geoscience.org.za

Abstract Historical and current gold, coal, Pt-Ni, and other mining activities severely affected the scarce water resources of South Africa. A multidisciplinary project is underway on a catchment area scale to assess mine impacts and delineate pollution hotspots. Subsequently nineteen "pollution influence areas" are delineated in the Olifants River Catchment Area. A catchment pollution atlas is then generated for ease of proper rehabilitation/remediation planning. This study proved catchment-scale multidisciplinary investigation is useful in identifying pollution sources faster and cheaper than conventional mine area approach especially for large catchments where mining are widespread, heterogeneous and of many decades of mine history.

Keywords Olifants River Catchment Area, mine pollution, pollution hotspot, pollution influence area, pollution atlas.

Introduction

In South Africa, mining pollution has historically been a major source of degradation of natural resource systems such as surface and groundwater resources and land use. Unfortunately, the current information on mining externalities is insufficient to be useful for policy setting. Extensive and systematic studies should be undertaken to fill this information gap, particularly in the development of policy instruments, which require information on social costs of mining, and partly to assist in the formulation of guidelines on damage assessment and compensation for the mining sector.

There is a need to nationally co-ordinate research, development, and application of AMD assessment and remediation techniques. In this regard, the Environmental Geosciences Unit (EGU) of the Council for Geoscience (CGS) has embarked upon a project focusing on a national holistic strategy for rehabilitation and remediation of environmental impacts and critical pollution problems from the mining industry affecting the environment and ecosystem with a particular focus on the scarce water resources.

The impact assessment component of the project began on catchment-based approach. Two major river catchment areas, the Olifants and the Komati-Crocodile, which are known to be severely affected by historical and current mining activities, have been investigated to date. The results of the investigation in the Olifants River Catchment Area (ORCA) are the subject of this paper.

The ORCA is one of the major river basins in South Africa constituting roughly 87,000 km^2 area, 85 % of which is within the South African territory and the rest in Mozambique (Ashton *et al.* 2001). It has nine secondary, 90 tertiary and 145 quaternary catchments (Fig. 1).

The Olifants River has a relatively dense network of tributary rivers and streams though most of the tributaries in the lower reaches of the catchment only have either sea-

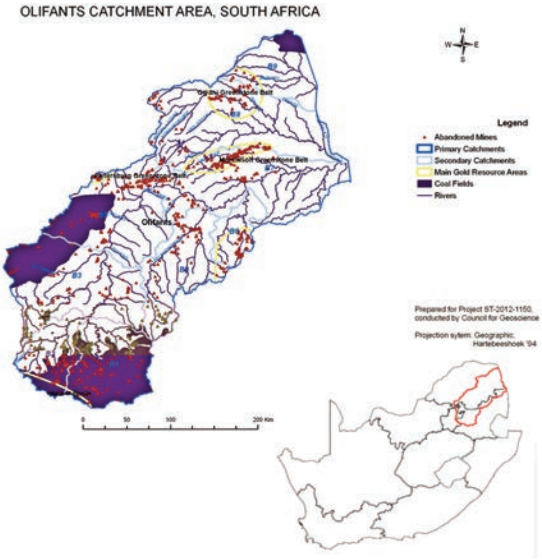

Fig. 1 *The Olifants River Catchment Area with its historical and active mines; in set -location of the catchment area within South Africa.*

sonal or episodic flows. The Olifants River flows north up to the middle portion of the catchment and makes a sharp turn towards east until it leaves the South African territory.

The geology of ORCA is part of the eastern lobe of the Kalahari Craton, which comprises predominantly crystalline granitic and gneissic rocks, intruded by various greenstone belts, dolerite dykes and sills. Silicified sedimentary formations also form part of the Archaean Craton. Karoo System rocks overlie large areas of the southwestern portion of the basin and these are associated with younger sedimentary and crystalline rocks consisting predominantly of sandstones, carbon-rich mudstone, and conglomerate and shale units. Recent sedimentary deposits line most of the river valleys and provide important farming areas (Netshitungulwana and Yibas 2012a).

The Olifants River Catchment Area hosts significant number of metallogenic (geo-environmental) provinces namely, the Archaean Greenstone Belts, the Bushveld Complex and the Witbank Coalfield, among others, which host a number of major goldfields, platinum-chromium and other PGE metal mines, coalmines, and mines of other mineral commodities such as copper and heavy minerals (Fig. 1).

Approach and Methodology

A multidisciplinary project which includes remote sensing & GIS, hydrology & water quality, hydrogeology, geochemistry, acid mine drainage assessment, ecotoxicology and geophysics, have been applied to assess the qualitative and quantitative impacts of extensive mining activities mainly on the water resources of the Olifants River Catchment Area.

A catchment scale geochemical study of stream water underlying sediments was conducted to determine their metal and anion loadings and for their current and potential AMD as well as to understand the sediment-water geochemical interaction.

Assessment of current and potential AMD from active and inactive mine infrastructures such as mine residue deposits, open pits and underground workings, have been carried out.

Hydrogeological studies including evaluation of existing data, delineation of major aquifers and qualitative characterization of surface and borehole water in and around the mine areas were undertaken based on existing information and newly acquired hydro census data. The data then was integrated and preliminary assessment of human induced flow patterns due to pumping as well as injection (if any) was done.

A catchment-scale hydrological simulation was performed to estimate runoff and infiltration.

Ground based electromagnetic and electrical geophysical methods namely frequency domain electromagnetic (FDEM) and electrode resistivity tomography (ERT), were used for mapping the depth and lateral extent of subsurface pollution plumes in areas where subsurface plumes were suspected. Geological structures were delineated using the magnetic method. In the northeastern part of the study area, geophysical surveys were carried out along the peripheral zones of mine locations.

Results and Discussions

Geochemistry

About 119 stream water and similar number of stream sediment samples were collected from systematically distributed positions in the various streams within the Olifants River Catchment Area. These samples were then analysed to assess the concentration, migration and dispersion of potentially toxic metals and anions using XRF, ICP-MS and IC methods. The sediment samples were also subjected to acid base accounting (ABA) test for current and potential AMD. Leachates have also been extracted from the sediment samples using standard water extraction technique and analysed using ICP-MS and IC methods.

On the basis of the interpretation of the geochemical data 19 pollution hotspots have been delineated throughout the ORCA in terms of metal signatures and their current and potential AMD. These hotspots drains largely on various mining areas such as the Witbank coalfield mines, the greenstone hosted gold mines such as the Sabie and Pilgrim's Rest area, the Sn and Cu mines of the Rooiberg Felsites, the copper deposit in the Phalaborwa Carbonatite Complex and small scale heavy mineral mines (Netshitungulwana and Yibas 2012a, 2012b). This study enables fingerprinting of sources of contaminants and therefore mining impact on the geochemistry of the stream water and sediment.

Acid Mine Drainage (AMD)

The main objective of the AMD assessment task is to characterize the quality and quantity of mine water drainage from operational and non-operational mine infrastructures such as surface or underground mines, mine residues deposits; and also determine the potential of the mine infrastructures to generate AMD in the future.

Fieldwork which involved site characterisation and sampling was conducted in the Olifant River Catchment Area. The fieldwork covered the mining areas of Giyani and Murchison greenstone belts, Pilgrim Rest Goldfield, eastern Limb of the Bushveld Complex, and the Witbank Coalfield (Novhe *et al.* 2013).

The gold mineralisation in Giyani Greenstone Belt is associated with quartz veins, with minor suphides, asscoaited with banded iron foramtions (BIF), and carbonate veins. Most of the gold mines are left with abandoned and unrehbilatated mine tailings deposits, open pits and shafts. Owing to the climate of the area most of the mine residue deposits are dry although the high percentage of sulphur (0.3 – 2.5 %) indicates acid generating potential of the tailings deposits. This was cofirmed during a follow up visit immediately after heavy rain, which revealed that the run-off water from one of the deposits (Osprey Gold Mine) was acidic.

The majority of antimony and gold mines of the Murchison Greenstone Belt are abandoned and only few are still operational. Large part of the inactive mine residue deposits do not show any seepage which could be attributed to the dry climate and weather of the area. However, the sulphur content ranges from 0.05 to 4 %, averaging at 0.9 % and leachates extracted from the samples yield low pH (>4) and high conductivity (> 400 mS/m). Sb, Fe, Al, Mn, Cr, As, and Co have been identified as potential pollutants.

Gold mineralisation in the Pilgrim's Rest Goldfield principally occurs within the Malmani dolomite of the Transvaal sediments. Onsite analyses of leachates from the active mine residues and return water dam showed near neutral (pH ≈ 7) which could be atributed to the buffering capacity of the carbonate host rocks. The sulphur percentage (2.6 – 18 %, averaging at 9 %) indicates, however, acid generating potential.

In the Eastern part of the Bushveld Complex, most of the mines exploit platinum and chrome from the Merensky Reef and the UG2 layer, respectively. During the the field investigation most of the mine residue deposits shows seepages of alkaline drainage with pH of 8 or higher. ABA test conducted on the collected samples indicated no potential to generate AMD. This is also evident from the very low sulphur content (0.02 – 0.04 %, averaging at 0.03 %) of the samples.

The Witbank Coalfield, situated in the southern part of the Olifant Catchment, is one of the major coal mining areas in South Africa. Coal is extracted by means of both open cast and underground mining method from depths of a few meters to about 300 metres. Both abandoned and operational mines dischrage acid mine drainage (AMD) in various forms. In some cases AMD discharges directly into the streams. Generally, the AMD in the Witbank Coalfield is characterised by low pH (<3) and high concentration of metals (Fe, Al, Mn) and sulphate and TDS. The sulphur content ranges from 0.4 to 7 %, averaging at 2.7 %, pyrite as the major sulphide mineral. Acid base accounting (ABA) tests indicate high acid generating potential (AP) and low neutralization potential (NP). Leachates extracted from the samples indicate Fe, Al, Mn, Cr, and As as potential pollutants (Novhe *et al.* 2013).

The AMD assessment summarised above is used to delineate AMD hotspots in the Olifants River catchment area. The AMD hotspots identified tied well with and corroborated the pollution hotspots identified from surface water and stream sediment geochemistry.

Hydrogeology

Preliminary hydrogeological assessment was conducted in the Murchison, Giyani and Pilgrim's Rest greenstone gold mines, in the Burgersport platinum (and chromium) mines in the eastern part of the Bushveld Complex, and in the Phalaborwa Carbonatite copper and phosphate mine area.

Groundwater samples collected from mines monitoring boreholes and from farm boreholes as well as surface water samples from within and around the mining areas, showed elevated cocentrations of certain species such as NO_3, As, Fe, Al, Mn, and rarely Cu, SO_4, Cl, F, albeit variably, in the different mines of the catchment. Aresenic (As) is the most common contaminant cation exceeding both drinking water as well as SANS (South African National Standard) limits in the five out of the six mine areas investigated. Al, Fe and Mn each showed elevated concentrations in three out of the six mine areas. The most common anion contaminants are NO_3 and Cl, each of which show elevated concentration in three out of the six mine areas. SO_4, F and Cl show elevated concentrations in the three separate mine areas co-elevated only in one.

The pollution hotspots identified using the hydrogeological investigation in the six mining areas in the Olifants River Catchment Area are well in agreement with the pollution hotspots delineated using the stream water and sediment geochemistry as well as from AMD potential assessment studies.

Ground Geophysical Survey

The depth and lateral extents of contaminant plumes were mapped in the southern and northern parts of the catchment using geophysical techniques that comprised Frequency Domain Electromagnetic (FDEM) and electrical resistivity tomography (ERT). Contaminant pathways associated with high electrical conductivity values were delineated at some mining locations in the northeastern part of the study area (Nyabeze *et al.* 2012). The results confirmed the existence of near surface high electrical conductivity zones that were interpreted as shallow AMD plumes. Dykes, faults and geological contacts were delineated from magnetic profile data. The use of geophysical techniques proved to be an effective tool for mapping out contaminant plumes specifically in the Barberton, Giyani and Witbank areas.

Hydrology

Catchment-scale annual and single event runoff depth and infiltration distribution were simulated for the Olifants River Catchment Area using the GIS based RINSPE (Runoff, Infiltration and Non-point Source Pollution Estimation) model (Thomas *et al.* 2010). The total annual rainfall volume received in the catch-

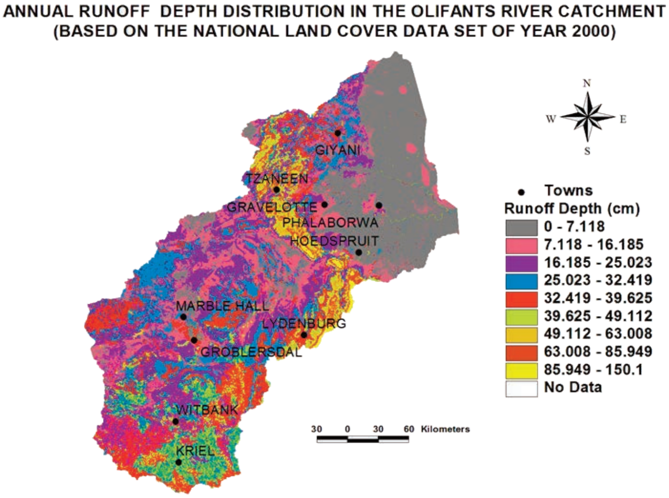

***Fig. 2** Annual runoff simulation results for the Olifants Catchment.*

ment is 44.6 Gm³. The total volume of cumulative infiltration in a year is 6.4 Gm³ (14.46 % of the rainfall volume whereas the total annual volume of surface runoff (direct runoff) is 16.6 Gm³ (37.2 % of the rainfall volume). The runoff modeling result (Fig. 2) showed that high annual runoff depths characterize the Greenstone Goldfield mine areas in the central part of the catchment (near Tzaneen) and the Witbank Coalfield area in the south. This indicates the contribution of polluted runoff from these areas of intense past and current mining activities towards downstream of the catchment is high (Fig. 2). The Kruger National Park area has the lowest runoff (0 – 7.118 cm) whereas the area around Tzaneen has maximum runoff (85.949 – 150.1 cm).

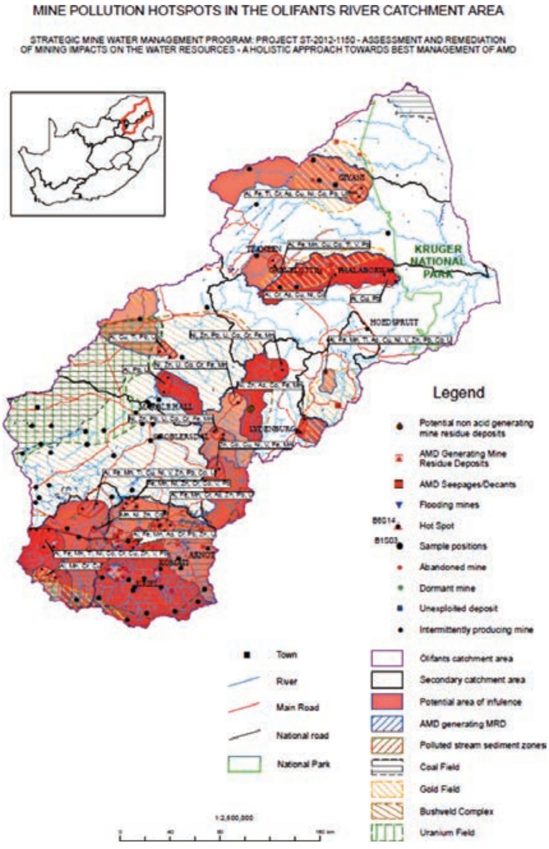

***Fig. 3** Pollution atlas of the Olifants Catchment area generated based on multidisciplinary pollution characterization.*

Summary and Conclusions

Catchment Pollution Atlas

Mine pollution atlas map has been prepared for the Olifants River Catchment Area after integrating the findings of: a) catchment-scale stream water and sediment geochemistry, b) catchment-scale hydrological study for runoff and infiltration estimation; c) mine area-scale investigations of hydrogeology, current and potential AMD assessment, and ground geophysical surveys for shallow subsurface plumes. The atlas (Fig. 3) shows in addition to the polluted areas, pollution sources and the pollution pathways, together forming what is herein termed as "mine pollution influence areas". Nineteen such pollution influence areas are delineated. Eight of the 19 pollution influence areas are within the Witbank Coalfield confirming the severity of mining pollution in the coalfield. The eight pollution influence areas could be integrated into two major pollution areas.

Conclusion

This study shows that catchment-scale mine pollution study using a multi-disciplinary approach with the understanding of geo-environmental provinces proved powerful and meaningful than focusing on a number of separate localized mine-scale studies.

Such catchment-scale investigation provides a holistic understanding of mine pollution from pollution source to pathways to receiving environment (source-pathways-recipient dynamics) – herein termed as "mine pollution influence areas". Nineteen such pollution influence areas have been delineated. Eight of the 19 pollution influence areas are within the Witbank coalfield confirming the severity of mining pollution in the coalfield.

The multi-disciplinary approach also proved effective in providing multiple source of scientific information and integrating such multi-disciplinary scientific data improves the reliability and accuracy of the findings. The study provides a powerful management tool for the remediation and rehabilitation of pollution influence areas, which encompasses the source, the pathways and the receiving areas of pollution. This is particularly relevant in mining countries such as South Africa where the legacies of over a century of mining activities affected not only mining areas but also areas of tens of square kilometers which crosses catchment boundaries.

Acknowledgements

The authors thank the Department of Mineral Resources of South Africa for funding the project. We would also like to thank all CGS colleagues and project team members involved in field activities, sample preparation and analysis. The authors also acknowledge the assistance of Harold Weepener of the Institute for Climate and Water of ARC for providing various spatial (*e.g.* annual rainfall, National Land Cover (NLC) 2000, SRTM elevation) and Daniel Sebake and Dirk Grobbelaar of CGS for providing GIS services. Lastly yet importantly, the authors thank an anonymous reviewer whose critical comment on the first version of the manuscript prompted us to improve the write-up.

References

Ashton P, Love D, Mahachi H, Dirks P (2001) An overview of the impact of mining and mineral processing operations on water resources and water quality in the Zambezi, Limpopo and Olifants catchments in southern Africa, Contract Report to the Mining, Minerals and Sustainable Development (SOUTHERN AFRICA) Project, by CSIREnvironmentek, Pretoria, South Africa and Geology Department, University of Zimbabwe, Harare, Zimbabwe. Report No. ENV-P-C 2001–042. xvi + 336 pp

Netshitungulwana R and Yibas B (2012a) Investigations of the stream sediments geochemistry for the metal pollution sources of the Olifants River Catchment, Technical Report, Council for Geoscience, unpublished report, pp87.

Netshitungulwana R and Yibas B (2012b) Stream sediment geochemistry of the Olifants catchment, South Africa: Implication for acid mine drainage. In: McCullough CD, Lund MA, Wyse L, 2012 International Mine Water Association Symposium, Bunbury, Western Australia, 257–264

Novhe NO, Netshitungulwana R, Yibas B, Motlakeng, T, Sakala E (2013), Metal pollution sources and transport in mined watershed: an insight from Ermelo Coalfield, South Africa (IMWA 2013, this volume).

Nyabeze P. K., Yibas B. and Sakala E. (2012). Conference Paper: Investigation of contaminant plumes emanating from residual mine deposits in the Limpopo Province of South Africa, results from geophysical surveys. GeoManitoba 2012 Conference, Manitoba, Canada.

Thomas, A., Chingombe, W., Ayuk, J. and Scheepers, T. 2010. 'A Comprehensive Investigation of the Kuils-Eerste River Catchments Water Pollution and Development of a Catchment Sustainability Plan'. Water Research Commission (WRC) Report No. 1692/1/10. ISBN 978-1-4312-0016-0. September 2010.

RELIABLE MINED HYDROCARBON WATER

RELIABLE MINED HYDROCARBON WATER

7

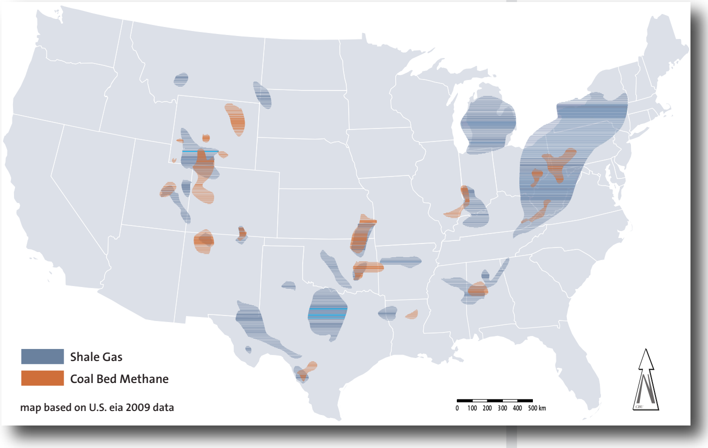

Low Salinity Hydrocarbon Water Disposal Through Deep Subsurface Drip Irrigation: Leaching of Native Selenium

Carleton R. Bern[1], Mark A. Engle[2,3], Adam R. Boehlke[4], John W. Zupancic[5]

[1]*U.S. Geological Survey, Denver Federal Center, Denver, Colorado, USA, cbern@usgs.gov*
[2]*U.S. Geological Survey, 12201 Sunrise Valley Drive, Reston, Virginia, 20191, USA, engle@usgs.gov*
[3]*University of Texas at El Paso, Dept. Geological Sciences, El Paso, Texas, 79968, USA*
[4]*U.S. Geological Survey, Denver Federal Center, Denver, Colorado, USA, aboehlke@usgs.gov*
[5]*BeneTerra LLC., 1415 N. Main Street, Sheridan, Wyoming, 82801, johnz@beneterra.com*

Abstract A subsurface drip irrigation system is being used in Wyoming's Powder River Basin that treats high sodium, low salinity, coal bed methane (CBM) produced water with sulfuric acid and injects it into cropped fields at a depth of 0.92 m. Dissolution of native gypsum releases calcium that combats soil degradation that would otherwise result from high sodium water. Native selenium is leached from soil by application of the CBM water and traces native salt mobilization to groundwater. Resulting selenium concentrations in groundwater at this alluvial site were generally low (0.5–23 µg/L) compared to Wyoming's agricultural use suitability standard (20 µg/L).

Keywords coal bed methane, coal bed natural gas, produced water, sodium adsorption ratio

Introduction

Coal bed methane (CBM) is rapidly expanding worldwide as a source of energy. Production is achieved by drilling into a flooded, subsurface coal bed, pumping out water, and collecting the natural gas liberated as a result of reduced pressure in the bed. Volumes of co-produced water are largest during early development. CBM generates greater volumes of water per volume of gas compared to other natural gas resources. In 2011, 7.8 × 10^7 m^3 of water were produced in the Wyoming portion of the Powder River Basin (PRB; Wyoming Oil and Gas Conservation Commission 2012). As a result, management and disposal of produced water is an important challenge for developing CBM resources.

Waters produced with CBM in the PRB generally have $Na\text{-}HCO_3$ compositions. The waters have low to moderate salinity in the form of total dissolved solids (TDS 200–4000 mg/L), but often have relatively high sodium adsorption ratios (SAR 5.6–69). The SAR of a water or soil extract can be calculated according to equation 1 with $mmol^{1/2}\,L^{1/2}$ as the resulting units, although common convention in reporting data is to omit them.

$$\mathrm{SAR}=\frac{[\mathrm{Na}^{+}]}{\sqrt{\left([\mathrm{Ca}^{2+}]+[\mathrm{Mg}^{2+}]\right)}} \qquad (1)$$

Waters with low salinity and high SAR can damage soil by dispersing clay particles, which results in breakdown of soil structure, crusting, and decreased infiltration and permeability (fig. 1). Such problems can be particularly severe for soils containing high percentages of expansive clays; such soils are common in the PRB. Interactions of SAR, salinity, and soil properties make thresholds for soil damage difficult to define, but significant problems are generally expected to occur with SAR >15.

Disposal of CBM waters in the PRB is most commonly achieved by placing them in unlined impoundments to evaporate and infiltrate into the subsurface. One issue with such impoundments is that the infiltrating waters can mobilize native salts, including Se-bearing salts, and negatively impact groundwater quality (Healy *et al.* 2011). Selenium mobilization

Fig. 1 *Photograph on the left shows the physical effects of raw CBM produced water on soil. To the left of the felt tipped marker is unaffected soil and to the right is soil on which CBM produced water was spilled. Photograph on the right shows an aerial view of the Headgate SDI site. Bare patches in fields are herbicide carryover from landowner treatment of noxious weeds prior to SDI installation.*

can be a particular concern because when it reaches the surface environment in sufficient concentrations the resulting bioaccumulation negatively impacts wildlife health (Skorupa 1998).

A desire to derive beneficial use from CBM waters while simultaneously disposing of them spurred the development of the deep subsurface drip irrigation (SDI) method studied here (Zupancic *et al.* 2008). By this method, CBM water is allowed to oxidize, degas and settle out in a surge pond, then acidified with H_2SO_4, and applied year-round to agricultural land through drip-tubing buried 0.92 m deep. Oxidation results in the loss of redox sensitive elements (*e.g.* Fe and As) while degassing increases pH through CO_2 loss. Acidification with H_2SO_4 removes alkalinity and thus combats the precipitation of calcite in soil which would otherwise result from irrigating with a $Na\text{-}HCO_3$ type water. Losses of Ca^{2+} to calcite precipitation can drive SAR values in soil solution higher, exacerbating problems with clay dispersion. Installation of the drip tubing at 0.92 m helps retard the rise of SDI solutes to the soil surface and prevents frost damage during year-round operation. However, such deep placement necessitates that the crop planted in the fields be a deep-rooted perennial like alfalfa or grass.

Several studies have examined different aspects of these SDI systems in the PRB (Bern *et al.* 2013a, Bern *et al.* 2013b, Bern *et al.* accepted, Engle *et al.* 2011, Engle *et al.* submitted). Here we assess mobilization of native selenium from soil beneath fields at a site irrigated by the SDI system described above.

Site description and SDI operation

The Headgate Draw SDI site (fig. 1) is located in Johnson County, Wyoming, and was constructed on a series of alluvial terraces at the confluence of Crazy Woman Creek and the Powder River (Engle *et al.* 2011). Installation of the SDI system was completed in October 2008 and fields were planted with alfalfa. High density polyethylene tubing for water application was buried at the 0.92-m depth and spaced 1.4 m apart, with pressure compensating emitters located every 0.92 m along the tubing. A total of 81 ha were covered by the SDI system. Produced water was pumped to a surge pond at the site from dozens of CBM wells. Acidification of CBM water was achieved by in-line addition of H_2SO_4, resulting in an injectate pH of ≈ 6.1. Injectate was applied year-round at an average rate of 0.026 m/month in 2008 and 2009, and increased to 0.100 and 0.084 m/month in 2010 and 2011, respectively. Natural precipitation and injectate application combined provided 0.34 m less water than potential evapotranspiration demand in 2009, but 0.56 and 0.45 m more than potential evapotranspiration demand in 2010 and 2011, respectively (Bern *et al.* accepted). Initial depths to groundwater below the fields were 3.2 to 3.8 m.

Soils at the site are generally silt loams and sandy loams, typical for the alluvial terrace setting (Bern *et al.* accepted). Clay mineralogy was dominated by illite and smectite, and both calcite and dolomite were ubiquitous in soil. Although soil contained little gypsum above 1 m depth, gypsum concentrations were often >2 % in deeper soil and ranged up to 6.9 %.

As with other SDI operations of this type, the SAR of surface soil increased little in response to injectate application, but SAR of soil near the depth of the drip tubing increased substantially (Bern *et al.* 2013b, Bern *et al.* accepted). Preventing the increase of SAR at the soil surface is a significant advantage of the described SDI method over surface irrigation methods using similar CBM waters and also allows disposal of greater volumes of water (Johnston *et al.* 2008). With continued injectate application, problems with SAR at and below the soil surface might be predicted (Bern *et al.* 2013b). However, CBM water production from any given set of wells declines with time and the SDI sites are designed to be operated only for several years. As of late 2012, the Headgate Draw SDI system was transitioning to use waters from an adjacent stream.

Methods

Data presented here were collected as part of a larger research and monitoring project (Engle *et al.* 2011). Ceramic tipped suction lysimeters were installed at depths of 0.5, 1.0 and 2 m at three sites (21, 23 and 24) within SDI fields in October 2008. Lysimeter samples were collected four times between May 2009 and March 2011, but not all lysimeters yielded enough water on all dates for all planned analyses. Fourteen groundwater monitoring wells inside and outside the boundaries of the SDI fields were sampled quarterly starting in May 2008. Injectate pumped to the fields was sampled on the same schedule. Sampling methodology, analytical protocols, and QA/QC results for water chemistry are described in Geboy *et al.* (2011). The saturation index for gypsum was calculated using the PHREEQC software. Depth to groundwater was continuously monitored at three wells installed within SDI fields using *in situ* pressure transducers.

Soil cores were collected at three sites (21, 22 and 23) within SDI fields. Cores were collected in October 2008, prior to SDI operation (pre-SDI), and again in October 2011 after three years of operation (post-SDI). Selenium in soil was measured by extraction at 1:1 water soil ratio on selected depth increments. Depth increments were selected to represent the zone with highest pre-SDI salt content based upon extract electrical conductivity. Extracts were filtered to <0.2 µm and selenium was analyzed by hydride generation at the U.S. Geological Survey in Denver.

Results

Injectate had high concentrations of Na compared to Ca and Mg, giving it an average SAR value of 24 (Table 1). Average specific conductance of injectate was 2,550 µS/cm. The combination of high SAR and low specific conductance indicates that the water would cause moderate to severe infiltration problems due to clay dispersion if used for surface irrigation (Ayers and Westcot 1985). The Se content of injectate averaged only 0.6 µg/L, indicating low concentrations in both CBM produced water and the H_2SO_4 used for acidification.

Soil water collected by lysimeter had lower SAR values compared to injectate, with one exception (fig. 2). Generally, soil water SAR varied between 0.5 and 10, indicating a substantial decrease in the risk of clay dispersion once injectate had equilibrated with subsur-

pH	Spec. Cond. (µS/cm)	TDS (mg/L)	Alkalinity† (mg/L)	SAR	Se µg/L
6.1±1.0	2550 ± 500	2200 ± 300	560 ± 470	24 ± 5	0.6 ± 0.2

Na (mg/L)	Ca (mg/L)	Mg (mg/L)	K (mg/L)	Cl^- (mg/L)	SO_4^{2-} (mg/L)
560 ± 81	17 ± 3	15 ± 9	13 ± 2	32 ± 33	790 ± 480

†mg/L as $CaCO_3$

Table 1 *Averages and standard deviations of chemical parameters for injectate water.*

face soil. The gypsum saturation index of injectate varied from -2.7 to -1.5. Saturation indices for soil water were higher and generally varied from -0.9 to 0.3, with many values close to zero.

Groundwater concentrations of SO_4^{2-} varied over a narrow range in most of the 14 individual monitoring wells with no obvious trends (fig. 3). Exceptions were two wells within SDI fields where SO_4^{2-} increased toward the end of the monitoring period, and another located outside that had high values early on that decreased with time. In contrast, Se in groundwater showed distinct trends that were remarkably correlated between wells (fig. 3). Concentrations rose to a first peak in the middle of the 2009 growing season, and then dropped over the winter. Concentrations rose again sharply in early 2010, continued to increase moderately through the growing season, then dropped abruptly by early 2011.

Groundwater levels in monitoring wells within the SDI fields also showed trends with time (fig. 4). Injectate application rates in 2009 produced only moderate rises in groundwater. Substantial increases in injectate application rates in 2010 and 2011 caused groundwater levels to rise more rapidly. Peaks in groundwater levels occurred in early spring of 2010 and 2011, with an intervening decrease that corresponded to the summer growing season.

Concentrations of water-extractable selenium in pre-SDI soil varied from 11 to 557 µg/kg, generally increasing by site in the order 21, 23, 22 (fig. 5). Post-SDI soil showed a much narrower range of concentrations, from 18 to 107 µg/kg and much less differentiation between sites.

Discussion

A crucial geochemical process in the SDI fields is indicated by the combination of gypsum saturation indices closer to zero and lower SAR values in lysimeter water as compared to injectate. Dissolution of native gypsum releases Ca^{2+} and lowers the SAR of injectate as it equilibrates with soil (Bern *et al.* 2013b). By lowering the SAR, and simultaneously raising the salinity, native gypsum dissolution reduces the risk of clay dispersion and associated problems with soil permeability. Acidification of injectate extends the duration of gypsum influence by combating losses of Ca^{2+} to calcite precipitation, and keeps SAR lower if gypsum becomes depleted (Bern *et al.* 2013b).

Injectate application has been shown to increase salinity in two of the three monitoring wells located within SDI fields, despite the fact that the injectate had a lower salinity than the native groundwater (Bern *et al.* accepted). However, trends in SO_4^{2-} in the larger dataset from 14 wells across the site were generally dif-

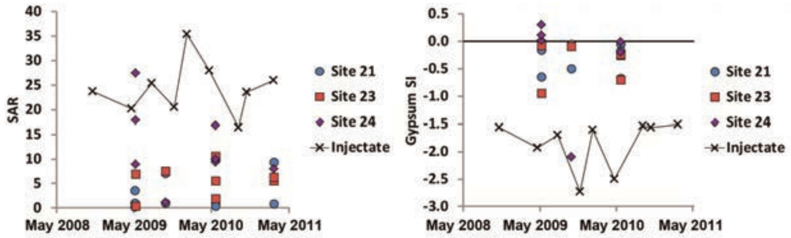

Fig. 2 *Time series of sodium adsorption ratio (SAR) and gypsum saturation index (SI) values for injectate and lysimeter samples.*

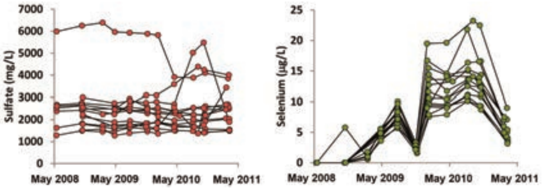

Fig. 3 *Time series of concentrations of sulfate and selenium in the 14 monitoring wells.*

ficult to discern (fig. 3). The same was true for the other major anions Cl^- and HCO_3^- (data not shown). Selenium, by contrast, showed dramatic shifts in concentration with conspicuous correlation in timing across all wells (fig. 3). A substantial decrease in soil concentrations of water-extractable Se between the pre-SDI and post-SDI cores (fig. 5) strongly suggests the SDI fields as the source of increased Se in groundwater.

Timing of the changes in groundwater Se concentrations relative to irrigation rates and groundwater levels can provide some insight into Se mobilization. Redox processes have the potential to confound such interpretations by conversions between soluble selenate (SeO_4^{2-}), selenite (SeO_3^{2-}), and less soluble selenide (Se^{2-}). However, a lack of corresponding changes in SO_4^{2-} (fig. 3), with which SeO_4^{2-} shares redox similarities, allows Se concentration changes to be more confidently attributed to physical mobilization.

Initial increases in groundwater Se (fig. 3) corresponded to the moderate irrigation rates and rise of groundwater in 2009 (fig. 4). The Se peak in August of 2009 was likely generated by injectate leaching Se from soil directly beneath the drip tubing. Lower concentrations in the following winter may have reflected dispersion or dilution of the leached Se. The abrupt increase in groundwater Se in January 2010 correlated with an abrupt increase in injectate application rates. Subsequent moderate increases in Se occurred as groundwater levels first rose and saturated more soil, and then decreased due to crop water usage in the 2010 growing season. The sharp drop in groundwater Se over the 2010–2011 winter corresponded to another sharp rise in groundwater levels, again possibly reflecting dispersion or dilution. That decline, combined with decreased water extractable Se in soil (fig. 5), may indicate little potential for additional Se mobilization.

As was shown by a study of groundwater near a CBM impoundment (Healy *et al.* 2011), Se can trace native solute mobilization in the subsurface of the PRB. In contrast to the impoundment study, which found unusually high Se concentrations in groundwater (>300 µg/L), concentrations at Headgate Draw were rather moderate. Only three samples exceeded Wyoming's 20 µg/L of Se groundwater quality standard for agricultural use, the most sensitive of the state's groundwater selenium standards (Wyoming Department of Environmental Quality 2005). By comparison, all groundwater samples (pre- and post-SDI) exceeded the 200 mg/L agricultural suitability standard for SO_4^{2-} (fig. 3).

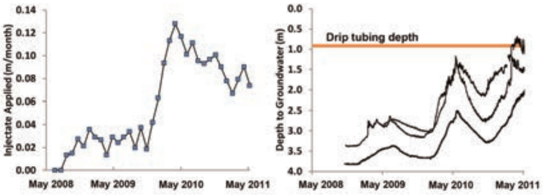

Fig. 4 *Time series of injectate application rates and, for three monitoring wells, depths to groundwater below SDI fields.*

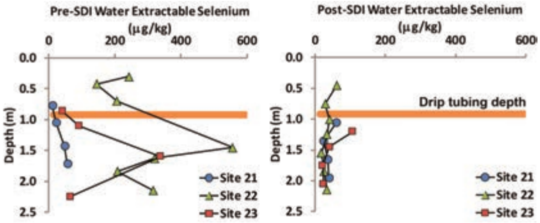

Fig. 5 *Depth profiles of water extractable selenium in SDI field soil before and after irrigation. Yellow line marks the depth of the drip tubing.*

Conclusions

High SAR values in injectate derived from CBM produced water were lowered by dissolution of native gypsum in subsurface soil. Lowering of the SAR values, and increasing electrical conductivity of soil waters, reduced the risk of soil permeability problems. Injectate application mobilized native selenium from the soils in the SDI fields and raised concentrations in groundwater. Selenium appears to be a good tracer for native salt mobilization in the PRB. Even at their peak, selenium concentrations at the Headgate Draw SDI site were generally below Wyoming’s agricultural suitability standard for groundwater.

Acknowledgements

We are grateful for assistance with sampling and analysis from numerous employees of BeneTerra and the U.S. Geological Survey. We also thank Kenneth Knudson for access to the property and Richard Healy for helpful review comments.

References

Ayers RS and Westcot DW (1985) Water Quality for Agriculture: FAO Irrigation and Drainage Paper No. 29 rev. 1. Rome, Food and Agriculture Organization of the United Nations

Bern, C, Breit GN, Healy RW, Zupancic JW (2013a) Deep subsurface drip irrigation using coal-bed sodic water: Part I. Water and solute movement. Agr Water Manage 118: 122–134, doi:10.1016/j.agwat.2012.11.013

Bern, C, Breit GN, Healy RW, Zupancic JW, Hammack R (2013b) Deep subsurface drip irrigation using coal-bed sodic water: Part II. Geochemical processes. Agr Water Manage 118: 135–149, doi: 110.1016/j.agwat.2012.11.014

Bern, CR, Boehlke, AR, Engle MA, Geboy NJ, Schroeder KT, Zupancic JW (accepted) Shallow groundwater and soil chemistry response to three years of subsurface drip irrigation using coalbed methane produced water. Hydrogeol J

Engle MA, Bern CR, Healy RW, Sams JI, Zupancic JW, Schroeder KT (2011) Tracking solutes and water from subsurface drip irrigation of application of coalbed methane produced waters, Powder River Basin, Wyoming. Environ Geosci doi:10.1306/eg.03031111004

Engle MA, Gallo M, Schroeder KT, Geboy NJ, Zupancic JW (submitted) Three-Way Compositional Analysis of Water Quality Monitoring Data. Environmental and Ecological Statistics

Geboy NJ, Engle MA, Schroeder, KT, Zupancic JW (2011) Summary of inorganic compositional data for groundwater, soil-water, and surface-water samples at the Headgate Draw Subsurface Drip Irrigation Site, Johnson County, Wyoming. U.S. Geol Surv Data Series 619: 6 p

Healy RW, Bartos, TT, Rice CA, McKinley MP, Smith BD. (2011) Groundwater chemistry near an impoundment for produced water, Powder River Basin, Wyoming, USA. J Hydrol 403:37–48 doi: 10.1016/j.jhydrol.2011.03.042

Johnston, CR, Vance GF, Ganjegunte GF (2008) Irrigation with coalbed natural gas co-produced water. Agr Water Manage 95: 1243–1252 doi: 10.1016/j.agwat.2008.04.015

Skorupa, JP (1998) Selenium poisoning of fish and wildlife in nature: Lessons from twelve real-world examples. Frankenberger Jr WT, Engberg RA (Eds.), Environmental chemistry of selenium, Marcel Dekker, New York pp. 315–354

Wyoming Department of Environmental Quality (2005) Water quality rules and regulations (Chapter 8) http://deq.state.wy.us/wqd/WQDrules/ Chapter_08.pdf, accessed Mar 26, 2013

Wyoming Oil and Gas Conservation Commission (2012) Basin statistics for the Powder River Basin: http://wogcc.state.wy.us/StatsForBasin.cfm (accessed August 27, 2012)

Zupancic JW, Roenbaugh JW, Mull GA, Nicholson CM (2008) System and method for dispersing of coal bed sodic water. Patent 7,320,559. BeneTerra, LLC, Pratt, Kansas, USA

Geotechnical centrifuge permeater for characterizing the hydraulic integrity of partially saturated confining strata for CSG operations

Steve Bouzalakos[1,2], Wendy Timms[1,2], Priom Rahman[3],
Dayna McGeeney[2,3], Mark Whelan[1,2,3]

[1]*Australian Centre for Sustainable Mining Practices (ACSMP), School of Mining Engineering, University of New South Wales, NSW 2052, Australia, s.bouzalakos@unsw.edu.au, w.timms@unsw.edu.au*
[2]*National Centre for Groundwater Research and Training (NCGRT), Australia*
[3]*Water Research Laboratory (WRL), University of New South Wales, Australia*

Abstract Vertical hydraulic conductivity (K_V) of aquitards is enabled under accelerated gravity in a Broadbent G-18 geotechnical centrifuge (2 m diameter). Expedited determination of K_V under saturated steady state flow required very high G-levels (up to 520 G) to force flow, providing evidence that intact shale core from deep sedimentary formations are very low permeability ($<10^{-12}$ to 4×10^{-10} m/s). New centrifuge instrumentation developments are proposed for experimentation under partially saturated conditions and transient flow to determine the extent to which vertical seepage is influenced. This may be a critical dynamic process that reduces potential impacts of depressuration or dewatering from CSG extraction.

Keywords Coalbed methane extraction, centrifuge core testing, confining strata, permeability, hydraulic integrity

Introduction

Hydraulic disconnection by low permeability confining strata (*i.e.* aquitards) can limit potential impacts of dewatering and contamination migration. An ideal aquitard is a deep or thick material of low permeability, that is laterally continuous and without preferential flow paths (*e.g.* fracture networks).

The volume of groundwater flow during coal seam gas (CSG) production can have implications for safe and efficient extraction and for potential impacts on shallow aquifers, or nearby rivers, lakes and wetlands. For example, extraction of water for CSG production is required to reduce the hydraulic head at the coal seam sufficiently to enable gas desorption. The feasible design of water extraction systems to achieve this low hydraulic head depends on many factors including the permeability of the coal seam, and the degree of vertical disconnection or connectivity through the overburden (Timms *et al.* 2012).

The flow of groundwater through aquitards is typically very slow, but could be significant at the large scale over long periods of time if underlying aquifers remain depressurized as a result of CSG extraction (Timms 2012). It is also well known that vertical flow depends on the degree of saturation of the pore space, with partially saturated aquitards having much lower hydraulic conductivity (*K*) than when fully saturated (Neuzil 1986, 1994). K is, therefore, an important factor for assessing whether or not vertical connectivity with overlying and underlying aquifers is significant.

Given the tight nature of aquitards, *K* measurements are not practical and time-efficient using standard test methods (*e.g.* falling/constant head permeameters). Expedited determination of their hydraulic integrity may be determined relatively rapidly using geotechnical centrifuge technology. For example, accelerating intact core samples at 100 times gravity makes it possible to observe in 1 day of centrifuge testing, flow that would occur in 10,000 days (≈ 27 years) under *in situ* conditions.

This paper reports geotechnical centrifuge measurements of vertical hydraulic conductivity (K_V) for intact shale core, assumed to be saturated, under steady state flow conditions. The cores are from the Surat Basin, Queensland, where there is particular interest in K_V determination as, at present, there is very little data available via indirect estimations from horizontal permeability assessments (Queensland Water Commission 2012). Further work and centrifuge instrumentation developments allowing for experimentation under partially saturated and transient flow is also mentioned.

Methods

A total of eight intact cores were tested at the National Centre for Groundwater Research and Training (NCGRT) geotechnical centrifuge facility located at the Water Research Laboratory (WRL), University of New South Wales (UNSW). Moisture content of cores was measured using methods adapted from AS 1289.2.1.1 (AS 2005), and K_V was tested using a method adapted from ASTM D6527-2000 (ASTM 2000) using a centrifuge permeameter (Zornberg and McCartney 2010; Timms and Hendry 2008).

Geotechnical centrifuge system

The NCGRT geotechnical centrifuge is a Broadbent Modular Geotechnical Centrifuge (2 m diameter) with a new centrifuge permeameter (2 × 4.7 kg permeameter sample at 556 G-max). A 22 kW motor drives a variable speed of 10–875 RPM. The centrifuge permeameter (CP) module was designed specifically for groundwater research, and is a relatively large module that allows on-board instrumentation and real-time monitoring of a range of parameters. Since a maximum of G-level of 471 applies at the centre of the sample weight, the rating of the centrifuge permeameter is 2.2 G-ton (471 × 4.7/1000). The total weight of one permeameter when empty is 12.7 kg plus an allowance of 1.0 kg of effluent in the reservoir. A large cross-sectional flow area (100 mm diameter), low volume influent pumps and a custom made effluent suction extraction system have enabled routine testing of low permeability matrix.

Each permeameter assembly (fig. 1) is configured to maintain a constant head of influent above the sample. The influent pumping and monitoring systems are connected to a PC via a Fiber Optic Rotary Joint (FORJ) and controlled using LabVIEW software. Effluent flows from the porous sample through drainage plate and into the effluent reservoir. Effluent is extracted via a syringe or peristaltic pump through a 'U' shaped tube that connects to the base of the effluent reservoir. This system enables samples to be extracted without the need for the permeameters to be taken off the beam. An air vent maintains zero pressure outflow boundary.

Hydraulic conductivity calculations

Using Darcy's Law ($v = -K \cdot \partial h / \partial L$), where h is hydraulic head (*i.e.* the sum of the pressure head and elevation head) and L is sample length (cm), the discharge velocity (v) during laminar flow of water through a porous media can be

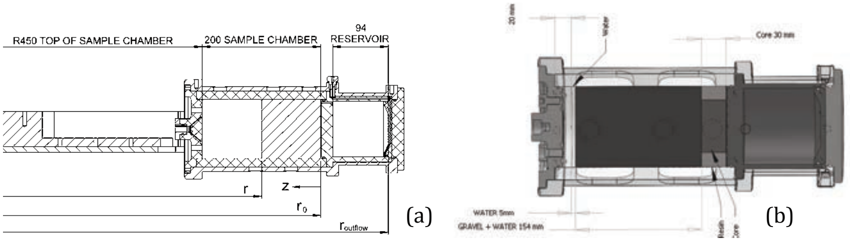

Fig. 1 *Cross section of the (a) centrifuge permeameter (CP) and beam showing new reservoir and reference points and (b) detail of core setup in new CP module.*

calculated as a function of the gradient in hydraulic head, and a constant of proportionality referred to as hydraulic conductivity (*K*). K_V calculations using the CP module are based on Equation 1 adapted from ASTM D6527 (2000), assuming that the hydraulic head gradient is negligible compared to the centrifuge force driving flow:

$$K_v = \frac{0.248Q}{A \times r_m \times (\text{RPM})^2} \quad (1)$$

where K_V is vertical hydraulic conductivity (m/s), Q is the fluid flux imposed by the flow control system (mL/h), A is the sample flow area (cm^2), RPM is revolutions per minute, and r_M is radial distance at the mid-point of the core sample (cm).

The centripetal acceleration, oriented outward in a radial direction and at a distance r from the axis of rotation, equals a:

$$\alpha = \omega^2 r = \frac{N}{g} \quad (2)$$

where ω is the angular velocity (rad/s), r is the radius from the axis of rotation (m), N is the ration between centripetal acceleration and gravity, and g is the acceleration due to gravity (9.8 m/s^2). The angular velocity is related to RPM as follows:

$$\omega = 2\Pi \times \frac{\text{RPM}}{60} \quad (3)$$

Substituting Equation 3 into Equation 2 and dividing by g yields Equation 4 which can be used to determine the N scale (or G-max) for a given RPM and radius:

$$N = 1.122 \cdot 10^{-3} \times (\text{RPM})^2 \times r \quad (4)$$

Core preparation

Rock cores from deep sedimentary basins were obtained using rotary mud drilling methods, using standard coring methods (65–80 mm diameter), with cores stored in open air trays. These cores were re-saturated with synthesized pore water (described below). Rock cores were set in the permeameter liners using resin (Megapoxy 240). The resin was selected due to ultra-low permeability, fast curing rate and strong adherence to acrylic. Potting rings (ID 90 mm and length 30 mm, hard anodized aluminum alloy AL6061), custom designed by UNSW, were used to ensure that the resin set sample precisely matched the top and base of the core. Flat core surfaces and uniform cross-sectional area were assumed in K calculations. The UNSW potting rings were then fitted within the acrylic liner via double O-ring seals (fig. 1b). Rock cores were connected to the CP drainage plate via a 1 mm thick A14 Geofabrics Bidim geofabric filter (110 micron, and permeability of 33 m/s) laid on top of a Whatman 5 Qualitative filter paper.

As the majority of the core samples were received from a depth in excess of 500 m below the surface, the centrifuge testing conditions could not replicate *in situ* stress levels. To increase stress imposed on the samples during testing, a dense porous medium (saturated gravel) was packed on top of the cores with an influent head of 10–50 mm ponded on the sample (fig. 1b).

Two core samples were tested simultaneously at either end of the centrifuge beam, and balanced to the nearest 500 G. Effluent water passing through the core samples was collected manually from a reservoir below the cores, with measurements of head and effluent volume (to the nearest 0.01 g) recorded during brief centrifuge stops.

The CP was operated at various speeds range from 10–400 G (depending on the *K* value of core – higher speeds being used for core with lower *K*). Testing typically commenced at 10 G and increased periodically until testing ceased. A typical increase in G-level over time is shown in Fig. 2. Each centrifuge run required approximately 2–4 days for each core specimen given the very low permeability nature.

Influent preparation and core re-saturation

Four influent waters were synthesized for K_V testing to approximate the groundwater chemistry at the depth of core collection. Dominant salts and carbonates were taken into account based on the water quality report for the respective drill sites supplied to WRL. Total ionic strength and major ion ratios (*i.e.* chloride, carbonate, sodium and potassium) were calculated for target solutions. Analytical grade reagents were prepared with Milli-Q water to target concentrations and the pH adjusted if necessary with concentrated sulphuric acid. Electrical conductivity (EC) and pH values of prepared solutions were measured with calibrated water quality probes as shown in Table 1.

Saturation of cores for K testing was assumed by preservation of drill core and vacuum plate saturation, and verified by monitoring weight changes during testing, and moisture tests before and after testing. A custom vacuum plate device was designed by UNSW to fit the CP liners containing the cores, drawing ponded water influent from the top to the base of the cores. After 12–48 hours, or upon effluent flow from the base, the liners were then transferred directly to the CP module without disturbing the sample.

Results and Discussion

Hydraulic conductivity assessment

According to Table 2, K_V ranged from $<10^{-12}$ – 4×10^{-10} m/s ($n = 12$), compared with a resin value of $<10^{-12}$ m/s. It is important to note that half of the values ($n = 6$) were less than the current detection limit of the instrumentation (*i.e.* $<10^{-12}$ m/s). In addition, there were two unreliable values of 3×10^{-8} and 10^{-5} m/s tested on cores from the Evergreen and Hutton formations, respectively, owing to leakage through micro-fractures and poor resin seals caused as a result of high G levels and defects in the drill core.

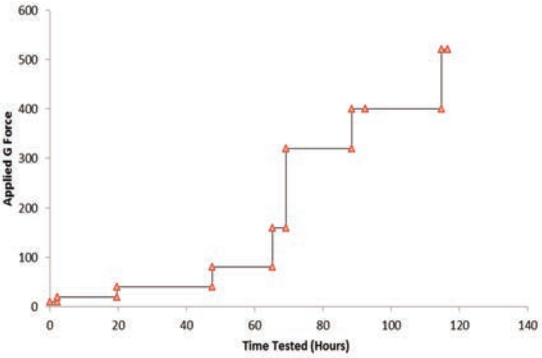

Fig. 2 *Typical G-level applied to core specimens versus testing time.*

In comparison to Fig. 3a, shale core tested in this study (*i.e.* Table 2 and fig. 3a – Shale 2) shows relatively low K_V, at least 10–100 times lower than some alluvial clay aquitards that have been tested with the NCGRT centrifuge. Further, measured K_V values are consistent with values typically reported for shales (*e.g.* Neuzil 1994). Fig. 3b compares data of K_V (from Table 2) and K_h from the APLNG project using various *in situ* and traditional laboratory techniques, and the newly-developed NCGRT centrifuge permeameters (APLNG 2013). Centrifuge-derived K_V are, in general, significantly lower than parameterized in previous groundwater modeling, whereas average K_h data are generally in agreement with model input values although a much greater spread is noted.

The natural variability of hydraulic conductivity within apparently homogeneous geological media is large. It was found that permeability commonly varies over 3 orders of magnitude for similar porosity (Neuzil 1994). On this basis, it is reasonable to report permeability measurements to the nearest order of magnitude. Laboratory techniques, however, may be able to report a more precise value to a tenth of an order of magnitude (or one sig-

Sample	Formation	Salts Added (g/L)	EC (µS/cm)	pH	pH Correction
A	Westbourne	Na_2CO_3: 0.55; NaCl: 0.47	1,930	8.80	H_2SO_4 added
B	Hutton	Na_2CO_3: 1.03; NaCl: 1.38; KCl: 0.90	6,720	8.30	H_2SO_4 added
C	Walloon	Na_2CO_3: 1.10; NaCl: 1.76	4,870	8.30	H_2SO_4 added
D	Evergreen	Na_2CO_3: 0.51; NaCl: 1.99; KCl: 0.85	8,770	8.05	H_2SO_4 added

Table 1 *Summary of influent chemistry.*

Formation	Core Depth (m)	Apparent K$_v$ (m/s)	Received w (%)	Final w (%)
QA test	Resin only	$<10^{-12}$	-	-
Westbourne	152.65-152.90	$<10^{-12}$	5.30	5.60
Westbourne	152.65-152.90	10^{-11}	5.30	5.60
Walloon	824.94-825.26	3×10^{-10}	2.50	5.40
Walloon	824.94 – 825.26	4×10^{-10}	2.50	3.50
Walloon	864.93-865.12	$<10^{-12}$	3.60	7.90
Hutton	1055.93-1056.15	$<10^{-12}$	6.40	3.60
Hutton	1111.86-1112.27	$<10^{-12}$	2.60	2.70
**Hutton*	*1111.86 - 1112.27*	10^{-5}	*2.60*	*2.70*
**Evergreen*	*1128.36-1128.68*	3×10^{-8}	*4.50*	*5.60*
Evergreen	1128.36-1128.68	5×10^{-11}	4.48	5.45
Evergreen	1153.34-1153.58	$<10^{-12}$	3.50	3.50
Evergreen	1153.34-1153.58	$<10^{-12}$	3.40	3.50
Evergreen	1184.25-1184.46	2×10^{-10}	3.89	3.93
Evergreen	1184.25-1184.46	$<10^{-12}$	3.80	3.90

*Note: *Unreliable values are given in italics.*

Table 2 *Summary of apparent hydraulic conductivity (K$_V$) and moisture content (w).*

nificant figure). Natural permeability variability, both within a core sample, and between core samples from adjacent depths are likely to be more variable than plausible laboratory measurement precision.

Based on current instrumentation capabilities, cores with K$_V$ between $10^{-9} – 10^{-6}$ m/s can be measured to a precision of half an order of magnitude, while measurements in the range of $10^{-12} – 10^{-10}$ m/s are subject to greater uncertainty. Centrifuge runs where no flow was induced for a testing period of up to 70 hours a value of $<10^{-12}$ m/s was reported in Table 2.

Quality assurance (QA) included cross-checking of core and permeability weights to monitor changes in moisture content, and cross-checking influent and effluent flow rates. An additional QA test confirmed that K of resin used to set cores in the permeameter liner was less than the detection limit (*i.e.* $<10^{-12}$ m/s).

Moisture content assessment and further work

K is a function of moisture content, with K at saturation higher than for partially saturated cores (*e.g.* Jougnot *et al.* 2010). It must be noted that increasing moisture content before and after testing suggests that the apparent K$_V$ values may not be representative of saturated rock. For instance, moisture content of core from 864 m depth (Walloon Formation) increased from 3.60 to 7.90 % before and after testing, respectively, even though a K$_V$ of $<10^{-12}$ m/s was measured.

Future work with very low permeability shale cores is currently underway to prevent moisture loss of cores, and further investigate the effect of moisture content, degree of saturation (θ) and inter-particle capillary pressure (ψ) of partially saturated matrix. Very few stud-

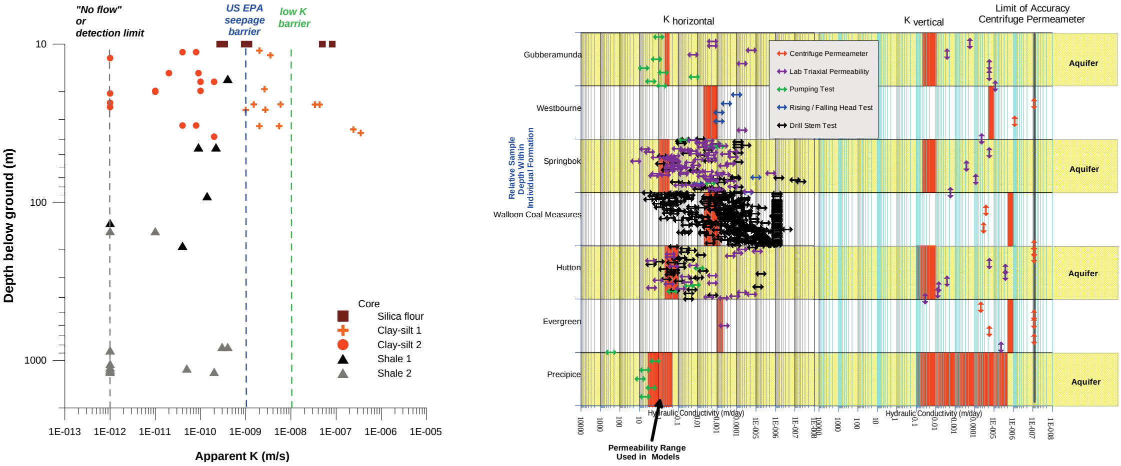

Fig. 3 *(a) Hydraulic conductivity as a function of depth for rock core samples (Shale 2) compared to more permeable matrix (i.e. silica flour and clayey sediments) at steady state flow in the NCGRT centrifuge; (b) Summary of APLNG hydraulic conductivity results, m/day (K$_V$ and K$_h$, various laboratory/field techniques).*

ies have attempted to determine the hydraulic properties of deep shale under unsaturated conditions as such measurements are extremely challenging. Instrumentation developments at the NCGRT geotechnical centrifuge, such as real-time moisture content measurement in high G environments, will enable *K* function investigations under transient infiltration and drainage of water under partially saturated core conditions. The extent to which vertical seepage is reduced by partially saturated conditions during CSG extraction may be a critical dynamic process that reduces potential effects on shallow aquifers.

Conclusions

The NCGRT geotechnical centrifuge enables *K* testing of low permeability geological material that would otherwise not be possible. Findings have so far highlighted the relatively low K_V of intact shale, consistent with larger permeability datasets typically reported for shales (*e.g.* Neuzil 1994) and at least 10–100 times lower than some alluvial clay aquitards. To date, there have been no published studies measuring K_V in deep shale of these formations. The K_V is also sensitive to moisture content and small fractures due to defects in drill core. Minimally disturbed core samples from depths greater than 500 m have been tested, although load restrictions in this centrifuge cannot match *in situ* lithostatic stresses at such depths. Nevertheless, permeability values are indicating that *in situ* stress for hard rocks may not be an important factor under high G environments. Instrumentation developments that are currently in progress will enable real-time monitoring of moisture content to enable transient flow under partially saturated core conditions deriving values of greater certainty for model inputs.

Acknowledgements

This work was funded by the Australian Research Council and National Water Commission, as part of National Centre for Groundwater Research and Training, Program 1B. Origin Energy is acknowledged for providing shale drill core for permeability testing.

References

APLNG (2013) Report – 2013 Groundwater Assessment, Australia Pacific LNG Upstream Project Phase 1, Q-LNG01-15-TR-1801, Australia Pacific LNG, 266 pp

AS (2005) Testing soils for engineering purposes. Method 2.1.1 – soil moisture content tests – oven drying method, Australian Standard 1289.2.1.1

ASTM (2000) Standard test method for determining unsaturated and saturated hydraulic conductivity in porous media by steady state centrifugation. American Society for Testing and Materials International, D 6527–00

Jougnot D, Revil A, Lu N, Wayllace A (2010) Transport properties of the Callovo-Oxfordian clay rock under partially saturated conditions. Water Resources Research 46(8) W08514

Neuzil CE (1994) How permeable are clays and shales? Water Resources Research 30(2):145-150

Neuzil CE (1986) Groundwater flow in low permeability environments. Water Resources Research 22(8):1163-1195

Queensland Water Commission (2012) Underground Water Impact Report for the Surat Cumulative Management Area, 18 July 2012, State of Queensland, 224 pp

Timms W, Acworth I, Hartland A, Laurence D (2012) Leading practices for assessing the integrity of confining strata: application to mining and coal seam gas extraction. In: McCollough CD, Lund MA, Wyse L (Eds) 2012 International Mine Water Association Symposium Proceedings, Bunbury, Western Australia, p 139–148

Timms WA, Hendry MJ (2008) Long term reactive solute transport in an aquitard using a centrifuge model. Ground Water 46(4):616-628

Timms WA (2012) Environmental 'time machine' – the integrity of aquitards overlying coal seams. AusIMM Bulletin, April 2012 issue, p 79–81

Zornberg JG, McCartney JS (2010) Centrifuge permeameter for unsaturated soils. I: Theoretical basis and experimental developments. J Geotech Geoenviron Eng 136(8):1051-1063

Decision support tool for management of produced and frac-flowback water

Tzahi CATH[1], Mengistu GEZA[2], Jörg DREWES[3], Pei XU[4]

[1]*Coloardo School of Mines, 1500 Illinois Street, Golden, Colorado, 80401, USA, tcath@mines.edu*
[2]*Coloardo School of Mines, 1500 Illinois Street, Golden, Colorado, 80401, USA, mgezanis@mines.edu*
[3]*Coloardo School of Mines, 1500 Illinois Street, Golden, Colorado, 80401, USA, jdrewes@mines.edu*
[4]*New Mexico State University, Box 30001, MSC-3CE, Las Cruces, New Mexico, 88003, pxu@nmsu.edu*

Abstract A decision support tool (DST) was developed for technology selection and decentralization of treatment facilities in the exploration and production oil and gas industry. Selection of water treatment processes is a complex task and has to consider many parameters including water quality and quantity and overall economics. Produced water quality is widely variable, and water may contain contaminants from diverse groups. The DST can help designers, utilities, and regulators to evaluate options for beneficial use of flowback and produced water from oil and gas production and select effective treatment trains that can be implemented for treatment of these streams.

Keywords Produced Water, Frac-flowback, Beneficial Reuse

Introduction

Beneficial Use refers to the use of reclaimed or impaired water for a secondary purpose that has a positive value. This may apply to produced water from oil or gas wells or other impaired water from industrial or domestic sources. Potential beneficial use options for produced water include domestic potable use, livestock watering, industrial, commercial, agriculture irrigation, fisheries and wildlife maintenance and enhancement, recreation, fire protection, dust suppression, and more. The determination of a specific beneficial use depends on federal and state jurisdiction and the circumstances of each case, and the availability and feasibility of conventional and advanced water treatment technologies.

Large volumes of produced water are pumped to the surface during production of oil and gas, including coalbed methane (CBM) and shale gas, throughout the United States. CBM basins are shown in Fig. 1. Water must be pumped out of the coal layers (referred to as dewatering) in order to reduce the hydrostatic head (*i.e.* reservoir pressure) and allow the release of methane. The produced water generated during these operations is by far the largest byproduct or waste stream associated with gas production. The quantity of water produced during the life of a well is typically from 1 to 3 barrels (bbl; 120–360 L) of water per thousand cubic feet (bbl/mcf; 28 m^3) of gas (4–13 L/m^3). Water production is greatest in the early stages of well production, and it diminishes over time.

Produced water is an inextricable part of the natural gas recovery process. If an operator cannot reduce water production rates or sufficiently minimize water management costs, CBM fields cannot be efficiently developed, and a valuable energy resource may be lost or diminished.

The costs of produced water management vary extensively depending on the location, disposal method, the type of waste (quality and quantity), and the extent of competition in the local or regional area. Direct discharge and impoundment/evaporation are the least expensive management options, while commercial hauling of water or brine disposal are

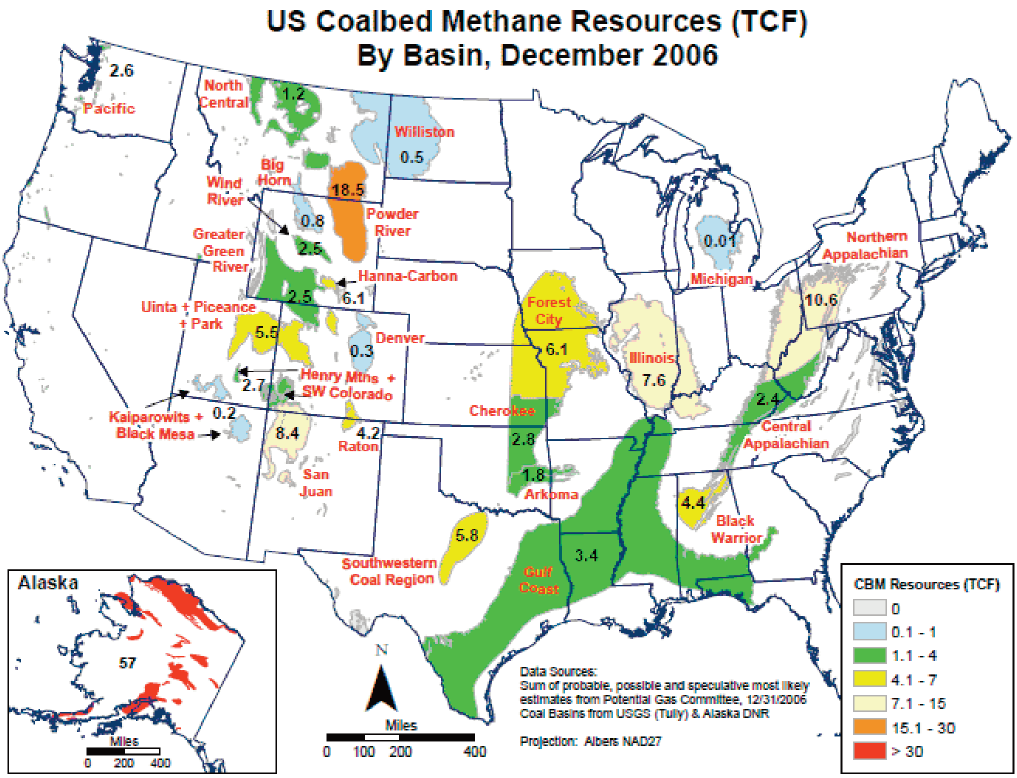

Figure 1 *Map of US coalbed methane resources by basin in trillion cubic feet of natural gas (eia 2013).*

the most expensive options for management of produced water.

Today, freshwater resources in the Western United States are fully allocated. Population forecasts suggest that the majority of U.S. population growth by 2020 will occur in western states, representing regions already lacking sufficient water resources. Increasing water demands associated with energy production and use exacerbate the situation in the West. While this scenario represents enormous challenges, it also provides opportunities for beneficial use of new water resources such as produced water. There are clear needs and strong economic drivers to develop integrative approaches to improve treatment, handling, disposal, and beneficial use of water brought to the surface during production of CBM, shale gas, and other unconventional gas resources.

Methods

In this project we have developed a computerized tool that can help users, including gas producers, water utilities, governments, and the public to learn about the characteristics of produced water and the major steps, costs, technologies, and environmental issues associated with production of water for beneficial use from coalbed methane produced water.

The CBM Produced Water Management Tool is a macro-enabled Excel workbook that contains four modules: Water Quality Module (WQM), Treatment Selection Module (TSM), Beneficial Use Screening Module (BSM), and Beneficial Use Economic Module (BEM). A flow diagram of the Tool is illustrated in Fig. 2.

The development of the decision support tool (DST) at CSM started in 2009 with the establishment of a comprehensive water quality and quantity database for CBM produced water for several major basins in the Rocky

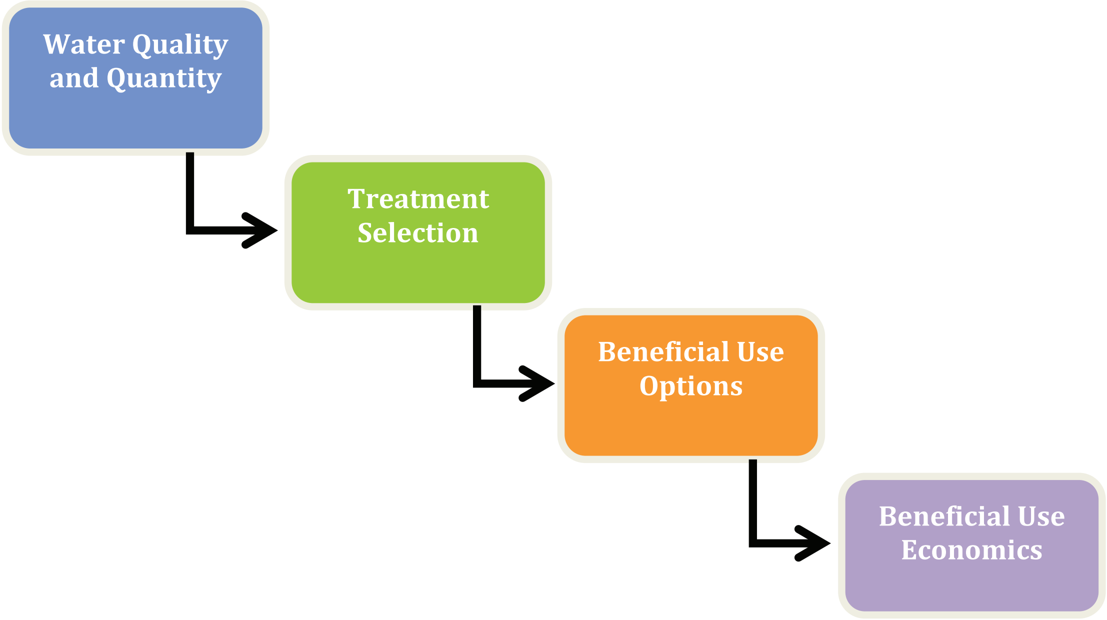

Figure 2 *The four internal modules of the DST for produced water treatment and beneficial reuse.*

Mountains region. The WQM enables access to this data (CSM/AQWATEC 2013b). To predict the water quality of wells based on location, the module incorporates known water quality information from a combination of public and private sources. Data is currently available for three major producing basins in the Rocky Mountain Region, including the Powder River, Raton, and San Juan basins.

The WQM (Fig. 3) is amenable to a broad range of user inputs, from limitation (location and basin of interest) to substantial (validation of user observed constituent concentrations). The WQM is capable of estimating produced water quality based on different levels of data available to the user.

The TSM (Fig. 4) is designed to suggest three treatment trains capable of treating produced water to a quality suitable for each of pre-programmed or user defined beneficial uses. The user inputs criteria such as water quality, water quantity, desired water recovery,

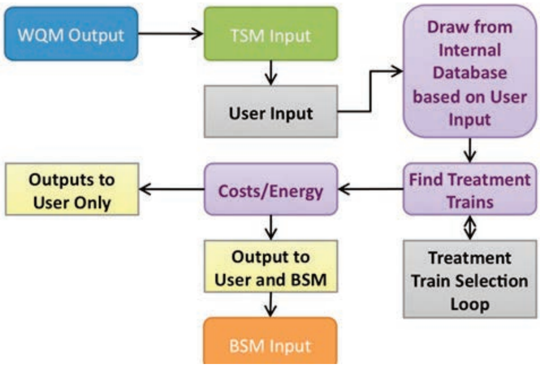

Figure 3 *Flow diagram of the WQM.*

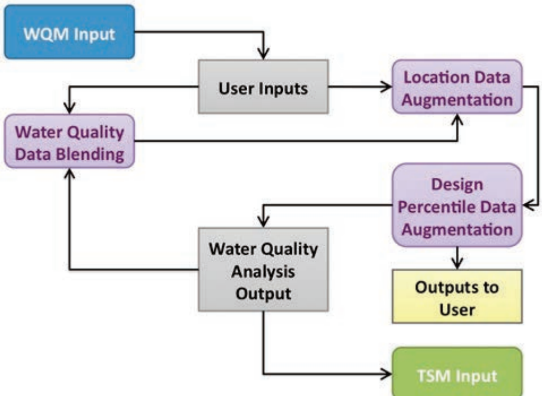

Figure 4 *Flow diagram of the TSM.*

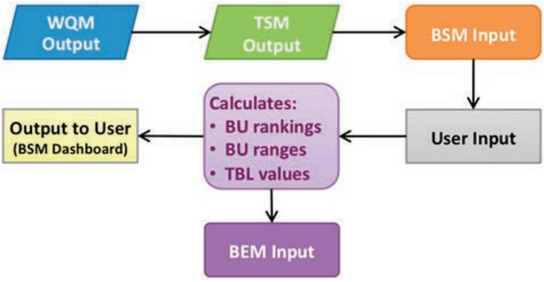

Figure 5 *Flow diagram of the BSM.*

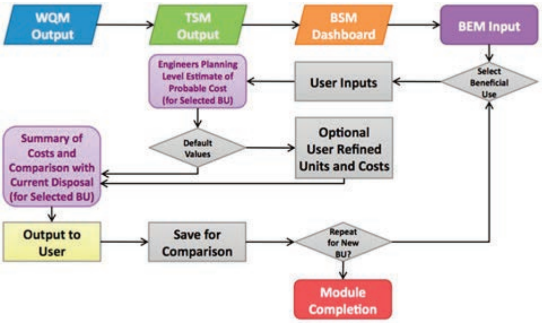

Figure 6 *Flow diagram of the BEM.*

and other site-specific operational objectives to assist in the selection of an integrated treatment process. Using these inputs, along with a robust selection methodology, the tool generates potential treatment trains from a set of >40 technologies (CSM/AQWATEC 2013a). The TSM preferentially selects the minimum number of processes, in a most logical order, required to treat a given feed water stream to either predefined or user defined beneficial uses. The TSM generates a report detailing three suggested treatment trains, estimated water quality and quantity, chemical and energy requirements, estimated brine quality and quantity, and a proposed brine management strategy for each beneficial use predefined or defined by the user.

The purpose of the Beneficial Use Screening Module (BSM; Fig. 5) is to help produced water generators, potential beneficial users, and other stakeholders identify key issues regarding different potential beneficial use projects. The user inputs information about water quantity, reliability and duration of flows for a potential project. Based on this information, the module screens potential beneficial uses and ranks them qualitatively. The rankings are output in a Screening Matrix, which provides a color-coded assessment of the feasibility and relative complexity between beneficial use categories. This can help the user to identify the top 2 or 3 beneficial uses that have a greater potential for feasibility or economic return. The user then can focus on these beneficial uses for additional assessment in the BEM.

The purpose of the Beneficial Use Economic Module (BEM; Fig. 6) is to help produced water generators, potential beneficial users, and other stakeholders identify estimated, planning-level capital and O&M costs for potential beneficial use projects. The evaluation can be performed for multiple beneficial use categories or variations on a single beneficial use category to allow for comparison of the relative costs between scenarios. Potential social, environmental and other benefits are also estimated quantitatively and/or qualitatively in the BEM to provide a non-economic assessment of beneficially using produced water (CSM/AQWATEC 2013b).

The BEM is the last module in the series of linked modules; it builds off of the output information from the WQM, TSM, and BSM. The BEM also uses scenario-specific user input variables (such as estimated project life, project area, and terrain) to build a cost estimate. The costs are outputted in both a detailed, line-item cost estimate table and a general cost summary. Default variables can be adjusted as necessary to refine the cost estimate or to change the basic scenario.

Results from the First Phase of the Study

During the first phase of the study the DST was developed and tested by operators and stakeholders. Then two hypothetical case studies were simulated on the DST to determine site-specific produced water treatment technologies and beneficial use options, using realistic conditions and assumptions. Case studies were located in the Powder River (WY) and San Juan (NM) Basins. Potential beneficial uses evaluated include crop irrigation, on-site use, potable use, and instream flow augmentation. The screening tool recommended treatment trains capable of generating the water quality required for beneficial use at overall project costs that were comparable to or less than existing produced water disposal costs, given site-specific conditions and source (produced) water quality. In this way, the tool may be used to perform a screening-level cost estimate for a particular site to determine whether the costs per barrel for beneficial use are more or less than site-specific disposal costs. The demonstrated technical and economic feasibility provide incentive to address the institutional and legal challenges associated with beneficial use of produced water.

The two comprehensive case studies were previously reported and can be accessed on the web at http://aqwatec.mines.edu/produced_water/tools/RPSEA_CBMPW_CaseStudies.pdf

Further Development of the DST

Encouraged by the results from the first phase of development, upgrade of the current version of the DST with more functions and user choices is being pursued. The DST is being further developed and enhanced beyond the CBM produced water management, and will incorporate databases and treatment of shale gas and tight sand. A comprehensive water quality database (including compositions of fracturing fluids, flowback, produced water, baseline groundwater and surface water) and a thorough examination of produced water and flowback water qualities are critical to evaluate the environmental impacts, alleviate public and regulatory concerns, and select pretreatment and treatment processes to meet beneficial use or disposal requirements.

The new version of the DST will include decentralization of treatment, enabling modeling and optimization of treatment for a wider variety of beneficial uses. Decentralized treatment refers to the implementation of water treatment for a single of a small cluster of wells, whereas centralized treatment refers to the collection and treatment of water from the entire basing of a large section of the basin. A decentralized system could be beneficial because it provides localized water reuse opportunities and reduces conveyance costs and could be cost effective when produced water sources are very scattered. On the other hand, there might be benefits from using a centralized system, driven by economy of scale. The decentralization module accounts for economic and environmental factors to make appropriate decisions on whether a decentralized or centralized system is more efficient for a specific basin or user and to make an optimal distribution of treatment plants at selected sites.

In the new version of the DST the user will have higher flexibility to define and include/exclude specific treatment technologies. This will open up the DST for use by other industries and by process developers.

DST for Urban Infrastructure Development

A third version of the DST is now being developed for selecting technologies and redesigning urban water infrastructure. The new DST includes new features that are critically needed in urban settings, but also in rural and industrial settings. These include (in addition to decentralization capabilities) selection of energy recovery systems and nutrient recovery systems. Thus, the third version of the DST can optimize water systems to facilitate net-positive energy use.

Conclusions

Computerized decision support tools are critical to better understanding water resources quality and quantity and improving the infrastructure through optimization of treatment processes and maximization of beneficial reuse of impaired water. In parallel to other

DSTs currently developed by other institutions, the Produced Water DST will enable better utilization of resources in critical industries and new urban settings.

Acknowledgements

The authors thank the “Ultra-Deepwater and Unconventional Natural Gas and Other Petroleum Resources Research and Development Program” as part of the Research Partnership to Secure Energy for America program administered by the U.S. Department of Energy’s National Energy Technology Laboratory for funding the project (Grant # 07122–12). The authors also thank the regional participating CBM producers for their technical assistance, support, and contributions of water quality and quantity data. The authors also thank the National Science Foundation for funding through the ERC/ReNUWIt.

References

CSM/AQWATEC (2013a) An Integrated Framework for Treatment and Management of Produced Water: Technical Aassessment of Produced Water Treatment Technologies, Colorado School of Mines. Available: http://aqwatec.mines.edu/produced_water/treat/

CSM/AQWATEC (2013b) Produced Water Treatment and Beneficial Use Information Center: Beneficial Use Matrix — CBM Produced Water Management Tool aqwatec.mines.edu/produced_water/tools/

Energy Information Administration (eia). www.eia.doe.gov/oil_gas/rpd/cbmusa2.pdf

Hydrogeological Aspects during Closure of an Underground LPG Storage

Anne-Julie Defossez[1], Louis Londe[2], François Cabon[3], Pierre Roux[4]

[1]GEOSTOCK, 2 rue des Martinets, Rueil-Malmaison, France, ajd@geostock.fr; [2]llo@geostock.fr;
[3]fca@geostock.fr; [4]pru@geostock.fr

Abstract This article presents the successive steps of the GEOVEXIN LPG underground cavern storage closure from the decision to stop the activity in April 2006 for economic reasons until the present situation. It describes the operation termination phase (product removal and water flooding of the cavern), the partial backfilling of the cavern and access tunnel, the modeling and specific hydrogeological studies (considering the vicinity of drinking water fields), the monitoring network adaptation and the water quality and level of groundwater supervisions. Each step has been successfully carried out by the company GEOSTOCK according to the Environmental French Administration requirements.

Keywords Underground cavern storage, closure, hydrogeology, monitoring

Introduction

Many hydrocarbon storage caverns are currently operated around the world. Few of them have been already closed and abandoned. The GEOVEXIN cavern provides a successful and recent example of such a closure, in spite of technical and hydrogeological constrains.

LPG storage of GEOVEXIN presentation

GEOVEXIN underground storage was located near a refinery site alongside the Seine River, 40 km west of Paris. The facility was initially planned for storing 3 products: propane, gasoline and heavy fuel oil. Priority was subsequently given to heavy fuel oil and the design proceeded on this basis. The planned caverns were arranged like a comb with the oil pumped in from small galleries at a higher level, circulating in the “forks” of the comb and then along the main connecting gallery and a central branch where it could be pumped to the surface (fig. 1). Due to the oil crisis of the mid 70’s, the initial planned oil storage project was converted into a smaller propane storage project. The cavern eventually built in 1975 consisted of 2620 m (8590 ft) of egg-shaped gallery of 47 m^2 cross section, with a storage volume of 130 000 m^3. Gallery depths ranged from

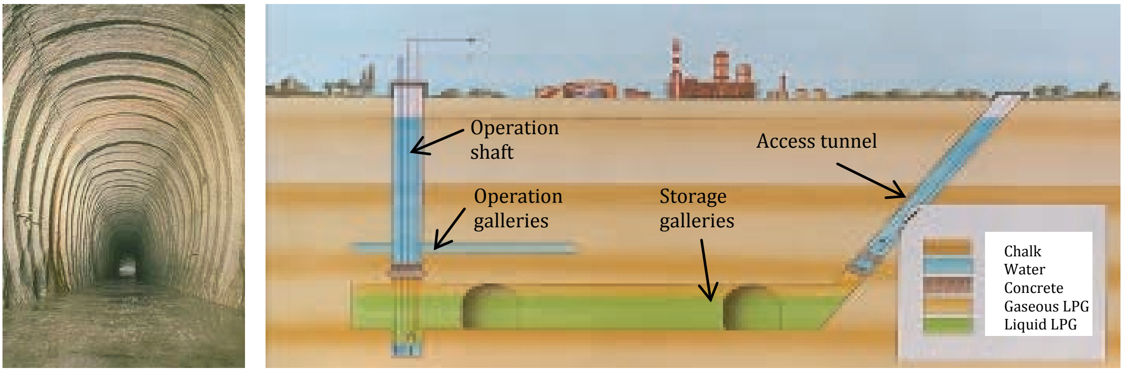

***Fig. 1** View of main gallery (left) and schematic cross section of underground storage (right).*

120 m (393 ft) to 145 m (475 ft). Access to the storage galleries was made through shafts and an access tunnel of 1045 m (3428 ft) long (Maury 1977).

Only chalk was suitable for such an underground storage in this area of the Paris basin. The Turonian chalk was selected. The geological section of the site starts at the top with about 100 m (328 ft) of Lower Senonian, a white chalk containing silex, with solution pockets at the higher levels. A more pervious detritic level is found near the top of the Turonian. The next layer is the Turonian chalk itself where the cavern is located, followed by the Cenomanian, a bed of sandy chalk about 50 m (164 ft) thick.

The hydraulic conductivity of the surface Quaternary zone and top of weathered chalk is several tens of Darcy (30 to 40 10^{-5} m/s). The hydraulic conductivity in the Turonian chalk is approximately 4 mD (4 10^{-8} m/s). The detritic level is sometimes much more permeable but is often not continuous. Lastly, a few irregular and discontinuous silex beds, a few centimeters thick, probably produce some anisotropy.

The hydrodynamic containment principle was used to obtain gas- tightness. A permanent flow of water from the surrounding rock is designed and maintained in such a way as it is always directed inwards, into the storage galleries, in order to oppose any outward migration of the propane. The storage facility must therefore be located at sufficient depth below the groundwater table and in the vicinity of a permanent source of groundwater recharge so that the natural hydrostatic head cannot be depleted by drainage into the cavern. Thus, the depth of the cavern is to be designed accordingly to the product pressure, approximately 8 bar gauge (116 psig) in the case of propane.

Once it was decided to use the facility for storing propane, the main service shaft was deepened 22 m (72 ft) and a concrete plug was built between the storage level and the operation galleries, which were subsequently filled with water. All the other shaft and adits were also sealed off. A double concrete plug with water seal at controlled pressure was built at the bottom of the access tunnel.

Operation termination (2006–2010)

Considered no longer economically viable for the LPG market, its shareholders decided to stop the GEOVEXIN activity on the 13 April 2006. At the time of the decision to stop the activity, the storage contained 123 000 m³ of product which represented approximately 2 000 tons at the cavern storage pressure of 7.4 bar gauge and the geothermal temperature of 16 °C.

The first action was to drain away the cavern of the liquid LPG by the usual means (pumping by means of the submerged pumps towards rail tanks) until reaching the low level and pump shut down.

Then the cavern was gradually flooded by the seepage water. At the same time, the residual gaseous propane was progressively evacuated and recovered by the recompression system available on the site and sent towards the rail tanks loading station. This operation was carried out with permanent control of the pressure in cavern and of the water level to guarantee the integrity of the storage. During the evacuation phase of the gaseous propane, the pressure of the cavern was monitored by successive stops and starts of the compression system. The pressure varied between the minimal value of 5.0 bar gauge (stop of the compressor) and 7.4 bar gauge (start of the compressor).

The seepage water filling was made up to a level very close to the roof of the cavern.

The next stage consisted of a flare operation which was introduced in November 2008, and ended in January 2009, which allowed extracting a remaining 148 tons of propane.

During this time, the company GEOSTOCK prepared a closure file for the DRIEE (French Environmental Administration). The technical definitive operation termination declaration defined the necessary works for placing the storage in safety mode, removing the LPG and supervising the storage installations. This closure declaration file was analysed by DRIEE in 2008 which resulted in the publication in September of the Prefect's first order which gave GEOVEXIN notice of the definitive operation termination declaration and listed the works to be carried out. This order which imposed that the seepage water pumping was maintained until an opposite decision is taken by an additional Prefect's order was then used as a basis for the definition of the closure works program.

After the flare operation was completed and during the closure file analysis by the Administration, the inerting gas phase was carried out. The goal was to reach a hydrocarbon content in the extracted mixture below 1 % molar. Three inerting cycles were necessary. Every inerting cycle consisted of a step of nitrogen injection to dilute the vapour phase, of a step of homogenization of the LPG/Nitrogen mixture and of a step of decompression and elimination of a fraction of the gaseous phase in the roof. The first inerting cycle lasted from April 2009 till October 2009 and allowed to lower the content in propane in the gas phase from 75 % to 11.5 % molar. The second inerting cycle took place from November 2009 till June 2010 and allowed to lower the content in propane from 11.5 % to 1.8 % molar. Finally the third and last cycle took place from July till August 2010 and allowed reaching a propane content lower than the target value of 1 % molar.

The inerting cycles took place under the permanent control of the pressure and the level of liquid in cavern to guarantee the integrity of the storage. The cavern pressure was monitored by successive stops and starts of the seepage water pumping system. The pressure varied between the minimal value of 5.5 bar gauge (stop of the pump) and 7.1 bar gauge (start of the pump) and the level of liquid was monitored between the high level of 8.1 m (start of the pump) and the low level of 5.1 m (stop of pump).

In December 2010, an additional Prefect's order was published in order to define the main condition of the seepage water pump stop authorization. The hydrocarbon content in extracted water must be lower than 5 mg/L and the parameter must be checked on three successive weekly analyses.

In preparation of this order, seepage water analyses were regularly made. The last three analyses carried out in October and November 2010 resulted in a propane content lower than the imposed value of 5 mg/L.

The definitive stop of the seepage water pumps took place on the 23 November 2010 and the seepage water gradually flooded the cavern up to its roof.

Partial backfilling of the cavern and access tunnel (2011)

The partial backfilling of the caverns and access tunnel was carried out through small diameter cased holes (5" diameter) fitted with a blow out preventer for the cavern.

This technique derived from conventional grouting works has allowed backfilling without having to gain access to the underground submerged parts. This is an advantage for various reasons, mostly worker's safety and environmental reasons: *e.g.* possible instabilities when rapidly discharging the cavern wall to atmospheric pressure, management of very large water volumes for working in dry conditions involving water table modifications, huge water treatment costs.

A very specific aspect of the project is the concept of partial backfilling. The cavern is globally stable and only sensitive areas have been treated. The sensitivity has been judged based on depth, shape and geological conditions.

Dams – isolating backfilled and non-backfilled underground areas – have been constructed by a specific grouting technique based on mixing at cavern level a rich cement mix with an accelerator. Grouting was made in separate tubes and mixing was obtained at dam level to avoid clogging in the long grouting tubes (120 meters). This relatively conventional technique has never been used before at such depths and distances and many tests and trials have been conducted with the Contractor (SOLETANCHE – BACHY) before starting the main works.

Once dams were constructed and their tightness checked by radar, backfilling was implemented using conventional grout mixes with low mechanical properties.

Works lasted five months working in two shifts. Two underground dams were constructed and some 15000 m³ of backfilling have been placed.

One must also note that the access tunnel constructed in the seventies is now covered with housings of the nearby suburban town. Drilling and grouting activities have consequently been realized in a dense urban environment.

Concerning the backfilling of the operation shaft, it was cleaned of all extractible equipment and backfilled with clean gravel using a tremie tube placed under water

The surface installations were dismantled. Operation shaft casings which are sealed in the bottom plug were cut at water table level and backfilled with cement grout as they cannot be reasonably extracted

At the end of the works the surface used by the facility can be returned to any other usage such as housings or road construction. Only a small area around the operation shaft has been declared “non- constructible”

Regional and local hydrogeological context

At a regional scale, the geological encountered formations are as follows i) Quaternary alluvial deposits from the Seine river, ii) Senonian white chalk with silex beds, more or less weathered on the upper part and iii) Turonian light grey chalk, fresh. On a local scale, the various investigation holes rapidly indicate after the top soil and decalcification clays a strongly weathered chalk (most productive part) then a fresher chalk (fig. 2).

The hydrogeological context is summarised as follows:

- The existence of the Seine river roughly flowing towards West South-West,
- One aquifer composed by the alluvial deposits and the upper weathered chalk part. Due to the lack of impermeable layer, these complex formations are interconnected and constitute the Chalk aquifer and are sensitive as regards to pollutions.
- The existence of an important drinking water field area on the left side of the Seine River (South-east part of the underground storage area).

Relations between the surface water and groundwater are directed in general from the aquifer towards the river but are sometimes inversed especially during floods or overproduction of water from the drinking fields.

The cavern seepage was around 60 m³/h at the beginning of operation and was close to

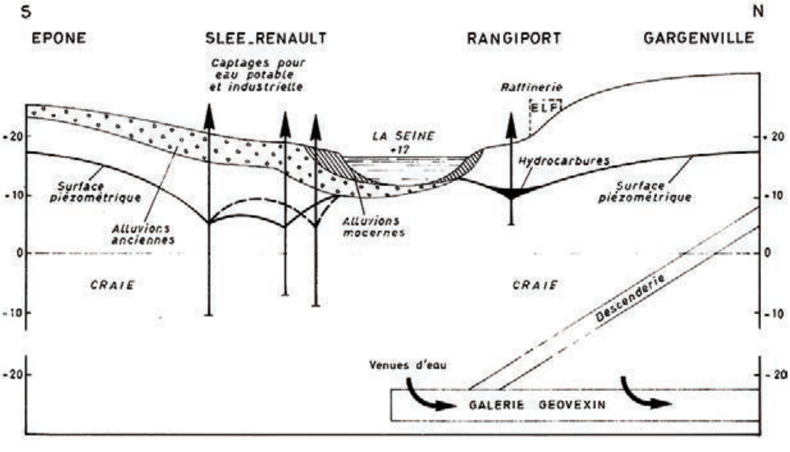

Fig. 2 *Schematic north-south hydrogeological cross section of the considered area (Mégnien 1979).*

20 m³/h just before the closure works. The withdrawal was low (200 times less than the water quantity taken from the drinking fields). The storage impact can be considered as negligible.

Monitoring network

Due to the hydrogeological context (vulnerability), the history of the area (existence of an oil refinery), the underground storage under operation and the vicinity of drinking water fields, an important monitoring network was located all around the underground facility in order to control the hydrogeological behaviour (fig. 3).

This network was composed of around forty monitoring points as shown in the following Fig. (piezometers, pumping wells and Seine river level).

For the post closure monitoring phase, several monitoring boreholes have been completed or abandoned.

Modeling and specific studies

During operation of underground storage, the hydraulic potential in the rockmass was higher than the cavern hydraulic potential and at that time the hydraulic gradients were directed towards the cavern. After the removing operations, the underground cavern was full of water and there was a modification of flow patterns around the cavern which do not seep into the cavern but go through the cavern and therefore lead to transportation of dissolved product.

Analytical and numerical modelling studies allowed to determine the distribution of the hydraulic potentials during these operations and to estimate the possible concentration of dissolved product at pumping well locations.

FEFLOW software was used (transient flow and mass transport considering free surface conditions). Modelling consisted of several steps and more specifically:

- a matching of the hydrodynamic parameters for the different considered layers in order to obtain an accurate distribution of the hydraulic potentials and
- a correct estimation of the seepage water compared to the operation measurements.

Migration of product by inversion of the flow gradients from the cavern is not taken into account according to the favourable hydrogeological situation during operation (hydrodynamic containment, hydrogeological monitoring, water seepage changes and water quality of undergroundwaters). An estimation of the potential quantity of product and of the propagation distance into the rockmass from the cavern walls were performed in order to quantify the pollution risk once the natural gradient is restored.

The main conclusions show that a limited quantity of dissolved product, around one

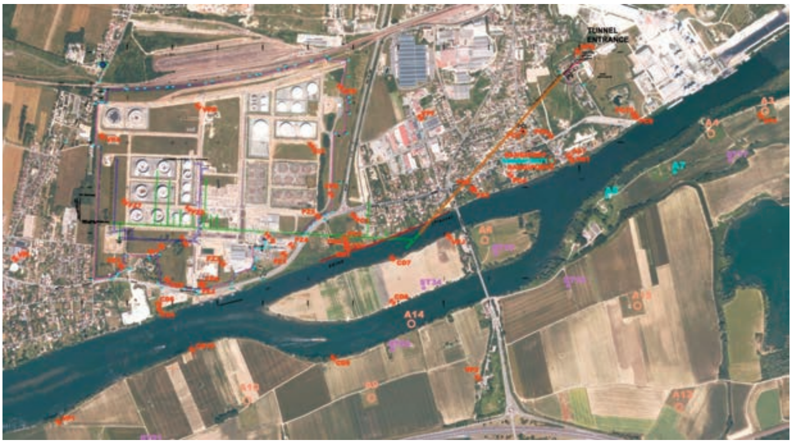

Fig. 3 *Monitoring point location and underground cavern location (green line for cavern)*

hundred kilogram, potentially moves into the aquifer and penetrates on several centimetres inside the rock mass. The impact on the drinking water wells will be negligible.

Post-closure and current situation

Once the closure works were ended, GEOSTOCK prepared an end of works file for the DRIEE. The technical file describes the various operations which were carried out. It was analysed by DRIEE in 2012 which resulted in the publication in December of a last Prefect’s order which gave GEOVEXIN notice of definitive works termination and maintained the follow-up of a set of reference parameters already imposed in the previous Prefect’s orders.

In particular, the supervision of the level of the groundwater and of the quality of surrounding waters of the storage was put into place (fig. 4).

The supervision of the work is effective since the end of 2011 but one should note that this takes place after technical follow-ups of the work which were carried out during the operation and then during the closure works. Indeed, a zero state of the gallery and piezometers water quality was already carried out at the end of the inerting operation. The program of supervision is thus an adaptation of the previous follow-ups of the cavern, and there has never been a break of the technical supervision of the work during all of the successive phases of its existence.

The supervision of the level of the groundwater is carried out by means of quarterly measures of the height of water in eight piezometers located around the storage and four wells in neighbouring potable drinking water fields. Two piezometers are also equipped with a daily recorder.

The supervision of the water quality consists of the analysis of the water taken from the eight surrounding piezometers, from the four wells of neighbouring potable drinking water fields and from the former storage gallery. These analyses are carried out every six months in periods of low waters and high waters and concern total hydrocarbons, methane, ethane, propane and butane. Mercaptans and BTEX (benzene, toluene and xylenes) are also analysed.

After two whole years of technical follow-up, the post-closure situation of the storage does not present any particular problem, whether it is from the hydrogeological or the chemical point of view.

References

Maury V (1977) An example of an underground storage in soft rock (chalk), Rockstore, September 1977, 681–689

Mégnien C (1979) Hydrogéologie du centre du bassin de Paris: contribution à l’étude de quelques aquifères principaux. Thèse Université Paris VI. Mémoires du BRGM Nº 98.

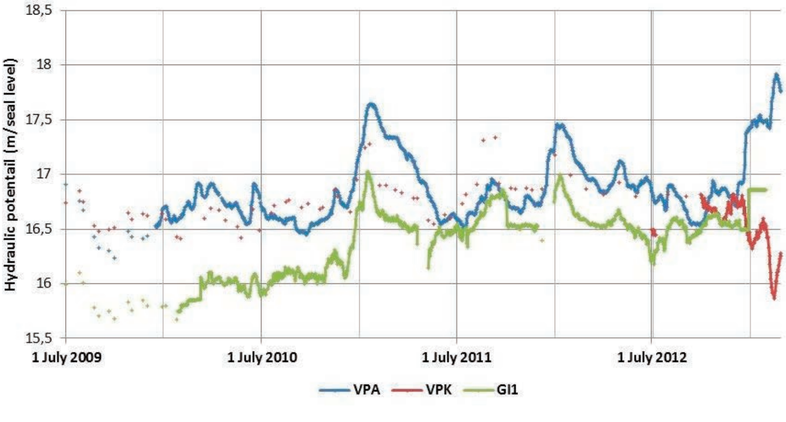

***Fig. 4** Variations of hydraulic potentials in some monitoring piezometers.*

Suitability of Central Utah's Navajo Sandstone for Disposal of Mined Hydrocarbon Water

Thomas LACHMAR[1], Kevin RANDALL[2]

[1]Utah State University, 4505 Old Main Hill, Logan, Utah, 84322, USA, tom.lachmar@gmail.com
[2]Geo Engineers Inc, 523 E 2nd Ave, Spokane, Washington, 99202, USA, kevinrandall@rocketmail.com

Abstract Water produced with coalbed methane in central Utah is disposed of primarily by injecting it into the Navajo Sandstone. High injection pressures have reversed the vertical hydraulic gradient from downward to upward, so the produced water may eventually mix with shallow groundwater. Three subsurface faults were identified, but shale smear factor calculations suggest that the fault sealing potential is high. Furthermore, chemical analyses of water samples from nine saltwater disposal wells and four shallow freshwater wells demonstrate that no mixing has occurred. Finally, the time estimated for the produced water to migrate to the surface is at least 2,000 years.

Keywords coalbed methane, water disposal, faults, hydrochemistry, Navajo Sandstone, Utah

Introduction

Coalbed methane is produced from the Ferron Sandstone in the Drunkards Wash, Helper and Buzzard Bench gas fields in central Utah (fig. 1) by pumping water from wells to lower the fluid pressure and cause methane to desorb from the coal, which then flows as a gas to the wells. Water from these three gas fields is very high

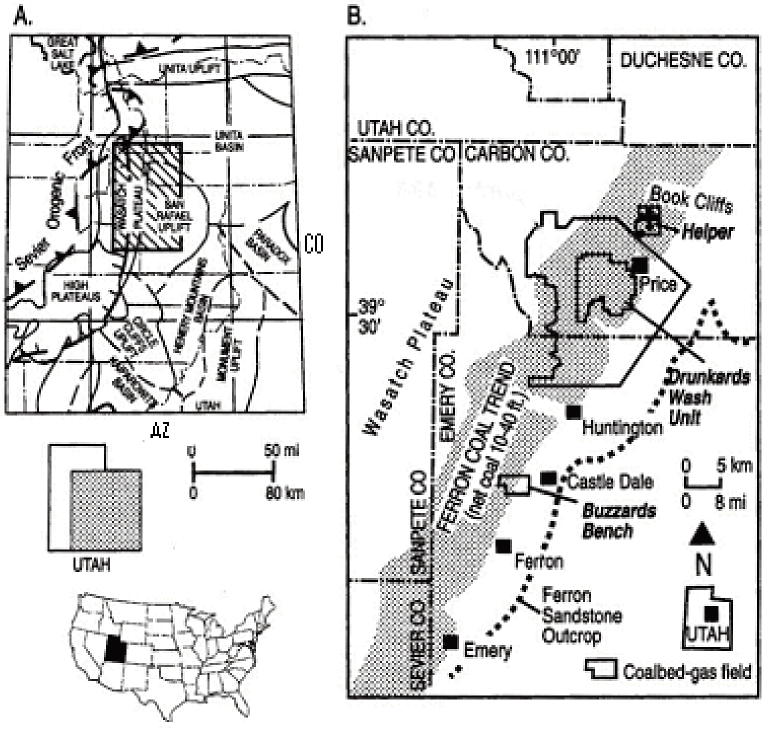

***Fig. 1** Location map of study area (A). Location map of the Drunkards Wash, Buzzard Bench and Helper gas fields (B) (Randall 2009).*

in total dissolved solids (TDS), especially sodium and chloride, and is disposed of by injecting it at depth, primarily into the Navajo Sandstone.

This research has been conducted to determine if the produced water is being safely sequestered from shallow groundwater. Structural data have been collected and analyzed to identify any subsurface faults. Chemical analyses of water samples from saltwater disposal wells (SWD) and shallow freshwater wells have been compared to determine if any mixing has occurred.

Methods

The structural analysis was accomplished using 418 digital well logs provided by ConocoPhillips in the Drunkards Wash gas field (fig. 2). Thirty-one east-west cross sections were constructed using the computer program PETRA to identify faults that displace sandstones at depth but not the shales overlying them. Gas and water production from faulted areas and areas where faults are thought not to exist have been compared as an estimate of the relative amount of fracturing.

The potential for clay as well as shale smearing for the faults also has been evaluated using an algorithm developed by Lindsay *et al.* (1993) called the shale smear factor (SSF). It is calculated by dividing the fault throw by the thickness of the clay/shale bed.

Nine SWD wells in the Drunkards Wash, Helper and Buzzard Bench gas fields were sampled because of their proximity to shallow freshwater wells (fig. 2). Two samples were collected from each SWD well and analyzed for: (1) major ions; and (2) the stable isotope ratios of deuterium (^{2}H) to hydrogen (D/H) and ^{18}O to ^{16}O (^{18}O/^{16}O).

Four shallow freshwater wells were also sampled (fig. 2), and were analyzed for major ions and the stable isotope ratios D/H and ^{18}O/^{16}O. The four wells are completed either in alluvium or the Upper Blue Gate Shale Member of the Mancos Shale.

Results

Three subsurface, north-south trending, downward to the west normal faults have been located in the Drunkards Wash gas field from the structural cross sections. An anticline has also been identified near the southern boundary of the gas field. These four structural features have been labeled alphabetically from north to south (fig. 3). Control areas where no faults are thought to exist have been designated adjacent to each faulted area (fig. 3).

The 24th-month average gas production per well and the maximum gas production of the highest producing well in the faulted and control areas are compared in Table 1, as are the average maximum water production per well and the maximum water production for the well with the highest production. The gas and water production data were obtained from the Utah Division of Oil, Gas and Mining (UDOGM) website (http://linux1.ogm.utah.gov).

The gas and water production data for the faulted and control areas have been compared using the Mann-Whitney nonparametric statistical test. Areas A, B and C show a statistically significant difference between faulted and control areas for both gas and water production. The probability of exceedence for gas production is <0.003 for area A, <0.0001 for area B and <0.001 for area C, whereas water production is <0.05, <0.0001 and <0.003 for areas A, B and C, respectively. This suggests that the faulted areas have higher fracture densities than their associated control areas.

The amount of throw for each fault has been measured from the offset of the beds shown on the cross sections. Fault throws range from a maximum of 40 m to a minimum of 3 m, both for fault B. Fault throws for faults A and C range from 33 to 5 m and 36 to 4 m, respectively.

Gamma ray logs for three wells, one each from areas A, B and C, were used to identify the net shale thickness along each fault. These three wells were selected based on their proximity to their respective faults, and the well log intervals chosen were selected specifically to

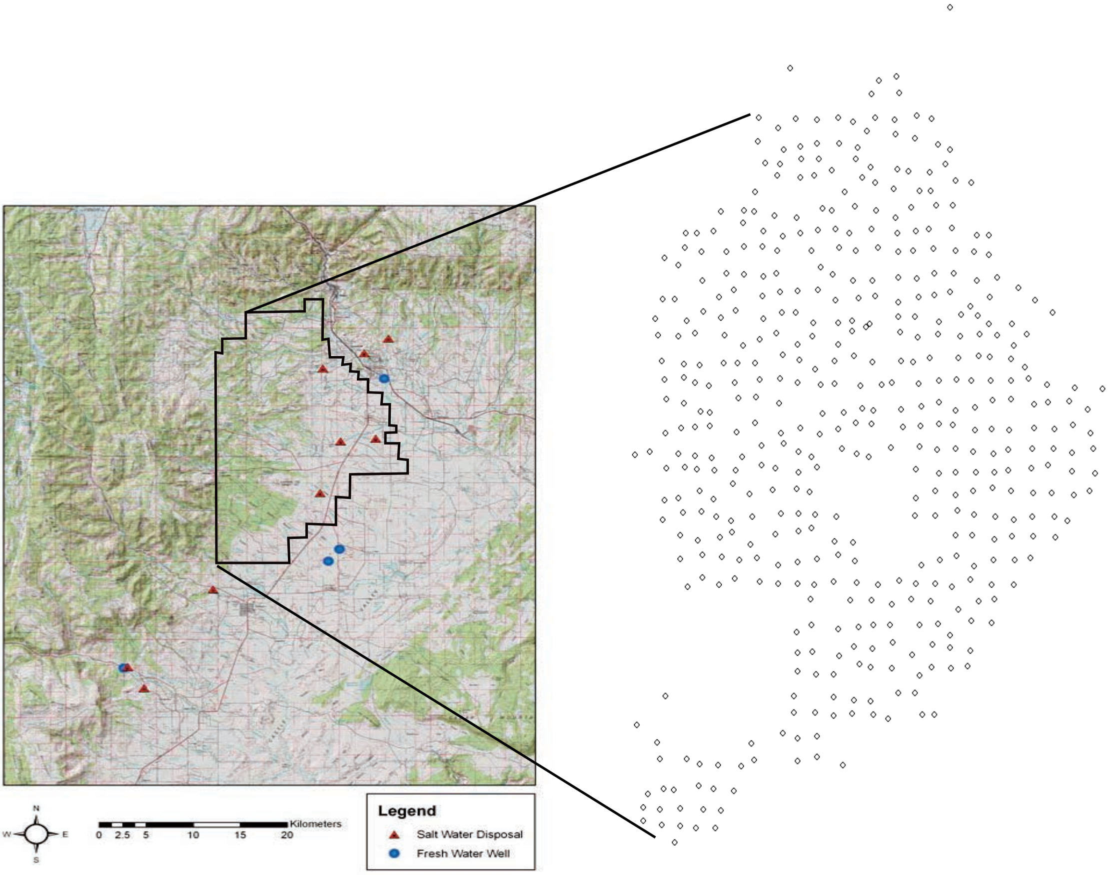

Fig. 2 *Map showing the locations of the four shallow freshwater wells, nine SWD wells, and the wells in the Drunkards Wash gas field used in the structural analysis.*

see the rocks above, below and within the Ferron Sandstone. Well logs were obtained from the UDOGM website.

The top 76 m of the log for the well in area A from 670 to 850 m has been identified as a single shale unit. The log for the area B well from 520 to 670 m shows 35 m of shale near the top and 23 m at the bottom; thus, a shale thickness of 58 m has been interpreted from this log. The top 116 m of the log for the area C well from 870 to 1,070 m appears to be almost entirely shales.

Calculated SSF values using the shale thickness and maximum throw for each faulted area are 0.43, 0.69 and 0.31 for areas A, B and C, respectively. Because the SSF values are all less than one, it can be presumed that the likelihood of fault sealing is quite high (Lindsay *et al.* 1993).

Concentrations of TDS, sodium and chloride for all nine SWD samples range from 4,278 to 14,244 mg/L, 2,400 to 4,106 mg/L and 1,117 to 9,974 mg/L, respectively, and are much higher than those for three of the four freshwater samples, which range from 843 to 1,595 mg/L, 117 to 225 mg/L and 69.1 to 94.6 mg/L, respectively. However, one freshwater sample has TDS, sodium and chloride concentrations of 11,337 mg/L, 3,382 mg/L and 7,619 mg/L, respectively, for TDS, sodium and chloride.

Delta D and $\delta^{18}O$ values for the SWD well samples range from -40 to -90 ‰ and from -1.3 to -9.9 ‰, respectively, and from -109 to -117 ‰ and -13.8 to -15.1 ‰, respectively, for the fresh-

Area	Number of Wells	Avg. 24th Month Gas Production/ Well (mcf)	Max. 24th Month Gas Production of Single Well (mcf)	Avg. Max. Water Production/ Well (barrels)	Max. Water Production from Single Well (barrels)
A	14	411	1,024	4,075	18,926
A-control	15	66	206	755	3,614
B	19	684	1,382	2,966	10,031
B-control	20	175	516	1,241	6,306
C	24	587	979	2,834	6,510
C-control	24	263	555	816	2,598

Table 1 *Summary of gas and water production for faulted and control areas.*

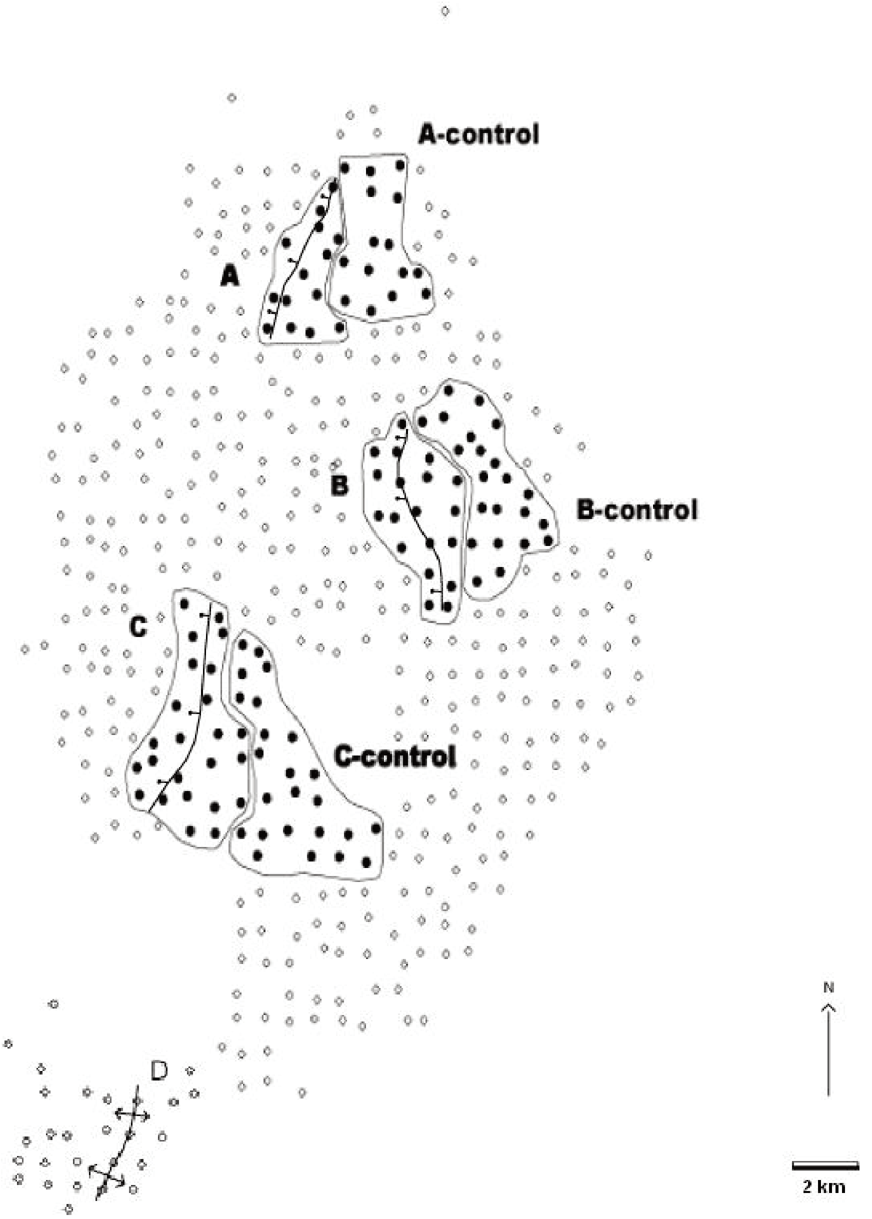

Fig. 3 *Faulted areas and associated control areas for gas and water production.*

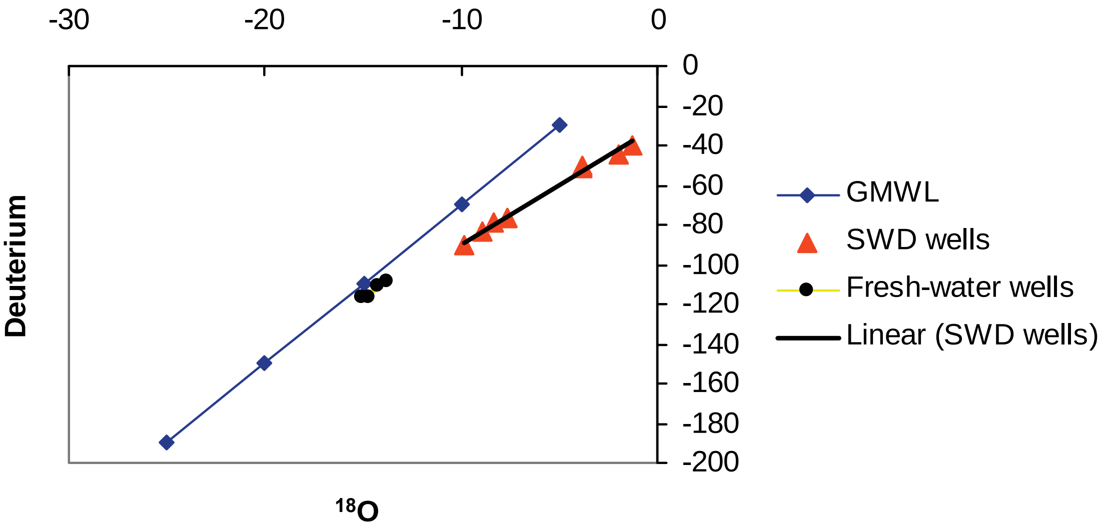

Fig. 4 *Delta D and δ*^{18}*O for SWD and shallow freshwater wells.*

water well samples. The four freshwater samples lie near the global meteoric water line (GMWL; fig. 4). However, the nine SWD samples plot far from the GMWL (fig. 4).

Discussion

The high TDS, sodium and chloride concentrations in the anomalous shallow freshwater well may be due to: (1) produced water mixing with shallow groundwater along a nearby fault; or (2) the well being completed in a formation that contains high concentrations of soluble salts. This well is completed in the Upper Blue Gate Shale Member of the Mancos Shale. Lines and Morrissey (1983) stated that water in the Blue Gate contains about 20,000 mg/L of TDS. Chemical analyses have also been done for two shallow freshwater wells identified as being completed in the Mancos Shale. One well is completed in the Blue Gate Member and has a TDS concentration of 4,040 mg/L (Waddell *et al.* 1978). The other well is only listed as being completed in the Mancos and has a TDS concentration of 6,964 mg/L (Sumison 1979).

Isotope data for D and ^{18}O are unambiguously distinct for the two types of water samples (see fig. 4). This provides additional evidence that the Upper Blue Gate Shale is the most likely source of the high TDS, sodium and chloride concentrations in the anomalous shallow freshwater well.

Injection of produced water has reversed the vertical hydraulic gradient from downward to upward. Reversal of the vertical hydraulic gradient may eventually cause the produced water to migrate upward and mix with shallow groundwater, and ultimately reach the surface.

The time required for the produced water to migrate from the Navajo Sandstone to the Upper Blue Gate Shale member of the Mancos Shale has been estimated by Randall (2009). The time estimated is approximately 730,000 days, or 2,000 years.

Conclusions

Three faults have been identified in the Drunkards Wash gas field. Wells in all three faulted areas produce more gas and water than wells in their respective control areas, presumably due to higher fracture densities. However, SSF calculations indicate that the likelihood of fault sealing is quite high.

Three of the four shallow freshwater wells sampled have low TDS, sodium and chloride concentrations, demonstrating that no mixing is occurring. The high concentrations for the fourth well are due to the dissolution of soluble minerals in the Upper Blue Gate Shale Member of the Mancos Shale.

Delta D and $\delta^{18}O$ values for the four shallow freshwater wells plot near the GMWL (fig. 4), indicating that meteoric water is the most likely source of recharge. However, all nine SWD wells plot far from the GMWL (fig. 4), implying that they have a different recharge source.

Because high injection pressures have reversed the vertical hydraulic gradient from downward to upward, mixing of produced water with shallow groundwater may eventually occur. However, the amount of time required for the produced water to migrate from the Navajo Sandstone to the Upper Blue Gate Member of the Mancos Shale is approximately 2,000 years, much longer than the life of the gas field.

References

Lindsay NG, Murphy FC, Walsh JJ, Watterson J (1993) Outcrop studies of shale smears on fault surfaces. surfaces. Spec Pub of the Int Assoc of Sed 15:113–123

Lines GC, Morrissey D J (1983) Hydrology of the Ferron Sandstone aquifer and the effects of proposed surface-coal mining in Castle Valley, Utah. USGS Water-Supply Paper 2195, Washington, DC

Randall KL (2009) A geologic and hydrochemical investigation of the suitability of central Utah’s Navajo Sandstone for the disposal of saline process water and CO_2. MS Thesis, Utah State Univ, Logan, Utah

Sumsion CT (1979) Selected coal-related groundwater data, Wasatch Plateau-Book Cliffs area,Utah. USGS Open-File Report 79–915, Utah Hydrologic Data Report 32, Salt Lake City, Utah

Waddell KM, Contratto PK, Sumison CT, Butler JR (1978) Selected hydrologic data from 1931–1977 of the Wasatch Plateau-Book Cliffs Coal-Fields area, Utah. USGS Open-File Report 78–121, Utah Basic Data Release 31, Salt Lake City, Utah

High Density Polyethylene (HDPE) Lined Produced/Flow-back Water Evaporation Ponds

Neil C. Nowak[1], John Briest[2]

[1]*Weaver Boos Consultants, LLC, 7340 East Caley Ave., Centennial, CO, 80111, USA, nnowak@weaverboos.com*
[2]*Weaver Boos Consultants, LLC, 7340 East Caley Ave., Centennial, CO, 80111, USA, jbriest@weaverboos.com*

Abstract The problem to be solved is the disposal of millions of liters (gallons) of production water and flow-back water generated annually from the Rocky Mountain Region oil and gas industry in an environmentally safe, low cost, and efficient manner. One such technology used is the evaporation of the water in lined containment ponds after separation and removal of the hydrocarbon component from the water. Three projects in Cisco, Utah; Dad, Wyoming; and Cheyenne, Wyoming as case studies were designed to evaporate water in a series of geomembrane lined ponds. The projects use high density polyethylene (HDPE) as the top layer to help protect the groundwater, and enhance evaporation.

Keywords Evaporation Ponds, Evaporation, Impoundments, Produced Water, Geomembrane

Introduction

The three projects are complete and have been operational for a number of years. The production and flow-back water from oil and gas wells in the area local to each site is trucked to the sites for disposal. The water is evaporated in ponds lined with high density polyethylene (HDPE) as the top liner by using a combination of factors that are favorable to the evaporative process, including the following:

- Natural characteristics of the site, including the arid climate, windy conditions, and numerous sunny days,
- The top layer in the ponds is black HDPE, which creates a hot surface hence evaporation is enhanced,
- HDPE liner was chosen to protect the surface and groundwaters of the area; it is durable and chemical resistant.

Also, these sites are favorable due to other factors, such as, remoteness from populated areas, accessible from highways for trucks, far depth to groundwater, and geology.

The projects provide oil and gas production companies in the area with a large commercial alternative to production water and flow-back disposal versus numerous small ponds that may service only one well pad, or expensive re-injection wells, or even more expensive water recycling or treatment facilities. The regulatory agencies are favorable to these type commercial facilities for centralization and protection of the state's waters. The facilities protect surface waters in the area due to the liner, large capacity of the ponds, and the freeboard that is above the maximum water level, which is 0.61 m (2 ft; Utah) and 0.91 m (3 ft; Wyoming). Also, secondary containment is used in case of catastrophic berm failure in Utah.

Project Location – Silo Field, Cheyenne, WY

The project is located in a semi-arid region of southeastern Wyoming in Laramie County, which is situated at approximately 1,738 m (5,900 ft) above mean sea level (amsl). The site is located above the High Plains Formation underlain by Pierre Shale at approximately 1,737 m (5,700 ft) thick which is dominant throughout the region. The primary aquifer includes the High Plains Aquifer, consisting of the Ogallala, Arikaree, and White River formations, which total approximately 451 m (1,480 ft) thick. The Ogallala is the first instance of usable groundwater at approximately 48.8 to 91.4 m (160 to 300 ft) below the site.

Climatological Data

According to the U.S. Department of Agriculture (USDA) Natural Resources Conservation Service (NRCS) map, the average annual precipitation is 38.1 cm (15.17 in). The National Weather Service developed an isopleths map of the Free Water Surface Evaporation (shallow lake evaporation) based on 24 years of data. The free water surface evaporation rate is the amount expected to evaporate from the disposal ponds, which is 114.3 cm (45 in) per year. Approximately 88.9 cm (35 in) of that rate occurs from May to October. The remaining 25.4 cm (10 in) would evaporate from November to April. This is based on a water containment that is not lined with black HDPE.

Project Location – Danish Flats, Cisco, UT

The project is located in an arid region of eastern Utah in the area known as Danish Flat, which is situated at approximately 1,405 m (4,610 ft) amsl. The site is located in the Mancos Shale lowland area including the Greater Cisco area. The Mancos Shale Formation is the predominant outcrop in this area. Due to the preponderance of fine-grained sediments and water soluble minerals found in this formation, it does not usually contain any fresh water. Groundwater that comes in contact with the Mancos Shale Formation almost always contains high levels of dissolved solids. Groundwater is usually limited to alluvial deposits along streams and drainages or to sandstone units, some of which are very localized with low recharge rates. Wells in the area are usually drilled with air and little or no water encountered until the Dakota Formation is penetrated (Hunt 1996).

The underlying Mancos shale is a dark grey to black soft shale with sandstone beds at various horizons. The maximum thickness of the Mancos shale is approximately 274.3 to 304.8 m (900 to 1,000 ft). The Mancos shale is considered a confining unit and provides a thick barrier to vertical and lateral groundwater flow. Below the Mancos shale is the lower to upper Cretaceous Dakota Sandstone, which are a yellow-brown and gray friable to quartzitic sandstone and conglomerate sandstone and interbedded gray to black carbonaceous shale with occasional lenticular coal beds (Cashion Map I-736). The Dakota Sandstone is considered to be the first encountered or shallowest aquifer in the area.

Climatological Data

According to the U.S. Department of Agriculture (USDA) Natural Resources Conservation Service (NRCS) map, the average annual precipitation is 15.2 cm (6 in). The National Weather Service developed an isopleths map of the Free Water Surface Evaporation (shallow lake evaporation) based on 24 years of data. The free water surface evaporation rate is the amount expected to evaporate from the disposal ponds, which is 127 cm (50 in) per year. Approximately 88.9 cm (35 in) of that rate occurs from May to October. The remaining 38.1 cm (15 in) would evaporate from November to April. This is based on a water containment that is not lined with black HDPE.

Project Location – Southern Cross, Dad, WY

The project is located in a semi-arid region of southwest Wyoming in the area known as Mexican Flat, which is situated at approximately 1,993 m (6,540 ft) amsl. The site is located in the Wasatch/Claron Formation. The Claron Formation also referred to as the “Pink Cliffs,” and forms the highest “step” of the Grand Staircase. This formation is also known as the Wasatch Formation. The site is located in the Cathedral Bluffs Tongue of the Wasatch Formation. This outcropping consists of claystone, mudstone and sandstone. The field investigation and laboratory analysis confirmed the published description to the depth of the deepest boring. The only known groundwater is at a depth of approximately 213.4 m (700 ft) based on a recent boring on the north side of the property.

Climatological Data

According to the U.S. Department of Agriculture (USDA) Natural Resources Conservation Service (NRCS) map, the average annual precipitation ranges between 25.4 and 30.5 cm (10 and 12 in). The National Weather Service developed an isopleths map of the Free Water Surface Evaporation (shallow lake evaporation) based on 24 years of data. The free water surface evaporation rate is the amount expected to evaporate from the disposal ponds, which is 114.3 cm (45 in) per year. Approximately 88.9 cm (35 in) of that rate occurs from May to October. The remaining 38.1 cm (15 in) would evaporate from November to April. This is based on a water containment that is not lined with black HDPE.

Methods

The main purpose of the projects is to evaporate the production water and flow-back water as quickly as possible while maintaining environmental controls and containment. The projects were planned and built in order to service the oil and gas industry for the disposal of production water and flow-back water from oil and gas production in the service areas local to each facility. Several water disposal options exist, including reinjection wells, frac injection, treatment for surface discharge, and evaporation. The evaporation technology was chosen for these projects due to the ideal site conditions for evaporation, including low precipitation, windy conditions, high ambient temperatures and solar radiation. Other factors that made the project sites ideal include the following; little or no residences within several kilometers (miles) of the site (other than consenting land owners), easy access to/from a major highway, long distance to open water at several kilometers (miles), deep groundwater, and relatively impermeable formations below the sites.

Selection of Technology: To enhance the evaporative quality of the projects and to adequately contain the production water, the primary/top layer of the pond lining needs to be a durable long-lasting material that is cost-effective and helps to enhance evaporation while being acceptable to the regulatory agencies involved. Some of the liner technologies considered include compacted clay, geosynthetic clay liner (GCL), polyvinyl chloride (PVC), polypropylene (PPE), and high density polyethylene (HDPE). While several lining technologies are allowed by the regulatory agencies, the HDPE liner was chosen for the top layer for several reasons, including, durability, resistance to ultraviolet (UV) degradation, chemical resistance, black color, and ease of construction.

The design properties of HDPE make it acceptable to be the primary/top layer of ponds. This material can be exposed to the elements (sun, freeze/thaw, and physical impact), therefore, the material needs to be resistant to UV degradation and be durable. The addition of the proper amount of high quality carbon black to the geomembrane during manufacturing is universally accepted as making the HDPE more resistant to significant deterioration caused by weathering. In addition to high quality carbon black, highly effective chemical UV stabilizers further extend the life of the liner, which is estimated to be approximately 20 years. These additives absorb incident radiation as well as terminate free radical production, thus protecting the HDPE against thermal degradation and possible chemical reactions with surrounding materials. Other factors that affect the potential UV resistance of a material include average density, density range or dispersion, chemical stabilizer system, catalyst type and amount of residue, copolymer type, combined chemical exposures, and failure criteria (GSE 2003). An existing study was conducted on an HDPE liner installed at a site in Colorado after 20 years of service where the liner was not buried and exposed to weathering, UV light and power plant cooling tower blow-down water. The material was tested for various properties and was found to have no significant reduction in the primary physical properties of the HDPE (Ivy 2002).

To enhance the evaporative quality (*i.e.* pan rates versus actual) of each facility, and to adequately contain the brine water, high density polyethylene (HDPE) was chosen as the top layer. The top/primary liner was designed with 1.5 mm (60 mil) thick textured HDPE to help ensure a durable long-lasting containment. The liner was textured to increase the safety factor for personnel using the facility (*i.e.* the textured surface increases traction and gripping to enable easier egress in case of someone falling into the pond). The facilities generally consist of the following components:

- Access road and truck off-loading pad,
- Piping and valves,
- Acceptance Pits (vaults) or advanced oil/water separation equipment,
- Sludge Pond covered with bird control netting at Danish Flats and Southern Cross, or no sludge pond, if advanced oil/water separation equipment used at Silo Field,
- Evaporation ponds (constructed or planned):

1. Silo Field, WY has 3 ponds out of the permitted 10 ponds in the process of being built at approx. 2.1 ha (5.2 ac) each and 7.6 m (25 ft) deep (double lined HDPE with leak detection in between the liners) with a water holding capacity and nearly 922 ML (24 Mgal) each for a total water holding capacity of approximately 277 ML (73 Mgal).
2. Danish Flats, UT has 14 ponds built at approx. 2.1 ha (5.2 ac) each (single HDPE liner underlain by compacted clay layer) shallow 3.7 m (12 ft) deep ponds 1–8 with nearly 38.2 ML (10 Mgal) each for a total capacity of approximately 317.9 ML (84 Mgal). Ponds 9 through 13 are 6.7 m (22 ft) of water holding depth and nearly 100.5 ML (26.5 Mgal) each for a total capacity of 502.4 ML (132.7 Mgal).
3. Southern Cross, WY has 4 ponds built at approx. 2.1 ha (5.2 ac) each and are 3.7 m (12 ft) deep (double lined HDPE with leak detection in between the liners) have 3.7 m (12 ft) of water holding depth and nearly 38.2 ML (10 Mgal) for a total capacity of approximately 152.6 ML (40.3 Mgal).

General Production water and flow-back water is delivered to the facilities via tanker trucks from well sites located within the geographic area local to each disposal facility, and dilivery depends on transportation costs and disposal fees when compared to other alternatives for water disposal in the area. The tanker trucks are off-loaded and the water is sent through an oil/water separation process, including separation vaults, gun-barrel tanks, or state-of-the practice treatment equipment. Shut-off valves have been installed on the crossover piping to allow for proper flow management. If necessary, portable gasoline powered pumps are used to transfer liquid to ponds that are not in the gravity flow line or to empty a pond for maintenance or liner repair. At Danish Flats and Southern Cross the sludge ponds and evaporation ponds have an interior slope of 3 horizontal to 1 vertical, and a maximum exterior slope of 2 to 1. At Silo Field, the pond interior and exterior slopes were designed with 4 to 1 slopes. The varying slopes are due to soil subgrade stability based on soil geotechnical characteristics.

Berm Design Surface water will not be allowed to enter the ponds because the constructed berms are several feet higher than the surrounding ground surface. Also diversion and control ditches are used to direct the run-on and control run-off for minimizing impact of storm water. The interior berm walls are covered with the liner system. The HDPE provides erosion control.

Leak Detection System Each site has a 1.5 mm (60 mil) thick HDPE primary liner installed as the top layer in all of the ponds. The pond floors slope toward sumps that are fitted with a riser monitoring pipe and leak detection equipment to monitor leaks through the primary liner. Double liners are installed at Silo Field and Southern Cross, and a single primary liner at Danish Flats. The leak detection system is inspected monthly and data recorded as required. A summary of the inspections are reported to the regulatory agencies on an annual basis, unless excessive water quantities in the leak sump indicate large leaks(s). Liquid from the sump can be pumped back into the pond, if excessive amounts accumulate then specific protocols for repairing the liner in place (*i.e.* the ponds need to be emptied to point of the liner leak) are required if the volume of the leak exceeds certain thresholds, such as, greater than 3,785 (L/d)/ha (400 (gal/d)/ac) of liner.

Project Results As an example, the Danish Flats data is presented in this results section. The partially completed and partially operational project at Danish Flats was photographed from the air on June 29, 2009 and is shown in Fig. 1 above. The water is distributed from the truck offloading area through the sludge pond to the evaporation Ponds 1 through 13, which appear as "black". Currently, 14 evaporation ponds are operational at Danish Flats.

In Cisco, UT in July and August the ambient air temperatures often exceeds 37.8 °C (100 °F) and it is the windy. The actual evaporation during the months of July and August 2008 at the site was estimated to be approximately 38.1 and 45.7 cm (15 and 18 in) per month, respectively. The facility operators observed very favorable evaporation of the water and measured the total evaporation for the year 2008 above the estimate of 127 cm (50 in) during approximately 6 months of operation. In year 2009, the Danish Flats facility was estimated to have 152.4 cm (60 in) of evaporation, which took place mostly in the months from April 1 to October 31, and again in year 2010 the evaporation total has exceeded 152.4 cm (60 in) over the entire water surface of the ponds. The deeper ponds at Danish Flats experienced an approximately 30 % lower evaporation rate due to the deeper water depth and the entire depth of water not able to be achieve warmer temperatures as did the shallower ponds. The water level in the ponds was estimated by site personnel with tape measure and the change in water level recorded over time.

In an effort to increase evaporation with low costs in mind at Danish Flats and Southern Cross, a "weep" system was added to the allow pumped water from the ponds to flow and fan out over the surface of the HDPE liner that is above the water line (*i.e.* within the freeboard liner area on the berms). This system utilizes the exposed HDPE liner to increase evaporation by using the heat generated from the exposed HDPE liner in combination with the increased surface area of the water fanning out as sheet-flow over the liner.

Additional: Some of the liner was installed during the summer months and due to the expansion and contraction of the liner with am-

Fig. 1. *Aerial Photo of Completed Project at Danish Flats, UT*

bient air temperature gradients, the anchor trenches were only filled during the coolest part of the day to reduce bridging. The leak detection system is used to capture leaks through the primary liner, which worked as designed at the Danish Flats site when a leak was propagated due to ice on the water and the level in the ponds changing which resulted in the ice grabbing onto the pipe and pulling on the pipe boot. The liner was repaired and the leak did not appear again.

Conclusions

The use of HDPE as the primary liner in the ponds appears to be favorably enhancing the evaporation of the water. At Danish Flats, the estimate of 127 cm (50 in) of evaporation per year was far exceeded given the 83.8 cm (33 in) of evaporation experienced in only July and August 2008, which may have totaled 177.8 cm (70 in) for 2008. In years 2009 and 2010, the evaporation rate was over 152.4 cm (60 in). In 2012, the evaporation rate was 106.7 cm (42 in) from May through August.

The "weep" system was an enhancement to increase evaporation, which was not quantitatively measurable, but was a factor with increasing the total evaporation. The deeper ponds at Danish Flats experienced approximately a 30 % lower evaporation rate due to cooler water at depth. Similarly, the actual evaporation experienced at the Southern Cross project was also more than the pan evaporation estimate based on ponds without the HDPE liner effects, including the increase in evaporation from the estimate of 114.3 cm (45 in) per year to nearly 139.7 cm (55 in). It is anticipated that the evaporation rates at Silo Field will also be enhanced with the use of the HDPE liner as the top layer and the use of the "weep" system along the exposed liner too.

The durability and resistance to UV degradation due to the proper amount of carbon black in the geomembrane and other factors as discussed above are the major reasons for the use of the HDPE geomembrane liner as the top layer. The increase with the rate of evaporation due to the black color of the HDPE has been a great benefit and in combination with the "weep" system has realized an increase with the total evaporation at each facility.

Acknowledgments

Thank you to R360 Environmental Solutions/ Waste Connections, Danish Flats Environmental Services, and Southern Cross Environmental Services for the use of their projects in this paper and to John Heap of Colorado Lining, Inc. who provided his installation expertise and also performed the construction of the HDPE liners at the ponds in field, which all are performing exceptionally well and without leaks due to construction.

References

Cashion WB. Geologic and Structure Map of the Grand Junction Quadrangle, Colorado and Utah, USGS Miscellaneous Geologic Investigations, Map I-736.

Gundle/SLT Environmental, Inc (GSE) (2003) Technical Note – HDPE, UV Resistance for GSE Geomembranes

Hunt GL (1996) Environmental Handbook, Environmental Regulations for the Oil & Gas Exploration and Production Industry.

Ivy N (2002) HDPE geomembrane after 20 years of service, GFR Magazine June/July 2002.

Addressing Legal, Regulatory, and Risk-Allocation Challenges for Water Reuse in Hydraulic Fracturing

Diane Elizabeth O’Neil

Weber Law Firm, LLC, 1580 Lincoln St., Suite 1280, Denver, CO 80203

Abstract Oil and gas producers have been reusing the water co-produced with oil and gas in their subsequent operations for years. Now they are also implementing produced water sharing arrangements among producers in nearby areas allowing them to share water resources. These arrangements maximize water usage and minimize waste, but the specific details of these arrangements must be well-defined and expressly stated to ensure compliance with applicable laws. Once the producers have addressed the legal challenges associated with the implementation of the sharing arrangement, they may use the basic framework to incorporate other unconventional water sources into the producer’s operations.

Keywords hydraulic fracturing, legal and regulatory, produced water, water sources

Introduction

With water becoming an increasingly precious resource, particularly here in the arid Rocky Mountain West, produced water in oil and gas operations is transitioning from a nuisance to a valuable resource. As demand for water increases for hydraulic fracturing operations while available supplies decrease due to drought conditions and other demands for water, oil and gas producers are paying greater attention to their own water use throughout their operations. As a result, the reuse of water co-produced with oil and gas in a producer’s subsequent operations has emerged as a best practice in the industry. In addition, flowback water obtained from the return of fluids following hydraulic fracturing stimulation is also commonly recycled and reused in subsequent stimulations. Unfortunately, recycling and reuse of a producer’s own water is not always feasible if timing it not right or the producers well locations are not nearby. Consequently, oil and gas developers have started identifying potential new and unconventional water sources for use in their operations including, for example, produced water sharing arrangements.

Two producers in Colorado have created and received regulatory approval on, a unique produced water sharing arrangement (“Sharing Arrangement”) where they have agreed to transfer volumes of produced as well as flowback water (collectively “Production Water”) to one another, on an as needed as requested basis, based on availability and proximity of the Production Water to the individual producer’s needs. The Sharing Arrangement has a number of potential significant benefits including, for example, minimizing truck traffic, shorter haul distances for transport, fewer fresh water withdrawals, and less reliance on injection wells for ultimate disposal. While the possibility of exchanging Production Water between the producers allows for more efficient use of the water resource because the producers have more water potentially available to them in an area, the actual implementation of the Sharing Arrangement brought significant legal, regulatory, and risk-allocation challenges.

The producers addressed these challenges by entering into a legally binding, comprehensive Produced Water Transfer Agreement (“Transfer Agreement” or “Agreement”) articulating the terms of the Sharing Arrangement prior to transferring any water. By entering into this Transfer Agreement and making a basic framework of the Agreement available to the public (via submittal to the applicable regulatory agency), the producers proactively addressed the potential problems and provided assurances to the applicable regulatory bodies that they will implement the Sharing Arrangement reasonably and responsibly.

Produced Water Transfer Agreement:

The Transfer Agreement is the contract between the parties, which documents and controls the Sharing Arrangement addressing the associated operational and legal concerns. This includes, for example, defining the allowed origin(s) of the water, required minimum water quality, and maximum transferrable quantities. In addition, it articulates the purposes behind the parties entering into the Agreement in support of the public initiatives and regulatory agencies' targets related to conservation of resources and waste minimization. The Agreement also establishes the procedures the producers will follow to initiate and effectuate transfers of Production Water.

In addition to the technical and operational requirements, the Transfer Agreement also addresses the regulatory agencies' concerns, ensures compliance with applicable laws and regulations, and allocates liabilities and obligations between responsible parties. Because the production, use, and consumption of water are highly regulated activities and of substantial public concern, it is very important that the Transfer Agreement addresses compliance with applicable laws and regulations in significant detail, and clearly designates which party is responsible in the event of a problem.

Finally, the Agreement includes a Record of Transfer document, as an exhibit to the Agreement, which serves as the template for record keeping under the Agreement as required by the agencies having jurisdiction over the transfers. A number of the key terms and provision of the Transfer Agreement are discussed in more detail below to better demonstrate how the specific operational challenges and legal requirements were addressed within the document.

Key Provisions of the Transfer Agreement:

Water Type/Source Identifying the original source and confirming the producer's right to use and consume the Production Water within the Transfer Agreement is vital to the success of the Sharing Arrangement. A producer's right to use, consume, and transfer water produced in its operations varies from state to state, and may even differ in different areas of the same state (See generally Thorne 2013). Therefore, the specific rights of each producer in the Sharing Arrangement, as well as the acceptable origin(s) of the water being transferred pursuant to the applicable state law, are specifically described within the Transfer Agreement.

As an example of the level of specificity that may be required to ensure compliance with state water law, consider the following. In Colorado, where the Sharing Arrangement is taking place, only nontributary water may be produced from oil and gas operations without a permit from the Colorado State Engineer (Colo. Rev. Stat. § 37-90-137(7) (2012)). As a result, in order to facilitate oil and gas development and minimize the administrative burdens on the Colorado State Engineer's Office, the Office designated areas of the state where the produced water is known to be nontributary thereby eliminating the need for a permit in these designated areas (Produced Nontributary Groundwater Rules 2 C.C.R. 402–17 (2010)). Because the Sharing Arrangement is within a nontributary designated area, the Transfer Agreement includes a provision stating that only nontributary water may be transferred as part of the Sharing Arrangement as neither producer has a permit for the production of tributary groundwater. In addition to the legal distinctions between tributary and nontributary groundwater, a Colorado Court has also distinguished water produced from coalbed methane wells from other oil and gas wells (Vance v. Wolfe, 205 P.3d 1165 (Colo. 2009)). Therefore, in order to ensure the parties are in compliance with Colorado water law, the Transfer Agreement also states that only water produced from noncoalbed methane wells can be transferred as a part of the Sharing Arrangement.

Below is a sample provision, similar to that which is included in the Transfer Agreement, identifying what type of water can be produced (nontributary and noncoalbed methane), and the noting each party's obligation to adhere to the specific water laws and regulations (note that the representations and warranties included in this provision are also discussed in more detail below):

> *"**Usage** The Transferor warrants and represents that it has the right to use and consume all of the water to be delivered to the Transferee and that such water will come from non-coalbed methane wells determined to be non-tributary in accordance with applicable laws and regulations. In addition, the Transferor warrants and represents that it has complied with all permitting and other legal requirements concerning its water, including but not limited to any requirements from the Colorado State Engineer's office.*

Water Quality Establishing the minimum water quality required for the Production Water to be transferrable is key not only to ensure adherence to applicable laws and regulations, but is also vital to ensure the beneficial purpose of the Sharing Arrangement is realized. Because water quality in produced water sources can vary dramatically among producing formations and or locations within the same basin, and because the quality of the water used in fracture stimulation may affect the other chemicals used, it is important that the quality of the Production Water is characterized and documented prior to its transfer. Importantly, the detailed description of the water quality must occur for each specific transfer. Therefore, the Transfer Agreement establishes a basic minimum water quality threshold for all Production Water transferred under the Agreement, and further accommodates for the exchange of additional information for each specific water transfer. The Transfer Agreement requires a minimum threshold quality of "a quality that can be reused for fracture stimulation," and obligates each producer to execute a Record of Transfer (as discussed in more detail below), to be completed for each individual transfer, detailing the specific quality of the actual Production Water being transferred.

Furthermore, the Water Quality provision in the Transfer Agreement also provides for instances where the transferring party may be required to treat the Production Water prior to the transfer. If the producer has Production Water available to be transferred, but it is not of a quality that can be reused for fracture stimulation, that producer is required to perform basic treatment the Production Water (*i.e.* adding bactericide and separating out solids) prior to the transfer under the terms of this Transfer Agreement. Note that while the producer may be required to perform basic treatment on its Production Water prior to transfer, it is not required to perform treatment beyond what is commercially reasonable.

Water Quantity In addition to the specific water quality, the Record of Transfer will also note the amount of Production Water being transferred. However, while the producers must record the actual amount of Production Water transferred on an individual Record of Transfer, a provision of the Transfer Agreement must also clarify when and if either producer has an obligation to transfer Production Water to the other producer. Based on the agreement between the parties of this specific Sharing Arrangement, any transfer made under the terms of the Transfer Agreement are to occur solely on an as needed as requested basis; provided however each producer has an obligation to use commercially reasonable efforts to provide the Production Water requested. Furthermore, neither party has the obligation to equalize or balance the number of transfers or amount of Production Water transferred between the producers. Therefore, the Water Quantity provision in the Transfer

Agreement formalizes the cooperative nature of the Agreement without creating binding transfer obligations, and further clarifies that the intent of the Sharing Arrangement is to provide a mechanism for water reuse between producers when the logistical considerations warrant without imposing difficult and costly obligations.

Compensation; Costs and Expenses As with most commercial arrangements, allocating the costs and expenses associated with the Sharing Arrangement are confidential business decisions that the parties negotiated based on the specific economics of their operations in a geographic area. Therefore, the actual fees assessed under the Sharing Arrangement remain confidential between the parties. However, it is important for purposes of this paper to note that any similar agreement should identify the costs and expenses associated with the transfer of water and should allocate these costs and expenses between the parties within the terms of the controlling agreement. For example, the Transfer Agreement determines which party (either the transferring or receiving party) is responsible for the out-of-pocket expenses associated with the transfer of Production Water (*e.g.* transportation costs, water quality testing). It also notes that the expenses associated with the transfer of the Production Water may be, at least partially, off-set by the expense the producer would have to pay to transport and dispose of the Production Water if the Production Water was not transferred to the other producer.

In addition to the actual costs and expenses incurred, the Transfer Agreement acknowledges the nonmonetary benefits of reusing the Production Water for an additional beneficial use rather than discarding it as waste. These nonmonetary benefits are become increasingly important as the value of conservation and reuse of resources continues to be acknowledged, and in some cases even required, by the regulatory agencies having jurisdiction.

Risk Allocation within the Transfer Agreement:

Some of the most important provisions of the Transfer Agreement deal with the assessment and allocation of risks between the parties. Due to the intricacies of the laws and regulations controlling oil and gas development and water resources, it is extremely important to clearly outline each party's duties and obligations, as well as identify which party is responsible at each stage of the transferring process in the event a problem arises. The Transfer Agreement addresses the allocation of risks through various contract clauses including Custody Transfer, Representations and Warranties, and Compliance with Laws.

Custody Transfer The physical and legal point or points at which the Production Water transfers from one producer to another have significant implications as to each party's liabilities and ongoing obligations. It is extremely important that a specific legal point of transfer is clearly identified, and the transition of obligations and responsibilities as between the parties are expressly described within the Agreement both pre and post transfer. In the Transfer Agreement, the parties agreed they would record the specific point of transfer on the Record of Transfer, but the point of transfer was generally understood to be the exact physical point when custody and control of the Production Water was transferred to the receiving party or its designee as well as the legal point of custody transfer. The Transfer Agreement then goes on to state that the party having legal custody and control of the Production Water shall be the party with primary responsibility for any spills or releases of the water, including notifications and clean-up, if and as applicable. Because the liabilities between the parties are different before and after the transfer takes place, the legal point of transfer must be a clearly identifiable point in time in order to determine which party is the responsible party in the event of a problem.

Representations and Warranties Representations and warranties within contracts are statements that the representing party is confirming as true and accurate, and therefore, the other party may rely on the representation. For that reason, the representations and warranties made in the Transfer Agreement (as is the case in most agreements) are limited to only those representations and warranties that are essential for the parties to enter into the agreement. For example, the parties represented and warranted in the Transfer Agreement that the transferring party has the rights necessary to use and consume any water being transferred under the Agreement (see the sample Usage provision provided above). Because a party can only transfer rights it possesses, it is imperative that each party warrants its rights to use and consume the water prior to transferring to the other party. Including this warranty in the Agreement allows each party to use the Production Water transferred without independent verification of the transferring party's rights to the Production Water. Without this warranty the parties may find the administrative burdens associated with verifying the other party's right to use the water outweigh the benefits received by sharing Production Water between the parties.

Compliance with Laws Finally, the last allocation of risk clause addressed in this paper is the parties' commitment to comply with all applicable laws and regulations of governmental entities having jurisdiction over the Production Water or the transportation process. This includes compliance with all laws and regulations related to the entire life cycle of the Production Water including the proper disposal of the Production Water at the end of its useful life. Upon accepting a transfer of Production Water the receiving party is committing to the eventual proper disposal. By each producer affirmatively agreeing to comply with the applicable laws, it establishes that each producer will conduct its operations in a responsible and legal manner, and therefore each party may be held individually accountable in the event of noncompliance. Furthermore, the Transfer Agreement provides the mechanism with which each producer may require actions in the event of noncompliance on the part of the other party.

In addition to a statement regarding the compliance with all laws and regulations, the Transfer Agreement also includes a provision stating that each party will comply with the policies of the other party pertaining to the point of transfer and the transfer process. This provision again ensures that the producers will perform their obligations under the agreement safely and responsibly, and further supports the cooperation envisioned by the Sharing Arrangement.

Record of Transfer

As briefly discussed above, the Record of Transfer is a document that the producers execute for each transfer occurring as a part of the Sharing Arrangement. The execution of the Record of Transfer incorporates the terms and conditions of the entire Transfer Agreement and creates one complete and binding agreement between the parties. It serves essentially as a bill of lading for each transfer of Production Water, and provides the producers the opportunity to exchange a detailed account of the specific Production Water involved in the transfer. Each Record of Transfer will document, at a minimum, the following:

1. the transferring party and the receiving party;
2. the amount of Production Water requested;
3. the amount of Production Water actually transferred;
4. the specific water quality of the Production Water transferred including where the water originated (*i.e.* the specific well where the water was produced);
5. the specific point of transfer with as much specificity as possible under the circumstances;
6. the proposed date for the transfer and the actual date of the transfer;
7. how delivery will be accomplished (*i.e.*

truck or pipeline); and
8. any special instructions for the specific transfer.

Each producer is required to keep a copy of every Record of Transfer to satisfy its individual record-keeping and reporting requirements. It is extremely important that the producers exchange accurate in-depth information on the Record of Transfer, as this information may need to be reported to regulatory agencies having jurisdiction. In the case of this Sharing Arrangement, each producer has the obligation to provide an annual report summarizing the transfers made under the Agreement to the Colorado Oil and Gas Conservation Commission. It is important to note that the reporting requirements for a similar arrangement may differ based on the specific transfers taking place and the applicable rules and regulations of the governing agencies.

Conclusion:

The major terms of the Transfer Agreement discussed above, although not an exhaustive list of the terms of the Agreement, indicate the significant complexities the parties had to negotiate and address in order to share produced water resources between their respective operations. By entering into the comprehensive Transfer Agreement to describe and control the terms of the Sharing Arrangement, the two producers were able to resolve the legal and operational challenges and allow for the transfer of Production Water in compliance with the numerous applicable laws and regulations. Outlining the requirements and procedures for the transfer, identifying and addressing the potential pitfalls, and allocating the liabilities and obligations between the parties in a legally binding agreement is crucial to ensure the ongoing success of the Sharing Arrangement. Before even a single transfer could take place, each producer had to clearly understand its role in the Sharing Arrangement and agree to adhere to the terms of the Transfer Agreement. Once these terms were understood and accepted, the parties could confidently transfer water to advance the economic and timing efficiencies of their operations, while minimizing waste and maximizing the utilization of the valuable water resource.

The basic concepts underlying the Sharing Arrangement can be replicated across the nation among producers developing oil and gas resources in the same region by applying similar practical solutions. However, in addition to produced water, the major terms and conditions included in the Agreement can be modified to apply to any number of unconventional water sources, including for example, acid mine drainage. The Transfer Agreement provides an example on how parties can address the legal and operational challenges and allocate liabilities and obligations among responsible parties which may be replicated in any type of water sharing arrangement. In addition, it provides the basic framework for how to integrate new water sources into oil and gas operations practically and efficiently.

As fresh water resources continue to dwindle while demands for water in industrial processes grow, the ability to incorporate new and unconventional water resources into operations will be essential for the continued advancement of these industries. With the significant technical advances in water treatment, in addition to the increasing costs to obtain fresh water, water resources previously determined to be unusable may now be economically treated and reused, but the parties involved must know and understand the risks and benefits of such use.

References

Colo. Rev. Stat. § 37-90-137(7) (2012)

Produced Nontributary Ground Water Rules 2 C.C.R. 402–17 (2010)

Thorne CL, Caile WH (2013) Produced Water Extraction From Oil and Gas Wells: Implications for Western Water Rights. Natural Resources and Environment ABA Section of Environment, Energy and Resources 27(3): 16–19

Vance v. Wolfe, 205 P.3d 1165 (Colo. 2009)

Water Associated with Oil and Gas Production – Produced Water Management and Water Needs

John Veil

Veil Environmental, LLC, 1081 Carriage Hill Ct., Annapolis, MD 21401, USA, john@veilenvironmental.com

Abstract Water plays an integral role in oil and gas production as a needed input and as a byproduct. Water is required to make up drilling fluids and hydraulic fracturing fluids, and in many fields is needed for water or steam flooding to produce more oil. Most wells generate produced water during production. This paper describes how water is a part of oil and gas production, with an emphasis on management of produced water.

Keywords produced water, oil and gas, hydraulic fracturing

Introduction

Oil and gas can be produced in a variety of ways. Each of these production methods has its own profile for water needs and wastewater (produced water) generation. Produced water is not a single, consistent commodity. In reality, it is quite variable, not only in its chemical/physical characteristics, but also in the volume of produced water generated by a single well and whether that volume increases or decreases over time. Table 1 shows a summary of how the water needs and the produced water

Type of Oil and Gas Production	Water Needs for Production	Produced Water Generated
Conventional Oil and Gas	• Modest needs for hydraulic fracturing • More needed for enhanced recovery later on	• Low volume initially • Increased volume over time • High lifetime pw production
Coalbed Methane	• Modest needs for hydraulic fracturing	• High volume initially • Decreases over time
Shale Gas	• Large needs for hydraulic fracturing	• Initial flow rate is high, but quickly drops to very low • Low lifetime flowback and produced water production
Heavy Crude	• Steam flood to help move heavy oil to production wells	• Much of the water results from the injected steam used in steam flooding
Oil/Tar Sands	• Steam (or water) injection used in large volumes	• In-situ production methods: some water is formation water, but much is from the injected steam • Oil sand mining production methods and subsequent processing steps also generate wastewater

Table 1 *Variations in Water Needs and Generation by Production Method*

outputs vary based on the hydrocarbon production method used.

What Is Produced Water?

Produced water is water brought to the surface along with oil or gas. In most cases, the water is natural water that was present in the formation for a long time, but it can also include water that was introduced to the formation by the oil and gas company for production purposes (*e.g.* water flood, steam flood, hydraulic fracturing). Produced water may also be referred to as "brine" or "salt water" (Veil *et al.* 2004).

The individual concentrations vary from well-to-well and over time, but the major constituents of concern in produced water are:

- Salt content (salinity, total dissolved solids [TDS], electrical conductivity) – TDS concentrations range from < 5,000 mg/L to > 250,000 mg/L.
- Oil and grease (this is not a single compound – rather it is an analytical method that measures the presence of many families of organic chemical compounds). Oil and grease is typically quite low in gas wells but is much higher in oil wells. Oil may be in separate state or may be emulsified.
- Various natural inorganic and organic compounds that are part of the rock from which the produced water originated, the hydrocarbon which was in contact with the produced water for centuries, or chemical additives that are used in drilling and operating the well. There can be hundreds of potential compounds in produced water, but most are present in low concentration. Some of the volatile organic compounds can lead to air emissions when produced water is stored in open ponds.
- Naturally occurring radioactive material (NORM). NORM ranges from extremely low levels in some formations to relatively higher levels in formations like the Marcellus Shale. Generally the concentration of NORM in produced water is below any public health concern levels, although if produced water is treated, any resulting sludges or concentrated brines will have higher concentrations.

Produced Water Volume

It is challenging to make a comprehensive and accurate estimate of the produced water volume generated in the entire United States over a year (there are nearly 1 million producing oil and gas wells in the country). The most recent detailed estimate was published in 2009 – it represents water volumes from the 2007 calendar year (Clark and Veil 2009). The total 2007 produced water volume, including onshore and offshore wells, was approximately $21 \cdot 10^9$ US bbl ($882 \cdot 10^9$ US gal; $3.3 \cdot 10^9$ m^3).

Water production profiles and lifetime total volumes vary depending on the method used to produce oil and gas. These differences are shown in Table 1.

Another important statistic is the water-to-oil ratio (WOR). Clark and Veil (2009), using data from only 14 states, found WOR values from 5.3 to 1 to 7.6 to 1. However, the data provided by several of the states with the largest number of wells could not be used for WOR calculation (water production was not separated by gas wells *vs.* oil wells). The authors noted that if data from those states with large numbers of older wells with presumably high WORs had been available and included, the actual national average WOR would most likely be greater than 10 to 1. Higher WOR values mean that the operator must devote more effort and cost to manage the water from those wells. Typically, wells with higher WOR are older, more mature wells.

Since 2007, many new wells have been drilled to produce oil and gas from tight shale formations. Some people believe this will cause the national produced water volume to increase dramatically. Typically, these wells require a significant volume of water for hydraulic fracturing, but once the well begins production, there is only a small ongoing volume of water produced. The newly abundant shale gas wells contribute far less produced water to the national total that other more conventional oil and gas wells. The national produced water total is unlikely to rise rapidly from its 2007 level.

Produced Water Management

Produced water management technologies and strategies can be described in terms of a three-tiered water management or pollution prevention hierarchy (*i.e.* minimization, recycle/reuse, and disposal). Companies are encouraged to first evaluate practices that reduce the volumes of produced water entering the well or being handled at the surface. In this water minimization tier, processes are modified, technologies are adapted, or products are substituted so that less water is generated. When feasible, water minimization can often save money for operators and results in greater protection of the environment. Examples of technologies followed include:

- Reduce the volume of water entering the wells using mechanical blocking devices (*e.g.* packers, plugs, cement jobs) or water shut-off chemicals.
- Reduce the volume of water managed at the surface by remote separation (*e.g.* downhole separation or sea floor separation).

For the water that is still produced following water minimization, operators move next to the second tier, in which water is reused in a beneficial manner or recycled. Examples of reuse include injection for enhanced oil recovery, irrigation water, industrial water supply, and even drinking water.

In some situations, these more desirable management options may not be practical, cost-effective, or permitted by the regulatory agencies. Then water must be disposed of by injection, discharge, evaporation, or removal offsite to a commercial water disposal facility.

Prior to reusing or disposing produced water, companies often must first treat the produced water. Many technologies are available that can be used to treat different components of the produced water. For removing inorganics and salinity the following technologies have been used:

- pH adjustment, flocculation, and clarification,
- Electrocoagulation,
- Membrane filtration (micro filtration, ultrafiltration, nanofiltration, reverse osmosis),
- Thermal treatment,
- Ion exchange, and
- Capacitive deionization.

For removing organics and oil and grease, the following technologies have been used:

- Physical separation (gravity separators, hydrocyclones, filters, centrifuges),
- Coalescence,
- Flotation,
- Combined physical and extraction processes,
- Solvent extraction,
- Adsorption, and
- Oxidation.

A detailed written description of technologies and practices is available at Veil (2011). A more readily available version of this information can be found on the Produced Water Management Information System (PWMIS) website, developed by the author and his former colleagues (PWMIS 2007).

Costs for produced water management vary widely from a few cents per barrel (1 barrel or bbl = 42 U.S. gallons = 0.16 m^3) to more than $10/barrel. They are very site-specific. The true cost includes many cost components (Table 2).

U.S. Regulations Concerning Produced Water

In 1988 and 1993 the U.S. Environmental Protection Agency (EPA) published notices stating

Category	Cost Component (Some or all may be applicable)
Prior to Operations	• Prepare feasibility study to select option (in-house costs and outside consultants) • Obtain financing • Obtain necessary permits • Prepare site (grading; construction of facilities for treatment and storage; pipe installation) • Purchase and install equipment • Ensure utilities are available
During Operations	• Utilities • Chemicals and other consumable supplies • Transportation • Debt service • Maintenance • Disposal fees • Management of residuals removed or generated during treatment • Monitoring and reporting • Down time due to component failure or repair • Clean up of spills
After Operations	• Removal of facilities • Long-term liability • Site remediation and restoration

Table 2 *Components Contributing to Total Cost of Wastewater Management*

that wastes resulting from oil and gas exploration and production (including produced water) would not be regulated as hazardous wastes under the Resource Conservation and Recovery Act. The notices clarified that most oversight of these wastes would be handled by state agencies.

The most common ways for managing produced water are discharge and injection. The EPA published national discharge standards (effluent limitations guidelines) for the oil and gas industry. Offshore platforms can discharge in conformance with the requirements of National Pollutant Discharge Elimination System (NPDES) permits. Nearly all offshore wells treat produced water on the platform then discharge it back to the ocean.

Most onshore wells, however, are prohibited from discharging produced water. This led most operators to inject their produced water. Clark and Veil (2009) report that more than 90 % of onshore produced water is injected into underground formations. Slightly more than half is injected into producing formations for enhanced recovery. The remainder is injected into non-hydrocarbon bearing formations for disposal. Injection wells are regulated by the Underground Injection Control (UIC) program. The EPA has primary authority for this program, but has delegated UIC authority to many states.

In a few locations, the salinity level of produced water is low enough that it can be economically treated and discharged. In these situations, the state NPDES permitting agencies would issue permits to control the discharges.

When there is an opportunity for beneficial reuse of produced water, there may or may not be regulatory requirements. Usually the level of treatment prior to reuse is set not by regulatory standards, but rather by the operational water quality needs of the end user.

Conclusions

Sizeable volumes of water are needed to drill and hydraulically fracture many wells. Produced water is generated at many U.S. locations in high volume. Various options are available for managing that water. The presentation provides more detail on how water is used to produce oil and gas, qualitative estimates of the water volume needed, how produced water is managed, and some discussion of hydraulic fracturing and flowback water.

References

Clark CE, Veil JA (2009) Produced Water Volumes and Management Practices in the United States, ANL/EVS/R-09/1, prepared for the U.S. Department of Energy, National Energy Technology Laboratory, September, 64 pp.

PWMIS (2007) Produced Water Management Information System website, developed by Argonne National Laboratory for the U.S. Department of Energy, National Energy Technology Laboratory, www.netl.doe.gov/technologies/pwmis.

Veil JA (2011) Produced Water Management Options and Technologies, chapter in Produced Water: Environmental Risks and Advances in Mitigation Technologies, edited by Lee K, Neff J, Springer.

Veil JA, Puder MG, Elcock D, Redweik RJ Jr (2004) A White Paper Describing Produced Water from Production of Crude Oil, Natural Gas, and Coal Bed Methane, prepared by Argonne National Laboratory for the U.S. Department of Energy, National Energy Technology Laboratory, January 2004, 87 pp.

8

FIELD TRIPS

FIELD TRIPS

IMWA 2013 Mid-Conference Tour to Leadville, Colorado: August 7th, 2013

Raymond H. Johnson

U.S. Geological Survey, Denver Federal Center, Denver, Colorado, USA, rhjohnso@usgs.gov

Abstract An itinerary, maps, and details about the IMWA 2013 mid-conference tour from Golden, Colorado to Leadville, Colorado on August 7, 2013, are provided.

Keywords IMWA 2013, mid-conference tour, Leadville

Introduction

A summary of the IMWA 2013 mid-conference tour to Leadville, Colorado is provided. This trip will be on Wednesday, August 7th, 2013. An itinerary, maps, and a few details about what we will see (along with web links) are provided below. North is toward the top of the page on all maps.

Itinerary

7:30 Leave Golden, CO

9:30 Arrive in Leadville, CO (fig. 1) at the National Mining Hall of Fame and Museum with a half hour break

10:00 – 12:00 One group will tour the National Mining Hall of Fame and Museum and one group will tour the nearby abandoned mine lands and drainage tunnels (fig. 2)

12:00 – 13:00 Lunch altogether in the National Mining Hall of Fame and Museum ballroom with an overview presentation of the Climax Molybdenum Mine (given by a Climax Mine employee)

13:00 – 15:00 Groups will switch and one

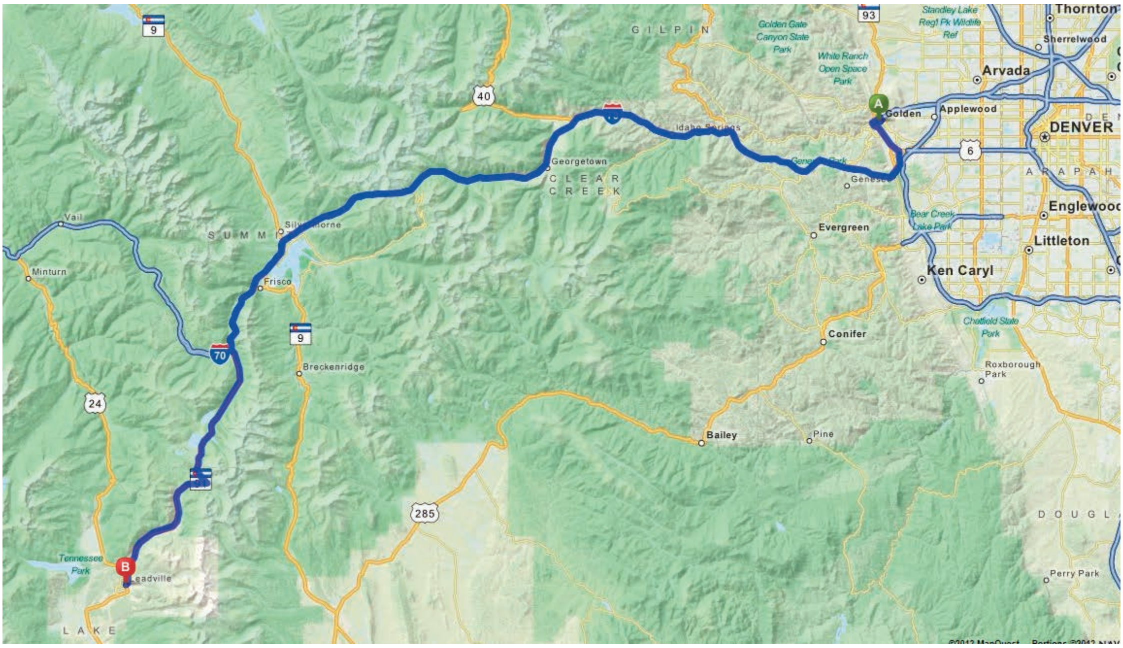

Fig. 1 Map of IMWA 2013 mid-conference field trip route. Golden, Colorado (A) to Leadville, Colorado(B). Distance from Golden to Leadville is approximately 148 km (92 mi). Map base is from www.mapquest.com.

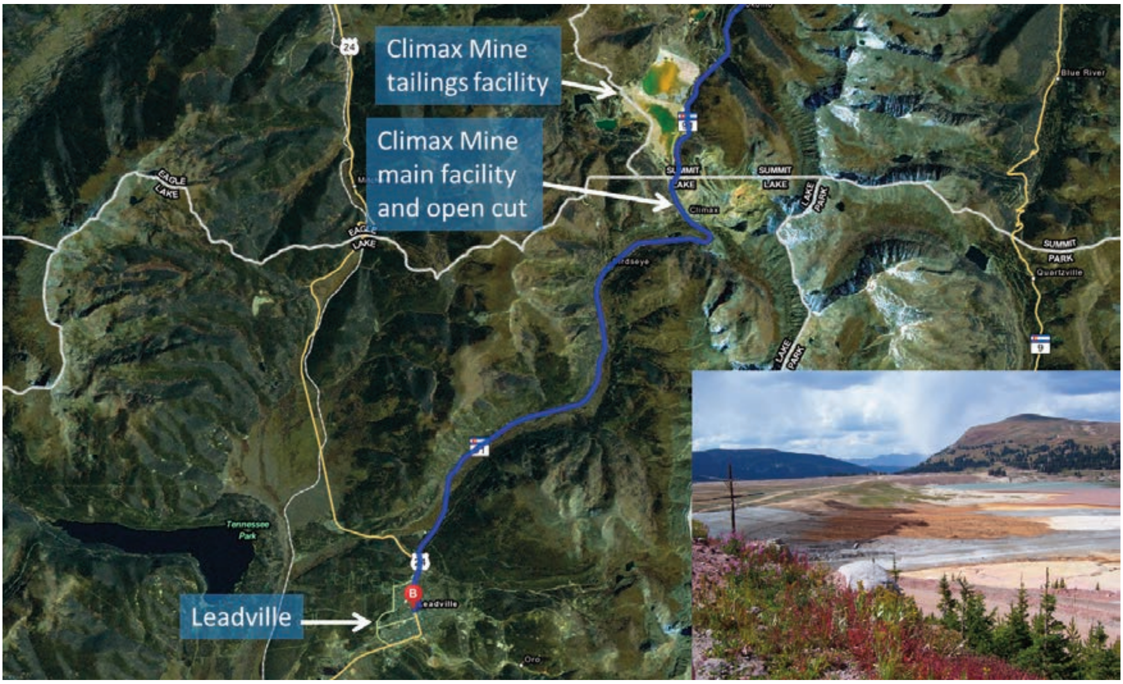

Fig. 2 Map of Leadville’s abandoned mine lands and mine drainage tunnels. Map source is the U.S. Department of Interior, Bureau of Reclamation (pdf link is provided in the text).

group will tour the National Mining Hall of Fame and Museum and one group will tour the nearby abandoned mine lands and drainage tunnels (fig. 2)

15:00 – 15:15 Travel by bus to the Climax Mine

15:15 – 16:15 Two stops: (1) overlook of Climax Mine operations, and (2) overlook of the Climax tailings disposal facility (fig. 3). At both stops a mine employee will be available to discuss the operations in more detail and answer questions.

16:15 – 18:00 Travel by bus back to Golden

Note: all times are approximate

Leadville, Colorado

Leadville, Colorado, has a colorful mining history with the discovery of gold in 1860, followed by silver-lead deposits in 1876. By 1880, Leadville had a population of over 40,000 as one of the world’s largest silver camps. As of 2010, the population in Leadville was 2,602. At 3,094 m (10,152 ft) Leadville is the highest incorporated city in the United States and has an alpine subarctic climate. Average high temperatures in August are 20.8 °C (69.5 °F), so bring a light jacket. Many additional details about Leadville, Colorado can be found at http://en.wikipedia.org/wiki/Leadville,_Colorado and www.visitleadvilleco.com.

Leadville National Mining Hall of Fame and Museum

This is a very extensive mining museum that covers the history of mining in the Leadville area. Details about the museum can be found at www.mininghalloffame. org. During the museum time, participants can also visit downtown Leadville if interested.

Abandoned Mine Lands: California Gulch and mine drainage tunnel

In 1983 the abandoning mining area around Leadville was added to the National Priorities List (Superfund) for environmental remediation due to past mining, milling, and smelting operations. The United States Envi-

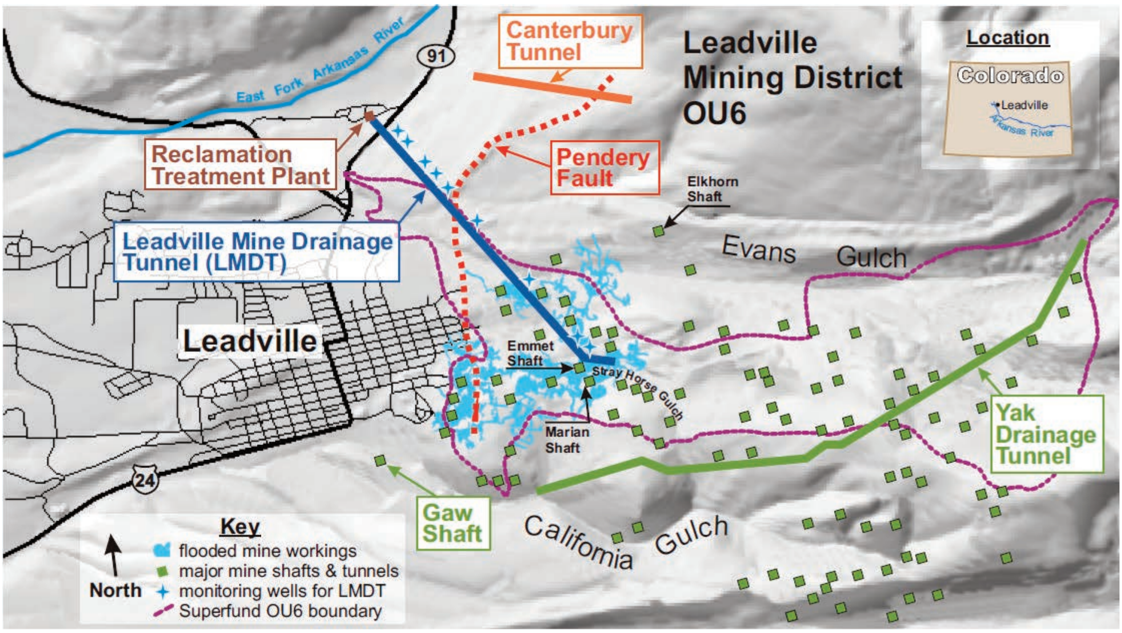

Fig. 3 *Location of the Climax Molybdenum Mine. Distance from Leadville to the Climax Mine is approximately 21 km (13 mi). Inset is a view of the tailings facility. Map base is from www.mapquest.com.*

ronmental Protection Agency (EPA) has a detailed web site on the remediation efforts (www.epa.gov/Region8/superfund/co/calgulch). The California Gulch Superfund listing is divided into 12 operable units and includes 46.6 km^2 of Lake County, Colorado. As of September 2011, remediation efforts at four of these operable units have been declared complete.

A brief overview on the mine drainage tunnels in the area (including the Yak Tunnel and the Leadville Mine Drainage Tunnel or LMDT, fig. 2) are provided in http://www.usbr.gov/gp/ecao/leadville/lmdt_overview.pdf. The Leadville Mine Drainage Tunnel was constructed in 1943 to 1952 to drain portions of the Leadville Mining District in order to continue development of strategic mineral reserves. In 1959, the U.S. Bureau of Reclamation acquired the tunnel in a failed attempt to use the flow for water supply purposes. In 1992 the U.S. Bureau of Reclamation completed a water treatment facility at the tunnel's portal. Subsequent collapses of the Leadville Mine Drainage Tunnel created water blockages that threatened sudden releases of mine drainage water into the nearby Arkansas River. Emergency response by the EPA included a relief well and pipeline construction in 2008.

The Yak Tunnel (fig. 2) is another main tunnel that drained the historic mining district and was a primary focus of studies and cleanup activities from 1989 to 1994 overseen by the EPA (EPA oversight in the area is still ongoing). The initial portion of the Yak Drainage Tunnel was constructed in 1895 to drain water from the surrounding mines. The Yak Tunnel treatment plant began operating in 1992 and prior to that date 210 tons of metals drained from the California Gulch area into the nearby Arkansas River each year. Water quality in the Arkansas River has now improved substantially.

Climax Molybdenum Mine

The history of the Climax Mine can be found at http://en.wikipedia.org/wiki/Climax_mine and in a book by S.M. Voynick (http://mountain-press.com/item_detail.php?item_key=615). This mine is located in what was the unincorporated mining village of Climax, Colorado (http://en.wikipedia.org/wiki/Climax,_Colorado). The Climax Mine produces molybdenum, which is used mainly to strengthen steel, but is also used as a solid lubricant. The Climax Molybdenum Mine first produced ore in 1915. The mine was recently closed, but reopened again on May 10, 2012 and is operated by Climax Molybdenum (www.climaxmolybdenum.com), which is part of Freeport-McMoRan Copper and Gold (www.fcx.com). The Climax Mine is an open-cut mine with an extensive tailings disposal facility (fig. 3).

Disclaimer

All mention of company names are for informational purposes only and do not constitute any endorsement by the author or the U.S. Geological Survey.

Mines, Mountains, and Hot Springs – IMWA 2013 Post-Conference Tour to Silverton, Colorado: August 10–13, 2013

Raymond H. Johnson

U.S. Geological Survey, Denver Federal Center, Denver, Colorado, USA, rhjohnso@usgs.gov

Abstract An itinerary, maps, and details about the IMWA 2013 post-conference tour from Golden, Colorado to Silverton, Colorado on August 10–13, 2013, are provided.

Keywords IMWA 2013, post-conference tour, Silverton

Introduction

A summary of the IMWA 2013 post-conference tour to Silverton, Colorado is provided. This trip will be from August 10–13, 2013. An itinerary, maps, and details about what we will see (along with web links) are provided below. North is toward the top of the page on all maps.

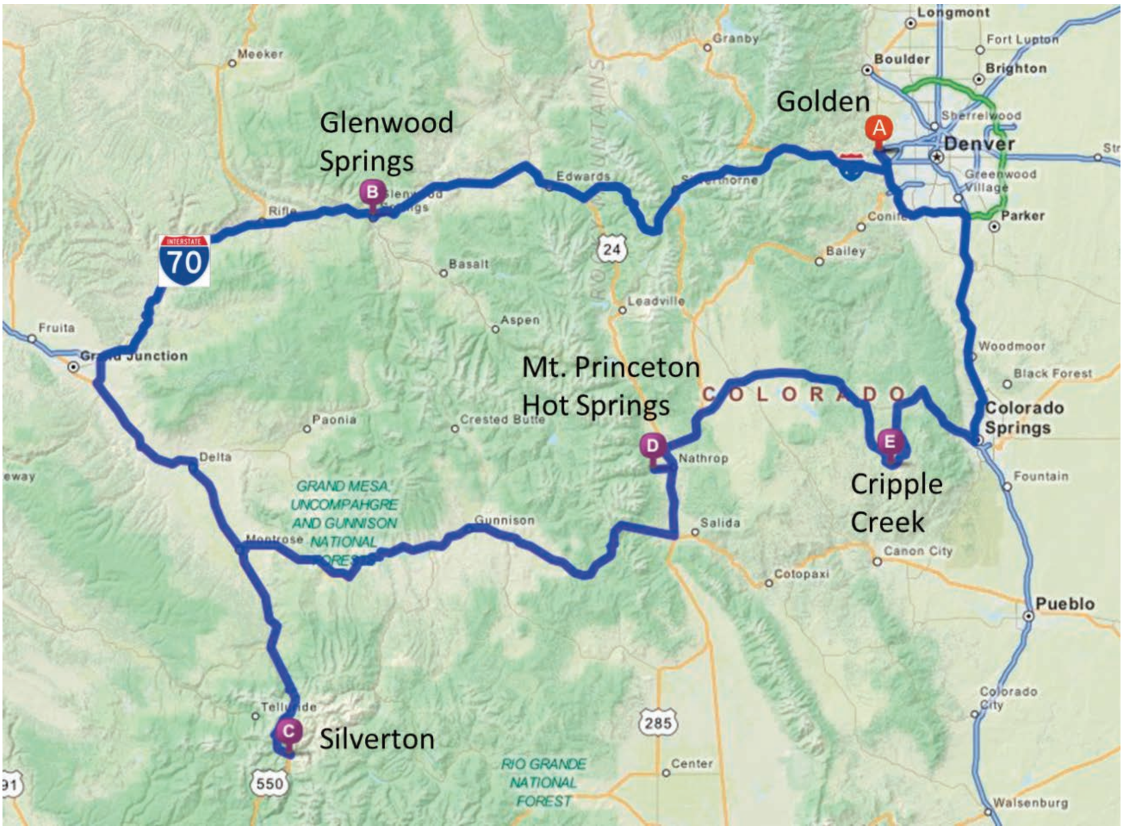

Fig. 1 *Map of IMWA 2013 post-conference field trip route. Golden, Colorado (A) to Glenwood Hot Springs (B) to Silverton (C) to Mount Princeton Hot Springs (D) to Cripple Creek (E) and back to Golden. Road distance from Golden to Silverton is approximately 560 km (350 mi). Map base is from www.mapquest.com.*

Itinerary

Map of full trip route is shown in Fig. 1.

August 10: Golden to Silverton (fig. 1)

07:30 Leave Golden

10:30 – 13:30 Glenwood Hot Springs

18:30 Arrive in Silverton

August 11: Silverton 4 × 4 tour (fig. 2)

08:00 – 17:00 All day in the San Juan Mountains in four-wheel drive, open-top vehicles

August 12: Silverton to Mount Princeton Hot Springs (fig. 3)

08:00 – 10:00 Overlook the Silverton caldera or free time to see the local sights

10:00 – 11:30 Tour of the Mayflower Mill

11:30 – 12:30 Lunch in the local park

12:30 – 17:30 Travel from Silverton to Mt. Princeton Hot Springs

17:30 Arrive at Mount Princeton Hot Springs

August 13: Mount Princeton Hot Springs, Cripple Creek and Victor Gold Mine, and back to Golden (figs. 1, 4)

08:00 – 10:30 Travel from Mt. Princeton Hot Springs to Cripple Creek

10:30 – 15:00 Tour the Cripple Creek area and the Cripple Creek and Victor Gold Mine

15:00 – 18:00 Travel back to Golden

Note: all times are approximate

August 10: Golden to Silverton

On the first day we will travel though the central Colorado Rocky Mountains (fig. 1), taking Interstate 70 over the Continental Divide, past Dillon Reservoir (part of Denver’s water supply), and through Glenwood Canyon (http://en.wikipedia.org/wiki/Glenwood_Canyon), which was carved by the Colorado River. We will have an extended lunch stop with time to swim in the Glenwood Hot Springs (www.hotspringspool.com). After Glenwood Springs, we will drive around the north and west sides of Grand Mesa, a 1,300 km^2 (500 square miles) flat topped mountain (3,454 m or 11,332 ft at its peak) capped with volcanic basalt (http://en.wikipedia.org/wiki/Grand_Mesa), before heading south towards Silverton. Hang on to your hats as we drive from Ouray to Silverton along the Million Dollar Highway (http://en.wikipedia.org/wiki/U.S._Route_550) believed to have gotten its name because it cost a million dollars a mile to build in the 1920s. The drop off from the edge of the road to the river below is pretty impressive. If you want a preview, you can take a look at www.youtube.com/watch?v=geLCaRlb3IM.

Throughout the day, we will discuss the geology of Colorado using the guidebook written by Chronic and Williams (2002). At the end of a long day, we will have time to relax in Silverton (http://en.wikipedia.org/wiki/Silverton,_Colorado) where we will be staying at the Grand Imperial Hotel (www.grandimperialhotel.com), which was built in 1882 and has Victorian-style architecture.

August 11: Silverton 4 × 4 tour

A full day touring the San Juan Mountains (fig. 2) in an open-topped four-wheel drive vehicle cannot be beat. This day will have lots of mountain scenery, but also a lot of information about the local geology (Yager and Bove 2002), as this area is rich in metal ores and is the center of the 28-million year old Silverton caldera. We will also visit some of the many abandoned mine sites and discuss the related acid-mine drainage and natural acid-rock drainage issues. In Fig. 2 you can see some of the red iron staining on the mountain sides to the west of Silverton, Cement Creek, and Gladstone.

We will start out from Silverton and go along Cement Creek (fig. 2), which got its name from the naturally cemented creek bottom. Historic mining in the area has degraded the stream water quality even more, resulting in increased metals in the surface water and loss of fish habitat downstream. The U.S. Geological Survey (USGS) has completed a variety of studies in the area, which will be discussed

Fig. 2 *Map of 4 × 4 route on from Silverton on August 11 (while line). Map base is from Google Earth.*

throughout the day. This area was part of the USGS abandoned mine land initiative (http://amli.usgs.gov and http://amli.usgs.gov/data/animas) and a series of scientific articles were compiled and published in Church *et al.* (2007). More recent studies have used geographic information systems (GIS) to better understand the rock/water interactions that occur in the area (Yager *et al.* 2008, Yager *et al.* 2013). In addition, the Animas River Stakeholders Group (www.animasriverstakeholders-group.org) has been responsible for overseeing abandoned mine reclamation projects and continues to monitor the water quality in the Upper Animas River watershed.

The first stop outside of Silverton along Cement Creek will be a zone of iron-cemented gravel, or ferricrete. This ferricrete was deposited during post-glacial times and is approximately 10,000 years old. It is near the road high above the stream that has since down cut into the valley. The next stop will be Prospect Gulch. Several abandoned mines are located in this small watershed, and it was selected by the USGS for focused studies on understanding the groundwater flow and its influence on the stream water quality (Johnson and Yager 2006, Johnson *et al.* 2007, Johnson 2008). In and around Prospect Gulch, we will visit: (1) some of the groundwater monitoring wells, (2) some natural springs with acid-rock drainage, (3) sites where stream tracers were completed to measure stream flow and groundwater discharge (Wirt *et al.* 2001, Johnson *et al.* 2007), and (4) the abandoned mines, and talk about the reclamation that has been completed, including a full encapsulation of the waste rock from the Lark Mine (completed by the U.S. Bureau of Land Management).

Our next stop will be at Gladstone (fig. 2) and the mouth of the American Tunnel. This tunnel was completed to drain the mines

Fig. 3 *Map of route on August 12 from Silverton (A) to Mount Princeton Hot Springs (B) near Nathrop, Colorado. Road distance is approximately 320 km (200 mi). Map base is from www.mapquest.com.*

above it and was part of the Sunnyside Mine complex (www.mindat.org/Loc-3687.html), which produced over $150 million dollars' worth of metals. It currently has several bulkheads in an attempt to back up the groundwater to pre-mining conditions. However, this bulkheading created new discharges in open mines up the hill (like the Red and Bonita Mine that we will see later in passing). Several stream tracer studies were also completed in this area (Kimball *et al.* 2002, 2007) to better understand the water flow and quality patterns, along with being a valuable tool to assess remedial options (Walton-Day *et al.* 2007, 2012). While the Animas River Stakeholders Group (ARSG) has seen improvements in stream water quality elsewhere, the discharge from in and around the American Tunnel is still a large source of metals draining into Cement Creek. ARSG and several federal entities are currently pursuing treatment options to improve stream water quality in the immediate area.

The trip from Gladstone to Animas Forks (fig. 2) is a rugged four-wheel drive road with amazing mountain scenery. Along the way, we will overlook the Red Mountains just outside of Gladstone, pass some interesting abandoned mines, go over Hurricane Pass, and then drop into the long glacially-carved California Gulch, just before Animas Forks (http://en.wikipedia.org/wiki/Animas_Forks,_Colorado).

Animas Forks is an old mining „ghost" town with many of the old houses still standing. As we come out of the rugged mountains into a broader braided-stream river valley, we will see the abandoned Eureka Mill site and

Fig. 4 *Map of route onAugust 13 from Mount Princeton Hot Springs (A) to Cripple Creek (B). Road distance is approximately 136 km (84 mi). Map base is from www.mapquest.com.*

pass by the Mayflower Mill (fig. 2), with a large tailings impoundment next to it.

August 12: Silverton to Mount Princeton Hot Springs

After a few hours in the morning to enjoy the town of Silverton or going to overlook the edge of the Silverton Caldera, we will be touring the historic Mayflower Mill maintained by the San Juan County Historical Society (www.silvertonhistoricsociety.org). Built in 1929, the Mayflower Mill is one of the last mills in the area that is still standing. On the way out of Silverton, we will follow Mineral Creek next to highway 550 (fig. 2), where a recent stream tracer study was completed by the USGS to determine stream and groundwater flows along with changes in metal loads after recent reclamation activities (Runkel at al. 2009a, b). In the afternoon, we will be on scenic roads through the Colorado Mountains (fig. 3) and again be using Chronic and Williams (2002) to inform us about the geology. Near Gunnison (fig. 3) we will be able to see cliffs of volcanic tuff that formed from the volcanic eruptions of the Silverton caldera 28 million years ago. We will be staying at the Mountain Princeton Hot Springs Resort (www.mtprinceton.com).

August 13: Mount Princeton Hot Springs, Cripple Creek and Victor Gold Mine, and back to Golden

This day will be more travel through the mountains (figs. 1, 4) with much of the day spent touring an open pit gold mine operated by the Cripple Creek and Victor Gold Mining Company (www.ccvgoldmining.com). We will have a chance to visit a regional mine drainage tunnel for the Cripple Creek Mining District, discuss mine water management issues, and will hopefully have some time to visit the historic gold mining town of Cripple Creek (http://en.wikipedia.org/wiki/Cripple_Creek,_Colorado).

Disclaimer

All mention of company names are for informational purposes only and do not constitute any endorsement by the author or the U.S. Geological Survey.

References

Chronic H, Williams, F (2002) Roadside geology of Colorado, 2nd ed. Mountain Press, Missoula, Montana, 399 p

Church SE, von Guerard P, Finger SE, eds. (2007) Integrated investigations of environmental effects of historical mining in the Animas River watershed, San Juan County, Colorado. U.S. Geological Survey Professional Paper 1651, 1,096 p. plus CD-ROM [In two volumes] (http://pubs.usgs.gov/ pp/1651/)

Johnson RH (2008) Geologic controls on metal transport in groundwater within an alpine watershed affected by historical mining (Chapter G) in Verplanck PL, ed., Understanding contaminants associated with mineral deposits. U.S. Geological Survey Circular 1328, 96 p (http://pubs.usgs.gov/ circ/1328/)

Johnson RH, Wirt L, Manning AH, Leib KJ, Fey DL, Yager DB (2007) Geochemistry of surface and groundwater in Cement Creek from Gladstone to Georgia Gulch and in Prospect Gulch, San Juan County, Colorado. U.S. Geological Survey Open-File Report 2007–1004 (http://pubs.usgs.gov/of/ 2007/1004/)

Johnson RH, Yager DB (2006) Completion reports, core logs, and hydrogeologic data from wells and piezometers in Prospect Gulch, San Juan County, Colorado. U.S. Geological Survey Open-File Report 2006–1030 (http://pubs.usgs.gov/of/2006/ 1030/)

Kimball BA, Walton-Day K, Runkel RL (2007) Quantification of metal loading by tracer injection and synoptic sampling, 1996–2000 (Chapter E9), in Church SE, von Guerard P, Finger SE, eds., Integrated Investigations of Environmental Effects of Historical Mining in the Animas River Watershed, San Juan County, Colorado. U.S. Geological Survey Professional Paper 1651, (1):417—495. (http://pubs.usgs.gov/pp/1651/)

Kimball BA, Runkel RL, Walton-Day K, Bencala KE (2002) Assessment of metal loads in watersheds affected by acid mine drainage by using tracer injection and synoptic sampling—Cement Creek, Colorado, USA. Applied Geochemistry 17(9):1183—1207, doi:10.1016/S0883-2927(02)00017-3

Runkel RL, Bencala KE, Kimball BA, Walton-Day K, Verplanck PL (2009a) A comparison of pre- and post-remediation water quality, Mineral Creek, Colorado. Hydrological Processes, 23(23):3319—3333, doi:10.1002/hyp.7427

Runkel RL, Kimball BA, Steiger JI, Walton-Day K (2009b) Geochemical data for upper Mineral Creek, Colorado, under existing ambient conditions and during an experimental pH modification, August 2005. U.S. Geological Survey Data Series 442, 41p (http://pubs.usgs.gov/ds/442/)

Walton-Day K, Paschke SS, Runkel RL, Kimball BA (2007) Using the OTIS solute-transport model to evaluate remediation scenarios in Cement Creek and the Upper Animas River (Chapter E24) in Church SE, von Guerard P, Finger SE, eds., Integrated Investigations of Environmental Effects of Historical Mining in the Animas River Watershed, San Juan County, Colorado. U.S. Geological Survey Professional Paper 1651, (2):973—1028 (http://pubs.usgs.gov/pp/1651/)

Walton-Day K, Runkel, RL, Kimball BA (2012) Using spatially detailed water-quality data and solute-transport modeling to support total maximum daily load development. Journal of the American Water Resources Association (48):950—969, doi:10.1111/j.1752-1688.2012.00662.x

Wirt L, Leib KJ, Melick R, Bove D (2001) Metal loading assessment of a small mountainous sub-basin characterized by acid drainage—Prospect Gulch, upper Animas River watershed, Colorado. U.S. Geological Survey Open-File Report 2001–0258, 36 p (http://pubs.usgs.gov/of/2001/ofr-01-0258/)

Yager DB, Johnson RH, Rockwell BW, Caine JS, Smith KS (2013) A GIS and statistical approach to identify variables that control water quality in hydrothermally altered and mineralized watersheds, Silverton, Colorado, U.S.A. Environmental Earth Sciences, doi: 10.1007/s12665-013-2229-y

Yager DB, Johnson RH, Smith BD (2008) Using a geographic information system (GIS) to determine the physical factors that affect water quality in the Western San Juan Mountains, Silverton, Colorado (Chapter M) in Verplanck PL, ed., Understanding contaminants associated with mineral deposits. U.S. Geological Survey Circular 1328, 96 p (http://pubs.usgs.gov/circ/1328/).

Yager DB, Bove DJ (2002) Generalized geologic map of part of the upper Animas River watershed and vicinity, Silverton, Colorado. U.S. Geological Survey Miscellaneous Field Studies Map MF–2377, scale 1:48,000 (http://pubs.usgs.gov/mf/2002/ mf-2377/)

LAGNIAPPE

YOUR GOODIES

LAGNIAPPE

YOUR GOODIES

L

Author Index

Volume I pages 29– 760 ❧ *Volume II pages 807–1246*

Keyword Index

***Volume I** pages 29– 760* ❧ ***Volume II** pages 807–1246*

This keyword index is based on the keywords submitted by the authors. It is not an index for the pages in these proceedings. Each keyword directs to the paper’s first page.

IMWA — 国际矿井水协会

申请表

www.IMWA.info

个人或学生申请表 (请发电子邮件或传真给司库)

名、姓 ______________________ 、 ______________________

职称或职位 ______________________

单位地址（公司名称）______________________

____

电话号码 ______________ 传真号码 ______________ 电子邮件 ______________

家庭地址（住所）______________________

____

电话号码 ______________ 传真号码 ______________ 电子邮件 ______________

学生会员需要填写学校名称和预期毕业时间

____

通讯地址: □ 公司名称 □ 住所

会员类型（请选一）: □ 个人 □ 学生(<30 岁)

出生日期 ______________ 出生国家 ______________

国籍 ______________________

签名 ______________________ 申请日期 ______________

随信附上 20 ... ...年会费

□ 个人:	欧元 €50.00	(用信用卡€53.00)
□ 学生:	欧元 €25.00	(用信用卡€27.00)

请按汇款时汇率将欧元换算成美元，不要给司库直接汇欧元

缴费方法:

□ 银行支票** □ 电汇*** □ 银行发票

□ Visa 卡* □ 万事达卡* □ 网上缴费: www.IMWA.info/card

* 持卡人姓名: ______________________ 安全码: ______________

卡号: ______________________ 有效至: ______________

签名: ______________________

** 请将可付支票寄给 IMWA 司库:

Dr. Lee C. ATKINSON (Treasurer)
c/o Itasca Denver, Inc.
143 Union Blvd. Suite 525
Lakewood, CO 80228, USA
电话号码: +1 303 969-8033
传真号码: +1 303 969-8357

*** 您也可以电汇美元至 IMWA:

请发送 E-mail 至
treasurer@IMWA.info
以得到汇款帐号
请注意银行将收取 7 美元的手续费

/...

IMWA 一 国际矿井水协会

申请表

训练和经验 (请使用额外的表，如果有必要 一 请以英文填写)

www.IMWA.info

The 2013 International Mine Water Association Conference at the Colorado School of Mines takes place at a time of rapid growth in global mining and concomitant increase in mine water use and discharge.

Sustainable mining requires reliable mine water technology, to ensure that mining will meet all resource and environmental protection goals, and to assure all stakeholders that their water resource interests will not be adversely impacted by mining.

IMWA 2013 covers the state of the art and practice in reliable mine water technology, with over 200 papers on mine water use, mine water flow and control, mine water treatment and quality protection. It showcases the remarkable progress achieved in regulation, evaluation, use, extraction, treatment, and discharge of mine water, which makes mine water use and protection reliable and mining hydrologically and geochemically sustainable.

CONFERENCE THEMES

RELIABLE

1 Mine Water Permits and Regulation
2 Mine Water Hydrology
3 Mine Water Geochemistry
4 Mine Water Treatment
5 Mine Water Operations
6 Mine Water Closure
7 Mined Hydrocarbon Water

ISBN 978-0-615-79385-6